"Arrhythmogenic right ventricular cardiomyopathy; a disease of the desmosome: genetic and functional studies."

Angeliki Asimaki

A thesis submitted for the degree of Doctor of Philosophy

Department of Medicine

University College London

October, 2007

ProQuest LLC
789 East Eisenhower Parkway
P.O. Box 1346
Ann Arbor, MI 48106-1346

I hereby solemly declare that the work presented in this thesis has been carried out by me only unless otherwise acknowledged in the text.

Signature:

Angeliki Asimaki

Abstract:

Arrhythmogenic right ventricular cardiomyopathy (ARVC) is an inherited disorder associated with arrhythmias and sudden death. Mutations in the desmosomal genes plakoglobin and desmoplakin have been associated with the disease, founding the hypothesis that ARVC is a disease of cell adhesion. The aim of this study was to identify novel ARVC-causing genes and mutations and elucidate the molecular pathogenetic pathways of selected mutations.

As part of this study, mutation analysis of the recognized ARVC genes and of further candidate genes was performed on a large cohort of ARVC patients. Several novel mutations were identified and three further desmosomal genes were linked to the disease: plakophilin2, desmocollin2 and desmoglein2. Heart and skin samples from ARVC patients were subjected to microscopic examination and immunohistochemistry to study the effect of the newly-identified mutations on the structure of cell adhesion complexes.

The functional effects of a particular novel mutation were thoroughly examined in vitro. S39_K40insS is the first dominant ARVC-causing plakoglobin mutation to be reported. Yeast-two-hybrid analysis was used to investigate the effect of S39_K40insS on the protein interactions established by plakoglobin. A HEK293 cell line stably expressing the mutant protein was generated and used to study the effects of S39_K40insS on desmosomal structure, cell proliferation, cell death, subcellular localization and expression levels of proteins involved in adhesion and signaling and cellular responses to defined mechanical load. A recombinant adenovirus expressing the mutant protein was generated and used to transfect neonatal rat ventricular cardiomyocytes, whose behavior and responses were subsequently analysed. The functional consequences of S39_K40insS were compared with those of PK2157del2, a previously reported recessive plakoglobin mutation known to underlie Naxos disease, a syndromic form of ARVC.

These results point towards novel mechanisms of disease pathogenesis, that apart from weakened cell-cell adhesion involve altered protein turnover kinetics and defects in signaling pathways. Similar studies should improve our understanding of ARVC and provide a more accurate diagnostic algorithm.

TABLE OF CONTENTS:

Genetic studies of familial ARVC: identification of novel causative mutations and genes

Acknowledgements:

Completing a PhD is truly a marathon event, and I would never have been able to bring this journey to an end if it was not for the people that stood by my side over the past 4 years. I first have to express my gratitude to my teachers, my mentors; Professor Steve Humphries, who opened the way, who made what seemed impossible in September 2003, become a reality. Professor William McKenna, who helped me open my wings, lifted me up and then watched me fly. Bill, you have been a true inspiration. Your guidance, your belief and trust in me have been invaluable! Your leadership has set an example I hope to match one day. Professor Jeffrey Saffitz who made the journey across the Atlantic truly worth it, who motivated me until the very end. Jeff, your advice, help and support have been priceless. Dr. Petros Syrris, who greeted a shy girl with a cup of coffee on the 7th floor of the Middlessex Hospital 4 years ago, and has steadily held her hand ever since. Petros, through hills and valleys, through smiles and tears, we brought this to the end.

I am also grateful to our numerous collaborators. Dr. Wichter, Dr. Matthias, what we seeded all this time ago has finally flowered! Nikos, Adalena, your enthusiasm and effort are truly admirable. A big "thank you" goes to Nicholas, Mihaela and Patricia for their help with the animal work and to Dr. Hughes for her help in histology. Many thanks also go to Dr. Guereta and Dr. Mogensen for both samples and enthusiasm. Hayden, I could not have hoped for a better colleague. I am looking forward to working with you in the future. Together, we still have way to go! At this point I have to mention the people that worked by my side on the lab benches, the people that warmed up the atmosphere and made this journey an unforgettable experience; Alison, Denise, Tony, Shiney, Kiyomi, Karen, Wei-Hui, Nicole, you have all been great! And since you can never build the roof unless you make sure that the foundations cannot be shaken; Dr. Papagiannis, Dr. Alexander, Dr. Leisner, Dr. Sofia, Jan, Carolyn, Fanis, all of you that made sure my heart was strong enough to beat at the rhythm of a PhD; to you all, I am eternally grateful...

A big thank you goes to George, for making the "crossing-over" smoother than I could have imagined. To Theodora, who had her own mountains to climb and was still strong enough to encourage me. To someone who has opened his wings to fly higher than I would ever dare, who is now facing tips of metal and glass somewhere in China; I wish you knew how much I owe you... Alexis, Despoina, Dimitra, Katerina, Maria, Athena; you simply asking: "When are you next coming to Greece?" has always been enough to give me strength to keep going. Antonis, I am sorry this PhD kept me away from you when you most needed me... To Cherloria, who has been a true friend over what is now approaching a decade. To Magda, for lifting my spirits when I most needed it. To Vasilis, for "Armenian" conversations, shopping trips and countless facebook

messages. To Stavronikos, for Wellesley nights and "material" in-depth conversations. To Jennifer, for traditional Friday afternoon scientific meetings at the Longwood Starbucks. To Nikos, Antonis, Apostolos, Giola and Fenia for making Boston a prettier city. To someone who is not with us anymore. Even if it has been over 7 years now, every single day I hope I am still making you proud...

Andreas, what you have done for me over the past two years could never be acknowledged in a single paragraph. For being "my family", "my home", "my shelter" at the other side of the world. For being there every time I was feeling lost, for holding me every time I was feeling scared, for giving me a reason to get up every morning, a reason to smile every night. To you, "thank you" shall never be enough...

It is difficult to overstate my gratitude to my sister, Dominic, who has protected me, encouraged me and put up with me all the way from the very beginning. Following the road you have paved has always been a challenge, but nevertheless, a worthwhile one!

Mum, dad, when I started writing the "acknowledgments section" I feared reaching this point, for I knew that when it came to you two, there would be no words for me to express the way I feel. This thesis is dedicated to you, for teaching me how to keep my feet to the ground and my gaze to the sky. This thesis is dedicated to you, for mere unconditional love through every step. If you can call the end of this journey a success, then it belongs to you as much as it belongs to me...Dad, when I first started this PhD, you said one word: "Αγάντα!". Four years down the line I reply by saying six words: "Δεν έχω λόγια να σας ευχαριστήσω..."

This thesis has been funded by the British Heart Foundation, the European Commission 5th Framework Programme and a grant from the March of Dimes. Their support is gratefully acknowledged.

INTRODUCTION:

1) Cardiomyopathies; definition and classification:

As John Goodwin has emphasized; classification serves to bridge the gap between ignorance and knowledge. Previously cardiomyopathies were defined as diseases of the heart muscle of unknown cause.[1] The recent revision by the World Health Organisation defined specific cardiomyopathies as ventricular dysfunction resulting from the inability of the myocardium to deal with volume or pressure overload related to valve disease, hypertension, ischemia or inflammation or secondary to systemic disease. Intrinsic cardiomyopathies on the other hand, are disorders of the myocardium associated with cardiac dysfunction that are subdivided based mainly on their pathophysiology as dilated cardiomyopathy (DCM), hypertrophic cardiomyopathy (HCM), restrictive cardiomyopathy (RCM) and arrhythmogenic right ventricular cardiomyopathy (ARVC). Such a functional rather than etiological classification has drawbacks but reflects our current level of knowledge.[2]

a) Dilated cardiomyopathy:

DCM is a myocardial disorder with an estimated incidence of 1 per 2000, characterized by dilatation and contractile dysfunction of the left and/or the right ventricle (Figure 1). Histological changes include increase in myocyte length, loss of intracellular contractile myofibrils, increase in nuclear size, polyploidy, myocyte death by apoptosis and/or necrosis, interstitial fibrosis and increased numbers of interstitial macrophages and T lymphocytes.[2] Many cases show increased expression of class II antigens in the myocardium while circulating auto-antibodies to a wide range of components of the myocyte are present. Whether these antibodies are the cause of myocyte injury or a secondary phenomenon constitutes a yet un-answered question.[2] Although DCM has traditionally been regarded as a sporadic non-genetic disorder ("idiopathic DCM"), more recent studies suggest inherited gene defects as an important cause ("familial DCM"). The natural history of the disease is variable both between and within families. Affected individuals may have a relatively benign course, develop progressive heart failure or experience sudden death.[3] The reported prevalence of familial DCM has varied between 10 and 35% according to the methods of detection and diagnostic criteria employed. De novo mutations, incomplete penetrance, small family size and the concurrent presence of conditions known to promote DCM, such as viral infection, alcohol excess and ischemia, may limit the recognition of the contribution that heritable gene mutations have in the overall incidence of DCM.[4]

Studies of families with DCM have revealed autosomal dominant, autosomal recessive, X-linked and maternal modes of inheritance.[3] Some cases of familial DCM are caused

by mutations in genes coding for cytoskeletal proteins such as dystrophin, desmin, metavinculin, β- and δ-sarcoglycan, implicating defects in contractile-force transmission as one mechanism underlying this disorder.[5] Sarcomere protein genes, previously associated with HCM, were shown to also underlie certain forms of DCM. These include the genes that code for β-myosin heavy chain (β-MHC), cardiac myosin binding protein C (cMyBP-C), cardiac troponin T and α-tropomyosin, suggesting that defects in force generation are also involved in the pathogenesis of the disorder.[6] The discovery that mutations in the genes coding for lamin A, lamin C and emerin caused DCM raised intriguing questions about the role of the nuclear lamina proteins in heart physiology and pathology. Currently, no data exist to suggest that nuclear envelope proteins participate directly in either force transmission or force generation in cardiac myocytes. One possibility though is that such mutations might promote DCM by disruption of nuclear function possibly through altered transcription regulation (Figure 2).[3] Point mutations in mitochondrial DNA have been found in a number of multi-system disorders that may have associated cardiac abnormalities, such as childhood-onset DCM.[3] Furthermore, mutations in G4.5, the gene encoding tafazzin, have been implicated in childhood-onset X-linked DCM.[3] In a recent study, mutations in the genes coding for presenilin-1 and presenilin-2, proteins previously associated with Alzheimer disease, were found to underlie DCM with poor or favorable prognosis respectively. Calcium signaling was altered in presenilin mutation carriers implicating novel mechanisms of myocardial disease. [7] Although multiple clinical parameters have been proposed as predictors of mortality in DCM, it appears that family genotype may be the strongest determinant of outcome. [3]

Figure 1: A heart in dilated cardiomyopathy compared with a normal heart at end-systole.[8]

Figure 2: Identified genes that result in dilated cardiomyopathy include cytoskeletal protein-encoding genes, sarcomeric protein-encoding genes and intermediate filament protein-encoding genes.[9]

b) <u>Hypertrophic cardiomyopathy:</u>

HCM is characterized by left ventricular hypertrophy that is usually asymmetric and can affect various regions of the ventricle (Figure 3). Typical histo-morphological changes include myocyte hypertrophy and myofibrillary disarray (Figure 4). The prevalence of HCM is as high as 1 in 500 young adults. Clinical presentation of the disease ranges from lifelong symptom-less forms to sudden cardiac death (SCD).[10] Estimates for the prevalence of SCD vary according to the population studied, ranging from <1% to 3-6%.[3] Diagnosis of HCM generally requires exclusion of secondary causes of hypertrophy such as hypertension or aortic stenosis.[3]

HCM is an autosomal dominant familial disease in about 50% of patients. Genetic analysis has causally linked several genes to HCM. The majority of these genes encode cardiac sarcomeric proteins that include α-MHC, β-MHC, troponin T, troponin I,

α-tropomyosin, myosin light chain-1, myosin light chain-2, cMyBP-C and titin while the more recently discovered PRKAG2 encodes the γ2 subunit of AMP-activated protein kinase. All these proteins have different roles within the contraction-relaxation cycle and contribute to energy homeostasis in the heart.[10] The defective protein may be integrated into the sarcomere and act in a dominant negative way resulting in diminished force production. Therefore, hypertrophy could possibly be a means of compensation for low force generation. Another potential mechanism for hypertrophy might be increased cardiac contractility. This mechanism occurs rarely with specific defects in myosin light chains 1 and 2 and α-tropomyosin genes that cause increased Ca^{+2} sensitivity and thus increased force production. By contrast with other HCM-causing defects, cMyBP-C mutants lacking the myosin-binding and titin-binding domains seemingly do not integrate into the sarcomere, causing HCM due to lack of functional protein (haploinsufficiency).[10] Calcium appears to be a critical link between mechanical dysfunction of the sarcomere and induction of the hypertrophic gene program.[3]

It is now recognized that cases exist in which there is an increase in LV mass, with striking asymmetric or symmetric LV wall thickening, yet disarray is absent and mutations in the myofibrillary genes are not found. These cases indicate that other genes outside the sarcomeric complex can produce thick-walled LV. Mitochondrial gene disorders, glycogen-storage disease and Fabry's disease are among the known causes of this phenomenon.[2] Recently, mutations in the gene encoding the cytoskeletal muscle LIM protein have also been implicated in the HCM pathogenesis.[3]

The extent of LV hypertrophy varies between different genes and even between members of a single family with the same gene mutation. These observations may be explained by a modifying role of additional genetic and/or environmental factors.[3] The genes that cause HCM can be associated with dysplastic changes in the small intramural arteries, leading to a decrease in the lumen size. Such changes are associated with fibrosis such that HCM may progress to a more DCM-like phenotype.[2]

Various risk algorithms based on clinical parameters have been proposed to identify individuals with an increased propensity for SCD. Given the complexity of the mechanisms that may precipitate SCD, it is not surprising that no single risk factor has been identified. In genotyped individuals though, prognosis varies considerably between different genes and between different mutations in the same gene. For example the Arg403Gln and Arg453Cys β-MHC mutations, cardiac troponin T mutations and some α-tropomyosin mutations are "high risk" mutations with reduced life expectancy and high rates of SCD, whereas the Val606Met β-MHC mutation and cMyBP-C mutations are associated with a relatively benign course.[3]

Figure 3: Illustrations of a normal heart (left) and a heart with hypertrophic cardiomyopathy. [11]

Figure 4: Photomicrograph of myocardium from a patient with familial hypertrophic cardiomyopathy. The normal parallel arrangement of myocytes has been replaced with myocyte disarray and increased connective tissue.[12]

c) Restrictive cardiomyopathy:

RCM is the least common of the four categories of cardiomyopathies and is characterized by restrictive filling and reduced diastolic volume of either or both ventricles with normal or near-normal systolic function and wall thickness.[13] It is most frequently caused by pathological conditions that stiffen the myocardium such as endomyocardial disease, hemochromatosis, amyloidosis, sarcoidosis, Gaucher's disease, Fabry's disease, glycogen storage disease or radiation damage, the most common form being myocardial amyloid (Figure 5).[3] It is usually easy to recognize amyloid on histology by its characteristic green color under polarized light after staining with Congo red dye. Other causes of restriction include diffuse perimyocyte fibrosis. This pattern of fibrosis is seen to a degree in many cases of DCM, but when it occurs in a uniform distribution it causes predominantly restriction. Another form of RCM is associated with myocyte disarray on biopsy, but without other clinical or morphological features of HCM. [2]

In some individuals RCM may occur in the absence of a precipitating condition. Idiopathic RCM is not generally recognized to have a familial predisposition; however several small families have been reported showing autosomal dominant or recessive patterns of inheritance. The prognosis in RCM varies according to the underlying cause, but the majority of individuals experience progressive deterioration due to congestive heart failure with a high incidence of premature mortality. The small size of the families reported precluded genetic linkage analysis and only one disease-causing gene, desmin, has been identified to date.[3]

Figure 5: Illustration of a heart with restrictive cardiomyopathy. Ventricles stiffen and lose their flexibility.[14]

2) Arrhythmogenic right ventricular cardiomyopathy:

a) A 45-plus year journey:

The very first cases of ARVC were supposed to have been published in 1961 under the term: "auricularisation of right ventricular pressure curve".[15] The first typical cases though, of adults with monomorphic ventricular tachycardia (VT) of left bundle branch block (LBBB) morphology, indicating its right ventricular (RV) origin, and an enlarged RV in the presence of normal pulmonary vasculature were reported in 1977 by Guy Fontaine.[16] Since the first description of 24 cases, the term dysplasia was applied to the condition, which was thought to arise from "an abnormality in the development of the RV musculature".[17] It was thus considered to be a malformation similar to that seen in Uhl's anomaly, a congenital condition characterized by "an almost total absence of the RV myocardium". Arrhythmogenic right ventricular dysplasia (ARVD) was at the time thought to be infrequent with an exceedingly low risk of sudden death (SD). [17]

In 1988, *Thiene et al.* conducted a postmortem series of individuals who had died suddenly in the Veneto region of North-eastern Italy. This study indicated that the incidence of the disease may be much higher than originally thought, while simultaneously drawing attention to the association with SD especially in young people engaged in strenuous activity. In fact in a large number of subjects, SD was the first manifestation of the disease. Two main histological patterns were identified; a lipomatous pattern characterized by partial or total replacement of myocytes primarily of the RV free wall with adipose tissue, mainly at the apex and infundibulum and a fibro-lipomatous pattern which featured large areas of fibrosis with or without fat infiltration. Signs of progressive myocardial degeneration and apoptosis with or without inflammatory infiltrates were also observed. [18] The strong familial preponderance of the disease became apparent in an extensive epidemiological study of ARVC in the same area.[19] These observations managed to shake the belief that the disease was caused by abnormal embryogenesis.[18] ARVC is now known to be a primary myocardial disease, as opposed to a developmental anomaly, and was included in the World Health Organization classification of cardiomyopathies in 1995.[1]

b) Natural history:

Early reports focused mainly on the peculiar RV involvement and the electrical instability precipitating VT and SD. Long-term follow-up data from clinical studies though, indicated that ARVC is a progressive heart muscle disease that with time may

lead to more diffuse RV involvement and LV changes and may culminate in heart failure (HF).[20] In fact, a study conducted by six collaborative medical centres showed macroscopic and/or histological LV involvement in 76% of the hearts analysed.[21] Four distinct phases have been documented in the natural history of the disease. In the concealed phase, patients are often asymptomatic, but may nonetheless be at risk of SD, notably during extreme exertion. Structural changes, when present, are subtle and may be confined to one region; the so-called "triangle of dysplasia": the inflow, outflow and apical portions of the RV. Symptomatic ventricular arrhythmia is seen in the overt phase, accompanied by more obvious morphological and functional abnormalities of the RV. The third phase is characterised by diffuse RV disease, which results in right HF with relatively preserved LV function.[22] Significant LV involvement with biventricular HF occurs in the advanced stage leading to a phenotype that may be difficult to distinguish clinically from DCM.[20]

c) Task Force diagnostic criteria:

Clinical diagnosis of ARVC is challenging owing to the non-specific nature of associated findings. Recognition of this difficulty led an international task force to propose standardised criteria for ARVC in 1994.[23] Structural, histological, electrocardiographic, arrhythmic and genetic features of the disease are incorporated into the criteria, which are sub-divided into major and minor according to the specificity of their association with ARVC (Table 1). The presence of two major, one major and two minor or four minor criteria from different categories is considered diagnostic.[22]

Electrocardiographic findings:

ECG findings associated with ARVC are subdivided into depolarization/conduction and repolarisation abnormalities. In a cohort of 265 patients who fulfilled Task Force criteria for ARVC, RBBB was observed in 6%, while a further 14% showed incomplete RBBB. However, the relatively common occurrence of these findings among normal subjects precludes their inclusion in the diagnostic criteria. [24] Delayed depolarization confined to the right precordial leads (RPL) is considered more specific for ARVC. Prolongation of the QRS complex to >110ms in leads V1 to V3 in the absence of RBBB, reflecting slow conduction in the RV free wall, is a major criterion for ARVC and was identified in 98% of the patients in the above study (Figure 6).[22,24] Epsilon waves are small amplitude deflections occurring between the end of the QRS complex and the beginning of the T wave and correspond to delayed electric potentials that originate in areas of healthy tissue surrounded by fibrofatty infiltrate (Figure 7).[25] Highly suggestive of ARVC when localized to the RPL, they were found in 23% of patients in the above series.[24] Epsilon

waves may go unnoticed, though the sensitivity for their detection can be increased by suitably preparing the skin and recording the ECG at double speed and double amplitude.[26] Also, a signal-averaged ECG (SAECG) facilitates detection of the equivalent sign of late potentials in 50-80% of established cases. [22]

Repolarization abnormalities are common in ARVC. The characteristic pattern of T-wave inversion beyond V1 was present in 54% of confirmed cases and represents a minor criterion for ARVC in probands (Figure 7).[24] The Task Force guidelines exclude T-wave changes secondary to RBBB, and stipulate age over 12 years, as altered repolarization may be a normal variant in children. Significantly higher prevalence of T-wave abnormalities has also been observed in apparently healthy Afro-Caribbean subjects and highly trained athletes. In the absence of a conspicuous family history and characteristic imaging abnormalities, these alterations should be considered most likely benign.[22]

Figure 6: Localised right precordial QRS prolongation with QRS duration ≥ 110ms.[24]

Figure 7: Electrocardiogram of a patient with ascertained ARVD showing T-wave inversions and epsilon waves (indicated by the arrow).[27]

Table 1: Diagnostic criteria for arrhythmogenic right ventricular cardiomyopathy.[22]

Arrhythmic findings:

Ventricular arrhythmia of LBBB morphology is a minor criterion in probands. Sustained monomorphic VT, defined as a consecutive run of beats lasting at least 30 sec, was present in up to 65% of live index cases, while a further 29% showed non-sustained VT. Frequent premature ventricular contractions in excess of 1000 over a 24-hour period, were documented in 42% (Figure 8). [28]

Figure 8: VT with LBBB morphology induced during exercise test.[26]

Histological findings:

The routine use of endomyocardial biopsy in the diagnosis of ARVC is not recommended for a number of reasons. The risks of perforation and tamponade preclude sampling from the thinned free wall of the diseased RV, the region prevalently affected by fibrofatty replacement. Instead, biopsies are taken from the RV portion of the inter-ventricular septum, which is relatively spared by ARVC. The presence of myocytes in various stages of cell death with evidence of fibrofatty replacement is one of the major criteria for ARVC. A negative biopsy is of no value excluding ARVC owing to the segmental nature of the disease, particularly in its early stages. Unequivocal positive findings may however confirm the diagnosis. [22]

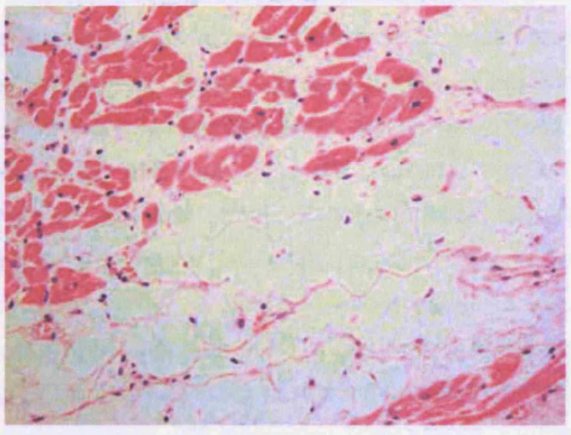

Figure 9: Histological sample: fibrofatty infiltration of the right ventricle (H&E).

Imaging findings:

Structural abnormalities in ARVC may be localized, in the form of patchy wall thinning and segmental dilatation, or diffuse with global dilatation of the RV. Functional impairment ranges from mild regional wall motion abnormalities to generalized hypokinesia.[22]

Right ventriculography offers clear views and was traditionally used as a diagnostic tool for ARVC as it can localize aneurysms and areas of dyskinesis particularly in the triangle of dysplasia.[29] Drawbacks though include the lack of information about LV involvement and the unsuitability of an invasive technique for serial follow-up studies.[22,27] Visualization of the right ventricle by echocardiography is not always satisfactory, particularly in the presence of thoracic deformities or obesity, but may be enhanced by the use of intravenous contrast.[22] However, it has the advantage of being non-invasive, readily available and inexpensive. Furthermore, echocardiography allows the study of family members, while differential diagnosis is possible with respect to other entities associated with arrhythmias and RV dilatation.[26] With the advance of imaging techniques and the development of software for objective analysis of the images obtained, echocardiography can help detect early abnormalities as well as progression of the disease.[26] M mode and pulse tissue Doppler techniques are also considered useful for detection of abnormalities in diastolic tricuspid annular motion.[30]

The non-invasive nature of cardiac magnetic resonance (CMR) and its unique ability to detect fatty tissue infiltration, while assessing volumes, function and regional wall motion has increased its popularity as a diagnostic tool but not without controversy.[29] High resolution CMR sequences are currently dependant on ECG gating. Multiple premature ventricular contractions or a highly variable heart rate result in poor image quality. The fast spin-echo sequences used to detect fatty replacement are also especially sensitive to respiratory and motion artefacts.[22] Since the RV free wall can be studied by CMR in several planes, greater detail is provided compared to echocardiography and right ventriculography, which may lead to false positive interpretation. The normally thin wall of the RV may also appear to have focal wall motion abnormalities, without any structural abnormalities actually being present.[29] Despite its excellence in detecting fat, CMR has difficulties differentiating between intramural and epicardial fat.[31] The hearts of most adults in the western countries contain varying physiological amounts of fat, found mainly in the sub-epicardial region (adipositas cordis).[32] This epicardial fatty tissue is more abundant on the RV surface, is thicker in women and increases with increasing body weight. Furthermore, in a normal heart, a certain amount of fatty tissue is always present within the myocardium of the RV free wall, particularly at the level of the antero-lateral and apical regions. Differing from adipositas cordis, this fatty RV infiltration seems independent of gender and body

weight while myocytes seem to be just pushed apart by the fat rather than degenerating.[32] Finally, the subjectivity related to reading and interpreting the images and the lack of a standard protocol for ARVC diagnosis have reduced the faith in the value of CMR even further. [31]A recent study has shown that the use of fat-suppressed in addition to non-fat-suppressed conventional T1-weighed spin-echo imaging increased inter-observer agreement and confidence in diagnosis and evaluation of intra-myocardial fatty infiltration in patients suspected for ARVC.[33] With newer imaging systems, better quality images and more comprehensive protocols, the accuracy of CMR is likely to improve.[29]

Further imaging techniques including nuclear ventriculo-scintigraphy, LV angiography, single photon emission and multi-detector row computer tomography have been used but were not sensitive or specific enough to become established as the gold standard for ARVC diagnosis.[27,34,35]

Electrophysiological testing (EP):

The invasive EP study, while not a routine component of the diagnostic work-up for ARVC may have a role in differentiating idiopathic right ventricular arrhythmias (IRVA) from ARVC. VT in ARVC is often inducible by programmed electrical stimulation, exhibits entrainment and is associated with fragmented diastolic potentials. In contrast, VT in IRVA frequently requires an isoprenaline infusion and/or burst pacing for provocation.[22] An EP-associated risk however is the possible induction of ventricular fibrillation (VF).[27] Ajmaline challenge during an EP study can also be used to differentiate ARVC from Brugada syndrome, since it can induce RPL QRS prolongation only in typical Brugada while it can unmask epsilon waves and induce RBBB with QRS prolongation in the left precordial leads only in ARVC. Still, the question remains whether systematic ajmaline challenge to exclude Brugada syndrome is of any value, especially since provocable ST-segment elevation in ARVC represents a risk factor of additional progressive conduction disease.[36]

d) Vast variation in ARVC:

The disease is thought to affect 1 in 5000 individuals in the general population; however this figure varies among different ethnic groups.[37] In the Veneto region of Italy, the incidence of ARVC is as high as 6 in 10000 inhabitants.[38] The true prevalence of the disease is not easy to estimate, as many cases undoubtedly remain undiagnosed, and the full spectrum of disease expression is only now being elucidated.[22] Two recent studies conducted in a non-referral centre in Germany and in South-East Korea

estimate that ARVC affects 1 in 1000 individuals. [39,38] ARVC shows male predominance and is usually manifested in adolescence or early adulthood. Typical symptoms include dizziness, palpitations and syncope episodes which first appear at 33 ± 14 years of age, ranging from 13 to 73 years. Paediatric cases have been reported, while a foetus with arrhythmia *in utero* exhibited the very early stages of the condition.[27]

The disease exhibits phenotypic variation both in its presentation and clinical course even amongst affected members of the same family. Some individuals may remain asymptomatic throughout life or experience minor symptoms, others may develop biventricular HF prompting heart transplantation, while in some cases SCD is the first manifestation of the disease.[40] In the United States, ARVC accounts for approximately 5% of SCDs in individuals under the age of 65 and is responsible for at least 3 to 4 % of deaths associated with physical activity in young athletes.[37] In the Veneto region of Italy though, ARVC is the most common cause of sudden arrhythmic deaths in individuals under the age of 35, and the overwhelming cause of SD associated with exertion in young athletes.[37] Still, because necropsy is not frequently performed in cases of SD in those aged 35 or older, the true incidence of the disease among cases of SD is probably under-estimated.[41] Moreover, given the progressive nature of the disease, diagnosis may be missed at autopsy if structural abnormalities have not yet developed (concealed phase).[22]

The annual mortality rate of ARVC has been estimated at 3% without treatment and at 1% with treatment.[37] In contrast with the recognition of strenuous exercise as a trigger of SD in patients with ARVC, in the study performed in South-East Korea, most of the cases were found dead in bed or died suddenly during ordinary daily activity.[39] A difference in the incidence of fatal ARVC may exist because of regional or genetic factors. Alternatively, it may be that autopsies are not always requested in Korea in cases of SCD during strenuous activity.[39] Furthermore these observations do not exclude the possibility of sudden unexplained nocturnal death syndrome or Brugada syndrome being mis-diagnosed as ARVC.[39] Interestingly, in the study conducted in Germany, patients experienced chest pain and tiredness, symptoms not commonly associated with ARVC, while the disease was shown to have a good prognosis with only 0.3% of annual SCD.[38] Finally, the average age of onset of the disease amongst Chinese patients was significantly higher than in other groups studied, though this could be due to late diagnosis or late clinical presentation.[42] Also, none of the patients in this study showed LV involvement, while 36.4% of the patients did not show any echocardiographic abnormalities. [42]

The spectrum of ARVC presentation and clinical course becomes even broader when familial cases are considered. In a study conducted in England, relatives of 67 ARVC

index patients underwent cardiac evaluation.[28] Of 298 relatives, 10% had ARVC based on the Task Force criteria, while a further 11% exhibited ECG, echocardiographic or Holter monitoring abnormalities without fulfilling the criteria for diagnosis. In the context of a familial disease, such subtle abnormalities may in fact represent early or mild disease expression.[28]

Unusual presentations:

Although typical ARVC first manifests with palpitations, syncope or sudden cardiac death in adolescence or early adulthood and is characterized by arrhythmias originating primarily from dilated, hypo-kinetic right ventricles, over the past few years, a number of cases of unusual disease presentation have been published.

In 1999, the case of two siblings with ARVC was reported.[43] The older sibling, previously considered healthy, died suddenly at age 17. The younger sibling developed congestive HF prompting cardiac transplantation at age 14. Macroscopic examination of the two hearts showed a thick cap of fibro-adipose tissue covering all of each RV. Microscopically, both left ventricles contained excessive myocyte disarray and multi-focal fibrosis. The coronary arteries displayed intimal hyperplasia with disruption of the internal elastic lamina, similar to fibro-muscular dysplasia. Typically, ARVC does not affect the coronary arteries, is not characterized by disarray and does not progress to such advanced stages at such a young age. [43] *Nemec et al.* described the case of two patients who underwent heart transplantation with a clinical diagnosis of idiopathic DCM, while pathology demonstrated the end stage of ARVC with major LV involvement.[44]

In 2000, *Suzuki et al.* presented the case of a 43-year old man admitted to hospital because of congestive HF following a common cold.[45] The RV function was preserved, but the LV function was severely and diffusely hypo-kinetic. An endomyocardial biopsy revealed mild infiltration of lymphocytes with focal myocyte necrosis. The observations were consistent with DCM and healing myocarditis. Progressive impairment, dilatation and thinning of both ventricles were observed on serial echocardiographic examinations; however the LV impairment had always been predominant in the patient's clinical course. He died suddenly of VF and pump failure. The autopsy revealed evidence of apoptosis and extensive fibrofatty replacement of myocytes in both ventricles extending from the outer layer to the inner layer of the myocardium in the RV and to the middle layer of the LV, observations compatible with ARVC.[45]

In 2001, the case of a 19-year old man, evaluated because of his sister's SD, was published.[46] He was given the diagnosis of ARVC based on electrocardiographic and echocardiographic abnormalities. The patient died at 33 years of age, while waiting for a heart transplant. At gross examination, huge cardiomegaly and paper-thin RV walls

with transmural myocardial loss were evident. A large calcified plaque, 7 x 9 cm in size, was found at the level of the RV outflow tract. Calcification has not previously been implicated in ARVC, while it is commonly associated with RCM.[46]

In 2002, the case of a 30-year old Caucasian woman presented with fatigue and dyspnoea on exertion was reported.[47] Twelve-lead ECG was remarkable for ST-segment elevation in V1-V2, negative T-waves in V1-V6 and fractionated low-amplitude spiking electrical activity extending 300ms beyond the QRS complex in all leads. Angiography revealed RV global dilatation and hypo-kinesis with multiple aneurysms and mild LV involvement. The histological picture was compatible with ARVC. The finding of multiple delayed after-potentials extending into the T-wave is a very unusual finding in ARVC, while the down-slopping ST elevation in V1 and V2 is often seen in Brugada syndrome.[47]

In 2004, a 49-year old man was admitted to hospital after experiencing chest pain, palpitations and dizziness.[48] On admission, ECG showed VT of LBBB morphology, which suddenly became unstable and prompted cardioversion. His post-conversion ECG showed inverted T-waves and Q-waves and he showed elevated cardiac markers indicative of myocardial infarction. Echocardiography showed a dilated RV. However based on chest pain of ischemic character, the finding of Q-waves with T-wave inversions at inferior leads and positive cardiac markers, the patient was treated as a case of acute coronary syndrome. An angiogram performed during follow-up showed normal coronary arteries but a dilated RV with dysplastic changes indicative of ARVC.[48]

Around the same time another unusual case of ARVC was reported.[49] A 76-year old woman with no previous history of disease, developed recurrent VT and VF, termed electrical storm as the first manifestation of ARVC. The diagnosis was confirmed post-mortem, suggesting a tremendous variation regarding the age of onset of symptoms in ARVC.[49]

Collectively, these observations suggest that ARVC is a disease characterized by vast phenotypic variation, age-related progression and incomplete penetrance. A quarter of a century has passed since ARVC was first recognized as an individual clinical entity, and yet, this vast variation combined with the lack of a single diagnostic test capable of differentiating ARVC from different, yet overlapping clinical entities, still make diagnosis problematic. In fact, in a large study conducted at the John Hopkins medical centre, out of 89 patients who were referred for a re-evaluation for diagnosis of ARVC, only 27% actually met the Task Force criteria.[50] This study demonstrated the high frequency of misdiagnosis of ARVC mainly due to over-reliance on the presence of intra-myocardial fat on MRI, incomplete diagnostic testing, lack of awareness of the Task Force criteria and a not yet clearly defined disease spectrum.[50]

e) Etiology

In addition to a genetic cause of ARVC, dysontogenic, degenerative, infectious or inflammatory, apoptotic and myocyte trans-differentiation theories have been proposed either as a cause of or as environmental factors facilitating disease expression.[37]

The dysontogenic theory is largely historical, but suggests that ARVC is a milder form of Uhl's anomaly. The degenerative theory suggests that ARVC is a consequence of myocyte death due to inherited metabolic or ultra-structural defects. The infectious or inflammatory theory maintains that the disease results from previous myocarditis. Inflammatory infiltrates are common in histological specimens from patients with ARVC.[37] *Fontaine et al.* found inflammatory infiltrates in 8 of 27 patients with ARVC[51] while *Calabrese et al* found foci of inflammatory infiltrates in 4 of 20 patients though all specimens were negative for enteroviral genomes indicating that enteroviruses may not be involved in the etiopathogenesis of the disease. [52] In agreement with this finding, BALB/c mice inoculated with Coxsackie virus B3 showed evidence of increased myocardial degeneration and necrosis, extensive inflammation, large numbers of inflammatory infiltrates and extensive fibrosis primarily in the pericardial side of the RV myocardium.[53] More recent studies though showed that myocarditis can mimic ARVC and that it may be super-imposed on an already affected heart accelerating disease progression, rather than being involved in the actual etiology of the disease.[54] The apoptotic theory is supported by the finding of apoptosis and a high level of CPP-32, a cysteine protease required for apoptosis, which were detected in the RV myocardium of 6 of 8 ARVC patients examined but not in 4 normal subjects.[55] Finally, the trans-differentiation theory is based on the hypothesis that myocardial cells can change from muscle to adipose tissue and the observation in one patient of "transitional cells" at the interface between cardiac muscle and adipose tissue.[37]

f) Syndromic ARVC:

Naxos disease:

Palmoplantar keratosis (PPK) is a familial ectodermal defect characterised by hyperkeratosis of the palms and soles. After recurrent VT developed in two young patients with non-epidermolytic PPK and peculiar woolly hair (Figure 10) from the Greek island of Naxos, *Protonotarios et al.* sought evidence of cardiac abnormalities in families on this island that included members with these cutaneous abnormalities.[56] A total of 9 individuals from 4 families were examined. The majority of the patients demonstrated ECG disorders including intra-ventricular conduction delays, T-wave inversions, abnormal Q waves, low voltage and arrhythmias of ventricular origin, mainly

frequent ventricular extra-systoles and VT of LBBB morphology. Echocardiographic abnormalities consisted of cardiac enlargement mainly of the RV, wall motion abnormalities, and an echodense muscular type band originating from the right apex. The occurrence of strikingly similar cardiac anomalies in most of the patients with PPK and woolly hair could not be regarded as a coincidence. Thus a new familial, possibly autosomal recessive, disease entity was recognised in 1986 involving hair and skin abnormalities as well as a form of cardiomyopathy, which at the time was thought to exhibit characteristics of either DCM or ARVC. [56] After the description of the first cases, further cases were identified in other Greek islands, Turkey[57] and Saudi Arabia.[58] The entity though was named Naxos disease due to the clustering of events in the island of Naxos.[59] Indeed, the prevalence of the syndromic disease in the Greek islands is as high as 1 in 1000 individuals.[60]

The peculiar woolly hair phenotype appears at birth, the dermatosis appears in the first year of life, interestingly at skin regions exposed to increased mechanical stress, such as the palms and the soles, while the cardiac phenotype does not appear until puberty.[59] Clinical and histological studies conducted over the past 20 years, comparing Naxos disease with ARVC showed that the heart disorder is identical in both cases (Figure 11).[60] Therefore, after 1995, according to the Classification of World Health Organisation, Naxos disease is considered to be a recessive form of ARVC. Naxos disease is a rather progressive disease with adverse outcome especially in the young. The annual disease-related and SD-related mortality rate is 3% and 2.3% respectively. Risk factors for SD include history of syncope, appearance of symptoms and severely progressed disease in the RV before the age of 35 and LV involvement. The prevalence of heterozygotes in the island of Naxos is as high as 5% of the population. Apart from a small fraction of heterozygous individuals who show woolly hair and some minor electrocardiographic and echocardiographic abnormalities, not diagnostic of ARVC, heterozygotes show a normal clinical phenotype.[60]

Figure 10: Cutaneous features of Naxos disease: Woolly hair (A), palmal (B) and plantar (C) keratoses.[60]

Figure 11: Two-dimensional echocardiogram of heart showing typical features of ARVC: right ventricular (RV) dilatation and multiple saccular aneurysmal segments (arrows). There is also right atrial (RA) dilatation. In contrast, left ventricle (LV) and left atrium (LA) are normal. Accompanying ECG shows abnormal T-wave inversion in leads V_1 through V_4, consistent with abnormal repolarization affecting RV.[61]

Carvajal syndrome:

In 1998, the case of three families from Ecuador showing evidence of autosomal recessive inheritance of a syndromic disease affecting the hair, skin and heart was reported.[62] The skin disease presented as a PPK with some non-volar involvement particularly at sites of pressure or abrasion. All epidermal lesions had the characteristic longitudinal hyperkeratosis of striated PPK. The hair was curly and woolly in texture (Figure 12). Cardiological investigation including ECG and echocardiographic examinations of a number of the affected family members reported the diagnosis of an LV-DCM often resulting in HF during adolescence. The newly-described entity was named Carvajal syndrome after the dermatologist who first described it.[62]

Figure 12: PPK and woolly hair in two affected family members.[63]

The heart of a child affected by Carvajal syndrome, who died of progressive HF at age 11 years, was examined macroscopically and microscopically.[64] The RV was only moderately dilated but it contained discrete inferior, apical and infundibular aneurysms with thin translucent walls. In contrast, the LV was widely dilated and contained shallow posterior and antero-septal aneurysms (Figure 13). Microscopic examination disclosed diffuse scarring of the free walls of both ventricles with extensive areas of myocardial loss and replacement fibrosis while there was no evidence of fatty infiltration in either ventricle. Myocyte hypertrophy and attenuation with bizarre nuclei and non-specific myocytolytic changes were prominent. Patchy foci of inflammatory cells were visible

adjacent to degenerating myocytes and TUNEL staining revealed increased apoptotic rates (Figure 14).[64]

Figure 13: Gross photographs of the right (A, B) and left (C–E) sides of the heart. Both ventricles contained discrete regions of aneurysmal wall thinning. Affected areas included the subtricuspid posterior right ventricle (B), the posterior basal portion of the left ventricle (marked by an asterisk in D), and the anteroseptal portion of the left ventricle (E).[64]

Figure 14: Panoramic views of the right (A) and left (B) ventricular free walls showing extensive myocardial loss and replacement fibrosis. Higher magnification views of left ventricular myocardium showing myocyte hypertrophy and myocytolysis with bizarre nuclei (C); focal inflammatory infiltrates surrounding dying myocytes (D); replacement fibrosis (E); and myocyte apoptosis (F).[64]

Overlapping syndromes:

Recently the case of a 17-year-old boy of Turkish origin was published.[65] The boy was referred to the coronary care unit of the local hospital after complaining for dyspnea and palpitations. He had curly hair and PPK, also confirmed by skin biopsy. An ECG showed right axis deviation, low voltage, T-wave inversions and epsilon waves in V1-V3. On echocardiographic examination both ventricles were dilated and showed global hypokinesia. On Holter monitoring there were frequent supra-ventricular tachycardia attacks, but no complex arrhythmias were recorded. His younger brother, who did not show any cutaneous abnormalities, was diagnosed with ARVC without LV involvement based on ECG, echo and CMR findings. The grandfather of the patient had PPK, curly hair and a mild enlargement and systolic dysfunction of the RV. A clear differential diagnosis between Naxos disease and Carvajal syndrome could not be established indicating that the two entities may indeed represent different existences of the same pathogenetic pathway. [65]

A unique form of syndromic ARVC in Israel:

In 2003, Alcalai et al. reported a clinical syndrome consisting of SD with hair and skin abnormalities in a family from Israel.[66] Family history was significant for 8 members who died suddenly during young adulthood. All of them had woolly hair and exceptionally dry skin in all parts of the body beginning at birth. During childhood, they presented with vesicular lesions on the extremities, particularly on the knees, palms and soles. Histological examination of a biopsy sample demonstrated features similar to pemphigus foliaceous. One living affected female, with similar cutaneous abnormalities presented with recurrent syncope at the age of 16. VT of RV origin was documented. 12-lead ECG demonstrated T-wave inversion with localized prolongation of the QRS complex. Echo revealed a mildly dilated RV without regional wall motion abnormalities or aneurysms and a normal LV. A diagnosis of ARVC was made based on ECG and echo abnormalities and a family history of SD. The constructed pedigree was suggestive of an autosomal-recessive inheritance pattern.[66]

The entities described above indicate that ARVC can be found in syndromic disease that involves a range of hair and skin abnormalities. They also highlight the broad spectrum of the disease, which despite being named arrhythmogenic *right* ventricular cardiomyopathy can in fact predominantly affect the LV resembling DCM.

g) Naturally-occurring myocardial disease in animals:

Cardiomyopathy/woolly hair syndrome (CWH) of Poll Hereford calves:

A lethal autosomal recessive cardiocutaneous syndrome of Poll Hereford calves has been reported in Australia.[46] Affected animals can be identified at birth by their distinctive woolly haircoat and ventricular arrhythmias. Electrocardiography has recorded low voltage, flat T-waves, complex ventricular extra-systoles and episodes of non-sustained VT. Death usually occurs within 12 weeks of birth and may be sudden (from VF often after physical exertion) or follow a period of congestive HF. In CWH, lesions can occur in both ventricles and include multi-focal to locally extensive myocardial loss with replacement fibrosis and occasionally areas of calcification (Figure 15).[67] The ventricular calcification is comparable to a phenomenon described also in a human patient, with calcification of the RV free wall. [46]

Figure 15: (A) Distinctive woolly haircoat. (B, upper) Cross section of the heart reveals sub-epicardial myocardial loss with fibrous replacement of the right ventricular free wall. (B, lower) Cross section of the heart reveals the same pathologic process in both ventricles associated with calcification. (C) Right ventricular free wall with extensive sub-epicardial myocyte loss and replacement fibrosis embedding surviving myocytes.[68]

Spontaneously-occurring ARVC in the domestic cat:

Between 1995 and 1998, pathology archives of the animal medical centre in New York were reviewed for cases in which death appeared to be due to congestive HF.[69] Of 26 cases, 12 were suspected of ARVC on the basis of marked RV and atrial enlargements with grossly identifiable wall thinning. Clinical features included right-sided congenital HF, supra-ventricular tachy-arrhythmias, VT, polymorphic ventricular arrhythmias and

RBBB. Out of the 12 cats, 8 died of cardiovascular disease. At autopsy, hearts of ARVC cats were characterised grossly by moderate to severe RV-cavity enlargement and wall thinning and apical aneurysm formation. Histology demonstrated pronounced RV lesions in all 12 cats, including marked myocardial injury (myocyte necrosis and atrophy) and repair (fibrous and/or fatty replacement). Injury and repair were also evident in the LV in 10 cats while 2 showed involvement of both atria. Evidence of increased apoptosis was detected in 9 animals. [69]

ARVC causing SD in Boxer dogs:

In a study performed at the Ohio State University College of Veterinary Medicine, ARVC was diagnosed in 23 Boxer dogs.[70] Clinical events included SD, ventricular arrhythmias of suspected RV origin, syncope and HF. RV enlargement and aneurysms were a common finding. Striking histo-pathological abnormalities were present in each dog including severe RV myocyte loss with replacement by fatty or fibrofatty tissue. MRI demonstrated bright antero-lateral and/or infundibular RV myocardial signal, confirmed as fat by histopathology. Evidence of myocarditis was present in 14 and familial transmission was evident in 10 dogs.[70]

Collectively, the forms of cardiomyopathy described in all calves, felines and Boxer dogs are remarkably similar to ARVC in human patients with respect to both clinical and pathological features. These naturally occurring disease models may be a potentially important investigative tool that could enhance our understanding of the complex clinical and patho-physiological mechanisms operating in ARVC, as well as the molecular mechanisms responsible for its genesis.[69]

h) Management of ARVC:

Pharmacological therapy:

No evidence currently exists for the efficacy of any anti-arrhythmic agent in preventing SD. Drug treatment may however alleviate symptoms such as palpitations and dizzy spells secondary to multiple PVCs or runs of VT.[22] The association of SD with strenuous activity, together with the observation that VT in ARVC is often preceded by an increased heart rate, suggests that sympathetic stimulation may be a precipitant. First-line use of beta-adrenergic receptor antagonists, where no contra-indications exist, is therefore reasonable. Amiodarone is recommended as add-on therapy if beta-blockers alone prove ineffective in suppressing VT.[22] Greater caution is justified before commencing amiodarone in patients with frequent PVCs as the risk of side effects may outweigh the potential benefits of symptom control.[22] After a clinical study conducted in

Japan, *Hiroi et al.* suggested carvedilol as a first-line drug for some patients with ARVC demonstrating sympathetic over-activity, drawing attention to the drug's ability to control arrhythmias while improving LV function.[71] Standard HF therapy is indicated in later stages of the disease for patients with impaired ventricular function. Anticoagulation should be considered in patients with atrial fibrillation, marked ventricular dilatation or ventricular aneurysms.[22]

Invasive treatment strategies:

The implantable cardioverter defibrillator (ICD) confers the optimal protection against SD.[22] Appropriate interventions occur frequently in ARVC patients, highlighting the likely survival benefit in this population. In current practice, an ICD is first-line therapy for all survivors of VF arrest, and is also offered to patients with VT that recurs or remains inducible in spite of drug therapy. Constraints to more widespread use include the potential complications of lead insertion into the diseased RV, infection, the requirement of multiple generator replacements, the risks of in-appropriate intervention and psychological repercussions associated with the device. [22] Sustained monomorphic VT may also be susceptible to radiofrequency ablation.[22] Owing to the progressive nature of the disease though, recurrence of VT is relatively common, and myocardial injury precludes repeated intervention.[22]

Disarticulation of the RV is used to completely isolate the RV free wall.[27] This operation is based on the principle that the RV makes only a small contribution to cardiac hemodynamics and that the isolation of its free wall will prevent the transmission of abnormal rhythms to the LV. The efficacy of this operation in the prevention of VT is un-questioned. Nevertheless, because of hemodynamic alterations, this extensive surgical approach should be used with caution. [27] Right ventricular cardiomyoplasty consists of wrapping the RV free walls with the left latissimus dorsi muscle flap.[72] The distal part of the latissimus dorsi muscle is fixed to the diaphragm and then electro-stimulated. The results of a long-term clinical study conducted in France demonstrated hemodynamic and functional improvements following this operation without peri-operative mortality, long-term malignant arrhythmias or RV dysfunction-related deaths indicating that RV cardiomyoplasty may in fact be an effective treatment for ARVC patients with severe RV failure.[72] Finally, heart transplantation is the ultimate form of therapy indicated in cases of extreme RV dilatation or severe LV involvement. [27]

3) Work leading to the current hypothesis:

The beginning:

The identification of the genetic determinants underlying ARVC has been slow due to the difficulties in diagnosis and the vast variation characterizing the disease. However Naxos families, where co-segregation of the hair and skin features with cardiomyopathy allow diagnostic status to be more confidently assigned, presented a powerful model for gene identification in ARVC.[73] Linkage analysis of 9 families mapped the disease locus to 17q21. A homozygously inherited disease haplotype was common to all the affected individuals supporting an autosomal recessive mode of inheritance as well as a founder effect.[61] *Coonar et al.* hypothesized that a common ancestor had introduced a single copy of the disease gene to the genetically isolated population of Naxos, and then as a result of inbreeding, homozygous individuals arose bearing the phenotype of Naxos disease.[61] The region of homozygosity was refined and found to contain the candidate gene plakoglobin, a member of the armadillo protein family and a constituent protein in adherens and desmosomal junctions, with adhesive and signalling properties.[73] Mice with null mutations in plakoglobin, exhibit heart and skin abnormalities analogous to Naxos disease.[74] A patient's cDNA was thus screened for mutations in plakoglobin. A 2 base pair deletion was identified at the 3' end of the gene (2057del2), predicted to cause a frameshift and premature termination of translation truncating the C-terminal domain of the putative protein by 56 residues. Western blot analysis with an anti-plakoglobin antibody confirmed the presence of the mutant protein in a cardiac biopsy sample from a patient. Mutant plakoglobin migrated with a molecular weight of 75kDa, whereas plakoglobin expressed in a normal heart migrated with a molecular weight of 82kDa. The plakoglobin deletion identified destroyed the Bst01 recognition site, allowing rapid screening in Naxos disease families through restriction digestion. [73]

Desmoplakin mutations underlying ARVC:

In 2000, a genome scan was performed on the three families from Ecuador, where Carvajal syndrome was first recognized.[63] All affected members showed homozygosity at 6p23-p24, where the gene coding for desmoplakin lies. Histology of affected patient skin revealed large inter-cellular spaces between supra-basal keratinocytes indicating a cell adhesion defect underlying the disease. Desmoplakin is the most abundant protein of desmosomes and is important in the attachment of the intermediate filament (IF) network to the plasma membrane and in inter-cellular adhesion. Functionally therefore, desmoplakin was a good candidate for the disease gene. Sequence analysis revealed a deletion of a G nucleotide at position 7901 (7901delG), which segregated with the

disease phenotype in all three families with all affected members homozygous for this variant.[63]

Following the recognition of 7901delG as the genetic determinant underlying Carvajal syndrome, a point mutation in desmoplakin was identified in the family from Israel presented with a similar cardiocutaneous phenotype, leading to a Gly2375Arg substitution in the protein.[66] Only the one living affected individual was homozygous for the substitution suggesting an autosomal recessive manner of inheritance.[66] In 2002, a genome scan in one Italian family affected by ARVC without associated cutaneous abnormalities was reported. An autosomal dominantly inherited mutation (S299R) was identified in exon 7 of desmoplakin, highlighting how different desmoplakin mutations may produce different clinical phenotypes with different modes of inheritance.[75]

Plakophilin2; another ARVC-causing desmosomal gene:

Plakophilins are proteins of the armadillo family that function in embryonic development and assembly of cell-cell junctions. *Grossmann et al.* ablated the plakophilin2 (PKP2) gene in mice. The resulting mutant mice exhibited lethal alterations in heart morphogenesis and stability at mid-gestation (E10.5-11), characterized by reduced trabeculation, disarrayed cytoskeleton, ruptures of cardiac walls and blood leakage into the pericardial cavity. In the absence of PKP2, desmoplakin dissociated from the plaques of adhering junctions that connect cardiomyocytes and formed granular aggregates in the cytoplasm.[76] Based on these findings and on the implication of two further junctional proteins in ARVC pathogenesis, *Gerull et al.* hypothesized that mutations in human PKP2 may account for ARVC.[77] Sequence analysis of 120 Caucasians, diagnosed with ARVC according to the Task Force Criteria, revealed 25 different heterozygous mutations in 32 probands. Of the 25 mutations, 12 were insertion/deletion mutations, 6 nonsense mutations, 4 missense mutations and 3 splice site mutations. Although the majority of mutations were detected in the carboxy-terminal half of the molecule, ARVC-causing PKP2 mutations were spread over the entire gene. Three mutations were observed in several unrelated patients suggesting an ancient founder effect or the presence of mutational hot spots throughout the gene.[77]

The implication of three junctional proteins in ARVC pathogenesis constituted the foundation for the hypothesis that ARVC may in fact be a disease of defected cell-cell adhesion, or more specifically a disease of the desmosome.

4) Further genetic background:

Apart from the three genes presented above, seven further chromosomal loci have been associated with autosomal dominant or autosomal recessive forms of ARVC through chromosomal mapping (Table 2).

Type	Chromosomal position
ARVC1	14q23-q24[78]
ARVC2	1q42-q43 [79]
ARVC3	14q12-q22[80]
ARVC4	2q32.1-q32.3[81]
ARVC5	3p23[82]
ARVC6	10p12-p14[83]
ARVC7	10q22[84]

Table 2: ARVC-associated chromosomal loci

Out of these seven ARVC forms, ARVC2 was different in that it showed high penetrance, a 1:1 male to female ratio in affected individuals and was characterized by a particular form of effort-induced ventricular arrhythmias. Three candidate genes were mapped on the chromosomal region previously identified by linkage analysis (1q42-q43), one of which was RyR2, the gene coding for the cardiac ryanodine receptor.[85] When a number of families diagnosed with ARVC2 were screened for mutations in RyR2, six missense mutations were identified at highly conserved positions of the gene.[86]

RyR2 is the only ryanodine receptor isoform expressed in the heart. It is a homo-tetramer with a molecular weight of 565kDa, which transverses the membrane of the sarcoplasmic reticulum (SR) and is involved in the excitation-contraction coupling of the cardiomyocytes.[87] Ca^{+2} that enters the cell during the plateau phase of the action potential through the L-type voltage-gated channels, activates the ryanodine receptors, which in turn release further calcium from the SR. The influx of Ca^{+2}, together with the release of Ca^{+2} from the intracellular stores, greatly increases the levels of Ca^{+2} within the cell, which in turn binds troponin C thus switching on the contractile machinery. Following contraction of the cardiomyocytes, the ryanodine receptor closes, Na/Ca exchangers pump Ca^{+2} out of the cell and Ca^{+2} ATPase pumps transfer Ca^{+2} back to the SR so that the intracellular Ca^{+2} levels can drop and the cell can relax.[88] The mutations identified in RyR2 were thought to increase the phosphorylation of the

protein, thus not allowing it to close properly.[89] This would result in Ca^{+2} leaking in to the cytoplasm. A prolonged increase in the intracellular level of Ca^{+2} could potentially provoke ventricular arrhythmias.[89] However, although this hypothesis can explain the exercise-related arrhythmias, it does not explain the structural abnormalities characterizing the disease. More recent reports suggest that mutations in RyR2 are more likely to be causing catecholamine-induced VT rather than ARVC.

ARVC1 was mapped to chromosomal region 14q23-q24. Amongst that critical region, five genes are expressed in the heart, one of which is TGFβ3. TGFβ3 was considered to be a plausible candidate gene as it is known to induce fibrosis *in vivo* in a number of tissues. When screening of a number of patients diagnosed with ARVC1 did not reveal any mutations in the coding region of TGFβ3, screening was extended to the regulatory regions of the gene.[90] As a result two point mutations were identified, a transition at the promoter region and another transition at the 3' un-translated region of the gene. *In vitro* studies using a luciferase reporter gene showed that both mutations increase the levels of expression of the gene two-fold compared to wild-type. The hypothesis was that if TGFβ3 is over-expressed, it could induce fibrosis in the myocardium, which is one of the morphological features of ARVC.[90] This finding, though interesting, raised a number of issues; no evidence was given that TGFβ3 was up-regulated *in vivo* as well as *in vitro* and despite the fact that TGFβ3 is known to induce fibrosis, there was no clear biological link between the mutations identified and ARVC.[91]

In 2003, a mouse model of ARVC was identified by chance, during the testing of anti-diabetic compounds on obese mice that were originally isolated on the basis of hyperglycemia.[92] Examination of the heart of these mice showed massive fibrosis of the RV wall, degradation of cardiomyocytes, and macrophage infiltration. A retroposon insertion encoding a mutant form of the nuclear protein laminin receptor 1 (LAMR1) was identified by positional cloning, and was considered to be responsible for the cardiac phenotype observed. LAMR1 is one of the ribosomal proteins localized in the nucleus and is involved in apoptosis. [92] To date though, there has been no report of LAMR1 contributing to the etiology of human ARVC.

5) Cell-cell junctions:

When cells bear the stress...

Cells organized in tissues are in contact with secreted extracellular macro-molecules referred to as the extracellular matrix whose function is to hold the cells together and provide a means in which cells can migrate and interact. In addition, cells are held together by cell-cell junctions. Connective tissues and epithelial tissues represent the two extremes in which the structural roles played by the cell-matrix and cell-cell adhesion are radically different. In connective tissues, the extracellular matrix is plentiful and the cells within it sparsely distributed. The matrix is rich in fibrous polymers, especially collagen, and bears most of the mechanical stress to which the tissue is subjected, therefore constituting direct cell-cell attachment relatively unimportant. On the contrary in epithelial tissues the extracellular matrix is scanty, consisting mainly of a thin layer referred to as the basal lamina, which underlies cells bound together into sheets. Within epithelial tissues, it is the cells that bear most of the mechanical stress. Strong intracellular protein filaments cross the cytoplasm of each cell transmitting mechanical forces to neighboring cells. To achieve this, the filaments are directly or indirectly attached to transmembrane proteins on the plasma membrane, where specialized junctions are formed between adjacent cells or between cells and the underlying basal lamina.

Anchoring junctions:

Anchoring junctions are widely abundant in animals, but are not found in plants. They allow groups of cells to act as robust structural units by connecting the cytoskeletal elements of one cell to the cytoskeletal elements of adjacent cells or to the extracellular matrix. They are mostly abundant in tissues subjected to increased mechanical stress, such as the heart and the epidermis.[93] Three types of anchoring junctions are recognized to date: the adherens junctions, which connect the actin microfilaments of one cell to the actin microfilaments of adjacent cells; the hemi-desmosomes, which connect the intermediate filaments of one cell to the matrix; and the desmosomes, which connect the intermediate filaments of one cell to the intermediate filaments of neighboring cells (Figure 16). All three types of anchoring junctions consist of two main groups of proteins: the intracellular attachment proteins, which connect the junction complex to the cytoskeletal elements of the cell, and the transmembrane linker proteins, which on the one end interact with the intracellular attachment proteins and on the other end associate with the matrix or with transmembrane linker proteins of a neighboring cell.[94]

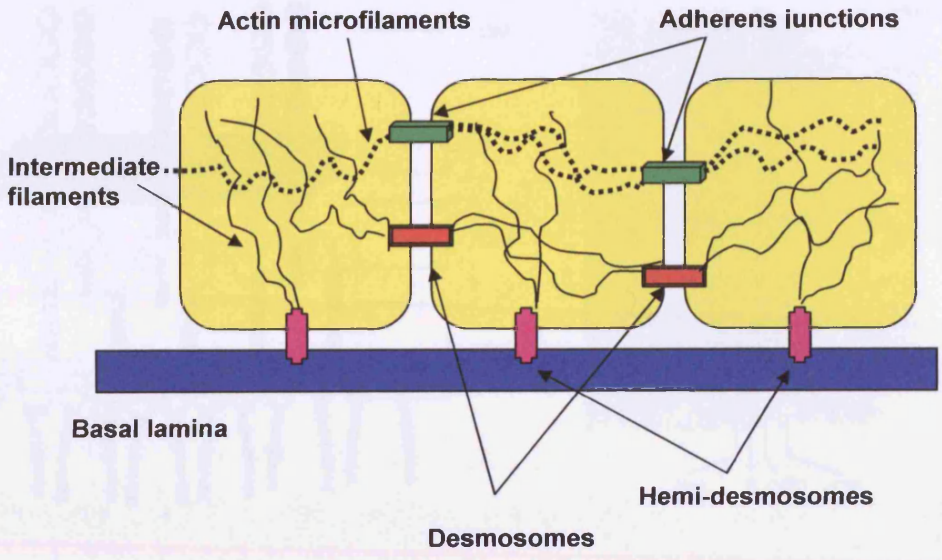

Figure 16: Anchoring junctions connecting adjacent cells to each other and to the basal lamina.

Desmosomes:

Of all the vertebrate intercellular junctions, desmosomes are perhaps the most specialized, arising later in metazoan evolution than their relatives, the adherens junctions. [93] Historically, desmosomes isolated from cow nose epidermis were separated to reveal a large number of bands by SDS-polyacrylamide gel electrophoresis, which indicated a level of complexity comparable to that shown for plasma membranes.[95] Although the analogy with the plasma membrane was short-lived, desmosomes do in fact bring together members of at least three protein families: the armadillo, the plakin and the cadherin protein families.[96]

Desmosomes are readily identified in transmission electron micrographs of conventional thin sections by their characteristic ultrastructural appearance. They consist of two principal domains: the extracellular core domain (ECD), or desmoglea, and the intracellular plaque. The intracellular plaque is commonly described as consisting of two regions: the outer dense plaque (ODP), 15-20nm wide and separated by an electron-lucent zone from a slightly less dense inner plaque (IDP), into which the intermediate filaments are seen to insert. The region between the inner phase of the ODP and the IF domain has also been referred to as the satellite region. Differing values have been reported regarding the width of these domains. The orientation of IFs at desmosomes is also unclear, although in classical thin sections, IFs are reported to converge towards the plaque and then loop away from it (Figure 17).[97]

Figure 17: Desmosome ultrastructure and molecular model. An electron micrograph (right) and a molecular model (left) showing the various regions of the junction including the inner dense plaque (IDP), the outer dense plaque (ODP), the plasma membrane (P) and the dense midline (DM).[98]

Our current understanding of desmosomal structure comes from *in vitro* cell-culture domain mapping and reconstitution studies. The model driving these studies was based on adherens junctions, where microfilaments are tethered to the plasma membrane through a tripartite complex: a classic cadherin, such as E-cadherin, N-cadherin and P-cadherin, is coupled directly through its cytoplasmic tail to armadillo proteins, namely plakoglobin and beta-catenin, which in turn are linked to α-catenin, which binds to actin. Consequently it was predicted that IFs are also tethered to the plasma membrane by a linear complex. Desmosomal cadherins, mainly desmocollins and desmogleins, associate with armadillo proteins, mainly plakoglobin and plakophilins, which in turn bind members of the plakin family, primarily desmoplakin that links the cytoskeletal elements to the junction complex (Figure 18). [93] In agreement with this linear model, it was suggested that the N-terminal halves of desmocollins and desmogleins constitute the desmoglea; their C-terminal halves are embedded in the ODP along with plakoglobin, plakophilins and the N-terminal domain of desmoplakin, while the C-terminal domain of desmoplakin extends within the IDP.[99] Several studies have indeed provided data consistent with this model. However, more recent studies suggest a more complex molecular map than the linear chain originally predicted, where each protein has several points of contact for more binding partners than initially thought.[93] Moreover, apart from the major desmosomal protein components presented,

additionalminor components such as IFAP 300, pinin, desmocalmin, plectin, envoplakin and periplakin may also contribute to the plaque structure.[97]

Figure 18: Molecular model of the desmosome. This simplified model shows representative protein-protein interactions in which principal desmosomal components participate.[93]

Despite their critical role in maintaining adhesion and integrity, desmosomes are not static units. Instead, they are dynamic units that allow for cell motility and membrane elasticity, by assembling and disassembling in response to outside-in signalling from the micro-environment.[99] This intrinsic elasticity may explain the way in which desmosomal adhesion is maintained throughout the entire cell cycle and even during mitosis when complete restructuring of the cells is taking place.[100] The desmosomal canvas becomes even more colourful as different types of IFs bind desmosomal plaques in different tissue types. In epithelial tissues, desmosomes anchor keratin filaments to the membrane. In the myocardial and Purkinje fibre cells of the heart, they anchor desmin filaments to the membrane, while in the meningeal cells and the follicular dendritic cells of the lymph nodes, they associate with vimentin IFs.[93] In fact, the first experiments showing an interaction between desmoplakin and desmin in the heart were performed in 1983.[101] Desmin filaments not only attach to the membrane plaques, but remain attached to desmoplakin even after endocytotic internalisation of desmosomal domains by treatment of the cells with ethylene glycol tetra-acetic acid (EGTA).[101] Furthermore, different desmosomal plaque components are found in different tissues.[102] For instance, intestinal epithelial cells contain both plakophilin2 and

plakophilin-3, whereas hepatocytes express only plakophilin2, indicating that there probably are functional differences between desmosomes in different cell types.

Desmosome composition and structure not only varies from cell type to cell type but also during the process of differentiation and stratification in complex epithelia. In the epidermis, desmoglein1 and desmocollin1 are concentrated in the highly differentiated upper layer of the skin, while desmoglein3 and desmocollin3 are prominent in the basal and suprabasal layers (Figure 19). The specific distribution pattern of desmosomal components is not merely a result of differentiation but may in fact drive tissue morphogenesis. Alternating the ratio of desmoglein3 to desmoglein1 in the mouse suprabasal epidermis by forced expression of desmoglein3, resulted in the acquisition of mucous epithelial traits and led to peri-natal lethality due to severe trans-epidermal water loss.[98] Similar studies suggest that desmosomes are much more than tethers for intermediate filaments and that they have a role in tissue morphogenesis, organization and homeostasis and intracellular signalling. [98]

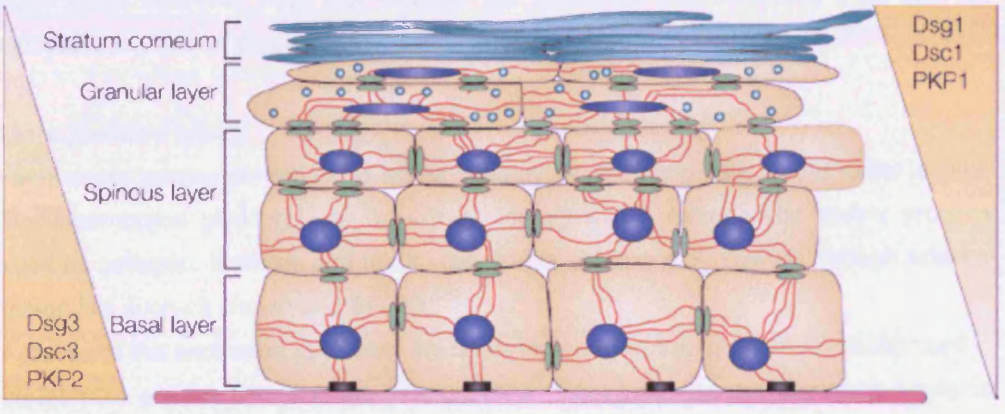

Figure 19: This schematic of the epidermis shows that proteins are expressed in a differentiation-dependent manner. For example, in the case of desmosomal cadherins, desmoglein1 and desmocollin1 are patterned in a gradient, with the highest level in the superficial layers and tapering off in the basal layers. Desmoglein3 and desmocollin3 show an opposite pattern. Likewise, the armadillo family member plakophilin1 is concentrated in junctions of the superficial layers, whereas plakophilin2 is found in desmosomes deeper in the epidermis.

Desmosomes in cultured cells assemble in response to cell-cell contact and increased levels of intracellular calcium. Perturbing intracellular Ca^{+2} stores with the Ca^{+2}-ATPase inhibitor thapsigargin interferes with intercellular junction assembly even when the cells are in contact.[93] Recently, Darier's and Hailey-Hailey disease have been shown to arise

from mutations in the calcium ATPases ATP2A2 and ATP2C1, respectively.[103] These disorders were long hypothesized to arise from defects in desmosomes, based on the loss of desmosomal structures and adhesion observed in patients. The finding that mutations in these molecular pumps cause these diseases supports the importance of intracellular Ca^{+2} homeostasis for desmosomal adhesion.[103,104] Desmosome assembly in response to Ca^{+2} is reversible during the early stages, but ultimately desmosomes mature and can no longer be dissociated and endocytosed due to Ca^{+2} depletion. They do however re-acquire their Ca^{+2} dependency at the free edge of wounded epithelial sheets, and this process has been shown to depend on activation of protein kinase C (PKC).[93] Indeed, treatment with 12-O-tetradecanoyl-13-acetate, which activates PKC, induces desmosomal formation even in cells grown in low Ca^{+2}- containing medium.[99] Interestingly, restoration of Ca^{+2} levels in Ca^{+2}-starved cultures does not lead to re-translocation of endocytosed assembled structures to the cell surface, supporting that desmosomes are assembled at the plasma membrane and not in the cytoplasm.[100] This observation however does not exclude the possibility that assembly may rely on cytoplasmic pools of plaque components.[100]

More junction types:

Hemi-desmosomes contribute to tissue integrity by attaching cells to the basal lamina. Transmembrane glycoproteins, known as integrins, link extracellular matrix proteins such as collagen, laminins and fibronectin, to the cytoskeletal network through adaptor molecules such as plectin and BP230.[105]

Apart from the anchoring junctions, the other major intercellular junctions recognized in vertebrates are the tight and the gap junctions. Tight junctions are occluding junctions that play a critical role in maintaining the concentration differences of small molecules across epithelial cell sheets.[106] In 1958, *Sjostrand et al* described an area of specialization of the cardiomyocyte adhering surface composed of "three dark lines with two intervening less dense lines", which he referred to as the "longitudinal connexion".[107] Years later, *Jean Paul Revel* coined the term "gap junctions" thus emphasizing the two key features: a gap between the cells and yet a junction between them. Of the various ways that cells "talk" to one another, communications via gap junctions is certainly the most direct. Composed of arrays of densely packed channels that link the cytoplasmic compartments of neighbouring cells, gap junctions provide a direct route by which cells can exchange ions and small molecules. In the heart, gap junctions are responsible for inter-cellular transfer of current and thus control the precise spatio-temporal pattern of electrical activation to coordinate the contractile activities of individual cells and ensure effective pump function.[108]

A gap junction is formed by multiple intercellular channels, each of them formed by two hemi-channels referred to as connexons, oligomeric transmembrane proteins built by 6 subunits that belong to the connexin family (Figure 20). Permeability and electric conductivity of gap junction channels is determined by molecular peculiarities of connexins, their capacity for phosphorylation and by extra- and intracellular factors.[109] The modern era of cardiac connexin biology began in 1987 with the cloning of connexin43 (Cx43), the major cardiac gap junction protein. With the advent of genomic sequencing, we now know that the human genome contains 21 different connexin genes. It has also become clear that with few exceptions, individual cells express multiple connexins. At least five connexins (Cx43, Cx40, Cx45, Cx31.9 and Cx37) are expressed in the heart. Four of these connexins are expressed by cardiac myocytes, but different regions of the heart express different amounts and combinations of the cardiac connexins. For example, atrial myocytes express abundant amounts of Cx43 and Cx40, but only a very limited amount of Cx45. In contrast, ventricular myocytes express large amounts of Cx43 but only trace levels of Cx45 and no Cx40.[110]

Cell-cell junction dependency and the concept of the intercalated disc:

The cardiac plasma membrane incorporates a specialized region termed the intercalated disc which coordinates and facilitates intercellular adhesion and communication by bringing together adherens, desmosomal and gap junctions.[111]

Adherens junctions arose first in evolution and also assemble first both during development and in individual cells that are stimulated to make junctions. When adherens junction formation is blocked through inhibitory antibodies, dominant-negative constructs or as a result of naturally-occurring mutations, desmosome assembly is inhibited or delayed. Adherens junction assembly is an active process that requires the engagement of N-cadherin and the active participation of the actin cytoskeleton. It has been proposed that desmosomes form passively, assembling in the gaps between adherens junctions.[93] The purpose of adherens junctions then could be to bring the membranes into close proximity, thereby allowing desmosomal molecules to engage and cluster. [93] In agreement with this hypothesis, cells that express desmosomal protein components but lack a classic cadherin or α-catenin are unable to assemble desmosomes.[98] However, activation of PKC appears to by-pass the requirement for adherens junction components in certain cell lines, resulting in the induction of desmosome formation, indicating that adherens junctions may also provide important chemical signals for the assembly of desmosomes.[98]

Figure 20: Gap junctions viewed by transmission electron microscopy: (A) by freeze-fracture to split membranes and (B) in ultra-thin sections. (C) A model of gap junction communication. [112]

Additionally, experiments on adult rat cardiomyocytes have shown that the formation of adhering junctions is a pre-requisite for the assembly of gap junctions in the cardiac intercalated disc.[113] This implies that during the establishment of cell-cell contacts, transmembrane cadherins form a zipper-like structure, coupled to a cytoplasmic protein plaque, thus strengthening the cell-cell contact and providing enough close membrane apposition to allow the assembly of connexins into gap junctions. This hypothesis is in good agreement with the observations that antibodies against classical cadherins, transfection of cells with cDNA encoding cell adhesion molecules and calcium depletion, which collectively inhibit cell-cell contact, significantly perturb the formation of communicating junctions.[113,114] In contrast, loss of electrical junctions has no effect on the establishment of mechanical junctions between cardiac myocytes.[115]

6) Major desmosomal components:

a) Desmosomal cadherins:

The family of the transmembrane desmosomal cadherins includes the desmocollins (Dscs) and the desmogleins (Dsgs). The genes coding for the members of this cadherin sub-family are clustered in chromosomal region 18q12.1 with the three desmocollin genes arranged in a head-to-tail orientation in opposite direction to the four head-to-tail oriented desmoglein genes. The order in which the genes are found in the cluster mirrors the spatial order in which the equivalent genes are expressed in the developing mouse embryo.[116] The close proximity of these genes in both the human and mouse genome may be indicative of the presence of a shared regulatory region, perhaps in the form of a locus control region (LCR).[117] Also, the fact that desmocollins show a higher sequence similarity to classical cadherins than to desmogleins may be mirroring the series of evolutionary events leading to the different cadherin sub-classes through gene duplication and mutation events.[118] Each isoform has characteristic expression patterns with the type 2 isoforms showing the widest tissue distribution in epithelia and also in desmosome-bearing non-epithelial tissues, being for example the only isoforms expressed in the heart. In contrast, type 1 and 3 isoforms are detected only in certain stratified epithelia, with desmocollin 1 being especially restricted to the epidermis[116] and desmoglein 4 being mostly abundant in the testes, the prostate gland and the salivary gland.[119]

At the amino acid level, the Dsc and Dsg isoforms within a single species exhibit 51-55% sequence identity and the specific isoforms between mammalian species are identical in the range of 73-83%.[120] The desmosomal cadherin extracellular domains are composed of four extracellular cadherin repeats (ECR) of about 110 amino acids in length and a membrane proximal extracellular domain, often named the extracellular anchor domain (EA). A major difference between Dscs and Dsgs resides in their cytoplasmic domains. Both reveal a membrane proximal intracellular anchor domain (IA) and an intracellular cadherin segment (ICS), which provides the binding site for plakoglobin. Specific for Dsgs is an extended intracellular domain containing a proline-rich region (IPL) followed by a repeated unit domain of 29 amino acid repeats (RUD) and a glycine-rich C-terminal desmoglein terminal domain (DTD).[120] Desmocollin isoforms differ additionally from desmoglein isoforms in that they can be alternatively spliced. When exon 16 is incorporated in the transcript, it contains a stop codon, which signals termination of translation, giving rise to isoforms "b". When exon 16 is excluded from the transcript though, termination of translation occurs within exon 17, giving rise to the longer isoforms "a". The C-terminus of the "b" splice variants lacks the ICS

domain and thus is unable to bind plakoglobin and assemble into desmosomal complexes (Figure 21). [121]

Figure 21: Schematic representation of desmosomal cadherin structure.[93]

Like classical cadherins, desmosomal cadherin interactions are calcium-dependent. However, unlike classical cadherins, in order for desmocollins and desmogleins from opposing cells to confer strong adhesion, they must form heterodimers,[122] with the first two ECRs of desmocollin isoforms and the first three ECRs of desmoglein isoforms being crucial for this interaction.[123] Surface force measurements and bead aggregation assays though have suggested that extensive inter-digitation of cadherin molecules, rather than interactions at their tips, may be required for strong adhesion.[124] X-ray structures of cadherin molecules have shown that all ECR domains adopt a β-sandwich form with calcium ions bound to the loops joining individual domains.[124] Furthermore, electron tomography examination of individual desmosomes has drawn attention to the importance of a Trp residue at the N-terminal domain of cadherins, which upon insertion into a pocket formed by 3 hydrophobic residues, highly conserved amongst all family members, confers both cis-adhesive and trans-intercellular bonding.[124] Numerous cis-interacting molecules propagating along the length of a junction indicate that full adhesion may in fact result from the sum of a large number of diverse, weaker interactions, and that even intracellular domains may be responsible for holding the groups together laterally (Figure 22).[124] The calcium-dependency of these interactions has been shown by experiments where increasing concentrations of EGTA significantly reduce the number of desmocollin-desmoglein complexes.[123] In 2001, *Ishii et al* provided evidence that desmosome assembly can tolerate large shifts in cadherin

stoichiometry but is very sensitive to isoform-specific differences exhibited by desmocollins and desmogleins. [125]

Figure 22: Schematic representations of cis- and trans-interactions between desmosomal cadherins conferring cell-cell adhesion.[124]

Certain members of the desmosomal cadherin family have been implicated in a number of acquired and inherited skin diseases.[126] Pemphigus foliaceous, fogo selvagem and pemphigus vulgaris are autoimmune diseases characterized by blisters and erosions of the skin with additional mucose membranes in pemphigus vulgaris. The auto-antigens recognized by the antibodies are specific to Dsg1 in pemphigus foliaceous and fogo selvagem and to Dsg3 in pemphigus vulgaris. The antibodies target the ECRs of desmogleins, especially ECR3, disrupting their association with desmosomal cadherins in adjacent keratinocytes.[127,128,129] Staphylococcal scalded skin syndrome affects primarily infants and young children and is characterized by fever, skin tenderness and erythrema leading to loss of large skin areas due to epidermal separation days or even hours after the onset of the disease. This reaction is induced by three exfoliative toxins,

secreted by *Staphylococcus aureus*: ETA, ETB and ETS.[127] The toxins target and cleave the glutamic acid residue at position 381 of Dsg1, causing disruption of adhesion between adjacent keratinocytes and thus allowing bacteria to enter and flourish within the skin.[127] Dominant mutations in the Dsg1 gene result in a completely different phenotype; striate palmoplantar keratoderma.[130] Mutations in the mouse Dsg3 gene lead to the so-called "balding phenotype" characterized by hair-loss, skin fragility and oral lesions.[131] Histological and ultra-structural examination of skin samples has shown widening of intercellular spaces, dramatic reduction in desmosomal number as well as changes in desmosomal size and structure.[131] Furthermore, desmosomal cadherins have been implicated in tumorigenesis, since loss of heterozygosity in the 18q12 locus has been observed in cases of human squamous cell carcinomas.[126] Finally, localized autosomal recessive hypotrichosis is a disorder characterized by hypotrichosis of the scalp, chest, arms and legs, less dense facial hair and the presence of ingrown hair in patches of the scalp. Deletions in the Dsg4 gene were found in two families presented with this disorder.[132]

When keratinocytes are exposed to pemphigus vulgaris serum, there is a transient and rapid increase of intracellular Ca^{+2} concentration and inositol triphosphate and a consequent activation of protein kinase C, which subsequently activates p38MAPK.[133] Interestingly, inhibition of phosphorylation of p38MAPK inhibits the cytoskeletal re-organization that takes place in the frame of pemphigus and also inhibits blister formation in animal models.[133] Furthermore, the balding mouse shows alterations in integrin expression, keratinocyte proliferation rates as well as inflammatory responses.[131] Finally, when Dsc3 is mis-expressed in spinous keratinocytes, there are defects in differentiation including hyper-proliferation, abnormal keratinization as well as increased beta-catenin stability and enhanced signaling.[133] Collectively, these observations suggest that the phenotypes described are not merely a result of defects in cell-cell adhesion, indicating a role of desmosomal cadherins in signaling cascades. Indeed, apart from their role as biological glues, desmosomal cadherins are now recognized to have a role in apoptosis, metastasis, cell-sorting, cell-positioning, morphogenesis and maintenance of ordered structures. [134,135]

b) <u>The armadillo family of proteins: plakoglobin</u>

Plakoglobin (PG), also known as γ-catenin is a major cytoplasmic protein that occurs both in a soluble and a membrane-associated form and is the only known constituent common to the sub-membranous plaques of both kinds of adhering junctions: the desmosomes and the adherens junctions.[136] PG is a representative of a large multi-

gene family of proteins defined by the occurrence of a variable number of "arm-repeats", so-called after the protein encoded by the armadillo segment polarity gene of *Drosophila melanogaster*. [137] Like its homologs, β-catenin and armadillo, plakoglobin has a tri-partite structure composed of an N-terminal, a central and a C-terminal domain. In their mostly highly conserved central region, all three proteins are composed of a series of 13 imperfect 42-amino acid arm-repeats (Figure 23). X-ray crystallography of the β-catenin central region gave important insights into the structural features of this domain.[120] A typical arm repeat consists of three α-helices which form a right-handed super-helix. The super-helical structure of the complete arm repeat region forms a long positively charged groove, representing the binding site for multiple ligands, including cadherins. Although the structure of the PG central domain has not yet been resolved, the high homology to β-catenin suggests that it forms a similar shallow basic groove. [120]

Mapped to the chromosomal region 17q12-q22, the plakoglobin gene consists of 15 exons, only 14 of which are translated and code for a 744 amino-acid protein. The 5' portion of the gene is rich in GC- dinucleotides and PG expression is decreased upon hyper-methylation of this region suggesting that expression of the gene varies depending on post-translational modifications. [138]

Figure 23: Schematic representation of the plakoglobin protein structure.[93]

When the plakoglobin gene is ablated in mice, animals die between days 12 and 16 of embryogenesis owing to defects in heart function.[139] Often, their ventricles burst, and pericardial tamponade appears to be the immediate cause of death. This tissue instability correlates with the absence of desmosomes and a redistribution of desmosomal proteins in the heart. In particular, typical desmosomes cannot be detected, and instead long mixed-types of junctions are observed, indicating that PG plays a crucial role in the architecture and stabilization of heart tissue as well as in the sorting of anchoring junction types. [139] Work performed on heart fibers obtained from PG-deficient embryonic mice suggests that PG is important for cardiac compliance but not necessary for the attachment of the myofibrillar apparatus to membrane junctions.[140] Apart from its association with Naxos disease, PG has also been implicated in the autoimmune disease pemphigus vulgaris. Binding of pemphigus auto-antibodies to Dsg3 causes phosphorylation of a serine residue on the cadherin

molecule resulting in the dissociation of PG from the junctional complexes.[141] Absence of PG from desmosomes leads to rapid depletion of Dsg3 from the membrane and hence the disease phenotype.[141] In PG-null cell lines, incubation with pemphigus antibodies does not lead to depletion of cadherin molecules thus sparing the major cytoskeletal re-organization characterizing the disease.[141]

In Xenopus, plakoglobin is shown to play a critical role in the assembly, organization and maintenance of the cortical actin cytoskeleton,[142] while over-expression of PG in embryos leads to neural axis duplication,[143],[144] indicating the currently widely recognized role of the armadillo protein in signaling pathways. In agreement with this belief, PG is recognized to have a role in cancer. Loss of heterozygosity in the PG gene has been observed in breast and ovarian tumors,[145,146] a missense mutation leading to a substitution of a serine by a leucine residue at the N-terminal part of the protein has been found to underlie cases of gastric and pancreatic cancers,[147] while PG expression is reduced or absent in a subset of human non-small cell lung carcinomas, indicating the putative tumor-suppressive role of the armadillo protein.[148] Further reports indicate that proteolysis and altered localization of γ-catenin are early markers for the response of cells to cisplatin, one of the most widely used anti-cancer chemo-therapeutic agents, and that reduced levels of γ-catenin in resistant cells may indicate an important role of γ-catenin in mediating or modulating the toxicity of cisplatin in cancer cells.[149,150] In contrast with these lines of evidence, histone deacetylase suppresses the expression of PG in human fibrosarcoma HT1080 cells, indicating a role of PG as an oncogene.[151] Collectively, these observations suggest that PG may have either a tumorigenic or a tumor-suppressing activity depending on the cell type and on its ability to activate downstream signaling pathways.

Plakophilins:

$P120^{ctn}$ is the prototypic member of the $p120^{ctn}$ subfamily of armadillo-related proteins.[152] Members of the $p120^{ctn}$ family share a characteristic organization of their arm repeat domain, which suggests an ancient evolutionary relationship. There are two groups that differ in the degree of sequence similarity and intracellular localization. The first group includes the prototype 120^{ctn} itself, ARVCF, δ-catenin/NPRAP and p0071/plakophilin4. These proteins share between 65 and 81.5% sequence similarity with each other in their arm domains and co-localize with classical cadherins at adherens junctions.[152] The second group includes plakophilins 1, 2 and 3 (PKPs). These proteins share between 51 and 60.9% sequence similarity with each other in their arm domains and around 50% sequence similarity with the $p120^{ctn}$ arm domain.[152] So far, no binding partner has been identified that interacts with members of both groups supporting the view of distinct molecular functions. Although the sequences of

all p120^{ctn}-related proteins are highly related, the corresponding genes are dispersed throughout the human genome, excluding the possibility of coordinated expression regulation as suggested for Dscs and Dsgs.[152] The PKP1 gene is located at 1q32, the PKP2 gene at 12p13, the PKP3 gene at 11p15 and the PKP4 gene at 2q24.[152]
Plakophilins are composed of an N-terminal head domain and a C-terminal domain containing 10 arm repeats separated by 3 conserved short insertions (Figure 24).[120] PKP1 localizes at the desmosomes of stratified epithelia, simple epithelia, urothelium and certain complex epithelia.[137] It is transcribed into two different mRNAs, one of 2.6kb and one of 5.3kb, the difference arising from alternative poly-adenylation of the 3' end of the mRNA transcript. PKP1 has two splice variants; the most common short variant, PKP1a, and the rarer longer PKP1b variant, which has a 21-amino acid insert at exon 7. The shorter isoform is found in all tissue types that form desmosomes, where it localizes both at the cell membrane and at the nucleus, while the longer isoform is confined to the nucleus.[137] Similarly to PKP1, PKP2 has two splice variants, the shorter one lacking a 44-amino acid motif between the second and third armadillo repeat. PKP2 is found in the desmosomes of most tissues, including simple one-layered epithelia and non-epithelial tissues such as the myocardium, the Purkinje fibers of the heart and the dendritic cells of the lymphatic nodes. [153] As is the case in PKP1, the shorter PKP2 isoform is found both at the membrane and in the nucleus, while the longer isoform shows a strict nuclear localization. PKP1 and PKP2 have been shown to have overlapping but distinct properties, indicating that they may be involved in the formation of functionally different desmosomes, tailored for the needs of different tissues or of different developmental stages.[154] PKP3 is found in all layers of stratified epithelia, in almost all simple epithelia apart from hepatocytes and in some non-epithelial tissues such as the dendritic cells of the lymph nodes. Finally, in mouse tissues, PKP4 is found in various epithelia, including the skin, the intestine and the liver and in non-epithelial tissues such as the heart and the brain. [155]

Figure 24: Schematic representation of the plakophilin protein structure.[93]

In 1997, *McGrath et al* first described the complete ablation of PKP1 in patients with a novel, autosomal recessive disorder that was termed skin-fragility ectodermal-dysplasia syndrome.[156] In early life, affected individuals exhibit skin fragility with trauma-induced

erosions and blistering, especially around the mouth and on the palms and soles. During childhood, hyperkeratosis of palmoplantar skin develops and there are plaques of crust-scale on the limbs and trunk. Scalp hair fails to develop normally and most patients show total or near-total alopecia. Histologically, there seems to be a "pinching off" of desmosomes with the plane of cleavage occurring immediately on the cytoplasmic side of the desmosomes. However, the presence of mostly intact, if somewhat fragile, epidermis indicates that PKP1 is only an accessory desmosomal component. [132]

It was recently shown that PKP2 is able to associate with β-catenin, and that over-expression of PKP2 up-regulates the activity of the endogenous T cell factor (TCF)/β-catenin transcription complex, indicating that PKP2 may in fact act as a transducer of signals between the cell surface and the nucleus. [154] Additionally, *Mertens et al* first showed that nuclear PKP2 associates with components of the RNA polymerase III holo-enzyme. [157] So far, the functional role of PKP2 in this complex remains elusive, although it is tempting to speculate that PKP2 might coordinate intercellular adhesion and growth control.[152] Recently, several RNA-binding proteins including poly A binding protein, fragile-X related protein and ras-GAP-SH3-binding protein were shown to partially co-distribute with PKP3 after sucrose gradient centrifugation. When cells are exposed to environmental stress, these proteins are found together with PKP3 in stress granules, cytoplasmic aggregates in which mRNAs accumulate in a stable, but translationally silenced state. Thus, PKP3 might have a function in post-transcriptional gene regulation through an interaction with RNA-binding proteins rather than a direct role in regulating gene transcription.[152] *Hatzfeld et al* had previously reported that although the head domain of PKP1 could play a role in organizing the desmosomal plaque, the armadillo repeat domain might be involved in regulating the dynamics of actin cytoskeleton.[158] Finally, like the other major desmosomal components described above, plakophilins seem to have a role in cancer. PKP1 mRNA expression was significantly elevated in head and neck squamous cell carcinoma, while PKP3 can function as an oncogene and may serve as a prognostic marker and therapeutic target for lung cancer.[152] Regulatory mechanisms that shift the balance between cell contact association and nuclear or cytoplasmic functions might contribute to a role in tumorigenesis. [152]

c) <u>The plakin protein family</u>

The plakin proteins represent a family of very large cytolinker proteins that have multiple functions in the cross-talk of cytoskeletal networks by cross-linking actin

microfilaments, microtubules and intermediate filaments to each other. They are also central components participating in the connection of different anchoring junctions with the cytoskeleton. Currently, seven plakin family members have been recognized: desmoplakin, plectin, envoplakin, periplakin, epiplakin, bullous pemphigoid antigen I and MACF1.[120] Ancestral members of this gene family are similar to the *Drosophila melanogaster* protein shot, which contains both actin and microtubule-binding domains and has an essential role in a variety of morphogenetic processes. [159] Although several plakin family members bind IFs and localize to desmosomes, genetic studies indicate that only desmoplakin is indispensable for these intercellular junctions.[159]

Desmoplakin:

Desmoplakin (DP) consists of an N-terminal domain essential for targeting the molecule to the membrane, a central coiled-coil rod domain involved in dimerization and a globular C-terminal domain, which anchors the intermediate filaments to the junctional plaque. Within the N-terminal domain, two major heptad-containing regions, predicted to be largely α-helical have been designated as V and Y while three minor regions have been designated as W, X and Z. The N-terminal heptad set is interrupted by short non-heptad sequences, which allow folding of the α-helical stretches onto each other. [160] The carboxy-terminal domain is composed of three plakin repeat domains (PRDs) named A, B and C, separated by a linker domain between repeat B and C. (Figure 25). Each repeat is composed of 4.5 copies of a 38-amino acid motif and forms a globular structure with a unique fold containing a conserved basic groove that may represent an IF binding site. Each PRD alone is able to bind vimentin filaments with relatively low affinity, while all three PRDs bind more strongly, consistent with the view that a sufficient number of weak but simultaneous interactions are required to confer stable adhesion. [120] Alternative splicing of the DP precursor mRNA generates two isoforms that differ in size (2871 residues in DPI versus 2232 residues in DPII) and cell type distribution. DPI and DPII have identical N- and C- termini but their central α-helical domains are of different lengths. DP binds all desmin, vimentin and keratin IFs; however these interactions involve distinct regions within each protein partner. Moreover, electrostatic interactions and post-translational modifications seem to influence IF binding. For instance, phosphorylation of a specific serine residue within the C-terminal DP domain has been shown to modulate binding to IFs. [161]

Figure 25: Schematic representation of the desmoplakin molecule structure.[93]

The first mutations to be described in DP were an heterozygous nonsense mutation (Q331X) and a donor splice site mutation (939+1G → A), in families with autosomal dominant striate PPK.[162,163] Following the description of the Carvajal syndrome, another recessive DP genodermatosis was reported.[164] The phenotype consisted of wooly hair, dystrophic nails and keratoderma without an associated cardiomyopathy and was thus termed skin fragility/wooly hair syndrome. Two unrelated cases were found to be compound heterozygotes for different combinations of nonsense/missense mutations (C809X/N287K and Q664X/R2366C).[164] Interestingly, individuals who were heterozygous carriers of the respective nonsense mutations were phenotypically normal. [164] Apart from inherited abnormalities in the DP gene, the DP protein may also be targeted in a number of autoimmune diseases.[165] Notably, antibodies to DP have been found in paraneoplastic pemphigus. There are also reports demonstrating the presence of anti-DP antibodies in pemphigus foliaceous, erythrema multiforme, bullous pemphigoid and mucosal dominant pemphigus vulgaris, although the significance of these auto-antibodies in the development of blisters remains unclear.[165]

DP-null mouse embryos proceed through implantation but do not survive beyond E6.5 owing to a loss or instability of desmosomes and tissue integrity.[166] When the DP function in the extra-embryonic ectoderm is rescued, these animals survive several days longer but die shortly after gastrulation with major defects in the heart muscle, neuroepithelium, skin epithelium and microvasculature.[167] Interestingly, endothelial cells of capillaries do not form desmosomes; however they possess unusual intercellular junctions composed of DP, PG and VE-cadherin.[167] DP-null keratinocytes isolated from an epidermis-specific DP mouse knockout, have few desmosomes and are unable to undergo actin re-organization and membrane sealing during epithelial sheet formation. [168] Moreover, knockdown of DP by siRNA in cultured endothelial cells prevents the formation of microvascular tubes.[169] Finally, loss of DP may be of potential importance in the progression of breast cancer and metastasis.[170] Collectively, these observations suggest that DP is much more than a molecular bridge that links the cell membrane to the cytoskeleton.[171]

There is more to plakins than desmoplakin:

Plectin is a high-molecular mass protein of approximately 500kDa that is associated with filamentous actin, microtubules and IFs.[172] Its structure resembles that of DP except that its plakin domain is preceded by an N-terminal actin-binding domain. Furthermore, plectin harbors 6 PRDs, denoted B1-5 and C. It is expressed in a variety of tissues, including the skin and striated muscle, where apart from its role as a cytolinker, it regulates actin and IF dynamics.[172] A role of plectin in controlling important signaling pathways is now beginning to be explored. For instance, it has been shown that the kinase activity of Erk1/2, c-Src, and PKCδ is up-regulated in plectin-deficient keratinocytes. Furthermore, plectin interacts with the non-receptor tyrosine kinase Fer and the regulatory γ1 subunit of AMP-activated protein kinase. [172] Mutations in the plectin gene have been implicated in epidermolysis bullosa, a heterogeneous group of genodermatoses characterized by fragility and blistering of the skin which is often associated with extra-cutaneous manifestations, such as muscular dystrophy and pyloric atresia. [173 ,174] Periplakin (190kDa) and envoplakin (210kDa) are closely related plakins that act as scaffolds for the formation of the cornified envelope and are also localized to desmosomes in differentiated keratinocytes. Since envoplakin does not contain a PRD, its association with IFs is likely to be indirect, possibly through the protein kazrin (Figure 26).[172] Envoplakin and periplakin are believed to be involved in desmosomal formation; however their role must be dispensable, since deletion of these genes has only minor effects on intercellular adhesion.[159]

Figure 26: Schematic representation of the plectin, envoplakin and periplakin protein structure.[93]

d) Intermediate filaments: the largest family in the cytoskeleton:

Intermediate filaments (IFs) are named such because their 7-10nm diameter is intermediate between that of actin (6nm) and tubulin (23nm).[175] More than 50 IFs are recognized to date and based on their gene structure, sequence homology, and immunological and/or assembly properties can be divided into six categories. With the clear exception of type V, the lamins, all form IF arrays. Types I and II include the epithelial IF proteins called keratins. Type III includes vimentin, expressed in cells of mesenchymal origin, desmin which is characteristic of muscle cells, GFAP, found in glial cells, and peripherin, which localizes at the peripheral nervous system. Type IV IF proteins are found in neurons and include the neurofilament proteins NF-L, NF-M and NF-H and α-internexin. The VI class may include depending on different group criteria, nestin, synemin, paranemin and tanabin.[176]

A basic molecular structure is common to all intermediate filaments.[177] A central a-helical rod domain is responsible for dimerization and higher order polymerization. This domain exists in four segments (1A, 1A, 2A and 2B) interrupted by three non-helical linkers (L1, L12 and L2) and a helix polarity reversal known as the stutter sequence, usually indicated as S. The rod domain is flanked by the more variable globular head and tail domains (V1, V2). The sequence prior to 1A, denoted helix initiation peptide (HIP/H1), and immediately after 2B, denoted helix termination peptide (HTP/H2), show a remarkable degree of evolutionary conservation (Figure 27).[177] All IF proteins share common structural features enabling them to self-assemble into 10nm filaments in vitro in the absence of auxiliary proteins or factors.[177] IFs are made of ~4.5nm protofibrils, which in turn are made of smaller protofilaments. Protofilaments contain linear arrays of IF dimers arranged in head-to-tail fashion. Most IF types are able to form homodimers. Keratins are unusual in that they form obligatory heterodimers of a type I and a type II subunit.[177] These keratin pairs show great tissue specificity. For instance the type I K14 and the type II K5 are the primary keratins of basal cells in stratifying squamous epithelia, while in more suprabasal layers they are gradually replaced by K1/K10 heterodimers.[175]

Figure 27: Schematic diagram of basic intermediate filament structure.[178]

Keratins have been implicated in a number of human diseases.[179] Point mutations in the K14 and K5 genes were found to underlie epidermolysis bullosa simplex, while mutations in K1 and K10 have been associated with epidermolytic hyperkeratosis. Moreover, mutations in the K9 gene form the basis for many epidermolytic PPK cases.[179] It is interesting how some of these human skin disorders are also caused by mutations in major desmosomal genes, indicating disorder genetic heterogeneity and highlighting the pivotal role of IF proteins in maintaining tissue integrity. Mutations in type IV IF proteins underlie a collection of motor neuron diseases, including familial and sporadic amyotrophic lateral sclerosis, infantile spinal muscular atrophy and hereditary sensory motor neuropathy. [179]

Desmin-related myopathy was originally described as skeletal and cardiac myopathy, morphologically characterized by abnormal accumulation of desmin within muscle fibers. This definition focused attention on desmin as a key molecule associated with a diverse group of clinically and pathologically related entities.[180] Molecular studies of these disorders demonstrated that some are truly caused by mutations in desmin, while another form is associated with mutations in αB-crystallin, a chaperone that stabilizes desmin molecules by preventing their aggregation.[181] Desminopathy may manifest as a relentlessly progressive skeletal myopathy with no signs of cardiac involvement. In other cases cardiomyopathy is the leading or even the exclusive feature, while respiratory insufficiency may also be a major manifestation and the cause of death.[180] Desmin-null mice develop and reproduce, indicating that desmin is not essential for myogenic commitment or for myoblast fusion and differentiation, but they show a number of abnormalities including heart fibrosis, ischemia and disorganized, distended and non-aligned skeletal and smooth muscle fibers.[182] As with all adhesion molecules, the function of IF proteins has long been thought to be merely structural. However, this single function does not explain their diverse tissue and differentiation-specific expression patterns and cannot explain all phenotypic abnormalities in IF-related human disease. Evidence is now emerging that IFs also act as an important framework for the modulation and control of essential cell processes, in particular signal transduction events.[176] Upon extracellular stimuli, signaling intermediates, in particular protein kinases and phosphatases are activated. These active molecules may interact with the IF cytoskeleton leading to different architectural alterations such as collapse, re-organization or altered solubilization of IF sub-units.[176] Alternatively, in some cases, the presence of specific subunits in the IF cytoskeleton may serve as an anchoring site for these signaling intermediates, precluding their transduction to other cellular compartments. [176]

HYPOTHESIS:

We propose that ARVC is a highly clinically and genetically heterogeneous disease caused by defects in cell-cell adhesion and disruption of signaling pathway cascades. Three lines of evidence indicate that ARVC is a disease of the desmosome: the identification of ARVC-related mutations in junctional components, the involvement of desmosomes in other forms of human disease and the phenotypic and histological abnormalities exhibited by knockout mice. Weakened cell-cell adhesion reduces the ability of cells to withstand physical stress, and as a result they dissociate from the beating myocardium and undergo programmed cell death. As the regenerative properties of the adult heart are limited, dying cells are replaced by fat and fibrous tissue, thus providing the substrate for the generation of fatal arrhythmias and the development of heart failure characterizing the disease. This hypothesis provides a potential explanation for the high prevalence of the disorder in athletes, the frequent occurrence of ventricular tachyarrhythmias and sudden cardiac death during exercise and the rare manifestation of the disease in infancy, as at this stage of development the heart is still capable of regeneration.

However, the involvement of all proteins implicated in ARVC pathogenesis in signaling processes and the spectrum of abnormalities exhibited both by humans and mouse models, cannot merely be explained by mechanical defects. Disruption of signaling pathways could provide a potential explanation for the predominant involvement of the right ventricle, the strikingly different phenotypes that may arise from similar genetic alterations, and the risk of fatal arrhythmias in the early stages of the disease when no structural or microscopic abnormalities are yet manifested. In conclusion we suggest that there is more to ARVC than adhesion. Defects in structural bonds are only part of the story, the rest of which includes multiple pathways and molecules, which have only recently started to be explored.

CHAPTER 1:

"Genetic studies of familial ARVC: identification of novel causative mutations and genes"

CLINICAL EVALUATION AND GENETIC SCREENING:

A weekly ARVC clinic, headed by W. J. McKenna, is currently operating at the Heart Hospital. All probands that fulfill ARVC diagnostic criteria undergo assessment at the time of diagnosis, and relatives are invited for clinical evaluation. The clinical assessment includes:

- RV and LV morphology and systolic function: 2D echo Doppler/tissue Doppler
- Diastolic function: Doppler tissue imaging, mitral & pulmonary venous flow
- Exercise capacity: symptom limited bicycle exercise with metabolic gas exchange measurements
- Electrocardiography: 12 lead, signal-averaged, exercise and 24h Holter
- CMR of selected patients

Thus far, approximately 220 probands and >600 relatives have been evaluated clinically. Following clinical evaluation, blood was obtained from each proband or family member, so that DNA could be used for mutation analysis. Following the same procedure, 70 probands were evaluated in Muenster, Germany and another 30 probands were evaluated in Greece and Cyprus, and DNA samples sent to our laboratory for genetic screening.

All probands were screened for mutations in the known ARVC-causing genes: desmoplakin I, plakophilin2a and plakoglobin and in the additional candidate genes: desmocollin2a, desmoglein2 and desmin. These specific isoforms were selected for screening as they constitute the major cardiac desmosomal components. Sequencing primers were designed and conditions were optimized for the amplification of each exon (Appendix: 1). Two hundred ethnically-matched non-ARVC control individuals were screened using the same methods to ensure that the newly identified mutations were indeed pathogenic. Whenever possible, relatives were screened and pedigrees were constructed.

METHODS:

1) DNA extraction from blood/body fluid and paraffin-embedded tissue blocks:

DNA extraction was performed using a QIAampmini Kit (QIAGEN) according to the instructions of the handbook. Briefly:

Blood/plasma:

Samples were equilibrated to room temperature. QIAGEN protease was added to 1.5ml micro-centrifuge tubes. Sample (200μl) followed by AL lysis buffer was added to each micro-centrifuge tube and mixed by pulse vortexing. Samples were then incubated at 56°C for 10min. Following incubation, the micro-centrifuge tubes were briefly centrifuged; ethanol was added and mixed by pulse vortexing.

Paraffin-embedded tissue:

Tissue (25 mg) was cut in small pieces and placed in 1.5ml micro-centrifuge tubes. ATL tissue lysis buffer was added to each tube followed by proteinase K and mixed by pulse vortexing. The samples were then incubated at 56°C for 1-4 hrs and occasionally mixed by vortexing until lysis was complete. Following incubation the samples were briefly centrifuged, AL lysis buffer was added and mixed by pulse vortexing. The samples were then incubated at 70°C for 10min. Following incubation the samples were briefly centrifuged, ethanol was added and mixed by pulse vortexing.

Blood, plasma and tissue:

The mixture was applied on Spin columns assembled to 2ml collection tubes and the tubes were centrifuged at 8000rpm for 1min. The filtrate was discarded, the Spin column was assembled to a new collection tube and AW1 wash buffer was added followed by centrifugation at 8000rpm for 1min. The filtrate was discarded, the Spin column was assembled to a new collection tube and AW2 wash buffer was added followed by centrifugation at 13200rpm for 3min. The collection tube was discarded, the Spin column was placed in a 1.5 ml micro-centrifuge tube and distilled water was added. The samples were equilibrated to room temperature for 1min and then were centrifuged at 8000rpm for 1min. This technique is predicted to yield 6μg of DNA in 200μl of distilled water (30ng/μl).

2) Polymerase chain reaction (PCR):

AmpliTaq Gold polymerase was used for fragments shorter than 400 base pairs. For each PCR reaction the following were added:

2.5μl of 10xPCR buffer containing 1.5mM $MgCl_2$ (Applied Biosystems)

1 μl of dNTP mix, 2.5mM each of dATP, dGTP, dCTP and dTTP (Invitrogen)
1 μl of 25mM $MgCl_2$ (Roche)
10 pmoles of forward primer (Invitrogen)
10 pmoles of reverse primer (Invitrogen)
0.1 μl of Ampli Taq Gold polymerase enzyme,5 units/μl (Applied Biosystems)
75 ng of DNA template. Distilled water was added to a total volume of 26.5 μl
PCR reactions were performed under the following program:

96°C for	10min	
96°C for	30 sec	35-40 cycles
45 - 68°C for	30 sec	
72°C for	1min	
72°C for	7min	
4°C	∞	

GC-rich PCR system was used for fragments with a high content in G and C bases.
For each PCR reaction the following were added:
5μl of GC-rich 10x PCR reaction buffer with dimethyl sulfoxide (DMSO, Roche)
1 μl of dNTP mix, 2.5mM each of dATP, dGTP, dCTP and dTTP (Invitrogen)
10 pmoles of forward primer (Invitrogen)
10 pmoles of reverse primer (Invitrogen)
2.5 μl of GC-rich resolution solution (Roche)
0.5 μl of GC-rich system enzyme mix,2 units/μl (Roche)
75 ng of DNA template. Distilled water was added to a total volume of 25 μl
PCR reactions were performed under the following program:

95°C for	3min	
95°C for	30 sec	35 cycles
60 - 68°C for	30 sec	
72°C for	45 sec	
72°C for	7min	
4°C	∞	

The annealing temperature and the number of cycles varied according to the fragment amplified. All PCR reactions were performed on a Gene Amp PCR System 9700 (Applied Biosystems) using Thermo-Fast 96-well plates (ABgene).

3) PCR product purification:

PCR products were purified using a GFX-96 PCR Purification Kit (Amersham Biosciences) or a QIAquick PCR purification Kit (QIAGEN) according to the handbook. Briefly:
A GFX-96 plate was assembled on a wash plate and binding buffer was added to each well. The PCR products were transferred to the wells and mixed with the binding buffer. The plate was then centrifuged at 1800rpm for 2min. Following centrifugation, the flow-through was discarded, the wash plate was re-assembled to the GFX-96 plate and wash buffer was added to each well. The plate was then centrifuged at 1800rpm for 5min, the flow-through discarded and the plate centrifuged again at 1800rpm for 1min to remove residual ethanol. The GFX-96 plate was assembled on a collection plate, 20 μl of distilled water was added to each well, the plate was left to equilibrate to room temperature for 1min and then centrifuged at 1800rpm for 2min. Alternatively:
Five volumes of PB binding buffer were added to one volume of PCR sample and mixed. A QIAquick spin column was assembled to a 2ml collection tube; the sample was transferred in the column and centrifuged at 13200rpm for 1min. Following centrifugation the flow-through was discarded and the spin column was re-assembled on the collection tube. PE wash buffer was added and the columns were centrifuged at 13200rpm for 1min. The flow-through was discarded; the column was assembled again on the collection tube and centrifuged for an additional 1min at 13200rpm. Following that, the column was placed on a 1.5 ml micro-centrifuge tube, 20 μl of EB elution buffer was added, the tubes were allowed to equilibrate to room temperature for 1min and then centrifuged at 13200rpm for 1min.

4) Agarose gel electrophoresis:

For small DNA fragments, 2% agarose gels were prepared from agarose powder (SIGMA) and 1x Tris borate EDTA (TBE, SIGMA) buffer. For larger DNA fragments, 1% agarose gels were prepared. PCR product (5-10 μl) was loaded on the gel along with 1KB Ladder Mix (Fermentas) for reference purposes. The voltage for electrophoresis was set at 100-150 Volts, while the duration varied according to the size of the DNA fragments.

5) Amplification reaction for direct sequencing:

For sequencing purposes, samples were amplified using a BigDye Terminator v3.1 cycle sequencing Kit (Applied Biosystems) according to the protocol. Briefly:
For each sample the following were added:
3-10 ng of forward or reverse primer.
1 μl of BigDye Terminator cycle sequencing mix (Applied Biosystems)
150-600 ng of DNA template. Distilled water was added to a total volume of 10 μl
Sequencing reactions were performed under the following program:

96°C for	2min	
96°C for	10 sec	25 cycles
50°C for	5 sec	
60°C for	4min	
4°C	∞	

6) Purification of sequencing reaction products:

Purification of sequencing reaction products was performed using a DyeEx 96 Kit (QIAGEN) according to the protocol. Briefly:
The DyeEx 96 plate was assembled on top of the collection plate and centrifuged at 2660rpm for 3min. The flow-through was discarded and the DyeEx 96 plate was placed on top of a Thermo-Fast 96-well plate (ABgene). The sequencing reaction products were transferred to the plate and the plate centrifuged at 2660rpm for 3min. The samples were then dried down at 70°C for 40min on a thermal cycler, formamide (Applied Biosystems) was added to each well and the samples were sequenced on an ABI3100 sequencer. DT3100POP6{BDv3}v1.mob was used as a mobility file, RapidSeq36_POP6DefaultModule was used as a run module and BC-3100POP6RR_SeqOffFtOff.saz was used as an analysis module. The data were analyzed by Sequencing analysis program v3.7 and viewed on SeqScape v1.1.

RESULTS AND DISCUSSION:

1) Desmoplakin I:

Family A1:

The proband (A1.4), a young woman, seeked cardiac evaluation following the SCD of her sister (A1.1). Histological examination of a heart autopsy sample obtained from A1.1 showed massive fibrofatty infiltration, with degenerating residual myocytes embedded within fat and scar tissue, consistent with a diagnosis of ARVC. A1.4 presented with palpitations and pre-syncope episodes. Her resting 12-lead ECG showed inverted T-waves in precordial leads V1 and V3, and flat T-waves in V2. She showed PVCs on Holter monitoring, which however did not exceed 1000 over a 24-hour period. On echo, her LV was normal and her RV showed slightly reduced tissue Doppler velocities. On MRI her RV was mildly dilated but with preserved function. An ICD, implanted in 2004, has since discharged appropriately.

A1.5 also presented with palpitations and pre-syncope. Her resting 12-lead ECG showed no abnormalities. However, she had >1000 PVCs/24 hr on Holter monitoring. Echocardiography showed RV wall motion abnormalities, which were subsequently confirmed by contrast echo and MRI. An ICD, implanted in 2005, has since discharged appropriately. Their mother (A1.2) was normal on ECG and echo. An MRI was not performed. Their father (A1.3) reported no symptoms but he showed increased QRS duration in right precordial leads on ECG and 1356 PVCs/24 hr on Holter monitoring. Echo and MRI showed a mildly dilated LV, a normal-sized RV but with one area of hypokinesia at the RV apex. Based on the modified diagnostic criteria, applied to relatives of an individual with documented ARVC at postmortem, the findings for A1.4, A1.5 and A1.3 were considered diagnostic. A1.17 (aged 14 upon examination) reported occasional "dizzy spells". His ECG was normal, but on echo he showed a mildly dilated LV. All other family members were normal as shown by ECG and echo studies.

A C to T transition leading to a substitution of an arginine codon by a stop codon in the desmoplakin gene was identified in the family (**R1113X,** Figure 1). The mutation is predicted to lead to premature termination of translation and subsequent truncation of the C-terminus and part of the central domain of the molecule. All affected individuals were heterozygous carriers for the mutation. A1.17 (aged 14), A1.18 (aged 12), A1.13 (aged 8) and A1.14 (aged 4) were also found to be carriers, however due to their young age do not show any phenotypic abnormalities (Figure 2). It was suggested that they undergo cardiac evaluation on a yearly basis. DNA was extracted from a heart sample of A1.1 preserved in paraffin and tested for the presence of R1113X. A1.1 was also found to be a carrier of the mutation.

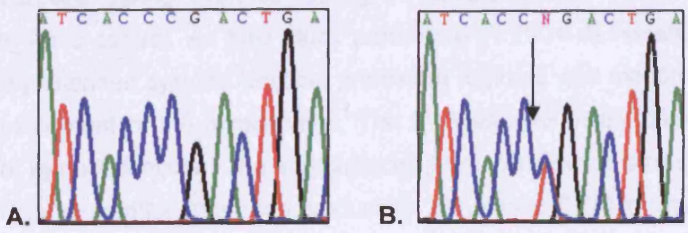

Figure 1: Electropherograms of the sense strand showing the wildtype (A) and mutant (B) sequences. C3337T is indicated by the arrow.

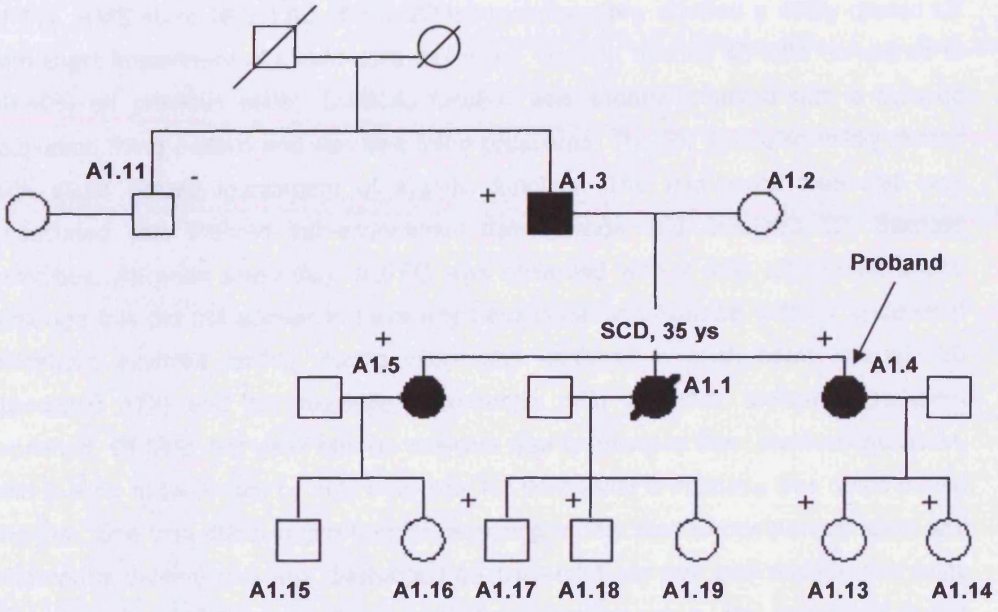

Figure 2: Pedigree of family A1 shows autosomal dominant mode of inheritance.

Family A157:

The proband (A157.1) was evaluated at the clinic following a longstanding history of palpitations and pre-syncope. Her sister died suddenly at age 26 and postmortem examination demonstrated features of acute cardiac failure. In 2003, A157.1 showed a dilated LV with impaired systolic function on echo, which was considered consistent with familial DCM. She was thus commenced on standard HF therapy with an ACE inhibitor and a beta-blocker. However, her arrhythmic symptoms persisted and ambulatory ECG monitoring documented in excess of 15,000 PVCs in a 24-hour period with occasional triplets and runs of non-sustained VT. Non-sustained VT of RV origin

was also observed during exercise testing. Amiodarone was thus commenced to improve arrhythmic control. An MRI study performed in 2004 demonstrated a dilated RV, with mildly impaired systolic function, prominent regional wall motion abnormalities and fatty replacement of the myocardium. The LV was also mildly dilated with slight impairment of systolic function. The appearances were considered strongly suggestive of ARVC, which as mentioned in the introduction, can mimic DCM in later stages. She was last seen in clinic in 2006. A 12-lead ECG demonstrated sinus rhythm with a rate of 53, left axis deviation and early transition. T-waves were attenuated in V1-V3 and inverted in V4-V6 and the inferior leads. There were signs of an intra-ventricular conduction delay in the inferior leads with an RSR complex in III and AVF. A SA-ECG using a 40Hz filter was positive for late potentials in all 3 parameters assessed (QRSD of 117, RMS 40 of 18.5, LAS of 37). 2D echocardiography showed a mildly dilated LV with slight impairment of global contractility (LV ejection fraction 45-50% compared to 30-40% on previous echo). Diastolic function was slightly impaired with a delayed relaxation filling pattern and elevated filling pressures. The RV was also mildly dilated with slight diffuse impairment of systolic function. The mid-lateral free wall was associated with marked sub-endocardial trabeculation and reversed TDI diastolic velocities. As seen previously, a PFO was observed with a mild left-to-right shunt, although this did not appear to have any hemodynamic influence. A157.1 underwent metabolic exercise testing, during which she achieved a peak heart rate of 120 (predicted 177) and her respiratory exchange ratio was 1.0, indicating sufficient workload. Of note, her peak rate on exercise was unchanged from previous occasion, and is likely to be limited by beta blockade. No ventricular arrhythmia was noted during the test. She was discouraged from participating in any kind of competitive sport and endurance training and was discharged on carvedilol, ramipril and amiodarone while the possibility of ICD implantation is currently under discussion. Her son (A157.3) and two daughters (A157.5 and A157.6) are completely asymptomatic and all their investigations were within normal limits.

The proband's sister (A157.2) has a longstanding history of intermittent sustained palpitation. The episodes are of variable duration and frequency with no identified specific triggers and are often associated with pre-syncopal symptoms. She is experiencing 3-4 episodes of light headedness and near-syncope per week and she also experienced one syncopal episode in 2001. There is no history of exertional dyspnea. A recent 12-lead ECG demonstrated sinus rhythm with a rate of 85, normal QRS axis, and preserved R wave progression. There were signs of an intra-ventricular conduction delay in the inferior leads and V3. T-waves were attenuated in V3-V6, in a pattern resembling that on A157.1's ECG. A SA-ECG fulfilled numerical criteria for late potentials in the Z lead. 2D echocardiography showed a slightly dilated LV with normal

wall thickness. However, the septum and distal apex appeared hypo-kinetic and global contractility was at the lower limit of normal (ejection fraction 50-55%). Of note, the mid posterior, mid lateral and posterior apical walls appeared heavily trabeculated with deep intra-myocardial recesses. The appearances were considered strongly suggestive of non-compaction cardiomyopathy. The RV appeared normal in both size and function. A157.2 additionally underwent metabolic exercise testing, during which she achieved a peak heart rate of 159 (predicted: 180) and her respiratory exchange ratio was 1.07. Frequent isolated ventricular extra-systoles of both RV and LV origin were observed during the test. An endo-myocardial biopsy consisting of 3 fragments was obtained in 2005. There was fibro-adipose infiltration in two of the fragments with increased fibrous tissue, consistent with ARVC. A skin biopsy showed no significant pathological abnormality. The specimen was bisected and a sample submitted for electron microscopy. Overall the architecture of the desmosomes appeared to be preserved, although there was focal loss of cohesion between some of the keratinocytes affecting maturation. The significance of this finding is uncertain but may be related to ARVC pathogenesis.

One of the proband's cousins (A157.11) was also diagnosed with ARVC in Belgium. His father had died of congestive heart failure, aged 56. Two more of the proband's cousins (A157.15 and A157.16) were also diagnosed with the disease after cardiac evaluation performed at their local medical facilities in Belgium. A157.17, A157.8, A157.9 and A157.10 were all seen in the clinic and found normal.

A deletion of a G nucleotide was found in the proband at exon 22 of desmoplakin (3045delG). The mutation changes the frame of translation, inserts eight novel amino acids downstream, followed by a stop codon, which is predicted to terminate translation within the central domain of the molecule (**S1015fsX1023**, Figure 3). A157.1, A157.2, A157.11, A157.15 and A157.16 were carriers of the novel mutation. A157.3 was also found to be a carrier. Given his young age and his positive genotype, his negative phenotype does not exclude the concealed phase of the disease (Figure 4).

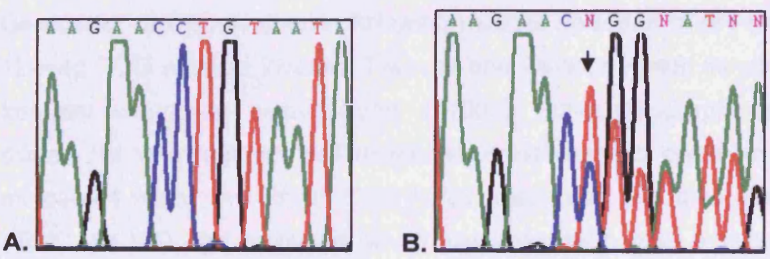

Figure 3: Electropherograms of the sense strands showing the wildtype (A) and mutant (B) desmoplakin sequences. 3045delG is indicated by the arrow.

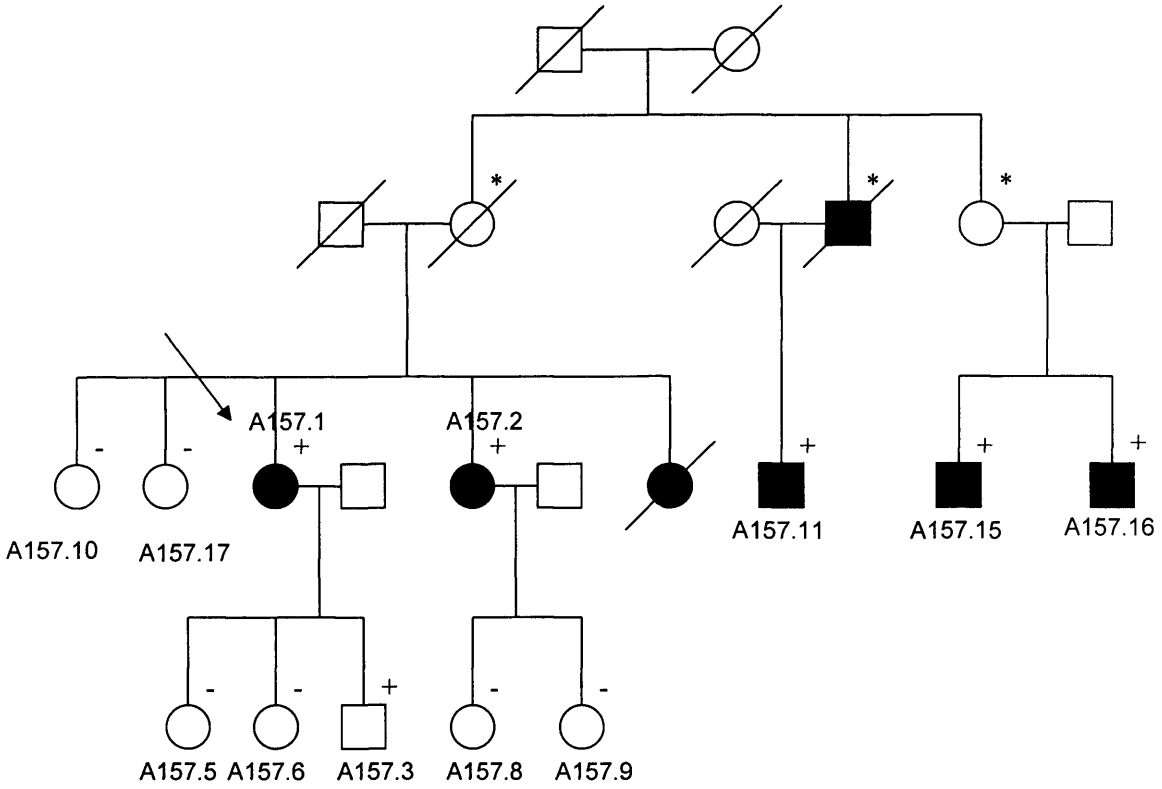

Figure 4: The pedigree of family A157 shows autosomal dominant manner of inheritance. The proband is indicated by the arrow. Obligatory carriers of 3045delG based on the constructed pedigree are indicated by the " * " sign.

Family A12:

The proband, a woman aged 19 upon examination, (A12.1) was referred to a hospital in Greece for cardiac evaluation following multiple episodes of pre-syncope. Her resting 12-lead ECG showed inverted T-waves and 24-hour Holter monitoring demonstrated frequent ventricular extra-systoles (>1000). Echocardiography showed a globally dilated RV with regional wall motion abnormalities and preserved LV function. She matched 1 major and 3minor Task Force criteria and was thus given the diagnosis of ARVC. An ICD was implanted, which has since discharged appropriately. Her mother (A12.2) demonstrated frequent ventricular extra-systoles and runs of non-sustained VT on 24-hour Holter monitoring and echocardiography revealed a mildly dilated LV with preserved RV function. She matched the modified diagnostic criteria for ARVC with

predominant LV involvement. The proband's grandfather died suddenly aged 29, however no postmortem data is available. The proband's brother (A12.3), aunt (A12.4) and grandmother (A12.5) were examined and found normal.

A T→A transition was identified in the family at exon 23 of desmoplakin (T4736A). The mutation alters a leucine residue for a stop codon and is predicted to terminate translation within the central domain of the molecule (**L1486X,** Figure 5). Both A12.1 and A12.2 were found to be carriers of the mutation. A12.3, A12.4 and A12.5 were homozygous for the wildtype allele. Since A12.5 was not a carrier of L1486X, the grandfather was considered an obligatory carrier of the mutation (Figure 6).

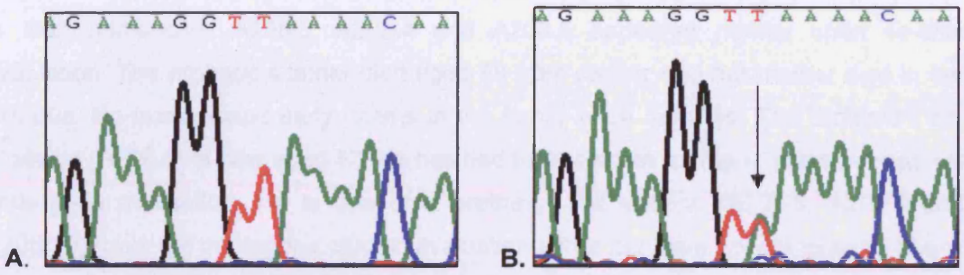

Figure 5: Electropherograms of the sense strands showing the wildtype (A) and mutant (B) desmoplakin sequences. T4736A is indicated by the arrow.

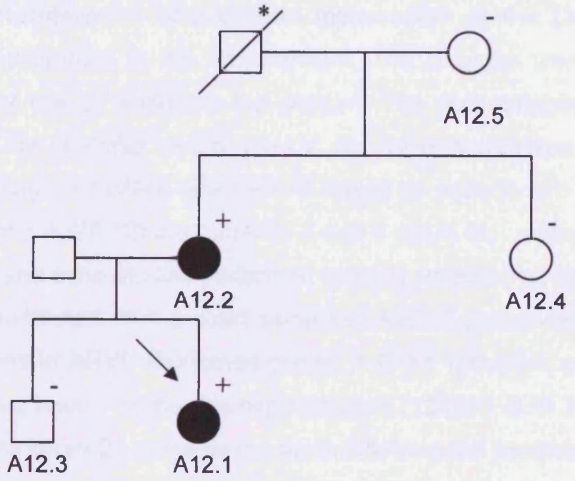

Figure 6: The pedigree of family A12 shows autosomal dominant manner of inheritance. The proband is indicated by the arrow.

Family A208:

The proband, a 48-year-old woman upon examination, (A208.2) has had ectopic beats for many years and had undergone cardiac evaluation including 12-lead ECG and 2D echocardiography on numerous occasions but no abnormalities other than isolated ectopics had been identified. The proband's daughter (A208.1) died suddenly while doing aerobics at home in 2003. She had a history of palpitation and exertional pre-syncope but had never fainted. She had not undergone medical evaluation for these symptoms. She was extremely fit and active and very health conscious. She was known to have a low blood pressure (90/50). The proband has re-married and has a 12-year son (A208.3). She also has a sister (A208.4) and a brother (A208.5), who are in their mid-sixties. A208.3, A208.4 and A208.5 appeared normal upon cardiac evaluation. The proband's father died aged 68 from cancer and her mother died in her mid-80s. No unexplained early deaths in the family were reported. The proband's ex-husband (A208.6) is now aged 53. He has had tachycardias for many years but has not undergone evaluation. He is one of 4 brothers. His siblings (A208.8, A208.9 and A208.10) have not undergone cardiac evaluation either but have not complained of any disease-related symptoms. A208.6's parents lived into their mid-70's to die from coronary artery disease and cancer. A208.6's mother though had had a brother, who apparently had died suddenly at a young age, although the details are sketchy (indicated with a grey symbol on the family pedigree). A208.6 has also re-married and has a 13-year old son (A208.7), who is well. The autopsy report of A208.1 reported striking circumferential fibro-adipose replacement of the LV myocardium advancing from the epicardium to the endocardium. The changes were present at all levels of sampling of the LV including the septum. The fibro-adipose replacement was more striking at the posterior wall of the LV. No RV abnormalities were detected. She was given the diagnosis of left-sided ARVC based on postmortem findings. Her two children (A208.11 and A208.12) are currently 8 and 5 years old, respectively, and they are both well. ECG and echo studies performed recently revealed no abnormalities (Figure 7).

DNA was extracted from a heart sample of A208.1 preserved in paraffin and screened for mutations in ARVC-implicated genes. A G→A transition was identified at the splice site following exon 7 of the desmoplakin gene (**1218+1 G → A**, Figure 8). The mutation is thought to insert 24 novel amino acids following the predicted end of exon 7 followed by a premature stop codon. All family members declined genetic screening and therefore the pattern of inheritance of 1218+1 G→ A could not be established and the individuals at potential risk of developing the disease could not be identified.

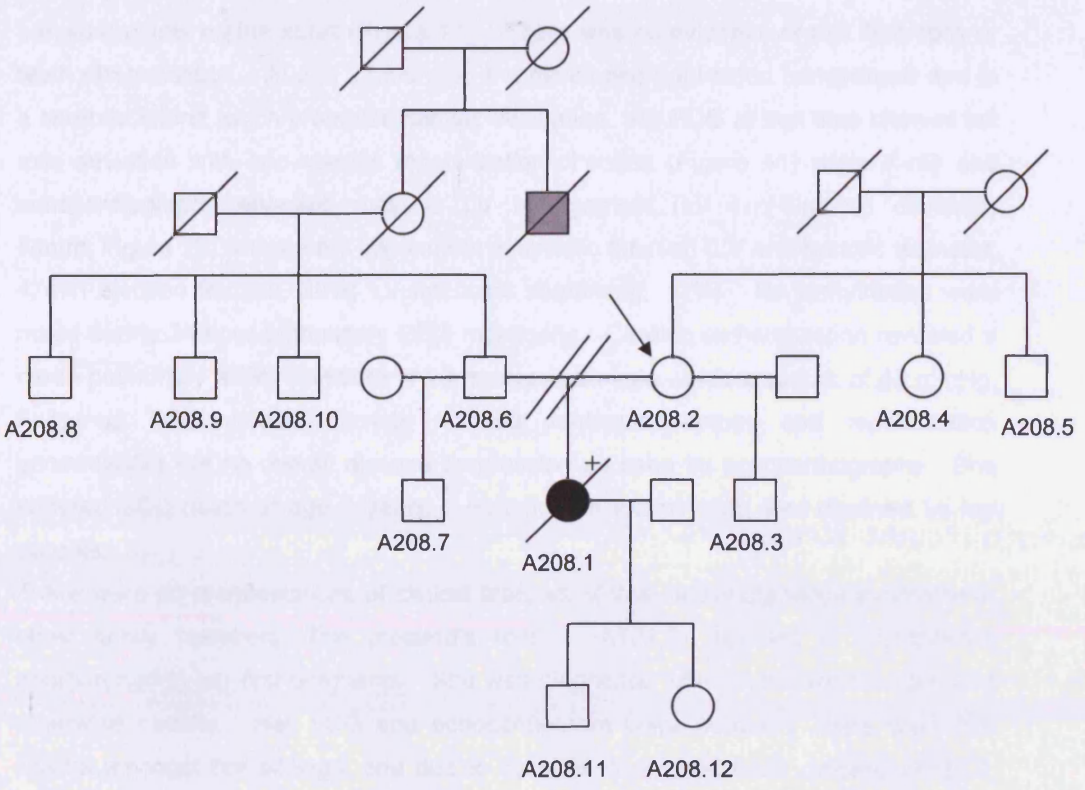

Figure 7: The pedigree of family A208. The proband is indicated by the arrow.

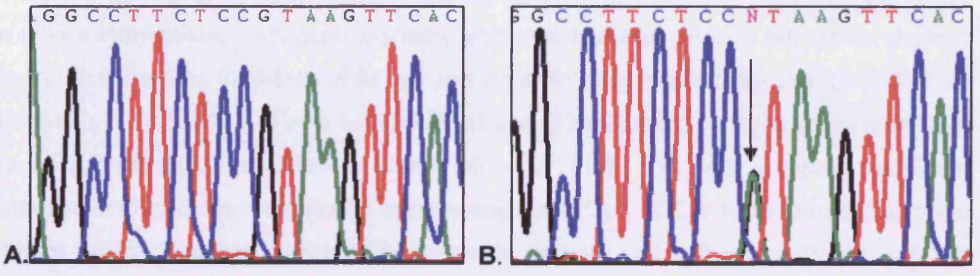

Figure 8: Electropherograms of the sense strands showing the wildtype (A) and mutant (B) desmoplakin sequences. 1218+1 G→ A is indicated by the arrow.

Family A131:

The index case (A131.1) was a girl who presented at birth with bullous dermatitis, pressure-related skin fragility and sparse, woolly scalp hair. By her first birthday, she had developed total alopecia (Figure 9) and PPK, which was more prominent over

pressure points on the soles (Figure 10). There was no evidence of nail dystrophy or teeth abnormalities. At age 27 months, she developed right-sided hemiparesis due to a cerebral infarct which prompted cardiac evaluation. An ECG at that time showed left axis deviation with non-specific repolarization changes (Figure 11) while X-ray and echocardiography revealed massive LV enlargement (LV end-diastolic diameter, 48mm, Figure 12) with severe impairment of systolic function (LV end-systolic diameter, 42mm ejection fraction, 28%; LV fractional shortening, 13%). No arrhythmias were noted during 24-hour ambulatory ECG monitoring. Cardiac catheterization revealed a mean pulmonary artery pressure of 20 mmHg and mean aortic pressure of 48 mmHg. Follow-up ECG studies showed isolated ventricular ectopy and repolarization abnormalities but no overall disease progression as seen by echocardiography. She suffered SCD death at age 9 years. Postmortem examination was declined by her parents.

There were no manifestations of clinical features of this cardiocutaneous syndrome in other family members. The proband's mother (A131.3) reported a spontaneous abortion during her first pregnancy. She was diagnosed with hyperthyroidism but was otherwise healthy. Her ECG and echocardiogram were normal. There were two deaths amongst her siblings, one due to cyanotic congenital heart disease (A131.9, indicated by a grey symbol on the family pedigree) and the other related to acute lymphoblastic leukemia at age 6 years (A137.10). One living sibling had ulcerative colitis (A131.7) and another was healthy (A131.8). The maternal grandmother (A131.11) had been diagnosed with idiopathic DCM but lived until age 74 years (indicated by a grey symbol on the family pedigree). She showed no evidence of hair or skin abnormalities. Echocardiography performed shortly prior to her death showed an LV end-diastolic diameter of 64mm and an estimated ejection fraction of 30%. The proband's father (A131.4) was healthy; ECG and 2D echocardiography studies showed no abnormalities. The paternal grandmother (A131.6) had had a breast neoplasm removed and had also reported a spontaneous abortion. ECG and echocardiography studies of the maternal siblings, the paternal parents (A131.6 and A131.5) and the proband's brother (A131.2) showed no cardiac anomalies.

Figure 9: The picture shows the proband's scalp. A131.1 had lost virtually all her hair by her first birthday.

Figure 10: A131.1 had developed profound PPK, more prominent at pressure points on the soles.

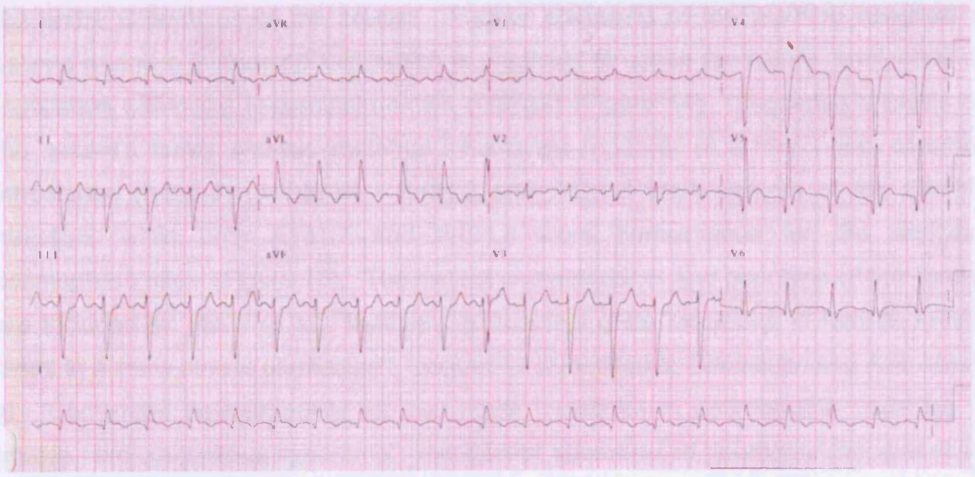

Figure 11: ECG of A131.1 obtained at age 27 months. Findings include left axis deviation and non-specific repolarization abnormalities indicative of ischemic heart disease.

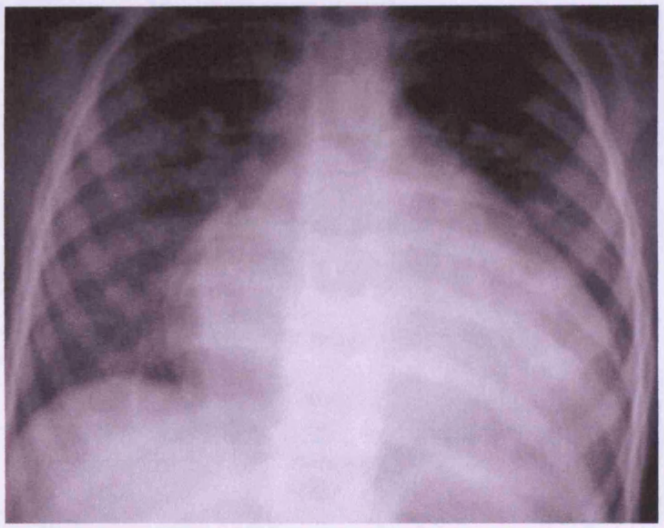

Figure 12: The proband's X-ray revealed massive cardiomegaly.

A131.1 was initially screened for mutations in plakoglobin, the gene known to underlie Naxos disease. Sequence analysis indicated the absence of the 2157del2 mutation or any other mutation in the plakoglobin gene. Thus, the proband was screened for mutations in other genes implicated in ARVC. We identified a C→T transition in desmoplakin, which is predicted to lead to a substitution of a glutamine codon with a stop codon within the central domain of the molecule (**Q1446X**) (Figure 13). This mutation is predicted to lead to premature termination of translation and truncation of

the entire C-terminus of the protein. Further screening of the proband revealed a second mutation in desmoplakin, which is predicted to cause premature termination of translation within the N-terminal domain (**Q673X)** (Figure 14). Sequence analysis of the patient's family showed maternal inheritance (A131.3) of Q1446X and paternal inheritance (A131.4) of Q673X. A131.2 and A131.6 were carriers of the Q673X mutation, while both A131.7 and A131.8 were homozygous for the wildtype desmoplakin allele (Figure 15). The clinical characteristics and genotype of this family are included in: *Ward et al.* "Multiple desmosomal gene mutations in familial ARVC result in a more severe phenotype"; manuscript submitted to *Circulation* and Asimaki et al. "Compound heterozygosity for two novel mutations in desmoplakin underlies a unique cardiocutaneous syndrome"; manuscript submitted to *Journal of the American Academy of Dermatology*.

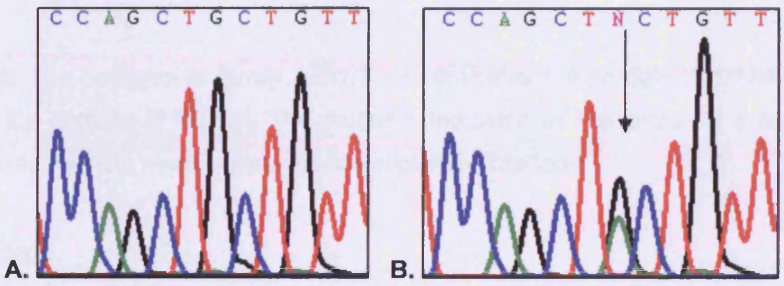

Figure 13: Electropherograms of the sense strands showing the wildtype (A) and (B) mutant desmoplakin sequences. Q1446X is indicated by the arrow.

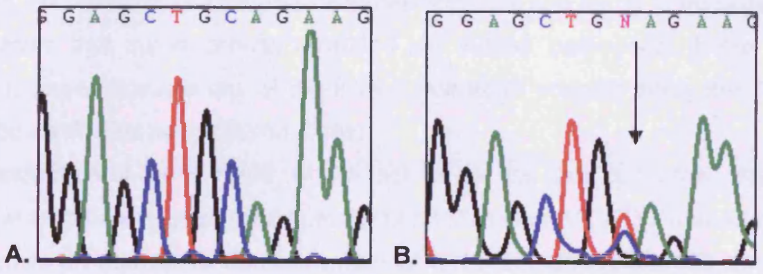

Figure 14: Electropherograms of the sense strands showing the wildtype (A) and mutant (B) desmoplakin sequences. Q673X is indicated by the arrow.

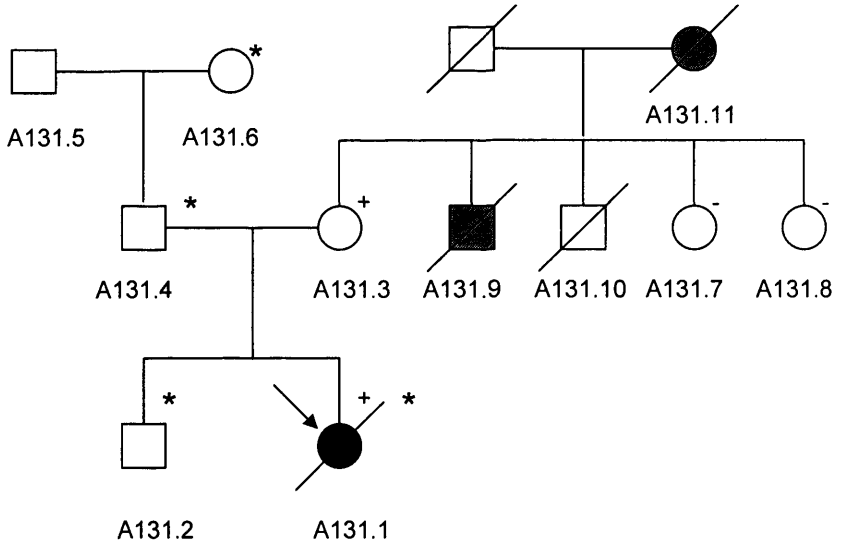

Figure 15: The pedigree of family A131.1. "+" indicates the carriers of Q1446X. " * " indicates the carriers of Q673X. The proband, indicated by the arrow, is a compound heterozygote for both novel nonsense desmoplakin mutations.

Discussion:

Collectively, 6 novel desmoplakin mutations were identified in 5 probands and their family members, wherever genetic screening was permitted. All mutations are predicted to cause premature termination of translation and sub-sequent truncation of variable lengths of the desmoplakin molecule (summarized in Table 1). The mutations were not found in 400 ethnically-matched control chromosomes, which eliminates the possibility of their being uncommon polymorphisms. All probands were screened for mutations in plakoglobin, plakophilin2, desmoglein2 and desmocollin2 and found to be negative. It is likely therefore that the mutations identified are indeed pathogenic. None of the 6 sequence changes disrupts any of the known restriction enzyme sites, and therefore, could not be confirmed by restriction digest.

With the exception of family A208, where lack of genetic data prevented establishing the mode of inheritance, desmoplakin mutations in families A1, A157 and A12 seem to be inherited in an autosomal dominant manner. R1113X, S1015fsX1023 and L1486X show high penetrance, with all carriers being affected by the disease apart from young individuals, who are though at risk of developing the disease later in life. Desmosomal mutations can exert pathogenic effects at three levels: the desmosome composition and function level, the intercalated disc level (given the interdependency between different junction types on these specialized heart regions) and by disrupting signaling pathways. At the desmosome level, mutations can have pathogenic effects due to

haploinsufficiency, and thus insufficient incorporation of the protein at the junctions, due to absence of formation of essential protein-protein interactions or due to mutated molecules getting incorporated in the junction thus leading to disrupted desmosome structure and reduction in the number of functional desmosomes.[183]

Family	Mutation	Predicted outcome
A1	R1113X	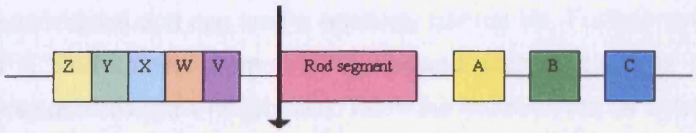
A157	S1015fs X1023	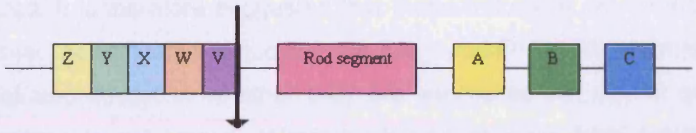
A12	L1486X	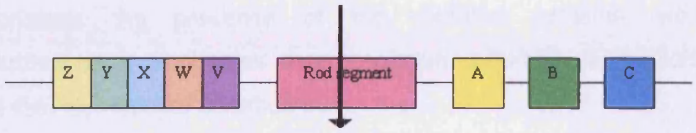
A208	1218+1 G→A	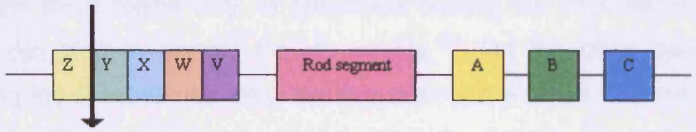
A131	Q1446X	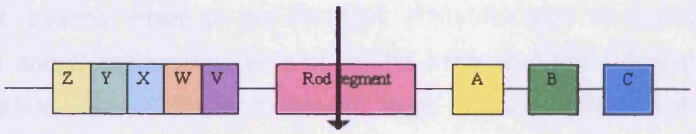
A131	Q673X	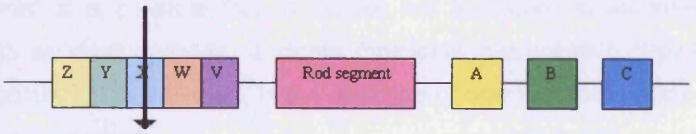

Table 1: All novel desmoplakin mutations identified signal premature termination of translation and are predicted to truncate the molecule at varying points (indicated by the arrows).

Bornslaeger et al. generated A431 cell lines stably expressing desmoplakin N-terminal only polypeptides. In these cells, the truncated molecule co-localized at cell-cell interfaces with desmosomal proteins, markedly disrupting the distribution of endogenous DP and leading to a total breakdown of the IF network.[184] Furthermore, in these cells, adherens junction components were found to co-localize with desmosomal components in mixed-type junctions.[184]

Carriers of R1113X, S1015fsX1023 or L1486X, show some form of cardiomyopathy but no further phenotypic abnormalities and can lead a relatively normal life. Furthermore, electron microscopy of a skin sample from A157.2 showed normal numbers of presumably functional desmosomes (data not shown). Were the mutations to be acting in a dominant negative manner, as described by *Bornslaeger et al*, a worse phenotype would have been expected. It is therefore suggested that these mutations act through haploinsufficiency. Whether the truncated molecules are not translated at all, because of mRNA nonsense mediated decay, or whether they are expressed but do not get incorporated in the junctions is not known. Western blotting analysis from patient samples would demonstrate the presence of the mutated proteins, while immunofluorescence studies using antibodies that recognize different desmoplakin domains, would indicate their sub-cellular distribution.

Lapouge et al recently reported that DP constructs encompassing the B-subdomain and the linker region, the linker region only, or constructs lacking the 51 C-terminal amino acid extremity, can bind to desmin though weakly.[185] On the other hand, constructs encompassing the C subdomain only, the C subdomain with the C-terminal extremity or the C-terminal extremity only cannot bind to desmin filaments.[185] Desmoplakin molecules bearing either of the R1113X, S1015fsX1023 or L1486X mutations lack all A, B and C subdomains as well as the linker and the C-terminal extremity region. Therefore, even if these molecules were indeed expressed and managed to localize to cardiac desmosomes, they would not have been able to anchor the intermediate filaments. It is possible that in tissues not subjected to increased mechanical stress, such as most epithelia, a single functional desmoplakin copy is sufficient to confer adhesion, but in the heart, in the absence of one functional copy, a cardiomyopathy phenotype emerges.

Early genotype-phenotype correlations suggest that when the C-terminal part of desmoplakin is missing, it is the LV that gets primarily affected, while missense mutations that disrupt desmosomal protein interactions sparing the cytoskeleton tend to cause a predominant RV phenotype.[186] In the cases presented herein, members of the same family, carrying the same mutation, may show either typical ARVC or left-sided ARVC mimicking DCM. Modifier genes or environmental factors are likely to affect the ultimate phenotype.

Fontao et al reported that the linker region between the B and C subdomain is important for the binding of DP to K8/K18 keratin heterodimers, while the C subdomain alone is crucial but not sufficient for the interaction of DP with K5/K14 pairs.[187] Collectively, it was shown that only residues amongst the C-terminal domain of desmoplakin are responsible for binding to all keratins.[187] Given the fact that the skin is also subjected to increased mechanical stress, it is curious that carriers of R1113X, S1015fsX1023 or L1486X do not show any gross cutaneous abnormalities. It may be that other plakins, such as plectin, envoplakin or periplakin, can compensate for the loss of DP in the skin only. It is also possible that one functional allele, although unable to confer strong adhesion in the heart, is able to do so at the skin. It may also be that the same mutation has different tissue-specific effects on downstream signaling pathways. Still, autosomal dominant desmoplakin mutations acting through haploinsufficiency have previously been shown to cause striated palmoplantar keratoderma without associated cardiomyopathy.[188] In these cases, Western immunoblotting failed to demonstrate the presence of the mutant protein. It may therefore be that the presence of both desmoplakin copies, even if one is truncated, protects from PPK and helps maintain the epidermal integrity. If this assumption is indeed true, then R1113X, S1015fsX1023 and L1486X should not activate nonsense mRNA decay, and the truncated proteins should therefore be present whether they manage to localize at the cell junctions or not. At this point though, these conclusions are merely speculations.

Of all cases presented above, family A131 is perhaps the most interesting. It is the first report of compound heterozygosity for two novel nonsense desmoplakin mutations identified in a child of Spanish origin who presented with palmoplantar hyperkeratosis, complete alopecia and early-onset cardiomyopathy leading to hemiparesis and SCD in childhood. The absence of cardiocutaneous abnormalities in carrier family members suggests that the mode of inheritance for Q1446X and Q673X is autosomal recessive or autosomal dominant with low penetrance. Genetic studies in mice indicate that desmoplakin is an indispensable protein. Desmoplakin-null embryos do not survive beyond E6.5 owing to a loss or instability of desmosomes. When provided with wildtype extra-embryonic tissue, these embryos die shortly after gastrulation due to major defects in heart muscle, neuroepithelium, skin epithelium and microvasculature. Despite the numerous phenotypic abnormalities, the compound heterozygosity presented herein did not lead to embryonic lethality. Instead, the proband managed to survive until 9 years of age, suggesting that at least one of the two truncated proteins is expressed and does make it to the desmosomes. Western blotting would be required though to confirm this hypothesis.

When keratinocytes come into initial contact during development and wound healing, filopodia extend into neighboring cells to form an adhesion zipper on which adherens junctions are formed to seal the sheet of epithelial cells. Desmosomes are formed passively along the long axis of filopodial associations. In the absence of desmoplakin, the cohesion cascade stops at the adhesion zipper stage. [189] However, this blockage in adhesion can be rescued by the lone expression of the N-terminal domain of desmoplakin. Indeed, the head of the plakin protein not only gets incorporated into desmosomal plaques and restores adhesion, but it also promotes the association of intermediate filaments with the plasma membrane in a parallel fashion.[190] Isolated N-terminal domains of desmoplakin can orient plakophilins such that intermediate filaments can associate with the cell junctions in a parallel orientation, whereas the full-length desmoplakin containing its C-terminal domain anchors the filaments in a vertical fashion.[191] It can therefore be suggested that tissue organization is disrupted only when cells bearing the truncated protein are subjected to stress. The N-terminal domain of desmoplakin is known to bind plakoglobin.[192] Q673X, apart from disrupting the interaction of DP to IFs, could also disrupt the interaction of DP with plakoglobin. Plakoglobin is shown to reduce proliferation in hair follicles by premature termination of the growth phase of the hair cycle.[192] If Q673X does indeed interfere with the normal interaction between DP and PG, it could have an effect on the hair phenotype as well, thus explaining the hair abnormalities exhibited by A131.1.

Recently *Jonkman et al* described a patient who died in the neonatal period due to transcutaneous fluid loss through erosions of large skin areas.[193] The child also presented with alopecia, nail loss and neonatal teeth but showed no cardiac or other internal organ abnormalities. This novel phenotype, named lethal acantholytic epidermolysis bullosa, was linked to compound heterozygosity for a nonsense/frameshift combination of desmoplakin mutations, both predicted to cause premature termination of translation. Although the molecular pathology of desmoplakin in Jonkman's report is comparable to that of the case presented here, the phenotype is strikingly different.[193] How similar changes at the genetic level can have such different effects at the phenotypic level is still not understood.

Since the identification of the mutations presented herein, additional ARVC-associated mutations were reported in the literature. In 2004, a novel dominant mutation in desmoplakin (2034insA) causing left-sided ARVC with arrhythmias of LV origin, lateral T-wave inversion and late gadolinium enhancement in the LV on MRI was presented.[194] In 2006, the case of a patient with a recessively inherited ARVC with left and right ventricular involvement, epidermolytic PPK and wooly hair was presented.[195] The patient showed a severe heart phenotype with an early onset and rapid progression to HF at 4 years of age. A homozygous nonsense mutation (R1267X) was found in exon

23 of the DP gene, which resulted in an isoform specific truncation, and subsequent instability and loss of only the longer DP isoform.[195] Finally, *Yang et al* reported 4 novel DP variants in ARVC patients: V30M, Q90R, W223X and R2834H.[196] In vitro analysis demonstrated that the N-terminal mutants (V30M and Q90R) failed to localize to the cell membrane and also failed to immunoprecipitate plakoglobin. Analysis of mouse embryos expressing cardiac-specific trans-genes, bearing either the V30M or the Q90R mutation, revealed evidence of profound ventricular dilatation resulting in early embryonic lethality. On the contrary, mice expressing the R2834H mutation, under a cardiac-specific promoter, did survive but showed increased cardiomyocyte apoptosis, cardiac fibrosis and lipid accumulation along with ventricular enlargement and cardiac dysfunction in both ventricles. These mice also displayed interruption of the DP-desmin interaction at intercalated discs (IDs) and marked ultra-structural changes of the IDs.[196] Collectively, these results identify desmoplakin as an important genetic determinant in ARVC pathogenesis, though many questions still remain unanswered.

2) Plakoglobin:

Family D0074:

The proband (II:1), a 48-year-old man of German origin upon examination, had first experienced syncope at the age of 39 years. After a documented episode of sustained VT, he was admitted to the University Hospital of Muenster, Germany for further diagnostic evaluation and management. ECG demonstrated QRS prolongation and T-wave inversion in right precordial leads and late potentials. Angiography showed moderate, global RV dilatation and regional wall motion abnormalities without LV involvement. Sustained monomorphic VT of LBBB morphology was induced at electrophysiological study. Endomyocardial biopsy showed extensive fibrofatty replacement of RV muscle with patchy mononuclear inflammatory infiltrate. He fulfilled the Task Force criteria for the diagnosis of ARVC. An ICD implanted in 1997 has since discharged appropriately. The proband's skin and hair appeared grossly normal upon physical examination. Individuals II:2 and II:3 were diagnosed with ARVC after cardiac evaluation at their local medical facilities based on 12-lead and 24-hour ECG and echo abnormalities. Both II:2 and II:3 have offspring who refused clinical and genetic screening and who were not included in the family pedigree. Individual I:1 died aged 70 of HF (indicated by a grey symbol on the family pedigree). Individual II:4 underwent cardiac evaluation and was found to be normal. We identified an insertion of 3 bases in the gene coding for plakoglobin (118_119insGCA). This mutation has not been previously reported. It does not disrupt the frame of translation but is predicted to result in the insertion of an additional serine residue at amino acid position 39 within the N-

terminal domain of plakoglobin (**S39_K40insS**, Figure 16). Individuals expressing the S39_K40insS mutation showed an autosomal dominant mode of inheritance of ARVC and the mutation co-segregated with the disease phenotype in the family (Figure 17). The clinical characteristics and genotype of this family are included in: *Asimaki et al.* "A novel dominant mutation in plakoglobin causes arrhythmogenic right ventricular cardiomyopathy"; manuscript in press, *The American Journal of Human Genetics.*

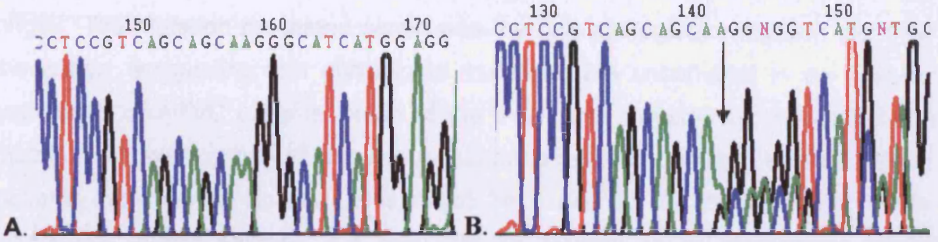

Figure 16: Electropherograms of the sense strands showing the wildtype (A) and mutant (B) plakoglobin sequences. S39_K40insS is indicated by the arrow.

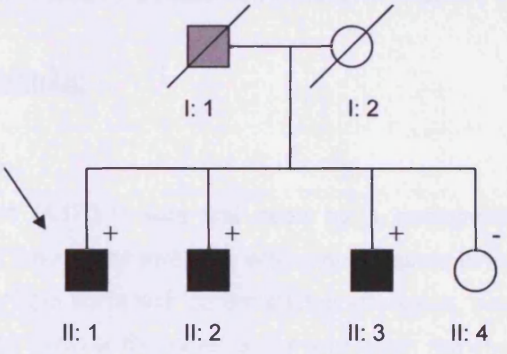

Figure 17: The pedigree of family D0074. The proband is indicated by the arrow.

Discussion:

A novel autosomal dominant plakoglobin mutation (S39_K40insS) was identified in a German family affected by ARVC. Recently, an uncommon polymorphism in plakoglobin (L697M) was shown to co-segregate with a nonsense mutation in desmoplakin (R1267X) in a family with early-onset ARVC.[195] It has been suggested that L697M could have a negative modifier effect on the cardiac phenotype in the presence of R1267X.[195] In the family presented herein the L697M polymorphism was

not present and genotyping of other desmosomal candidate genes including desmoplakin and plakophilin2 did not reveal additional mutations. S39_K40insS co-segregated with the disease phenotype and was not found in 400 ethnically-matched control chromosomes. It is likely, therefore, that this mutation is in fact pathogenic rather than a modifying polymorphism.

The index case was part of a larger cohort of ARVC patients who were screened for mutations in candidate desmosomal genes. The cohort included >200 individuals of English origin, 70 individuals of German origin and 30 individuals of Greek/Cypriot origin. The mutation presented herein was the only plakoglobin mutation identified in the cohort, suggesting that plakoglobin mutations are uncommon in an unselected population of ARVC patients. None of the individuals affected by the S39_K40insS mutation showed apparent cutaneous abnormalities, in contrast to those seen in patients with Naxos disease. This might be explained by the dominant mode of inheritance of S39_K40insS. It is likely that the different clinical phenotypes produced by S39_K40insS and 2057del2, the mutation known to cause Naxos disease, may result from differential effects of the mutations on the various plakoglobin binding partners and the downstream effects on signalling, but this must be analyzed in detail in future studies. In vitro investigations pointing towards the mechanisms of pathogenesis of this novel mutation are presented in detail in chapters 3 and 4.

3) Plakophilin2a:

Family A170:

The proband (A170.1) was first seen by a pediatrician at age 10 weeks due to shortness of breath and sweating with exertion since birth. Investigations demonstrated coarctation of the aorta with patent ductus arteriosus, severe LV hypertrophy and non-obstructive bicuspid aortic valve. Surgery to repair the coarctation was performed when A170.1 was 3 months old. He was discharged on furosemide and spironolactone but was readmitted at the hospital 1 week later due to persistent hypertension and treated with propanolol. Following the operation, he was followed regularly until the death of his father (A170.2), at 37 years of age. The postmortem examination at the time cited "floppy mitral valve" as the cause of death, although the RV was mildly enlarged. Subsequent review of histology revealed areas of fibrosis in both ventricles. ARVC was suspected as the cause of death of another relative (A170.10), who died suddenly during physical exercise at 22 years of age. His father (A170.9) refused clinical evaluation. Cardiac evaluation of other immediate family members (A170.4, A170.4, A170.6, A170.7 and A170.8) was unremarkable. The 89-year old paternal grandmother (A170.3) though was found to have an abnormal ECG of RBBB morphology, but it

could have been due to age-related conduction disease. Echocardiography showed no abnormalities and she refused further clinical evaluation. She did not fulfill the Task Force criteria but in the context of familial ARVC, these mild abnormalities may represent a mild form of the disease (indicated by a grey symbol on the family pedigree). In 2004, the proband died suddenly while playing rugby at 15 years of age. He was last seen in clinic 2 years prior to his death. His ECG was normal and his echo showed normal LV and RV size and systolic function. The postmortem examination showed cardiac enlargement with concentric LV hypertrophy. There were areas of fibrosis and thinning in the RV anterior wall extending to the inter-ventricular septum. The rest of the RV appeared normal apart from a mild dilatation. Histological examination showed extensive replacement of myocardial tissue by fibrosis in the macroscopically scarred area of the RV as well as in other random RV samples. There was also focal but histologically similar fibrosis in several samples from the LV.

A deletion of a C nucleotide was found in the family in the gene coding for plakophilin2 (1709delC). The mutation alters the frame of translation, inserts 6 novel amino acids downstream followed by a stop codon, which signals premature termination of translation within the fifth armadillo repeat domain of the protein (**V570fs576X**, Figure:18). The paternal grandmother (A170.3) and her brother (A170.9) were also carriers of the mutation. All other clinically normal family members were gene negative (Figure:19).[197]

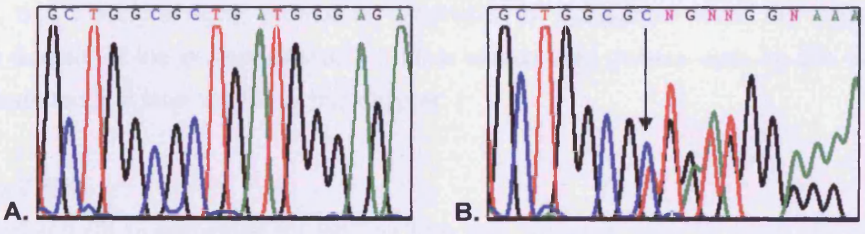

Figure 18: Electropherograms showing the wildtype (A) and the mutant (B) PKP2 sequences. 1709delG is indicated by the arrow.

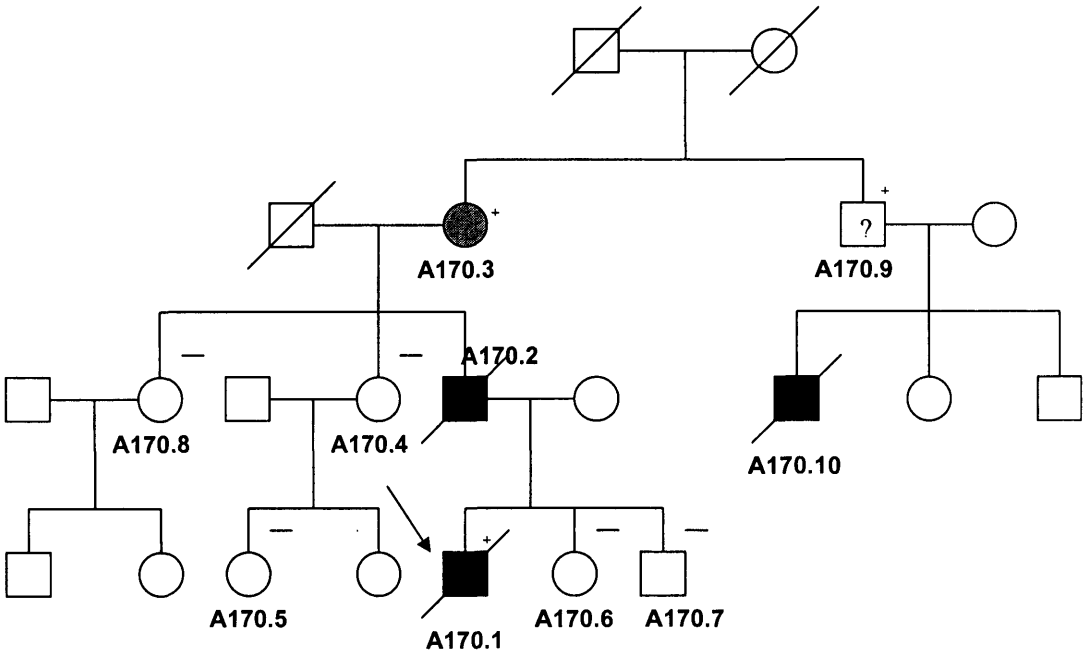

Figure 19: The pedigree of family A170 shows autosomal dominant manner of inheritance of V570fs576X with low penetrance. The proband is indicated by the arrow.

Family A198:

In this family, a C→T transition was identified in exon 5 of the plakophilin2 gene (1237C>T). The mutation is predicted to substitute an arginine residue with a stop codon, and therefore signal premature termination of translation within the armadillo repeat domain of the protein (**R413X**). Further clinical and genetic data on this family are presented in a later section of this chapter.

Family CYP1:

The proband (III:1) presented for the first time with syncope aged 16 years. His ECG was abnormal and on 24-hr Holter monitoring he showed episodes of non-sustained VT. Imaging studies showed evidence of typical ARVC with LV involvement. He fulfilled 2 major and 2 minor Task Force criteria. He died suddenly, aged 20 years. Post-mortem examination showed extensive fibrofatty replacement of both ventricles, confirming the original diagnosis. The proband's father (II:5) is affected by typical ARVC. His ECG shows prolongation of QRS duration and inverted T-waves in precordial leads V1-V3, he shows multiple ventricular extrasystoles and an electrophysiological study induced sustained VT. On echo, he shows global dilatation and hypokinesia of the RV without LV involvement. He is currently being treated with sotalol. The proband's brother (III:3) fulfils 2 major and 2 minor Task Force criteria. His ECG is abnormal with T-wave inversions and prolongation of the QRS duration, he has

documented frequent extra-systoles and episodes of non-sustained VT, and on echo he shows global RV involvement and hypokinesia of the LV antero-lateral wall. Recently, he had an ICD implanted. The proband's aunt (II:4) fulfils 2 major and 2 minor criteria for typical ARVC as well. Her ECG shows T-wave inversions in the right precordial leads, while on echo her RV is globally affected with preserved LV function. She also has frequent extra-systoles and a biopsy sample obtained from the inter-ventricular septum showed extensive fibrofatty replacement. All other family members examined were clinically normal.

A novel deletion of 10 bases was found in the family in exon 3 of the plakophilin2 gene (971_980del10). This mutation is predicted to cause a frameshift and introduce a premature stop codon in the N-terminal domain of the plakophilin2 molecule (**G324fsX348**, Figure:20). All affected members in the family (III:3, II:4 and II:5) are carriers of the novel mutation, while one family member (II:3) is genotype-positive but phenotype negative at 61 years of age (Figure:21).[198]

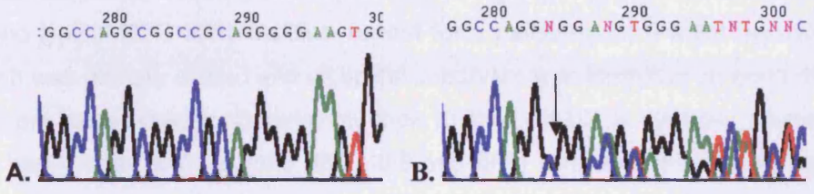

Figure 20: Electropherograms showing the wildtype (A) and the mutant (B) PKP2 sequences. 971_980del10 is indicated by the arrow.

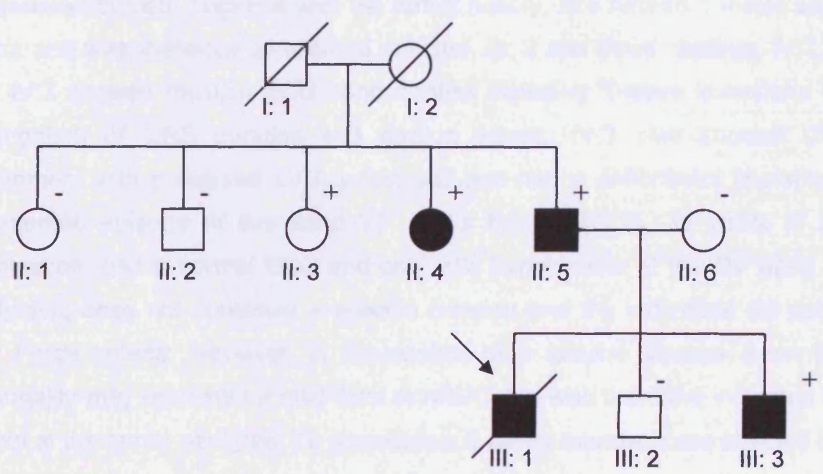

Figure 21: The pedigree of family CYP1 shows autosomal dominant manner of inheritance of G324fsX348 with low penetrance. The proband is indicated by the arrow.

Family CYP10:

The proband (III:12), a man of Cypriot origin, died aged 61 of non-cardiac etiology. Prior to his death, he showed T-wave inversions and prolongation of QRS duration on ECG and global dilatation and hypokinesia of the RV with preserved LV function on echo. A biopsy sample obtained showed fibrofatty replacement of the RV, consistent with an ARVC diagnosis. Ablation was performed successfully at the time to treat frequent episodes of sustained VT. The proband's daughter (IV:12), 29 years of age upon examination, showed T-wave inversions on ECG, segmental hypokinesia of the RV and frequent extrasystoles. Together with the family history of ARVC, she fulfilled 1 major and 3 minor Task Force criteria, and was therefore considered affected. The proband's nephew (IV:10) died aged 18. Post-mortem examination concluded sudden cardiac death, but further details are sketchy. Given the family history though, the possibility that he was also affected by ARVC is high (indicated by a grey symbol on the pedigree). Two of his siblings are also affected. IV:8 showed T-wave inversions in the right precordial leads, frequent extra-systoles and regional hypokinesia of the RV. IV:9 showed no typical ECG abnormalities, except for a pathological S-wave upstroke. His RV though was globally dilated and an apical aneurysm was identified on echo. He also had frequent extra-systoles. Surprisingly their mother (III:10) is clinically normal. The proband has 4 other siblings (III:5, III:7, III:8 and III:9) who are clinically normal. III:5 has three children (IV:4, IV:5 and IV:6) and two grand-children (V:1 and V:2) who are also clinically normal. The proband also has 7 first cousins (III:1, III:2, III:3, III:14, III:15, III:16 and III:17), all of whom are clinically normal apart from III:3. III:3 showed T-wave inversions in V1-V4 and segmental RV hypokinesia. No arrhythmic episodes have been documented though. Together with the family history, III:3 fulfilled 1 major and 2 minor criteria and was therefore considered affected. III: 3 has three children: IV:1, IV:2 and IV:3. IV:3 showed multiple ECG abnormalities including T-wave inversions in V1-V3, prolongation of QRS duration and epsilon waves. IV:3 also showed diffuse RV involvement with preserved LV function and has had a defibrillator implanted after a documented episode of sustained VT. IV:3's brother (IV:2), 39 years of age upon examination, had a normal ECG and only mild hypokinesia at the RV apex. By itself, this finding does not constitute a specific criterion and the individual did not fulfill the Task Force criteria. However, in the context of a familial disease, even this minor abnormality may represent a mild form of ARVC. He was therefore indicated by a grey symbol at the family pedigree. To summarize, 6 family members are affected by ARVC, one member shows only minor abnormalities, which may or may not represent a mild form of the disease, and one family member is suspected to have died of ARVC, aged 18, although clear post-mortem details are not available.

A novel deletion of 50 bases was identified in the family at exon 13 of the plakophilin2 gene (2569del50). This mutation is predicted to result in a frameshift and premature termination of translation within the C-terminal part of the protein (**R857fsX858**, Figure:22). 25 family members were genotyped, 10 of whom were carriers of the novel mutation. All living clearly affected individuals (III:3, IV:3, IV:8, IV:9 and IV:12) were carriers of R857fsX858. IV:2 was also a carrier. The remaining 4 carriers (III:10, III:14, IV:6 and V:2) were clinically normal. III:10, III:14 are in their late sixties, IV:6 is 39 years old, however V:2 is only 12 and may therefore be at risk of developing the disease later on in life. Interestingly, although IV:6 is a carrier, her mother (III:5), who is a sister of the proband, is not. IV:6's father (III: 6) had died of non-cardiac reasons and was unavailable for genotyping. He was thus considered an obligate carrier. Based on the constructed pedigree (Figure:23), three more deceased individuals (II:1, II:3 and II:6) were considered obliterate carriers. All 4 obliterate carriers were indicated with a diagonal-line pattern on the family pedigree. The fact that III:6 was considered an obliterate carrier of R857fsX858 though not directly related to the proband, may suggest a founder effect in the small, inbred society of Cyprus, or alternatively, a mutational hotspot in the plakophilin2 gene, indicating that ARVC-causing mutations may in fact be much more common that originally thought.[198]

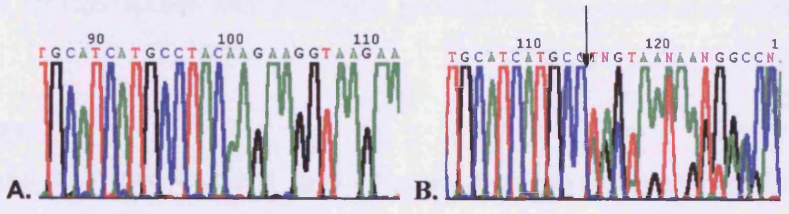

Figure 22: Electropherograms showing the wildtype (A) and the mutant (B) PKP2 sequences. 2569del50 is indicated by the arrow.

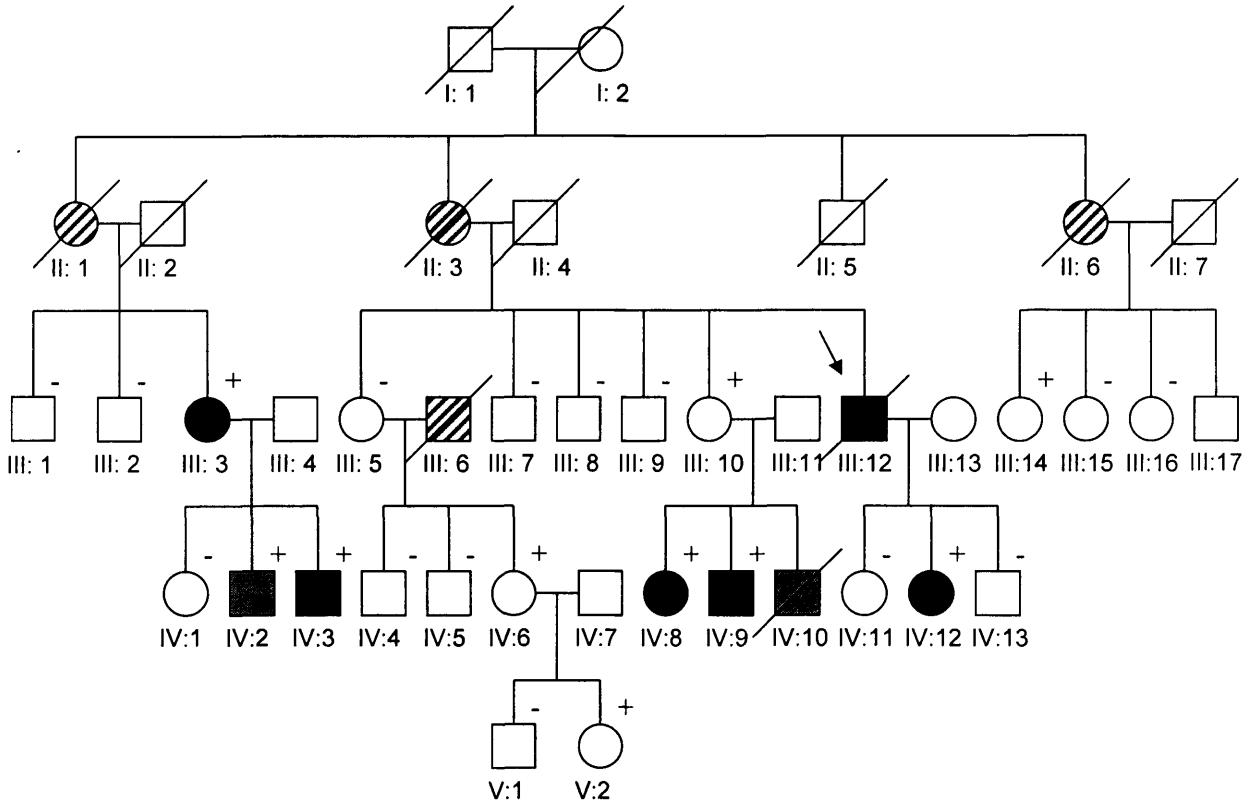

Figure 23: The pedigree of family CYP10 shows autosomal dominant manner of inheritance for R857fsX858 with incomplete penetrance. The proband is indicated by the arrow.

Family GR1:

The proband (III:2) died suddenly aged 23 years. Post-mortem examination showed typical features of ARVC. In particular, there was extensive fibrofatty replacement of the RV with degenerating myocytes embedded within areas of fat and fibrous tissue. An ECG performed a few months prior to the proband's death was pathological, showing inverted T-waves in V1-V4 precordial leads and low voltage. The proband's father (II:2) showed T-wave inversions in V1-V3 on ECG, minor hypokinesia of the RV on echo, late potentials on SA-ECG, and frequent extra-systoles on 24-hour Holter monitoring. He is currently being treated with sotalol. The proband's sister (III:1) is clinically normal. The proband's uncle (II:3) is also affected by typical ARVC. In particular he showed T-wave inversions on ECG, late potentials on SA-ECG, diffuse RV involvement on echo, a normal LV, documented episodes of non-sustained VT, and an electrophysiological study induced an episode of sustained VT. A proband's aunt (II:5) is clinically normal.

A deletion was identified in the family in exon 13 of the plakophilin2 gene (2509delA). The deletion, has been previously seen in ARVC patients, and is predicted to lead to

the introduction of a number of additional amino acid residues at the C-terminal domain of the protein (**V837fsX930**, Figure:24).[77] Both II:2 and II:3 are carriers of the mutation, while II:5 is homozygote for the wildtype allele. II:3 and II:4 have declined clinical examination and genotyping of their daughter (III:3), because of her young age (Figure:25).[198]

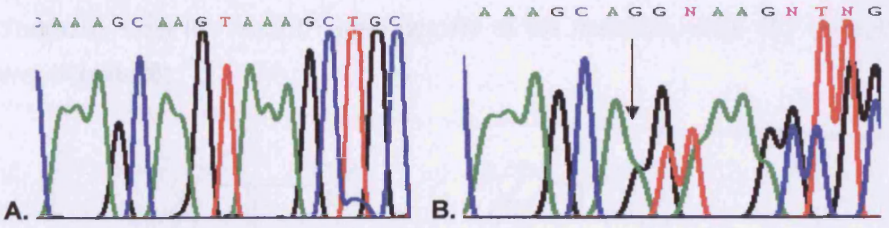

Figure 24: Electropherograms showing the wildtype (A) and the mutant (B) PKP2 sequences. 2509delA is indicated by the arrow.

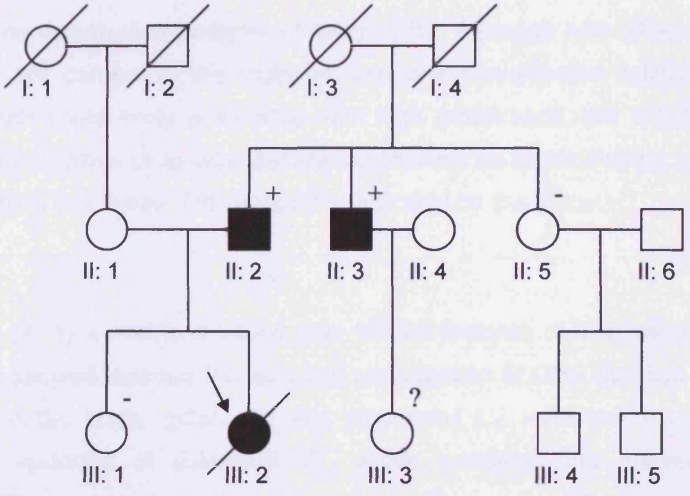

Figure 25: The pedigree of family GR1 shows autosomal dominant manner of inheritance for V837fsX930 with high penetrance. The proband is indicated by the arrow.

Family GR2:

The proband (III: 1), currently a young man, is affected by a severe form of ARVC. Specifically, he showed ECG abnormalities, which include T-wave inversions, prolongation of QRS duration and epsilon waves and imaging abnormalities, which include global dilatation and hypokinesia of the RV. The LV function though was

preserved. He also has had episodes of sustained and non-sustained VT and had a defibrillator implanted recently. His mother (II:1) is also affected by the disease. In particular, she had a pathological ECG, similar to that of the proband, ventricular arrhythmias, and diffuse RV involvement on echo and MRI. The proband's brother (III:2) is clinically normal.

The same mutation identified in family GR1 was also identified in family GR2 (**V837fsX930**). Both III:1 and II:1 were carriers of the mutation, while III:2 was gene negative (Figure:26).[198]

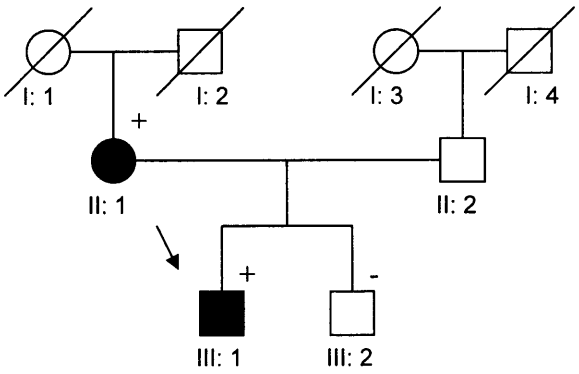

Figure 26: The constructed pedigree of family GR2. Although both affected members of the family are carriers of the mutation, and one non-affected individual is gene-negative, which could imply a mutation with high penetrance, the small size of the pedigree does not allow us to draw definite conclusions as to the manner of inheritance of V837fsX930 in this family. The proband is indicated by the arrow.

Family GR3:

The proband (II: 1), currently a young man, shows features of biventricular ARVC. In particular, he showed inverted T-waves and prolongation of QRS duration in both right and left precordial leads, global RV and segmental LV involvement on echo, and documented episodes of sustained VT, which prompted the implantation of a defibrillator. The proband's mother (I:1) is clinically normal. His father though (I:2) showed late potentials on SA-ECG and segmental RV hypokinesia on echo. He only matches two minor Task Force criteria and was thus indicated by a grey symbol on the family pedigree (Figure:27).

The proband is a carrier of the same mutation identified in families GR1 and GR2 (V837fsX930). Surprisingly, neither his father nor his mother are carriers of the mutation, indicating that V837fsX930 has arisen de novo in this family. The fact however that his father shows minor abnormalities, which are consistent with a mild form of ARVC, while his son shows a severe form of the disease should raise suspicions that the proband is a carrier of a second mutation. He was screened for

mutations in plakoglobin, desmocollin2, desmoglein2 and desmoplakin and found negative, but that does not exclude the possibility of him being a carrier of a mutation in a yet non-identified ARVC-related gene.[198]

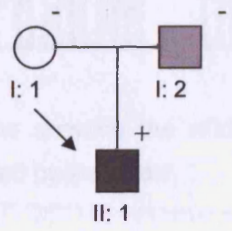

Figure 27: The constructed pedigree of family GR3 shows that V837fsX930 has arisen de novo in this case. The proband is indicated by the arrow.

Further plakophilin2 mutations:

Four further mutations were identified in 6 patients with a confirmed diagnosis of ARVC based on the Task Force criteria. A C→T transition was detected in exon 3 of plakophilin2, in the proband of family A191 (C419T). The mutation, which has previously been reported,[77] alters a highly conserved serine for a phenylalanine residue within the N-terminal domain of the protein (**S140F**, Figure:28). A C→T transition was detected in exon 11 of plakophilin2, in the proband of family A207 (C2203T). The mutation, which has also been reported previously,[77] alters an arginine residue introducing a premature termination codon within the armadillo repeat domain of the protein (**R735X**, Figure:29). The same splice site mutation was identified in the probands of three ARVC families; A203, A184 and A188 (**2146-1 G→C**, Figure:30). The mutation, also reported by *Gerull et al*,[77] is predicted to cause skipping of exon 11 during the translation of the plakophilin2 mRNA molecule. Finally, a splice site mutation was identified in the proband of family A193 (**2489+1 G→A**, Figure:31). The mutation, previously seen in a cohort of German ARVC patients,[77] is predicted to allow continuation of translation after the splice site of plakophilin2 exon12, possibly introducing a number of new amino acid residues.

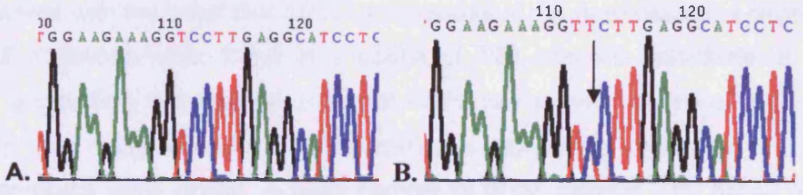

Figure 28: Electropherograms showing the wildtype (A) and the mutant (B) PKP2 sequences. C419T is indicated by the arrow.

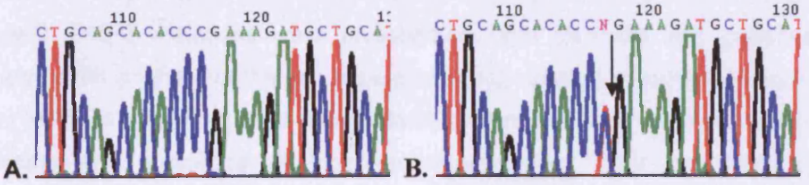

Figure 29: Electropherograms showing the wildtype (A) and the mutant (B) PKP2 sequences. C2203T is indicated by the arrow.

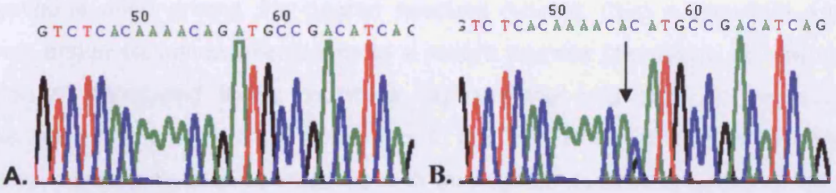

Figure 30: Electropherograms showing the wildtype (A) and the mutant (B) PKP2 sequences. 2146-1 G→C is indicated by the arrow.

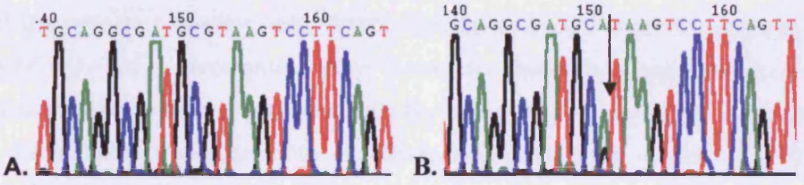

Figure 31: Electropherograms showing the wildtype (A) and the mutant (B) PKP2 sequences. 2489+1 G→A is indicated by the arrow.

Unfortunately, no further clinical or genotyping data on the probands' families is available yet.

Discussion:

In agreement with the belief that ARVC is a disease of the desmosome, a large number of PKP2 mutations were found in a cohort of 120 affected individuals of German origin,[77] suggesting that mutated forms of PKP2 are a major cause of the condition. However, that study lacked a detailed clinical evaluation of probands, and data on family members were limited. A large number of white patients with ARVC (in whom mutations in plakoglobin and desmoplakin had been excluded) were screened for mutations in PKP2. Fourteen disease-causing changes in 26 familial and sporadic

ARVC cases were found.[197,198] Furthermore, wherever possible, the families of those patients with PKP2 mutations were investigated both clinically and genetically to provide a detailed analysis of the genotype-phenotype relation in individuals carrying a mutation. PKP2 is known to bind desmoplakin and recruit it to the membrane, thus strengthening and stabilizing desmosomal interactions. [199] It can therefore be speculated that lack of or incorporation of mutated PKP2 into cardiac desmosomes impairs cell-cell contacts and as a consequence causes disruption of adjacent cardiac myocytes, particularly in response to mechanical stress.

The data presented herein show that clinical expression of PKP2 mutations is heterogeneous even among first-degree relatives ranging from a complete lack of symptoms and/or clinical manifestations to a severe disease phenotype. Retrospective evaluation of genotyped family members exposes the limitations of the currently available diagnostic criteria. Strict adherence to the Task Force criteria could have led to omitting many gene-positive relatives with incomplete disease expression, leading potentially to a less vigilant follow-up than may be desirable. Interestingly, in the families examined herein penetrance was higher in men than in women. This might be caused by factors such as exposure to vigorous athletic activity or biological factors such as the inhibitory effects of estrogens on myocardial cell apoptosis.[183] Also, a review of the affected families with PKP2 mutations shows that the majority have evidence of right-sided involvement only. It can be therefore suggested that PKP2 mutations are likely to result in predominantly RV disease but that exceptions do occur.

None of the patients investigated in our study had cutaneous involvement. This is consistent with the findings by *Gerull et al* in which probands carrying PKP2 mutations were apparently free of skin abnormalities.[77] In myocardial cells PKP2 is the only PKP isoform found in desmosomes, whereas PKP1a seems to be confined exclusively to the nucleus.[137] In contrast, in suprabasal cell layers of epidermis, PKP1a is detected in desmosomal plaques and PKP2 is located in the nucleus.[153] Therefore it seems possible that a compensatory mechanism involving PKP1a may explain the absence of a skin phenotype in individuals carrying a PKP2 mutation. Conversely, mutations in PKP1 result in ectodermal dysplasia/skin fragility syndrome characterized by skin, hair and nail abnormalities but no cardiac phenotype.[156] The identification of the same mutation in apparently unrelated probands may be due to an ancient founder effect or to mutational "hot spots" along the plakophilin2 gene. Nevertheless, the fact that some of the mutations identified by our group were also identified by *Gerull et al* in a cohort of different ethnical origin[77] may implicate the presence of recurrent mutations. However; unless haplotype analysis is performed this conclusion remains purely speculative.

Since the identification of the mutations herein presented, further ARVC-associated plakophilin2 mutations have been reported in the literature. *Dalal et al* reported 13

different PKP2 mutations in 43% of the ARVC probands investigated.[200] Genotype-phenotype correlations suggested that the presence of a PKP2 mutation correlates with earlier onset of symptoms and arrhythmia and that patients with a PKP2 mutation experience ICD interventions irrespective of the classic risk factors determining ICD intervention in ARVC.[200] *Kannankeril et al* reported a novel 28 base pair insertion in exon 11 of the PKP2 gene in a family showing incomplete penetrance and variable expression of ARVC.[201] *Nagaoka et al* reported a novel insertion in exon 8 of the PKP2 gene in an ARVC patient of Japanese origin.[202] Finally, *Van Tintelen et al* reported that the vast majority of Dutch patients fulfilling the ARVC criteria are carriers of PKP2 mutations.[203]

4) Desmoglein2:

Family A:

The proband (III:4), a 40-year old female aerobics teacher upon examination, had experienced episodes of sustained palpitation and recurrent pre-syncope. Her 12-lead ECG demonstrated sinus rhythm with poor R-wave progression, and inverted T-waves in V1-6 and the inferior leads (Figure 32). 2D contrast-enhanced echocardiography identified regional wall motion abnormalities in both ventricles and an LV apical aneurysm. A CMR study revealed biventricular dilatation, structural abnormalities, and multiple RV aneurysms in addition to the LV apical aneurysm (Figure 33). Ambulatory ECG (Holter) monitoring demonstrated 1400 ventricular extra-systoles in a 24 h period, including a triplet of non-sustained VT. An ICD was implanted. Histology of endomyocardial biopsy from the proband was characteristic of ARVC showing loss of myocardium and replacement by fibro-adipose tissue. The proband's mother (II:2, 79 years) was asymptomatic with a normal ECG and conventional 2D echo to the age of 75. However, she did not undergo specific ARVC evaluation due to other medical problems. The proband's daughter (IV:2, aged 11) was asymptomatic. Twelve-lead ECG showed sinus rhythm with T-wave inversion in V1, V2, and a biphasic T-wave in V3. In view of her age, this finding could be considered compatible with a juvenile repolarization pattern and is not valid for inclusion using the current diagnostic criteria. Transthoracic echocardiography, however, was abnormal with an area of hypokinesia in the RV lateral wall (indicated with a grey symbol on the family pedigree). Individuals III:1 and IV:1 were examined and found to be normal.

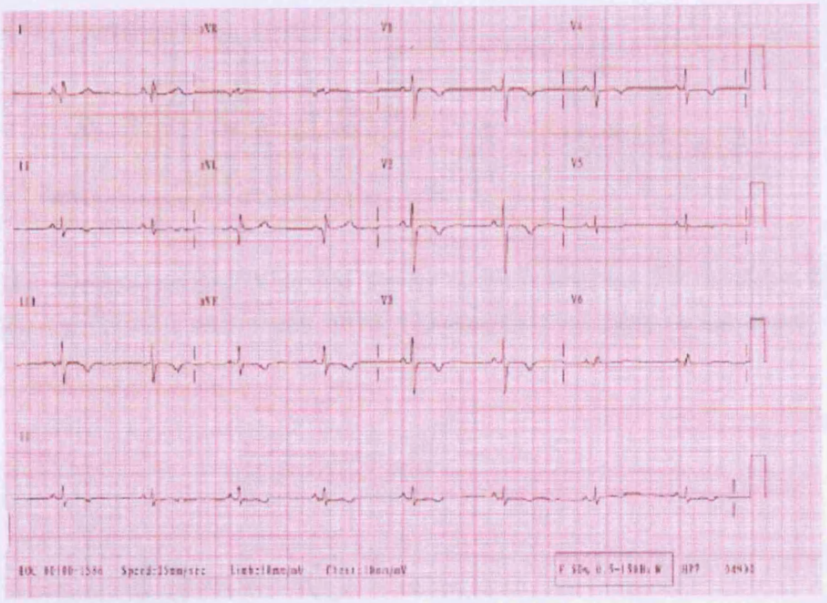

Figure 32: Electrocardiogram from individual III: 4 showing characteristic T-wave inversion, poor R-wave progression and diminutive voltages in V5-V6 consistent with LV involvement.

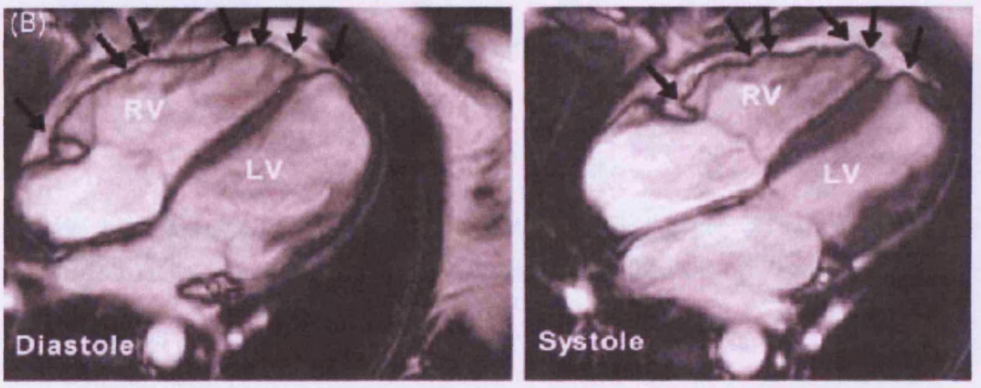

Figure 33: CMR images from individual III: 4, four chamber view in diastole and systole. The black arrows indicate regions of diastolic bulging and hypokinesia in the RV and LV apex.

A deletion of two bases in exon 12 of desmoglein2 (1773_1774delTG) was detected in the proband. This mutation results in a premature termination codon in the extracellular domain of the DSG2 protein (**C591X**, Figure 34). Both the proband's mother (II:2) and daughter (IV:2) were heterozygous for the mutation, while individuals III:1 and IV:1 were gene-negative (Figure 35).[204]

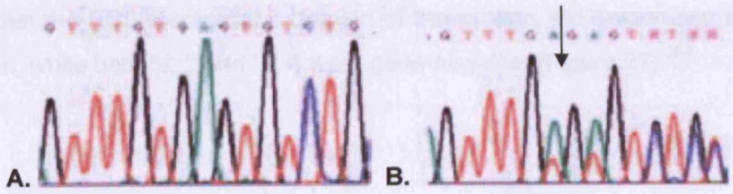

Figure 34: Electropherograms of the sense strands showing the wildtype (A) and mutant (B) desmoglein2 sequences. 1773_1774delTG is indicated by the arrow.

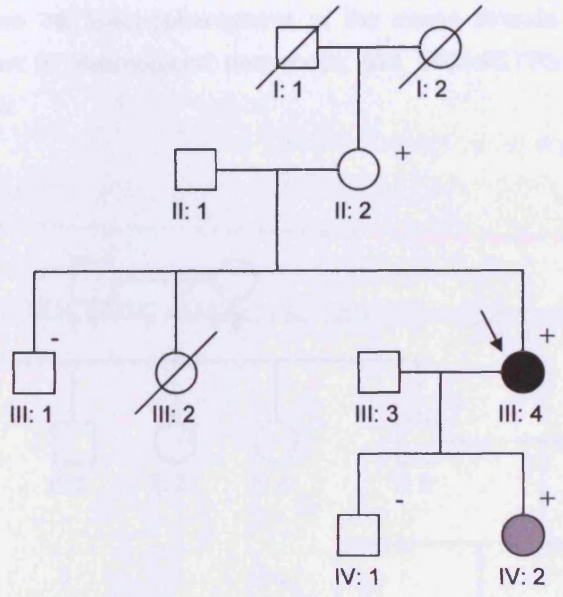

Figure 35: Pedigree of family A indicating an autosomal dominant pattern of inheritance for C591X with reduced penetrance. The proband is indicated by the arrow.

Family B:

The proband (III:1) died suddenly, aged 15, with ARVC identified as cause of death on post-mortem. Her brother (III:3) showed widespread T-wave inversion on ECG, LV and RV enlargement and impaired systolic function (LV ejection fraction 25%), a positive SA-ECG and an excess of 3000 ventricular ectopics on 24-hour Holter monitoring, with salvos of non-sustained VT of predominantly RV origin. He has an ICD which has delivered several appropriate therapies for VT. Two more siblings (III:2 and III:4) were found to be normal upon cardiac evaluation. The proband's mother (II:6) showed features of ARVC both on ECG and contrast-enhanced echocardiography. II:6's brother (II:7) was reported to have died as an infant but no post-mortem data is available. A deletion of 12 nucleotides (**829_840delCTTGAAGGGATG**) was detected in exon 8 of desmoglein2 gene in II:6 (Figure 36). The mutation is predicted to result in abnormal

splicing within the EC3 extracellular domain of the protein. III: 3 was also a carrier of the mutation, while both III: 2 and III: 4 were gene-negative (Figure 37).[204]

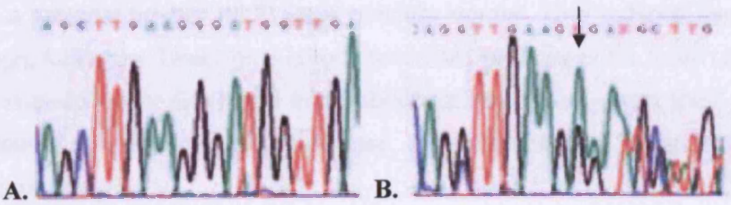

Figure 36: Electropherograms of the sense strands showing the wildtype (A) and mutant (B) desmoglein2 sequences. 820_840delCTTGAAGGGATG is indicated by the arrow.

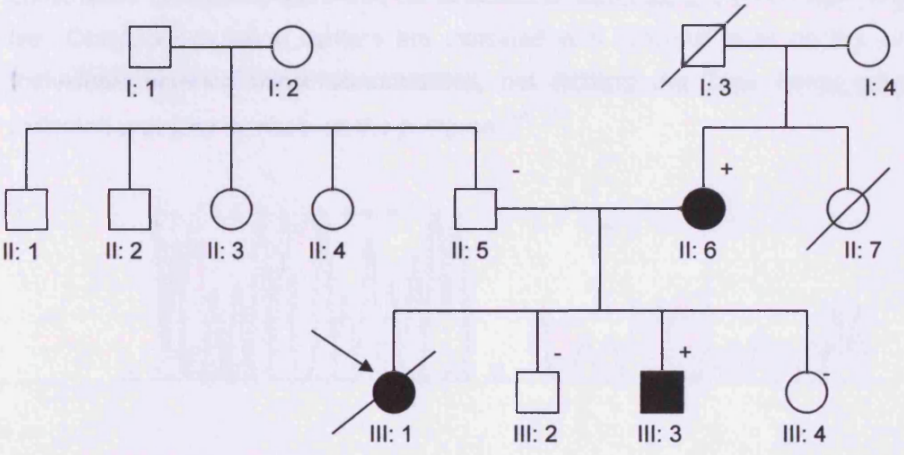

Figure 37: The pedigree of family B shows an autosomal dominant manner of inheritance for 820_840delCTTGAAGGGATG with high penetrance. All gene positive individuals are affected with ARVC. The proband is indicated by the arrow.

Family C:

The proband (IV:4), a young boy, was first presented with exertional syncope at age 14. He had diagnostic features of ARVC on ECG and imaging with gross biventricular enlargement and severe impairment of systolic function (LV ejection fraction 15–20%). An ICD was implanted following recurrent VT and there has been one appropriate discharge 2 years later for VF. Systolic function did not change during 10 years of

follow-up, and he remained clinically stable. His father (III:5) also had clinical features suggestive of disease expression. Echo showed predominantly LV dilatation with mildly impaired systolic function, but also RV wall motion abnormalities. The proband's sister (IV:5) and a paternal brother (III:7) were clinically normal. One paternal second cousin (III:1) though, fulfills the Task Force criteria for ARVC and two of his three children (IV:1 and IV:2) showed minor ECG and echo abnormalities, which given their young age, could represent an early form of the disease. His third child (IV:3) was examined and found to be normal.

A G→ C transversion was found in the start codon of the desmoglein2 gene in the proband (**3G>C**, Figure 38). This change alters the translation initiation codon ATG to ATC and leads to a substitution of a methionine by an isoleucine residue, predicted to abolish initiation of translation. III:1, III:5, IV:1, IV:2 and IV:3 were carriers of the mutation, while III:6, III:7 and IV:5 were gene-negative. IV:3 did not show any phenotypic abnormalities but given the high penetrance of the mutation, based on the constructed pedigree (Figure 39), he is at risk of developing the condition later on in life. Obligatory mutation carriers are indicated with diagonal lines on the pedigree. Individuals showing minor abnormalities, not fulfilling the Task Force criteria are indicated with grey symbols on the pedigree.[204]

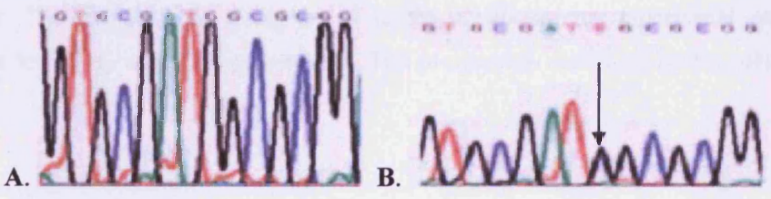

Figure 38: Electropherograms of the sense strands showing the wildtype (A) and mutant (B) desmoglein2 sequences. 3G>C is indicated by the arrow.

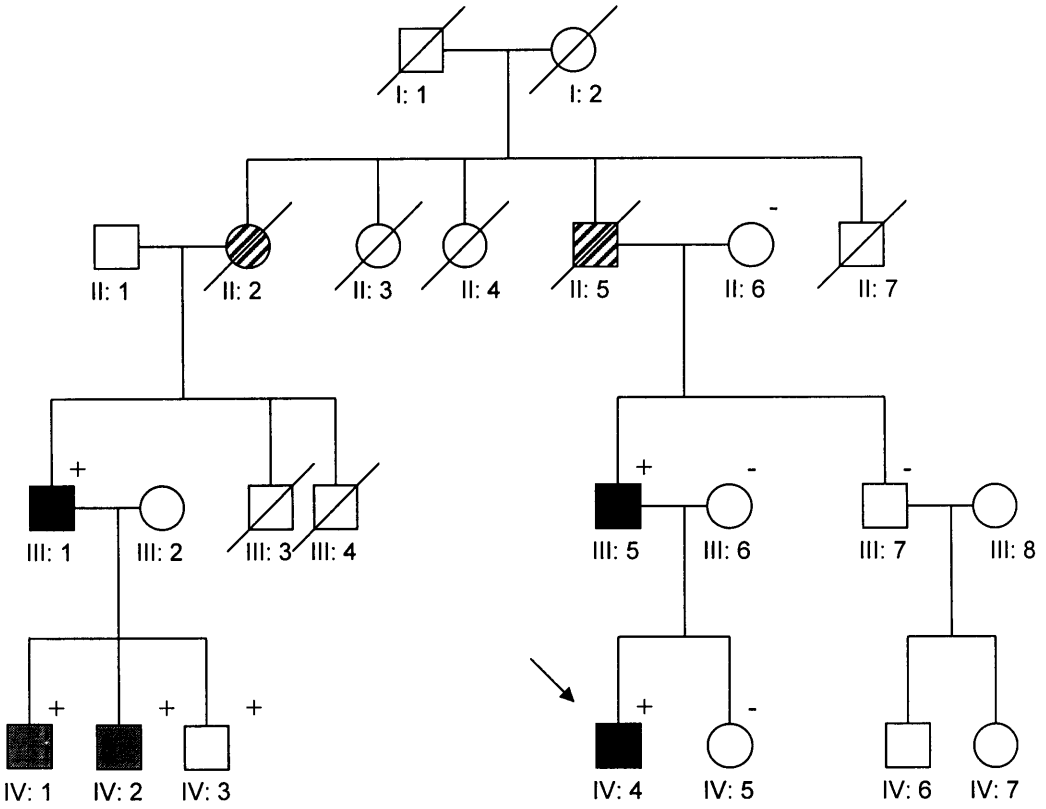

Figure 39: The constructed pedigree of family C shows an autosomal pattern of inheritance for 3G>C with high penetrance. The proband is indicated by the arrow.

Family D:

The proband (III:4), a young man, died suddenly, aged 26 and post-mortem findings were diagnostic of ARVC. His brother (III:3) had low voltage complexes and widespread T-wave inversion on ECG, RV wall motion abnormalities and fatty infiltration of both ventricles on CMR and non-sustained VT on exercise testing. Two sisters (III:2 and III:5) are clinically normal. The proband's mother (II:2) showed LBBB on ECG, but further specific clinical evaluation was not possible. A maternal sister (II:3) is clinically normal.

A C→ T transversion was found in exon 5 of the desmoglein2 gene in the family (462C>A). The mutation results in the substitution of an aspartic acid by a glutamic acid (**D154E**, Figure 40) within the EC1 extracellular domain of the protein. Both affected family members (III:3 and II:2) were carriers of the mutation, while both III:2 and III:6 were gene-negative. No genetic data on the maternal sister (II:3) is available (Figure 41).[204]

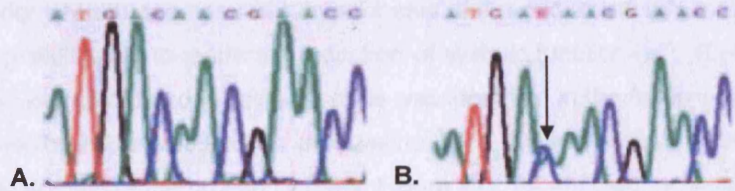

Figure 40: Electropherograms of the sense strands showing the wildtype (A) and mutant (B) desmoglein2 sequences. 462C>A is indicated by the arrow.

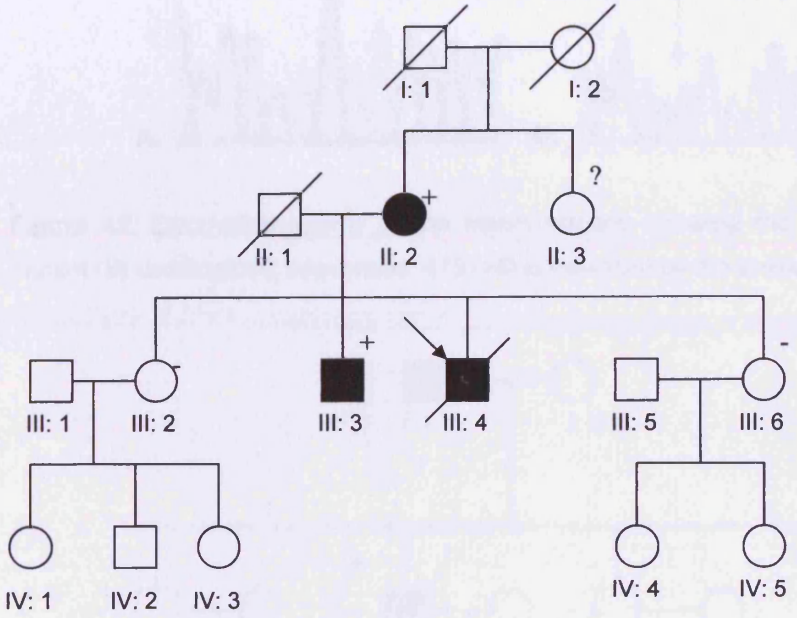

Figure 41: The constructed pedigree of family D shows an autosomal pattern of inheritance for D154E with a high penetrance. The proband is indicated by the arrow.

Family E:

The proband (II:3), a man of English origin, died suddenly at 48 years of age, and his post-mortem was consistent with a diagnosis of ARVC. In his family, two individuals fulfil the Task Force diagnostic criteria for typical ARVC. The proband's sister (II:8) showed positive findings on ECG, contrast-enhanced echo and CMR, while the proband's nephew (III:10) had positive findings on SA-ECG and imaging. The proband's daughter (III:4) fulfilled only the proposed modified diagnostic criteria, but given her young age, these minor abnormalities can be considered diagnostic (III:4 is indicated by a grey symbol on the family pedigree). The proband's father (I:1) showed changes confined to the LV. In particular, his cardiac imaging demonstrated an apparently normal RV but a dilated LV with regional wall motion abnormalities (akinesia

of the anterior septum and apex with hypokinesia of the mid-apical inferior and anterior walls) and globally mild-to-moderate reduction of systolic function (EF: 40-45%). A T→ G change in exon 5 of the desmoglein2 gene was identified in the family (473T>G). The mutation results in the substitution of a valine by a glycine residue within the EC1 extracellular domain of the protein (**V158G**, Figure 42). All affected individuals (I:1, II:8, IV:4 and IV:10) were heterozygous carriers of the mutation, while all clinically normal individuals were gene-negative (Figure 43).[204]

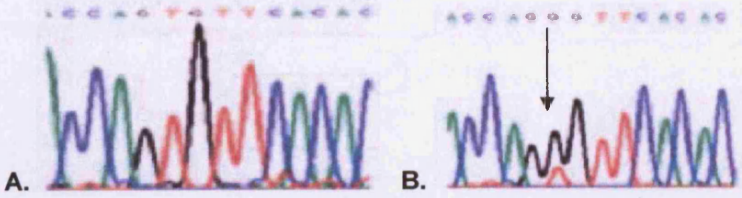

Figure 42: Electropherograms of the sense strands showing the wildtype (A) and mutant (B) desmoglein2 sequences. 473T>G is indicated by the arrow.

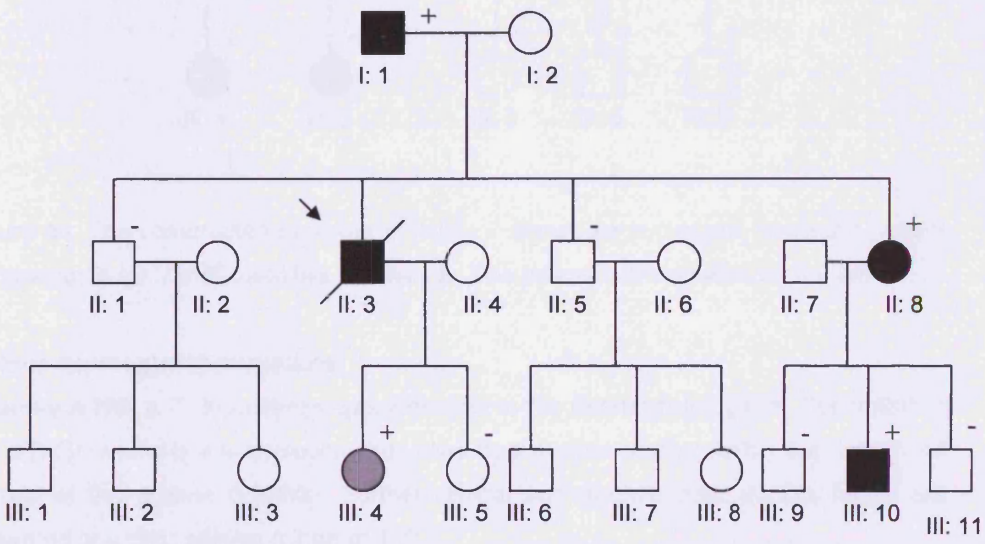

Figure 43:The constructed pedigree for family E shows an autosomal dominant pattern of inheritance for V158G with high penetrance. The proband is indicated by the arrow.

Family F:

The proband (II:3), a man of English origin, presented with recurrent syncope aged 45. His ECG demonstrated partial RBBB, T-wave inversion in V1-V3 and prominent epsilon waves. Cardiac imaging showed global enlargement of the RV with impaired systolic function. Recurrent VT of LBBB morphology was documented and an ICD was

implanted. The proband's sister (II:2) showed repolarization and depolarization abnormalities on ECG. II:2's daughters (III:1 and III:2) showed minor ECG abnormalities, which however do not fulfil the Task Force criteria. They are indicated by grey symbols on the family pedigree. The same mutation identified in family E (**V158G,** Figure 42) was also found in family F. All affected individuals (II:2, II:3, III:1 and III:2) were heterozygous carriers of the mutation. Clinical and genetic screening of the proband's children (III:3, III:4 and III:5) has been deferred for the present in view of their young age (Figure 44).[204]

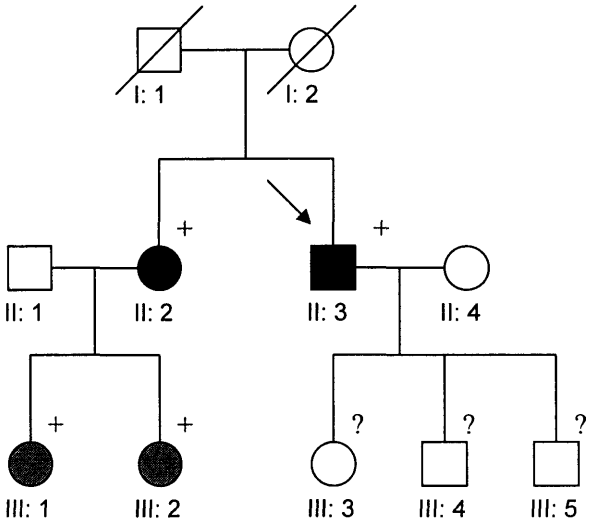

Figure 44: The constructed pedigree of family F shows an autosomal dominant pattern of inheritance for V158G, just like in family E. The proband is indicated by the arrow.

Further desmoglein2 mutations:

In **family A198**, a T →G change was identified in the desmoglein2 gene. The mutation (2759T>G) results in a substitution of a valine by a glycine residue within the repeat unit domain of the protein (**V920G**). Further clinical and genetic data on this family are presented in a later section (Chapter 1;7).

In **family H**, the proband, a woman of English origin, presented with recurrent syncope aged 45. Diagnostic findings included localized prolongation of QRS duration in V1-V3, T-wave inversion and a mildly dilated RV with regional wall motion abnormalities, in particular hypokinesia of the anterior RV outflow tract and of the apical lateral wall. The proband has had a prophylactic ICD implanted. She is a carrier of a G →A change in the desmoglein2 gene (165G>A). The mutation results in the substitution of a valine by a methionine residue within the EC1 extracellular domain of the protein (**V56M**).

In **family I**, the proband, a man of English origin, died suddenly aged 59 years. His post-mortem was consistent with a diagnosis of ARVC. The proband's asymptomatic

son, showed positive findings on ECG, SA-ECG and echo and he was found to be a carrier of a G→A change in the desmoglein2 gene (1174G>A). The mutation results in a substitution of a valine by an isoleucine residue within the EC4 extracellular domain of the protein (**V392I**). Other family members in families G, H and I were either unavailable for or declined clinical and genetic screening.[204]

Discussion:

The identification of ARVC-causing mutations in 3 desmosomal genes (PG, DP and PKP2), the implication of desmoglein isoforms in disease characterized by loss of epidermal adhesion, and the phenotype exhibited by animals expressing defective desmoglein molecules, led to the idea to screen ARVC probands for mutations in DSG2, the only DSG isoform expressed in the heart.

Eight novel mutations in the desmoglein2 gene are described herein. All gene-positive individuals were screened for mutations in other candidate ARVC-causing genes and found negative. Also, none of the mutations were found in 400 ethnically-matched control chromosomes examined, which eliminates the possibility of non-pathogenic polymorphisms. All mutations are predicted to disrupt functionally important parts of the DSG2 molecule. The C591X mutation in family A is predicted to cause truncation of the DSG2 protein with subsequent loss of the transmembrane and cytoplasmic components, where the binding sites for plakoglobin and plakophilin2 are found.[93, 120] A question is whether this mutation activates nonsense-mediated mRNA decay, resulting in the disease phenotype due to haploinsufficiency. The small size of the cardiac biopsy sample obtained, which was used for immunofluorescence studies (results presented in chapter 2) precluded supportive immunoblotting evidence.

The 829_840delCTTGAAGGGATG mutation in family B may cause skipping of exon 8 or alternatively activate a cryptic splice site in exon 8 or intron 8. Indeed, use of splice prediction computer programmes showed that the splice acceptor site for the mutant allele would be GTTTTGCAG//GTTG resulting in deletion of 5 amino acid residues. However, since heart or skin biopsies from an affected individual were not available for further analysis, these predictions remain purely speculative. The 3G>C mutation seen in family C is predicted to affect the initiation of translation of the DSG2 protein. Beginning of mRNA translation in eukaryotes takes place via a scanning mechanism, based on the first AUG codon and its flanking sequences. Studies of diseases caused by mutations that destroy the normal start codon have shown that translation may in fact start from alternative AUG codons, or be entirely abolished.[205] In the case of the 3G>C mutation it is unclear what the precise effect on the DSG2 protein would be. Unfortunately, cardiac tissue, which could have provided an answer, was not available from affected individuals in family C.

The five missense mutations found in families D, E, F, H, I and A198 affect amino acid sequences highly conserved among DSG2 homologues (mouse, dog, chimpanzee and human). Mutations V56M and V392I disrupt conserved regions in EC1 and EC4 extracellular domains, respectively. The extracellular domains of DSG2 and in particular EC1 and EC2 are involved in the formation of heterodimers between desmogleins and desmocollins in a Ca^{+2} dependent manner.[123] Such interactions are thought vital in achieving desmosomal adhesion.[93] Desmogleins contain conserved sequence motifs in the extracellular domains which represent putative calcium binding sites (DXNDN and A/VXDXD).[119] The fact that all gene-negative individuals were clinically normal provides further evidence to support disease causation.

Although DSG2 is expressed in the epidermis, none of the individuals carrying a DSG2 mutation had clinical evidence of hair or skin abnormalities. It is likely that other desmoglein isoforms expressed in the skin, specifically DSG1 and DSG3 functionally substitute DSG2 providing a potential explanation for the lack of cutaneous phenotype in DSG2 mutation carriers.

The penetrance of DSG2 mutations in the families described in this study is relatively high. Using the Task Force criteria as the definition of complete penetrance, DSG2 mutations are 58% penetrant. Using the proposed modified diagnostic criteria, penetrance rises to 75%. ARVC is a progressive cardiac disorder and younger individuals with few or no clinical features may develop disease later in life. If we separate the gene positive individuals into age groups (20-40 and >40years of age), the older group shows significantly higher penetrance. It can be argued that strict adherence to Task Force criteria, which by definition excludes LV disease, is no longer defensible. In family C, individual III:5 had almost exclusively left-sided disease, both on imaging and in T-wave inversion on ECG. Similarly, in family E, individual I:1 had disease which clinically was restricted to the LV. If we included those with isolated LV involvement, the penetrance would increase to 83%. The only gene positive patient with no evidence of ARVC on clinical investigation was the 79-year old mother of the proband in family A (II:2).Our clinical information on her is limited to a previous ECG, which did not show features of ARVC. However, further clinical investigation in her now would not be informative, as she has undergone intervention for complex coronary disease. This was complicated by RV perforation by a temporary pacing lead, which could have resulted from pre-existing structural abnormalities. Therefore, we can neither prove nor disprove gene penetrance in her case. Differential clinical findings even among members of the same family reflect once again the heterogeneity of disease expression in ARVC, even within individuals carrying the same mutation. The probands described herein, were part of a study population comprised of 86 unrelated patients with ARVC. The identification of DSG2 mutations in 8 families, suggests that

DSG2 mutations contribute genetically to ARVC pathogenesis in 9.3% of the cases, although further studies in larger cohorts are required to confirm these numbers.
Since the identification of the mutations presented herein, further ARVC-associated desmoglein2 mutations have been reported in the literature. *Pilichou et al* reported nine heterozygous DSG2 mutations in 8 probands from a series of 80 unrelated ARVC patients.[206] Of these mutations, 5 were missense, 2 were insertions-deletions, 1 was nonsense and 1 was a splice site mutation. Their identification of DSG2 mutations in 10% of ARVC individuals examined is in agreement with the number presented in our study.[206] Shortly after, *Awad et al* reported DSG2 mutations in 4 unrelated ARVC individuals, three of which are heterozygous carriers for missense mutations and one is a compound heterozygous for a missense and a nonsense DSG2 mutation.[207]

5) Desmocollin2a:

Family i:
The proband (III:1), a 44-year-old woman upon examination, was referred to the clinic for cardiac evaluation following episodes of syncope. She showed prolongation of QRS duration in both the right and left precordial leads, but no depolarization abnormalities on ECG. 24-hour Holter monitoring recorded frequent extra-systoles and on echo she showed global biventricular dilatation. She fulfilled one major and two minor Task Force Criteria and was thus given the diagnosis of ARVC. Following the proband's diagnosis; her mother was referred for cardiac evaluation. She had long experienced palpitations but had never been examined. Her ECG was normal but on echo she showed mild segmental RV and LV hypokinesia. She thus fulfilled two minor criteria, which were not diagnostic, but in the context of familial ARVC may represent a mild form of the disease. She is indicated by a grey symbol on the family pedigree. The proband's uncle (II:3) had died of non-cardiac reasons. II:3's daughters though (III:3 and III:4) were examined and found normal. Also, the probands' sister (III:2) was clinically normal.
A deletion of a single nucleotide was detected in exon 10 of the desmocollin2 gene (1430delC) in the family. The mutation leads to a frameshift and is predicted to insert a premature termination codon at position 480 of the protein (**M477fsX480**, Figure:45). Both the proband and her mother were carriers of the mutation while all clinically normal family members were gene negative (Figure 46).[208]

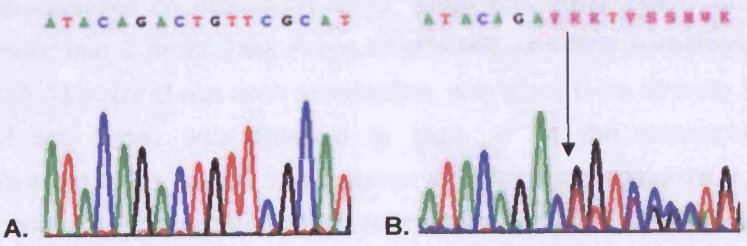

Figure 45: Electropherograms of the sense strands showing the wildtype (A) and mutant (B) desmocollin2 sequences. 1430delC is indicated by the arrow.

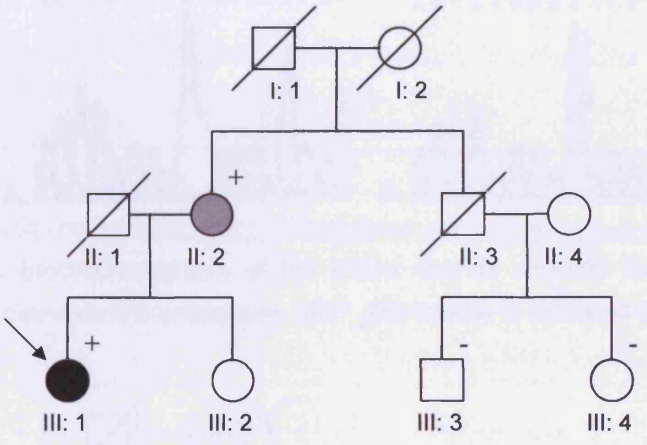

Figure 46: The constructed pedigree of family i shows an autosomal dominant manner of inheritance of M477fsX480 with incomplete penetrance. The proband is indicated by the arrow.

Family ii:

The proband in family ii (III:2) died suddenly at age 15 years. Shortly prior to her death she had experienced a syncope episode. Her ECG at the time showed T-wave inversions and 24-hour ambulatory ECG showed runs of non-sustained VT. Her post-mortem examination showed extensive fibrofatty replacement of the RV and LV myocardium, consistent with a diagnosis of ARVC. The proband's father (II:1), aged 59, was also affected by the disease. In particular he had experienced episodes of syncope and palpitations; he showed prolongation of QRS duration in V1-V3 on ECG and segmental RV hypokinesia on echo. No arrhythmic episodes have been recorded. The proband's sister (III:1), currently 19 years old, also showed mild RV hypokinesia and

frequent extra-systoles on ambulatory ECG. Given the family history of SCD, she fulfilled 1 major and 2 minor Task Force criteria and was thus considered affected. Individual III:3, 13 years of age upon examination, was found to be clinically normal. An insertion of two bases was detected in exon 17 of the desmocollin2 gene (2687_2688insGA) in the family. The mutation is predicted to generate a premature termination codon 4 amino acid residues downstream (**E896fsX900**, Figure:47). Both affected individuals (II:1 and III:1) were heterozygous carriers of the mutation. DNA was extracted from cardiac tissue preserved at autopsy of III:2, and the presence of E896fsX900 was also confirmed in the proband. Individual III:3 declined genetic testing (Figure:48).[208]

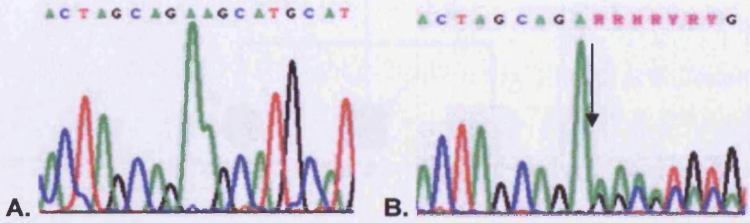

Figure 47: Electropherograms of the sense strands showing the wildtype (A) and mutant (B) desmocollin2 sequences. 2687_2688insGA is indicated by the arrow.

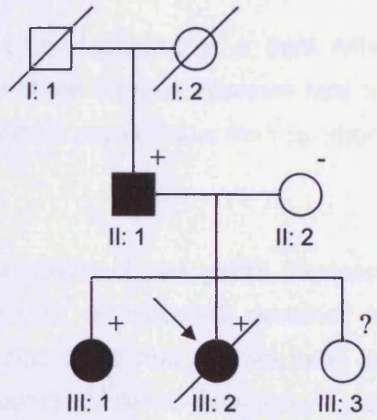

Figure 48: The constructed pedigree of family ii shows an autosomal dominant manner of inheritance for E896fsX900 with high penetrance. The proband is indicated by the arrow.

Two further carriers of E896fsX900:

The proband (II:1) in family iii, aged 42 upon examination, showed major structural abnormalities of the RV, consistent with ARVC, as well as multiple episodes of non-

sustained VT on ambulatory ECG. Her 12-lead resting ECG though was normal. II:1's brother (II:2), had died suddenly, at age 40, and his post-mortem examination was consistent with biventricular ARVC. Therefore II:1 fulfilled 2 major and 1 minor criteria and was thus considered affected by the disease. II:1's sister, 43 years of age upon examination was found to be clinically normal. The proband was a carrier of the same mutation also detected in family ii (**E896fsX900**, Figure:47). Unfortunately no tissue was preserved from the autopsy of individual II:2 and thus genotyping could not be performed. Individual II:3 was gene negative (Figure:49).[208]

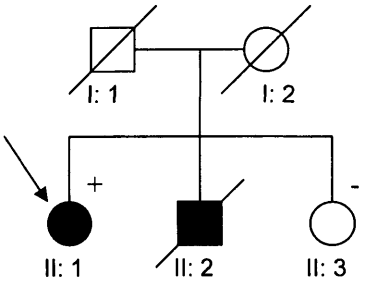

Figure 49: The constructed pedigree of family iii. Since the proband is only an heterozygous carrier of the mutation, E896fsX900 is dominantly inherited, however the small size of the pedigree does not allow us to draw conclusions as to the degree of penetrance of the mutation in this family. The proband is indicated by the arrow.

E896fsX900 was also detected in a third ARVC proband who presented with a biventricular form of the disease. However lack of clinical and genotyping information on her family members prevented us from constructing a pedigree (Family iv).

Discussion:

Following the association of plakoglobin, desmoplakin, plakophilin2 and desmoglein2 mutations with ARVC, desmocollin2 remained the only major desmosomal protein expressed in cardiac tissue that had not been implicated in the pathogenesis of the disease. Consequently, 77 ARVC patients who were screened for mutations in all other candidate genes and found negative, were screened for mutations in the desmocollin2 gene. Two heterozygous DSC2 mutations, a deletion and an insertion, were detected in 4 unrelated probands and 3 family members. Neither mutation was found in 400 ethnically-matched control chromosomes examined. This is the first time that mutations in the DSC2 gene have been described in families with ARVC. Interestingly, to date, no mutations in other human desmocollin isoforms have been reported. Of the three isoforms, only DSC1 has been implicated in human disease, since it was identified as an auto-antigen for sub-corneal pustular dermatosis-type IgA pemphigus.[209] This is in marked contrast to the involvement of desmoglein isoforms in several diseases,

including ARVC, striate PPK, and autoimmune disorders. However, animal studies have shown that Dsc1-null mice exhibit severe skin abnormalities due to loss of cell-cell adhesion.[210]

The two DSC2 mutations presented herein are considered to be pathogenic since they result in frameshift and premature termination codons. In particular, mutation M477fsX480 is in the fourth extra-cellular cadherin repeat and is predicted to truncate approximately one half of the desmocollin2 protein, with loss of the transmembrane and cytoplasmic components. It can be speculated that this leads to a completely non-functional mutant protein; however it is more likely that the deletion causes DSC2 haploinsufficiency by nonsense-mediated mRNA decay.

It is believed that the binding site for plakoglobin is located within the ICS domain of the DSC2a isoform.[211] In particular, the last 37 amino acids in the carboxy-terminal domain of DSC2 are essential for binding plakoglobin. Experiments in epithelial cells have shown that desmocollin mutants lacking this short segment in their C-terminus could not bind plakoglobin or effect the formation of the desmosomal plaque and the IF anchorage.[211]

Mutation E896fsX900 is located in exon 17 and would affect the C-terminus of DSC2 by altering 4 amino acid residues before a termination codon introduced prematurely. In the absence of functional studies, it is difficult to predict exactly how these two mutations would affect desmosomal formation. However, since desmocollins are crucial in cell-cell adhesion and tissue morphogenesis, it can be speculated that the absence of DSC2 or the incorporation of mutant DSC2 in desmosomes would result in structurally and functionally impaired desmosomes.

The presence of the E896fsX900 mutation in three families indicated either that this insertion is recurrent in patients with ARVC who harbour DSC2 mutations or that families ii, iii and iv have a common founder. However, haplotype analysis with use of microsatellite DNA markers in close proximity to the DSC2 locus in individuals carrying E896fsX900 identified no allele sharing, suggesting that E896fsX900 is a recurrent mutation. Although DSC2 expression in tissues is widespread, individuals carrying a DSC2 mutation did not show clinical evidence of hair or skin abnormalities. This is consistent with previous studies in which only a cardiac phenotype was present in patients with PKP2 and DSG2 mutations. Therefore, it seems likely that DSC1 and DSC3 compensate for a dysfunctional DSC2 isoform in epithelial cells, but not in cardiac myocytes where only DSC2 is expressed.

It is striking that five of seven individuals in this group had evidence of significant LV involvement which was more obvious than the RV disease in two individuals. The current Task Force criteria do not account for LV disease but the results presented herein would suggest that DSC2 mutations may be more frequently associated with a

predominantly LV phenotype of ARVC. However, since this study was limited by the small number of mutation carriers, this observation needs to be confirmed in larger kindreds in future studies. In conclusion, this part of the study identified DSC2 as the fifth desmosomal gene causing ARVC providing further evidence that ARVC is a disease of cell adhesion.

6) Desmin, an ARVC-causing or simply a modifier gene?

A213V:

The proband (III:3) in family A174 has had documented episodes of sustained VT, also induced on an electrophysiological study. She underwent an ablation procedure in 1997, following which VT recurred, necessitating cardioversion. Her most recent ECG showed inverted T-waves in both right and left precordial leads while a previous MRI investigation showed a grossly dilated RV with wall motion abnormalities and prominent fibrosis in the LV infero-lateral wall. Given the severity of the disease expression, she is now being considered for an ICD implantation. The proband's father (II:4) also had a history of palpitation. His ECG and SA-ECG were normal; however he showed isolated premature ventricular contractions of predominantly LV origin during exercise. On contrast echo, he presented with a mildly dilated RV. He is currently being treated with flecainide. The proband's brother (III:1) presented with late potentials on SA-ECG and an MRI investigation showed a mildly dilated RV with regional wall motion abnormalities. Exercise testing and 24-hour Holter monitoring showed only rare PVCs. The proband's mother (II:5) and sister (III:2) showed only minor abnormalities of uncertain significance and were not considered to be affected by ARVC. Individual III:4 presented with late potentials on SA-ECG, multi-focal PVCs on exercise testing and 256 PVCs on Holter monitoring. An MRI scan showed mild RV and LV dilatation. Individual III:5 was suspicious but not diagnostic of ARVC. She had a history of palpitations and syncope, although the latter was usually triggered by pain or fever. Her ECG showed inverted T-waves in V1-V2, an MRI showed mild wall motion abnormalities while her Holter and exercise testing were unremarkable.

A transition was detected in the proband in the gene coding for desmin. The mutation substitutes an arginine for a valine residue within the highly conserved 1B helix of the rod domain (**A213V**, Figure:50). Seven family members were genotyped, and other than the proband, none was a carrier of the mutation. It seemed therefore, that A213V had arisen de novo (Figure:51). Of note is that A213V was also identified in 1 of 200 ethnically-matched control individuals examined, raising doubts concerning the pathogenecity of the mutation.

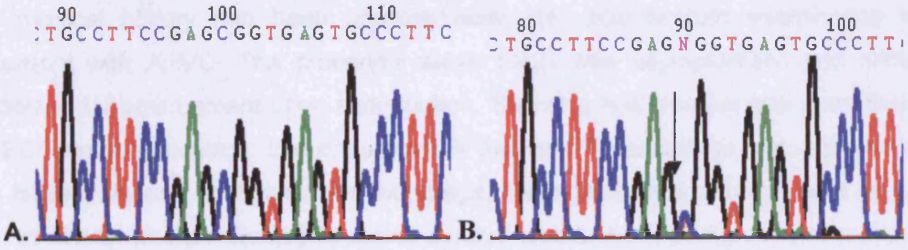

Figure 50: The electropherograms show the wildtype (A) and mutant (B) sequences of the desmin gene. A213V is indicated by the arrow.

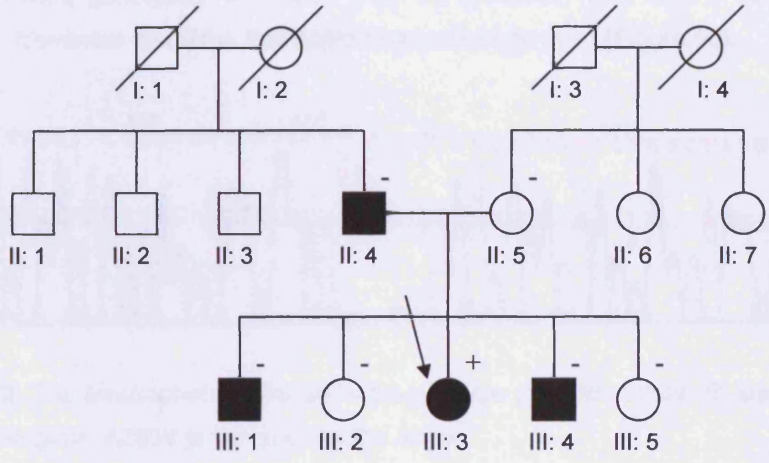

Figure 51: The constructed pedigree of the family A174 shows that A213V has arisen de novo and does not co-segregate with the disease phenotype in the family. The proband is indicated by the arrow.

A213V was also detected in two more probands with early disease onset and biventricular involvement since a young age. Like in the case of family A174, A213V seemed to have arisen de novo, and did not co-segregate with disease expression in the families (data not shown).

A285V:

The proband (III: 1) in family A19, was first referred for cardiac evaluation following a syncope episode at age 15. His ECG was consistent with an ARVC diagnosis, showing T-wave inversions in V1-V4, prolongation of QRS duration and epsilon waves. On echo, he showed global dilatation and hypokinesia of both ventricles, also confirmed by MRI. An SA-ECG performed recently, showed late potentials and he also had previous

documented episodes of non-sustained VT. His mother (II:2) died suddenly at age 40. Her medical history had been unremarkable. Her post-mortem examination was consistent with ARVC. The proband's sister (III:2) was asymptomatic and showed borderline LV enlargement upon examination. She also had positive late potentials on SA-ECG on one occasion. She does not fulfil the Task Force criteria, but in the context of a familial disease, and given her young age, these findings could represent an early form of ARVC. She is indicated by a grey symbol on the family pedigree. The proband's grandmother (I:2) was also affected by the disease based on both ECG and echo abnormalities. Individuals II:2, II:5 and II:7 were clinically normal. A transition was detected in the gene coding for desmin in III:1. The mutation substitutes an arginine for a valine residue within the 2A helix of the rod domain **(A285V**, Figure:52). Six family members were genotyped, and other than the proband, none was a carrier of the mutation. It seemed therefore, that A285V had arisen de novo (Figure:53).

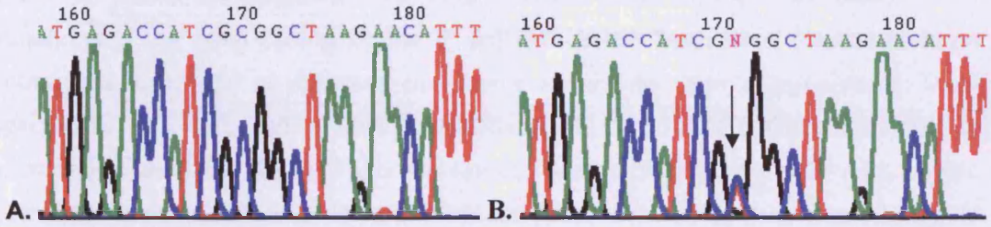

Figure 52: The electropherograms show the wildtype (A) and mutant (B) sequences of the desmin gene. A285V is indicated by the arrow.

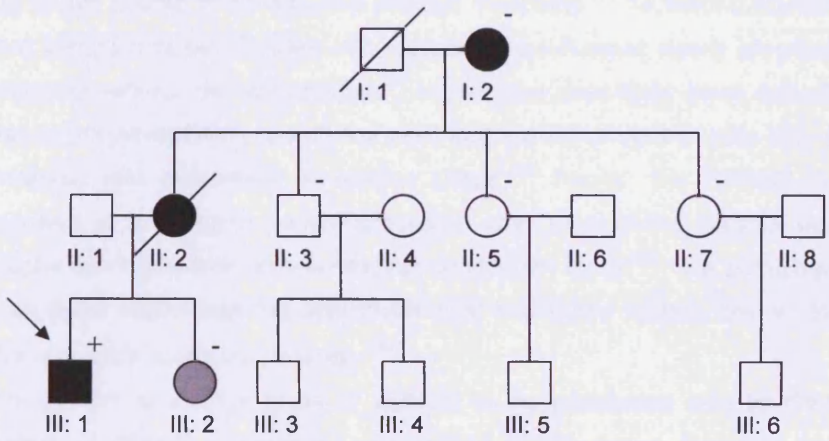

Figure 53: The constructed pedigree of the family A19 shows that A285V has arisen de novo and does not co-segregate with the disease phenotype in the family. The proband is indicated by the arrow.

A285V was also detected in one more proband with early disease onset and biventricular involvement since a young age. Like in the case of family A19, A285V seemed to have arisen de novo, and did not co-segregate with disease expression in the family (data not shown).

Discussion:

Pathogenic mutations in the type I and II epidermal keratins occur within regions thought to be involved in keratin intermediate filament assembly, namely the H1 domain, the helix initiation motif, the L12 linker region and the helix termination motif.[178] Mutations in these regions of the supra-basally expressed keratins K1 and K10 underlie bullous congenital ichthyosiform erythroderma/epidermolytic hyperkeratosis. However, two missense mutations outside the "hot spots" have been identified in exon 9 of the gene coding for keratin 1 (KI) in individuals presented with striated PPK. Both mutations seem to affect intermolecular connections rather than filament assembly.[178, 212] Mutations in the gene coding for the IF protein desmin have been implicated in an heterogeneous group of diseases collectively known as desmin myopathies. More specifically, two splice site mutations (IVS3+3A→G and IVS-1G→A) were found to underlie two unrelated cases of sporadic skeletal and cardiac myopathy.[213] Also, two in-frame deletions (E359_S361del and N366del) were associated with three cases of skeletal or cardio-skeletal myopathy.[214] A337P was identified in a family with adult-onset skeletal myopathy and mild cardiac involvement, while compound heterozygosity for A360P and N393I was detected in another family characterized by childhood onset aggressive course of cardiac and skeletal myopathy.[215] Mutations N342D and I451M were identified in two families with features of adult-onset slowly progressive skeletal myopathy without cardiomyopathy.[216] I451M has previously been associated with a case of idiopathic DCM, raising the point that the tail of desmin may play an important functional role exclusively in cardiac tissue.[217] Finally, the R406W mutation was identified in a sporadic patient presented with symmetrical muscle weakness and atrophy combined with atrio-ventricular conduction block.[218] The pathological hallmark of all these cases was the accumulation of mis-folded mutant desmin forming toxic, insoluble cytoplasmic aggregates. [180]

Although the anchorage of the IF network to the membrane may be disrupted in the context of ARVC, cytoplasmic aggregation of mis-folded filaments has not been reported. However, given the high similarity of desmin and keratin I and the implication of desmin C-terminal mutations in cases of cardiomyopathy without skeletal muscle involvement [217], it has been suggested that mutations in exon 9 of desmin may be affecting the intermolecular connections, rather than the assembly of the IF network, thus causing ARVC instead of a more generalized cardio-skeletal myopathy.[217] ARVC

probands that were previously screened for mutations in desmoplakin, plakoglobin, desmoglein2, desmocollin2 and plakophilin2 and found negative were screened for mutations in exon 9 of the desmin gene. After no sequence changes were identified, the same cohort of patients, was screened for mutations along the entire length of the desmin gene.

Two mutations were identified, A213V and A285V, in a total of 5 ARVC probands. Both mutations had arisen do novo, as is the case with many previously reported desmin mutations, and did not co-segregate with the disease phenotype in the families. A213V has previously been implicated in a case of restrictive cardiomyopathy,[219] and in a case of progressive skeletal myopathy without cardiac involvement (*M.de Visser, unpublished data*[180]). In particular, *Bowles et al.* have performed in vitro experiments to establish the pathogenetic mechanism of A213V.[219] Cells expressing the mutant protein are able to assemble IFs under resting conditions. However the IF network breaks down when the cells are exposed to mechanical stress.[219] This observation is in agreement with the hypothesis that desmosomal ARVC-causing mutations affect primarily the cardiac myocytes since they are constantly subjected to mechanical stress. Interestingly, a recent study comparing the phenotypic, molecular and functional characteristics of seven desmin mutations including A213V, suggested that A213V exhibits a pathogenic potential only if combined with other mutations in desmin or other genes and should therefore be considered conditionally pathogenic.[220] Based on this suggestion, and on the observation that the probands carrying either mutation show a much more severe phenotype than their ARVC-affected relatives, it can be speculated that A213V and A285V are not pathogenic. Instead, they act synergistically with other yet un-identified mutations to worsen the expression of the disease.

Of note is a publication by *Melberg et al* in 1999 concerning a family with both myofibrillar myopathy and ARVC.[221] Although limited by the small number of mutation carriers, these results indicate that desmin mutations, though not disease-causing per se, may still play a role in ARVC pathogenesis.

7) Mutations in two desmosomal genes:

Family A198:

The proband (III:1) presented with SCD at age 15 years. Initial post-mortem examination did not identify a cause of death. However, subsequent expert review of histology identified fibro-fatty replacement predominantly of LV myocardium. The proband's mother (II:4) had experienced an isolated unexplained syncope episode at age of 42. Her ECG showed T-wave inversion in precordial leads V1-V3 and

flat/inverted T-waves in precordial leads V4 and V5. There was localized prolongation of QRS duration in V1 to V4 and poor R-wave progression. SA-ECG was positive for late potentials. Cardiac imaging identified RV dilatation with aneurysms of the RV free wall, and the LV was mildly dilated with mild systolic impairment. She had frequent ventricular ectopics and couplets at low workloads on exercise testing (LBBB morphology). 24-hour ECG showed less than 50 ventricular ectopics during 24 hours of recording. The mother's siblings have declined screening investigations or genetic testing. One nephew (III:3) has been evaluated and shows no evidence of disease expression. The proband's father (II:3) has never experienced cardiac symptoms. His ECG was unremarkable but SA-ECG was reproducibly positive for late potentials. Cardiac imaging showed regional wall motion abnormalities of the RV. Specifically he showed segmental hypokinesia of the anterior RV outflow tract and apical free wall. He also showed global mildly reduced systolic function. The proband's brother (III:2), his father's siblings (II:1 and II:2) and extended family have refused clinical or genetic testing.

Mutation analysis in the mother revealed a nonsense mutation (1237C>T) in exon 5 of the plakophilin2 gene. The mutation is predicted to signal premature termination of translation within the armadillo repeat domain of the protein (**R413X**, Figure:54). Mutation analysis in the father revealed a missense mutation (2759T>G) in desmoglein2. The mutation alters a highly conserved valine for a glycine residue within the repeat unit domain of the protein (**V920G**, Figure:55). A small amount of tissue from the proband was made available for DNA extraction. Unfortunately, DNA of adequate quantity was not obtained so we suspect but cannot confirm whether the proband had inherited both mutations (Figure:56). The clinical characteristics and genotype of this family are included in: *Ward et al.* "Multiple desmosomal gene mutations in familial ARVC result in a more severe phenotype"; manuscript submitted to *Circulation*.

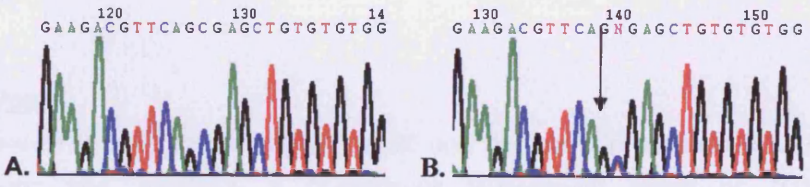

Figure 54: Electropherograms of the sense strands showing the wildtype (A) and mutant (B) plakophilin2 sequences. 1237C>T is indicated by the arrow.

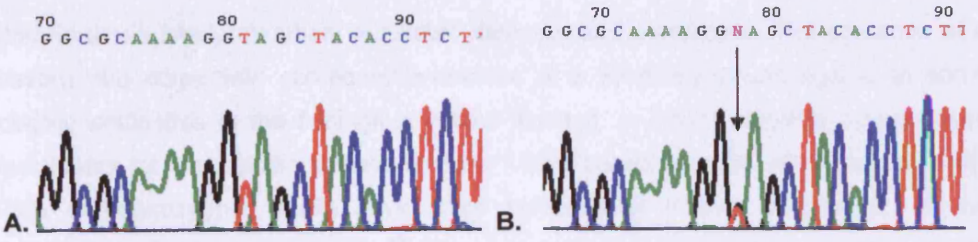

Figure 55: Electropherograms of the sense strands showing the wildtype (A) and mutant (B) desmoglein2 sequences. 2759T>G is indicated by the arrow.

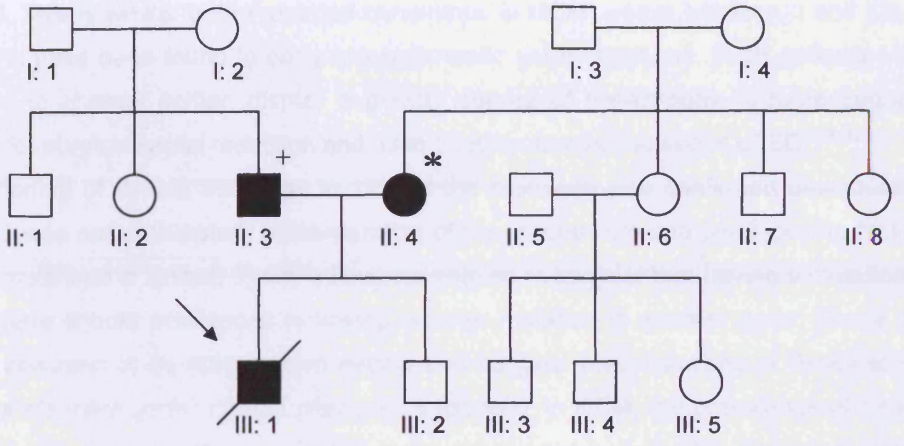

Figure 56: The constructed pedigree of family A198. " + " indicates a carrier of the V920G mutation in the desmoglein2 gene. " * " indicates a carrier of the R413X mutation in the plakophilin2 gene. Unfortunately, lack of genetic data did not allow us to establish the mode of inheritance or the penetrance of the two mutations. The proband is indicated by the arrow.

Discussion:

The presence of 2 mutations in A198.1 could only be assumed because of his SD at a very young age, evidence of biventricular involvement based on histological examination of an autopsy sample and both his parents being carriers of different disease-causing mutations. A case of confirmed compound heterozygosity for two novel nonsense desmoplakin mutations was presented in detail above (Chapter 1:1). From the ARVC cohort examined, compound heterozygosity for two desmosomal mutations was confirmed in 6 probands and assumed in 1 (*not all cases presented herein*). The clinical presentation in these 7 probands was significantly more severe

than in those family members evaluated clinically and genetically. The presence of a severe phenotype with compound mutations at a relatively young age is to some degree analogous to the findings in Naxos disease. In Naxos families, homozygous individuals for plakoglobin mutations have 100% penetrance by adolescence, while 20% of heterozygous adults have some evidence of disease expression without fulfilling the Task Force criteria.[60] This suggests that at least in young patients presenting with significant arrhythmia and marked morphological changes, the possibility of 2 mutations should be considered.

Although only a small percentage of the cohort examined had two documented mutations, this represents 13% of all families in whom any desmosomal mutation was found. This is similar to the reported occurrence in HCM, where between 3 and 5% of cohorts have been found to carry two sarcomeric gene mutations. Such patients were shown to present earlier, display a greater degree of hypertrophy, a more frequent need for surgical septal reduction and have a higher familial incidence of SD.[222, 223]

The finding of double mutations in 13% of the probands with confirmed desmosomal ARVC was not anticipated. Understanding of the mechanism and predisposing factors for 2 mutations is limited. There is however nothing to suggest that having a mutation in one gene should predispose to having another mutation in another gene. These are then assumed to be independent events and suggest that mutations in desmosomal genes are more common than previously estimated. In HCM, the prevalence of clinical disease in young adults is estimated to be approximately 1 in 500. Though mutation analysis has only been performed in small numbers, studies revealed that between 5-17% of patients with confirmed sarcomeric HCM have more than one mutation.[222] The fact that at least as many ARVC patients appear to have 2 mutations, in a clinical condition with an estimated prevalence that is only one tenth of that of HCM, may relate to the clinical difficulties of making an accurate diagnosis and reliance on diagnostic criteria which are recognized to be very specific but insensitive. Patients with ARVC may suffer disease-related complications including SCD during what is considered to be the concealed phase of the disease. Clinical diagnosis based on existing criteria is problematic for recognition of early disease. This highlights the importance of developing more sensitive clinical diagnostic criteria and the potential importance of mutation analysis of all the recognized genes in the assessment of families.

Finding a mutation may help the diagnostic clarification of "borderline" cases. Also, although the clinical course of the disease cannot be predicted from DNA analysis, it can help identify individuals at risk, thus facilitating timely diagnosis, with the subsequent possibility of preventing complications and reducing morbidity and mortality. Genetic predisposition may lead to alteration in lifestyle such as avoiding strenuous exercise. Given the low penetrance, however, a mutation carrier is not

automatically assumed to be destined for the severe phenotype that once was encountered in a family member. However, advances in molecular biology will enable cascade screening in family members with a high negative-predictive value. It is common practice to cardiologically screen close relatives of an index case at regular intervals. Identifying a pathogenic mutation in a family, would allow family members who have not demonstrated abnormalities and do not carry the respective mutation to be dismissed from regular cardiological follow-up.[183]

Finally, it is important to mention that of the 47 cases in which a single mutation was identified, 4 probands who presented with a more severe phenotype than other mutation carriers in their families, had additional desmosomal mutations, now recognized as polymorphisms. The possibility exists that these supposed polymorphisms are frequently occurring mutations which in isolation are not significantly pathogenic, but in the presence of other mutations may have a synergistic effect on disease expression.

Moving to the next step:

Early daguerreotype photographs required long exposure times, so long that the only visible features were permanent and stationary, such as roads, bridges and buildings. The lack of dynamic features, such as crowded streets, rendered the scenes empty and lifeless. The rest had to be imagined. So it is sometimes with genetics. The identification of mutations gives invaluable information when it comes to genetic disorders. However, we still have a daguerreotype in which we have to imagine the dynamic processes leading from the mutation to the actual disease phenotype.[224] Discovering gene mutations provides a strong foundation. However, considerable in vitro and animal work is needed before we can transfer this translational research from the laboratory bench to the bedside.[225]

CHAPTER 2:

"Histopathology and immunohistochemistry studies of heart and skin samples from ARVC patients"

FOUNDATIONS AND OVERVIEW:

In 2004, the heart of an 11-year-old girl diagnosed with Carvajal syndrome was macroscopically and microscopically examined.[64] Histological investigation disclosed diffuse scarring of the free walls of both ventricles with areas of extensive myocardial loss and replacement fibrosis in the outer third of the LV. There was no evidence of fatty infiltration in either ventricle. Myocyte hypertrophy and attenuation with bizarre nuclei and non-specific myocytolytic changes were prominent. Scant, patchy foci of inflammatory cells were visible adjacent to degenerative myocytes and TUNEL staining revealed an increased apoptotic index in both ventricles. The distribution of intercalated disc proteins was characterized by immunohistochemistry and confocal microscopy. Immunoreactive signal for desmoplakin, the mutant protein in Carvajal syndrome, was virtually undetectable at intercellular junctions where abundant signal was seen in controls that had undergone similar fixation and processing. Immunoreactive signal for plakoglobin was also markedly diminished as was signal for Cx43, the major cardiac gap junction protein. The amount and distribution of selected transmembrane adhesion proteins including N-cadherin and desmocollin2 appeared to be normal. Finally, desmin failed to localize at intercalated discs, suggesting that interactions between desmin and desmoplakin are disrupted in Carvajal syndrome.[64]

Similarly, the amount of Cx43 immunoreactive signal localized to intercalated discs was markedly reduced in both right and left ventricular samples from 4 patients with Naxos disease compared to controls.[226] Quantitative analysis showed that Cx43 signal at junctional sites was diminished to a greater extent in pathologic areas of the RV than in the LVs of patients with Naxos disease, and that it was significantly reduced even in a young patient who did not exhibit clinical or pathologic features of structural heart disease. The amount of immunofluorescence signal for plakoglobin, the mutant protein in Naxos disease, was also dramatically reduced at cell-cell junctions, while N-cadherin, desmoplakin, desmocollin2 and α-catenin, all exhibited normal localization. [226]

Pathologically, ARVC is characterized by the presence of fat and fibrous tissue embedded within degenerative, apoptotic cardiac myocytes with the occasional presence of inflammatory infiltrates. Following the publications described above, it appears that mutations in one desmosomal gene have cascade effects on the amount and localization of further mechanical and electrical proteins at cell-cell junctions. A number of heart and skin samples from ARVC patients with known or yet un-identified mutations have been analysed by histological examination, immunostaining and confocal microscopy. Herein we shall present the results obtained and discuss their implications in understanding and managing the disease.

METHODS:

1) Tissue acquisition and processing for microscopy and immunohistochemistry:
The tissue samples were excised, rinsed in phosphate buffered saline (PBS) and fixed in 10% neutral-buffered formalin. Each formalin-fixed sample was subsequently cut into transverse slices ~1mm thick, dehydrated in a series of alcohols, embedded in paraffin, sectioned at a thickness of ~6μm, and mounted on gelatin-coated slides (VWR International). The slides were deparaffinised and re-hydrated by serial immersion in xylene, 100% ethanol, 70% ethanol, 50% ethanol and distilled water (dH_2O).

2) Hematoxylin and eosin staining (H&E):
Sections were over-stained with hematoxylin for 3-5min. Sections were then differentiated and de-stained through serial immersions in acidic alcohol (usually 4-5 immersions) until they looked red. The sections were immersed in blueing agent for 2min until the nuclei were stained sharp blue, following which they were rinsed with dH_2O and immersed in 70% ethanol for 3min. Slides were then immersed in eosin for 2min and cleared through a series of 95% ethanol solutions. The hematoxylin stain is made from hematoxylin powder (6.4g), ammonium alum (60g), ethanol (200ml), glycerol (160ml) and dH_2O (640ml). Acidic alcohol is made by mixing 4 ml of hydrochloric acid with 396ml of 95% ethanol. Eosin stain is made by mixing 1 g of Eosin Y, with 5 ml of glacial acetic acid and 1 lt of dH_2O and subsequently diluting the solution 1:1 with 70% ethanol. Finally, blueing agent is made by diluting 1 g of bicarbonate blue in 1 lt of dH_2O. This technique stains fat white, nuclei dark blue/purple and residual tissue (cardiac myocytes or epithelial cells) light red.

3) Masson's trichrome staining:
Deparaffinised and re-hydrated sections were stained first in Weiger's iron hematoxylin working solution and then in Biebrich scarlet-acid fuchsin solution. The sections were then differentiated in phosphomolybdic-phosphotungstic acid solution and transferred to aniline-blue solution. The slides were then further differentiated in 1% acetic acid solution, dehydrated through 95% ethyl alcohol, absolute ethyl alcohol and xylene before being mounted with resinous mounting medium. Weiger's iron hematoxylin solution is prepared by mixing equal parts of stock solutions A (1 g hematoxylin, 100ml 95% ethanol) and B (4ml 29% ferric chloride in dH_2O, 95 ml dH_2O, 1 ml 1M HCl). Biebrich scarlet-acid solution is prepared by mixing 90ml 1% aqueous Biebrich scarlet, 10ml 1% aqueous acid fuchsin and 1ml glacial acetic acid. Phosphomolybdic-phosphotungstic acid solution is prepared by mixing 25 ml 5% phosphomolybdic acid solution with 25ml 5% phosphotungsitc acid solution. Aniline blue solution is made by

dissolving 2.5g of aniline blue and 2ml of glacial acetic acid in 100 ml dH_2O. Finally, 1% acetic acid solution is prepared by diluting 1ml of glacial acetic acid in 99ml of dH_2O. This technique stains collagen fibers blue, fat white, nuclei black and residual myocytes red.

4) Immunohistochemistry

In preparation for immunohistochemistry, deparaffinised, re-hydrated slide-mounted sections were placed in citrate buffer (10mmol/l, pH 6.0) and heated in a microwave oven until boiling for 10min to enhance specific immunostaining. After being cooled to room temperature, the tissue sections were rinsed in PBS (5min) and simultaneously permealised and blocked by incubating them in PBS containing 1% Triton X-100, 3% normal goat serum (Jackson Immunoresearch) and 1% bovine serum albumin (BSA, SIGMA). The sections were then incubated with the primary antibody (diluted 1:10-1:2000 in blocking buffer depending on preliminary data for condition optimization) overnight at 4°C, brought to room temperature, washed three times in PBS and incubated with indocarbocyanine-conjugated goat anti-rabbit or anti-mouse IgG (diluted 1:400 in PBS) for 2 hours at room temperature. Following incubation with the secondary antibody, the sections were washed three times in PBS and mounted with mounting medium made by mixing equal volumes of PBS and glycerol.

Primary antibodies included: mouse monoclonal anti-connexin43 (Chemicon), mouse polyclonal anti-desmoplakin I & II (Fitzgerald), mouse monoclonal anti-plakoglobin (SIGMA), mouse monoclonal anti-pan cadherin (SIGMA), mouse monoclonal anti-desmoglein2 (AbCam), mouse monoclonal anti-desmocollin2/3 (ZYMED), rabbit monoclonal anti-connexin43 (SIGMA), rabbit polyclonal anti-connexin43 (ZYMED), rabbit polyclonal anti-beta catenin (AbCam) and mouse monoclonal anti-pan desmoglein (AbCam). Secondary antibodies included cyanine 3 (Cy3) conjugate affini-pure goat anti-mouse IgG (H+L, Jackson Immunoresearch) and Cy3 conjugate affini-pure goat anti-rabbit IgG (H+L, Jackson Immunoresearch). Immunostained preparations were analysed by laser scanning confocal microscopy (Sarastro model 2000, Molecular Dynamics, Figure:1) as described below.[227]

5) Analysis of immunoreactive signal by confocal microscopy:

Stained sections from each tissue sample were examined by fluorescence microscopy at a magnification of x400 using a x40 oil immersion lens with numerical aperture of 1.0, lateral resolution of 0.23 µm, and depth resolution of 1.06µm. Use of this lens in combination with a 50-µm pin hole resulted in a full-width, half-maximal focal plane with a thickness of ~1.0 µm. Each individual test area encompassed ~26.400 μm^2 and included profiles of 30-50 cells. Five test areas were analysed for each antibody in each

tissue sample. Each test area was scanned by the laser at the approximate mid-depth of the section and digitized into a 1024 x 1024 matrix. In general, the level of background fluorescence was low and the immunoreactive material recognized by all antibodies was concentrated in discrete spots at points of intercellular apposition. The low background and highly localized intense signal facilitated the identification of a signal intensity threshold exceeded only by the specific discrete spots of signal at appositional membranes. Accordingly, an arbitrary threshold was identified for each set of sections stained with a given primary antibody that clearly distinguished the high-intensity signal concentrated in discrete spots from all other areas in the test field. Any structures with a signal intensity that exceeded this threshold were assumed to represent electrical or mechanical adhesion components of the intercalated discs. A much lower threshold value was also identified below by which only areas of the slide not covered by cells were defined. Thus, the proportion of total tissue area occupied by gap junctions or anchoring junctions was defined as the number of pixels with signal intensity exceeding the high threshold divided by the total number of pixels exceeding the lower threshold. The percentage of total test area occupied by tissue was defined as the total number of pixels exceeding the low threshold divided by the total number of pixels in the image space.[227]

6) Tissue processing for electron microscopy:

The tissue samples were excised, rinsed in PBS and fixed for 24 hours in 2% glutaraldehyde in 0.1mmol/l cacodylate buffer (pH 7.4). The fixed tissue was then post-fixed in 1% OsO_4, dehydrated in ethanol and embedded in Spurr's low-viscosity epoxy resin. After the resin had been polymerized, ultra-thin (50-100 nm) sections were prepared and examined by electron microscopy.[227]

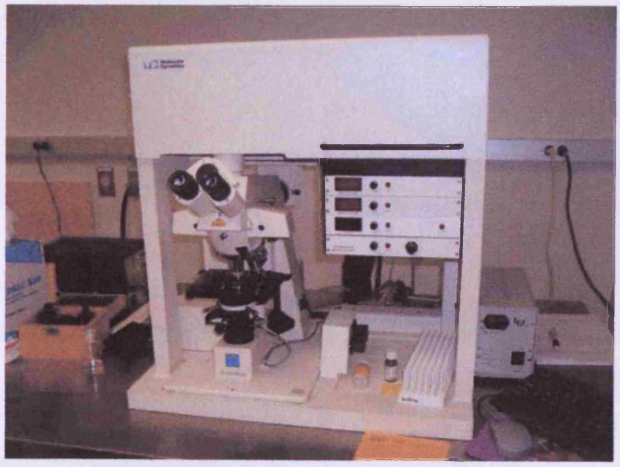

Figure 1: Confocal microscope, Sarastro model 2000, Molecular Dynamic

RESULTS AND DISCUSSION:

1) Histological examination of heart samples:

Heart biopsy samples from individuals diagnosed with ARVC according to the Task Force criteria and heart autopsy samples from individuals with confirmed ARVC postmortem were stained with hematoxylin& eosin and Masson's trichrome for microscopic examination. Heart autopsy samples from individuals with no history of heart disease were stained using the same conditions for control purposes. Representative images and observations are presented below.

Control A, B, C and D:

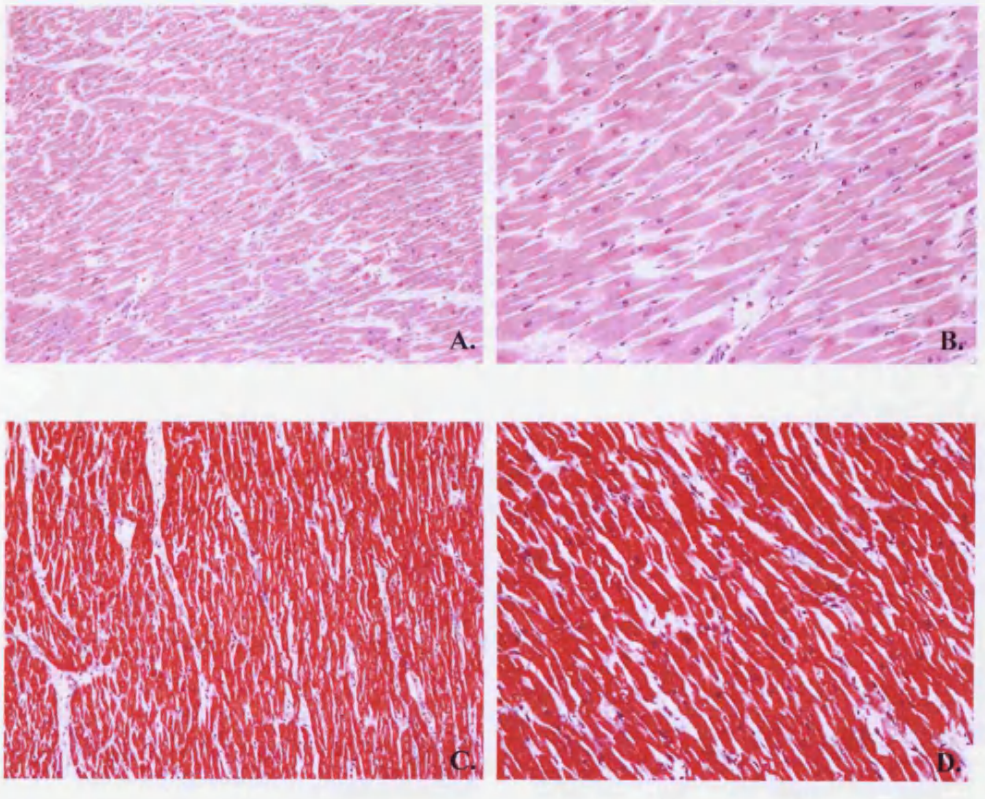

Figure 2: Heart autopsy samples from individuals with no history of heart disease, who died of non heart-related etiology were stained with H&E (A and B) and Masson's trichrome (C and D). Magnification 10x (A and C) and 20x (B and D). Samples A, B and C were obtained from the LV, while sample D was obtained from the RV.

A1.1: case presented in Chapter 1 (**pg. 67-68**)

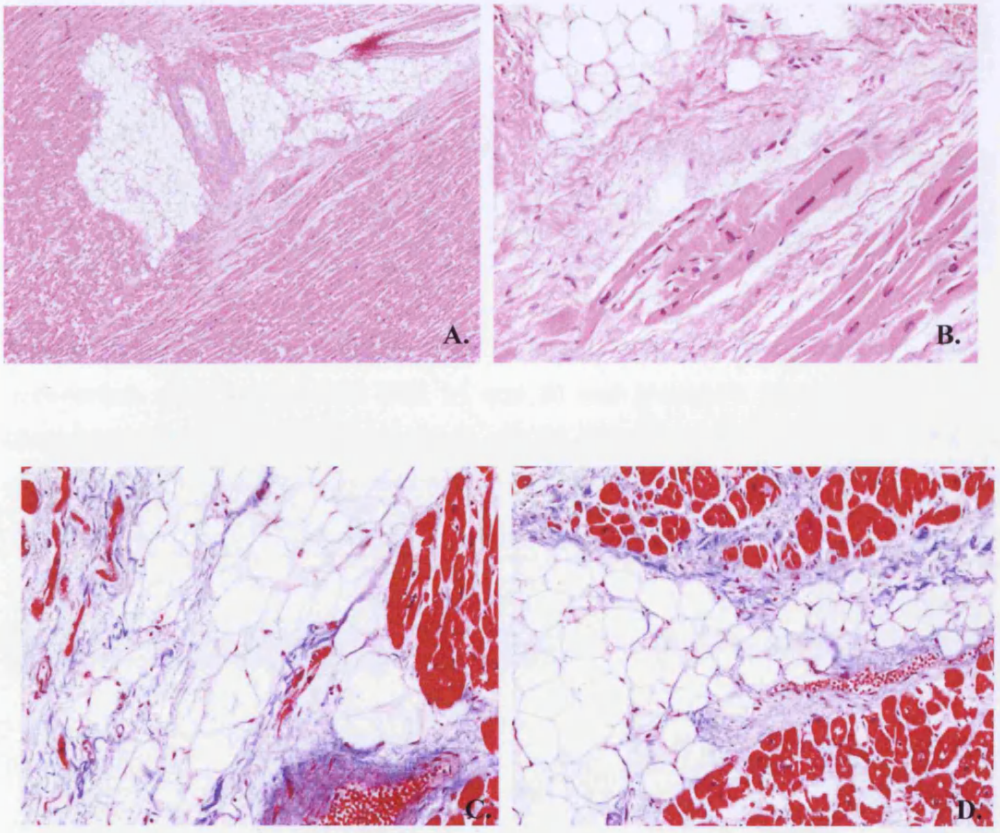

Figure 3: Heart autopsy samples from a female who was diagnosed with ARVC postmortem were stained with H&E (A and B) and Masson's trichrome (C and D). Magnification x4 (A) and x20 (B, C and D). All samples were obtained from the RV.

A208.1: case presented in Chapter 1 (**pg. 73-74**)

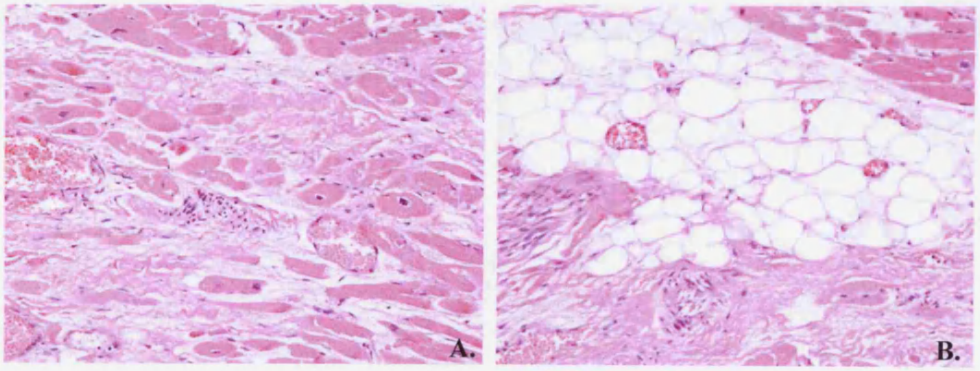

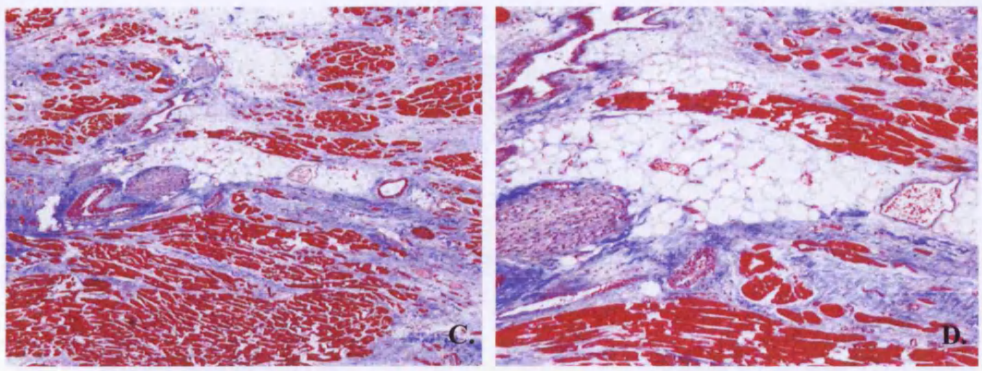

Figure 4: Heart autopsy samples from a female who was diagnosed with ARVC postmortem were stained with H&E (A and B) and Masson's trichrome (C and D). Magnification x4 (C), X10 (D) and x20 (A and B). Sample A was obtained from the LV, while samples B, C and D were obtained from the RV.

D0074: case presented in Chapter 1 (**pg. 84-85**)

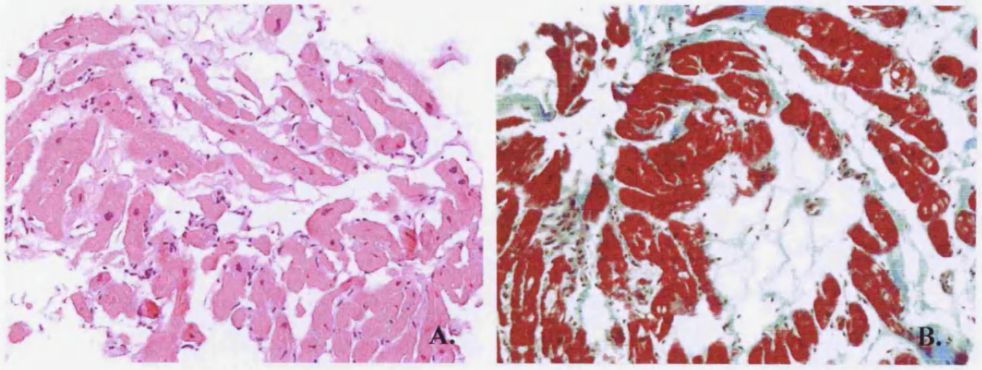

Figure 5: Heart biopsy samples from a male diagnosed with ARVC in his early-40s were stained with H&E (A) and Masson's trichrome (B). Magnification is x20 in both images. Both A and B were obtained from the affected RV.

GR3: case presented in Chapter 1 (**pg. 94-95**)

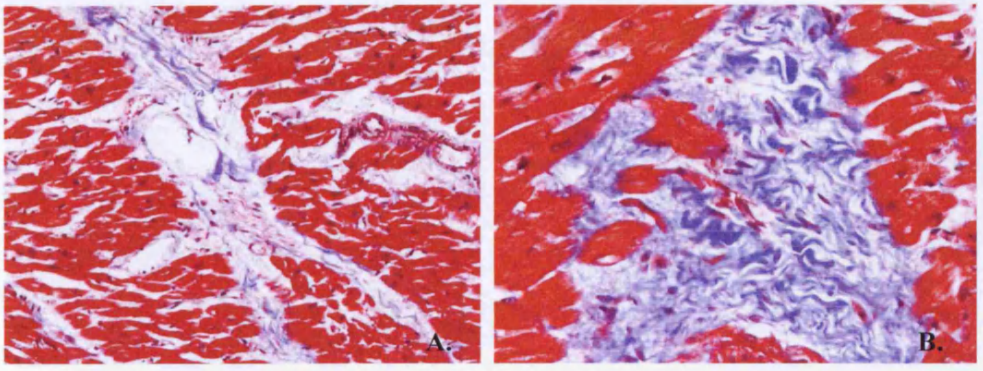

Figure 6: Heart biopsy samples from a male diagnosed with biventricular ARVC in his teens were stained with Masson's trichrome. Magnification x20 (A) and x40 (B). Both A and B were obtained from the RV.

A188.1: case presented in Chapter 1 (**pg. 95-96**)

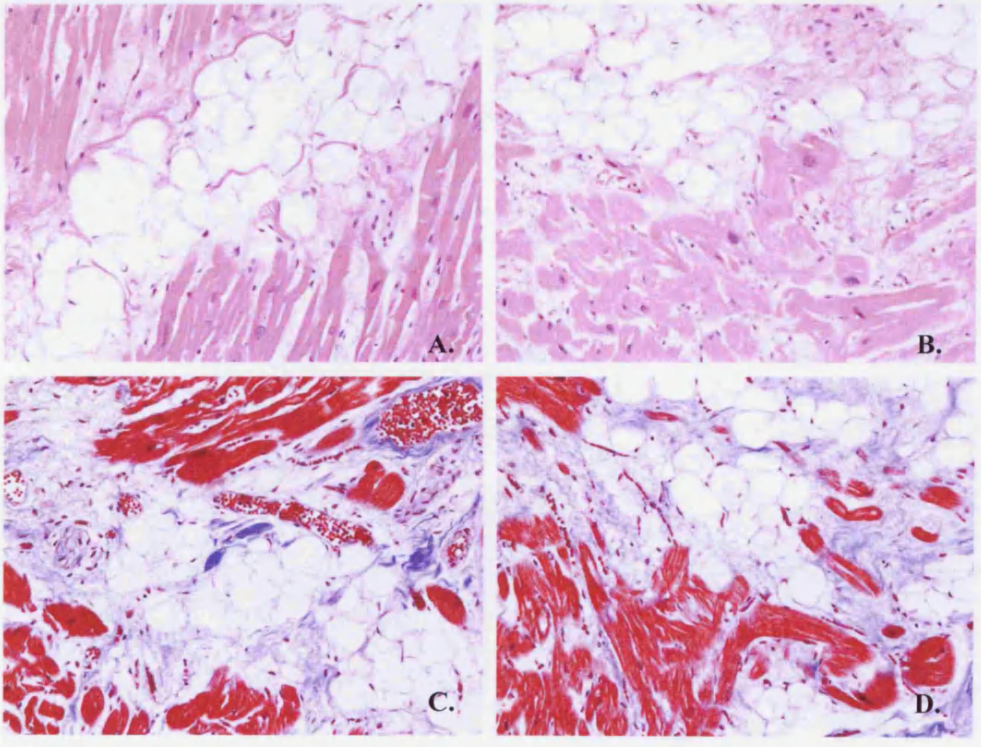

Figure 7: Heart autopsy samples from a young male who was diagnosed with ARVC postmortem were stained with H&E (A and B) and Masson's trichrome (C and D). Magnification x20 in all images. Samples A and C were obtained from the LV, while samples B and D were obtained from the RV.

Family A, Individual III: 4 case presented in Chapter 1 (**pg. 98-100**)

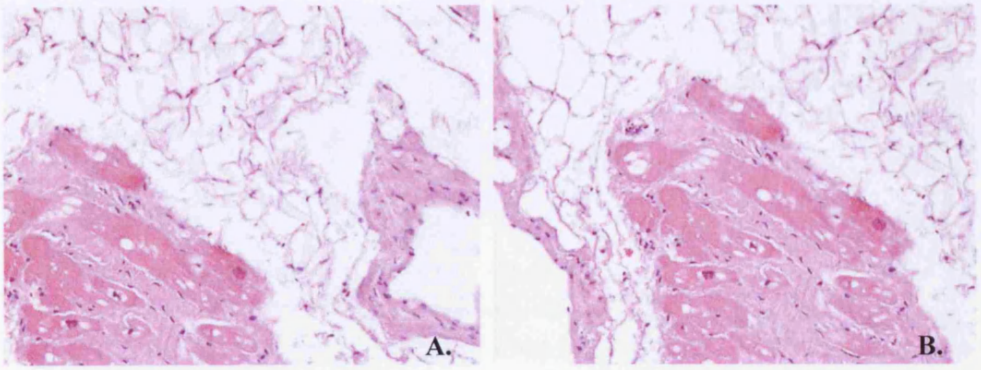

Figure 8: Heart biopsy samples from a female diagnosed with biventricular ARVC in her early-30s were stained with H&E. Magnification is x20 in both images. Both A and B were obtained from the affected LV.

A176.1:

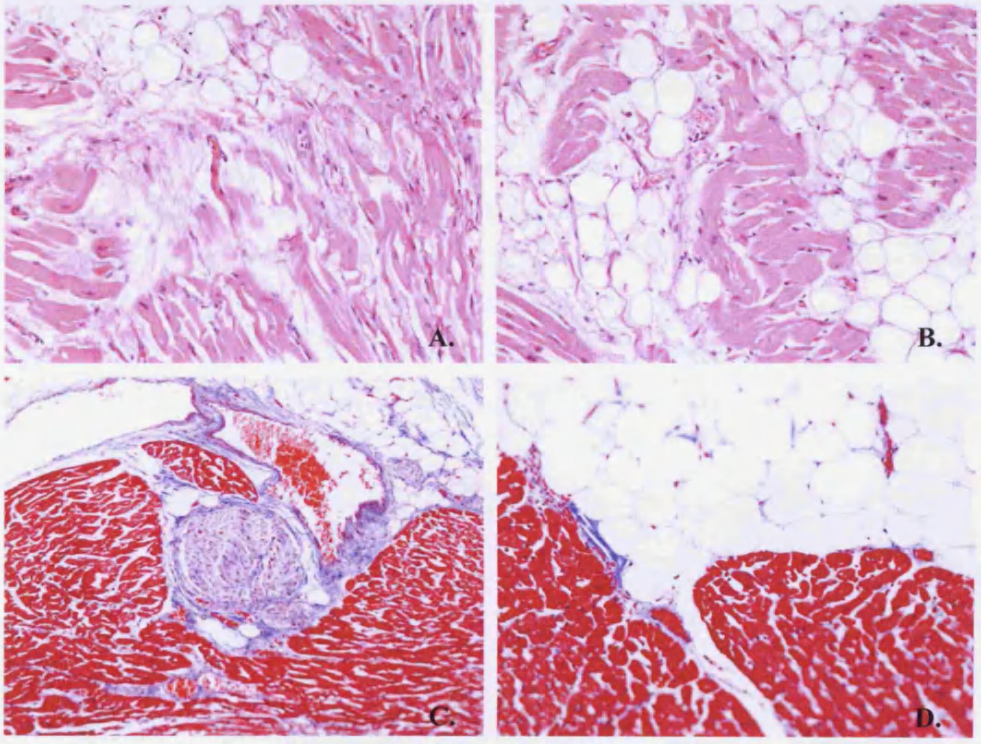

Figure 9: Heart autopsy samples from a male who was diagnosed with ARVC postmortem were stained with H&E (A and B) and Masson's trichrome (C and D). Magnification x20 (A, B and D) and x10 (C). Samples A and C were obtained from the LV, while samples B and D were obtained from the RV.

A223.1:

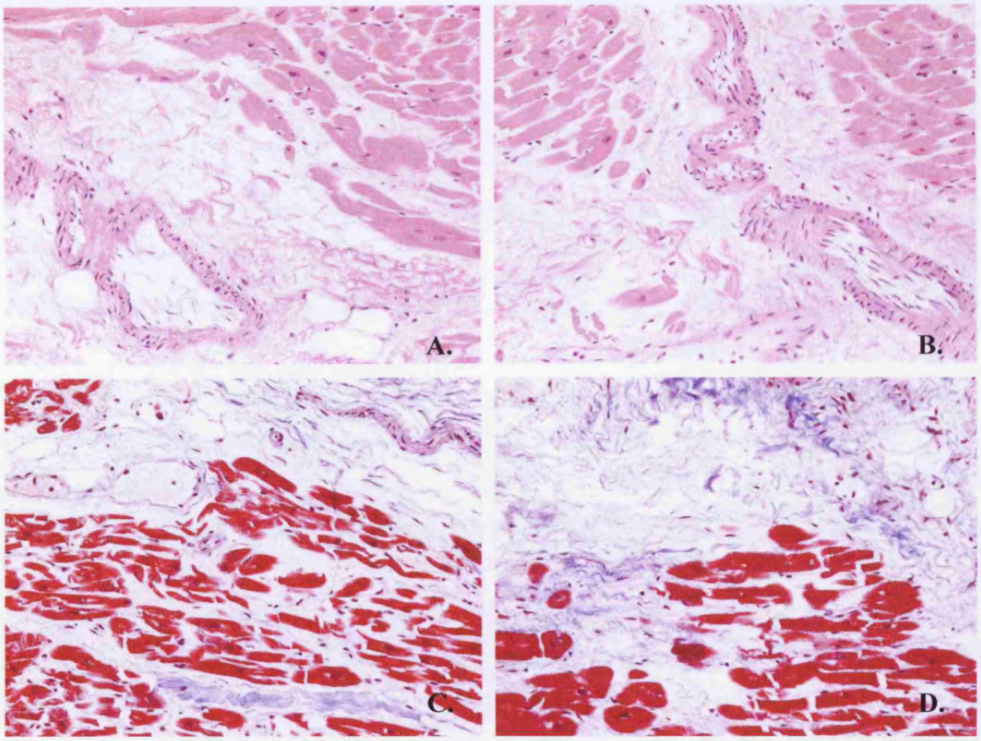

Figure 10: Heart autopsy samples from a male in his early teens who was diagnosed with ARVC postmortem were stained with H&E (A and B) and Masson's trichrome (C and D). Magnification x20 in all images. Samples A and C were obtained from the LV, while samples B and D were obtained from the RV.

A220.1:

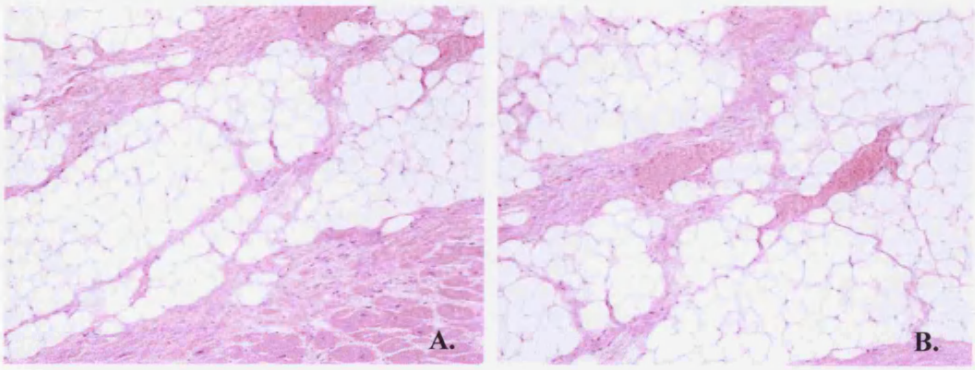

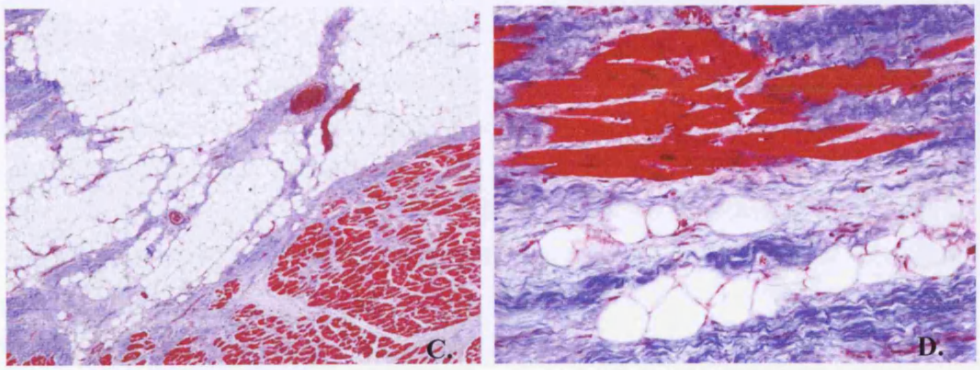

Figure 11: Heart autopsy samples from a male in his mid-40s who was diagnosed with ARVC postmortem were stained with H&E (A and B) and Masson's trichrome (C and D). Magnification x4 (C), x10 (A and B) and x20 (D). Sample D was obtained from the LV, while samples A, B and C were obtained from the RV.

Among the 9 individuals examined, 2 were carriers of desmoplakin mutations, 1 was a carrier of a plakoglobin mutation, 2 were carriers of plakophilin2 mutations, 1 was a carrier of a desmoglein2 mutation and 3 individuals, diagnosed with ARVC postmortem, were at the time screened for mutations in plakoglobin and desmoplakin and found negative (Table 3).

ARVC case	Figure	Mutation	Outcome
A1.1	**3**	**DP**: R1113X	Nonsense, premature truncation
A208.1	**4**	**DP**: 1218+1G→A	Splice site, premature truncation
D0074	**5**	**PG**: S39_K40insS	Insertion, additional serine residue
GR3	**6**	**PKP2**: V837fsX930	Deletion, premature truncation
A188.1	**7**	**PKP2**: 2146-1G→C	Splice site, exon skipping
Family A, III: 4	**8**	**DSG2**: C591X	Nonsense, premature truncation
A176.1	**9**	Unknown	-
A223.1	**10**	Unknown	-
A220.1	**11**	Unknown	-

Table 3: ARVC-causing mutations of patients examined histologically.

In A208.1 (Figure 4), A1.1 (Figure 3) and A176.1 (Figure 9) there is massive fibrofatty infiltration in the RV while in the LV, cardiac myocytes are primarily replaced by fibrotic tissue. In A188.1 (Figure 7), A III: 4 (Figure 8) and A2201. (Figure 11) there is extensive fibrofatty replacement in both ventricles. In particular, in A188.1 there is also evidence of disarray amongst the residual myocytes of the RV, but not of the LV, which is typically a characteristic of HCM instead of ARVC. This case provides another piece of evidence for the great phenotypic variation characterizing the disease. In D0074 (Figure 5), there is fibrofatty replacement in the RV. A biopsy from the LV was not obtained. Clinically, the proband does not show evidence of left ventricular disease however this does not preclude the possibility of minor histological abnormalities being present in the LV muscle. Finally, in GR3 (Figure 6) and A223.1 (Figure 10) there is only fibrous tissue embedding residual myocytes in the RV and in both ventricles respectively. Collectively in all cases, a marked decrease in myocardial fibers with myocardium usually replaced with an inconstant amount of fat and/or fibrous tissue was evidenced. Noteworthy, at higher magnification, degeneration of the remaining myocytes with dystrophic and pyknotic nuclei was detected; a typical characteristic of cell death.

Discussion:

Embryologically the heart, like the rest of the cardiovascular system, develops from a tubular channel. Its basic organization of tissues is divided into three layers: the endocardium, the myocardium and the epicardium. The myocardium is the thickest layer and consists primarily of cardiac myocytes with intervening connective tissue, blood vessels and nerves. In the normal heart, a certain amount of fatty tissue is always present within the myocardium of the RV free wall particularly at the level of the antero-lateral and apical regions. However, this fatty infiltration is not associated with fibrosis, is confined to specific areas, occupies less than 3% of the myocardium and the cardiac muscle fibers seem to be pushed apart by the fat rather than degenerating.[228] Histologically, cardiac muscle consists of myocytes (fibers) of about 15-20 μm diameter and 120 μm length. Cells are branched and are joined to each other at their ends by intercalated discs. Under a light microscope, cardiac muscle shows a number of cross-striations which represent the Z-discs. Each myocyte has one or two nuclei, sited centrally. The region around each nucleus is filled with mitochondria, Golgi apparatus and glycogen (Figure 2).[229]

The analysis of a large series of SCDs from the Veneto region of Italy prompted the subdivision of the ARVC pathology into 2 distinct patterns based on the nature of myocardial replacement: if myocytes are replaced by fat it is recognized as the fatty or

lipomatous pattern, while if myocytes are replaced by fat as well as by fibrous tissue, it is recognized as the fibrofatty or the fibrolipomatous pattern.[230] In the fatty variant, the adipose tissue reaches the endocardium (transmural infiltration) and the wall thickness may even increase (pseudo-hypertrophy). The antero-lateral and infundibular regions are usually affected, whereas the postero-inferior wall appears normal. Small areas of fibrous tissue, usually focal and only detectable at higher magnification power may exist but could be overlooked with limited histological sampling. This fatty pattern is usually confined to the RV, sparing both the septum and the LV, with only occasional cases of aneurysms. [231,232] *Burke et al.* reviewed 25 hearts from SCD with either pattern.[233] Most of the patients with the lipomatous pattern were female, they were significantly older, none had a history of arrhythmia or family history of arrhythmia and SCD and in almost every case, there were one or more factors present that could possibly have contributed to the SCD of the patient.[233] In the fibrofatty variant, the wall is thinner and translucent, and in nearly 50% of the cases, saccular aneurysms are visible at the apex, the infundibulum or at the postero-inferior wall. Involvement of the ventricular septum occurs in 20% and of the LV in 47% of the cases. At histology, myocardial substitution by extensive replacement-type fibrosis and fatty tissue is evident, with aspects of myocyte degeneration, features indicating an injury and repair process. The fibrofatty variant also exhibits in two thirds of the cases inflammatory cell infiltrates associated with focal myocyte necrosis. This pattern seems more prone to electrical instability and SD and may progress with time to heart failure.[232] Following this distinction though, the controversy arose as to whether pure fatty replacement of the RV actually represented a true pathologic entity.[234]

The current belief is that pure fatty infiltration is an entity that should not be considered as ARVC and that is not necessarily a cause of death when identified at autopsy. A diagnosis of "sudden cardiac death in a heart with extensive RV fatty infiltration" would be better, because it does not imply a cause-effect relationship and leaves the door open for other hypotheses on the final cause of death. [235] Fat is possibly the least reliable criterion for the diagnosis of ARVC and should be viewed in conjunction with other histopathological features that refer to both myocytes and fibrous tissue deposition. In keeping with the current belief, all cases presented herein are of the fibrolipomatous pattern and involve a wide spectrum of histological abnormalities in association with the evident fatty infiltration. When a pathologist is dealing with a case of SCD in which the only morphologic finding consists of an increased amount of fat, a more convincing arrhythmogenic substrate, such as myocardial inflammatory infiltrates, fibrosis, anomalous pathways and ion channel disease should always be searched for to avoid over-diagnosis of ARVC. The expectation is that molecular biology will make a difference in cases where the differential diagnosis is difficult to consent to a

postmortem genetic diagnosis. Meanwhile, the need to adopt strict diagnostic criteria is warranted not only in the clinical setting, but also in the pathology arena. These criteria are mandatory both for epidemiological purposes and for clinical implication, since the identification of a genetic disease as the cause of an individual's death is the starting point for familial screening and consequently timely disease management and prevention of SCD. [228]

Of note is that the individuals where only fibrotic replacement was observed (GR3 and A223.1) were significantly younger than the rest of the group. Also, in A208.1, A1.1 and A176.1 there was fibrofatty replacement in the RV, while there was primarily fibrous tissue embedding the residual myocytes in the LV. These observations help enlighten our knowledge when it comes to the evolution of ARVC. The disease advances with age, and the LV involvement becomes increasingly severe. *Fletcher et al.* suggested that in the context of ARVC, muscle is gradually replaced by fibrosis first in the RV and then in the LV, which changes to fat as the disease advances. The presence of fat may explain why older people present with heart failure, while the predominance of fibrosis in the younger age may explain sudden death.[236] This hypothesis, currently widely accepted, is in contrast with the evolutionary pathway suggested by *Fontaine et al*, according to whom myocarditis is superimposed on the background of myocardium interspersed by fat, eventually transforming the fatty to the fibrofatty form.[237]

The question therefore arises whether there is a role for myocarditis in the frame of ARVC. The inflammatory/infective theory supports that the disease is expressed in the presence of a viral trigger. This theory does not exclude a familial occurrence, since genetic alteration regarding host immunological status or myocyte receptor may predispose the patient to viral infection. However, this theory can not explain the large number of ARVC cases where no evidence of inflammation and/or infection is present. It is therefore more likely that a genetic alteration, instead of predisposing the patient to viral infection, may bring about by itself changes of structural and functional proteins. In this case, the possible viral genome or inflammatory infiltrate detection in ARVC should be interpreted differently. The viral agent might either be an innocent bystander or play a secondary but still important role, such as promoting ventricular arrhythmias by itself.[238] *Hoffman et al.* studied reperfusion arrhythmia and demonstrated for the first time the role played by the activation of neutrophils in producing early after-depolarizations.[239] These results demonstrate a direct link between inflammation and an electrophysiological phenomenon that is a possible trigger of arrhythmias.[240]

In 2000, a 40-year old woman with a clinical diagnosis of DCM underwent cardiac transplantation. [241] Upon gross examination of the heart, the clinical diagnosis was challenged and the pathologic diagnosis of ARVC was given instead. Histologically,

myocytes adjacent to the adipose tissue showed multiple sarcoplasmic vacuoles, ultrastructurally confirmed as lipid droplets. This case posed a dilemma when it comes to the foundations of ARVC: do cardiac muscle cells transform into adipocytes, or do they undergo apoptosis and subsequently get replaced by fat and fibrous tissue?

In 1996 the case of an infant, who died aged 7 weeks from heart failure was presented.[242] Microscopic examination of the heart showed massive apoptotic destruction of the RV, sparing the LV and both atria. *James et al.* argued that postnatal, the RV wall is excessively but disadvantageously thick and that programmed cell death is responsible for reducing the thickness of the wall to achieve optimal conduction and function.[242] *James et al.* suggested that in the case of this infant, apoptosis started but was not "turned off".[242] ARVC is rarely manifested in infancy and becomes fully penetrant in adolescence. It would therefore seem impossible that non-switching off of the postnatal apoptotic process is responsible for this entity. There is however a role for apoptosis

Apoptosis in all metazoan cells is mediated by caspases, a multi-gene family of cysteine proteases that hydrolyze peptide bonds. Synthesized as zymogens, pro-caspase activation involves cleavage and re-association of two fragments into a functional holo-enzyme. Caspases can be activated by at least two mechanisms: either already activated upstream caspases cleave pro-caspases or certain pro-caspases can be auto-activated when forced in close proximity through interactions with other proteins.[243] *Nishikawa et al.* examined the apoptotic index in a number of pediatric ARVC cases, where no profound structural abnormalities were present versus a number of adult cases, where significant fibrofatty replacement was evident.[244] There was no statistically significant difference in the numbers obtained suggesting that apoptosis was a primary phenomenon that preceded fibrofatty degeneration.[244] The precise triggering factors for apoptotic myocardial death though, remain to be elucidated.[55] If we accept that mutations in the RyR2 gene may underlie certain cases of ARVC, we could claim that altered levels of Ca^{+2} could be triggering apoptosis. Moreover, plakoglobin, the gene found to underlie Naxos disease, is an apoptotic inhibitor,[245] thus a mutation that impairs the function of this protein, could be affecting the balance of programmed cell death. As mentioned at the beginning of the chapter, mutations in one junctional component may alter the expression levels and distribution patterns of other adhesion molecules. It can therefore be hypothesized that alterations in the localization of plakoglobin due to primary defects in other desmosomal proteins, could promote myocyte cell death. Furthermore in certain cases the super-imposed presence of inflammatory infiltrates could be involved in the propagation of programmed cell death. Finally, mutations in genes involved in programmed cell death, such as CPP-32 cannot be ruled out and have to be examined in the future.

2) Histological and microscopic examination of ARVC skin samples:

Skin biopsy samples were obtained from an ARVC patient bearing a nonsense mutation in DSG2 (A, III: 4, **pg. 98-100**) and an ARVC patient, found to be a compound heterozygous for two novel nonsense desmoplakin mutations (A131.1, **pg. 74-79**). The skin samples were stained with H&E and examined under a light microscope. An additional skin sample was obtained from A III: 4 and processed accordingly for electron microscopy examination. Characteristic images and observations are presented below.

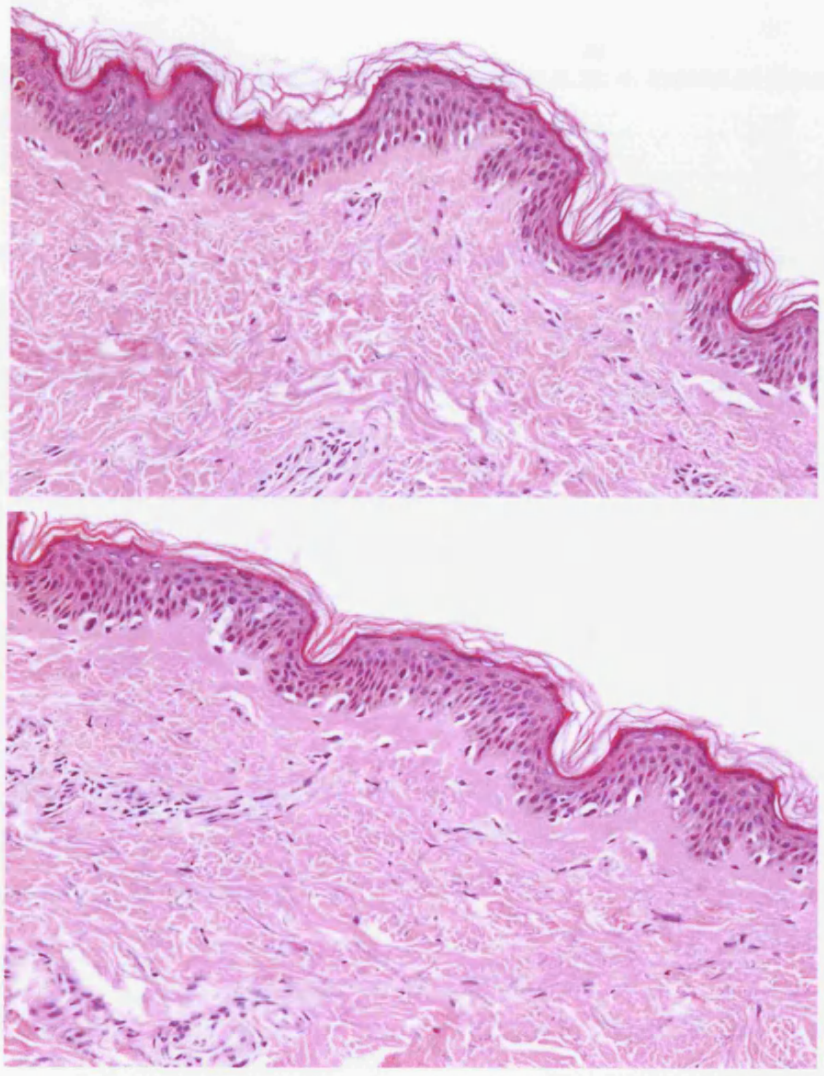

Figure 12: H&E staining of a skin biopsy sample obtained from A, III: 4 (magnification x20).

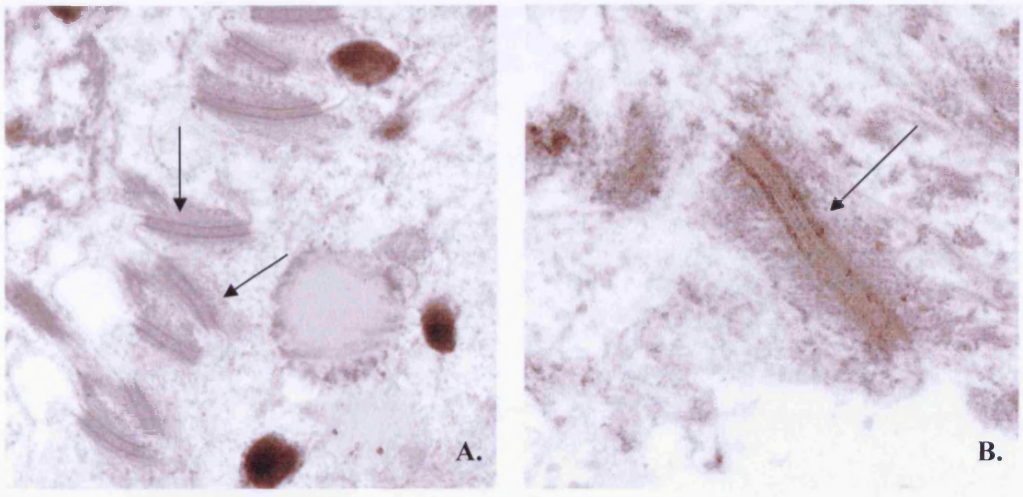

Figure 13: Electron microscopy of a skin section from A III: 4. Individual desmosomes are indicated by the arrows.

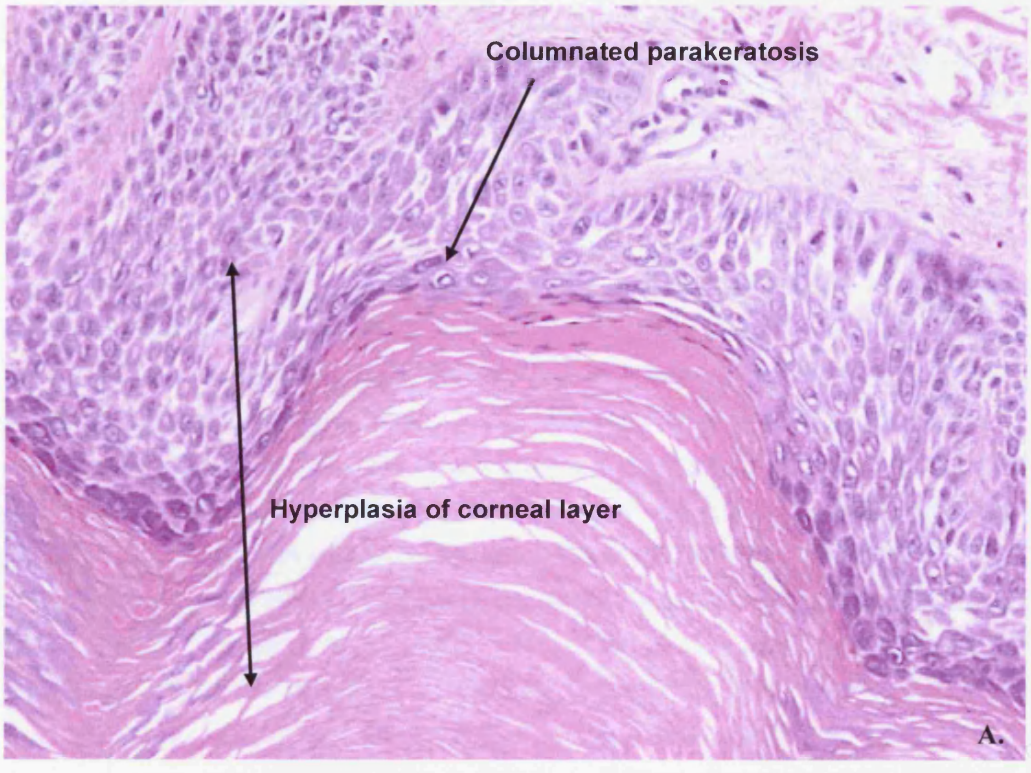

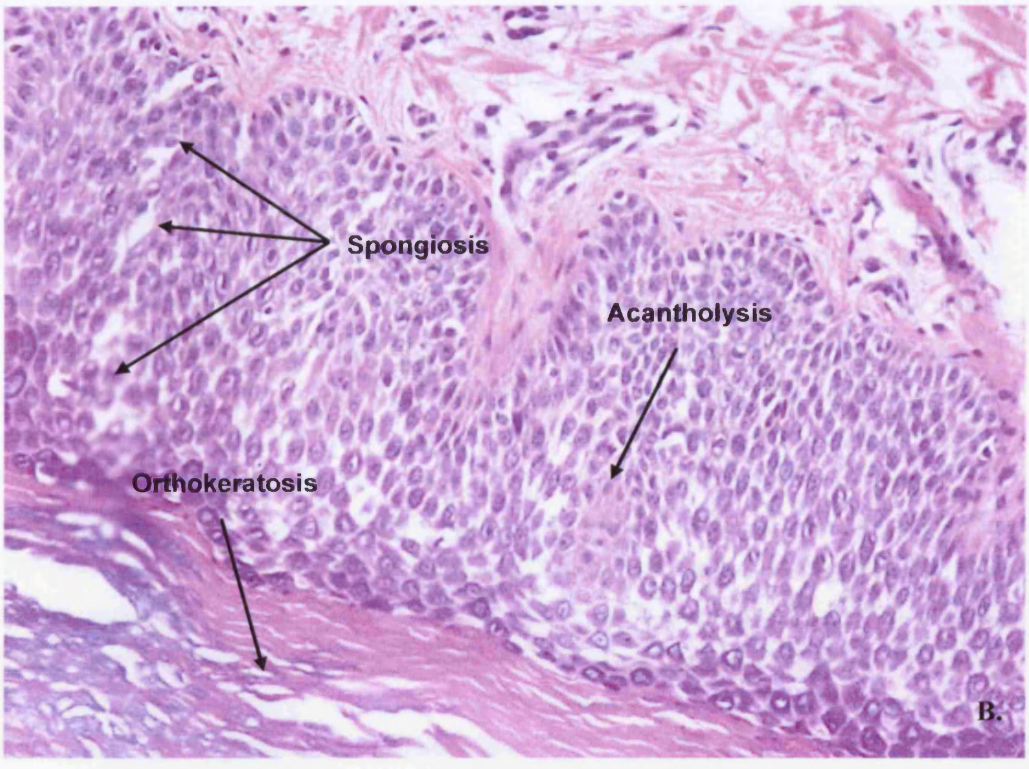

Figure 14: Microscopic appearance of a plantar skin biopsy sample obtained from A131.1 (magnification x40).

Discussion:

The human skin is composed of three primary layers: the epidermis, the dermis and the hypodermis. The epidermis, the outermost layer of the skin, forms the waterproof protective wrap over the body's surface and is made up of stratified squamous epithelium and an underlying basal lamina. The main type of cells that make up the epidermis are keratinocytes while melanocytes and Langerhans cells are also present. It can be further sub-divided into the stratum corneum, the stratum lucidum, the stratum granulosum, the stratum spinosum and the stratum germinativum, also known as the stratum basale. Cells are formed through mitosis at the basale layer. The daughter cells move up the strata changing shape and composition as they die due to isolation from their blood source. The cytoplasm is released, keratin is inserted while the cells finally reach the stratum corneum and slough off, a process known as desquamation.[246]

A skin sample was obtained from a female individual diagnosed with ARVC and processed for histological and electron microscopy examination. A III: 4 (**pg. 98-100**) is a carrier of a nonsense mutation in DSG2, which causes premature termination of translation within the extracellular portion of the protein. No microscopic abnormalities

were evident under the light microscope (Figure 12), and similarly, both the number and structure of desmosomes appeared normal under the electron microscope (Figure 13). The observations indicate that possibly other desmoglein isoforms (primarily DSG1 and DSG3) can compensate for the defect in DSG2 in the patient's skin, therefore preventing the development of cutaneous abnormalities.

On the other hand, the plantar skin biopsy sample obtained from A131.1 (**pg. 74-79**) showed marked hyperplasia of the corneal layer (hyperkeratosis) and suprabasal clefting between the granular and keratin layers, mimicking acantholysis. The stratum spinosum demonstrated widening of the intercellular spaces, a feature known as spongiosis, supporting the finding of a cell adhesion defect underlying the disease. The basal cells however appeared normal (Figure 14). The proband was a compound heterozygote for two desmoplakin mutations (Q673X and Q1446X), which both lead to premature termination of translation within the N-terminal and the central domain of the protein respectively. Lack of desmoplakin tails can be compatible with life as cells bearing the truncated protein can still assemble unless they are subjected to stress. This can explain why the proband's basal epidermal layer appeared normal in the histological examination, as it is subjected to less stress compared to the suprabasal layers. Another plausible explanation could be that the lack of an intact desmoplakin peptide can be compensated by another member of the plakin family or that IF assembly is differentially controlled at the basal layers. No other desmoplakin mutation carrier of those presented in Chapter 1 showed any gross cutaneous abnormalities. This can be explained by the fact that apart from A131.1, all other patients examined had one complete functional desmoplakin allele which might have been enough to maintain epidermal integrity. However, skin samples from individuals bearing the desmoplakin mutations presented in Chapter 1 were not obtained; therefore the presence of minor histological or ultrastructural abnormalities cannot be excluded.

3) Immunohistochemistry; mechanical adhesion molecules:

A number of tissue samples from individuals diagnosed with ARVC, were stained for selected mechanical adhesion proteins and examined by confocal microscopy. Samples were obtained both from patients with an identified ARVC-causing mutation and from patients with an un-identified pathogenic mechanism. A total of 13 heart and 4 skin samples were examined. Three heart and three skin samples from individuals with no history of heart disease were subjected to the same immunostaining protocol and used for control purposes. Since only once specimen per case was available, statistical analysis could not be performed.

Naxos disease & Carvajal syndrome:

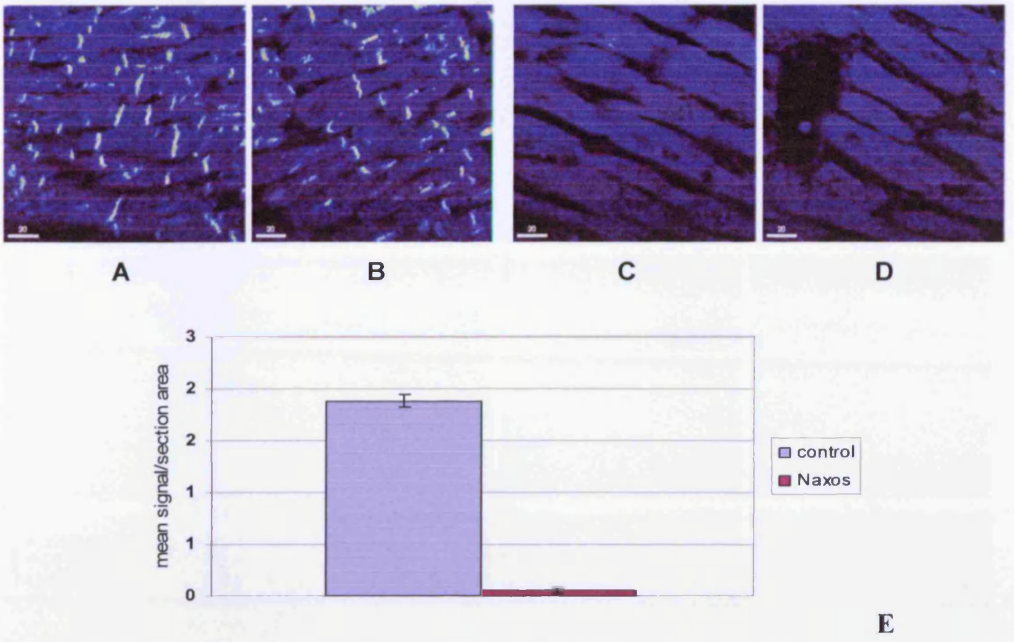

Figure 15: Immunostaining against plakoglobin in control heart tissue (A, B) and in tissue from a patient with Naxos disease (C, D). Confocal quantitative analysis (E). The error bars represent standard deviations.

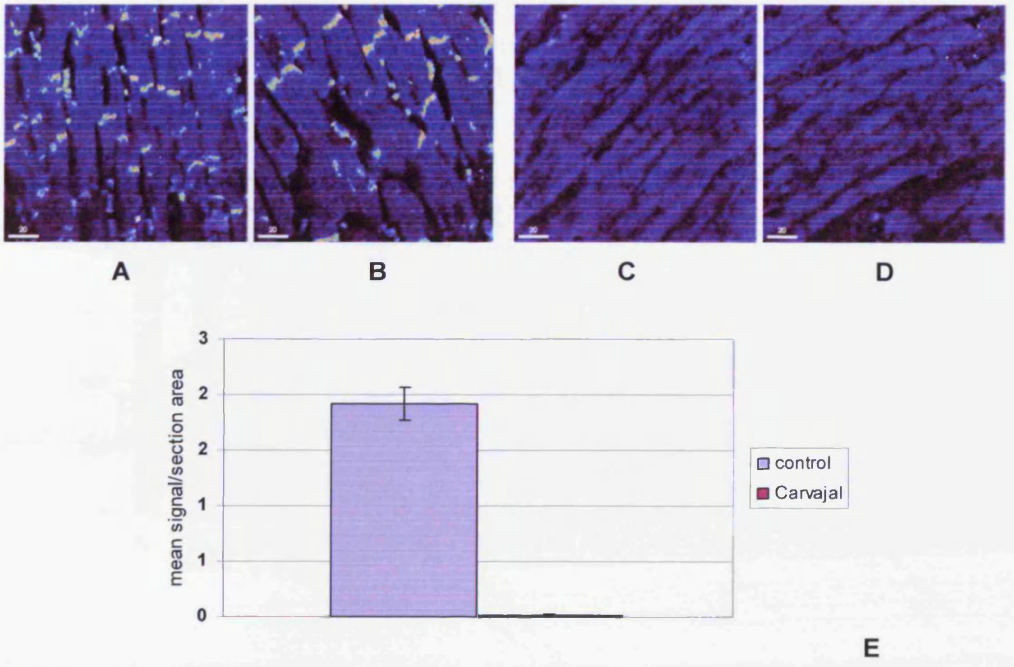

Figure 16: Immunostaining against desmoplakin in control heart tissue (A, B) and in tissue from a patient with Carvajal syndrome (C, D). Confocal quantitative analysis (E). The error bars represent standard deviations.

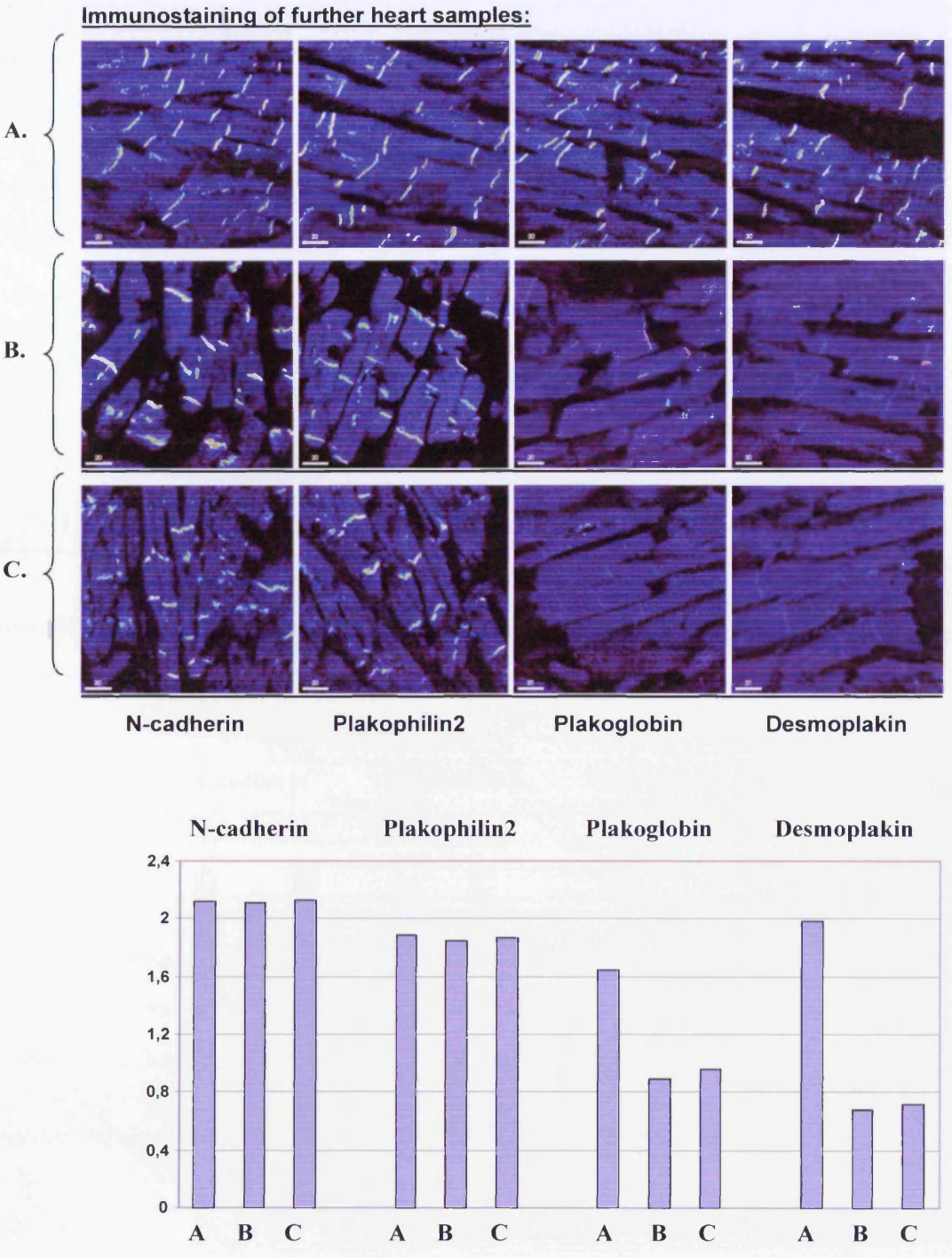

Figure 17: Immunostaining against N-cadherin, plakophilin2, plakoglobin and desmoplakin in control heart tissue (A) and in two ARVC patients with identified desmoplakin mutations (B and C). The graph shows quantitatively the mean signal per protein, per sample as measured by confocal microscopy.

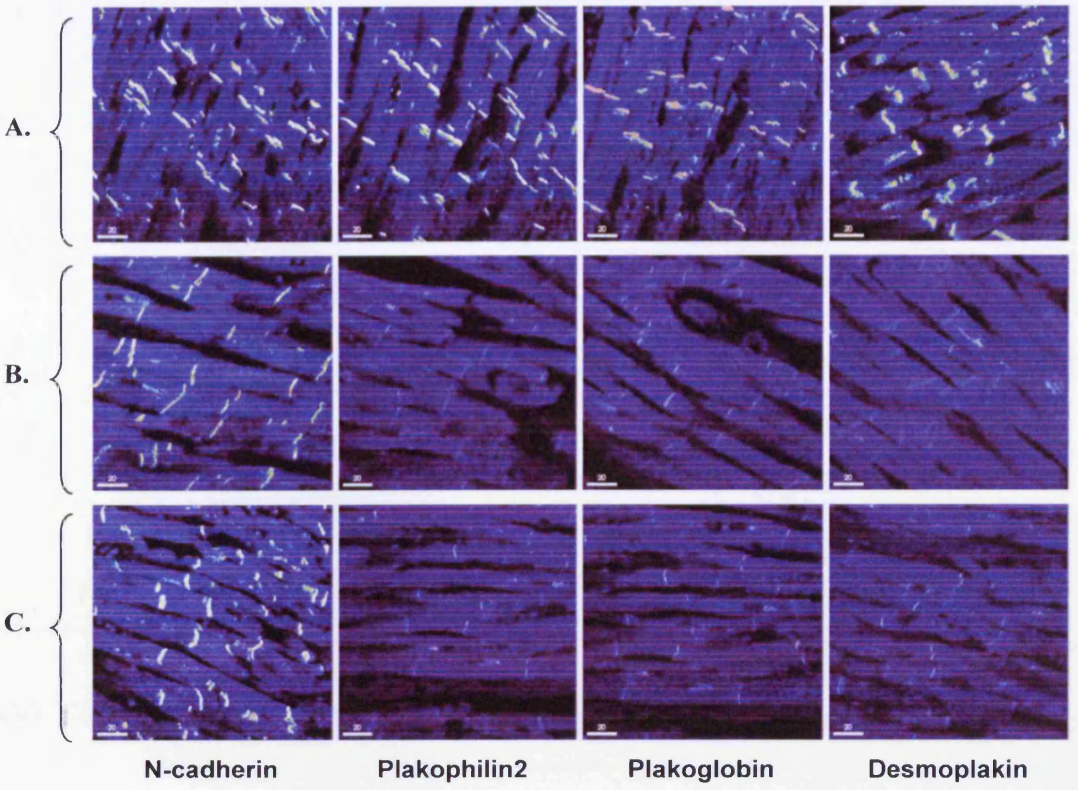

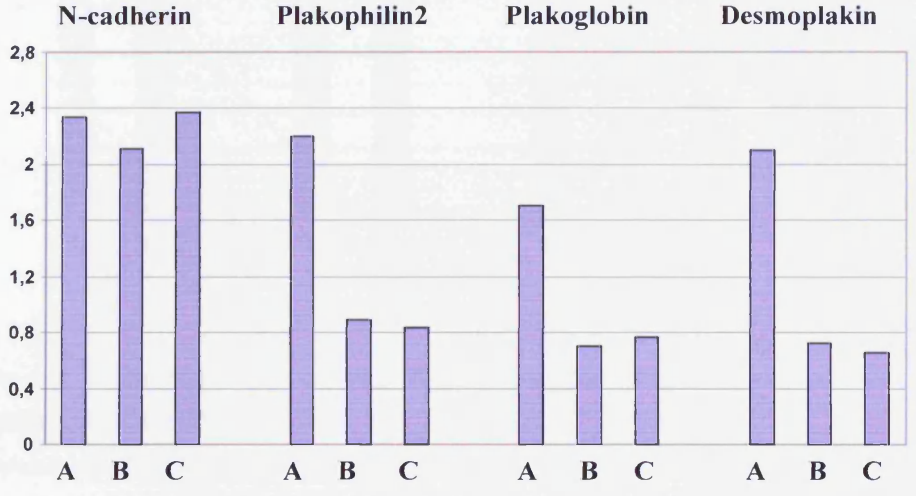

Figure 18: Immunostaining against N-cadherin, plakophilin2, plakoglobin and desmoplakin in control heart tissue (A) and in two ARVC patients with identified plakophilin2 mutations (B and C). The graph shows quantitatively the mean signal per protein, per sample as measured by confocal microscopy.

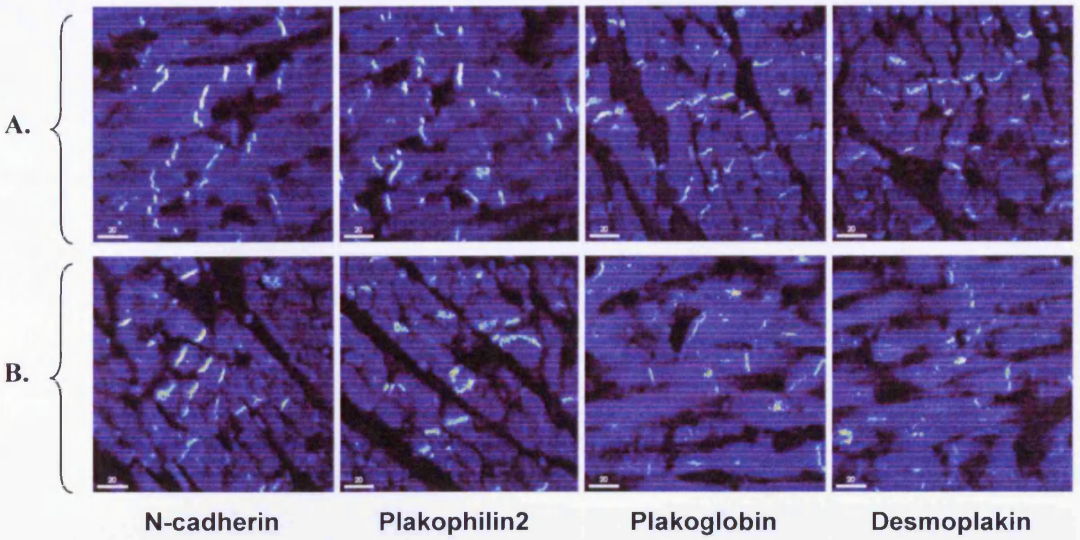

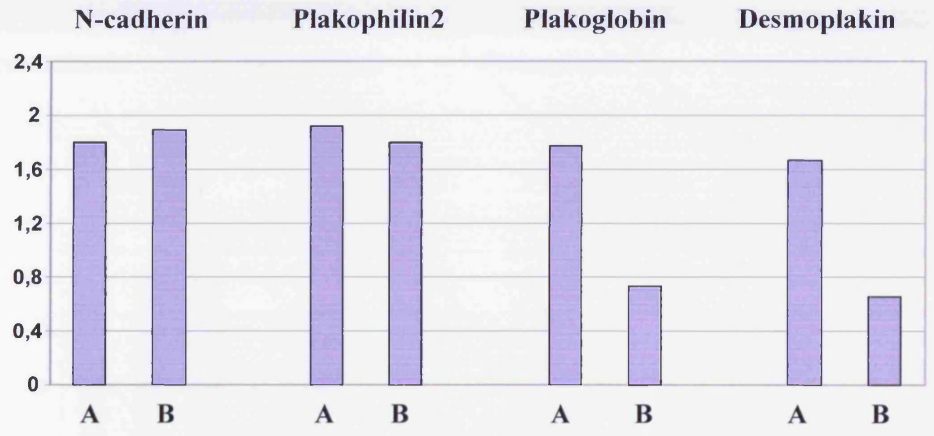

Figure 19: Immunostaining against N-cadherin, plakophilin2, plakoglobin and desmoplakin in control heart tissue (A) and in an ARVC patient with an identified plakoglobin mutation (B). The graph shows quantitatively the mean signal per protein, per sample as measured by confocal microscopy.

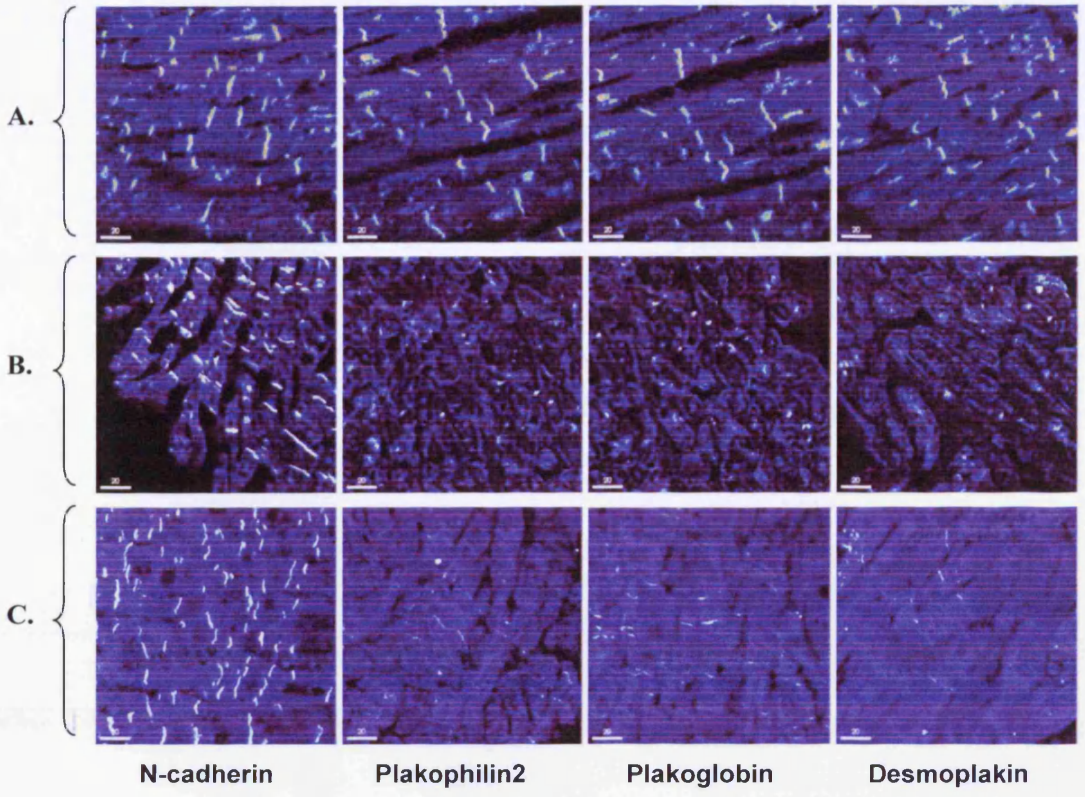

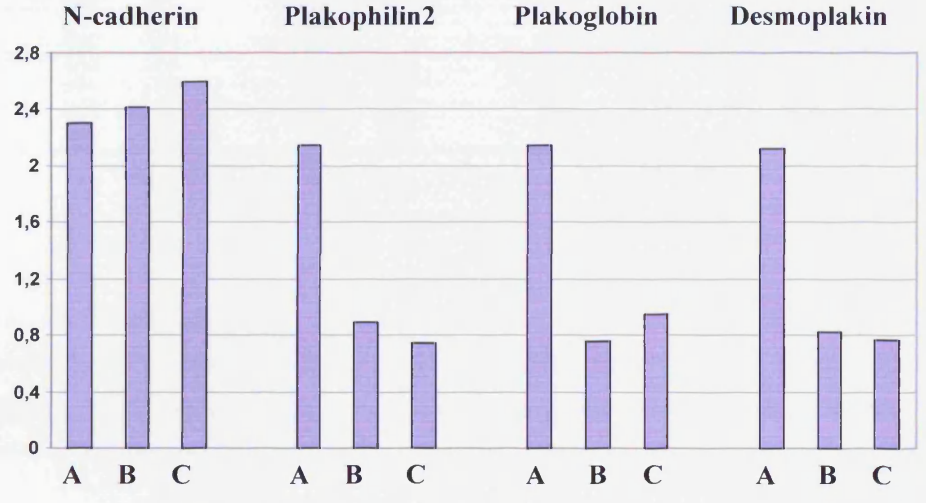

Figure 20: Immunostaining against N-cadherin, plakophilin2, plakoglobin and desmoplakin in control heart tissue (A) and in two ARVC patients with identified desmoglein2 mutations (B and C). The graph shows quantitatively the mean signal per protein, per sample as measured by confocal microscopy.

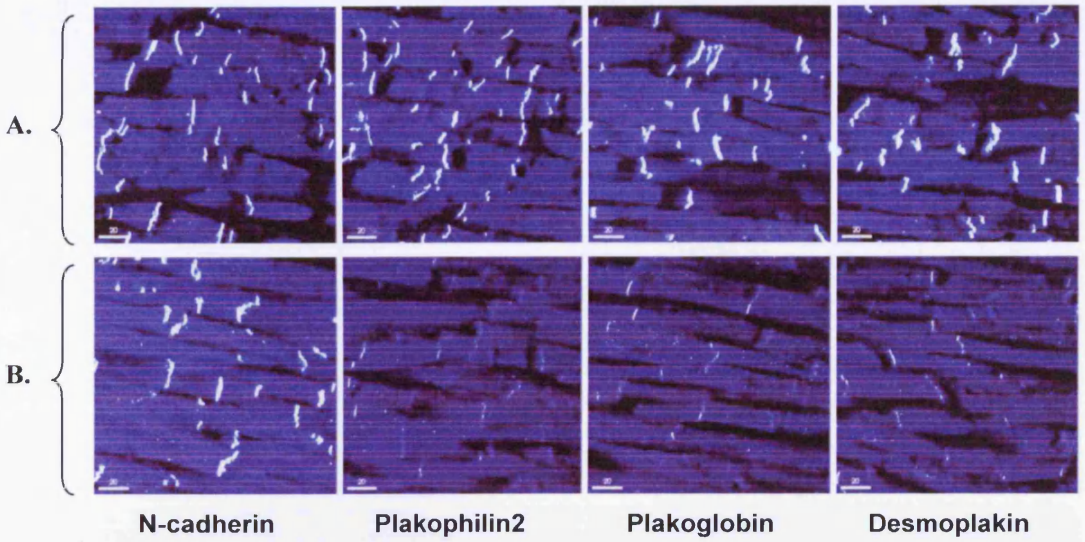

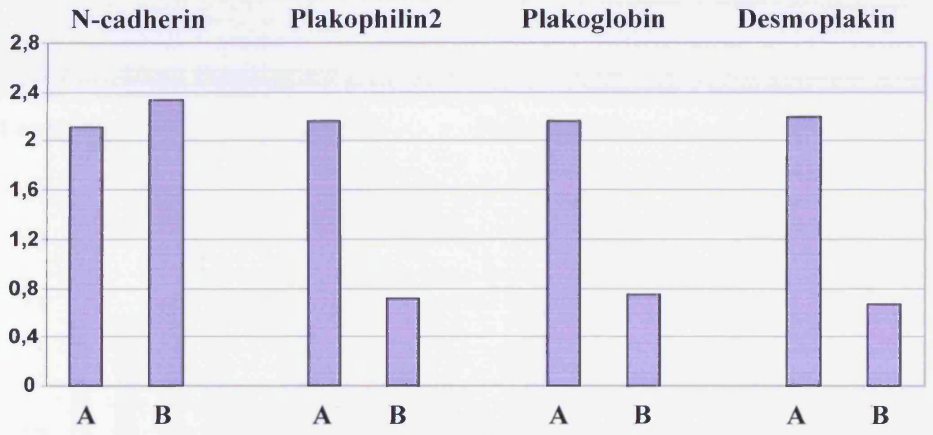

Figure 21: Immunostaining against N-cadherin, plakophilin2, plakoglobin and desmoplakin in control heart tissue (A) and in an ARVC patient bearing a desmoplakin and a plakophilin2 mutation (B). The graph shows quantitatively the mean signal per protein, per sample as measured by confocal microscopy.

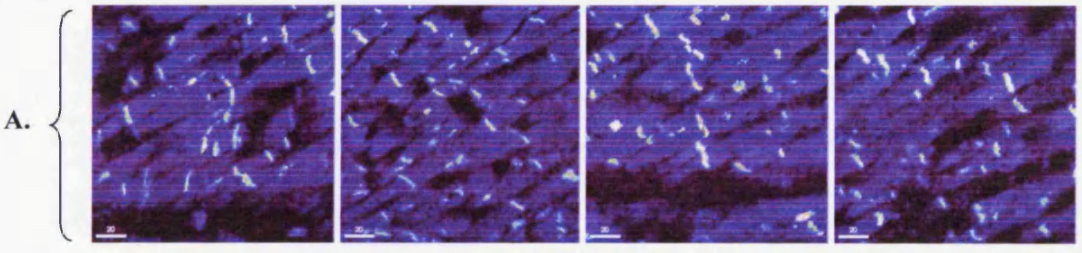

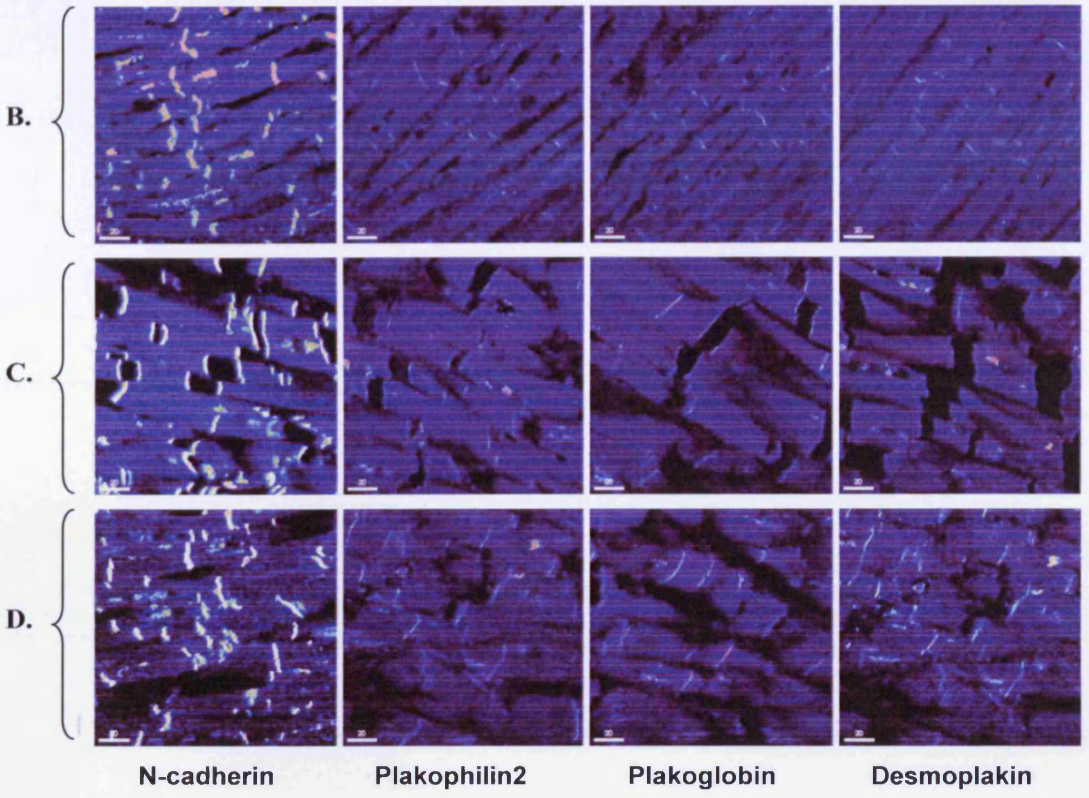

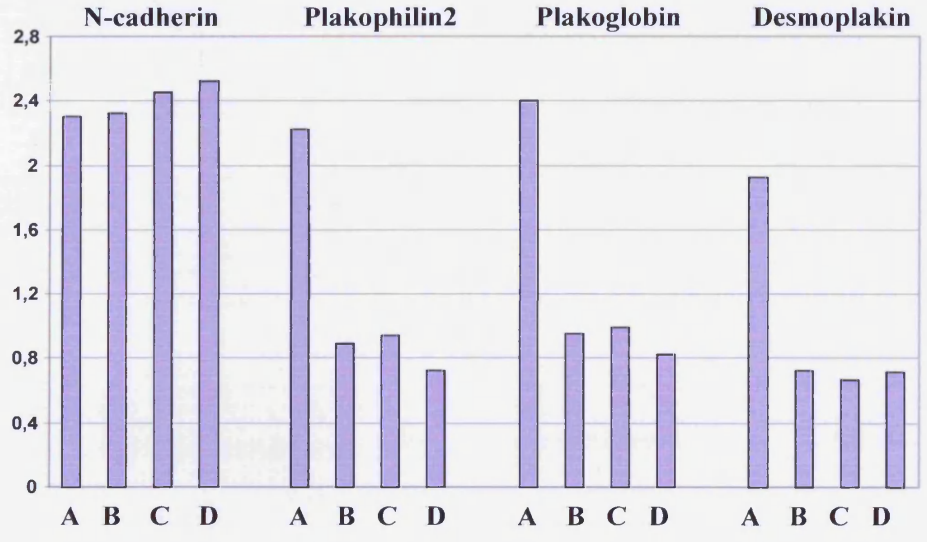

Figure 22: Immunostaining against N-cadherin, plakophilin2, plakoglobin and desmoplakin in control heart tissue (A) and in 3 ARVC patients with non-yet identified pathogenic mutations (B, C and D). The graph shows quantitatively the mean signal per protein, per sample as measured by confocal microscopy.

In both specimens obtained from individuals with an identified ARVC-causing desmoplakin mutation (1218+1 G→A, R1113X), the immunoreactive signal for desmoplakin and plakoglobin was significantly reduced at cell junctions compared to controls, while there was no obvious difference in the expression levels of N-cadherin and plakophilin2 (Figure 17). The same was true for the sample obtained from the individual with a plakoglobin ARVC-causing mutation (S39_K40insS, Figure 19). In both specimens obtained from individuals with an identified ARVC-causing plakophilin2 mutation (2146 -1G→C, V837fsX930), the immunoreactive signal for all plakophilin2, desmoplakin and plakoglobin was significantly reduced at cell junctions compared to controls, while there was no obvious difference in the expression levels of N-cadherin (Figure 18). The same was true for the samples obtained from the two individuals with a desmoglein2 ARVC-causing mutation (C591X, T335A, Figure 20) and from the compound heterozygous for a desmoplakin and a plakophilin2 mutation (DP R270X, PKP2 R735Q,Figure 21). Finally, in all three specimens with unidentified molecular changes, plakophilin2, desmoplakin and plakoglobin were all down-regulated at the cell junctions compared to controls, while the levels of N-cadherin were undistinguishable (Figure 22). All 8 positively genotyped individuals were heterozygous carriers of the respective mutations. Though reduced, there was still immunoreactive signal at cell junctions corresponding to the "pathogenic" protein (i.e. the protein encoded by the mutant gene). Conversely, immunostaining for plakoglobin in a Naxos disease specimen (Figure 15) and desmoplakin in a Carvajal syndrome specimen (Figure 16) rendered no signal, highlighting the difference between homozygous and heterozygous carriers of ARVC-causing mutations. The results obtained are summarized in Table 4.

Specimen	N-cadherin	PKP2	DP	PG
Carvajal syn.	Not examined	Not examined	**Immeasurable**	Not examined
Naxos disease	Not examined	Not examined	Not examined	**Immeasurable**
A208.1 (DP)	Unaltered	Unaltered	**Reduced**	**Reduced**
A1.1 (DP)	Unaltered	Unaltered	**Reduced**	**Reduced**
D0074 (PG)	Unaltered	Unaltered	**Reduced**	**Reduced**
A188.1 (PKP2)	Unaltered	**Reduced**	**Reduced**	**Reduced**
GR3 (PKP2)	Unaltered	**Reduced**	**Reduced**	**Reduced**
A,iii:4 (DSG2)	Unaltered	**Reduced**	**Reduced**	**Reduced**
DanA (DSG2)	Unaltered	**Reduced**	**Reduced**	**Reduced**
A176.1 (u/a)	Unaltered	**Reduced**	**Reduced**	**Reduced**
A220.1 (u/a)	Unaltered	**Reduced**	**Reduced**	**Reduced**
A223.1 (u/a)	Unaltered	**Reduced**	**Reduced**	**Reduced**

Table 4: Immunoreactive signal of ARVC specimens compared to control.

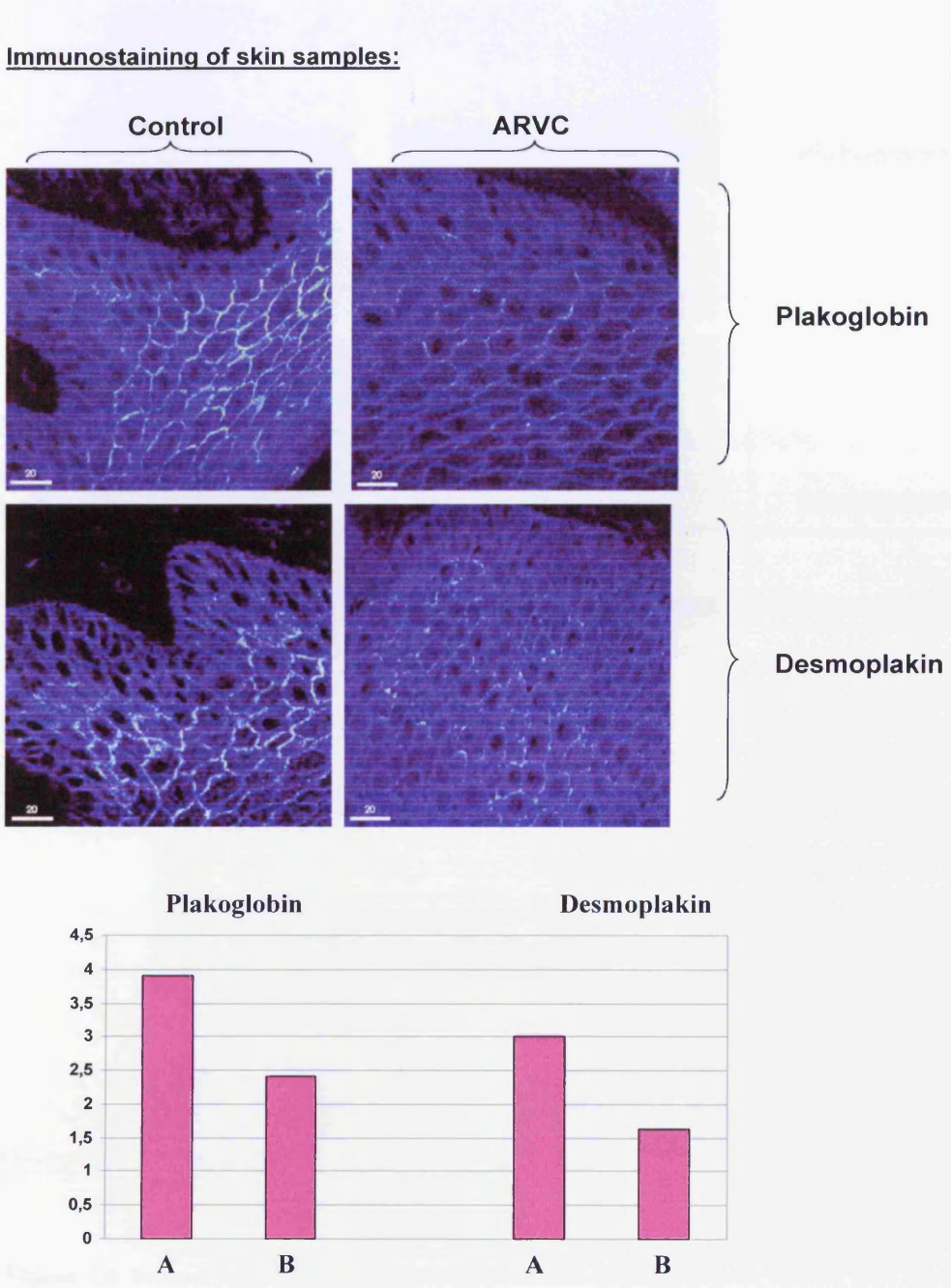

Figure 23: Immunostaining against plakoglobin and desmoplakin in control plantar skin tissue and in a plantar skin sample from an ARVC patient identified as a compound heterozygote for two nonsense desmoplakin mutations. The graph shows quantitatively the mean signal per protein, per sample as measured by confocal microscopy.

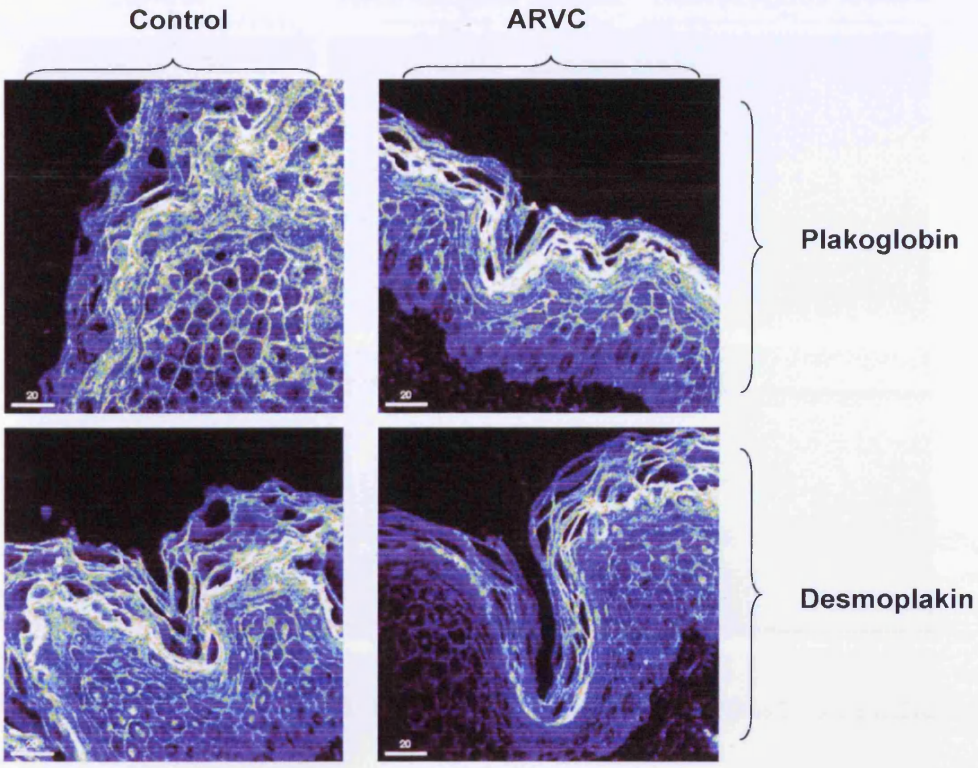

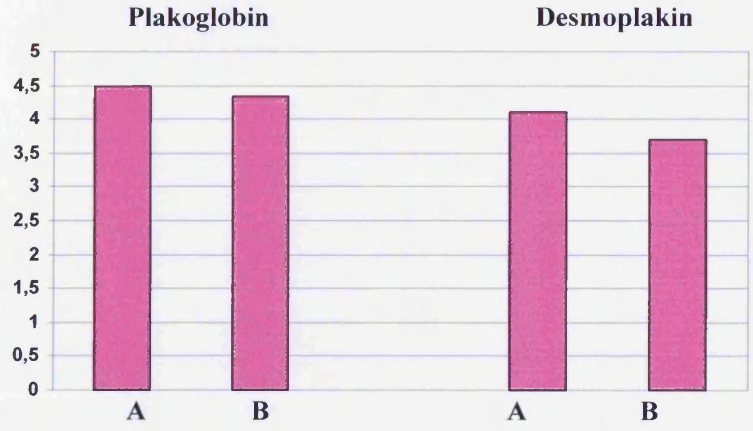

Figure 24: Immunostaining against plakoglobin and desmoplakin in control skin tissue and in a skin sample obtained during an ICD implantation procedure from an ARVC patient heterozygous for a desmoglein2 mutation. The graph shows quantitatively the mean signal per protein, per sample as measured by confocal microscopy.

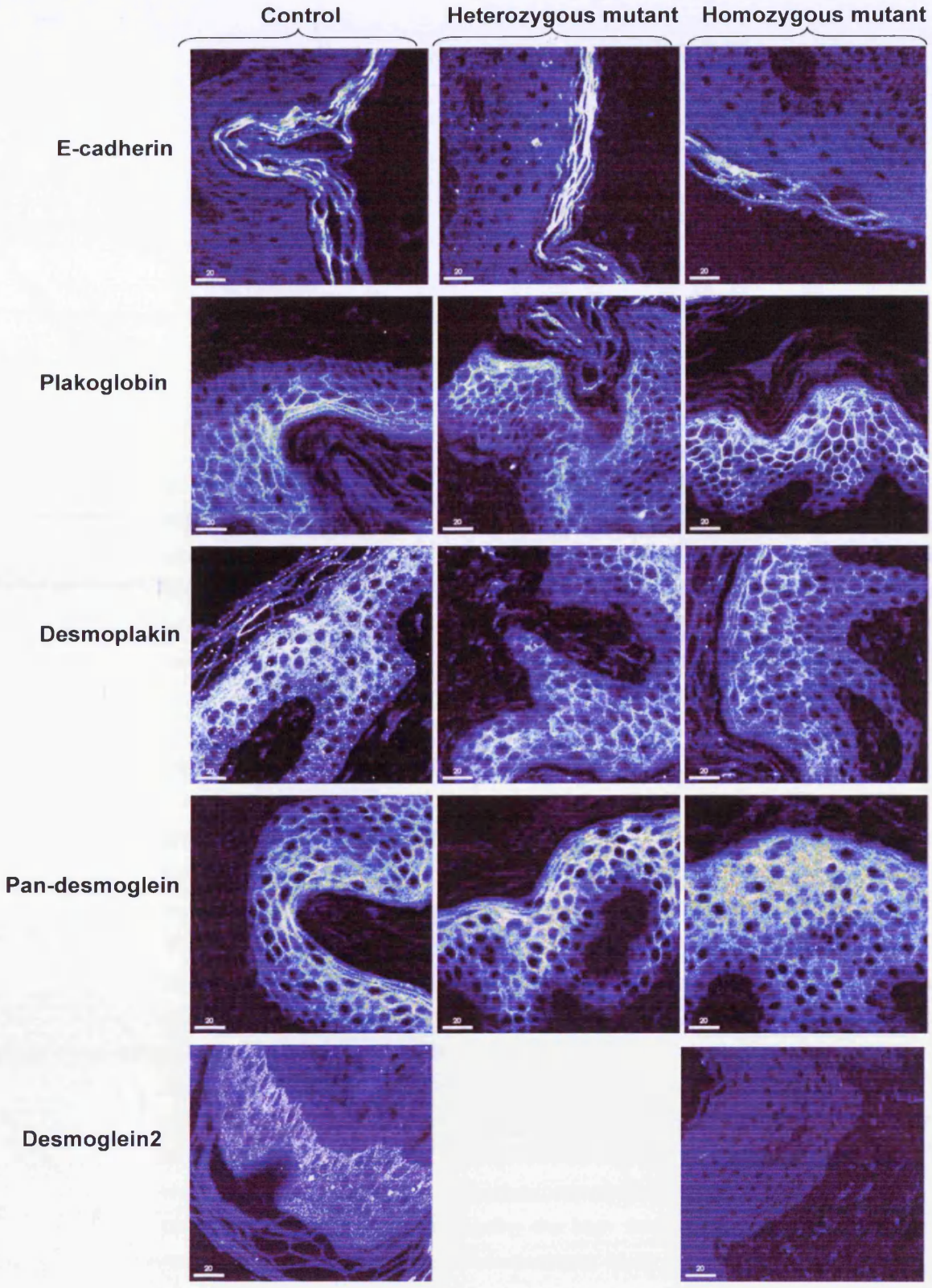
Control
Heterozygous mutant
Homozygous mutant
E-cadherin
Plakoglobin
Desmoplakin
Pan-desmoglein
Desmoglein2

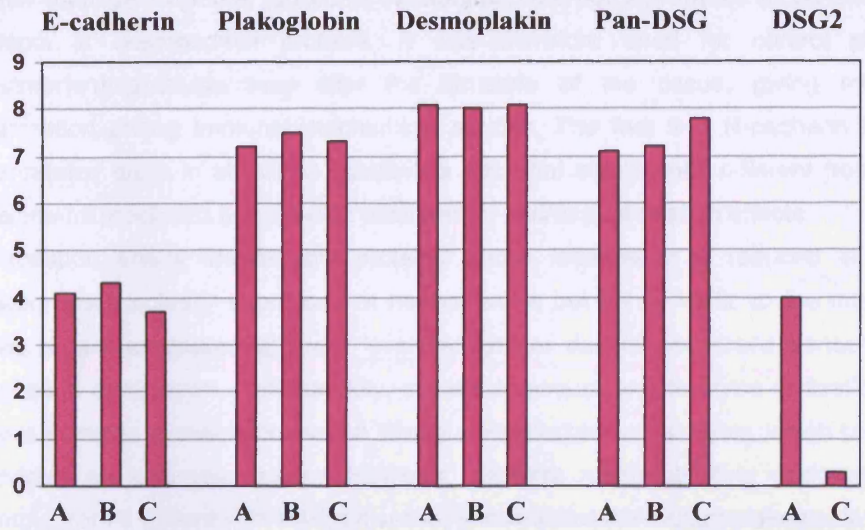

Figure 25: Immunostaining against E-cadherin, plakoglobin, desmoplakin, pan-desmoglein and desmoglein2 in control skin tissue (A), in a skin sample obtained from an ARVC patient heterozygous for a desmoglein2 mutation (B) and an ARVC patient homozygote for the same desmoglein2 mutation (C).The graph shows quantitatively the mean signal per protein, per sample as measured by confocal microscopy.

Discussion:

Immunohistochemistry of heart specimens with antibodies against adhesion molecules gives characteristic images where intercalated discs stand out decorating and adjoining myofibrils. Immunostaining of heart samples from patients with Carvajal syndrome[64] and Naxos disease[226] showed a significant decrease in the immunoreactive signal for desmoplakin and plakoglobin, and for plakoglobin, respectively, leading to the hypothesis that a molecular defect in one structural adhesion molecule may have effects on the localization pattern and expression levels of other desmosomal proteins. A total of 11 heart autopsy/biopsy samples from individuals diagnosed with ARVC were stained for N-cadherin, plakophilin2, desmoplakin and plakoglobin to add further evidence to this hypothesis and draw conclusions that could in the future facilitate timely disease diagnosis and guide genetic screening. Five sections of each specimen were examined quantitatively by confocal microscopy. For each section, the number of pixels with signal intensity exceeding the high threshold was divided by the total number of pixels exceeding the lower threshold. Mean values were then calculated and used to compare protein expression levels between ARVC and control heart samples. All specimens were stained for N-cadherin. Being a major component of adherens,

rather than desmosomal junctions, N-cadherin was not anticipated to be affected by defects in desmosomal proteins. It was therefore used for control purposes. Postmortem autolysis may alter the structure of the tissue, giving misleading information during immunohistochemical studies. The fact that N-cadherin levels at intercalated discs in all ARVC specimens were not significantly different from control specimens precluded non-specific postmortem and/or post-fixation effects.

A question arises whether the proteins whose localization is reduced at the cell junctions are actually expressed at normal levels but fail to traffic to the intercalated discs or are expressed at lower levels altogether due to decreased transcription or increased destruction. Unfortunately, the small amount and the type of fixation of the tissue samples available precluded Western immunoblotting analysis, which could have provided an accurate answer. However, Western immunoblotting performed on a sample from a patient with Naxos disease, showed that the mutant plakoglobin is in fact expressed at control levels in the patients' hearts but fails to make it to the cell membrane.[226] We could therefore hypothesize that the same is true for the cases presented herein, however considering the lack of supporting immunoblotting evidence, at this point, this hypothesis is purely speculative. A possible explanation for the abnormal distribution of desmosomal proteins is outlined below.

It is believed that desmosome assembly depends on the formation of cadherin/catenin complexes as cells which lack E-cadherin/plakoglobin complexes cannot form desmosomes.[247] The head domain of PKP2 is known to bind the N-terminal part of desmoplakin and target it to the membrane.[248] Both individuals A188.1 (Figure 18B) and GR3 (Figure 18C) bear PKP2 mutations that do not affect the head of the protein. Nevertheless since, as shown by the images presented, mutant PKP2 fails to localize at the cell borders in these cases, localization of desmoplakin is expected to be altered as well. The same stands for individual D0074 (Figure 19B), who bears a mutation in plakoglobin. In plakoglobin-deficient keratinocytes, both localization of DP at the cell membrane as shown by immunohistochemistry and expression levels of DP as shown by Western immunoblotting are significantly reduced.[249] Plakoglobin is known to bind desmoplakin and recruit it to the desmosomes. It is therefore understandable how a defect in the gene coding for plakoglobin could lead to altered distribution of desmoplakin in this patient's heart. In another study though, desmoplakin was shown to be able to bind desmosomal cadherins even in the absence of plakoglobin,[250] which could explain the presence of immunoreactive signal, though reduced, at the cell junctions of D0074's heart sample. Furthermore, the head domain of plakophilin2 is able to bind the tails of desmosomal cadherins including DSG1, DSG2, DSC1 and DSC2, and this interaction seems sufficient to drive PKP2 to the cell borders.[154] These

data may explain why PKP2 levels at the cell membrane are not altered in the presence of the S39_K40insS plakoglobin mutation.

Binding of desmogleins to plakoglobin is facilitated by a small region in the cytoplasmic domain of the cadherin molecules and particularly in the intracellular cadherin segment domain.[251] This part of DSG2 would be absent in the specimen obtained from individual A iii: 4 (C591X, Figure 20B), thus impairing interactions between DSG2 and plakoglobin. The cytoplasmic part of DSG2 is also responsible for its interaction with PKP2,[154] which could explain why PKP2 is down-regulated in this specimen. Desmoplakin binds desmosomal cadherins either directly, or through plakophilin2 and plakoglobin. In any case, since DSG2, PKP2 and PG are all mis-localized in the patient's sample, distribution of desmoplakin would also be expected to be affected. Desmosomal adhesiveness is a multi-step process mediated by heterophilic interactions between desmocollins and desmogleins. In particular, the N-terminal domains of the two desmosomal cadherin types bind in a Ca^{+2}-dependent manner.[252] C591X does not affect the N-terminal part of the protein. It could therefore be speculated that the interaction of DSC2 with DSG2 would not be affected. Still, the mere binding of a desmocollin to a desmoglein isoform is not adequate to provide adhesion.[253] Expression of DSG and DSC in the absence of plakoglobin in mouse L cells resulted in no adhesion.[254] Individual Dan1 (Figure 20C) bears a missense mutation which affects a crucial, highly conserved amino-acid within the extracellular domain of the cadherin (T335A). In the presence of this mutation, binding of DSG2 to DSC2 would be disrupted consequently leading to mis-localization of all 3 plaque proteins.

It is known that the plakin repeat domains of desmoplakin are responsible for binding intermediate filaments and anchoring them to the membrane.[255] Since desmoplakin localization is altered in all specimens examined, irrespective of the pathogenic mutation underlying the disease, it would be logical to hypothesize that the IF network in all these samples would be affected and that the desmin protein would be re-distributed. Immunostaining with a desmin antibody could help prove this hypothesis. It is of note that desmin failed to localize at intercalated disks in Carvajal syndrome myocytes suggesting that interactions between desmin and desmoplakin are disrupted in the presence of this desmoplakin mutation.[64]

Although the number of the specimens examined was small, certain preliminary conclusions could be drawn. It seems that when an ARVC patient is harboring a desmoplakin or a plakoglobin mutation, only the distribution of desmoplakin and plakoglobin is altered. On the other hand, when an ARVC patient is harboring a mutation in plakophilin2 or in a desmosomal cadherin, plakophilin2, desmoplakin and plakoglobin are all down-regulated at intercalated discs. In all three specimens obtained

from individuals with non-yet identified mutations (A176.1, A220.1 and A223.1, Figure 22B, C, D) all 3 plaque proteins were mal-distributed. Could we therefore hypothesize that these three patients are harboring mutations either in PKP2 or in a desmosomal cadherin? A much higher number of specimens would have to be examined before these preliminary conclusions can be confirmed. Screening a patient for mutations in all ARVC-candidate genes is a time-consuming and uneconomical procedure, while immunostaining of a tissue sample is relatively quick and inexpensive. If in the future, immunostaining could guide genetic screening, so that time and expenses could be reduced, it would be a highly significant step forwards towards an accurate and timely disease diagnosis and possibly genotype-related prognosis. Still, obtaining a heart biopsy is an invasive procedure to be performed merely for the purpose of research immunostaining. However, all desmosomal proteins are also present in the skin and even if an ARVC patient does not show any gross cutaneous abnormalities, similar re-distribution of selected adhesion molecules would be expected to be also found in keratinocytes.

Immunohistochemistry of a sample obtained from the affected plantar skin of an ARVC patient bearing two nonsense desmoplakin mutations (Q673X, Q1446X) showed diminished expression levels of desmoplakin and plakoglobin (Figure 23). Since both mutations lead to premature termination of translation and truncation of the C-terminal domain of desmoplakin, an antibody directed against the head domain of the protein was used. The presence of signal corresponding to desmoplakin at the cell membrane, albeit reduced, suggests that Q1446X and/or Q673X do not lead to nonsense-mediated mRNA degradation. Immunoblotting studies to measure the presence of either or both truncated peptides in the proband's epidermis were not possible due to the limited amount of tissue obtained. However, because the first 584 amino acids of the desmoplakin N-terminal domain are known to bind plakoglobin and cluster the desmosomal cadherin-plakoglobin complexes[256] it can be speculated that even the peptide bearing the Q673X mutation could, if present, localize at the cell membrane.

Immunohistochemistry of a skin sample obtained from the chest of an ARVC patient bearing a DSG2 nonsense mutation (C591X) did not show altered expression levels or distribution for both plakoglobin and desmoplakin (Figure 24). As mentioned earlier in the chapter, DSG2 though the only desmoglein isoform expressed in the heart, is not the major isoform expressed in keratinocytes. A defect in DSG2 could be compensated by other isoforms, particularly DSG1 and DSG3 at the epidermis, which could explain the unaltered expression of both plaque proteins compared to control tissue. Similarly, immunohistochemistry of a skin sample from an ARVC patient heterozygous for a missense DSG2 mutation and a patient homozygous for the same missense mutation (T335A) using antibodies that recognize E-cadherin, desmoplakin, plakoglobin and an

epitope present in all desmoglein isoforms did not show any significant differences in protein expression compared to control samples (Figure 25). It was only when an antibody specifically directed against DSG2 was used, that the signal was virtually absent in the homozygous mutation carrier (Figure 25). The lack of profound differences in the localization of mechanical adhesion molecules in the 3 latter specimens may explain the lack of cutaneous manifestations in these patients.
Of note is that in all specimens examined, plakoglobin expression was depressed at the cell junctions whether the sample was obtained from the heart or from the epidermis, possibly suggesting a final common molecular pathogenetic pathway underlying ARVC. Indeed, plakoglobin is shown to increase stability and recruitment of all desmosomal components and is also known to act as a rheostat that tunes the strength of connections in response to environmental cues.[249] Whether down-regulation of plakoglobin is merely due to its adhesive properties or could also be related to its signaling role remains to be elucidated. Also, prior to concluding that mis-localization of plakoglobin is specifically related to ARVC, samples from individuals diagnosed with other heart conditions, such as DCM, HCM or even ischemic heart disease must be subjected to the same staining protocol and examined quantitatively by confocal microscopy. If however this finding is indeed confined to ARVC cases, it would provide a very useful tool in assigning a definite diagnosis. Given the vast phenotypic variation of ARVC, and its overlapping clinical features with other conditions, such a molecular tool could greatly help resolve the existing problems in differential disease diagnosis.

4) Immunohistochemistry; electrical coupling molecules:

As mentioned in the introduction a number of experiments have shown that the assembly of mechanical adhering junctions is a pre-requisite for the assembly of electrical coupling junctions.[113,114] A question therefore arises whether in the frame of ARVC a defect in desmosomes would also disrupt the formation and maintenance of gap junctions. Indeed, the amount of Cx43 immunoreactive signal localized at cell junction sites was markedly reduced in heart samples obtained both from patients with Naxos disease[226] and Carvajal syndrome.[64] To investigate whether reduction of Cx43 at intercalated discs is a consistent feature in diverse genetic forms of ARVC, 10 heart and 1 skin samples were immunostained for Cx43, the major ventricular gap junction protein, and examined quantitatively by confocal microscopy. Since only once specimen per case was available, statistical analysis could not be performed. Representative images are presented below.

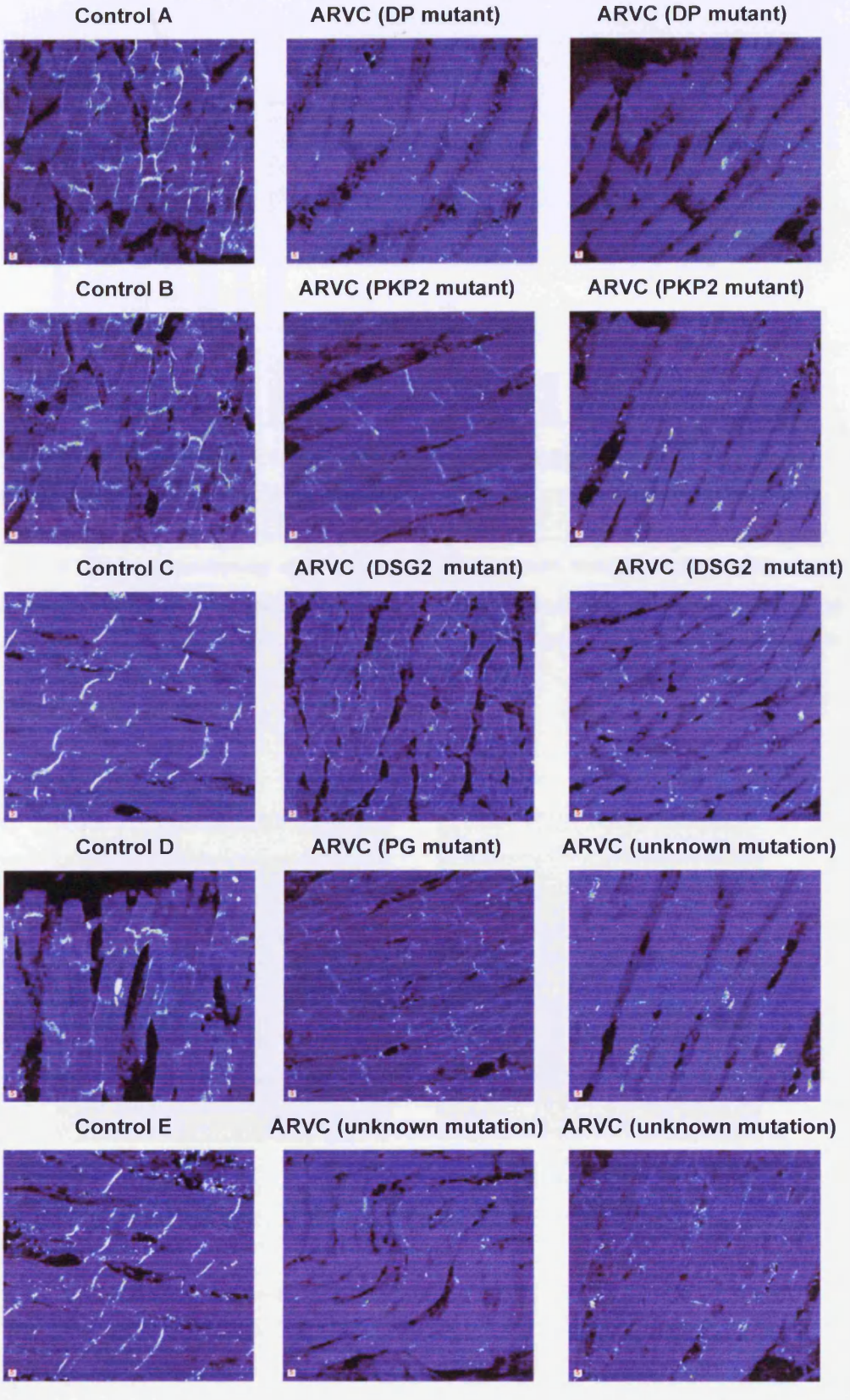
Control A
ARVC (DP mutant)
ARVC (DP mutant)
Control B
ARVC (PKP2 mutant)
ARVC (PKP2 mutant)
Control C
ARVC (DSG2 mutant)
ARVC (DSG2 mutant)
Control D
ARVC (PG mutant)
ARVC (unknown mutation)
Control E
ARVC (unknown mutation)
ARVC (unknown mutation)

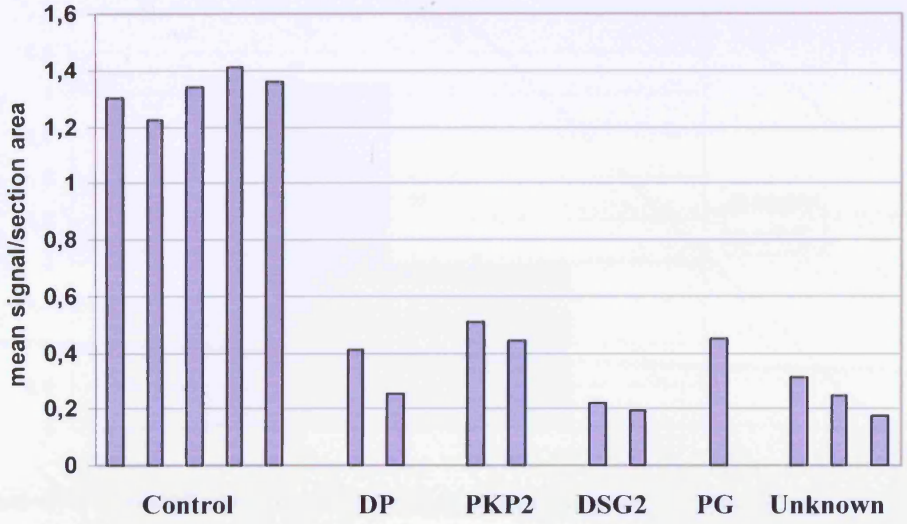

Figure 26: Immunostaining against Cx43 in control heart tissue samples (A-E) and in heart specimens obtained from ARVC patients with known or yet-non identified mutations. The graph shows quantitatively the mean Cx43 immunoreactive signal per sample as measured by confocal microscopy.

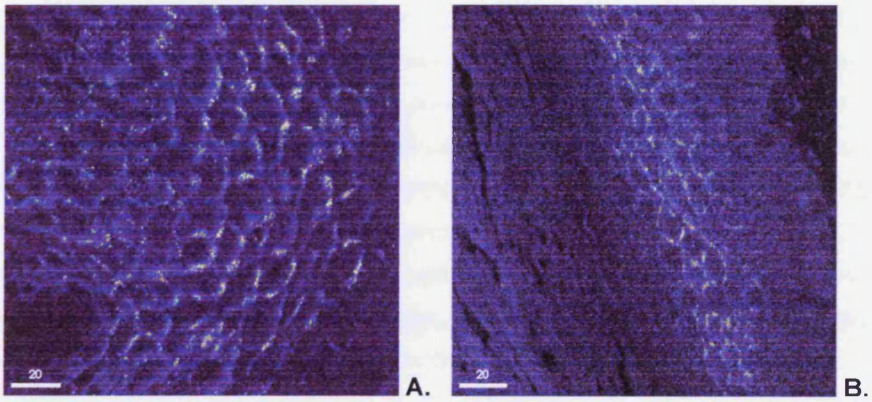

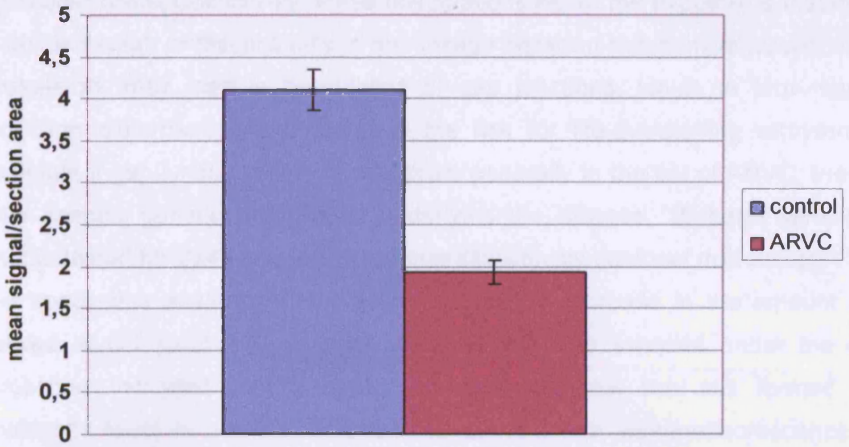

Figure 27: Immunostaining against Cx43 in control plantar skin tissue (A) and in a plantar skin sample from an ARVC patient identified as a compound heterozygote for two nonsense desmoplakin mutations (B).The graph shows quantitatively the mean Cx43 immunoreactive signal per sample as measured by confocal microscopy.

Discussion:

Mammalian ventricular myocytes are connected by numerous gap junctions. More than enough current flows across the borders, so that conduction in the normal ventricular muscle occurs in a highly continuous fashion as if current is flowing through a uniform conductive medium rather than across a network of discrete, individual conducting units. However, because the membrane containing the gap junctions is potentially susceptible to disruption due to shear stress, there is a risk that the gap junctions may encounter deleterious effects, caused by contractile activity. This may explain why gap junctions are always surrounded by cell-cell adhesion junctions, which presumably stabilize the sarcolemmas of the inter-connected cells and create membrane regions conducive to the formation and maintenance of large arrays of gap junctions.[257] The degree to which neighboring cells are coupled by gap junctions depends on the structure and function of adhesion junctions. Cells with limited mechanical connections are unable to maintain normal gap junction communication. For instance, highly malignant tumors, typically composed of dys-cohesive cells, are also communication-deficient.[258,259] A similar situation occurs in cardiomyocytes. When freshly disaggregated rat ventricular cardiomyocytes are placed in culture and allowed to re-form cell junctions, the initial event in the re-formation of the intercalated disc is the development of adherens junctions and it is not until adherens junctions are well formed that gap junctions develop.[260,113] In Naxos disease[226] and Carvajal syndrome,[64] there is a marked decrease of immunoreactive signal for Cx43 at the cardiac

intercalated discs. Collectively, these observations led to the hypothesis that defects in cell-cell adhesion or discontinuity in the linkage between mechanical junctions and the cytoskeleton, may lead to remodeling of gap junctions, which in turn may cause conduction disturbances and increase the risk for life-threatening arrhythmias. To investigate if gap junction remodeling occurs generally in the set of ARVC, irrespective of the specific genetic background underlying the disease, 10 heart samples were immunostained for Cx43 and examined quantitatively by confocal microscopy.

In all specimens analyzed, there was a significant decrease in the amount of Cx43 localized at cell junctions. Careful observation of the samples under the confocal microscope indicated that normal-sized gap junctions are still formed, though significantly fewer in number. This is in agreement with immunofluorescence studies performed on ventricular myocytes isolated from heterozygous Cx43 knockout mice. In this animal model, ventricular myocytes become interconnected by a reduced number of normally sized gap junctions, rather than a normal number of smaller junctions. Maintenance of normally sized electrical junctions may be an adaptive response supporting safe ventricular conduction.[261] In Naxos disease, although Cx43 signal at the cell borders is reduced, the protein is still abundantly expressed in the myocardium, but just fails to localize at the intercellular junctions. These results suggest that in Naxos disease, remodeling of gap junctions is not due to reduced expression of Cx43, but due to defects in gap junction assembly and/or trafficking.[257] Immunoblotting studies that would have supported this hypothesis in the cases presented herein were not possible due to the limited amount of tissue available. Nevertheless, though the numbers examined were small, a new horizon is emerging, where gap junction remodeling seems to be characterizing ARVC regardless of the causative mutation.

Remodeling is a change in the structure of an organ in response to injury or disease. In the heart, remodeling starts with alteration in gene expression, which in turn leads to alterations in the types and amounts of proteins expressed. Alterations in structure are accompanied by alterations in function, although the structure-function relationships have only recently started to be unraveled. Remodeling happens to aid adaptation of an organ to change.[262] For instance, formation of scar tissue following a myocardial infarct is a beneficial response, as it helps avoid ventricular rupture. Similarly hypertrophy, as a response to increased mechanical load, may also be beneficial as it aids the heart deal with the increased pressure it is subjected to. However, though beneficial, these changes have maladaptive consequences. In the frame of ARVC, remodeling of gap junctions, which may diminish communication between healthy tissue and apoptotic, dys-cohesive cells, may change the electrical activation of the heart and offer the substrate for lethal ventricular arrhythmias.[263,264]

Still, are gap junction alterations by themselves enough to promote arrhythmogenesis? An approximately 50% reduction causes significant conduction velocity slowing in the Cx43 +/- mouse heart but no spontaneous arrhythmias.[265] However, reduced expression of Cx43 accelerates the onset and increases the incidence, frequency and duration of ventricular tachyarrhythmias after coronary artery occlusion.[266] In the absence of secondary stimuli, in the absence of an appropriate trigger, just the presence of the substrate, such as decreased Cx43 localization at intercalated discs is not enough to bring about arrhythmias.[267] Analysis by positron emission tomography and I-meta-iodobenzylguanidine (I-MIBG) scintigraphy have shown significantly increased amounts of nor-epinephrine at the synaptic clefts and markedly reduced density of postsynaptic beta-adrenergic receptors underlying myocardial sympathetic dys-innervation and arrhythmogenesis in ARVC patients.[268,269] Dying cells in the ARVC heart may themselves exhibit transiently increased automaticity, while the mere presence of fat and fibrous tissue within the myocardium would alter the normal route of RV activation, thus providing an anatomic substrate for micro-reentrant or macro-reentrant circuits.[242] What if these defects are coupled with alterations in electrical communication? Gap junction remodeling may by itself not be arrhythmogenic. However, super-imposed on the structural and functional abnormalities characterizing ARVC, it may act synergistically to cause ventricular tachycardias, late potentials and epsilon waves that may lead to SCD.[226]

Eight different connexins, including Cx43 are expressed in the epidermis with overlapping expression patterns in different epidermal layers.[270] A plantar skin sample obtained from an ARVC patient bearing two nonsense desmoplakin mutations was immunostained for Cx43 and examined by quantitative confocal microscopy. Not only was the signal for Cx43 markedly reduced in the affected skin sample, but the protein was also mis-localized, being restricted mainly to the spinal layer, instead of across all epidermal layers as demonstrated by controls (Figure 27). Abnormal distribution of Cx43 in keratinocytes has also been observed in mouse skin carcinogenesis,[271] while transgenic mice lacking the C-terminal region of Cx43 demonstrate a defective epidermal barrier.[272] Though not the mere causative agent, the altered Cx43 expression observed in the sample examined may in fact contribute to the profound cutaneous abnormalities demonstrated by the patient (case discussed in Chapter 1).

Altered patterns of cardiac electrical junction distribution have also been observed in HCM,[273] DCM[274] and ischemic cardiomyopathy.[275] In fact, gap junction remodeling seems to be a common finding in the failing heart. Though not exclusive to ARVC, the results presented herein may contribute to the understanding of the mechanisms of arrhythmogenesis underlying the disease and open new horizons for future investigations.

5) Beta catenin: another player in ARVC?

Beta-catenin null mice die during gastrulation due to abnormalities in the development of all embryonic structures[276] while plakoglobin null mice on a C57BL/6 genetic background, develop further and die around birth due to severe heart defects.[74] The two armadillo proteins are structurally very similar with occasionally overlapping adhesive and signaling properties. As discussed above, down-regulation of plakoglobin at intercalated discs seems to be a constant feature in ARVC. The redundancy between the two catenins suggests that beta-catenin may be up-regulated in ARVC cell-cell junctions thus compensating for the reduced amounts of plakoglobin. To investigate this hypothesis, 4 ARVC heart samples with known mutations were immunostained for beta-catenin and examined by confocal microscopy. The samples were also stained for N-cadherin to preclude non-specific postmortem effects.

N-cadherin:

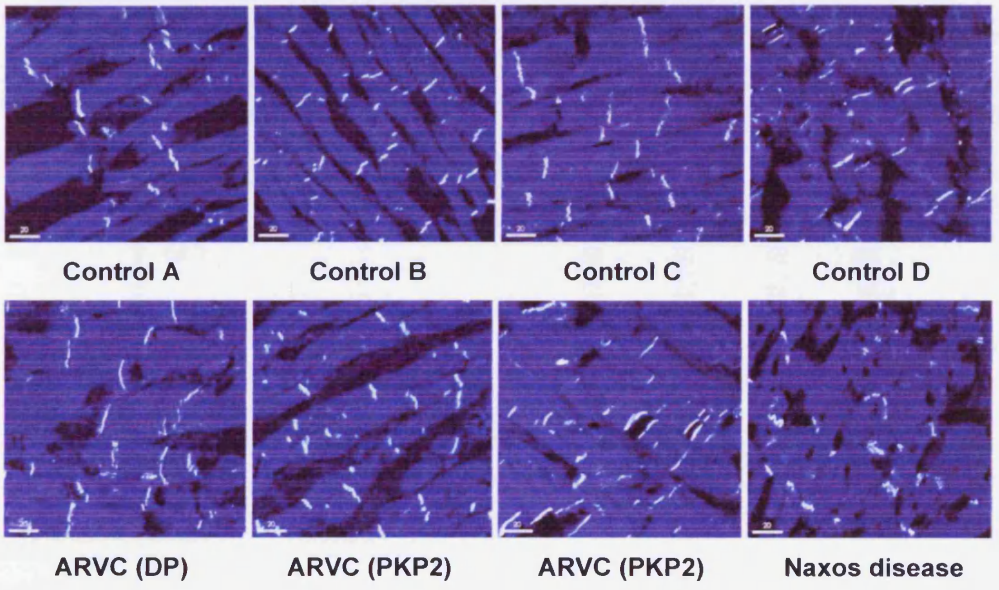

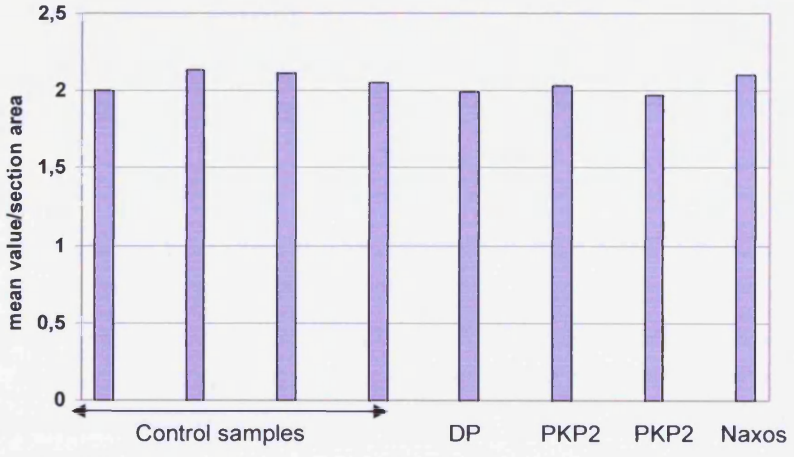

Beta catenin:

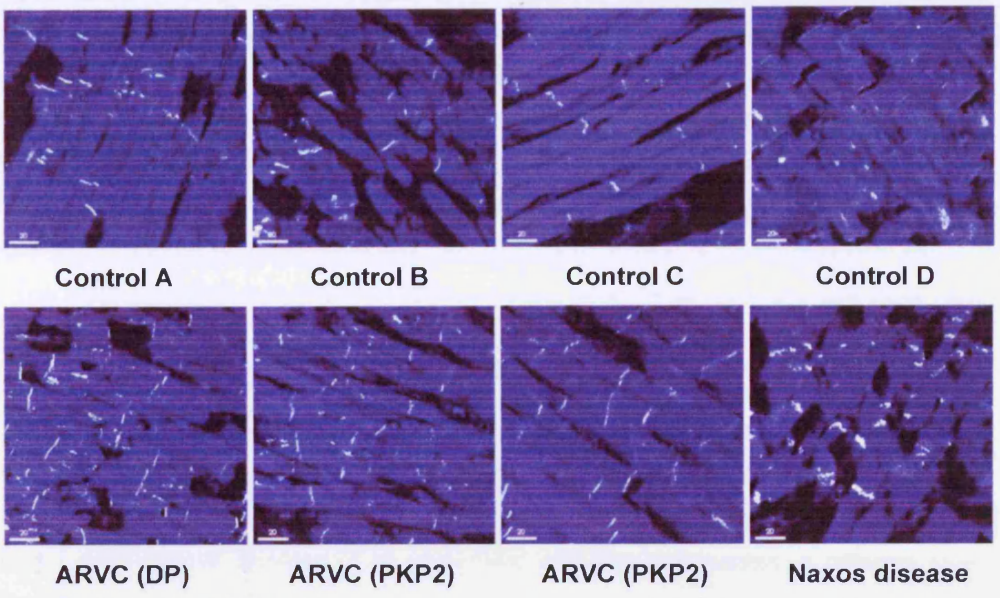

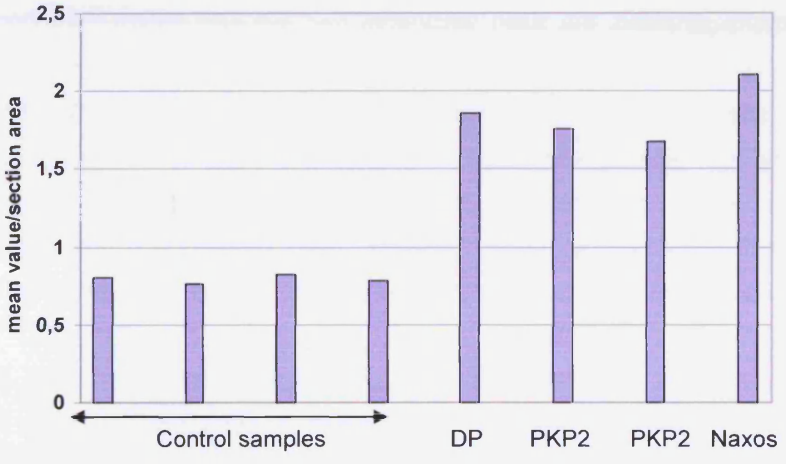

Figure 28: Immunostaining against N-cadherin and beta-catenin in control heart tissue samples (A-D) and in heart specimens obtained from ARVC patients with known mutations. The graphs show quantitatively the mean immunoreactive signal per protein, per sample as measured by confocal microscopy.

Discussion:

A major lesson learned from gene knockout studies in mice is that functions of many proteins overlap significantly, which enables the organism to carry out many physiological processes when a key component in a biological pathway is genetically eliminated. Another lesson has to do with the "other side of the coin", namely the multi-functionality characteristic of certain proteins which enables cells to coordinate the

regulation of what sometimes appear to be unrelated biochemical processes. In these cases, the same protein participates in several different processes, which are often carried out at different locations in the cell and form an independent network of cellular events. Beta-catenin provides an intriguing example of both these lessons. It combines the features of a major structural protein at cell-cell junctions with those of a transcription factor in the nucleus. Its close homolog, plakoglobin, shares with beta-catenin common protein partners and can fulfill some of the same functions.[277] There is a fine balance between the two armadillo proteins where they compete with each other both at the nucleus and at the membrane while one may at least partially compensate for the other when either is eliminated.

Although under physiological conditions beta-catenin's junctional role is confined to the adherens junctions, in plakoglobin-null keratinocytes, beta-catenin has been shown to localize at the desmosomes, associate with desmoglein1 and promote the assembly of further desmosomal proteins.[278] In agreement with this observation, a different study showed that over-expression of beta-catenin in plakoglobin-null skin increased the Triton-insoluble pool of desmoplakin.[249] Furthermore the contractile parameters of heart fibers obtained from plakoglobin-deficient embryonic mice are indistinguishable from those of control mice, suggesting that beta-catenin may be taking over this role in the absence of plakoglobin.[140] Similar seems to be the case in the opposite situation. When the beta-catenin gene is specifically ablated from adult mice cardiac myocytes, the expression levels of plakoglobin are significantly elevated as shown both by immunohistochemistry and Western immunoblotting suggesting that plakoglobin may in fact compensate for the loss of beta-catenin to maintain cardiac structure and function.[279]

Beta-catenin was significantly elevated in all ARVC samples examined herein compared to controls (Figure 28). It is not known however, whether this increased localization of beta-catenin at intercalated discs is due to increased gene expression, decreased degradation or increased sequestering of the catenin at the cell borders. To our knowledge, this is the first immunohistochemical study for beta-catenin on ARVC heart samples. However, a larger number of samples have to be examined before we can conclude that this compensation between the two armadillo proteins is in fact a consistent finding in all ARVC cases. More importantly, the significance of this finding still remains unclear. Whether this increased localization of beta-catenin at the cell membrane is merely rescuing the depressed adhesive function of plakoglobin or it also has effects on downstream signaling pathways is a big challenge that still has to be faced.

CHAPTER 3:

"Unraveling the effects of the ARVC-causing S39_K40insS plakoglobin mutation"

Why S39_K40insS?

As presented in Chapter 1, a novel mutation in plakoglobin was identified in a German family affected by ARVC. The 3-base insertion does not alter the frame of translation but is predicted to result in the insertion of an additional serine residue within the N-terminal domain of the protein. S39_K40insS co-segregated with the disease phenotype in the family and was absent in 400 ethnically-matched control chromosomes. It is likely therefore that it is in fact pathogenic. The proband was part of a large cohort of ARVC patients who were screened for mutations in known disease-causing and other candidate genes. A high number of ARVC-causing mutations in desmoplakin, plakophilin2, desmoglein2 and desmocollin2 were identified amongst patients of this cohort. S39_K40insS was the only mutation in plakoglobin identified in the cohort and the only other mutation in plakoglobin ever to be reported, after the identification of 2057del2 as the underlying cause of Naxos disease. In contrast to 2057del2, S39_K40insS is inherited in an autosomal dominant manner and is not associated with any gross cutaneous abnormalities. It therefore presented a good opportunity to investigate how two mutations in the same gene can have different, yet similar effects at the clinical phenotype level. Moreover, many of the mutations presented both in this project, and generally in the literature, cause premature termination of translation. Very little work has been done to date to functionally characterize these sequence changes. It would be logical to assume that their mechanism of action stems at least in part from the inability of the truncated proteins to interact with their protein binding partners. This could compromise the formation and maintenance of desmosomes and consequently the strength and stability that allow adjacent cardiomyocytes to deal with increased levels of mechanical stress. S39_K40insS is a unique mutation, whose mechanism of action would be more challenging to unravel since its only obvious effect seems to be the insertion of an additional amino acid. Furthermore, plakoglobin is a unique protein amongst all desmosomal molecules, because it has a well recognized role in all desmosomes, adherens junctions and nucleus thus encompassing both structural and signaling properties.

People with Marfan syndrome live with a ticking bomb. Unless surgically corrected, their aortas gradually enlarge and weaken until they fatally rupture. In 1991, mutations in the gene coding for fibrillin-1 were reported as responsible for this syndrome.[280] Such mutations could explain the aortic aneurysms, lung problems and many other features of Marfan syndrome. Interestingly though, there was still a number of features that could not be explained by a mere structural defect. Ten years later, a signaling molecule, TGF-β was implicated in the disease.[280] Fibrillin-1 binds TGF-β keeping it

inactive. In the presence of a fibrillin-1 mutation though, the growth factor is unleashed, exerting effects that could in fact justify the "unexplainable" features.[280]

Similar could be the case for plakoglobin. Given its dual role both at the membrane and nuclear sites and its seemingly ubiquitous involvement in ARVC, functionally characterizing S39_K40insS would allow us to understand whether the features of disease are merely due to structural defects at the cell-cell junctions or also due to disruption of signaling pathways.

METHODS AND MATERIALS:

1) Polymerase chain reaction (PCR)

Platinum PfX DNA polymerase or EXL DNA polymerase was used for the amplification of large DNA fragments (>400kb). For each PCR reaction with **PfX DNA polymerase**, the following were added:

5 μl of 10x PfX Amplification Buffer (Invitrogen)

10 pmoles of forward primer (Invitrogen)

10 pmoles of reverse primer (Invitrogen)

1.5 μl of dNTP mix, 2.5mM each of dATP, dGTP, dCTP and dTTP (Invitrogen)

1 μl of $MgSO_4$, final concentration: 50mM (Invitrogen)

1 μl of Platinum PfX DNA polymerase enzyme, 2.5 units/μl (Invitrogen)

150-500 ng of DNA template. dH_2O was added up to a total volume of 50 μl

PCR reactions were performed under the following program:

95°C for	10min	
95°C for	1min	25-30 cycles
50-55°C for	1min	
72°C for	x min	
72°C for	10min	
4°C	∞	

For each PCR reaction with **EXL DNA polymerase**, the following were added:

5 μl of EXL Reaction Buffer (Stratagene)

200 ng of forward primer (Invitrogen)

200 ng of reverse primer (Invitrogen)

2.5 μl of dNTP mix, 2.5mM each of dATP, dGTP, dCTP and dTTP (Invitrogen)

1 μl of stabilizing solution (Stratagene)

0.5 μl of DMSO (Stratagene)

1 μl of EXL DNA polymerase enzyme, 5 units/μl (Stratagene)

150-500 ng of DNA template. dH_2O was added up to a total volume of 50 μl

PCR reactions were performed under the following program:

92°C for	2min	
92°C for	20 sec	25-30 cycles
50-55°C for	45 sec	
68°C for	x min	
68°C for	20min	
4°C	∞	

The annealing temperature, extension time and number of cycles varied according to the fragment amplified. All PCR reactions were performed on a TE-412 PCR block (TECHNE) using 0.5 ml Thermo-Tubes (ABgene).

2) DNA gel extraction:

DNA gel extraction was performed using a QIAquick gel extraction Kit (QIAGEN) according to the protocol. Briefly:
The DNA fragment was excised from the agarose gel with a sterile scalpel and placed in a micro-centrifuge tube. The tube was filled with QG solubilization buffer and incubated on a heated block at 50°C until the gel was dissolved. The contents of the tube were mixed by pulse vortexing, loaded on a spin column assembled on a collection tube, centrifuged and the flow-through discarded. PE wash buffer was added to the column, centrifuged and the flow-through discarded. An additional centrifugation step was performed to remove residual ethanol following which, the column was assembled on a micro-centrifuge tube and EB elution buffer was added. The mixture was allowed to equilibrate to room temperature, was centrifuged and kept at -20°C.

3) Site-directed mutagenesis:

For each sample the following was added:
5 μl of PFU buffer (Invitrogen)
125 ng of forward mutagenic primer (Invitrogen)
125 ng of reverse mutagenic primer (Invitrogen)
1 μl of dNTP mix, 2.5mM each of dATP, dGTP, dCTP and dTTP (Invitrogen)
3 μl of Quick solution (Invitrogen)
50 ng of DNA template

1 μl of Pfu DNA polymerase enzyme (2.5 units/μl). dH_2O was added up to a total volume of 50 μl

PCR reactions were performed on a TE-412 PCR block (TECHNE) using 0.5 ml Thermo-Tubes (ABgene) under the following program:

95°C for	1min	
95°C for	50 sec	18 cycles
50-55°C for	50 sec	
68°C for	x min	1min per Kb of template DNA.
68°C for	10min	
4°C	∞	

The number of amplification cycles used was kept to no higher than 18, so as to eliminate the possibility of introduction of unwanted sequence changes.

4) Cloning

a) Gateway-compatible cloning:

Primers flanking the DNA fragment of interest were designed so that they contained the Gateway-compatible attB sites. This allows the BP clonase enzyme to perform a site-specific recombination reaction and insert the DNA fragment of interest into the linearized vector carrying the complementary attR sites. The following were added in a micro-centrifuge tube:

150 ng of pDONR vector (Invitrogen)

150-450 ng of DNA template

2 μl of BP clonase enzyme mix (Invitrogen)

TE buffer, up to a final volume of 8 μl

The recombination reaction was performed either over 1 hr at room temperature or for 12-16 hrs on a thermal cycler at 16°C. Following the recombination reaction, 1μl of proteinase K (Invitrogen) was added to the mixture and the tube was incubated at 37°C for 10min to denature the enzyme.

To convert a final destination vector into a Gateway-compatible form, a Gateway vector conversion reagent system Kit (Invitrogen) was used. Briefly:

A restriction enzyme was selected to linearize the vector creating blunt ends. The following were added in a micro-centrifuge tube:

1-5 μg of final destination vector

2 μl of digestion enzyme buffer

5 μl of digestive enzyme. dH_2O was added to a total volume of 20 μl.

The reaction mix was incubated and subsequently the digestive enzyme was inactivated according to the instructions of the enzyme used. The correct Gateway reading frame cassette was selected (A, B or C.1). The three reading frame cassettes provided with the Kit differ by one nucleotide to allow generation of attR sites in all three reading frames. The following were added in a micro-centrifuge tube:

20-50 ng of linearized destination vector

2 μl of the selected Gateway reading frame cassette

2 μl of T4 ligase buffer (Invitrogen)

1 μl of T4 ligase enzyme (Invitrogen). dH_2O was added to a total volume of 10 μl

The ligation reaction was performed either over 1 hr at room temperature or for 12-16 hrs on a thermal cycler at 4°C.

To perform a recombination reaction between pDONR and a Gateway-compatible final destination vector, the following were added in a micro-centrifuge tube:

300 ng of the DNA fragment of interest in pDONR vector

300 ng of the Gateway-compatible final destination vector

4 μl of LR clonase enzyme mix (Invitrogen)

TE buffer was added up to a final volume of 16 μl

The recombination reaction was performed either over 1 hr at room temperature or for 12-16hrs on a thermal cycler at 16°C. Following the recombination reaction, 2μl of proteinase K (Invitrogen) was added to the mixture and the tube was incubated at 37°C for 10min for the enzyme to be denatured.

This system was used in order to clone plakoglobin cDNA (purchased from OriGene) first into pDONR and subsequently into the pcDNA4/His-Max and the pDEST^{TM}32 vectors (Invitrogen).

b) Zero blunt TOPO PCR cloning:

The DNA fragment of interest was first amplified using Taq, PfX or EXL polymerase. For the ligation reaction, the following were added in a micro-centrifuge tube:

0.5 - 4 μl of purified PCR product

1 μl of TOPO vector (Invitrogen)

2 μl of T4 ligase enzyme (Invitrogen) and

TE buffer to a final volume of 8 μl

The reaction was performed either over 5min at room temperature or at 16°C overnight.

This system was used in order to clone TGF-beta induced apoptosis protein-2 cDNA (purchased from Biosearch Technologies, USA) into the PCR blunt TOPO vector.

c) Restriction enzyme-based cloning:

Wherever possible, 2 restriction enzymes were used to avoid self-ligation of the vector. For linearization of the vector DNA, the following were added in a micro-centrifuge tube:

5 μl of 10X restriction enzyme buffer

0.5 μl of 100X BSA (optional, depending on the enzymes selected)

7.5 μg of vector DNA

2.5 μl of restriction enzyme A (10-20 units/ μl)

2.5 μl of restriction enzyme B (10-20 units/ μl)

dH_2O to a final volume of 50 μl

The reaction mixture was incubated at 37°C for 1-4 hrs according to the enzyme manufacturer's instructions. Following digestion, the mixture was loaded on a 1% agarose gel, and the DNA fragment of interest excised as described above.

Primers bearing recognition sites for the selected enzymes were designed and used for amplification. The PCR product was digested in the same way as the vector, and purified by agarose gel electrophoresis and subsequent excision.

For the ligation reaction the following were added in a micro-centrifuge tube:

100 ng of the digested DNA fragment of interest

100 – 300 ng of the linearized digested vector

2 μl of T4 ligase (Invitrogen)

TE buffer to a final volume of 20 μl

The reaction was performed either over 2hrs at room temperature or at 16°C overnight.

Following these instructions, plakoglobin was sub-cloned into the pcDNA5/FRT/TO vector (Invitrogen, UK) using the BamHI and EcoRV restriction sites and in the pGFP-C3 vector (Clontech, USA) using the BamHI and EcoRI restriction sites. Similarly, TGF-beta induced apoptosis protein-2 was sub-cloned into the pcDNA V5 His 3.1 vector (Invitrogen, UK) using the EcoRI restriction sites.

d) Transformation of chemically competent *E.coli* cells:

Chemically competent *E.coli* cells (100 μl) were mixed with the recombination/ligation reaction (7.5 μl) in a micro-centrifuge tube, left on ice for 45min and then heat-shocked in a water bath according to the bacterial cell type used. For instance, DH5a cells get heat shocked at 42°C for 30 sec while DB3.1™ cells get heat shocked at 42°C for 45 sec. Following the heat-shock, SOC medium (Invitrogen) was added to the cells and the micro-centrifuge tube was shaken in an incubator at 275rpm. The duration of the shaking varied according to the antibiotic resistance gene the vector was expressing. For instance, kanamycin and ampicillin resistance genes get expressed within 1 hr of shaking, while a gemtamycin resistance gene requires 3 hrs to be efficiently expressed. Following shaking, three dilutions of the transformation reaction were plated on appropriate plates (antibiotic concentration: 50-100μg/μl), which were then incubated for 12-16 hrs at 37°C.

Each colony selected was placed in falcon tubes along with LB broth and the appropriate antibiotic (concentration: 50-100μg/μl). The tubes were shaken (12-16 hrs, 275rpm, 37°C), centrifuged and the plasmid extracted from the cell pellets using a QIAprep Spin mini Prep Kit (QIAGEN) according to the protocol. Briefly:

P1 re-suspension buffer was added to each pellet and mixed by pulse vortexing. The mix was transferred to 1.5 ml micro-centrifuge tubes, P2 lysis buffer was added and the tubes inverted vigorously. N3 neutralization buffer was added, the tubes were inverted vigorously, centrifuged and the supernatant was placed in a spin column assembled to a 2 ml collection tube. The spin columns were centrifuged and the flow-through discarded. PE wash buffer was added; the spin columns were centrifuged twice and transferred on 1.5 ml micro-centrifuge tubes. 55 μl of EB elution buffer was added. The columns were allowed to equilibrate to room temperature, centrifuged and kept at -20°C. The A260 of each sample was measured using a spectrophotometer in order to estimate the DNA concentration. The technique is predicted to yield 5-15 μg of DNA. Two μl of each sample was digested with an appropriate enzyme under the conditions suggested by the manufacturer to ensure the correct recombination or ligation reaction had taken place. Following incubation with a digestive enzyme, the entire reaction mixture (total volume: 10μl) was loaded on a 1% agarose gel for electrophoresis. Specific samples were selected according to the band pattern obtained from digestion and 500-600ng of DNA was used to set up a sequencing reaction. Samples were sequenced on an ABI3100 sequencer as described above.

e) Midi/Maxi plasmid purification:

Plasmid (100-250 μg) was added to 50 μl of DH5a chemically competent *E.coli* cells in a micro-centrifuge tube and incubated on ice for 45min. The mixture was heat-shocked in a water bath (42°C for 30 sec), SOC medium (Invitrogen) was added and the tube shaken at 37°C at 275rpm. The duration of the shaking varied according to the antibiotic resistance gene the plasmid was expressing. The contents of the micro-centrifuge tube were mixed with LB broth and the appropriate selective antibiotic (concentration: 50-100μg/μl) and shaken at 275rpm at 37°C for 24-36 hrs. Following shaking, the culture was poured in falcon tubes and centrifuged. Plasmid purification from cell pellets was performed with a QIAGEN Midi Plasmid Purification Kit according to the protocol. Briefly:

The bacterial pellets were first re-suspended in P1 re-suspension buffer, then in P2 lysis buffer and incubated at room temperature for 5min. P3 neutralization buffer was added to the lysate which was then poured in a QIAfilter cartridge (QIAGEN) and incubated at room temperature for 10min. QBT equilibration buffer was added to a QIAGEN-tip, pre-assembled to a 50-ml falcon tube, and the column was allowed to empty by gravity flow. The lysate was then allowed to enter the resin of the previously equilibrated QIAGEN-tip by gravity flow and the flow-through was discarded. The QIAGEN-tip was washed twice with QC wash buffer, the column was allowed to empty by gravity flow and the flow-through was discarded. Following the washes, the QIAGEN-tip was assembled to a new 50ml falcon tube, QF elution buffer was added and the column was allowed to empty by gravity flow. Isopropanol was added to the flow-through, the mixture was centrifuged, the pellet re-suspended in 70% ethanol and transferred to a micro-centrifuge tube. The tube was then centrifuged and the pellet allowed to air-dry in a 37°C incubator before being eluted in 55 μl of TE elution buffer. The A260 of the sample was measured using a spectrophotometer. The technique is predicted to yield 20-100 μg of DNA. The samples were kept at -20°C.

5) Cell culture:

a) Maintenance of Flp-In 293 cells:

The cell line is supplied from Invitrogen in vials containing 3 x 10^6 cells in 1 ml of freezing medium (90% complete medium and 10% DMSO). The cells were thawed in a 37°C water bath and transferred to a T-75 flask containing 10 ml complete medium. Complete medium consisted of Dulbeccois Modified Eagle Medium (DMEM, GIBCO) supplemented with 10% Foetal Bovine Serum (FBS, GIBCO), 2mM L-glutamine (GIBCO) and 1% penicillin-streptomycin (GIBCO). The cells were incubated at 37°C, 5% CO_2 in order for them to attach to the flask. Twelve to sixteen hours later, the

medium was replaced with new growth complete medium supplemented with 15μg/ml blasticidin and 100μg/ml zeocin. The growth medium was then replaced after every 48-72 hours. When 80-90% confluent, the cells were washed with PBS and trypsinized with 50% versene (GIBCO)-50% trypsin-EDTA 1x (GIBCO). Following incubation (37°C, 5-7min), 10 ml of complete medium lacking antibiotics was added to stop trypsinization and the entire mixture was aspirated from the flask and transferred to a falcon tube. The tube was centrifuged, the pellet re-suspended in complete medium and part of the mixture transferred to a new T-75 flask containing complete medium supplemented with blasticidin and zeocin at the recommended concentrations. The flasks were incubated in a humidified, 37°C, 5% CO_2 incubator.

b) Transfection and selection of Flp-In 293 cells:

Flp-In-293 cells were transfected using the Flp-In system (Invitrogen). Briefly:

The cells were harvested as described above and 1/20 of the cell suspension was transferred in a P90 plate, containing complete medium supplemented with blasticidin and zeocin. The plate was incubated in a humidified, 37°C, 5% CO_2 incubator until the cells became 30-40% confluent. Four μg of the pcDNA5/FRT/TO vector containing the gene of interest along with 4 μg of pOG44 (Invitrogen), which expresses the Flp recombinase gene were added to a micro-centrifuge tube. DMEM and polyfect transfection reagent (QIAGEN) were also added to the tube and the mixture was incubated at room temperature for 20min, during which it was occasionally mixed by pulse-vortexing. Following incubation, the contents of the tube were poured in a falcon tube containing complete medium supplemented with blasticidin only (15μg/ml). The old growth medium was aspirated from the P90 plate, replaced with the new medium and the plate was incubated in a humidified, 37°C, 5% CO_2 incubator. Twenty-four to 48 hours after transfection, the growth medium in the P90 plate was replaced with fresh complete medium supplemented with blasticidin (15μg/ml) and hygromycin (100μg/ml). The medium was aspirated and replaced with fresh medium every 48-72 hrs for 10-14 days until distinct surviving cell colonies could be detected.

In order to further grow and characterize the individual colonies that had survived selection with hygromycin, the colonies were transferred to a 24-well plate. Briefly, the old growth medium was aspirated from the P90 plate and the cells were washed with 5 ml of DMEM. Following the wash, a cloning disc immersed in 50% versene-50% trypsin-EDTA 1x was placed above each colony and the plate was incubated for 5-7min at room temperature. Once the cells had detached from the surface of the plate, the cloning disc was transferred to a well of the 24-well plate containing complete medium supplemented with blasticidin and hygromycin. The growth medium was replaced every

48-72 hours until the cells became confluent, after which they were trypsinized and transferred first to a T-25 flask and subsequently to a T-75 flask.

When the cells in the T-75 flask reached 80% confluence, stocks were made and maintained in liquid nitrogen. Briefly: the cells were harvested as described above, however after centrifugation the pellet was re-suspended in freezing medium (95% FBS and 5% DMSO). The suspension was then transferred in cryo-vials, which were kept at -80°C for 12-16 hours before immersion in liquid nitrogen. The cell line was maintained in 2 T-75 flasks, one containing 10 ml of complete medium supplemented with blasticidin, hygromycin and tetracycline (100ng/ml medium) and the other containing 10 ml of complete medium supplemented with blasticidin, hygromycin and 70% ethanol (10μl/ ml medium). Tetracycline was added to the first flask to induce expression of pcDNA5/FRT/TO, while the second flask was used for control purposes.

6) Immunostaining of stably transfected Flp-In 293 cells:

Flp-In 293 cells, transfected to stably express the gene of interest were seeded on plastic coverslips. Forty-eight hours following seeding, the cells were washed with PBS and incubated with 4% paraformaldehyde in PBS at room temperature for 10min. Following fixation, the cells were washed first with PBS, then with 0.5% Triton-X/PBS and again with PBS. To block non-specific signal, the cells were incubated with 10% fetal calf serum/PBS for 30min. The primary antibodies were added diluted in the same blocking buffer and the cells incubated at 4°C overnight. The following day, the cells were equilibrated at room temperature for 30min, washed first with PBS, then with 0.1% Tween/PBS and again with PBS. The secondary antibodies were added diluted in blocking buffer and the cells were incubated at 4°C overnight. On the third day of the procedure, the cells were equilibrated at room temperature for 30min, washed first with PBS, then with 0.1% Tween in PBS and again with PBS. The coverslips were then placed on slides and mounted with 50% glycerol-50% PBS.

7) Western immunoblotting:

In preparation for Western immunoblotting, the cells were harvested as described above and the cell pellets re-suspended in RIPA buffer. RIPA buffer was prepared with 50mM Tris-HCl pH 7.4, 1% NP-40, 0.25% Na-deoxycholate, 150mM NaCl, 1 mM EDTA, 1mM Na_3VO_4, 1mM NaF and protease inhibitor cocktail (Roche: 1 tablet per 7 ml of buffer). The mixture was transferred in a micro-centrifuge tube, incubated on ice for 45min, mixed by pulse vortexing and centrifuged. Following centrifugation, a spectrophotometer was used to measure the A540 of the supernatant and the value was compared to a standard curve in order to estimate total protein concentration. The

standard curve was generated by measuring the absorbance values of solutions with known protein concentrations (Protein standard set, SIGMA).

The following were then added to a micro-centrifuge tube:

50 mg of protein lysate

6 μl of Laemmle dye, previously denatured at 96°C for 10min

dH_2O was added up to a total volume of 22μl.

The samples were incubated at 96°C for 5min and were then loaded on a 1.5mm 10% Tris-Glycine gel (Invitrogen) along with 8 μl of Precision Plus Protein Dual Color Standards (BIO-RAD). Tris-glycine buffer 1x (Fisher Scientific) was used for electrophoresis, while the current and duration varied according to the size of the protein of interest. Eight 6x8 cm pieces of absorbent paper (Whatman paper) and one similar size piece of nitrocellulose membrane (Amersham Biosciences) were cut and wetted with transfer buffer. For proteins larger than 100KDa, 1x Tris-glycine buffer was used while for proteins smaller than 100KDa, 1x CAPS buffer was used (SIGMA). The semi-dry Western blot method was used to transfer the protein bands from the gel to the membrane. The gel was removed from the container and the modules were assembled starting from the bottom electrode plate in the following order: four layers of absorbent paper, followed by the membrane, the polyacrylamide gel and another four layers of absorbent paper. The current and the duration of the transfer depended on the size of the protein of interest. The blot was then blocked with PBS-5% skimmed dried milk on a rotating shaker for 30min and then incubated at 4°C overnight. Following incubation, the blot was washed twice with PBS and incubated with the primary antibody in a plastic bag for 1 hr at room temperature or overnight at 4°C on a rotating shaker. The blot was then washed three times in PBS and incubated with the secondary antibody in a plastic bag for 1 hr on a rotating shaker. The antibodies were diluted in PBS-5% milk according to the instructions of the manufacturer. Following incubation with the secondary antibody, the blot was washed three times with PBS and blocked with 500 μl of each of the two Western blotting detection reagents (Amersham Biosciences) in a plastic bag. The blot was then exposed to X-ray film. The duration of exposure before the development of the film was optimized for each protein individually.

8) Cell-proliferation assay:

Proliferation rates in Flp-In 293 cells transfected to stably express the gene of interest were measured using the CellTiter 96 Cell proliferation assay (Promega, UK) according to the manufacturer's instructions. Briefly:

Cells (150,000, as measured with the aid of a haemocytometer) of each cell line were seeded in each of 20 wells (13mm diameter) supplemented with complete selective

medium and incubated overnight. Selective medium was added in 5 cell-free wells for control purposes. The following day the growth medium was aspirated from 4 cell-containing wells and 1 cell-free well, and replaced by 250 μl non-selective medium and 50 μl of CellTiter 96 Aqueous One Solution Reagent. The plate was incubated for a further 1 hour, following which the contents of the 5 pre-treated wells were aspirated and their absorption at 490nm measured by spectrophotometry. On the 3^{d}, 4^{th}, 5^{th}, and 6^{th} day of the experiment, the same procedure was repeated for a further 4 cell-containing wells and 1 cell-free well at a time. For each day, the absorbance value obtained from the control cell-free well was subtracted from the absorbance values obtained from each of the 4 cell-containing wells. The mean values per day were calculated and plotted on a graph.

9) Caspase-3 assay:

Cells were grown in 10-cm dishes, harvested and re-suspended in cell lysis buffer (10 mM HEPES pH 7.4, 2 mM EDTA, 0.1% CHAPS, 5 mM DTT, 1 mM PMSF, 10 μg/ml pepstatin A, 10 μg/ml aprotinin, and 20 μg/ml leupeptin). After repeated freeze-thaw cycles, lysates were centrifuged and aliquots of the supernatant fraction equivalent to 40 μg of protein were obtained. Caspase-3 activity was measured using the CaspACE assay system (Promega, UK) according to the manufacturer's instructions. Briefly, for each sample the following were added in a micro-centrifuge tube:

32 μl of assay buffer

2 μl DMSO

10 μl DTT (100mM)

40 μg sample

2 μl DEVD-pNA (10mM). dH_2O was added to a final volume of 100μl.

A mixture containing the same amounts of assay buffer, DMSO, DTT and DEVD-pNA but no sample was prepared and used for control purposes. The tubes were incubated at 37°C for 4 hours, following which the absorbance of their contents at 405nm was measured by spectrophotometry. A standard curve for pNA amounts was constructed using serial dilutions of the 10mM pNA stock provided. The following mixtures were prepared:

1) 20 μl DMSO and 80 μl dH_2O

2) 10 μl pNA (10μM), 10 μl DMSO and 80 μl dH_2O (final concentration 1 μM)

3) 20 μl pNA (10μM) and 80 μl dH_2O (final concentration 2 μM)

4) 5 μl pNA (100μM), 15 μl DMSO and 80 μl dH_2O (final concentration 5 μM)

5) 10 μl pNA (100μM), 10 μl DMSO and 80 μl dH_2O (final concentration 10 μM)

6) 5 μl pNA (1 mM), 15 μl DMSO and 80 μl dH_2O (final concentration 50 μM)

7) 10 μl pNA (1 mM), 10 μl DMSO and 80 μl dH_2O (final concentration 100 μM)
The absorbance of all 7 mixtures at 405nm was measured by spectrophotometry and the values plotted on a graph against the solutions' final concentrations. The slope of the best-fit line and the Y-axis interception were estimated from the graph.
The caspace-3 activity for each sample was calculated using the following formula:

X = [(ΔA – Y)/ time] x volume/slope
Where, ΔA = (the absorbance value of each sample) – (the value of the control)
Y = the intercept of the pNA curve constructed
Time = the incubation time of the tubes (4 hours)
Volume = the volume of each sample (100 μl)
And slope = the slope estimated from the pNA curve constructed.

Finally, the specific caspase-3 activity for each sample was calculated using the following formula:
Specific activity = X/ amount
Where X= the caspase activity calculated as described above and
Amount= the μg of protein contained in 100 μl of each sample (40 μg).

10) Transient transfection of human embryonic kidney (HEK) 293 cells:
The cells were seeded in 10cm P90 dishes and grown in complete medium until 40-60% confluent. On the day of the transfection the following were added in a micro-centrifuge tube:
300 μl of DMEM
80 μl of polyfect transfection reagent (QIAGEN)
8 μg of total DNA
The reaction was mixed by pulse vortexing and equilibrated at room temperature for 10min. The reaction solution was then diluted with 1 ml DMEM, mixed gently and added to the cells along with fresh complete medium.

11) Electron microscopy of cultured cells:
Cells were grown to confluence on glass coverslips and then fixed for 24 hr in 2% glutaraldehyde in 0.1 mM cacodylate buffer (pH 7.4). Fixed cells were post-fixed in 1% OsO_4, dehydrated in ethanol and embedded in Spurr's low-viscosity epoxy resin. Ultra-thin sections were cut in a plane parallel to the plane of the culture dish and examined with a JEOL 100SX transmission electron microscope. The number and size of individual desmosomes was measured in 10 randomly selected electron micrographs (final magnification x9000) of each cell line examined.

12) Yeast-two hybrid (Y2H):

a) Preparing dsDNA from a plasmid cDNA library:

Terrific Broth (500 ml) containing 100mg/μl ampicillin was inoculated with 2.5 x 10^9 cells from the library (16 hours, 30°C, 275rpm). The cells were supplied in 80% SOB medium-20% glycerol from Invitrogen, while Terrific Broth was prepared in the following way: Tryptone (6g, Fisher Scientific), yeast extract (12g, Fisher Scientific) and glycerol (2 ml, AnalaR) were dissolved in dH_2O and adjusted to a final volume of 450 ml. KH_2PO_4 (1.15g, SIGMA) and K_2HPO_4 (6.25g, SIGMA) were dissolved in dH_2O and adjusted to a final volume of 50 ml. Both solutions were autoclaved on liquid cycle for 20min, allowed to cool to 55°C and mixed. The chosen antibiotic was added at the desired concentration and Terrific Broth was stored at 4°C. Following the incubation period, a sample from the culture was taken and its A590 was measured using a spectrophotometer. The predicted value is within 0.2 and 0.8. The culture was then centrifuged, the supernatant discarded and the pellets stored at -20°C. Plasmids were extracted from the pellets using a MEGA QIAGEN plasmid purification kit according to the instructions given. Briefly:

The yeast pellets were re-suspended first in P1 re-suspension buffer, then in P2 lysis buffer and allowed to equilibrate to room temperature for 5min. A QIAfilter Mega-Giga cartridge (QIAGEN) was assembled onto a 45mm-neck glass bottle and connected to a vacuum source. P3 neutralization buffer was added to the lysate which was poured into the cartridge. The lysate was incubated at room temperature for 10min and then the vacuum source was switched on. FWB2 wash buffer was added to the cartridge and the vacuum source was switched on again until the liquid had passed through completely. QBT equilibration buffer was added to a QIAGEN-tip, pre-assembled onto a beaker, and the column was allowed to empty by gravity flow. The lysate was then applied onto the equilibrated QIAGEN-tip, allowed to enter the resin by gravity flow and the flow-through was discarded. The QIAGEN-tip was washed with a total of 200ml of QC wash buffer, the column was allowed to empty by gravity flow and the flow-through discarded. Following the washes, the QIAGEN-tip was assembled to a falcon tube, QF elution buffer was added and the column was allowed to empty by gravity flow. Isopropanol was added to the eluted DNA and the mixture was centrifuged. Following centrifugation, the supernatant was discarded, the pellet was re-suspended in 70% ethanol and centrifuged again. The pellet was allowed to air-dry in an incubator at 37°C and then eluted in TE elution buffer. The A260 of the sample was measured. The predicted value was 0.5-2.5mg of DNA. The samples were kept at -20°C.

b) Preparation and transformation of competent *S.cerevisae*:

The desired *S.cerevisae* strain was plated on Yeast Extract Peptone Dextrose (YPD, Fisher Scientific) plates at 30°C for 48 hours until isolated, single colonies had grown. In order for competent *S.cerevisae* cells to be generated, the S.c. EasyComp Transformation Kit (Invitrogen) was used according to the instructions provided. Briefly:

A single yeast colony was inoculated in YPD (30°C, 275rpm, 16-18 hrs). Following the inoculation period, a sample was taken from the culture and its OD_{600} was measured using a spectrophotometer. The predicted value is between 3 and 5. The cells from the overnight culture were then diluted to an OD_{600} value of 0.2-0.4 in a total volume of 10 ml of YPD. The cells were grown at 30°C in a shaking incubator for 3-6 hours until the OD_{600} reached a value of 0.6-1.0. The cells were pelleted by centrifugation and the pellet re-suspended in Solution I. The mixture was again centrifuged, the supernatant discarded and the cell pellet re-suspended in Solution II.

Competent *S.cerevisae* cells were transformed with the plasmid of interest using the S.c. EasyComp Transformation Kit (Invitrogen) according to the instructions provided. Briefly: Vector DNA (1-5μg) was added to 50 μl of competent yeast cells. Solution III was added to the mixture and mixed by vortexing. The transformation reaction was then incubated for one hour (30°C) during which it was occasionally mixed by vortexing. Following the incubation period, the tube was centrifuged, the supernatant discarded, the pellet re-suspended in YPD medium and plated on YPD plates.

c) Co-transformation of Library-Scale MaV203 Yeast cells:

Library-Scale Frozen Competent MaV203 Yeast cells (Invitrogen) were co-transformed with the:

1) pDEST^{TM}32 plasmid (expresses the DNA-binding domain and the gene of interest)

2) pEXP-AD502 plasmid (expresses the activation domain and the cDNA library)

Both the competent MaV203 yeast cells and the PEG/LiAc solution (Invitrogen) were thawed. A 250μl cell aliquot was transferred to a Falcon tube. pDEST^{TM}32 (10μg) and pEXP-AD502 (10μg) were added to the cells and mixed gently. PEG/LiAc solution (1.5 ml) was added and mixed well by swirling. The solution was incubated in a 30°C water bath for 30min, during which the tube was occasionally swirled. Following incubation, 88μl of DMSO (Fisher Scientific) was added and mixed by swirling. The cells were then heat-shocked (42°C, 20min) with occasional swirling. The solution was centrifuged, the supernatant discarded, the pellet re-suspended in sterile saline (0.9% NaCl) and two dilutions (1:800 and 1:8000) of the transformation reaction were plated on two 10-cm SC-Leu-Trp-plates to estimate the total number of transformants. Aliquots (400μl) of the transformation were then plated on twenty 15-cm SC-Leu-Trp-Ura-His+3-Amino-1,2,4-

Triazole (3AT, SIGMA) plates and incubated for 60-72hrs at 30°C. The optimum concentration of 3AT for the DNA binding domain vector was previously determined by titrating HIS3 activity on plates lacking histidine containing 3AT at concentrations: 10mM, 25mM, 75mM and 100mM to a point at which growth in the absence of histidine was inhibited. The number of transformants was estimated by multiplying the number of colonies on the 10-cm plates by the dilution factor. The colonies that grew on the twenty 15-cm SC-Leu-Trp-Ura-His+3AT plates were picked individually and plated on two replica YPD plates under the same selective conditions.

d) Beta-galactosidase filter assay:

Beta-mercaptoethanol (150µl, SIGMA) was added to 50ml of Z-buffer. (Z buffer was made by adding 4.26g of Na_2HPO_4, 2.76g of $NaH_2PO_4H_2O$, 0.4g KCl and 0.1g of $MgSO_47H_2O$ in dH_2O at pH7, final volume: 500ml). 5-bromo-4-chloro-3-indolyl-beta-D-galactopyranoside (X-gal, 100mg, Fermentas) was dissolved in 2ml of formamide (Applied Biosystems). 200µl of the X-gal solution was added to 10ml of the beta-mercaptoethanol-Z-buffer solution and mixed gently. A circular piece of nitrocellulose filter cut to fit a 15-cm plate was placed across the master plate of yeast colonies and allowed to equilibrate to room temperature for 2min. The filter was removed from the yeast plate and placed in an aluminium foil "boat", colonies facing up. The foil was slowly lowered into liquid nitrogen and raised again after 10 sec. Immersion of the filter in liquid nitrogen was repeated three times. A circular piece of absorbent paper was placed in an empty clean 15-cm plate and soaked with Z-buffer-X gal solution. The nitrocellulose filter was allowed to warm in room temperature for 2min and transferred colony side up, on top of the absorbent paper. The dish was covered and incubated (30°C, 3-4 hrs) during which it was regularly checked. The colonies that turned blue after the beta-galactosidase filter assay were marked, picked from the master yeast plate, plated on non-selective yeast medium and incubated at 30°C for 72hrs (Figure 1).

e) Characterization of yeast two hybrid protein interactions:

Yeast cells were mixed with TE buffer (QIAGEN). Lyticase (SIGMA) was added and the lysate was incubated at 37°C for 1 ½ hr during which it was occasionally mixed by vortexing. Following incubation, the plasmids were extracted using a QIAprep SpinminiPrep Kit (QIAGEN) as described above. The eluted product (5µl) was then used to transform 100µl of competent *E.coli* cells as described above and the cells were plated using the appropriate antibiotic for selection of the pEXP-AD502 plasmid. The plates were incubated at 37°C for 16-18hrs, colonies were picked and grown individually in LB broth containing the appropriate antibiotic and the plasmid was

isolated using a QIAprep Spin mini Prep Kit (QIAGEN) as described above. DNA (500-600ng) was used to set up a sequencing reaction and samples were sequenced on an ABI3100 sequencer. In order to identify putative interacting partners of the protein of interest isolated by the yeast-two-hybrid library screening, the data obtained were compared against the Human Reference DNA Sequences by a sequence similarity searching computer program (BLAST)

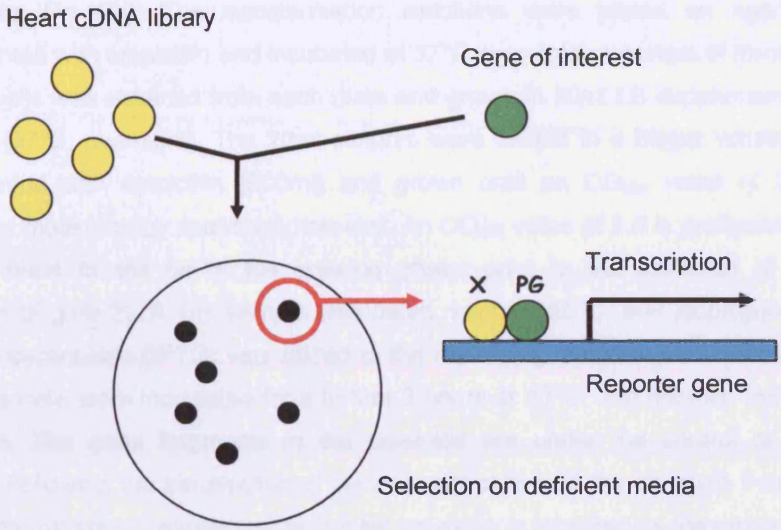

Figure 1: The basic concept of the Y2H technique: The gene of interest, which acts as a bait, is fused to a vector also expressing a DNA binding domain, while a heart cDNA library is fused to a vector that also expresses the activation domain. When the protein of interest interacts with any protein encoded by the heart cDNA library, the DNA binding domain and the activation domain are brought together and the complete transcription factor can drive the expression of a reporter gene.

13) Co-immunoprecipitation:

HEK293 cells were transiently transfected with epitope-tagged plasmids (A and B) expressing the proteins of interest as described above. The cultures were grown to confluence, harvested and the pellets washed in PBS. Cells were lysed by re-suspension of the pellets in IP buffer (25 mM Hepes-KOH pH 7.5, 150 mM KCl, 1 mM EDTA, 12.5 mM $MgCl_2$, 0.1% NP-40), sonicated and centrifuged. Aliquots of the supernatant fraction (equivalent to 2mg of protein) were mixed with an antibody raised against the epitope expressed by plasmid A and protein G-Sepharose beads slurry (Santa Cruz Biotechnology) in IP buffer and rotated overnight at 4°C. Following centrifugation, the supernatant was discarded; the pellet was washed three times and re-suspended in IP buffer. Western immunoblotting was performed using an antibody

raised to recognize the epitope expressed by plasmid B. Similarly, the procedure was repeated using the two antibodies in the reverse order.

14) In vitro protein binding assay:

BL21 star cells (Invitrogen, UK) were transfected with recombinant plasmids constructed for the expression of GST as well as the GST-fused N-terminal, central and C-terminal domains of the histidine-rich calcium binding protein (HRC-BP, *kindly donated by Dr. Ho*). The transformation reactions were plated on agar plates supplemented with ampicillin and incubated at 37°C overnight. A scrape of transformed bacterial cells was obtained from each plate and grown in 20ml LB supplemented with ampicillin (37°C, overnight). The 20ml cultures were diluted in a bigger volume of LB supplemented with ampicillin (500ml) and grown until an OD_{600} value of 2.0 was reached as measured by spectrophotometry. An OD_{600} value of 2.0 is preferable, since the cells need to still be in the growing phase prior to the induction of protein expression (Figure 2). A 1ml sample was taken, kept at -20°C, and isopropyl-beta-D-thiogalactopyranoside (IPTG) was added to the remaining cultures (final concentration 1mM). The cells were inoculated for a further 3 hours at 30°C, and another 1ml sample was taken. The gene fragments in the plasmids are under the control of the lac promoter. Following the transfection of the bacterial cells with the plasmids though, the gene fragments are not expressed as the lac promoter is inhibited by the presence of a repressor molecule. IPTG acts by binding the repressor and allowing transcription and therefore expression of the proteins of interest (Figure 3). IPTG is used instead of lactose (the natural activator of the lac promoter) since it is an artificial substance and cannot be metabolized by the cells. After induction of expression by IPTG, the cultures are incubated at 30°C, so as to avoid over-expression of the exogenous proteins, which may have deleterious effects to the cells.

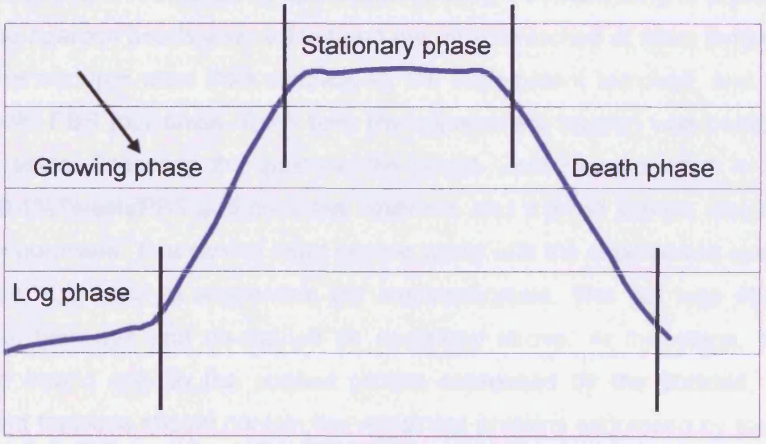

Figure 2: Bacterial growth curve showing the four typical phases of growth.

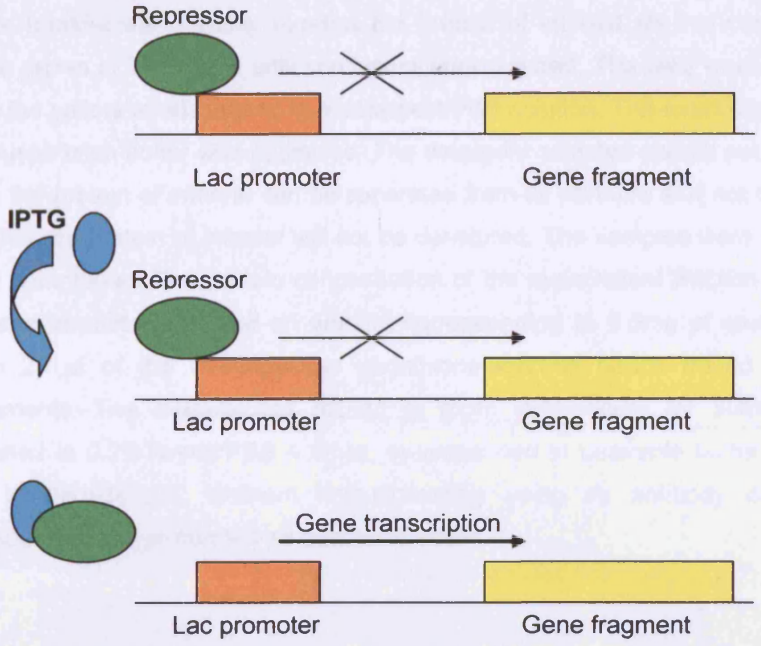

Figure 3: Mechanism of action of isopropyl-beta-D-thiogalactopyranoside (IPTG).

The two 1ml samples taken from the culture, one prior and one after induction by IPTG, were centrifuged, the pellets re-suspended in Laemmle buffer, heated, loaded on an acrylamide gel and subjected to electrophoresis. The gel was subsequently stained with Coomassie blue dye and de-stained with 20% acetic acid- 80% ethanol. The remaining cultures were centrifuged and the pellets re-suspended in a solution made of 50mM Tris-HCl, 1% Triton-X 100, 100mM NaCl and protease inhibitors (pH=8.0). The re-suspended samples were sonicated, centrifuged and the protein concentration of the supernatant fraction measured by spectrophotometry. For each 2mg of protein, 50µl of glutathione-agarose beads were added and the mixture rocked at room temperature for 30min. The mixtures were then centrifuged, the supernatant removed, and the beads washed with PBS four times. Each time the supernatant fraction was being removed and kept aside. Following the washes, the beads were re-suspended in a solution made of 0.1%Tween/PBS and protease inhibitors, and a small sample was kept aside for control purposes. This control bead sample along with the supernatant samples kept aside were subjected to acrylamide gel electrophoresis. The gel was stained with Coomassie blue dye and de-stained as described above. At this stage, the beads should be bound only to the purified protein expressed by the plasmid, while the supernatant fractions should contain the remaining proteins expressed by the bacterial cells.

Cells transfected to stably express the protein of interest (in this case, plakoglobin) were grown in T75 flasks until confluency was reached. The cells were then harvested and the pellets re-suspended in a detergent/PBS solution. The exact composition of the re-suspension buffer was optimized. The detergent selected should not be too mild, so that the protein of interest can be separated from its partners and not too harsh either so that the protein of interest will not be denatured. The samples were sonicated twice and centrifuged. The protein concentration of the supernatant fraction was measured by spectrophotometry and an amount corresponding to 0.5mg of protein was mixed with 25 µl of the re-suspended glutathione-agarose beads bound to the protein fragments. The mixture was rocked at room temperature for 30min, centrifuged, washed in 0.2%Tween/PBS 4 times, re-suspended in Laemmle buffer and loaded on an acrylamide gel. Western immunoblotting using an antibody directed against plakoglobin was performed as described above.

METHODS VALIDATION, RESULTS AND DISCUSSION:

1) S39_K40insS; effects on the binding properties of plakoglobin:

Plakoglobin cDNA was amplified by PfX and EXL polymerase and inserted into the pDONR™221 vector. (Figure 4).

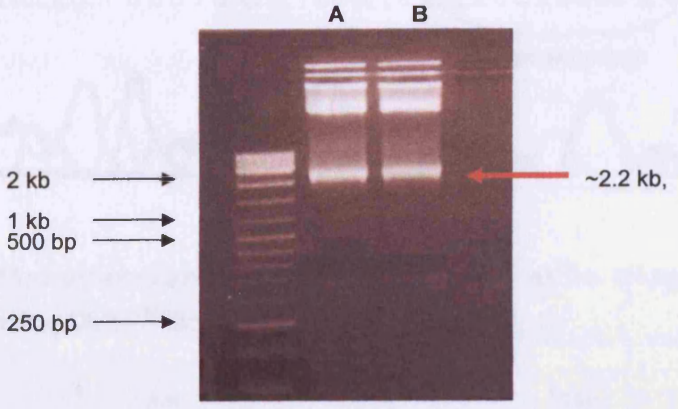

Figure 4: The bands indicated by the red arrow, correspond to plakoglobin cDNA amplified by PfX (A) and EXL (B) polymerase. The higher bands correspond to super-coiled DNA, which tends to migrate at a lower speed during electrophoresis. The lower, fainter bands may represent amplification products stemming from non-specific primer binding.

Following the generation of the pDONR™221-plakoglobin entry clone, site-directed mutagenesis was performed in order to create an entry clone expressing the mutant plakoglobin protein. Both wildtype and mutant genes were then transferred to the pDEST™32-DNA binding domain containing-vector (Figures 5 & 6).

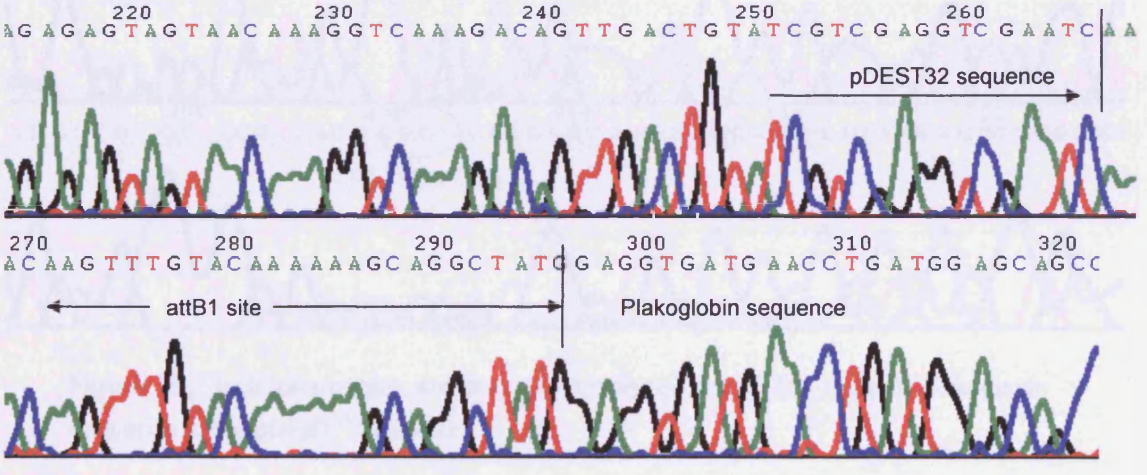

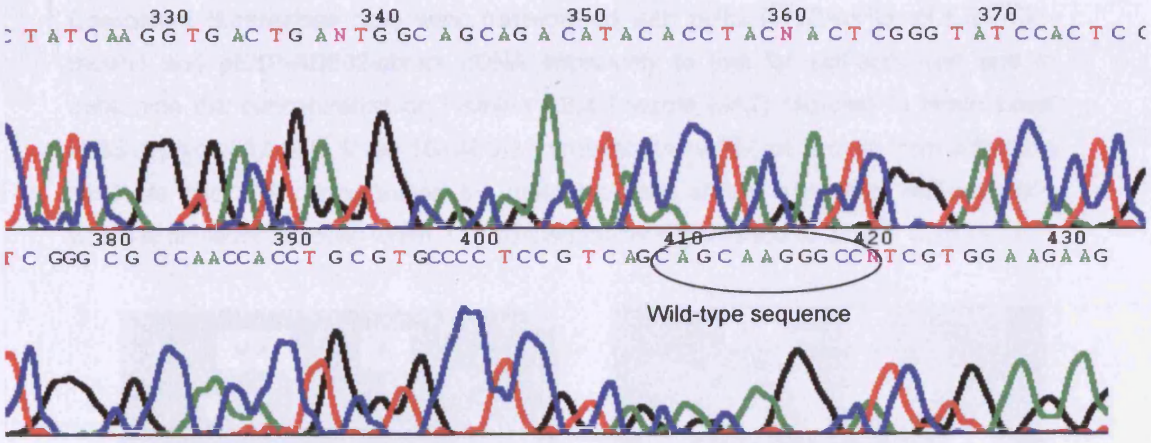

Figure 5: Electropherogram showing the incorporation of the wildtype plakoglobin sequence in the pDEST^{TM}32 vector.

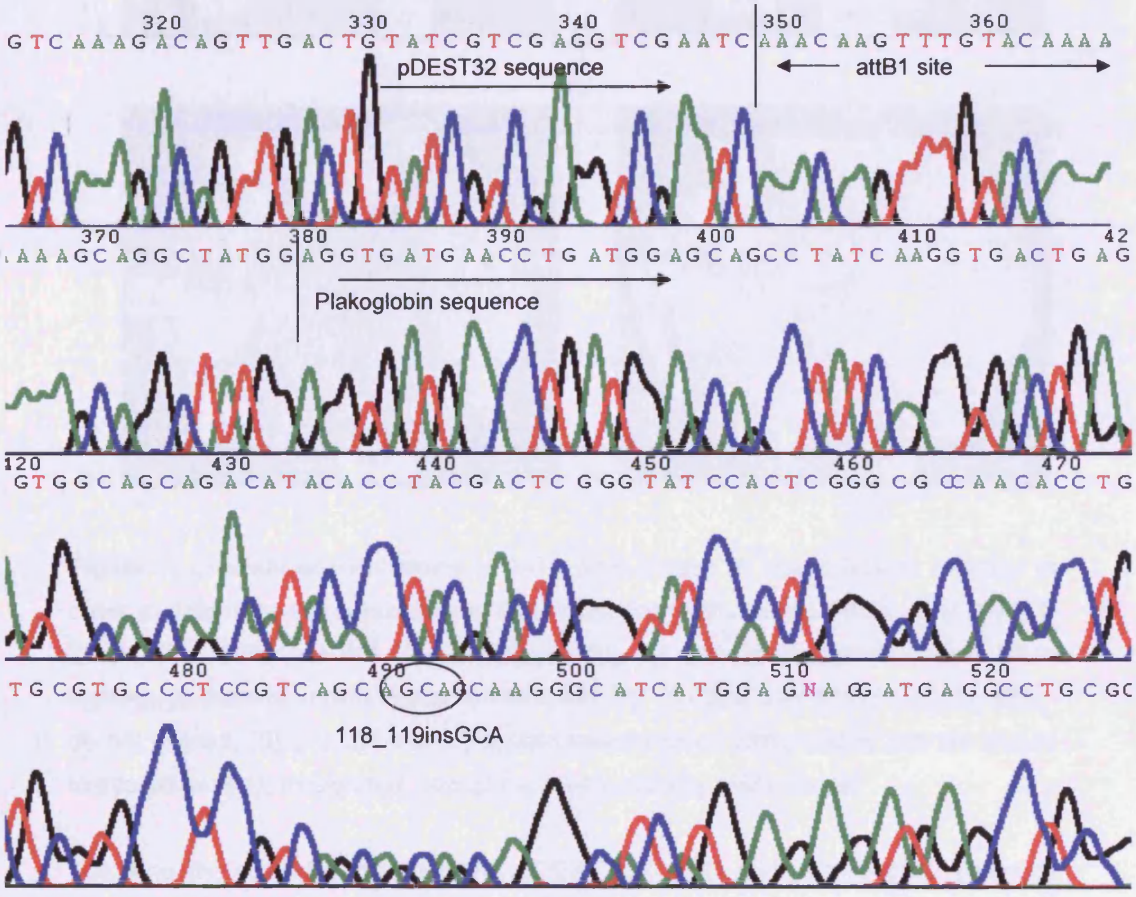

Figure 6: Electropherogram showing the incorporation of the mutant plakoglobin sequence in the pDEST^{TM}32 vector.

Competent *S.cerevisae* cells were transformed with pDEST^{TM}32-wtPG, pDEST^{TM}32-mutPG and pEXP-AD502-library cDNA separately to test for self-activation and to determine the concentration of 3-Amino-1,2,4-Triazole (3AT) required to titrate basal HIS3 expression levels. Even 10mM 3-AT prevents the wild-type protein from activating HIS3. At this 3AT concentration the mutant protein shows a level of self-activation which is however inhibited when 3AT concentration is increased to 25mM. (Figure 7).

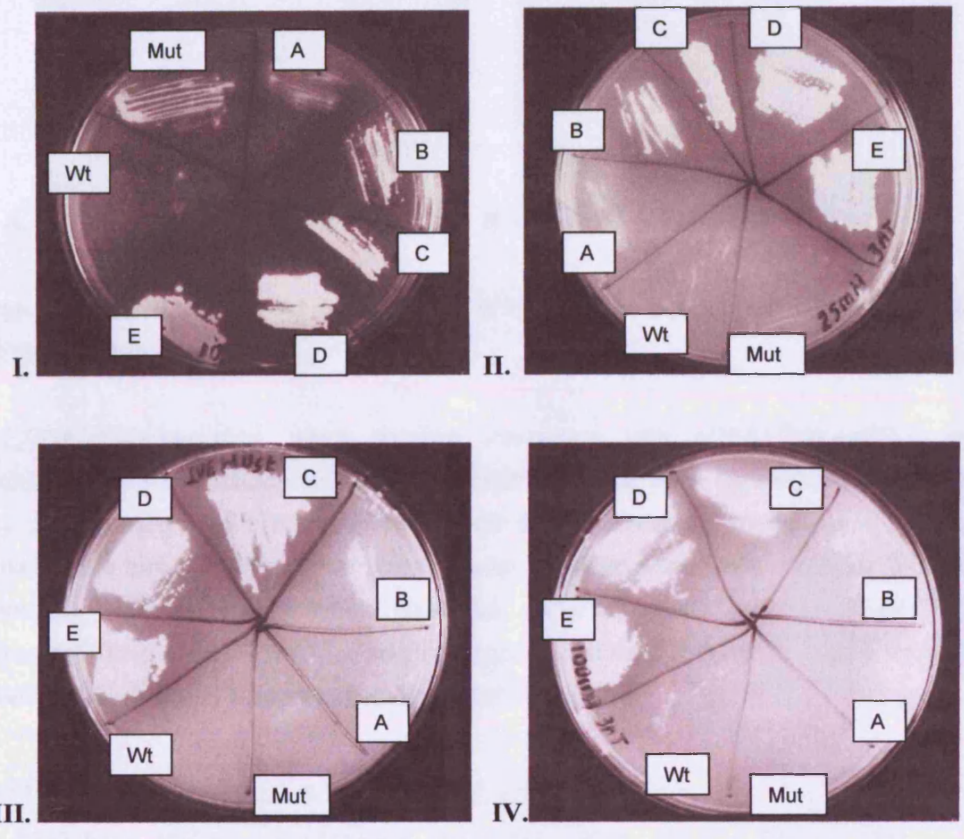

Figure 7: Different concentrations of 3-AT were titrated in plates lacking histidine in order to determine the concentration that inhibits self-activation of HIS3. (I) 10mM, (II) 25mM, (III) 75mM and (IV) 100mM. [A], [B], [C], [D] and [E] are control strains which express proteins of known interaction strength. [A] contains only empty vectors, which do not interact. [B], [C] ,[D] and [E] contain vectors fused with proteins that are known to interact weakly, moderately, strongly and very strongly respectively.

Following the control transformations, pDEST^{TM}32-wtPG and pEXP-AD502 plasmids were introduced into yeast cells and plated on SC-Leu-Trp-His+ 10mM 3AT plates. Similarly, pDEST^{TM}32-mutPG and pEXP-AD502 were introduced into yeast cells and plated on SC-Leu-Trp-His+ 25mM 3AT plates. The total number of transformants was

estimated to be 3.6 x 10^4 and 1.2 x 10^4 colonies per 250- µl transformation in the WT and the MUT reactions respectively (Figure:8).

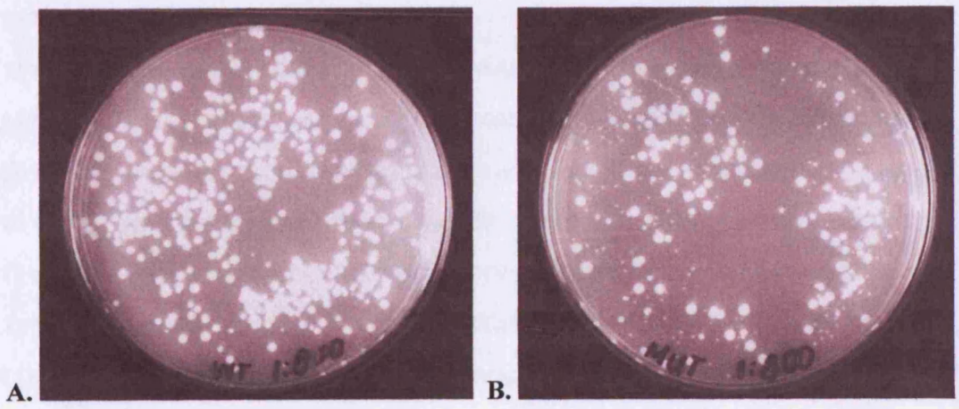

Figure 8: Estimation of transformation efficiency for pDEST™32-wtPG (A) and pDEST™32-mutPG (B).

pEXP-AD502 plasmids, which through interaction with pDEST™32-wtPG or pDEST™32-mutPG could induce the transcription of lacZ were isolated and identified by direct sequencing. The yeast-two-hybrid library screening showed that mutant plakoglobin interacts with all the proteins wildtype plakoglobin does. However, it also interacts with two clones which have not previously been associated with the desmosomal protein: TGF-beta induced apoptosis protein 2 (TAIP-2, Figure 9) and histidine-rich calcium binding protein (HRC-BP, Figure 10).

```
Features: TGF-beta induced apoptosis protein 2

Score = 3690 bits (1998),Identities = 2002/2004 (99%), Gaps = 0/2004 (0%)
 Strand=Plus/Plus

Query  1576      AGGTGGATCGTATGTCTTTCCCATGCGGCTGCACTAAAGAAGGATGTAGTAACACAGCAG
                  ||||||||||||||||||||||||||||||||||||||||||||||||||||||||||||
Sbjct  16744627  AGGTGGATCGTATGTCTTTCCCATGCGGCTGCACTAAAGAAGGATGTAGTAACACAGCAG

Query  1636      GTAGAATTGAATTTAATCCTATCCGTGTTCGGACTCACTTTTTGCACACAATAATGAAAC
                  ||||||||||||||||||||||||||||||||||||||||||||||||||||||||||||
Sbjct  16744687  GTAGAATTGAATTTAATCCTATCCGTGTTCGGACTCACTTTTTGCACACAATAATGAAAC

Query  1696      TTGAACTGGAGAAAAACCGAGAGCAGCAAATCCCCACGCTGAATGGCTGCCACAGTGAGA
                  ||||||||||||||||||||||||||||||||||||||||||||||||||||||||||||
Sbjct  16744747  TTGAACTGGAGAAAAACCGAGAGCAGCAAATCCCCACGCTGAATGGCTGCCACAGTGAGA
```

Figure 9: Alignment of a mutPG-binding plasmid sequence with human TGF-beta induced apoptosis protein-2 as shown by BLAST.

Features: histidine-rich calcium-binding protein precursor

Score = 3552 bits (1923),Identities = 1944/1953 (99%), Gaps = 6/1953 (0%)
Strand=Plus/Minus

```
Query  537      AAAGGACAAAGGAGAGACACAGAGaaaaaaaGAGACCAACCCCAAAGGGACAAAGACCCC
                 ||||||||||||||||||||||||||||||||||||||||||||||||||||||||||||
Sbjct  1199197  AAAGGACAAAGGAGAGACACAGAGAAAAAAAGAGACCAACCCCAAAGGGACAAAGACCCC

Query  597      AACGTTTGTCCACATTGCCGCAGAGGCAGCTGGAGCCAGTGCTGCCTGTCCGTCCCCATG
                 ||||||||||||||||||||||||||||||||||||||||||||||||||||||||||||
Sbjct  1199137  AACGTTTGTCCACATTGCCGCAGAGGCAGCTGGAGCCAGTGCTGCCTGTCCGTCCCCATG

Query  657      GGCCACCATAGGCCATGGCTGCACGCTTCTGTCCTCTGGGCTGGGGTGGCCAGCCTGCTC
                 ||||||||||||||||||||||||||||||||||||||||||||||||||||||||||||
Sbjct  1199077  GGCCACCATAGGCCATGGCTGCACGCTTCTGTCCTCTGGGCTGGGGTGGCCAGCCTGCTC

Query  717      CTCCCCCCGGCCATGACCCAGCAGCTCAGAGGGGATGGGCTAGGCTTCAGAAACCGGAAC
                 |||||||||||||||||||||||||||||||||||| ||||||||||||||||||||
Sbjct  1199017  CTCCCCCCGGCCATGACCCAGCAGCTCAGAGGGGATGGGCTGGGCTTCAGAAACCGGAAC
```

Figure 10: Alignment of a mutPG-binding plasmid sequence with human histidine-rich calcium-binding protein as shown BLAST.

Although the beta-galactosidase assay typically offers a high degree of confidence as to the true existence of the interactions revealed by Y2H screening, all interactions identified should be confirmed by further in vitro methods prior to drawing conclusions as to their implications in human physiology and pathology.

The plakoglobin-TAIP2 interaction was tested by co-immunoprecipitation. In contrast to the results obtained from the Y2H screening, both wildtype and mutant plakoglobin were shown to bind the TAIP2 protein (Figures 11, 12).

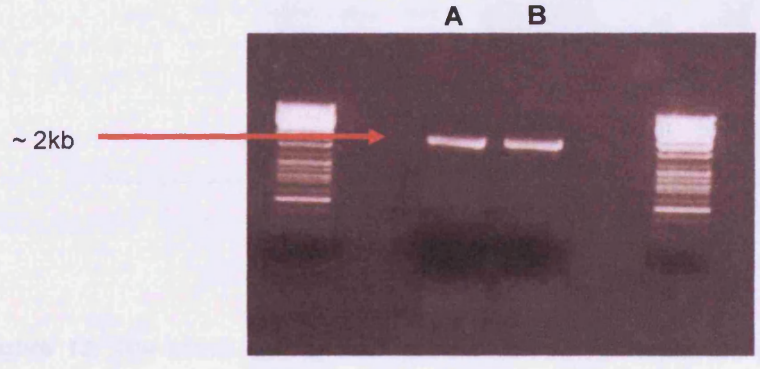

Figure 11: The bands indicated by the red arrow correspond to TAIP2 cDNA as amplified by PfX (A) and EXL (B) polymerase.

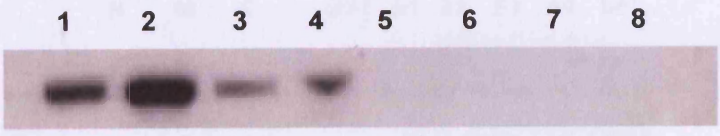

Figure 12: Lysates of cell lines induced to express wildtype (lane 1) and mutant plakoglobin (lane 2) were loaded for control purposes. Co-immunoprecipitation of wildtype PG and TAIP-2 (lane 3), mutant PG and TAIP-2 (lane 4), wildtype PG and V5 vector (lane 5), mutant PG and V5 vector (lane 6) His Max vector and TAIP-2 construct (lane 7) and His Max vector and V5 vector only (lane 8).

The plakoglobin-HRC BP interaction was tested by an in vitro protein binding assay. Four recombinant plasmids, encompassing glutathione-s-transferase (GST) as well as the GST-fused N-terminal, central and C-terminal domains of HRC-BP were used to transfect competent bacterial cells and their expression was induced by IPTG (Figure 13). Subsequently the lysates were incubated with glutathione agarose beads, which couple GST (Figure 14).

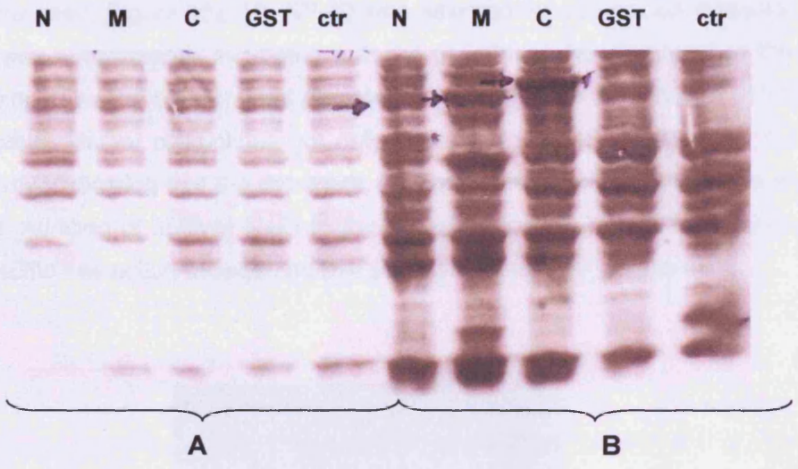

Figure 13: The bands on the Coomassie blue-stained acrylamide gel represent the proteins expressed by the cells prior (A) and after (B) induction by IPTG. [N] stands for the N-terminal HRC BP domain, [M] stands for the central (middle) protein part, while [C] stands for the C-terminal protein domain.

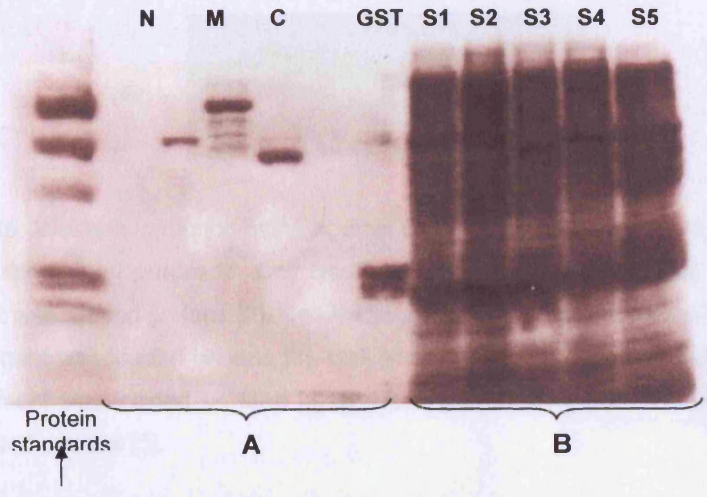

Figure 14: Purified glutathione agarose beads bound to the protein constructs of interest (A), and non-bound proteins present in the 5 supernatant fractions isolated during the bead purification (B).

A number of detergent solutions were used to optimise solubilization of mutant plakoglobin from a stably-transfected cell line. The largest amount of plakoglobin, as shown by Western immunoblotting, was isolated when 1% Tween/PBS or 1% NP-40/PBS were used (Figure 15). 1% NP-40 was selected for optimal solubilization. The cell lysate was subsequently incubated with the glutathione beads bound to the HRC BP fragments, to test whether mutant plakoglobin interacts with any domain of the HRC binding protein. Mutant plakoglobin not only interacted with all 3 fragments, but also with GST only, indicating that the detergent solution selected was not stringent enough (Figure 16). Addition of 250mM NaCl to the solubilization 1% NP-40 buffer prevented the non-specific interaction between mutant plakoglobin and GST (Figure 17).

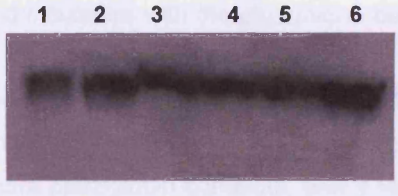

Figure 15: The bands represent plakoglobin solubilised from a stably transfected cell line using a number of different detergent solutions: [1] 0.5% Tween/PBS, [2] 1% Tween/PBS, [3] 0.5% Triton-X/PBS, [4] 1% Triton-X/PBS, [5] 0.5% NP-40/PBS and [6] 1% NP-40/PBS.

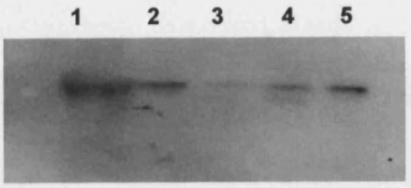

Figure 16: Western immunoblotting against plakoglobin. Cell lysate only was loaded on lane [1] for control purposes. Cell lysate along with beads bound to the N-HRC BP fragment was loaded on lane [2]. Cell lysate along with beads bound to the middle-HRC BP fragment was loaded on lane [3]. Cell lysate along with beads bound to the C-HRC BP fragment was loaded on lane [4] and cell lysate along with beads bound to GST was loaded on lane [5].

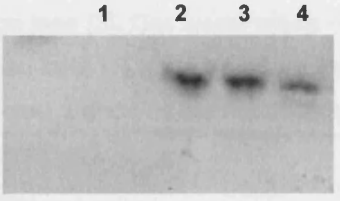

Figure 17: Western immunoblotting against plakoglobin. Cell lysate along with beads bound to GST was loaded on lane [1]. Cell lysate along with beads bound to the N-HRC BP fragment was loaded on lane [2]. Cell lysate along with beads bound to the middle-HRC BP fragment was loaded on lane [3]. Cell lysate along with beads bound to the C-HRC BP fragment was loaded on lane [4].

The pGFP-C3-wtPG plasmid, which expresses GFP-tagged wildtype plakoglobin was used to transiently transfect HEK293 cells. Plakoglobin was solubilised by the same detergent solution used for isolation of the S39_K40insS bearing protein (1% NP-40/PBS-250mM NaCl) and incubated with the glutathione beads bound to the HRC BP fragments.

Wildtype plakoglobin does not bind any of the three HRC BP fragments. Western immunoblotting of the control cell lysate gave two bands, a higher one corresponding to the GFP-bound recombinant plakoglobin construct, and a lower one, corresponding to the endogenous plakoglobin naturally expressed the HEK293 cells. The size of GFP (27 kDa) may explain the difference between the two bands observed (Figure 18).

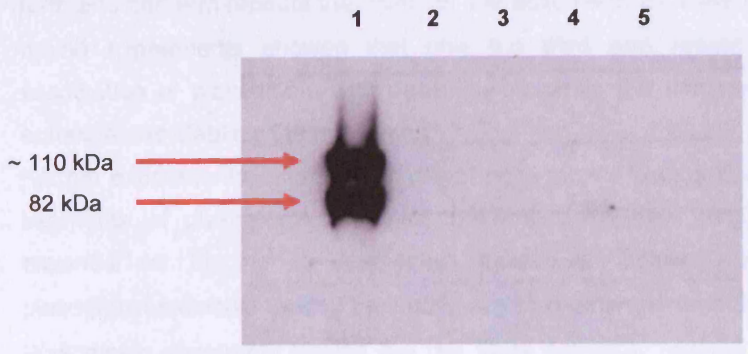

Figure 18: Western immunoblotting against plakoglobin. Cell lysate only was loaded on lane [1] for control purposes. Cell lysate along with beads bound to the N-HRC BP fragment was loaded on lane [2]. Cell lysate along with beads bound to the middle-HRC BP fragment was loaded on lane [3]. Cell lysate along with beads bound to the C-HRC BP fragment was loaded on lane [4] and cell lysate along with beads bound to GST was loaded on lane [5]. Protein standards are not shown.

Discussion:

Plakoglobin consists of three structurally distinct regions: the unique amino- and carboxy-terminal segments and a 560- amino acid long central region comprising 13 arm repeats. Specific regions along the plakoglobin protein are involved in a complex pattern of interactions with other proteins.[281] In transfected human A-431 carcinoma cells, a chimeric protein combining the cytosolic vesicle-forming glycoprotein synaptophysin with the complete human plakoglobin sequence localized at the cell borders and was incorporated into desmosomal structures. This strong topogenic effect was driven by associations of plakoglobin with desmosomal cadherins.[282] To determine the sites of plakoglobin responsible for this topogenic effect, a synaptophysin insertion mutagenesis approach was undertaken. Synaptophysin was inserted at various parts of the plakoglobin protein resulting in the formation of plakoglobin-coated vesicles, where one domain was functionally affected while the remaining domains maintained their ability to engage in protein-protein interactions. Chimeras containing a synaptophysin insertion in any of the three first arm repeats of plakoglobin were unable to interact with either desmocollins or desmogleins. On the contrary, chimeras containing a synaptophysin insertion in either the forth or the fifth arm repeat could interact with desmocollins and desmogleins, however their association with E-cadherin was abolished. These data clearly indicate that the first three armadillo repeats of plakoglobin are responsible for interaction with desmosomal cadherins, while it is the

forth and fifth arm repeats that mediate interaction with E-cadherin.[281] In fact, yeast-two hybrid experiments showed that only the third arm repeat is essential for the association of plakoglobin with desmogleins, while the first two arm repeats merely enhance and stabilize the interaction.[283]

Further experiments, where segments of beta-catenin were substituted by homologous segments of plakoglobin indicated that the plakoglobin sequence Arg^{142}-Arg^{233} is essential for binding to desmoglein molecules. Similar studies showed that a plakoglobin molecule lacking the Leu^{304}-Arg^{320} segment is unable to bind E-cadherin.[281] Plakoglobin constructs lacking the last three armadillo repeats do bind desmosomal cadherins though weakly, indicating that the C-terminal part of the arm region has a role in stabilizing and strengthening these interactions.[282] Moreover, these last arm repeats were shown to have a role in targeting the protein to the cell borders.[282] Transfections of carboxy-terminal plakoglobin deletion constructs into the human fibrosarcoma HT-1080 cells suggested a gradual decrease in the ability of plakoglobin and N-cadherin to associate as plakoglobin was shortened from the end of repeat 8 to the end of repeat 6 (amino acids: 375-458).[284]

It has been reported that a plakoglobin construct encompassing only the first 114 amino acids does not immunoprecipitate α-catenin. However, when plakoglobin was truncated at 161 amino acids it could readily associate with α-catenin, suggesting that the 47 residues from 115 to 161 play a major role in the interaction of the two catenins. Plakoglobin's binding site for α-catenin partially overlaps with the site required for association with desmosomal cadherins. This may be a way to ensure that only the right components are incorporated into each junction type. If plakoglobin binds α-catenin, it is unable to bind desmosomal cadherins and will therefore be incorporated into adherens junctions. Conversely, if plakoglobin binds desmosomal cadherins, it is unable to bind α-catenin and will therefore anchor intermediate filaments instead of actin microfilaments.[285] Plakoglobin constructs lacking the C-terminal domain do incorporate into desmosomes. However, extremely long junctions are formed, indicating a role of the C-terminus in limiting the size of desmosomes.[286] S39_K40insS is predicted to lead to the insertion of a serine residue at position 39 of plakoglobin. Despite the numerous bonds that plakoglobin establishes with many adhesion proteins, this part of the protein does not seem to be involved in any of the above-mentioned protein-protein interactions (Figure 19). In fact, *Palka et al.* have shown that an N-terminal truncation of plakoglobin does not affect the protein's incorporation into junctional complexes and does not have a dramatic effect on the structure of desmosomes.[286] A question therefore arises: since S39_K40insS does not seem to affect the interaction of plakoglobin with its known adhesion partners, how does it cause ARVC?

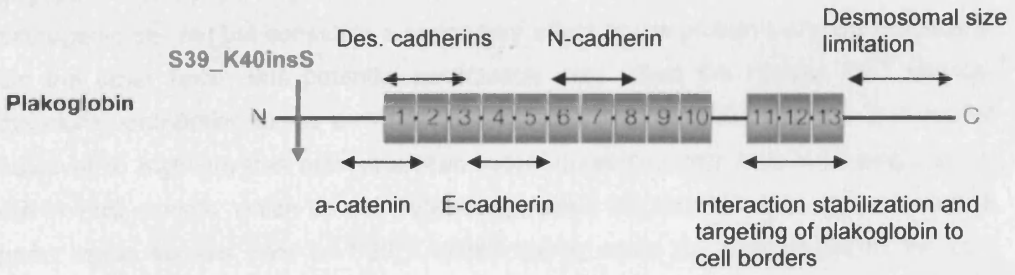

Figure 19: Schematic representation of plakoglobin domains involved in adhesive interactions in comparison to mutation localization.

The S39_K40insS-bearing protein was shown to interact with two additional proteins that have not previously been associated with plakoglobin: histidine-rich calcium binding protein (HRC-BP) and TGF-β induced apoptosis protein 2 (TAIP-2). HRC-BP localizes at the sarcoplasmic reticulum of cardiac and skeletal muscle cells, where it controls Ca^{+2} release during excitation-contraction coupling.[287] The first phase of the cardiac action potential is the depolarization of the cell membrane initiated by the influx of sodium. Membrane depolarization activates the L-type voltage-activated Ca^{+2} channels resulting in the influx of Ca^{+2} inside the cell. The Ca^{+2} entry activates the ryanodine receptors at the SR membrane, leading to further Ca^{+2} release from the SR stores to the cytoplasm. The influx of Ca^{+2} together with the Ca^{+2} release from the intracellular stores, contribute to the increase of Ca^{+2} concentration in the cell. As a result, Ca^{+2} binds troponin C switching on the contractile machinery. In order for the cell to relax, Ca^{+2} must dissociate from troponin C. The ryanodine receptor channels close, the release of Ca^{+2} from the stores stops, the Na/Ca^{+2} pumps pump Ca^{+2} outside the cell and the Ca^{+2} ATPase pumps force calcium back to the SR stores.[88] Recently, it was shown that HRC-BP binds to triadin and is able to control Ca^{+2} release through the ryanodine receptor.[288]

This is not the only time that ARVC has been associated with the excitation-contraction coupling mechanism. As mentioned in the introduction, one of the first genes associated with ARVC2 was RyR2, the gene coding for the cardiac ryanodine receptor.[85] Mutations in RyR2 were thought to permit leakage of Ca^{+2} into the cytoplasm, thereby causing electrical instability that could trigger arrhythmias.[89] RyR2 mutations are currently believed to be underlying catecholaminergic VT rather than ARVC. However, recent studies suggest that certain polymorphisms in the RyR2 gene can contribute to arrhythmogenesis and HF in a subset of ARVC patients bearing specific genotypes.[289] The fact that mutant plakoglobin binds a sarcoplasmic reticulum protein in vitro might reflect a change in the protein's structure, which would allow it to

engage in non-physiological interactions. This association may therefore be not pathogenic per se, but constitute a secondary effect of the protein's altered properties. On the other hand, this potential association may affect the normal Ca^{+2} release, therefore contributing to the arrhythmogenesis characterizing the disease. It is crucial however to highlight that both yeast-two-hybrid screening and protein binding assays are in vitro models, which do not necessarily reflect the situation that exists in vivo. A heart tissue sample from an S39_K40insS carrier could be immunostained for both mutant plakoglobin and HRC-BP. Co-localization of the two proteins in this case would provide solid evidence in support of the finding presented herein. Nevertheless, though not "waterproof" as yet, this result constitutes a provocative observation in understanding the mechanism of ARVC pathogenesis that is certainly worth further investigation.

Although TGFβ-induced apoptosis protein 2 (TAIP-2) has not previously been associated with ARVC, there is evidence that links plakoglobin to the mechanism of apoptosis. Plakoglobin regulates the expression of BCL-2, a prototypic member of apoptosis-regulating proteins, which prevent the proteolytic activation of caspases, the major executors of programmed cell death. [290,291] Desmin-null mice develop a type of cardiomyopathy characterized by extensive cardiomyocyte death, fibrosis, calcification and eventual heart failure. Over-expression of Bcl-2 in these hearts inhibits apoptosis thus decreasing the occurrence of fibrotic lesions, restoring cardiomyocyte ultrastructure and significantly improving the overall cardiac function.[292] The anti-apoptotic function of plakoglobin is independent of its role in mediating cell-cell adhesion.[293] Still, the fact that both wildtype and mutant plakoglobin co-immunoprecipitate with TAIP-2 suggests that this interaction may in fact not play a vital role in the development of ARVC. The significance of this novel finding may therefore lie in exploring the complex functions of plakoglobin rather than unraveling the mechanisms of disease pathogenesis. Nevertheless, the question still remains of how S39_K40insS causes ARVC.

2) S39_K40insS; effects on the subcellular localization of plakoglobin and desmosomal structure.

To investigate the functional consequences of a plakoglobin molecule bearing an additional serine residue, mammalian cell lines stably expressing the wildtype or the S39_K40insS-bearing protein were generated (Figure 20).

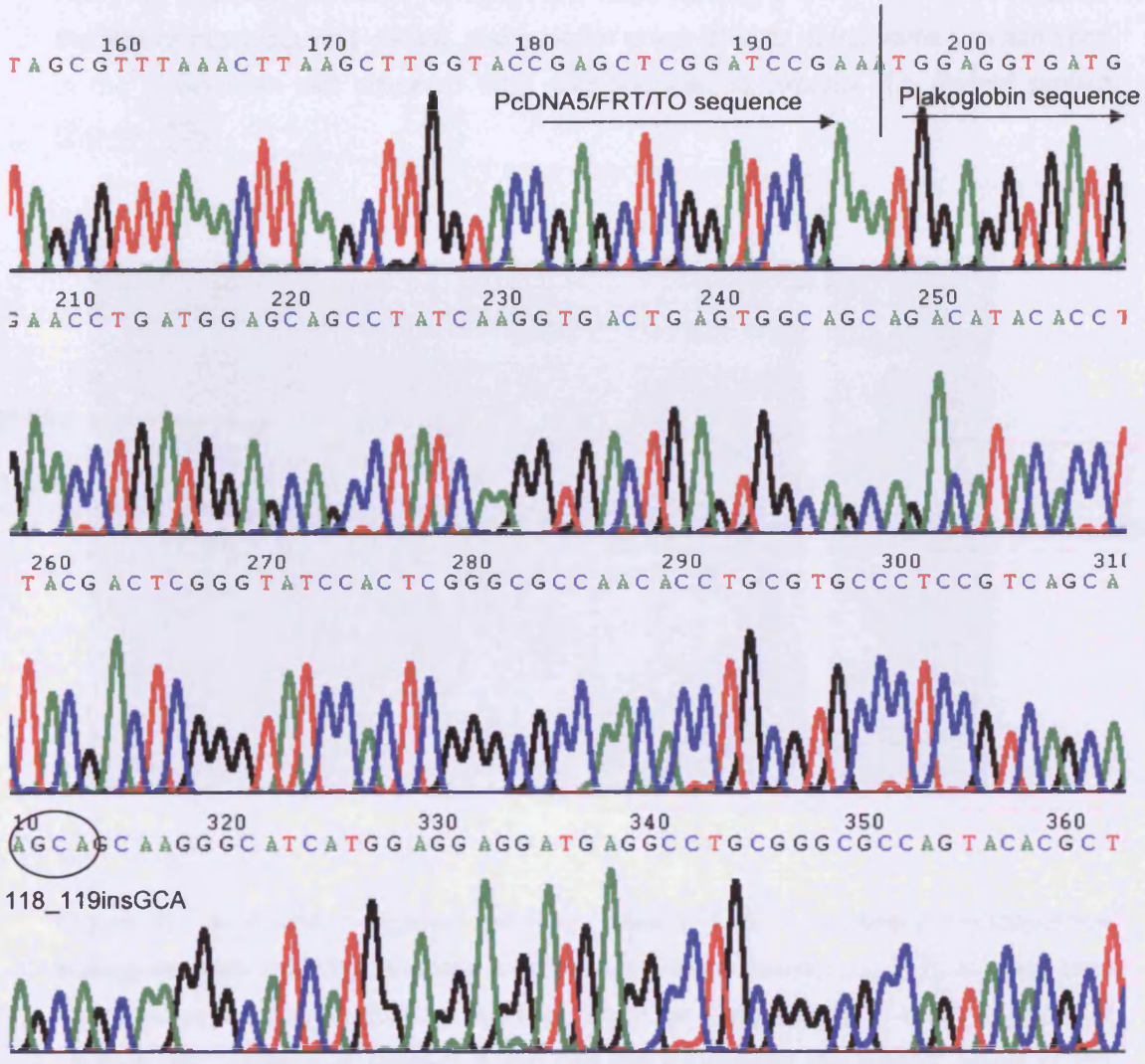

Figure 20: Electropherogram showing the incorporation of the mutant plakoglobin sequence in the pcDNA5/FRT/TO vector.

Western blotting revealed differences in the electrophoretic mobility of plakoglobin expressed by the transfected cells. In non-induced control cell lines, one band was observed which matched the predicted size of plakoglobin (82kDa) and corresponded to the endogenous protein naturally expressed by HEK293 cells. In contrast, two bands were observed in cells induced to express the S39_K40insS mutation; a lower

band (82kDa) corresponding to native plakoglobin and a higher band (~90kDa) which was the mutant protein (Figure 21A). Because cytoplasmic plakoglobin is degraded by the ubiquitin-proteasomal system,[294] we investigated the possibility that the mutant protein migrated with an apparent molecular weight of ~90kDa because it was bound to ubiquitin. Western blotting with an anti-ubiquitin antibody typically reveals a smearing band pattern reflecting the abundance of ubiquitin and its numerous interactions. However, brief film exposure revealed two major bands, a lower one which matched the size of free ubiquitin (~8kDa), and a higher one (~90kDa) at the same position seen in the plakoglobin blot prepared from cells induced to express the mutant protein (Figure 21B).

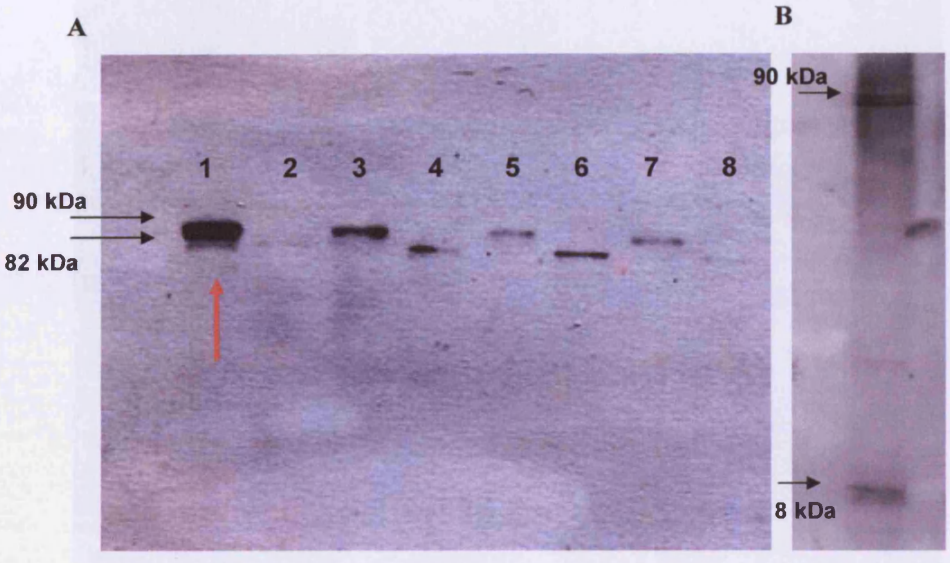

Figure 21: (A) Four non-induced cell lines (lanes 2, 4, 6, 8) express the endogenous plakoglobin only (82kDa), whereas 4 induced cell lines (lanes 1, 3, 5, 7) express both endogenous plakoglobin (82kDa) and the mutant form of plakoglobin which migrates at ~90kDa. (B) Ubiquitin is present in the cell line expressing the highest levels of the exogenous construct (indicated by the red arrow) both in its free form (8kDa) and at a form (~90kDa) consistent with it being covalently bound to mutant plakoglobin.

If S39_K40insS does indeed enhance the interaction of plakoglobin with ubiquitin, then the mutant protein might be expected to show increased cytoplasmic localization. To investigate the cellular distribution of S39_K40insS plakoglobin as distinguished from endogenous plakoglobin, HEK293 cells were transiently transfected to express wildtype

or mutant plakoglobin tagged with GFP. Transfected cells were counter-stained with DAPI to mark nuclei before being examined by confocal microscopy to visualize the GFP-tagged plakoglobin. In cells expressing wildtype plakoglobin, GFP signal was localized mainly at cell junctions. In contrast, signal in cells expressing mutant plakoglobin was markedly shifted to the cytoplasm (Figure 22)

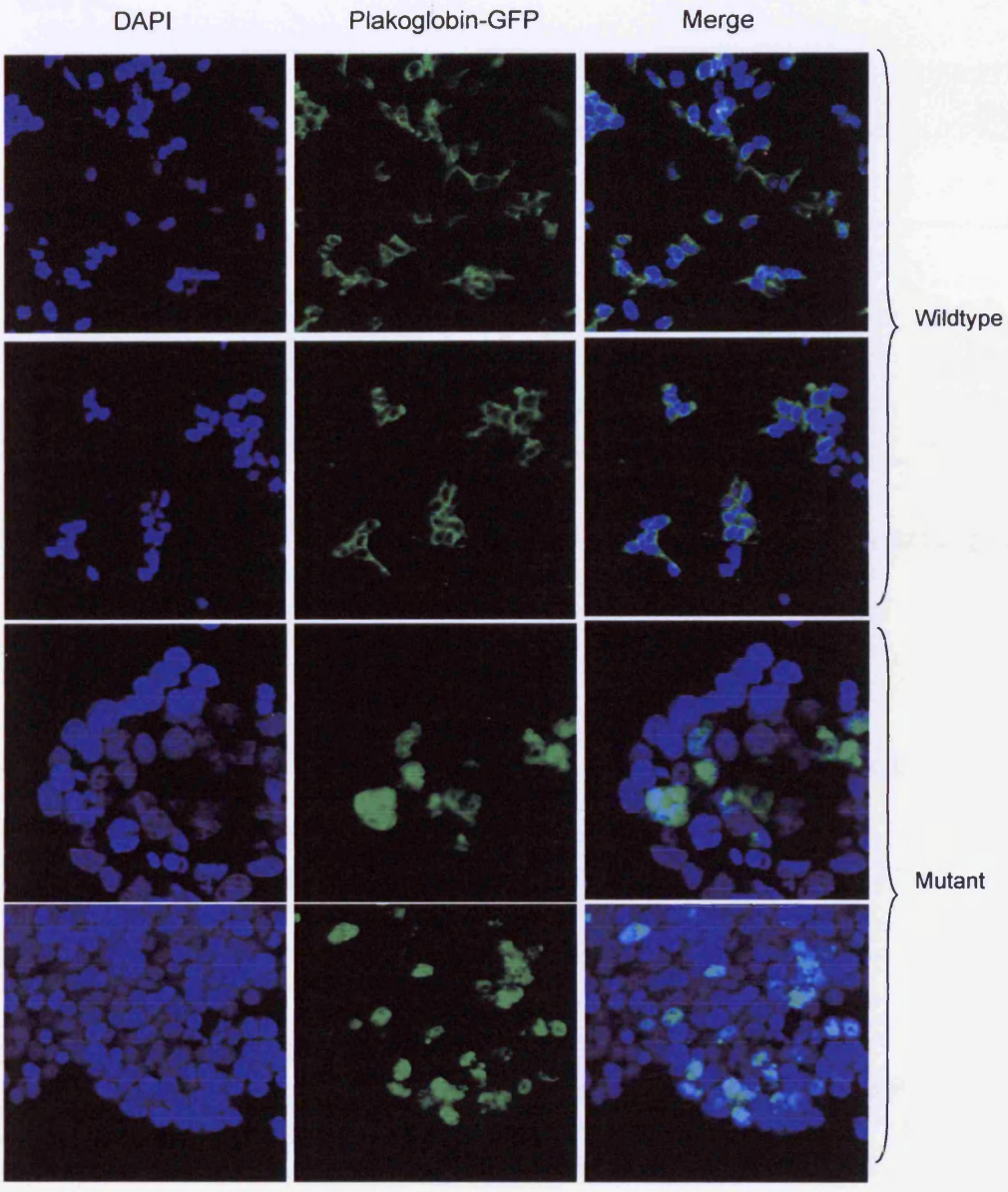

Figure 22: Confocal microscopy showing the distribution of wildtype and mutant plakoglobin in transiently transfected HEK293 cells.

Reduced amounts of S39_K40insS plakoglobin at junctional sites, as suggested by fluorescent microscopy, might affect desmosomal formation. To investigate this hypothesis, HEK293 cells stably expressing wildtype or mutant plakoglobin were examined by electron microscopy. The mutant cells form fewer and smaller desmosomes that wildtype cells (Figure 23). Representative micrographs are shown in Figure 24.

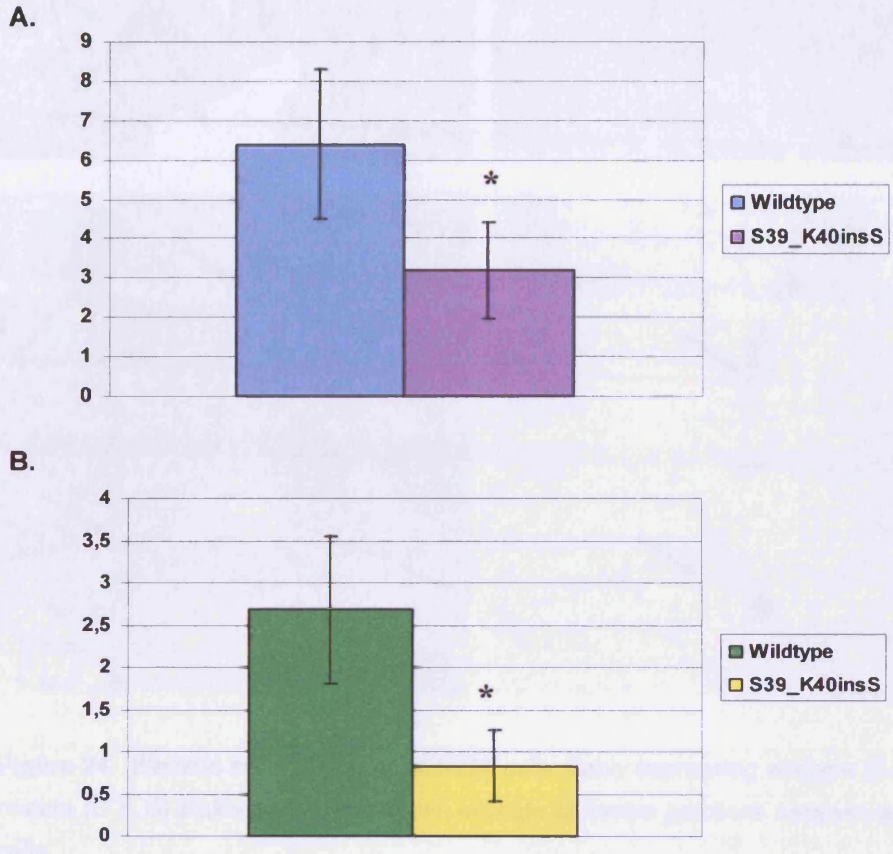

Figure 23: The number and size of individual desmosomes was measured in 10 randomly selected electron micrographs (final magnification 9000) of each cell line. Mutant cells formed fewer (3.2 ± 1.2 vs. 6.4 ± 1.9 desmosomes per micrograph, $p < 0.001$, graph A) and smaller (0.87 ± 0.42 vs. 2.68 ± 0.83 µm per desmosome profile, $p < 0.001$, graph B) desmosomes than wildtype cells. The bar lines represent standard deviations.

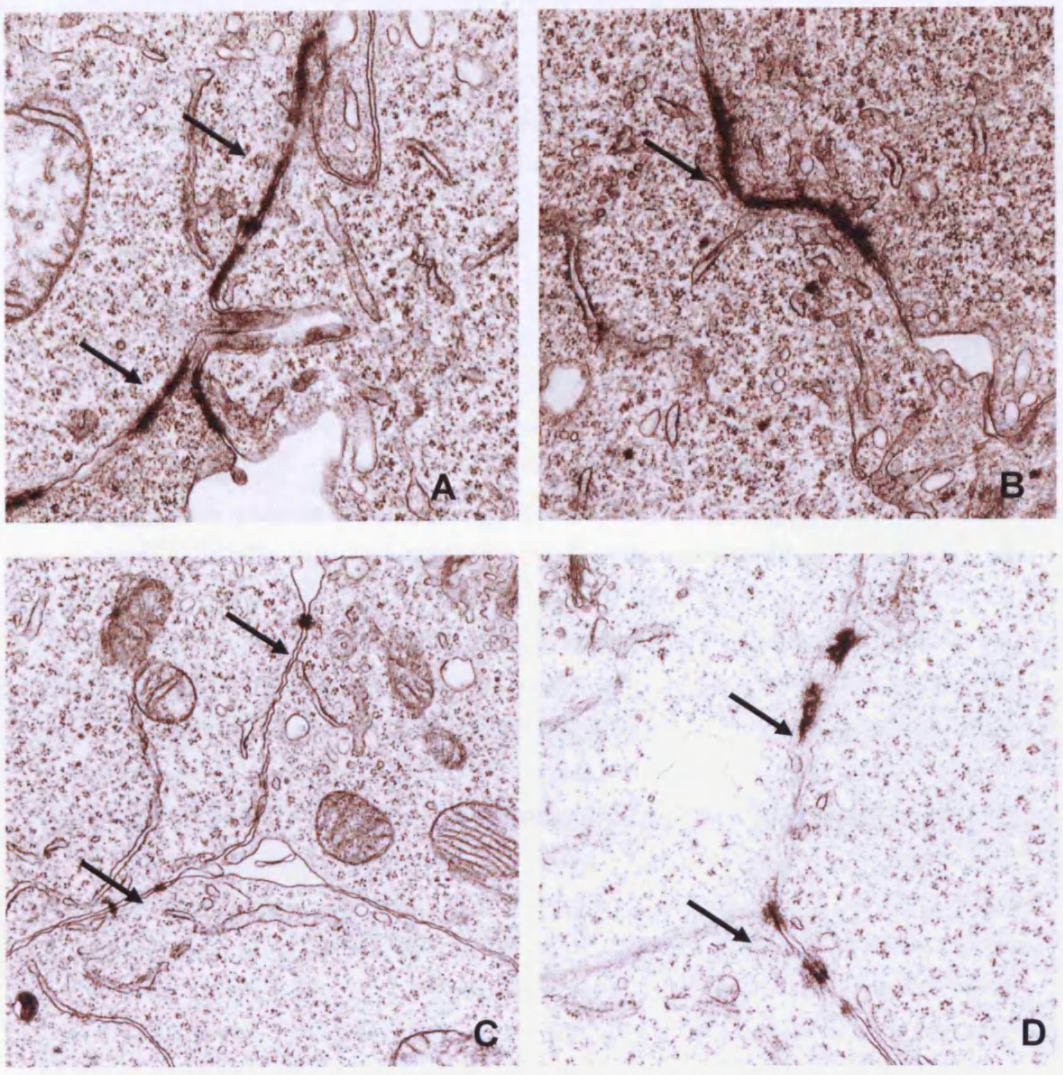

Figure 24: Electron micrographs of HEK293 cells stably expressing wildtype (A & B) or mutant (C & D) plakoglobin. The arrows indicate adhesive junctions between adjacent cells.

Discussion:

The N-terminus is known to play an important role in determining the stability of armadillo proteins. This region appears to be a target for O-glycosylation by N-acetylglucosaminyltransferase (O-GlcNAc). O-GlcNAc modification has been proposed to counteract phosphorylation, provide protection from proteasomal degradation, mediate signal transduction, silence transcription and regulate multi-molecular protein assembly.[295,296] Investigations using a number of plakoglobin deletion constructs indicated that the site for O-GlcNAc modification lies within the first 32 amino acids of the protein. A total of six threonine and serine residues are found within this stretch of

the molecule, however it appears that only when Thr14 gets mutated, O-glycosylation is totally abolished.[297] Since S39_K40insS does not affect this site, it is unlikely that the ARVC-causing mutation identified disrupts the O-GlcNAc modification of the plakoglobin protein.

Apart from regulating stability though, the N-terminus is also known to control the turnover kinetics of armadillo proteins. The ubiquitin-proteasomal system is the major non-lysosomal pathway for intracellular protein degradation, generally requiring a covalent linkage of one or more chains of polyubiquitins to the protein intended for degradation.[298] Ubiquitin is a highly conserved globular protein consisting of 76 amino acids that is expressed in all eukaryotes but very few prokaryotes. Proteasomes on the other hand, have a highly conserved architecture and are found in one form or another in all forms of life. The complete eukaryote proteasome is composed of two complexes of proteins: the proteolytic core, or 20S proteasome (on the basis of its sedimentation value), containing 28 subunits and having a molecular mass in excess of 700kDa, and one or two regulatory complexes, also known as the 19S complexes, consisting of at least 17 additional proteins and having a molecular mass of almost 900kDa. Association of the proteolytic core with the regulatory complex results in the formation of a macro-molecular structure that has become known as the 26S proteasome (Figure 25).[298] Experiments utilizing inhibitors of different degradation pathways have proven that the ubiquitin-proteasomal system is the major regulator of both plakoglobin and beta-catenin turnover.[299] Ubiquitination proceeds along a three-step cascade. In the first step, the ubiquitin-activating enzyme, E1, uses ATP to activate ubiquitin to a higher energy state. The activated ubiquitin is then transferred onto one of several ubiquitin-conjugated proteins, E2, by the formation of an additional high-energy bond and then covalently linked, generally at a lysine residue, to a protein substrate, which in turn is bound to a specific ubiquitin protein ligase, E3. In general, if the substrate is to be degraded by the 26S proteasome, it must be poly-ubiquitinated, which occurs via the successive addition of activated ubiquitins to internal lysine residues of the previously conjugated ubiquitin. In some instances, poly-ubiquitin chain formation is facilitated by a multi-ubiquitin elongation factor, E4. Once a substrate is poly-ubiquitinated, it is either recognized directly by the proteasome or bound to some shuttling protein, which will transport it to the proteasome (Figure 26).[300]

Figure 25: Structure of the mammalian 26S proteasome.[298]

Figure 26: The ubiquitin-proteasome pathway.[298]

When not engaged in cell-cell adhesion or nuclear signaling pathways, plakoglobin is recognized by glycogen synthase kinase 3b (GSK-3β). GSK-3β forms a complex with two further scaffolding proteins: axin and adenomatous polyposis coli (APC) and together they phosphorylate the target armadillo protein at a series of serine residues within its N-terminus.[294] Five residues (S28, T32, S36, S38 and S39) at the amino terminal part of plakoglobin form the consensus site for phosphorylation by GSK-3β,

come to be known as the "destruction box".[301] The phosphorylated plakoglobin may then interact with the ubiquitin ligase E3 complex, consisting of Skp1, Cullin and b-TRCP.[302] b-TRCP, whose homologue in Drosophila is Slimb, is an F-box protein, which can bind both Skp1 through its F-box domain and the phosphorylated target protein through a series of C-terminal WD repeats (Figure 27).[303]

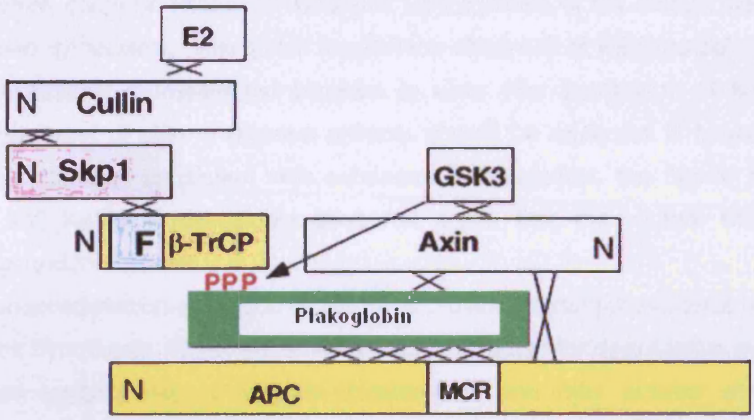

Figure 27: Proteolysis of plakoglobin by the ubiquitin-proteasomal system.

In response to Wnt signaling though, GSK-3β is prevented from phosphorylating plakoglobin, which therefore becomes stabilized, enters the nucleus and participates in regulating gene expression.[304] There is a fine balance between the amount of plakoglobin engaged in cell junctions, the fraction of plakoglobin involved in signaling and the quantity of plakoglobin that is degraded. A plausible hypothesis is that S39_K40insS disrupts this balance, perhaps because the presence of an extra N-terminal serine increases the protein's turnover rate. The resultant decrease in the total amount of plakoglobin may limit its accumulation at cell junctions leading to impaired intercellular adhesion and development of ARVC. This hypothesis could also explain the increased levels of β-catenin observed at the intercalated discs of the proband's cardiac tissue (Chapter 2). Plakoglobin and β-catenin compete at all junctional, nuclear and proteasomal sites maintaining a constantly dynamic balance. When plakoglobin is over-expressed, β-catenin gets released from the junctions and displaced to the cytoplasm, where it becomes available for degradation. Similarly, mutations that perturb the function of the β-catenin degradation complex, lead to increased accumulation of β-catenin in the nucleus, and subsequent displacement of plakoglobin.[305] If S39_K40insS plakoglobin is indeed driven away from the cell borders by its increased association with the degradation machinery, β-catenin could conversely be driven away from the saturated proteasomes and recruited at the cell junctions.

To test this hypothesis, HEK293 cell lines were transfected to stably express the mutant protein. Cells containing the S39_K40insS mutation expressed plakoglobin with a greater molecular weight than the wildtype protein. This could be explained by a number of post-translational modifications However, confocal microscopy showed that more of the S39_K40insS protein was localized in the cytoplasm and less at the cell junctions, which could be related to enhanced ubiquitylation of the mutant plakoglobin. The increased cytoplasmic plakoglobin localization observed at HEK293 cells does not however necessarily represent the situation in vivo. The distribution of the mutant protein in the heart or skin of affected patients should be analysed in future studies. Furthermore, although consistent with enhanced ubiquitylation, the higher molecular weight of S39_K40insS plakoglobin does not prove that the mutant molecule is covalently bound to ubiquitin.

A co-immunoprecipitation approach would have provided stronger evidence in favor of the proposed hypothesis. Moreover, since a protein targeted for degradation by the 26S proteasomes typically has to be poly-ubiquitinated, one may wonder why only a ~90kDa form (consistent with mono-ubiquitination) is observed at the Western immunoblot prepared from the mutant cell line. It could be speculated that poly-ubiquitinated forms of the mutant protein get degraded and therefore cannot be traced in the cell lysates. Also, even if the mutant protein is indeed covalently bound to ubiquitin, this does not necessarily mean that its turnover rate is increased. A way to approach this question would be to generate a recombinant construct of wildtype or mutant plakoglobin fused to the HaloTag protein (Promega) and use it to transiently transfect cells. A synthetic ligand, tagged with a fluorescent molecule can then be added to trace HaloTag and consequently the protein under investigation. Serial microscopy could be used to investigate the turnover rates of the target mutant molecule and compare them with those of its wildtype counterpart. Finally, even if S39_K40insS does not seem likely to affect the action of O-GlcNAc, the question still remains of whether the mutation can disrupt other types of post-translational modification. The consensus sequence for phosphorylation by GSK-3β overlaps with a potential N-glycosylation site, although modification at this site has not been proved experimentally.[297] To examine the possibility that S39_K40insS disturbs the potential N-glycosylation, the cell line stably expressing mutant plakoglobin should be treated with tunicamycin prior to Western immunoblotting. Tunicamycin is an antibiotic that blocks the reaction of UDP-GlcNAc and Dol-P in the first step of glycoprotein synthesis, thus inhibiting the synthesis of all N-linked glycoproteins. If following tunicamycin incubation, S39_K40insS plakoglobin still migrates at a higher molecular weight than the wildtype protein then this possibility could be ruled out. Also, the hypothesis that the additional

serine does get phosphorylated and disrupts the degradation pathway has to be investigated further.

Another approach would be to develop an antibody specifically recognizing a plakoglobin molecule phosphorylated at this additional residue and apply it to heart tissue from affected individuals. Still, even if the additional residue does get phosphorylated, it does not necessarily mean that it alters the turnover kinetics of plakoglobin. For instance, phosphorylation of specific plakoglobin C-terminal tyrosine residues following epidermal growth factor receptor activation leads to dissociation of desmoplakin from the desmosomal plaques without affecting the degradation pathway.[306] Though fascinating and plausible, the "altered turnover kinetics" hypothesis still contains gaps and unless they get filled it remains purely speculative. On the other hand, immunohistochemistry of cardiac tissue obtained from the actual proband showed altered localization of both structural and electrical coupling molecules (Chapter 2). In support of this observation, electron microscopy showed that mutant HEK293 cells form significantly fewer, smaller and less distinct desmosomes than wildtype cells. Whether through altered turnover kinetics or not, S39_K40insS does compromise cell-cell adhesion, and does lead to the development of ARVC.

3) S39_K40insS; effects on cell proliferation and cell death:

Apart from its role in cell junctions, plakoglobin is also known to participate in Wnt signaling pathways where it associates with Tcf/Lef transcription factors and regulates functions such as cell proliferation and apoptosis. To investigate the effects of S39_K40insS on cell proliferation, a CellTiter 96 Cell Proliferation Assay was performed. HEK293 cells stably expressing the mutant plakoglobin showed higher proliferation rates than cells expressing the wildtype protein, the difference being statistically significant in the fourth and fifth day of the assay (Figure 28). The effect of S39_K40insS on programmed cell death was examined using the CaspACE™ Assay method. HEK293 cells stably expressing S39_K40insS plakoglobin showed significantly less caspase activity than cells expressing the wildtype protein (Figure 29), suggesting lower rates of apoptosis in cells expressing the mutant protein.

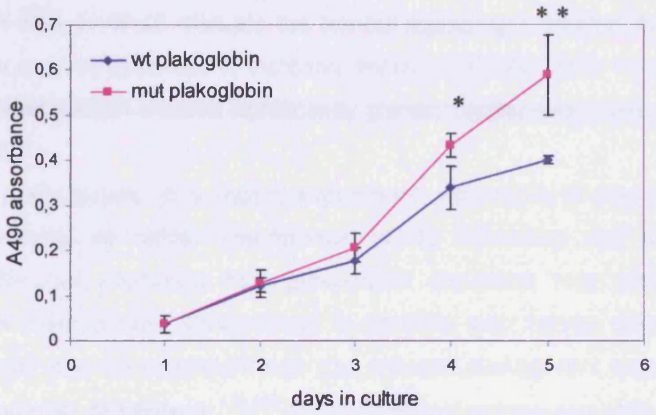

Figure 28: CellTiter 96 Cell Proliferation Assay over the course of five consecutive days; * p=0.014, ** p= 0.006.

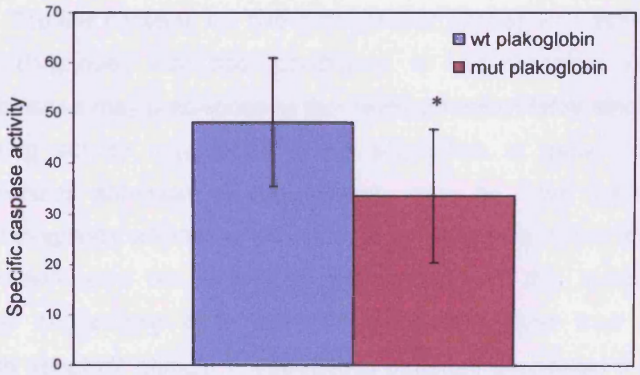

Figure 29: CaspACE™ assay. Specific caspase activity was measured in 10 individual wildtype and mutant cultures; * p=0.038.

Discussion:

Plakoglobin, β-catenin and *Drosophila* armadillo are closely related multi-functional proteins that regulate cell adhesion and participate in signal transduction cascades. All three proteins are found in cytoplasmic and nuclear complexes where they direct cell fate and govern aspects of cell proliferation.[307] Up-regulation of β-catenin, either by mutations in regulatory genes involved in degradation and signaling pathways or by direct mutations in the β-catenin gene, has been implicated in hyper-proliferation and tumor formation.[308,309] To investigate the role of plakoglobin in these functions, a full-length and an N-terminally truncated form of plakoglobin have been expressed in mouse epidermis and hair follicles, tissues which undergo continuous and easily observed postnatal renewal and remodeling.[192] Expression of these constructs resulted in stunted hair growth, and reduced proliferation of epidermal cells, indicating that plakoglobin suppresses epithelial proliferation and hair growth in vivo.[192] It is possible therefore that if S39_K40insS disrupts the normal signaling mediated by plakoglobin, cell proliferation may be expected to increase. Indeed, HEK293 cells induced to stably express the mutant protein showed significantly greater proliferation rates than wildtype cells (Figure 28).

Consistent with our results, in a recent experiment, desmoplakin down-regulation in HaCaT keratinocytes by siRNA interference led to increased cell proliferation.[310] Increased proliferation stemming from plakoglobin disruption may also explain the development of palmoplantar keratoderma in patients with Naxos disease. Such a mechanism would also be consistent with the reduced plakoglobin expression levels observed in a number of cancers. [146,148] In 2002, *Polychronopoulou* et al. suggested a possible pathogenetic association between myelodysplasia and Naxos disease. The myelodysplastic syndromes (MDS) are an heterogeneous group of blood disorders characterized by ineffective hemopoiesis and an increased tendency for evolution into acute leukemia. The link between the two pathogenetic entities was based on the case of two siblings diagnosed with both conditions. It was therefore suggested that plakoglobin dysfunction may predispose to the development of MDS since a decreased tumor suppressing activity may facilitate the acquisition of genetic lesions, while disrupted intercellular adhesion in the marrow may by itself contribute to the establishment of dysplastic alterations once the neoplastic clone has emerged.[311]

Dusek et al. investigated the effects of plakoglobin on the survival of mouse keratinocytes by challenging both plakoglobin-null cells and their heterozygous counterparts with apoptotic stimuli.[312] The results obtained suggested that plakoglobin deletion protects keratinocytes from apoptosis, with null cells exhibiting delayed mitochondrial cytochrome release and activation of caspase-3, and increased levels of the anti-apoptotic molecule Bcl-X_L compared to heterozygous controls. Collectively

these observations indicated that plakoglobin may function to potentiate death in cells damaged by apoptotic stimuli, perhaps limiting the potential for the propagation of mutations and cellular transformations.[312] To investigate the effect of S39_K40insS on plakoglobin-mediated apoptosis, a caspace-3 assay was used.

Consistent with the results of *Dusek et al.,* HEK293 cells expressing the mutation exhibited lower caspace-3 activity than wildtype cells, consistent with decreased rates of programmed cell death (Figure 29). In contrast to our results though, suppression of desmoplakin expression using siRNA in atrial myocyte cell lines or heterozygous desmoplakin-deficient mice led to increased rates of apoptosis, related to increased nuclear plakoglobin translocation and inhibition of the canonical Wnt signaling pathway.[313] This controversy may be explained by the fact that S39_K40insS seems to increase the cytoplasmic, rather than the nuclear accumulation of the mutant plakoglobin molecule (based on results presented earlier in this chapter). Translocation of S39_K40insS to the cytoplasm but not the nucleus, may lead to activation of the canonical Wnt signaling pathway and therefore decreased rates of apoptosis. Still, our results do not agree with the increased cardiomyocyte apoptotic rates reported in patients with ARVC.[55] The discrepancy therefore may well be cell type-specific instead of mutation-specific.

Although HEK293 cells have certain advantages, such as their rapid division rate and their ability to form desmosomes and therefore incorporate an exogenous desmosomal protein into cell junctions, we hasten to point out that the effects of S39_K40insS on signaling pathways in HEK293 cells cannot necessarily be translated to cardiac myocytes. Further studies will be needed to determine whether this ARVC-related mutation disrupts the signaling properties of ventricular myocytes. Furthermore, *Garcia-Gras et al.* also reported that suppression of desmoplakin expression using siRNA in atrial myocyte cell lines or heterozygous desmoplakin-deficient mice led to increased expression of genes involved in adipogenesis and collagen generation therefore shifting cells from a myocyte to an adipocyte fate.[313,314] If expression of S39_K40insS in ventricular myocytes is shown to have similar effects on cell fate, it would add further evidence to the hypothesis that a final common pathway involving plakoglobin is underlying ARVC pathogenesis.

Since the discovery of Wnt1 as an oncogene, the Wnt gene family, which includes 19 members in the human genome, has been found in all animal species examined.[315] As mentioned above, in the absence of a Wnt ligand, the level of cytosolic β-catenin is kept low by its amino terminal phosphorylation-dependent ubiquitination/proteasomal degradation. However, in the presence of a Wnt ligand, transmembrane lipoprotein receptors such as LRP5, LRP6 and their *Drosophila* homolog Arrow, activate the frizzled receptor. This receptor binds a molecule known as disheveled, which in turn

anchors axin, thus preventing the phosphorylation and subsequent degradation of β-catenin.[316,317] In response to activation of the Wnt signaling pathway, β-catenin accumulates in the nucleus, where it cooperates with lymphoid enhancer factor and T-cell factor (LEF/TCF) transcription factors to activate gene expression.[318] LEF/TCF factors are sequence-specific DNA-binding proteins which lack classical trans-activation domains.[319] *Hecht et al.* showed that β-catenin serves as a transcriptional co-activator of the DNA-binding proteins, thus driving expression of genes such as c-Myc and cyclinD1 (Figure 29).[320]

Although the signaling role of β-catenin is well established, a major controversy remains as to the involvement of plakoglobin in the Wnt pathway. *Simcha et al.* report that plakoglobin is unable to bind the Tcf/Lef transcription factors and therefore its role in the Wnt signaling pathway is confined to antagonizing β-catenin at the junctional and proteasomal sites, therefore allowing it to enter the nucleus.[321] *Miravet et al.* though report that while plakoglobin does bind Tcfs it does not compete with β-catenin for the same binding sites on the transcription factors.[322] Its inhibitory action is brought about because the Tcf/plakoglobin complex is unable to bind DNA sequences and thus activate transcription.[323] In this way, by antagonizing β-catenin, plakoglobin can inhibit proliferation and prevent cancer and metastasis.[324] Augmenting the existing controversy, *Rubenstein et al.* report that plakoglobin has its own transcriptional activity, independently of β-catenin.[325] Members of the Tcf/Lef family are characterized as architectural transcription factors, since they bind DNA bending it in such a way so that transcription is inhibited. *Rubenstein et al.* showed that plakoglobin can alleviate this inhibition driving the expression of genes.[325] Actually, *Maeda et al.* suggested that the downstream genes of plakoglobin may be different than those of β-catenin,[326] while *Kolligs et al.* presented evidence that plakoglobin can in fact drive the expression of oncogenes, possessing a tumorigenic activity itself equivalent to, but distinct from that of β-catenin.[327]

Figure 30: A simplified prevailing view of Wnt/β-catenin signaling.[315]

Even if all the genes recognized to date as disease-causing encode desmosomal proteins and even if a lot of the disease characteristics are indeed stemming from defects in cell-cell coupling, ARVC is more than a disease of the desmosome. Compromised cell-cell adhesion is only the beginning if not merely a part of the whole story. The results reported in this chapter are included in: *Asimaki et al.* "A novel dominant mutation in plakoglobin causes arrhythmogenic right ventricular cardiomyopathy"; manuscript in press, *The American Journal of Human Genetics*.

CHAPTER 4:

"S39_K40insS versus 2057del2; differential effects on cellular responses to mechanical load and cellular biomechanics"

ARROWS POINTING THE WAY:

In 2005, *Wlodarska et al.* described the case of a patient diagnosed with ARVC after episodes of non-sustained polymorphic VT and multiple premature ventricular beats of LBBB morphology.[328] Clinical investigation showed RV enlargement, focal apex hypokinesia and evidence of adipose tissue in the RV free wall. Identical RV morphology was seen in the proband's asymptomatic monozygotic twin brother. The symptomatic proband had been training in rowing for years, while his asymptomatic brother had never practiced any sport.[328] *Kirchhof et al* studied the cardiac effects of heterozygous plakoglobin deficiency (+/-) in mice.[329] Ten-month old +/- mice had increased RV volume, reduced RV function and spontaneous ventricular ectopy. Isolated perfused +/- hearts had spontaneous VT of RV origin and prolonged RV conduction times compared to wildtype hearts. Interestingly, endurance training (8 weeks of daily swimming) caused premature RV dilatation and dysfunction in the +/- mice at 5 to 6 months of age while training intensity correlated with training-induced RV enlargement in the plakoglobin deficient animals.[329] The precise incidence of sudden cardiac death in young athletes is unknown. Estimates from the United States suggest 1 in 200.000 although the true incidence is likely to be much higher.[330] It seems though that the vast majority of SCD in young athletes occur either during or immediately after strenuous physical activity.[331] In the first chapter, the case of an aerobics teacher bearing a mutation in the desmoglein2 gene (C591X) was presented. The 40-year old woman had evidence of severe biventricular ARVC, while her mother, a carrier of the same mutation, was asymptomatic and had a normal ECG and conventional 2D echo at the age of 75. Collectively, these observations suggest that sports per se are not a cause of enhanced mortality; they may however promote fatal arrhythmias or speed-up disease progression in individuals affected by certain cardiac disorders. In other words, physical activity may act as a trigger in the presence of an underlying cardiovascular disorder.[332] Despite the broad expression pattern of desmosomal proteins, all mutations identified to date affect only the heart and in specific cases the epidermis, presumably because these organs are subjected to increased mechanical stress. An increase in wall stress is known to be inversely proportional to wall thickness. This may explain why disruption of cell-cell adhesion may predominantly affect the thin-walled but highly-pressurized RV.[333]

Exercise, physical activity, training, stress, pressure; they all seem to have a role in ARVC, although the molecular path through which they bring about their effects is yet poorly defined. To investigate the relationship between stress and disease expression, HEK293 cells transfected to stably express plakoglobin bearing either the novel dominant S39_K40insS mutation or the 2057del2 mutation (previously identified to

underlie Naxos disease) were subjected to increased mechanical stress. In this chapter, we shall describe the effects of defined mechanical load on the expression and distribution of intercalated disc proteins as well as the signaling pathways through which stretch brings about its effects in the cellular model developed. S39_K40insS and 2057del2 are two mutations in the same gene that have different yet similar effects at the clinical phenotype level. We compared the effects the two mutations have at the cellular level, in an attempt to unravel the path that leads from the cell to the overall disease phenotype and ultimately from the laboratory bench to the bedside.

Despite the high number of mutations currently recognized to be underlying clinical ARVC, most previous studies have not rigorously characterized the effects of desmosomal protein mutations on cell biomechanics. As part of this project, the biomechanical properties of HEK293 cells expressing the two mutant variants of plakoglobin were characterized. Wound-healing, individual cell migration, cell stiffness and cell-cell adhesion were examined to assess the similarities and differences in cell mechanical behavior. However, as mentioned at the end of the previous chapter, although HEK293 cells constitute an advantageous model for studying desmosomal gene mutations, it should be emphasized that the results obtained cannot necessarily be applied to cardiac myocytes. To overcome this limitation, a recombinant adenovirus expressing the S39_K40insS plakoglobin has been generated and used to transfect neonatal rat ventricular cardiomyocytes. In this chapter, we shall present the effects of this novel mutation on cardiac myocytes, thus getting a step closer to accurately modeling this highly complex cardiac disorder.

METHODS AND MATERIALS:

1) Stretch and immunofluorescence protocol for HEK293 cells:

HEK293 cells were plated on collagen IV-pre-coated silicone membranes and grown to confluency before experimentation. The cultures were then subjected to linear pulsatile stretch using a custom-designed apparatus, illustrated in Figures 1 and 2. The lateral borders of a rectangular sheet of silicone membrane (C, thickness 0.01 inch) were fixed to bars (A) that could move freely in the *x* direction along two stainless steel axes (B). The two bars were in contact with an elliptical Teflon wheel (E) mounted in the centre of the device. The silicone membrane was cut to a length that produced tension slightly above the slack length when the short diameter of the wheel was in contact with the Teflon bars. The 1.1/1 ratio of the long to the short diameter of the elliptical wheel produced stretch of 10% during a 90° rotation of the wheel. The frequency of the stretch pulsations (half a wheel cycle) was monitored by a photodiode mounted on the stretch apparatus and controlled from outside the tissue culture incubator. A stretch frequency of 3 Hz was used in the present experiments. Transverse compression (shrinkage) in the *y* direction during linear stretch in the *x* direction was prevented by attaching 2 clamps (F) that stretched the membranes slightly along the transverse central axis. Cells were cultured in a chamber created by fixing a ring of silicone tubing (D, thickness 2 mm, diameter 24 mm) at the centre of the membrane with silicone sealant. Transverse deformation of the membrane at maximal longitudinal stretch was <1%, hence stretch was uniaxial.[334]

Figure 1: Schematic representation of the custom-fabricated stretch apparatus.[334]

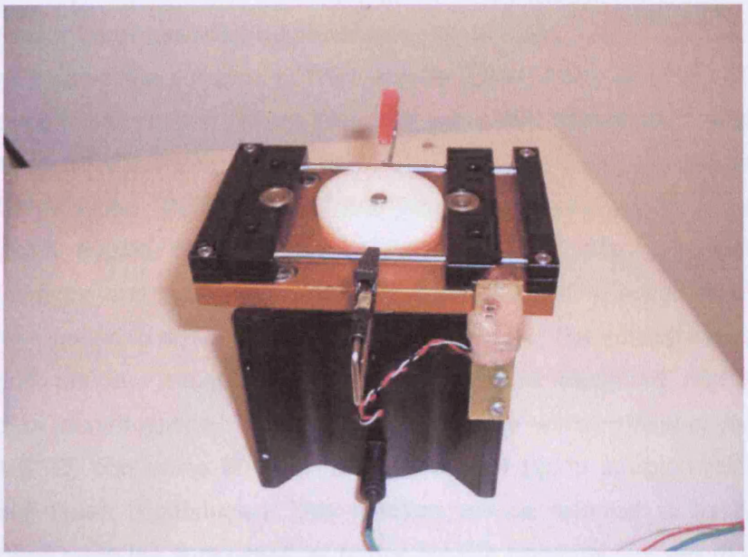

Figure 2: Image of the custom-fabricated stretch apparatus.

Following stretch, the medium was aspirated and the cells washed with PBS and incubated with 4% paraformaldehyde in PBS at room temperature for 10min. Following fixation, the cell-covered silicone membranes were cut in quadrants and placed in 24-well plates along with PBS. The cells were washed first with 0.5% Triton-X/PBS and then with PBS. To block non-specific signal, the cells were incubated with 10% fetal calf serum/PBS for 30min. The primary antibodies were added, diluted in the same blocking buffer, and the cells incubated at 4°C overnight. The following day, the cells were equilibrated at room temperature for 30min, washed first with PBS, then with 0.1% Tween/PBS and again with PBS. The secondary antibodies were added diluted in blocking buffer and the cells incubated at 4°C overnight. On the third day of the procedure, the cells were equilibrated at room temperature for 30min, washed first with PBS, then with 0.1% Tween/PBS and again with PBS. The membrane quadrants were then placed on slides, mounted with 50% glycerol-50% PBS and examined by quantitative confocal microscopy as described above.

In selected experiments, stretch-conditioned medium obtained from cultures previously stretched for 1-4 hours was collected and applied to other cultures that had not been stretched. In another set of experiments, cultures were incubated with a mouse monoclonal anti-VEGF antibody (directed against recombinant human $VEGF_{165}$, R&G systems).[335] In all experiments, control cultures that were neither stretched nor exposed to any exogenous reagent were grown on silicone membranes under the same conditions and incubated in serum-free medium for 1-4 hours (depending on the length of the experimental procedure).

2) Primary cultures of neonatal rat ventricular myocytes:

Primary cardiac myocyte cultures (NRVM) were prepared from ventricles of 1-day old Wistar rat pups (Charles River, Indianapolis) as previously described.[336] Briefly, hearts from 8-10 neonatal rats were removed and finely minced. The pieces were immersed in a dissociation solution (Ca^{+2} and Mg^{+2}-free Hanks' balanced salt solution, GIBCO) containing 0.1% trypsin, 60µg/ml pancreatin (SIGMA), 20 units/ml penicillin and 20 µg/ml streptomycin and repeatedly stirred for 15min at 37ºC. Four to five incubation periods were required to dissociate the mixture completely. The solutions obtained after all incubation periods, except for the first one, were decanted into tubes and sedimented by centrifugation. The resulting cell pellets were re-suspended in M199 medium (GIBCO) containing 20 units/ml penicillin, 20 µg/ml streptomycin and 10% neonatal calf serum (Boehringer). This medium will be referred to as high serum medium (HMS), while the same medium containing 5% neonatal calf serum only will be denoted as normal serum medium (NMS). The fibroblast content of the cell suspension was reduced by a differential attachment method. Briefly, the cell suspension was transferred to a T-75 culture flask and incubated in a 37 ºC, 0.1% CO_2 incubator for 2 hours. During this incubation period the fibroblasts preferentially attach to the flask. The remaining myocytes were counted with a haemocytometer and diluted in HMS to achieve a concentration of 3 x 10^5 cells/ml. Simultaneously with the differential attachment procedure, silicone membranes pre-coated with collagen I, were washed in PBS and incubated with HMS for 2 hours under UV-light. This procedure increases the number of adhering cells. After the pre-incubation medium was withdrawn from the silicone membranes, 2 ml of the enriched myocyte solution was plated onside each ring, and the cultures transferred to a 37 ºC, 0.1% CO_2 incubator for 24 hours. After this incubation period, the silicone membranes were shaken gently to suspend un-attached cells and the HMS medium was removed and replaced with NMS. Thereafter, medium exchanges with NMS were performed every other day.[336]

3) Stretch and immunofluorescence protocol for NRVMs:

Neonatal rat ventricular myocytes isolated as described above, were plated on collagen-coated silicone membranes and grown for 4 days prior to experimentation. Monolayers of ventricular myocytes were subjected to linear pulsatile stretch for 1 hour in serum-free medium (M199) using the custom-designed apparatus presented above. Non-stretched myocytes were also incubated in M199 medium for 1 hour and used for control purposes. Following stretch, the cultures were immunostained and examined by quantitative confocal microscopy. Primary antibodies included polyclonal rabbit anti-connexin43 (Cx43) (SIGMA, UK), monoclonal mouse anti-plakoglobin (Sigma, UK) and monoclonal mouse anti-N-Cadherin (Sigma, UK) antibodies. In preparation for

immunostaining, cultures were rinsed in serum-free medium (M199) and fixed in 4% paraformaldehyde/PBS for 5min at room temperature. Following fixation, the cell-covered membranes were cut, placed in 24-well plates and washed in PBS three times. To block non-specific signal, the cultures were incubated in PBS containing 0.1% Triton X-100, 1% bovine serum albumin (BSA) and 3% normal goat serum at room temperature for ~40min. The cultures were then incubated with the primary antibody overnight at 4°C, brought to room temperature, washed 3 times with PBS, and incubated with indocarbocyanine (Cy3)-conjugated goat anti-mouse or anti-rabbit IgG (diluted 1:400 in PBS) for 2 h at 25 °C. Following incubation with the secondary antibodies, the membrane quadrants were washed 3 times in PBS, transferred onto glass slides and mounted with 50% glycerol- 50% PBS.

4) Generation and amplification of recombinant adenoviral constructs:

Recombinant adenoviral constructs were created using the ViraPower Adenoviral Expression system (Invitrogen). This system allows creation of a replication-incompetent adenovirus that can be used to deliver and transiently express a gene of interest in either dividing or non-dividing mammalian cells, such as ventricular myocytes. An overview of the system is presented below:

The gene of interest is first transferred from pDONR221 to the Gateway-compatible pAd/CMV/V5-DEST vector through LR clonase-mediated recombination. The recombinant plasmid is then introduced in 293A cells. These cells contain a stably integrated copy of E1 that supplies the E1 proteins (E1a and E1b) *in trans* required for the production of an adenovirus. The viral particles enter the target cells by binding to the Coxsackie/Adenovirus receptors (CAR). After the initial binding, the particles are internalized through integrin-mediated endocytosis, followed by active transport to the nucleus. Once in the nucleus, the early events are initiated, such as the transcription and translation of the E1 genes, followed by expression of the adenoviral late genes and viral replication. The crude adenoviral stock produced is then used to transfect 293A cells in order to create an amplified adenoviral stock which is then titred, and used to promote expression of the recombinant protein of interest in the mammalian cell line of choice (Figure 3).

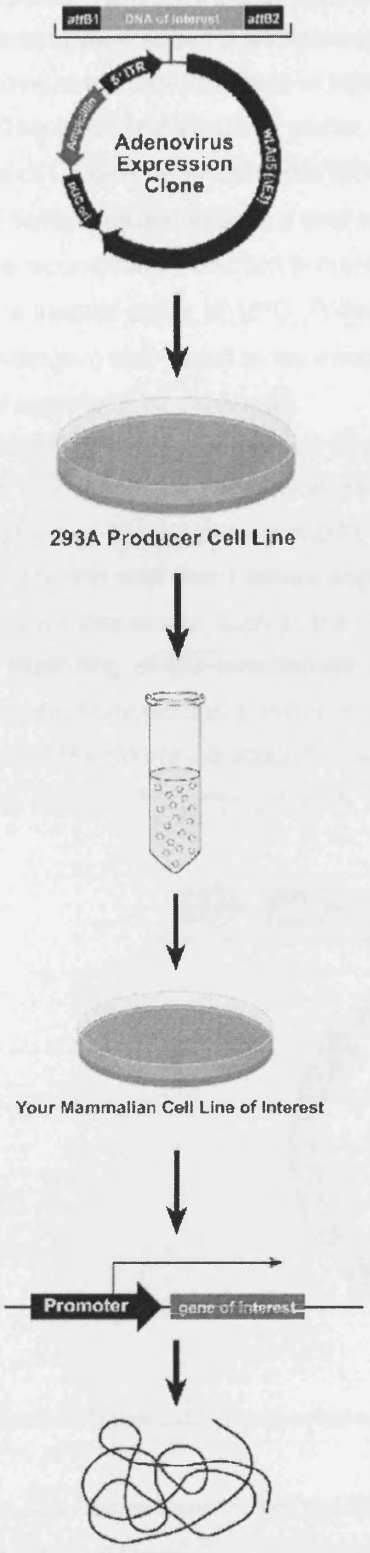

The adenoviral expression clone containing the gene of interest is generated and used to transfect 293A cells.

The transfected cells are harvested and the crude viral lysate is produced.

The adenovirus is amplified by infecting the producer 293A cells with the crude viral lysate. The amplified stock is then tittered.

The viral supernatant is then added to the mammalian cell line of interest.

Expression of the recombinant protein of interest can be assayed with a number of ways, including Western immunoblotting.

Figure 3: Schematic representation of the ViraPower Adenoviral expression system.

To perform a recombination reaction between pDONR221 and pAd/CMV/V5-DEST, the following were added in a micro-centrifuge tube:

300 ng of the DNA fragment of interest in pDONR vector

300 ng pAd/CMV/V5-DEST vector

4 μl of LR clonase enzyme mix (Invitrogen)

TE buffer was added up to a final volume of 16 μl

The recombination reaction occurred for either 1 hr at room temperature or for 12-16hrs on a thermal cycler at 16°C. Following the recombination reaction, 2μl of proteinase K (Invitrogen) was added to the mixture and the tube was incubated at 37°C for 10min for the enzyme to be denatured.

Prior to using the recombinant pAd/CMV/V5-DEST plasmid to transfect 293A cells, the left and right viral ITRs must be exposed to allow for proper viral replication and packaging. The pAd/CMV/V5-DEST vector contains Pac I restriction sites. Digestion of the plasmid with Pac I allows exposure of the left and right ITRs and removal of the bacterial sequences, such as the pUC origin and ampicillin resistance genes (Figure 4). At least 5μg of the recombinant plasmid was digested with Pac I according to the enzyme manufacturer's instructions and the digested DNA was then purified using phenol/chloroform extraction followed by ethanol precipitation. The purified plasmid was then eluted in TE buffer, pH = 8.0, to a final concentration of 0.1 – 3 μg/ μl.

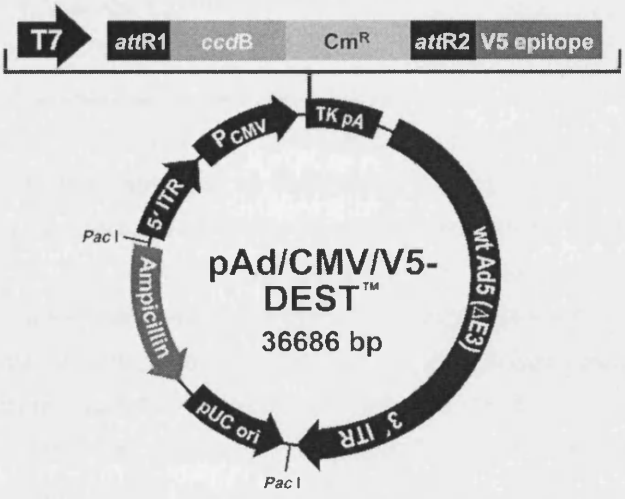

Figure 4: Schematic representation of the pAd/CMV/V5-DEST vector.

The day before transfection, the 293A cells were trypsinized and plated at 5 x 10^5 cells per well in a 6-well plate in complete medium. On the day of the transfection the culture medium was withdrawn from the 293A cells are replaced with 1.5 ml of normal growth medium containing serum but lacking antibiotics. For each transfection sample, 1 μg of

Pac I digested pAd/CMV/V5-DEST plasmid was diluted in 250 µl DMEM. Lipofectamine 2000 (3µl, Invitrogen) was diluted in 250 µl DMEM in a separate tube and incubated at room temperature for 5min. The two solutions were then mixed and incubated at room temperature for 20min, in order for lipofectamine complexes to be formed. Following the incubation period, the lipofectamine complexes were added drop-wise to each well, and the cells incubated in a 37°C incubator overnight. Twenty-four hours post-transfection the lipofectamine-containing medium was removed and replaced by complete medium. Forty-eight hours post-transfection the cells were trypsinized and transferred to 10cm culture plates containing complete medium. The culture medium was replaced every 2-3 days thereafter, until clear regions of cytopathic effects were observed (usually 7-10 days post-transfection). The infections were allowed to proceed until approximately 80% of the culture showed regions of cytopathic effects (usually 10-13 days post-transfection). The adenovirus-containing cells were then harvested and transferred to 15 ml tubes.

The tubes were placed at -80°C for 30min, followed by a 15-minute incubation in a 37°C water bath. The freeze-thaw cycle was repeated twice. The cell lysate was centrifuged to pellet the cell debris, and the adenoviral stock supernatant was transferred to cryo-vials and stored at -80°C. In order for the adenoviral stock to be amplified, 293A cells were once again used. The day before the infection, 293A cells were trypsinized and plated at 3 x 10^6 cells per 10cm plate. On the day of the infection the desired amount of crude adenoviral stock was added to each plate. The plates were then incubated in a 37°C incubator until 80-90% of the cells were rounded up and floating or just lightly attached to the tissue plate, implying that they were loaded with adenoviral particles (usually 2-3 days post-infection). The adenovirus-containing cells were then harvested and transferred to 15 ml tubes. The tubes were placed at -80°C for 30min, followed by a 15-minute incubation in a 37°C water bath. The freeze-thaw cycle was repeated twice. The cell lysate was centrifuged to pellet the cell debris, and the adenoviral stock supernatant was transferred to cryo-vials and stored at -80°C. Before expressing the recombinant protein of interest in the mammalian cell line of choice, the titer of the adenoviral stock had to be determined. The day before the infection, 293A cells were plated on 6-well plates and incubated in a 37°C incubator until 80-90% confluent. On the day of the infection, ten-fold dilutions of the adenoviral stock in complete medium were prepared to a final volume of 1 ml. The culture medium was withdrawn from the 293A cells, replaced with the adenoviral dilution and the plate incubated at 37°C overnight. Twenty four hours post-infection the medium containing the virus was removed and the cells were over-layed with 2ml of agarose solution (4% agarose solution was prepared in dH_2O, autoclaved at 121°C for 20min, equilibrated to 65°C in a water bath and used immediately). Forty eight hours following the initial over-

lay, the cells were over-layed with an additional 1 ml of agarose solution and returned to a humidified 37°C incubator. The plates were monitored thereafter until plaques were visible (usually 8-12 days post-infection). Then 5 µg/ml 3-[4,5 Dimethylthiazol-2-yl]- 2,5 –diphenyltetrazolium bromide; Thiazolyl blue (MTT) solution was evenly distributed on top of the solidified agar to stain the plaques and the plates were incubated for 3 hours at 37°C. The stained plaques were then counted and the titer of the adenoviral stock was thus determined. MTT (Sigma), 5ml/ml solution was prepared in PBS, filter-sterilized and kept at 4 °C in 5ml aliquots.

5) Adenoviral transfection and immunostaining of NRVMs:

MOI (multiplicity of infection) is defined as the number of virus particles per cell and generally correlates with expression. Typically expression levels increase linearly as the MOI increases. A number of factors can influence determination of MOI including the nature of the mammalian cell line, its transduction efficiency and the nature of the gene of interest. A range of MOIs (1, 5, 10, 20 and 50) were used on NRVMs to determine the MOI required to obtain optimal expression of the recombinant protein. pAd/CMV/V5-DEST expresses the V5 epitope as a C-terminal fusion to the protein of interest, therefore allowing detection of the recombinant protein by Western immunoblotting or immunostaining. NRVMs were plated on silicone membranes as described above and incubated in a humidified 37°C incubator overnight. The cultures were transfected with the pAd/CMV/V5-DEST plasmid 18 hours after initially being plated. Cells were rinsed twice in NMS and infected with the replication-defective adenovirus diluted in M199 for 1 hour at room temperature. Thereafter, the cells were rinsed and cultured for an additional 72 hours before being subjected to experimental protocols. In preparation for immunostaining, cultures were rinsed in PBS and fixed with ice-cold methanol for 10min at -20 °C. Following fixation, the cell-covered membranes were allowed to dry, cut, placed in 24-well plates and washed in PBS three times. To block non-specific binding, the cultures were incubated in PBS containing 1% bovine serum albumin at room temperature for ~30min. The cultures were then incubated with the primary antibody (diluted in PBS/albumin) overnight at 4°C, brought to room temperature, washed 3 times with PBS, and incubated with indocarbocyanine (Cy3)-conjugated goat anti-mouse or anti-rabbit IgG (diluted 1:400 in PBS/albumin) for 2 h at 25 °C. Following incubation with the secondary antibodies, the membrane quadrants were washed 3 times in PBS, transferred to glass slides and mounted with 50% glycerol- 50% PBS. In all experimental procedures, non-transfected cultures were used for control purposes.

The following methods were developed/ applied to study the effects of known plakoglobin mutations on cellular biomechanics. These experiments were performed by Dr. Hayden Huang, PhD, at the Cardiovascular Division, Brigham and Women's Hospital, Harvard Medical School, Boston in close collaboration with us.

6) Magnetic micromanipulation:

Receptor-dependent cell adhesiveness and cell stiffness were measured using a previously described magnetic micromanipulator.[337,338,339] Briefly, this apparatus consists of a core of CMI-C rod (CMI-C metals) which was machined to a sharp chisel tip, annealed and coated with a thin gold film to minimize corrosion, and wrapped with 300 turns of 18 gauge copper wire. Magnetic beads, 4.5 μm in diameter (M-450, Dynal, Invitrogen) were coated with antibodies against beta-1 integrins (HACD29, Fitzgerald) according to the manufacturer's protocol. A limiting number of beads were added to dishes of confluent HEK293 cells such that a cell had no more than one bead on its surface. After being incubated for 30min at 37°C, the cells were rinsed to remove unattached beads and placed on a temperature controlled stage (Warner Instruments, Hamden, CT) maintained at 37°C on an inverted microscope (Olympus IX-71, Center Valley, PA). The tip of the magnetic micromanipulator was brought into close proximity of a bead identified on the surface of a cell. Magnetic force was applied in five increasing steps to a maximum of 5 nN. Bead detachment rates were recorded, along with the maximum displacement of the beads during the step-wise application of magnetic force using custom Matlab tracking algorithms.[338,340] To measure the amount of beta-1 integrins expressed on the surface of HEK293 cell lines expressing wildtype or mutant forms of plakoglobin, flow cytometry was used as previously reported.[341] Cells were re-suspended in 1 ml Hanks balanced salt solution and split into 2 aliquots. One was incubated with an FITC-conjugated anti-rat CD29 (beta-1 integrin) antibody and the other was incubated with an Alexa488-conjugated anti-rat IgG antibody to control for non-specific binding. Cells were incubated on ice for 1 hr, centrifuged, re-suspended in 1 ml Hanks solution, and analyzed using a Becton-Dickinson flow cytometer.

7) Wound-healing experiment protocol:

HEK293 cells were plated on 35mm fibronectin-coated plastic dishes and grown to confluence. A linear wound approximately 1 mm in width was created by scraping the tip of a P-1000 pipette across each dish. The extent to which cells had filled in the wound was determined at 2 and 24 hr post-wounding by imaging at the same location at 4x magnification. To determine whether cells expressing mutant forms of plakoglobin

exhibited different rates of cell division in response to wounding, cells were plated on fibronectin-coated glass coverslips (to permit use of a high-NA water immersion objective for fluorescence microscopy), grown to confluence and wounded as before. At 24 hr post-wounding, cells were loaded with BrdU (Sigma) for 30min, and then fixed in 4% paraformaldehyde (Sigma) for 15min at room temperature. Cells were made permeable in 0.1% triton-X100 for 5min at room temperature, and then incubated with G3G4, an antibody against BrdU (Developmental Studies Hybridoma Bank[342]) in PBS containing 1% BSA for 1 hr at 37°C. The cells were then incubated with a fluorescent secondary antibody, washed several times and loaded with propridium iodide for 5min at room temperature to label nuclei. The cells were examined by fluorescence microscopy under the green channel to identify dividing cells (BrdU-positive)) and red channel to identify all nuclei (propridium iodide staining). The percentage of BrdU-positive nuclei in cells near the wound was then calculated. Four representative images were taken in each of three separate dishes.

8) Cell migration assay protocol:

To assess the speed of migration of isolated cells, HEK293 cells were plated at low density (20,000 cells/cm^2) on fibronectin-coated plastic dishes and allowed to attach overnight. The dishes were placed on the temperature-controlled microscope stage and images of individual cells were acquired every 10min at 10x for 2.5 hr. Displacements between successive cell centroids were measured using a custom Matlab program and averaged to yield a measure of cell migration speed.

9) Cell-cell adhesion assay using a deform-drag method:

HEK293 cells were plated on fibronectin-coated glass coverslips and grown to confluence. Cell nuclei were labelled by incubating them in a 1:10,000 dilution of Hoechst. The dishes were placed on a temperature-controlled microscope stage and imaged at 10x magnification. A 1 mm diameter glass rod in a motorized micromanipulator (Eppendorf) was positioned so that the tip was just touching the cell surface. The rod was moved by the manipulator at a constant rate of 100 μm/sec across the field of view. Images were acquired using the CoolsnapHQ at 1 frame/sec throughout the entire interval of rod motion and for several sec thereafter. The detachment and dragging of cells in the rod's path resulted in deformation of the cell monolayer adjacent to the cells being dragged. The extent of this deformation is an indicator of the relative strength of cell-cell adhesion and cell-matrix adhesion. To quantify this parameter, the frames acquired during each second were merged into a single image and the vertical extent of nuclear smearing was used as a quantitative measure of cell-cell adhesion.

10) Immunohistochemical analysis of cytoskeletal proteins:

HEK293 cells on fibronectin-coated glass coverslips were grown to confluence, fixed in 4% paraformaldehyde and permealised with 0.1% Triton x100 at room temperature. For actin staining, cells were incubated with Alexa488-conjugated phalloidin according to manufacturer's instructions. For identification of intermediate filaments and microtubules, cells were incubated for 1 hr in PBS containing 1% BSA and either anti-vimentin (Sigma) or anti-alpha tubulin (University of Iowa NIH repository) antibodies followed by incubation with Alexa488-conjugated anti-mouse secondary antibody. After being rinsed in PBS, cells were imaged using a confocal microscope.

RESULTS AND DISCUSSION

1) HEK293 cells subjected to stretch:

To determine the effect of S39_K40insS on the way HEK293 cells respond to defined mechanical load, cells induced to stably express the mutant plakoglobin variant were subjected to pulsatile stretch (110% of resting length, frequency 3Hz) for 1 or 4 hours. HEK293 cells stably expressing the wildtype protein, and non-stretched cultures of both cell lines were used for control purposes. The amount of signal at intercalated discs corresponding to the mechanical junction proteins N-cadherin and plakoglobin as well as the electrical junction protein Cx43 was analysed by immunostaining and quantitative confocal microscopy (Figures 5-7).

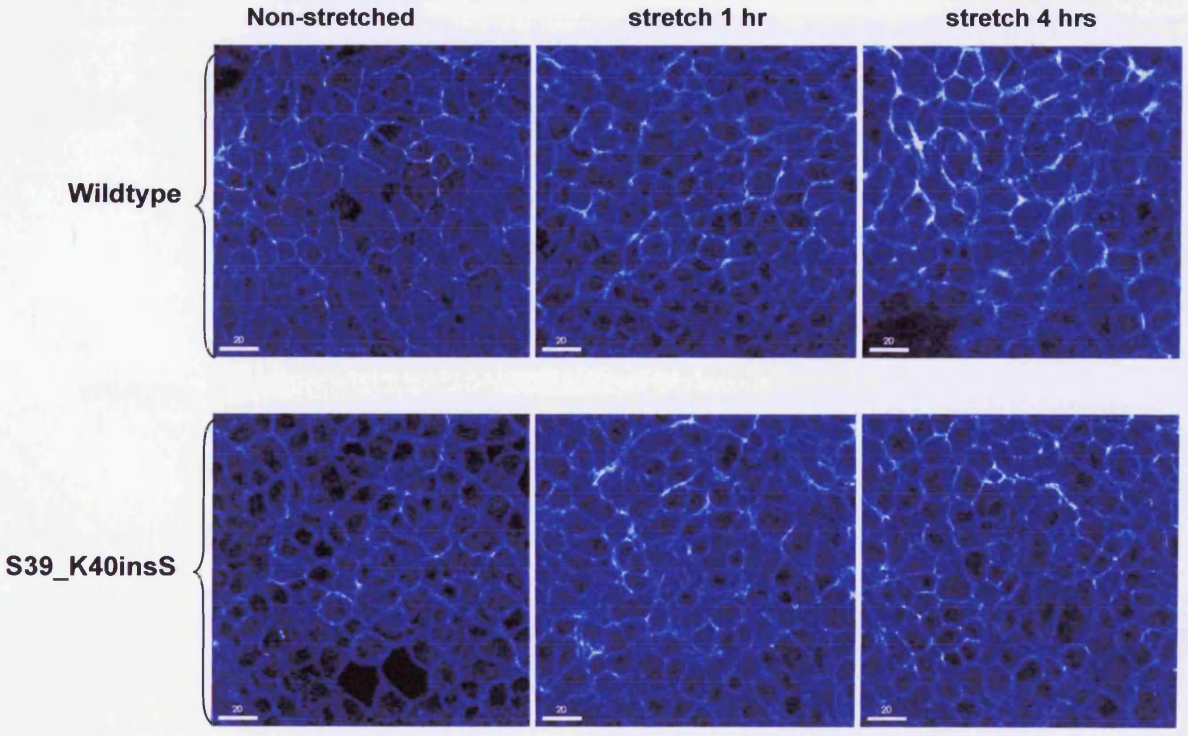

In all figures presented in this sub-chapter, the error bars represent standard deviations.

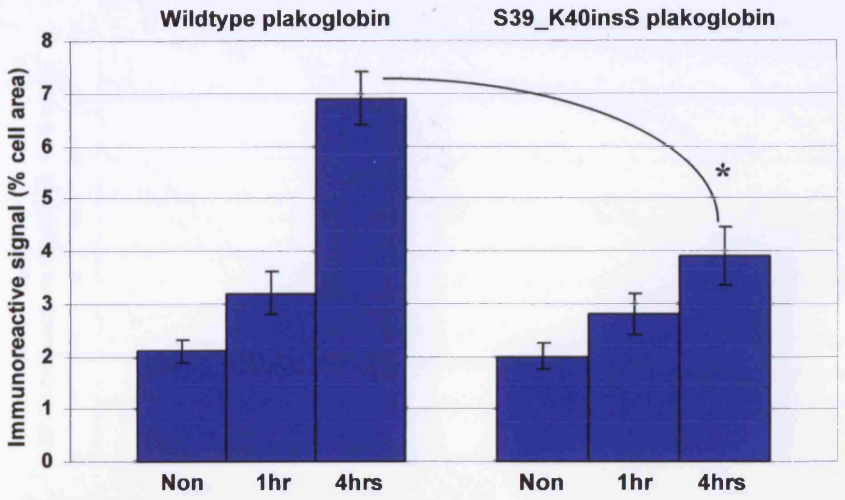

Figure 5: Representative confocal immunofluorescence images and quantitative confocal microscopy data showing the effects of stretch on expression of N-cadherin in HEK293 cells expressing wildtype and S39_K40insS plakoglobin. n=5 for each line, *p<0.05 compared with wildtype cells subjected to 4 hours of stretch.

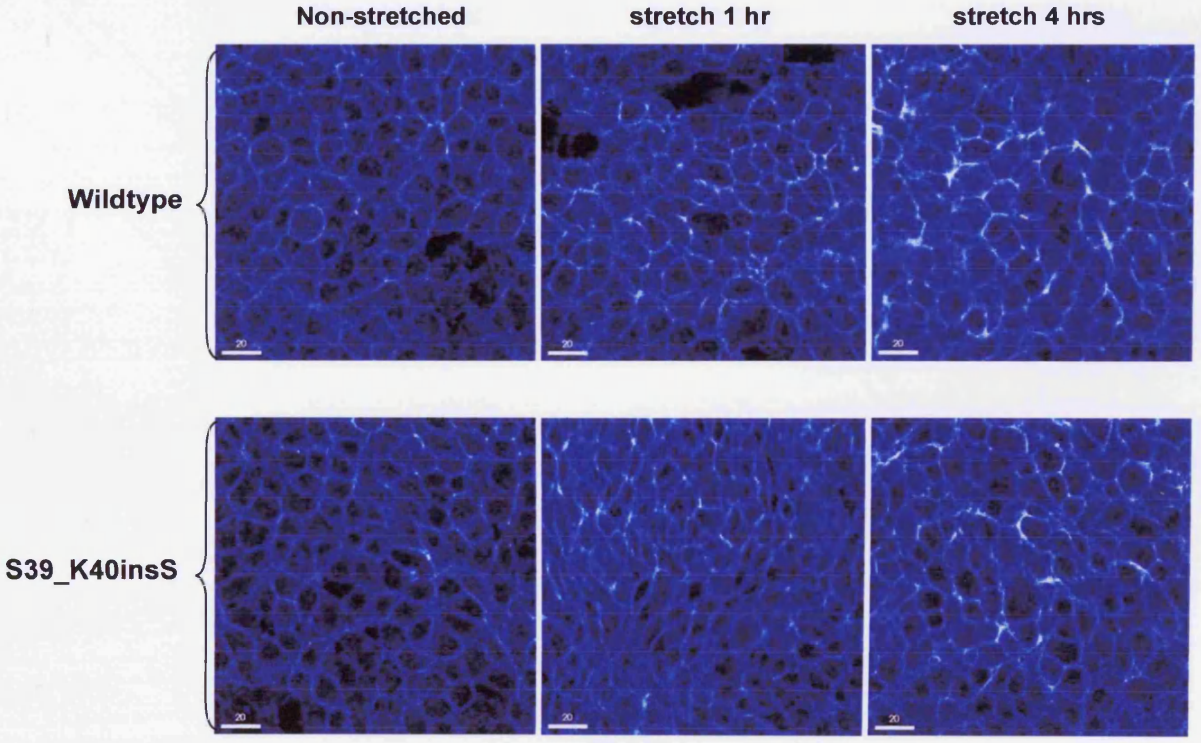

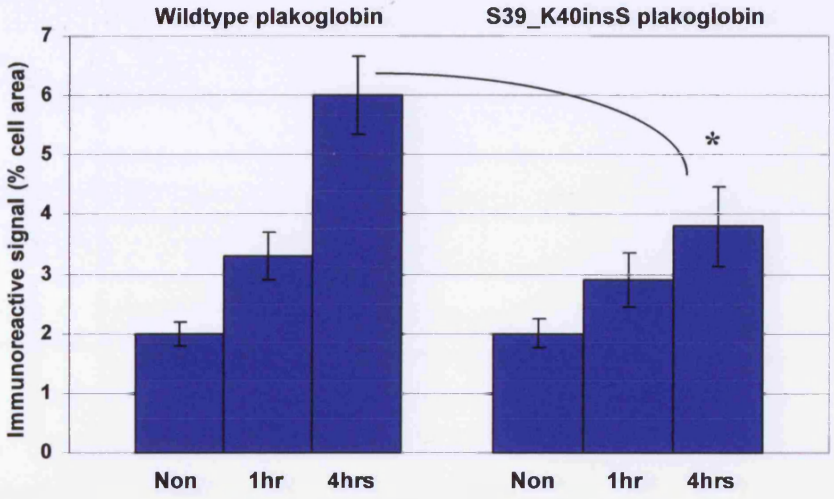

Figure 6: Representative confocal immunofluorescence images and quantitative confocal microscopy data showing the effects of stretch on expression of JUP in HEK293 cells expressing wildtype and S39_K40insS plakoglobin. n=5 for each cell line, * $p<0.05$ compared with wildtype cells subjected to 4 hours of stretch.

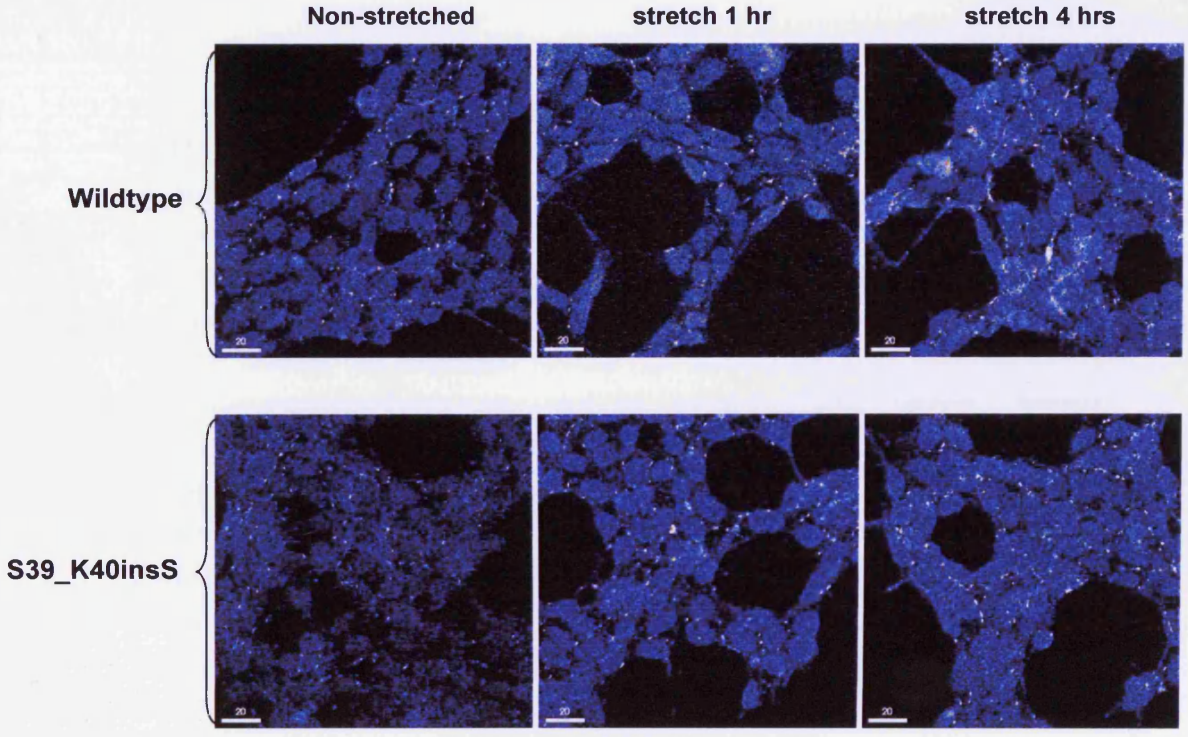

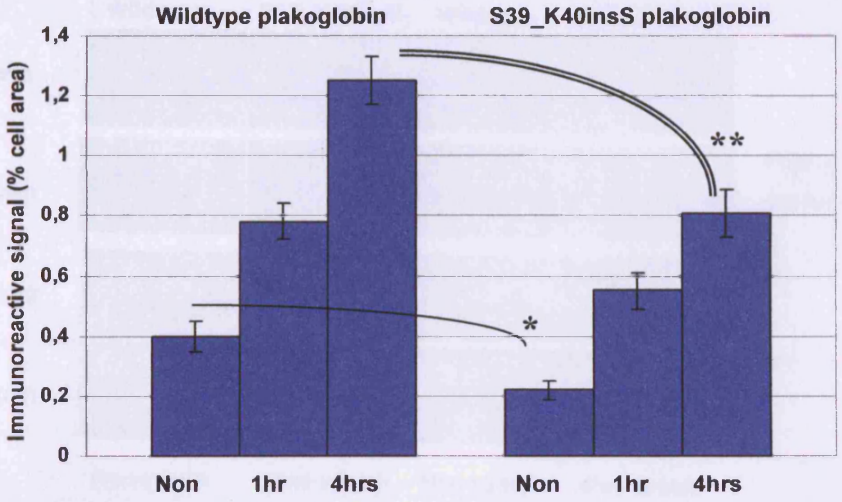

Figure 7: Representative confocal immunofluorescence images and quantitative confocal microscopy data showing the effects of stretch on expression of Cx43 in HEK293 cells expressing wildtype and S39_K40insS plakoglobin. n=5 for each cell line, * $p<0.05$ compared with wildtype baseline levels. **$p<0.05$ compared with wildtype cells subjected to 4 hrs of stretch.

The amount of signal at intercalated discs corresponding to N-cadherin, plakoglobin and Cx43 was highly increased in response to stretch (~3-fold in cells expressing the wildtype protein). However, stretch-induced signal up-regulation corresponding to both mechanical and electrical junction proteins was significantly blunted in cells bearing the S39_K40insS mutation. Interestingly, even the baseline expression levels of Cx43 at intercalated discs were significantly down-regulated in mutant cells compared to wildtype controls. To investigate whether the blunted response observed in the S39_K40insS-bearing cells was due to reduced protein content, Western immunoblotting was used. Expression of N-cadherin, plakoglobin and Cx43 seemed to be higher in wildtype than in mutant cells following exposure to 4 hours of pulsatile stretch (Figure 8). Glyceraldehyde-3-phosphate dehydrogenase (GAPDH) is a catalytic enzyme involved in glycolysis. Since its levels of expression are not anticipated to be affected by mechanical stress, it may be used as a loading control in these experiments. Indeed, all stretched and non-stretched, wildtype and mutant cells expressed similar levels of GAPDH (Figure 8).

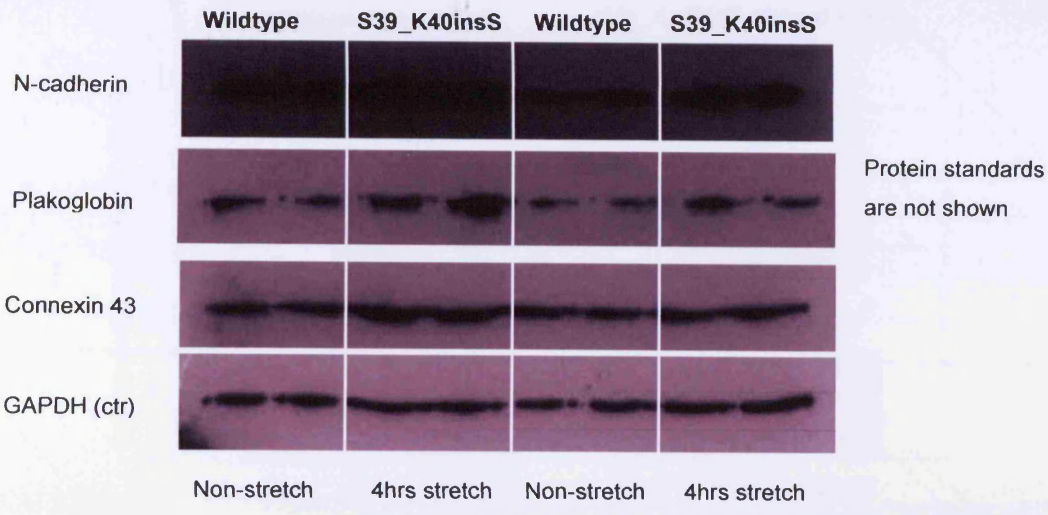

Figure 8: Expression levels of N-cadherin, plakoglobin, connexin43 and GAPDH in HEK293 cells bearing wildtype or S39_K40insS plakoglobin in response to 4 hours of pulsatile stretch. Non-stretched cells were subjected to Western immunoblotting for control purposes.

To investigate the mechanism of junctional protein stretch-induced up-regulation, conditioned medium was removed from cultures stretched for 4 hours, and added to non-stretched cells. The distribution of all 3 proteins was subsequently examined by immunostaining and quantitative confocal microscopy (Figures 9-11).

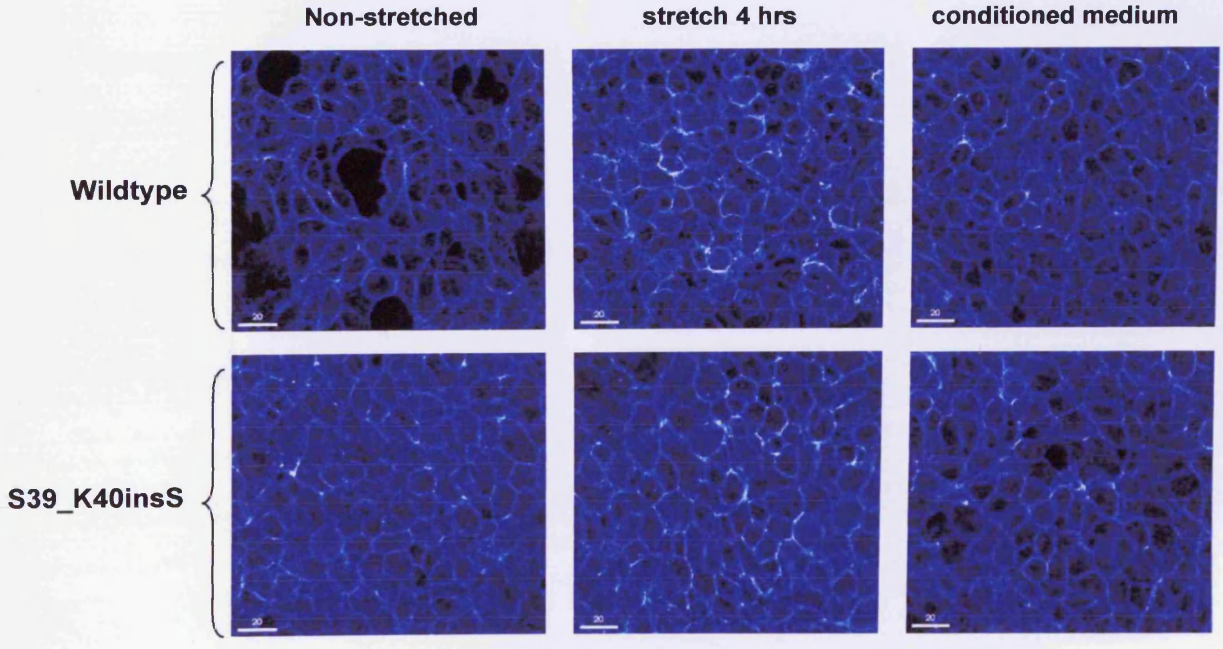

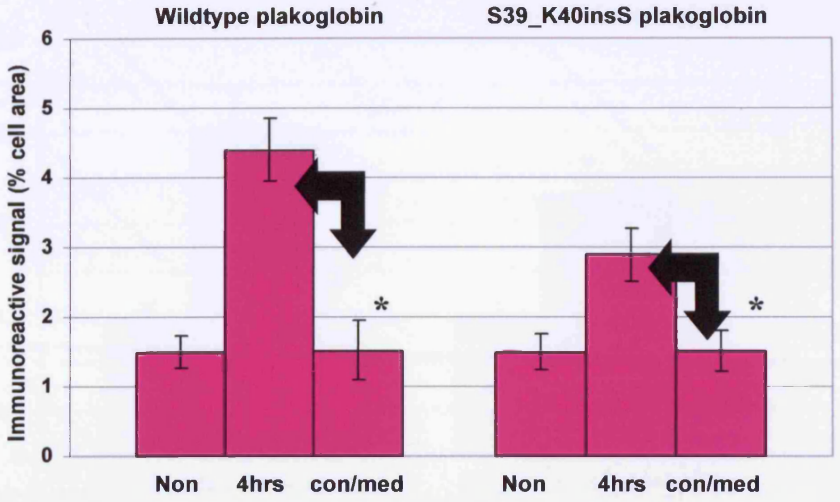

Figure 9: Representative confocal immunofluorescence images and quantitative confocal microscopy data showing the effects of stretch (4hrs) and conditioned medium (con/med) application on the expression of N-cadherin in HEK293 cells expressing wildtype and S39_K40insS plakoglobin. n=5 per experiment, per cell line. For each cell line: * $p<0.05$ compared with protein expression following 4 hours of stretch.

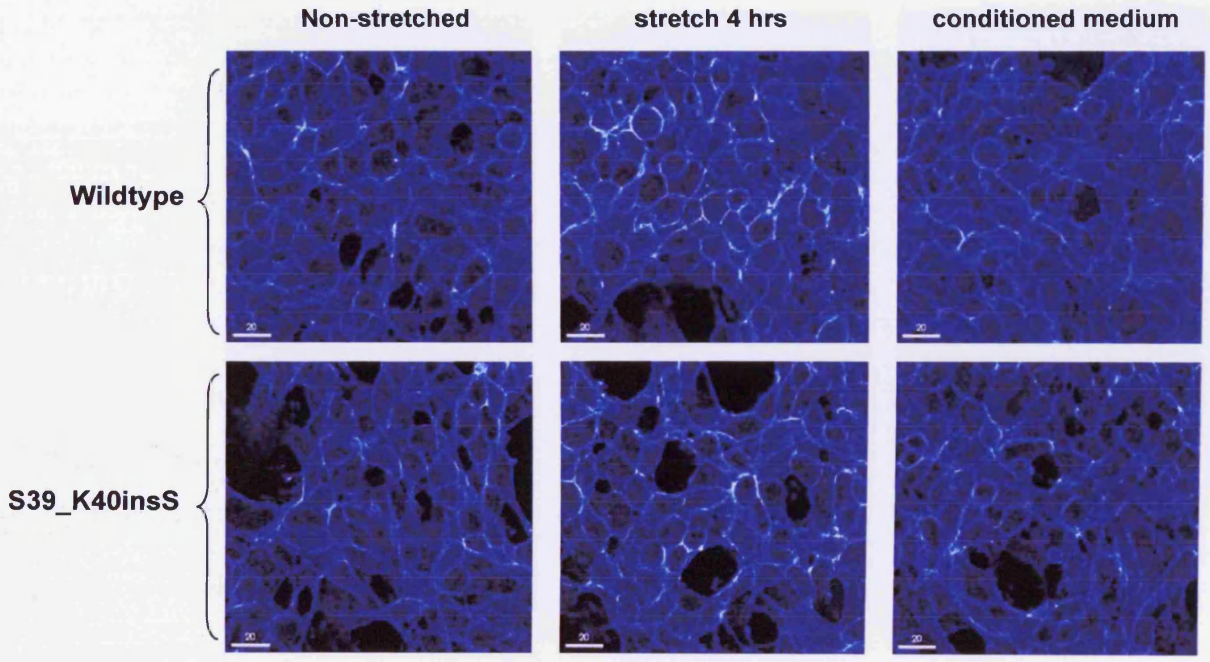

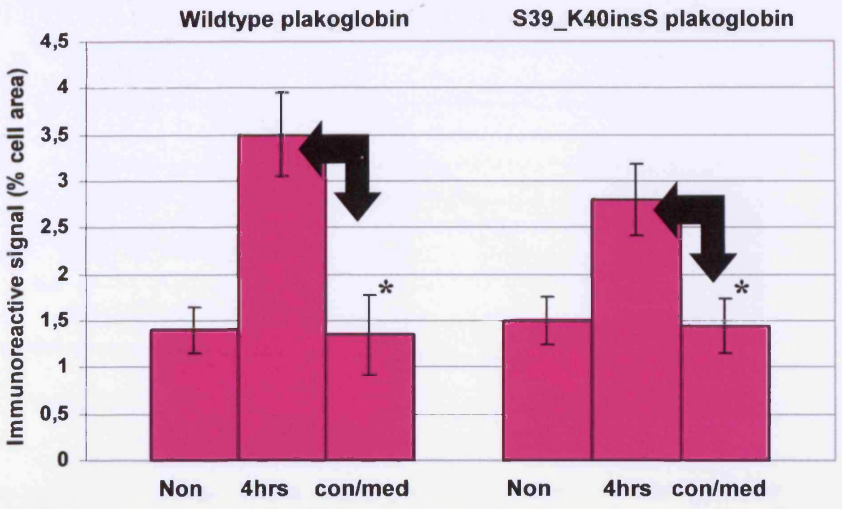

Figure 10: Representative confocal immunofluorescence images and quantitative confocal microscopy data showing the effects of stretch (4hrs) and conditioned medium (con/med) application on the expression of plakoglobin in HEK293 cells expressing wildtype and S39_K40insS plakoglobin. n=5 per experiment, per cell line. For each cell line: * $p<0.05$ compared with protein expression following 4 hours of stretch.

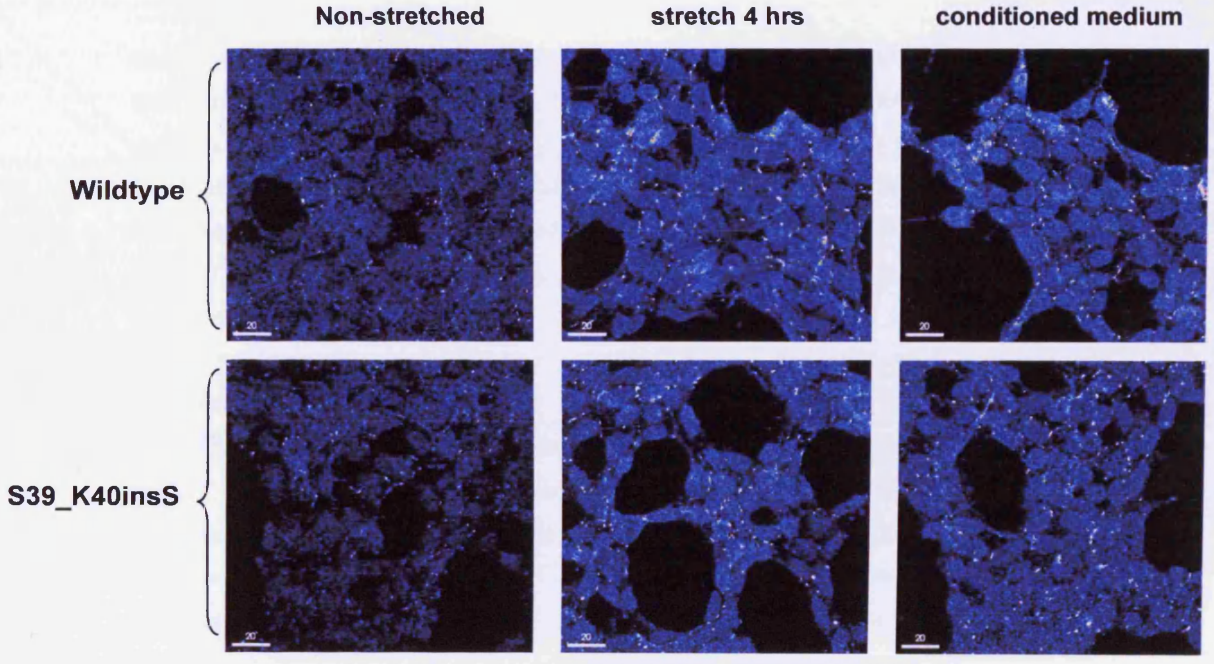

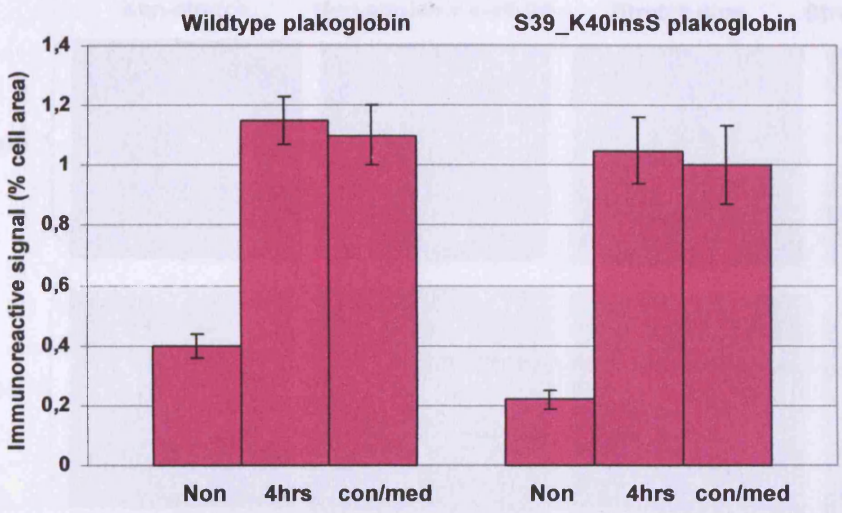

Figure 11: Representative confocal immunofluorescence images and quantitative confocal microscopy data showing the effects of stretch (4hrs) and conditioned medium (con/med) application on the expression of Cx43 in HEK293 cells expressing wildtype and S39_K40insS plakoglobin.

Localization of Cx43 at intercalated discs was significantly elevated in both wildtype and mutant HEK293 cells when stretch-conditioned medium was applied to the cultures. Conversely, the levels of expression of both mechanical junction proteins at the membrane sites remained unchanged. These observations indicate that stretch-induced up-regulation of Cx43 is mediated by a secreted chemical signal, while in the case of N-cadherin and plakoglobin, intracellular mechanotransduction pathways are involved.

It was previously shown that in neonatal rat ventricular myocytes, stretch-induced up-regulation of Cx43 is mediated by secretion of vascular endothelial growth factor (VEGF).[335] To investigate whether in HEK293 cells Cx43 expression in response to stretch is mediated through the same signalling pathway, cells stably expressing wildtype or mutant plakoglobin were incubated with an anti-VEGF antibody prior to being subjected to pulsatile stretch. Cx43 up-regulation was completely blunted in both cell lines, indicating that in HEK293 as well, expression of the gap junction protein in response to mechanical stimuli is mediated by VEGF secretion (Figure 12).

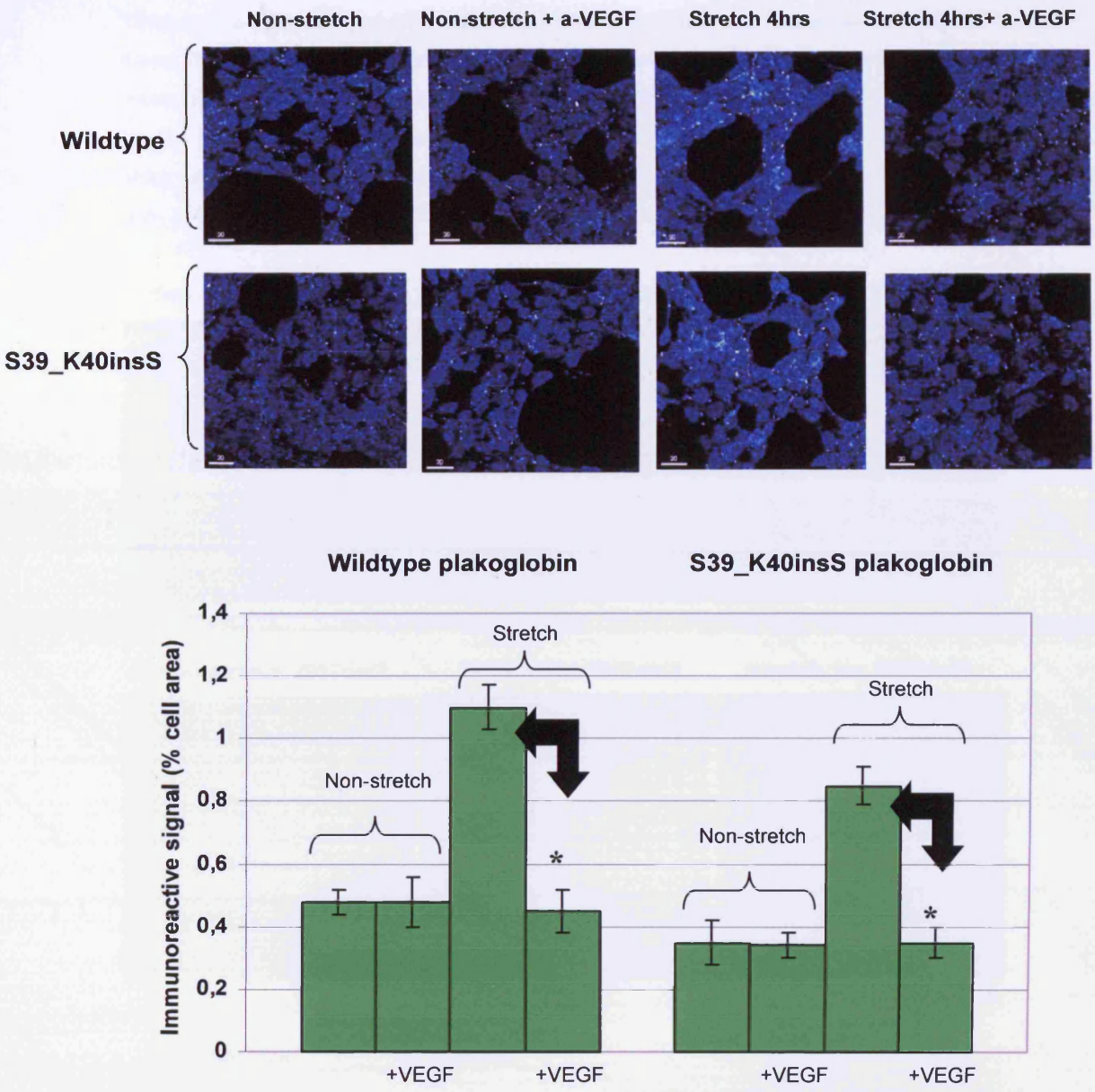

Figure 12: Representative confocal immunofluorescence images and quantitative confocal microscopy data showing the effects of stretch (4hrs) and incubation with an anti-VEGF antibody on the expression of Cx43 in HEK293 cells expressing wildtype and S39_K40insS plakoglobin. Non-stretched cells and cells not incubated with the antibody were used as controls. n=5 per experiment, per cell line. For each cell line: * $p<0.05$ compared with cells subjected to 4 hrs of stretch in the absence of an anti-VEGF antibody.

To compare the effects of S39_K40insS on cellular responses to mechanical load with those of 2057del2, the plakoglobin mutation previously identified to underlie Naxos disease, HEK293 cells induced to stably express 2057del2 plakoglobin *(kindly donated by Denise Lo*) were subjected to pulsatile stretch (110% of resting length, frequency 3Hz) for 1 hour. Cells expressing the wildtype protein, and non-stretched cultures of both cell lines were used for control purposes (Figures 13-15).

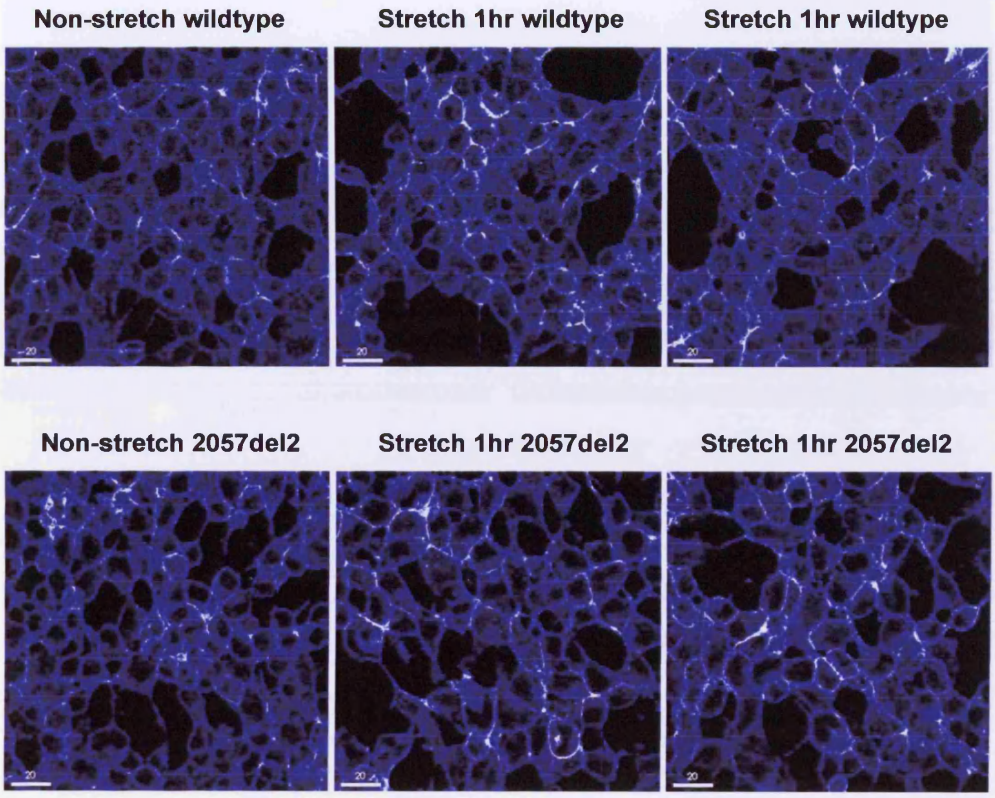

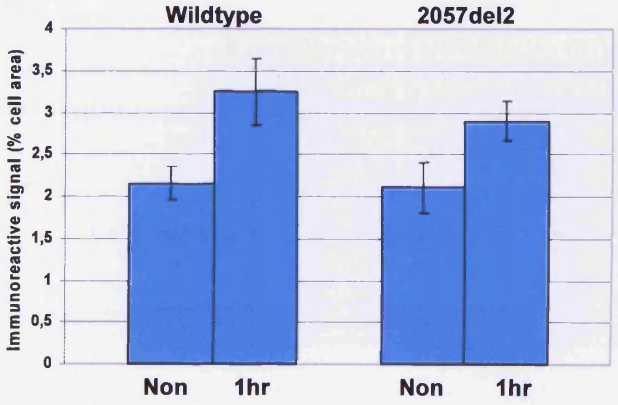

Figure 13: Representative confocal immunofluorescence images and quantitative confocal microscopy data showing the effects of stretch on expression of N-cadherin in HEK293 cells expressing wildtype and 2057del2 plakoglobin. n=5 for each cell line.

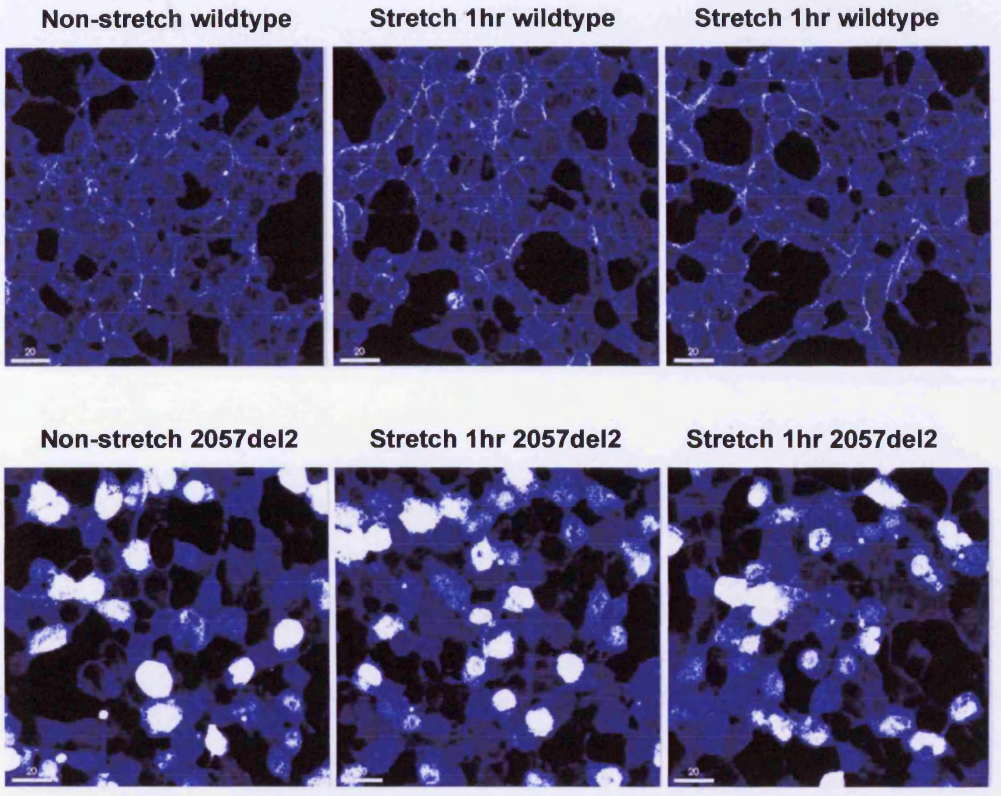

Figure 14: Representative confocal immunofluorescence images showing the effects of stretch on expression of plakoglobin in HEK293 cells expressing wildtype and 2057del2 plakoglobin.

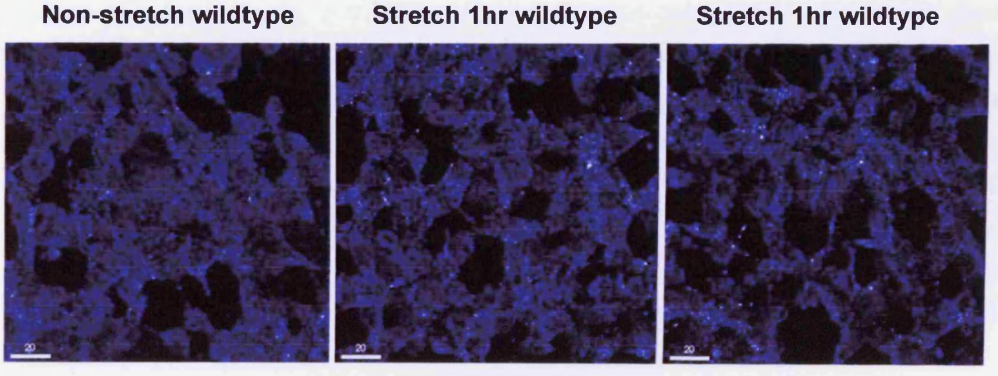

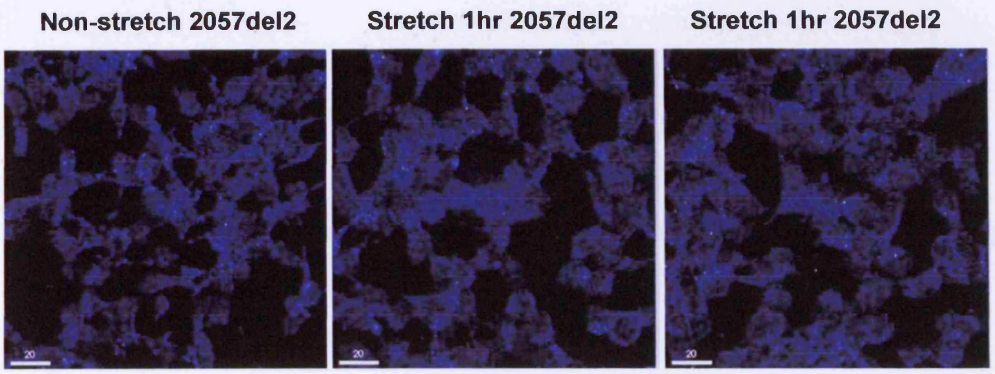

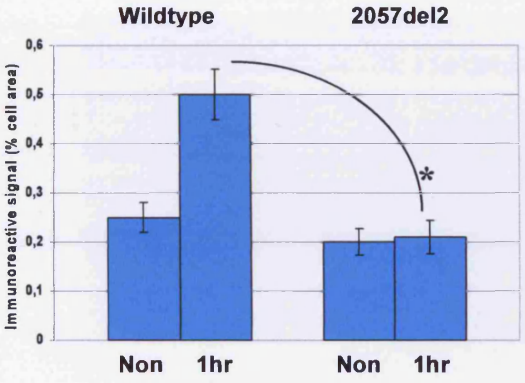

Figure 15: Representative confocal immunofluorescence images and quantitative confocal microscopy data showing the effects of stretch on expression of Cx43 in HEK293 cells expressing wildtype and 2057del2 plakoglobin. n=5 for each cell line. *p<0.05 compared with wildtype cells subjected to 1 hr of stretch.

Stretch-induced up-regulation of signal corresponding to N-cadherin is slightly reduced in cells bearing the 2057del2 mutation compared to wildtype controls, though the difference is not statistically significant (Figure 13). On the contrary, 1 hour of pulsatile stretch does not up-regulate the signal corresponding to Cx43 at intercalated discs (Figure 15). Interestingly, 2057del2 plakoglobin forms cytoplasmic aggregates, thus prohibiting quantitative confocal microscopy analysis (Figure 14).

Subsequently, HEK293 cells induced to stably express 2057del2 plakoglobin were subjected to pulsatile stretch (110% of resting length, frequency 3Hz) for 4 hours. Cells expressing the wildtype protein, and non-stretched cultures of both cell lines were used for control purposes. Analogously, the amount of signal corresponding to N-cadherin, plakoglobin and Cx43 at junctional sites was investigated by immunostaining and confocal microscopy (Figures 16-18), while protein content in response to defined mechanical load was assayed by Western immunoblotting (Figure 19).

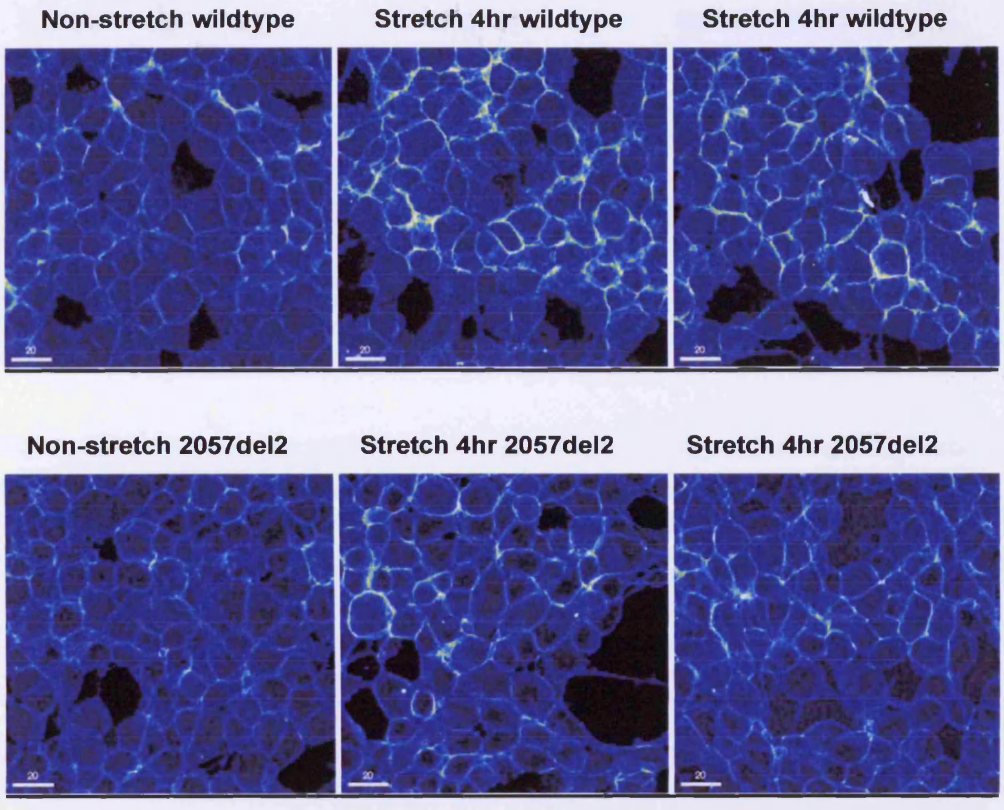

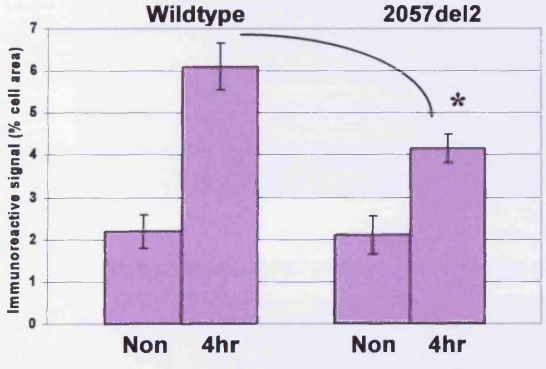

Figure 16: Representative confocal immunofluorescence images and quantitative confocal microscopy data showing the effects of stretch on expression of N-cadherin in HEK293 cells expressing wildtype and 2057del2 plakoglobin. n=5 for each cell line, * $p<0.05$ compared with wildtype cells subjected to 4 hrs of stretch.

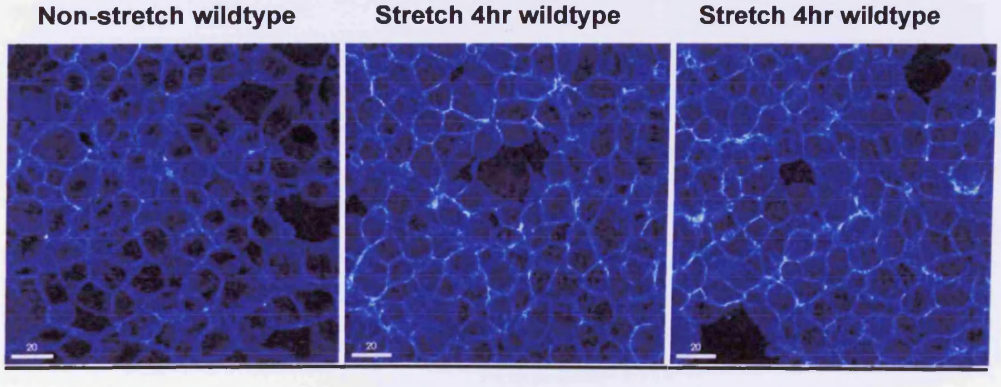

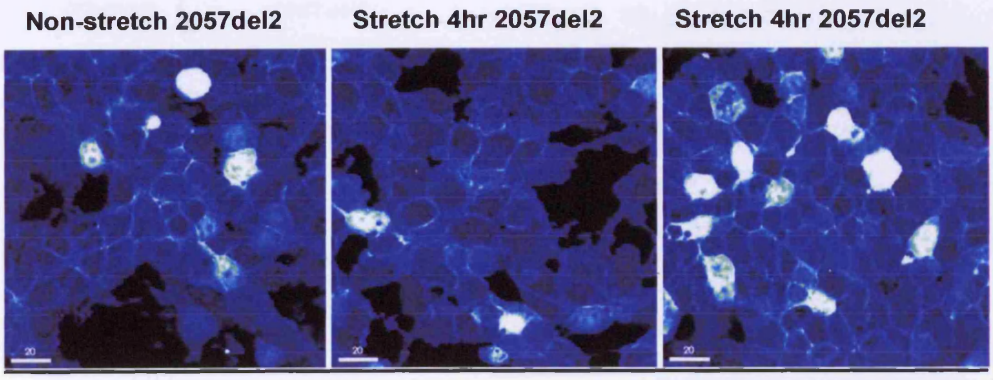

Figure 17: Representative confocal immunofluorescence images showing the effects of stretch on expression of plakoglobin in HEK293 cells expressing wildtype and 2057del2 plakoglobin.

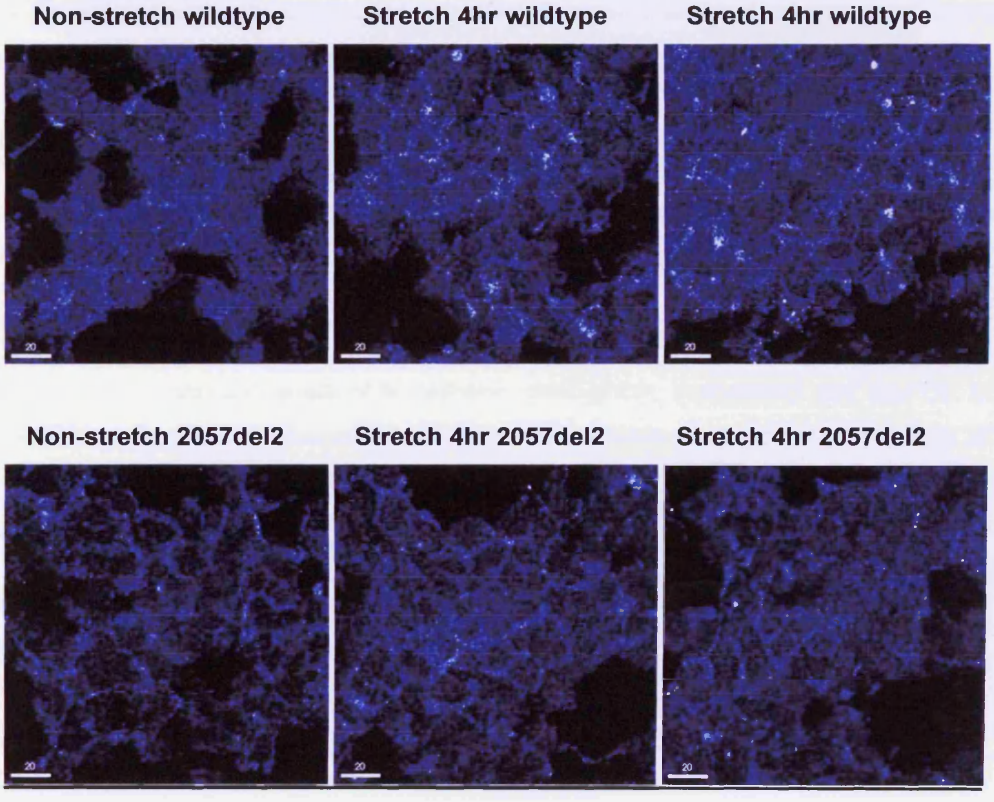

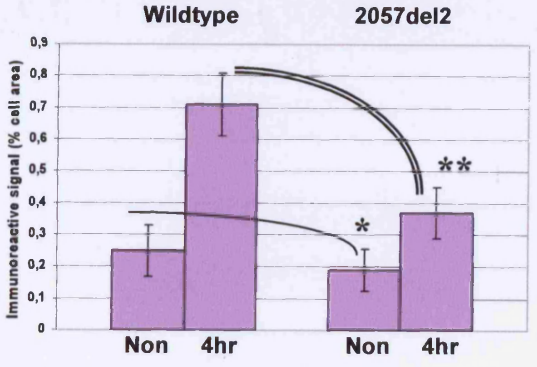

Figure 18: Representative confocal immunofluorescence images and quantitative confocal microscopy data showing the effects of stretch on expression of Cx43 in HEK293 cells expressing wildtype and 2057del2 plakoglobin. n=5 for each cell line, *p<0.05 compared with wildtype baseline levels. **p<0.05 compared with wildtype cells subjected to 4 hrs

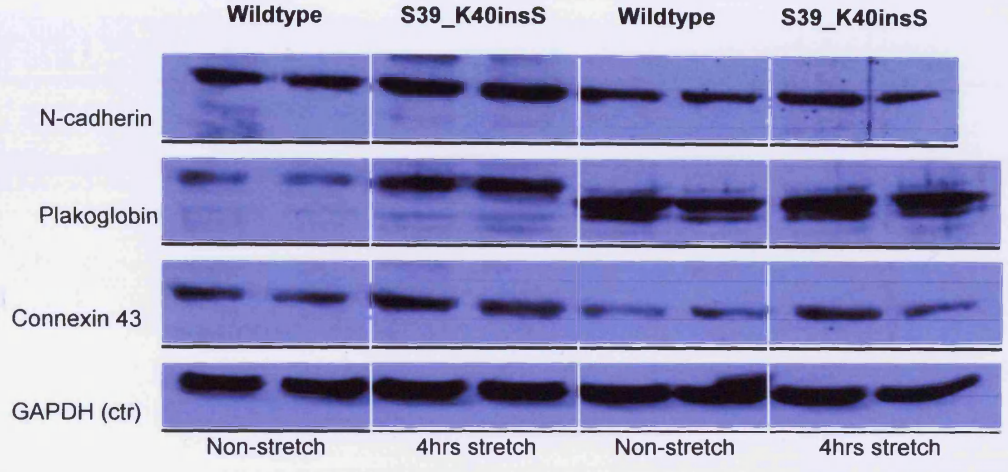

Figure 19: Expression levels of N-cadherin, plakoglobin, connexin43 and GAPDH in HEK293 cells bearing wildtype or 2057del2 plakoglobin in response to 4 hours of pulsatile stretch. Protein standards are not shown.

Similarly to S39_K40insS, 2057del2 inhibits the stretch-induced up-regulation of N-cadherin and Cx43, as shown both by confocal microscopy (Figures 16 & 18) and Western immunoblotting (Figure 19). As mentioned above, 2057del2 plakoglobin forms cytoplasmic aggregates. Therefore the effects of this mutation on cellular responses to mechanical load could not be evaluated by quantitative confocal microscopy (Figure 17). Western immunoblotting though, showed that even 4 hours of pulsatile stretch, does not up-regulate expression of the plakoglobin gene bearing the Naxos deletion. There were differences in the electrophoretic mobility of wildtype and 2057del2 plakoglobin. As mentioned in the introduction, the mutation underlying Naxos disease

introduces a premature stop codon, leading to the production of a C-terminally truncated protein which migrates with a molecular weight of 75 instead of 82kDa (Figure 19).

Discussion:

It is now well established that both gene expression and protein synthesis are subject to regulation by mechanical forces, resulting in alterations of growth and differentiation in a number of tissues and cells.[343,344] The responses of neonatal rat ventricular cardiomyocytes (NRVMs) to uniform pulsatile and static stress were previously investigated using an innovative approach developed in the laboratory of Dr. Andre Kleber. These experiments demonstrated a dramatic up-regulation of intercellular junction proteins after only 1 hour of pulsatile stretch, with a further increase after 6 hours accompanied by a concomitant increase in propagation velocity.[334] Following the generation of the cell line models described in the previous chapter, it was natural to wonder how HEK293 cells respond to mechanical load and whether these responses are altered in the presence of an ARVC-causing mutation. To our knowledge, there are only two ARVC-causing plakoglobin mutations identified to date: 2057del2, a deletion previously identified to cause Naxos disease, and S39_K40insS, a recently-described insertion shown to cause a dominant form of the cardiomyopathy without associated cutaneous abnormalities (Chapter 1). HEK293 cells induced to stably express wildtype plakoglobin or either mutant protein variant were grown on a flexible foundation constructed of thin silicone rubber. Typically, human embryonic kidney-derived cells are capable of producing extracellular matrix proteins and can therefore adhere to surfaces when cultured. Previous experiments though have shown that these cells tend to detach from silicone substrates when stretched, and that they have difficulties surviving and growing thereafter.[345] Therefore in all experimental procedures performed, the flexible foundations were pre-coated with collagen IV prior to cell seeding. Once the cells were firmly attached to this surface, the edges of the silicone membrane were connected to a mechanical device that would deform the silicone base in a controlled fashion. Experiments on NRVMs have shown that stretching cells at 110% of their resting length at a frequency of 3Hz is enough to bring about changes in the distribution of intercalated disc proteins.[334] The same protocol was therefore maintained when HEK293 cells were subjected to linear pulsatile stretch.

There was a marked up-regulation of the mechanical junction proteins N-cadherin and plakoglobin and of the major ventricular gap junction protein Cx43 in wildtype HEK293 cells in response to 1 hour of pulsatile stretch, which became significantly more profound following 4 hours of stretch as shown by confocal microscopy. However, is the increase in signal intensity observed a result of increased gene expression, decreased

degradation or increased trafficking of already present protein molecules to the membrane sites?[334] To clarify this issue, protein expression in response to 4 hours of linear pulsatile stretch was assayed by Western immunoblotting. Indeed, it appears that expression of all three genes examined is up-regulated as a consequence of mechanical forces. Still, is the increase in the immunoreactive signal observed due to increase in junction number or individual junction size? When interpreting immunoreactive signals, it is important to remember that there is a complex non-linear relation between the amount of antibody bound to an epitope and the intensity of the secondary detection signals. Therefore, the number and size of those signals do not necessarily represent the number and dimension of the immunoreactive target. It is possible that the immunofluorescent signal that is emitted from several closely spaced junction plaques would appear as a single spot. This would artificially lower the number of target structures while raising their apparent size. In addition, it is also possible that small junctions, especially gap junctions, below the resolution of the detection system could be missed. On the other hand, an over-estimation of the number of junctions could occur as a result of non-uniform staining of individual junction plaques. Despite these limitations, it is likely that changes in the total immunoreactive signal parallel the changes in the total content of each preparation.[334,346] Electron microscopy studies would be required though to determine whether it is the number of junctions, their size, or both that increase in response to stretch.

In the present experiments, cells were stretched at 110% of their resting length for 1 or 4 hours. Since changes in the distribution of intercalated disc proteins were significantly greater in the 4-hour stretch protocol, compared to the 1-hour stretch protocol, it is logical to assume that the duration of stretch is correlated with the magnitude of the adaptive response. However, is this relationship linear? We could speculate that the response observed after 1 hour of stretch, is primarily due to increased trafficking of already synthesized protein molecules and their increased incorporation to the junctional sites. Lengthier stretch regimes could promote transcription further, increasing the synthesis rate of novel protein particles. Further stretch regimes should be applied to identify the point where observable responses plateau.

Stretch-induced up-regulation of all intercalated disc proteins examined was significantly blunted in cells expressing the S39_K40insS mutation. Western immunoblotting showed that apart from trafficking, gene expression in response to stretch is also disrupted in the presence of S39_K40insS. Furthermore, even the baseline expression levels of Cx43 are reduced in the mutant cells compared to the wildtype controls as shown by both confocal microscopy and protein assays. Reduced accumulation of Cx43 at membrane sites, was also observed in the cardiac biopsy of the proband expressing this mutant plakoglobin variant (Chapter 2). Additionally,

decreased baseline localization of Cx43 at gap junctions was observed in HEK293 cells expressing the 2057del2 plakoglobin variant. Similarly to S39_K40insS, 2057del2 inhibits up-regulation of Cx43 in response to 4 hours of pulsatile stretch. In contrast to S39_K40insS though, 2057del2 totally abolishes Cx43 up-regulation in response to 1 hour of pulsatile stretch. On the other hand, expression levels of N-cadherin seem to be altered similarly in response to mechanical load in the presence of both mutant plakoglobin variants. Alterations of the localization patterns of 2057del2 plakoglobin at intercalated discs could not be examined by confocal microscopy, as the mutant protein tended to form cytoplasmic aggregates of very high signal intensity. Western immunoblotting though showed that in contrast to S39_K40insS, 2057del2 totally abolishes up-regulation of the plakoglobin gene expression in response to stretch. S39_K40insS and 2057del2 are two mutations in the same gene underlying different manifestations of apparently the same disease. Could the differences observed in the experiments presented herein, account at least in part for the differences in the clinical phenotype manifested by individuals with Naxos disease and ARVC patients bearing the S39_K40insS mutation?

In cultured human endothelial cells, there is a rapid up-regulation of c-Fos and Egr-1 mRNA following a mere 10min of stretch.[347] In cultured rat cardiac myocytes, pulsatile stretch rapidly phosphorylated p44/p42 mitogen-activated protein kinases (MAPKs), stress-activated protein kinase (SAPK), p38MAPK and $p125^{FAK}$.[348] Similar studies have shown that stretch enhances production of brain natriuretic peptide through calcineurin and calmodulin-dependant kinase II activation in cultured myocytes,[349] and increases adrenomedullin production through activation of the rennin-angiotensin system.[350] It is therefore already well-established that numerous complex signaling pathways respond to mechanical forces, and from the results presented herein, that both ARVC-causing plakoglobin mutations disrupt communication through these pathways. Whether and to what extent however, this disruption is related to the development of the actual phenotype characterizing the disease is yet to be determined. In 2004, *Liao et al* described the responses of both neonatal rat ventricular myocytes and cardiac fibroblasts to 24 hours of stretch (20% of resting length).[351] Cardiac myocytes underwent mitochondria-dependent apoptosis as evidenced by cytochrome c release, and showed increased expression of the pro-apoptotic Bcl-2 family proteins. Furthermore, p21 was up-regulated and cyclin B1 was down-regulated in cardiac fibroblasts, which seemed to be associated with G_2/M accumulation.[351] It appears therefore, that mechanical stress can be associated with physiologically increased apoptosis and fibrosis in *in vitro* models. What if the presence of a desmosomal mutation alters these responses causing them to become pathological? Could that partially explain the increased levels of apoptosis and the accumulation of fibrotic tissue

characterizing ARVC? Experiments on cardiac myocytes would be needed to address these questions.

When conditioned medium is removed from stretched cultures and added to non-stretched cultures, the localization of Cx43 at intercalated discs is increased, while the levels of expression of N-cadherin and plakoglobin remain unchanged. This observation implies that distinct pathways regulate expression of electrical and mechanical junction proteins in response to stretch, and in particular that stretch-induced up-regulation of Cx43 is mediated by secreted chemical signals, while in the case of mechanical junction proteins, intracellular mechanotransduction pathways are involved. It has been shown that in response to stretch, transforming growth factor-β (TGF-β) levels increase promoting increased secretion of vascular endothelial growth factor (VEGF).[352] It has also been shown that stretch-induced up-regulation of Cx43 in cultured myocytes is blocked by either anti-VEGF or anti-TGF-β antibodies, indicating that VEGF is in fact the secreted chemical molecule mediating this stretch-induced response in cardiac myocytes.[335] To investigate whether the same is true for HEK293 cells, cultures were incubated with an anti-VEGF antibody prior to being subjected to pulsatile stretch. Stretch-induced up-regulation of Cx43 was totally abolished in the presence of the antibody, indicating that the same signaling pathway is operating in both cardiac myocytes and human embryonic kidney-derived cells. Stretch induces remodeling of the heart, thus helping it cooperate with increased functional demands. One adaptation is gap junction remodeling, which was shown to be inhibited in HEK293 cells in the presence of either S39_K40insS or 2057del2. Could this inhibition be contributing to disruption of electrical signal transmission and thus the increased risk of arrhythmogenesis characterizing ARVC? Experiments on cultured rat myocytes have shown that a major mechanism underlying stretch-induced up-regulation of structural junction protein expression involves mechanotransduction by integrin activation via FAK and src kinase pathways.[353] To examine if the same signalling pathways are operating across different cell types, HEK293 cells should be incubated with inhibitors of FAK- and src kinase-dependent signalling prior to being subjected to mechanical stretch. Distribution of junctional proteins could then be examined by immunostaining and quantitative confocal microscopy.

As mentioned in the previous chapter, plakoglobin and β-catenin are both found at the membrane mediating adhesion and at the nucleus regulating the Wnt signalling pathway. It is natural therefore to wonder whether the effects exerted by S39_K40insS and 2057del2 on cellular responses to stretch are in part mediated by alterations in Tcf/Lef activity. Future experiments will be needed to address this question.

2) S39_K40insS versus 2057del2: effects on cellular biomechanics:

The experiments described in this sub-chapter were performed by Dr. Hayden Huang, PhD, at the Cardiovascular Division, Brigham and Women's Hospital, Harvard Medical School, Boston in close collaboration with us and are included in: *Huang H, Asimaki A et al.* "Disparate effects of different mutations in plakoglobin on cell mechanical behavior", manuscript submitted to *the American Journal of Physiology; Cell Physiology.*

No obvious difference in cell size or morphology was observed when HEK293 cells expressing wildtype, S39_K40insS, or 2057del2 plakoglobin were grown and passaged. However under sub-confluent conditions, it was readily apparent that cells expressing the 2057del2 plakoglobin showed a lower degree of clustering than cells expressing either the wildtype or the S39_K40insS-bearing protein (Figure 20). This observation provided the first hint that cells expressing the 2057del2 mutation exhibited abnormal cell-cell adhesion.

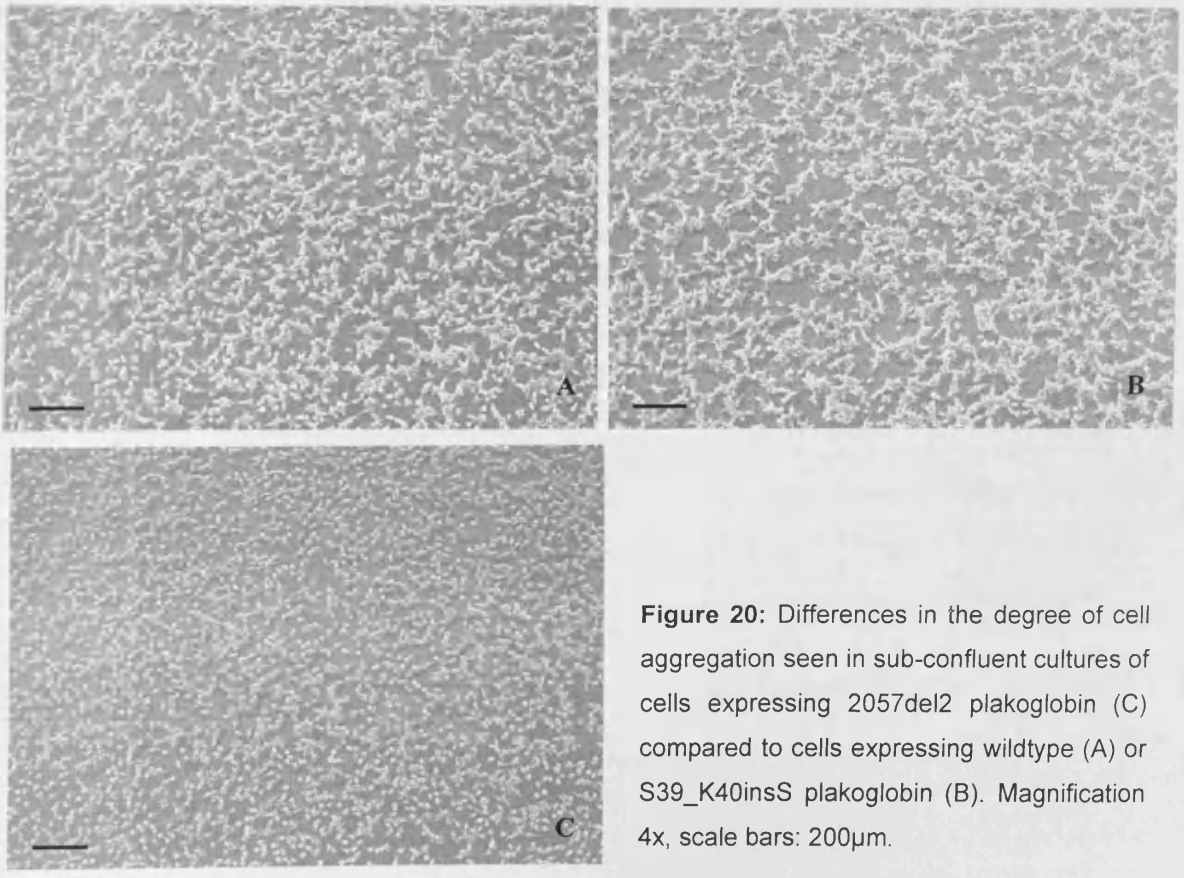

Figure 20: Differences in the degree of cell aggregation seen in sub-confluent cultures of cells expressing 2057del2 plakoglobin (C) compared to cells expressing wildtype (A) or S39_K40insS plakoglobin (B). Magnification 4x, scale bars: 200µm.

To determine whether the presence of either mutant plakoglobin variant affects the cell-extracellular matrix adhesiveness or the cell stiffness, magnetic micro-manipulation was used. Measurements were made on confluent cells incubated with magnetic beads coated with anti-beta-1 integrin antibodies. Such beads would bind to cell surface receptors that link common matrix components to the actin cytoskeleton. The strength of cell-matrix adhesion was first assessed by measuring the rate of bead detachment. The tendency for beads to detach from the cell surface is a reasonable surrogate for the strength of adhesion of the cell to the surface of the culture dish. Bead detachment rates were similar for all three cell lines (28 of 90 beads detached from S39_K40insS cells versus 25 of 88 for wildtype controls and 24 of 90 beads detached from 2057del2 cells versus 29 of 90 for wildtype controls, $p>0.05$ for both experiments). To determine whether there is any difference in the amount of beta-1 integrins expressed by the three cell lines, flow cytometry of cells labeled with fluorescently-conjugated antibodies against beta-1 integrins was employed. No differences were seen (data not shown). Taken together, the bead detachment and flow cytometry data indicate that the strength of cell-matrix adhesion was roughly similar in cells expressing the wildtype or either of the two mutant plakoglobin variants.

To assess cell stiffness the extent of bead displacement from the cell surface with step-wise increases in magnetic force was measured. Only firmly attached beads were included in the analysis. Beads that detached or moved more than one bead diameter (indicating loose attachment) were excluded from the analysis. Greater bead displacement indicated lower cell stiffness. Cells expressing S39_K40insS plakoglobin were significantly less stiff than wildtype controls, while there was no significant difference in stiffness between cells expressing wildtype and 2057del2 plakoglobin (Figure 21).

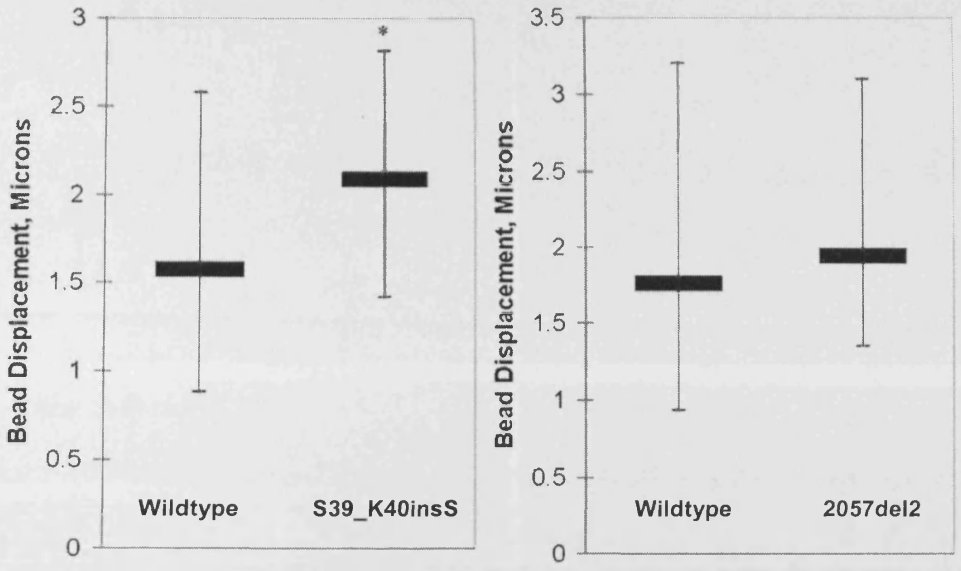

Figure 21: Magnetic micromanipulation experiments revealed differences in cell stiffness as measured by bead displacement. Cells expressing the S39_K40insS plakoglobin are significantly less stiff than cells expressing the wildtype protein (*$p<0.05$), while cell stiffness is not significantly different between cells expressing the 2057del2 and the wildtype molecule ($p>0.05$).

To determine whether ARVC-causing plakoglobin mutations alter cell mobility, two assays were used: a wound-healing and a single-cell migration assay. Cells grown to confluence were wounded with a pipette tip and allowed to heal. The wound-healing rate was measured by determining the distance of closure between the two leading edges of the wound. As shown in Figure 22, would healing occurred more rapidly during the first 24 hours in cell expressing either mutant form of plakoglobin compared with cells expressing wildtype plakoglobin ($p<0.01$ for both).

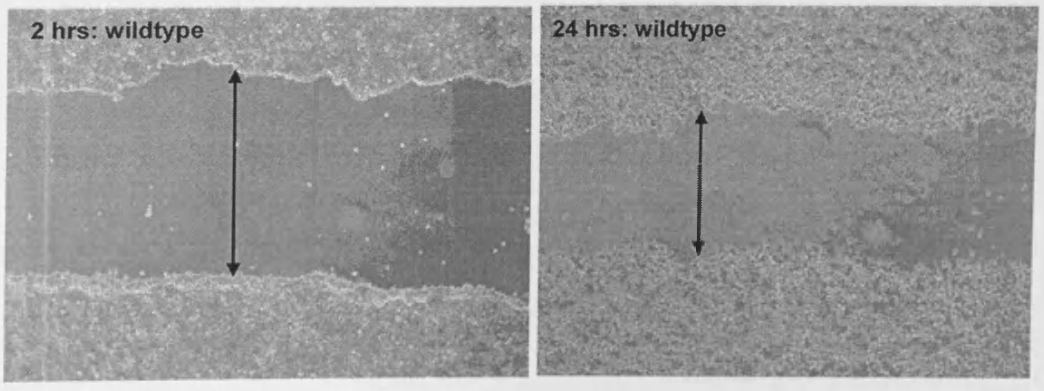

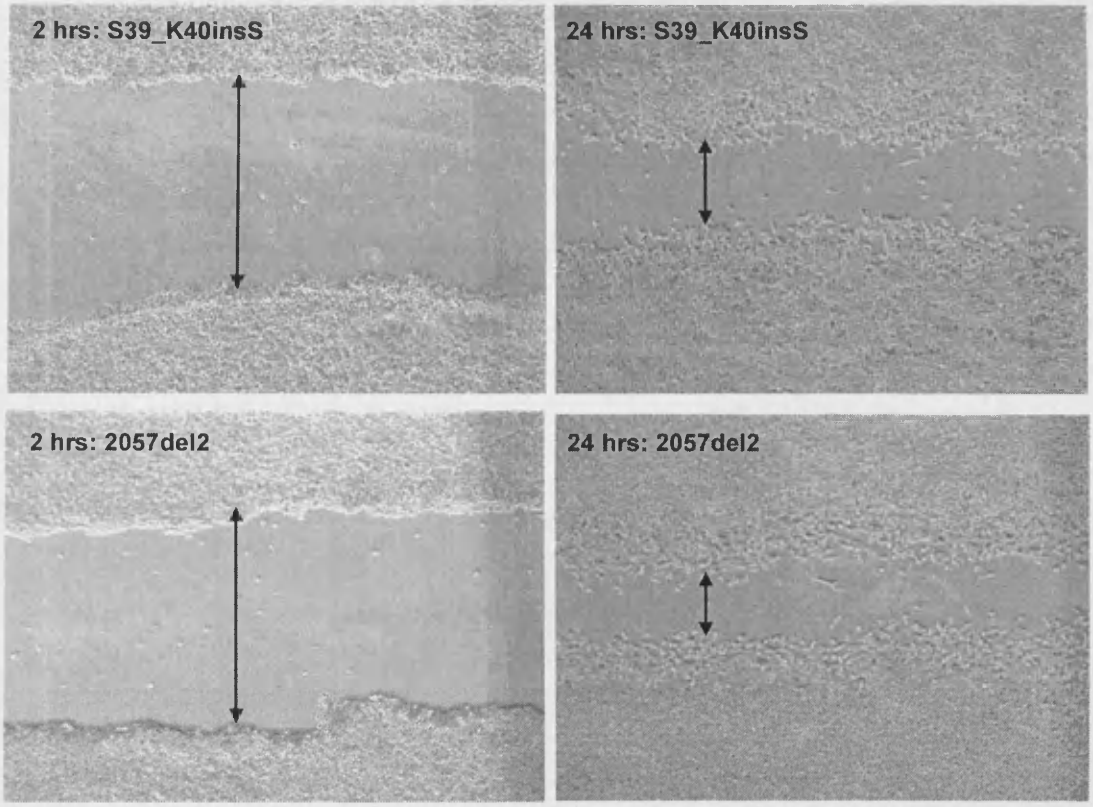

Figure 22: Wound healing is significantly accelerated in cells expressing either mutant plakoglobin variant compared to wildtype controls (magnification 4x).

To determine if increased rates of wound-healing are related to increased rates of cell division in the two mutant cell lines, cultured cells were labeled with BrdU during active wound-healing and the number of labeled nuclei was counted. Cell division rates were similar in all cell lines over the first 24 hours (Figure 23). Therefore, increased wound-healing is not related to increased rates of proliferation.

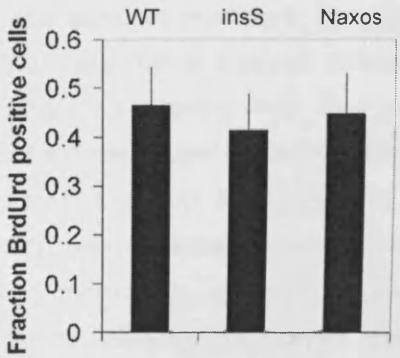

Figure 23: The graph shows the proportion of BrdU-positive nuclei in the vicinity of the wound, n=12 for each group, $p>0.05$.

To determine whether changes in the speed of cell migration contributed to the increased wound-healing, the movements of cells grown in low density were tracked over 2 hours. Cell expressing either mutant plakoglobin variant exhibited greater rates of migration compared to wildtype cells ($p<0.05$, Figure 24). These results indicate that increased wound-healing rates are related, at least in part, to enhanced cell mobility caused by expression of either ARVC-causing mutation.

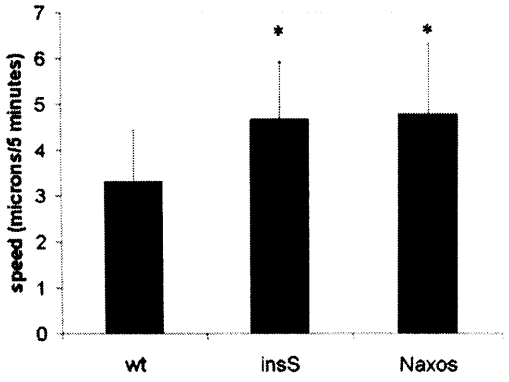

Figure 24: The speed of migration of individual cells in low density cultures is significantly increased in cells expressing either mutant form of plakoglobin compared with cells expressing the wildtype protein, $n>11$ for each group,*$p<0.05$.

Since magnetic micro-manipulation experiments did not show any differences in the strength of cell-matrix adhesion, we turned our attention to the effects of the plakoglobin mutations on cell-cell adhesion. Such analysis is of obvious relevance, given the role of abnormal inter-cellular adhesion in ARVC pathogenesis. However, we were unaware of any specific assays designed to directly measure pure cell-cell adhesion forces. Accordingly, Dr. Hayden Huang designed a new method was and named it: deform-drag method. A glass rod is dragged across a cell monolayer and the extend of deformation of the adjacent monolayer is assessed (Figure 25). By taking images in sequence as the glass rod is dragged across the field of view, and then merging the images together, neighboring cells that moved significantly could be detected by the smearing of a nuclear label across the field of view. The distance of the deformation, as assessed by this nuclear label smearing, was used as a quantitative measure of the strength of cell-cell adhesion across the monolayer. As shown in Figures 26 and 27, the deformation was equivalent between cells expressing wildtype and S39_K40insS plakoglobin. However in marked contrast, cells expressing the 2057del2 plakoglobin variant exhibited virtually no smearing at all, indicating that compared to the other two cell lines, these cells had dramatically reduced inter-cellular adhesion.

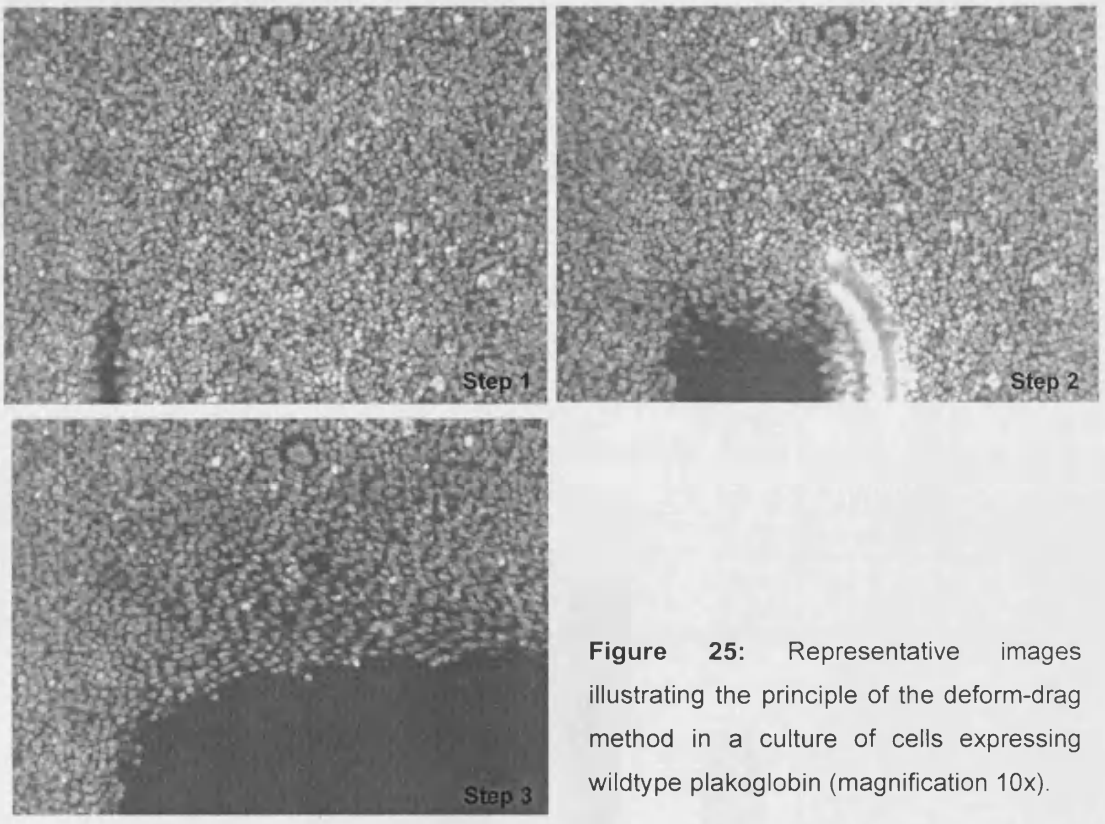

Figure 25: Representative images illustrating the principle of the deform-drag method in a culture of cells expressing wildtype plakoglobin (magnification 10x).

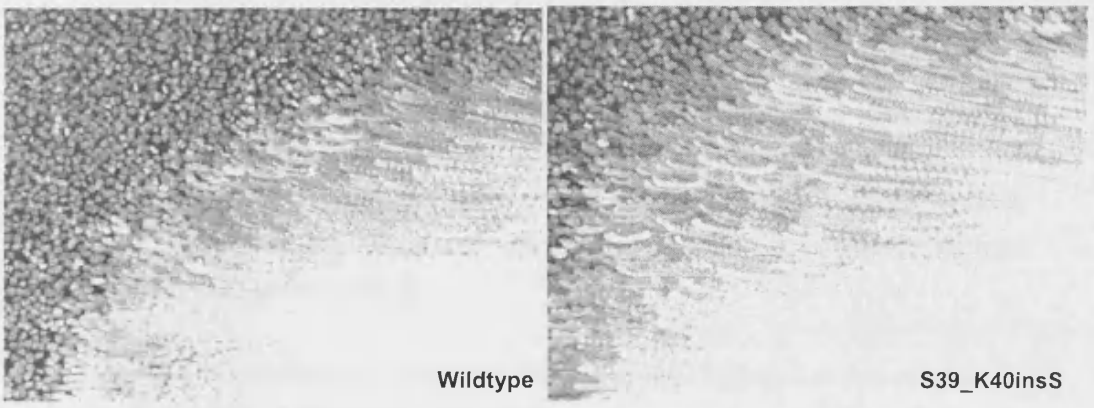

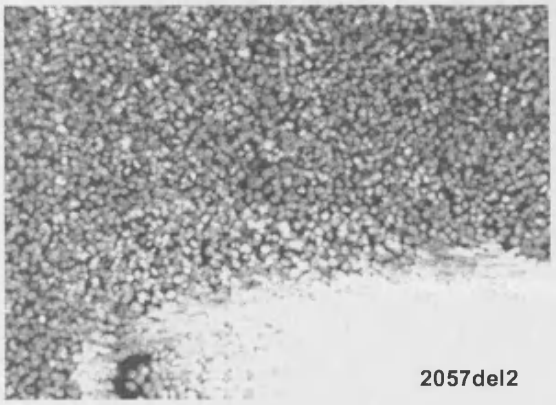

2057del2

Figure 26: By merging the frames acquired during dragging, the motion of nuclei in adjacent cells from cultures expressing wildtype or either mutant form of plakoglobin can be visualized and quantified.

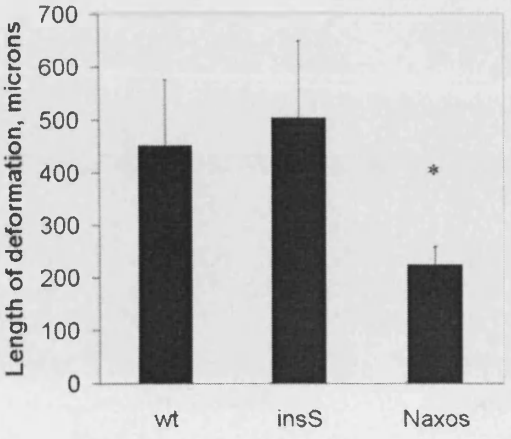

Figure 27: The extent of motion in the vertical direction (perpendicular to the direction of the wound) can be used as a measure of the strength of cell-cell adhesiveness. The graph shows that cells expressing the 2057del2 mutation, but not the S39_K40insS mutation, exhibit markedly diminished cell-cell adhesiveness compared to wildtype cells, n=6 for each group, *$p<0.05$.

To determine if mutations in plakoglobin cause apparent changes in the structure or distribution of the cytoskeleton, cells were grown to confluency and stained with antibodies against actin, alpha-tubulin and vimentin. Examination by confocal microscopy showed no obvious differences in cytoskeletal density, distribution or structure (Figure 28).

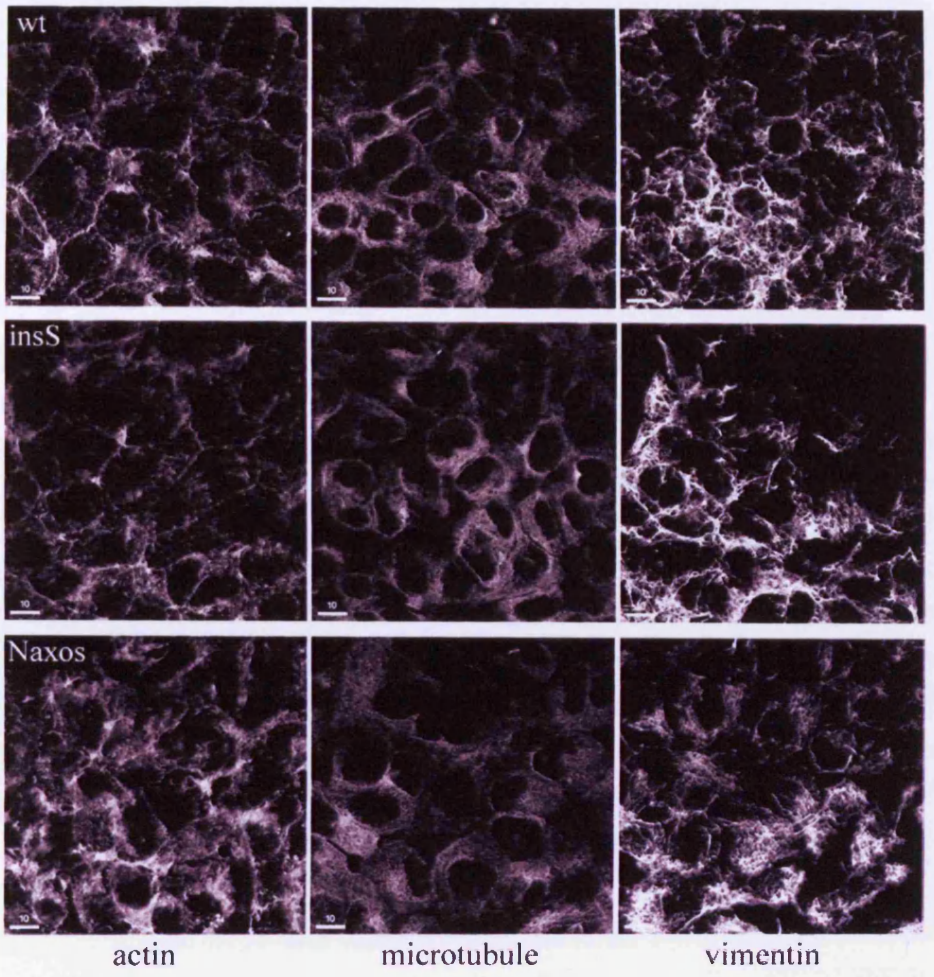

Figure 28: Representative confocal microscopy images of cells expressing all three forms of plakoglobin stained with antibodies against actin, alpha-tubulin and vimentin to visualize actin, microtubule and intermediate filament components of the cytoskeleton respectively. Scale bars= 10μm.

Discussion:

While significant progress has been made in identifying ARVC-causing mutations, much less is known about the mechanisms by which these mutations lead to the disease. One leading hypothesis involves loss of mechanical integrity within the heart; defects in linkage lead to injury and ultimately degeneration of cardiac myocytes and their replacement by fibrofatty tissue. Although the importance of cell-cell coupling in the setting of ARVC has been well-established, to our knowledge there has not been a study describing the effects of pathogenic mutations on cellular biomechanics. In this part of the project, the effects of two ARVC-causing mutations on cellular biomechanical properties have been characterized; the first is a C-terminal mutation in

the gene coding for plakoglobin (2057del2), previously identified to underlie Naxos disease, a syndrome characterized by ARVC, palmoplantar keratoderma and wooly hair and the second is an N-terminal mutation in the same gene (S39_K40insS), recently shown to underlie a form of late-onset typical ARVC without associated cutaneous abnormalities (Chapter 1).

Both standard and novel techniques were used to study mechanical behavior of HEK293 cells expressing different plakoglobin mutations. For instance, in order to assess the relative strengths of cell-cell and cell-matrix interactions, a novel technique was developed by Dr. Hayden Huang and named "deform-drag method". It was assumed that the interaction between cells and a fibronectin-coated culture dish surface is mediated by beta-1 integrins. Since magnetic micromanipulation experiments did not manifest any significant differences in such cell-matrix interactions, the dramatic differences obtained from the deform-drag experiments was interpreted as being primarily due to changes in cell-cell adhesion. This conclusion is significantly strengthened by the markedly decreased degree of cell clustering seen in sub-confluent cultures of cells expressing the 2057del2 mutation. It is possible though that slight differences in adhesion via beta-1 integrins or differences mediated by other cell-surface receptors could contribute to overall changes in cell-matrix adhesion. Further work to isolate these effects and to elucidate the mechanism of action in regulating cell mechanics is currently underway.

The experiments performed demonstrated that cells expressing either plakoglobin mutant exhibited increased wound-healing rates and higher cell migration speed compared to cells expressing the wildtype protein and that these changes are not due to differences in cell proliferation rates, at least not over the first 24 hours examined. While these results are generally consistent with results previously reported by *Yin et al*,[249] who observed both cell-cell adhesion-dependent and –independent changes in keratinocyte mobility mediated by plakoglobin, this is the first time that clinically-relevant mutations have been assessed. Additionally, *Yin et al* found that expression of an N-terminal variant of plakoglobin, but not a C-terminal truncation, suppressed cell mobility in keratinocytes lacking wildtype plakoglobin.[249] The results concerning cells expressing the 2057del2 mutation are consistent with those of *Yin et al.* On the contrary though, we showed that an S39_K40insS-bearing plakoglobin, which contains an additional N-terminal serine residue but has otherwise intact N- and C-termini, does not suppress cell mobility in a manner similar to wildtype plakoglobin. These data suggest that the presence of an excess serine affects cell mobility in an active manner. Simply removing the entire N-terminus does not apparently have the same effect as a single amino-acid residue insertion.

Interestingly, the observations presented above indicate that the S39_K40insS insertion in plakoglobin significantly diminishes cell stiffness without affecting cell-cell adhesion, while the 2057del2 deletion in the same gene has the opposite effect; it significantly reduces cell-cell adhesion strength without affecting cell stiffness. The disparate effects on cell biomechanical behavior are significant because they underlie potential differences in the pathogenesis of ARVC. They suggest for example that myocardial injury may arise from loss of cell-cell adhesion in Naxos disease, whereas similar problems could, amongst others, arise from diminished cell stiffness in the S39_K40insS form of ARVC. Diminished cell stiffness could for instance indicate persistently increased mechano-sensitive responses. However, although analysis of HEK293 cells has several advantages, we once again hasten to point out that the effects of different plakoglobin mutations on the biomechanical behavior of HEK293 cells cannot necessarily be translated to cardiac myocytes. Future studies will be needed to determine whether these known ARVC-related mutations alter the biomechanical properties of ventricular myocytes. Additional insights though may be gained by studying keratinocytes. These cells contain abundant desmosomes and are subjected to significant mechanical stress. As mentioned in the introduction, apart from 2057del2, further recessive mutations in desmosomal genes have been associated with syndromes that affect both the heart and the skin.[63,66] Similarly, a case of compound heterozygosity for two novel nonsense desmoplakin mutations underlying a unique cardiocutaneous syndrome was presented in Chapter 1. Future work involving keratinocytes may provide new insights into the biomechanical mechanisms by which mutations in desmosomal genes promote cell injury and cause human disease. Obtaining human cardiac myocytes from patients bearing ARVC-causing mutations would require an invasive heart biopsy procedure and such cells would not even be able to be maintained and propagated in culture. On the contrary, obtaining human keratinocytes from affected individuals would require a simple skin punch-biopsy procedure and they could potentially be immortalized and utilized in *in vitro* experiments. For instance, in 2003, *Chamulitrat et al* described a detailed method through which human epidermal cells can be isolated, immortalized and maintained in culture.[354] Although desmosomal junctions are formed throughout the entire epidermis, in such syndromic forms of ARVC it is mainly the palms and soles that are affected, presumably because these parts of the skin are subjected to increased mechanical stress. It would be fascinating to be able to recapitulate this "keratoderma" phenotype by subjecting cultured immortalized keratinocytes to stress *in vitro*. In this way we may be able to understand the pathways and mechanisms through which abnormalities emerge in response to increased mechanical load.

This part of the project showed that different mutations in the same gene, both of which known to cause the same disease, lead to different biomechanical responses at the cellular level. It therefore seems that there may not be a single common pathway by which ARVC develops. There are still many unanswered questions in this disease. It is becoming increasingly clear though, that ARVC cannot be fully characterized without considerations of cell mechanics and mechanotransduction.

3) Expressing S39_K40insS in ventricular myocytes:

Cardiomyocytes are terminally differentiated cells that to date have been characterized as poor targets for non-viral gene transfer. Therefore, to achieve high transfection efficiency, a recombinant adenoviral construct was generated. S39_K40insS plakoglobin was cloned into the pAd/CMV/V5-DEST vector via an LR clonase-mediated recombination reaction. A virus expressing the mutant gene was subsequently generated, amplified and titred. Similarly, a virus expressing the wildtype gene was generated and used for control purposes. Neonatal rat ventricular myocytes (NRVMs) were isolated and seeded on collagen I pre-coated culture chambers. A series of viral transfections were set up to determine the optimal MOI (multiplicity of infection). Cells were transfected 18 hours post-seeding and incubated for 72 hours prior to experimental procedures. Optimization studies showed that this time period was sufficient for expression of the exogenous gene and its targeting to the appropriate cellular compartment, in this case, the membranous cell-cell junctions. The pAd/CMV/V5-DEST vector expresses the V5 epitope as an C-terminal fusion to the inserted gene, therefore allowing immuno-localization of the exogenous protein separately from the endogenous protein, naturally expressed by the cells. Transfection efficiency was first tested with immunostaining and fluorescent or confocal microscopy. Using an MOI=10, >90% of the myocytes expressed the recombinant plakoglobin (Figure 29). Lower MOIs decreased transfection efficiency, while higher MOIs increased cell death rates in the transfected cultures. Therefore an MOI of 10 was interpreted as optimal for all experimental procedures. Though non-transfected control myocytes did not express V5, there was abundant signal corresponding to the epitope in cells transfected with both the wildtype and the S39_K40insS plakoglobin viruses (Figure 29).

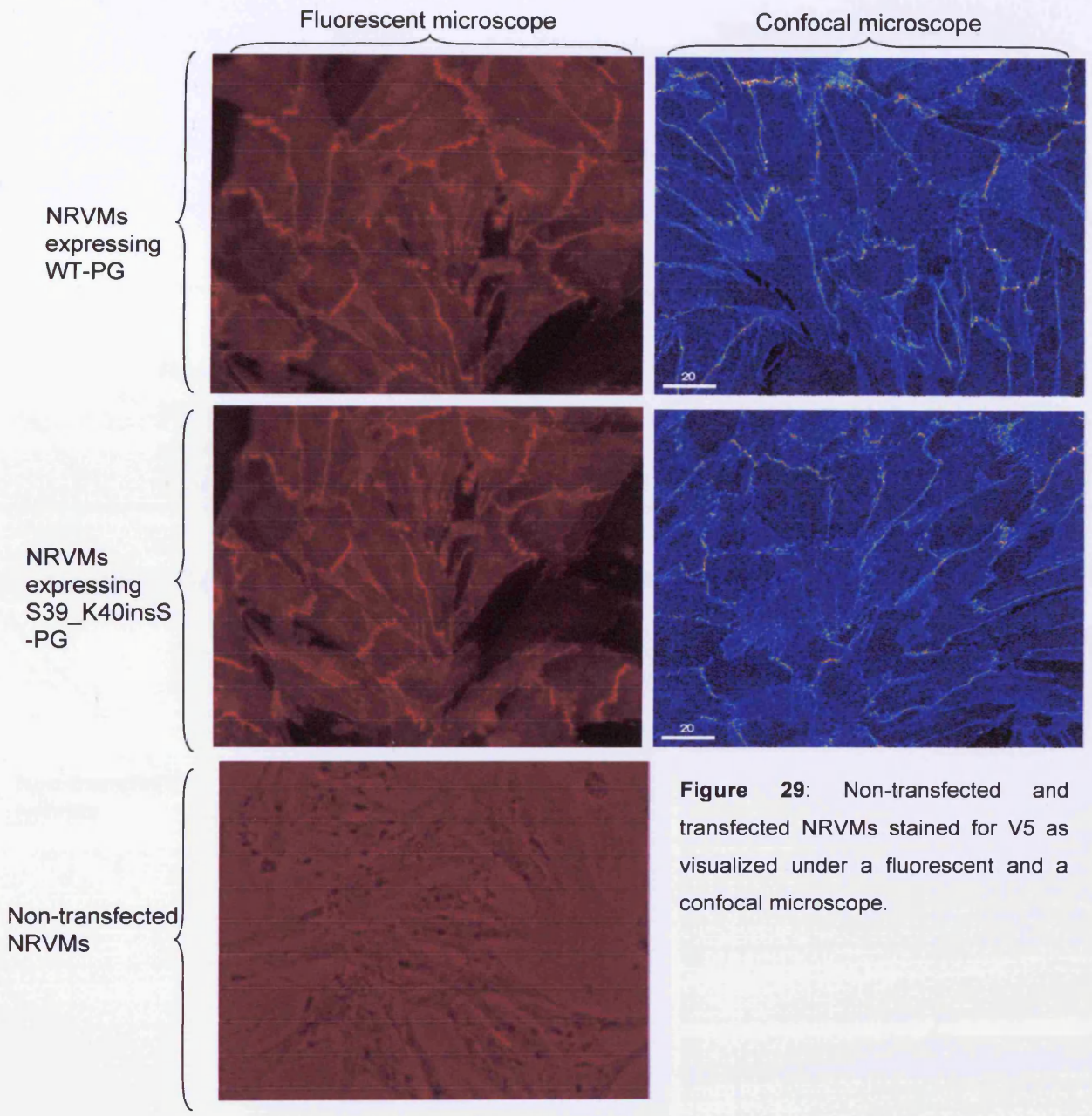

Figure 29: Non-transfected and transfected NRVMs stained for V5 as visualized under a fluorescent and a confocal microscope.

Transfection efficiency was also tested by Western immunoblotting. NRVMs transfected with either viral construct express significantly higher amounts of total plakoglobin protein compared to non-transfected controls (Figure 30). Subsequently, the effects of the adenoviruses on the distribution of N-cadherin were examined by immunostaining. Transfected myocytes show comparable levels of expression of the major adherens junctions' protein with non-transfected controls, indicating that the plasmids do not have non-specific deleterious effects (Figure 31).

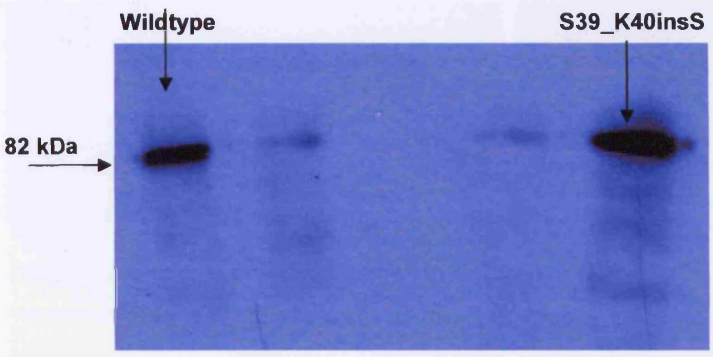

Figure 30: Western immunoblotting against plakoglobin in NRVMs transfected with a wildtype plakoglobin-pAd/CMV plasmid and an S39_K40insS plakoglobin-pAd/CMV plasmid. The middle lanes were loaded with lysate from non-transfected myocytes and used for control purposes. Protein standards are not shown.

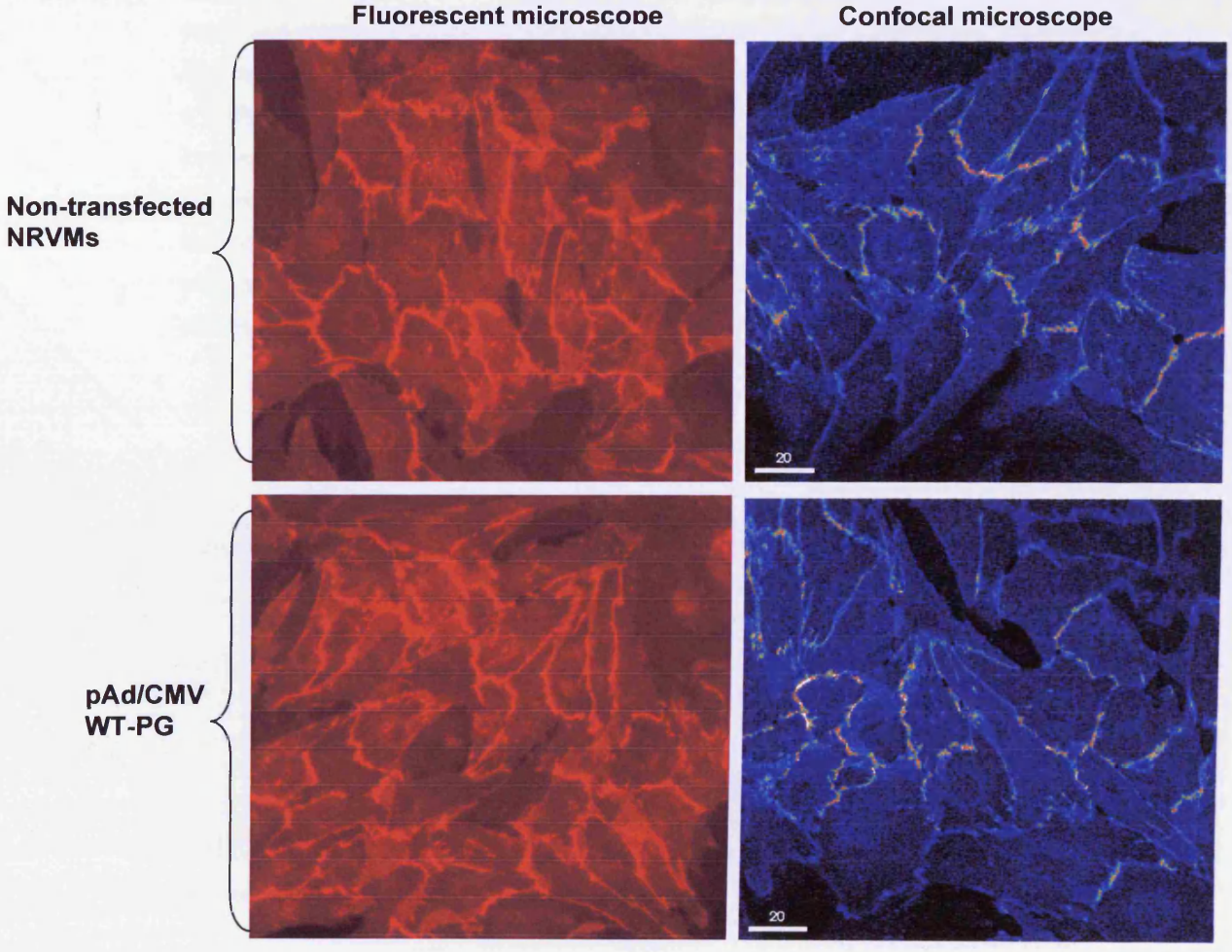

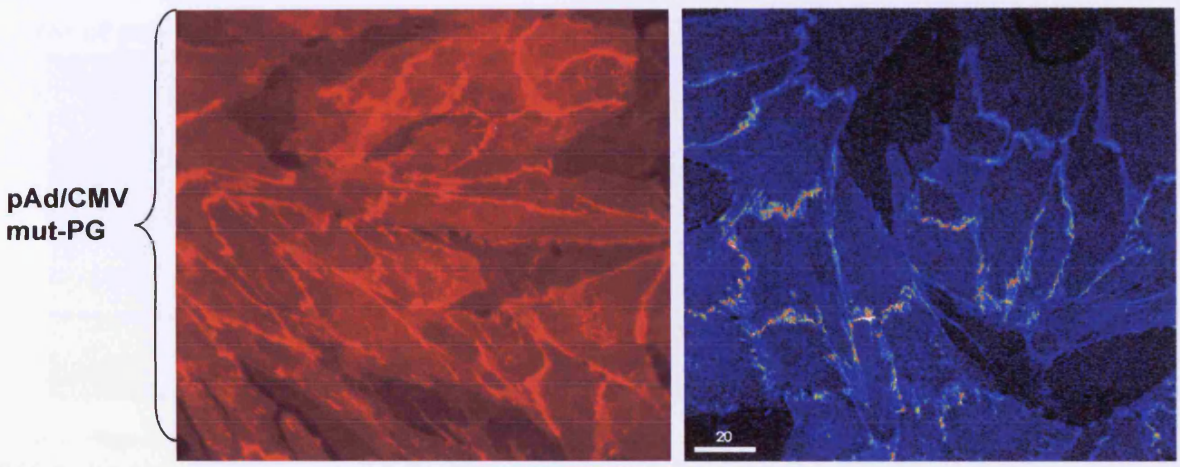

Figure 31: Non-transfected NRVMs and NRVMs transfected with pAd/CMV WT-PG plasmid or the pAd/CMV S39_K40insS-PG plasmid stained against N-cadherin.

To examine the effects of S39_K40insS on the responses of cardiac myocytes to increased mechanical load, NRVMs were seeded on silicone membranes, incubated for 18 hours, transfected with the mutant plakoglobin-expressing adenovirus, incubated for a further 72 hours and subsequently subjected to 1 hour of pulsatile stretch in serum-free medium (frequency 3Hz). Non-transfected myocytes, myocytes transfected with the wildtype plakoglobin-expressing adenovirus and non-stretched cultures were used for control purposes. Following exposure to mechanical stress, the cultures were fixed with ice-cold methanol, immunostained and examined by quantitative confocal microscopy (Figures 32-35).

N-cadherin

Resting conditions

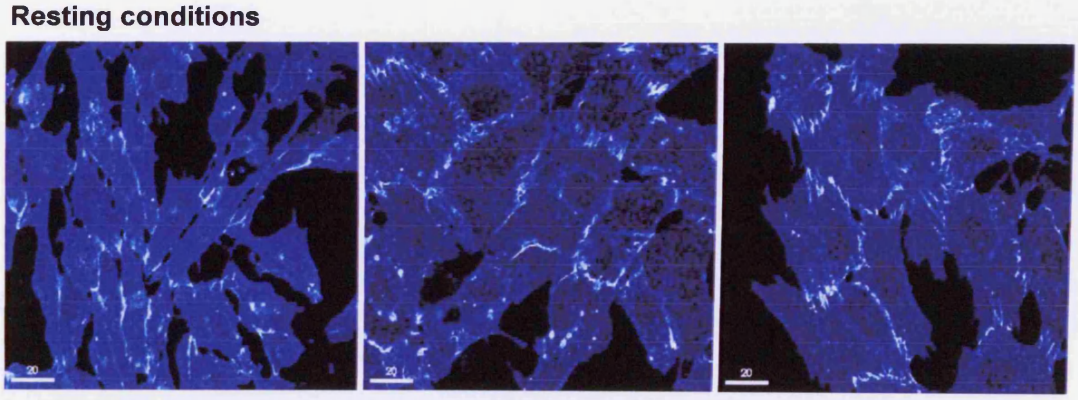

Non-transfected controls **Wildtype virus** **S39_K40insS virus**

1hr of pulsatile stretch

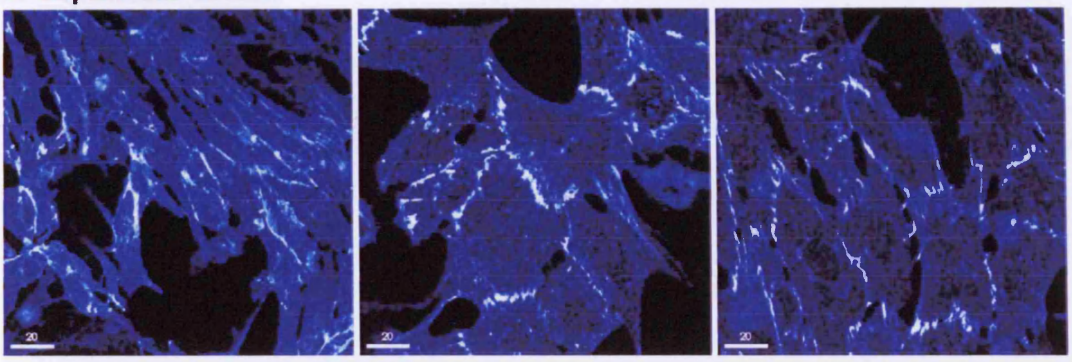

Non-transfected controls **Wildtype virus** **S39_K40insS virus**

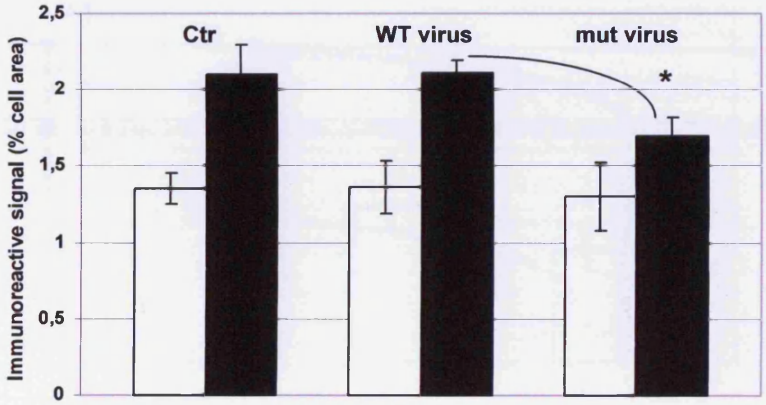

Figure 32: Representative confocal immunofluorescence images and quantitative confocal microscopy data showing the effects of stretch on expression of N-cadherin in NRVMs cells. The error bars represent standard deviations. n=5 for each group, * $p<0.05$ compared with WT virus-transfected NRVMs subjected to stretch.

Cx43

Resting conditions

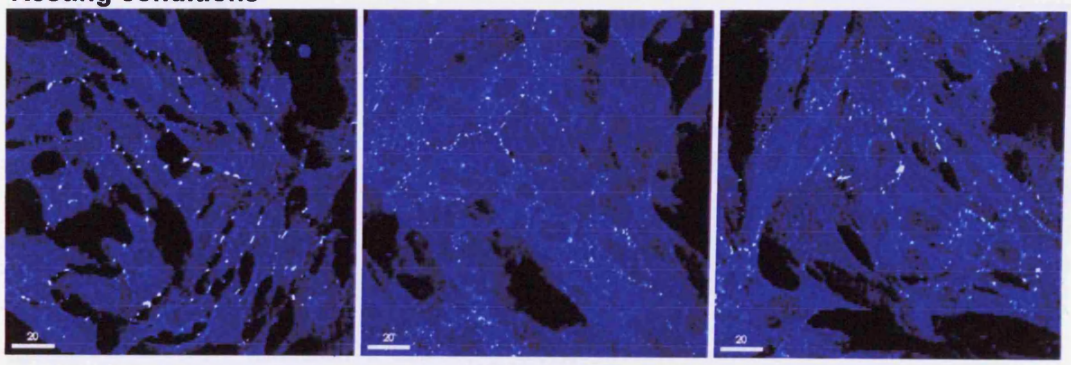

Non-transfected controls **Wildtype virus** **S39_K40insS virus**

1hr of pulsatile stretch

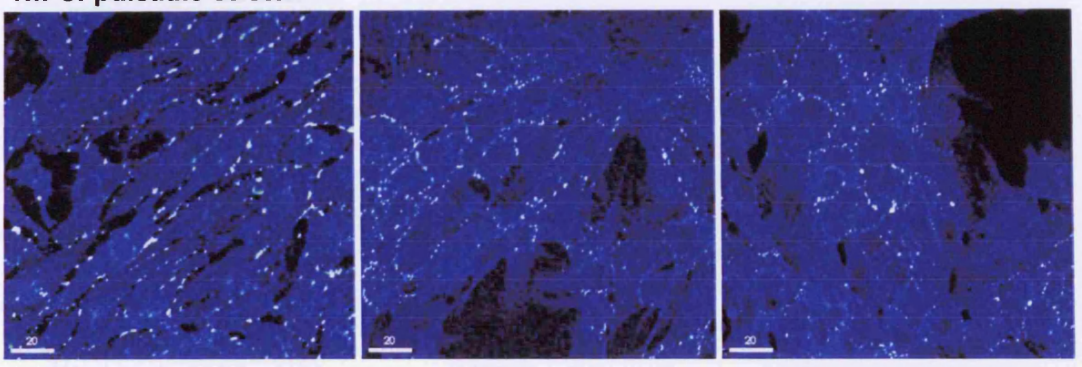

Non-transfected controls **Wildtype virus** **S39_K40insS virus**

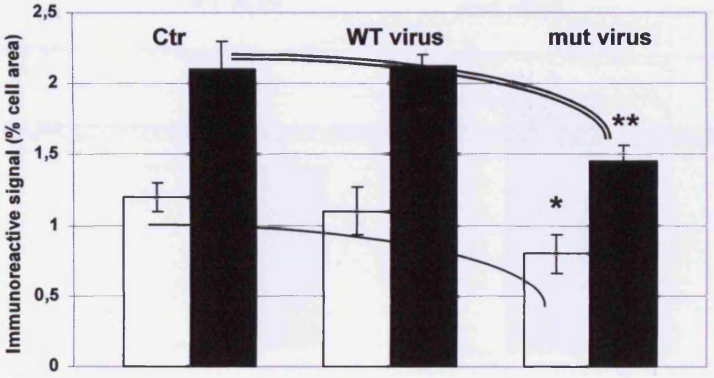

Figure 33: Representative confocal immunofluorescence images and quantitative confocal microscopy data showing the effects of stretch on expression of Cx43 in NRVMs cells. The error bars represent standard deviations. n=5 for each group, * $p<0.05$ compared with non-transfected control baseline levels. ** $p<0.05$ compared with WT virus-transfected NRVMs subjected to stretch.

V5 epitope

Resting conditions

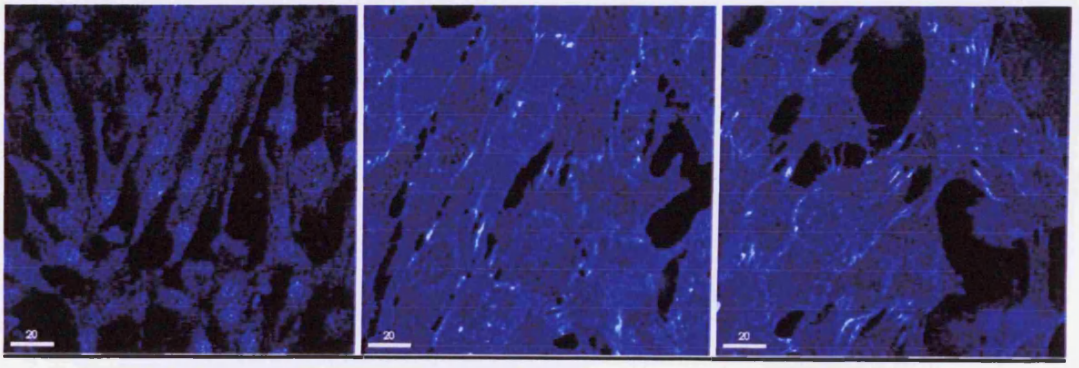

Non-transfected controls **Wildtype virus** **S39_K40insS virus**

1hr of pulsatile stretch

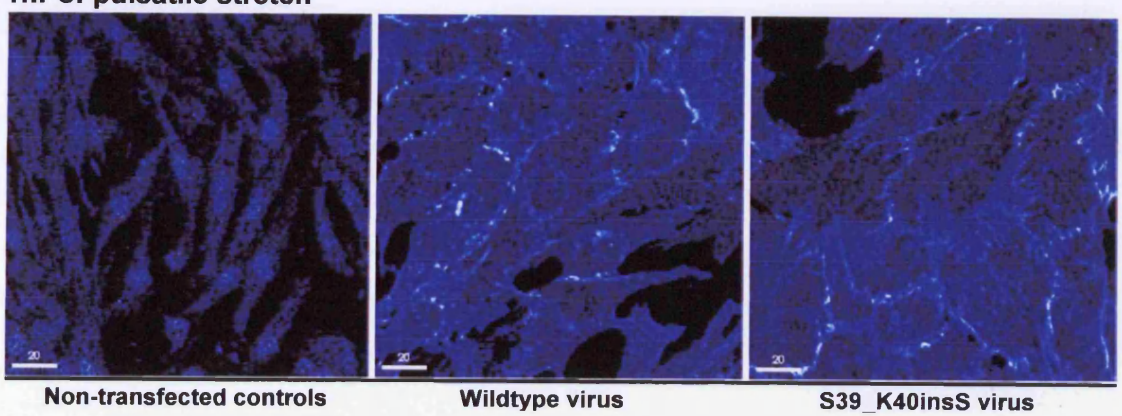

Non-transfected controls | Wildtype virus | S39_K40insS virus

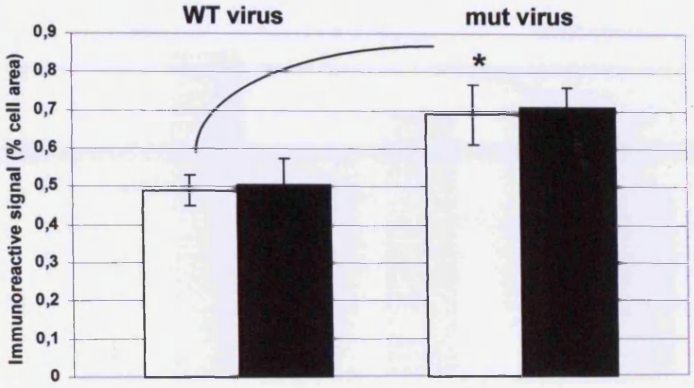

Figure 34: Representative confocal immunofluorescence images and quantitative confocal microscopy data showing the effects of stretch on expression of the V5 epitope in virally transfected NRVMs cells. The error bars represent standard deviations. n=5 for each group, * $p<0.05$ compared with wildtype transfectants.

Total plakoglobin

Resting conditions

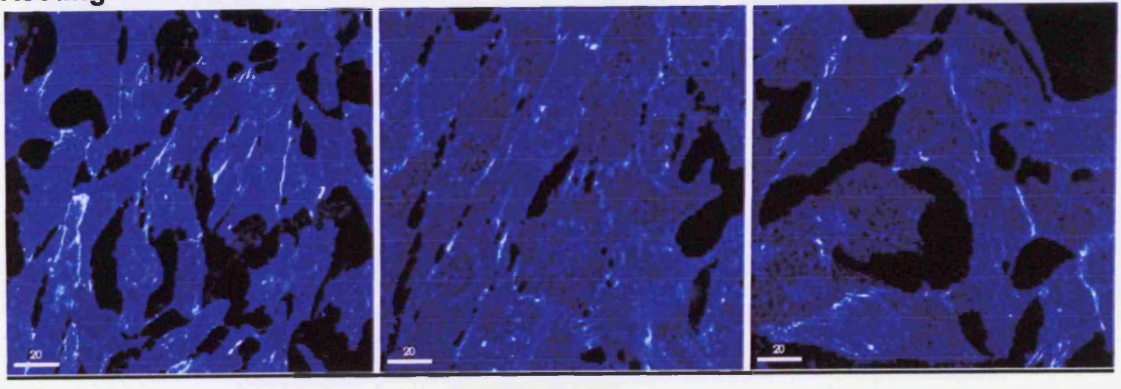

Non-transfected controls | Wildtype virus | S39_K40insS virus

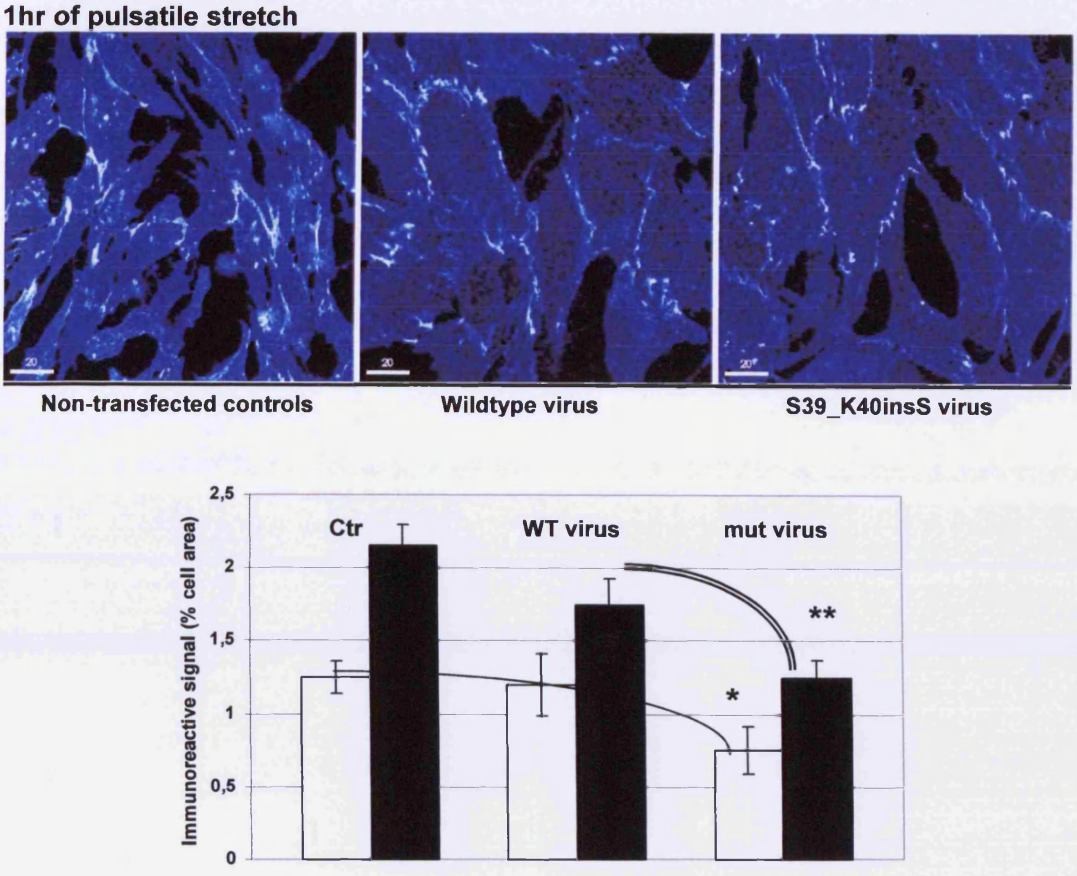

Figure 35: Representative confocal immunofluorescence images and quantitative confocal microscopy data showing the effects of stretch on expression of total plakoglobin in NRVMs cells. The error bars represent standard deviations. n=5 for each group, * $p<0.05$ compared with non-transfected control baseline levels. ** $p<0.05$ compared with WT virus-transfected NRVMs subjected to stretch.

The resting levels of N-cadherin are not affected by the presence of either viral construct. However, in marked contrast to the wildtype exogenous plakoglobin, the S39_K40insS-bearing exogenous plakoglobin significantly inhibits the stretch-induced up-regulation of the adherens junctions' protein (Figure 32). Furthermore, the resting levels of Cx43 and its stretch-induced up-regulation are not affected by the wildtype exogenous protein. However, both the resting levels of the gap junction protein and its up-regulation in response to 1hr of pulsatile stretch are significantly reduced in the presence of S39_K40insS (Figure 33). As expected, the distribution of the V5 epitope at the cell membrane, corresponding to the exogenous protein expressed, is not affected by stretch. However, a higher amount of the exogenous protein seems to be incorporated at the cell junctions in myocytes transfected with the mutant virus

compared to those transfected with the wildtype virus (Figure 34). The amount of total plakoglobin protein localizing at intercalated discs is comparable between non-transfected controls and myocytes transfected with the wildtype virus. On the contrary, total plakoglobin at intercalated discs is significantly reduced in myocytes transfected with the S39_K40insS virus. Finally, stretch-induced up-regulation of total plakoglobin seems to be reduced in myocytes transfected with the wildtype viral construct compared to non-transfected controls but the difference is not statistically significant. On the other hand, plakoglobin up-regulation in response to stretch is markedly inhibited in the presence of the ARVC-causing mutation (Figure 35).

4) <u>Generating a "Naxos" virus:</u>

To compare the effects of S39_K40insS on cardiac myocytes with those of 2057del2, a recombinant adenoviral construct bearing the Naxos disease-causing mutation was generated. The pDONR221-plakoglobin plasmid was first subjected to site-directed mutagenesis and the mutant plakoglobin sequence was subsequently cloned into the pAd/CMV/V5-pDEST vector via an LR clonase-dependent recombination reaction (Figures 36 & 37).

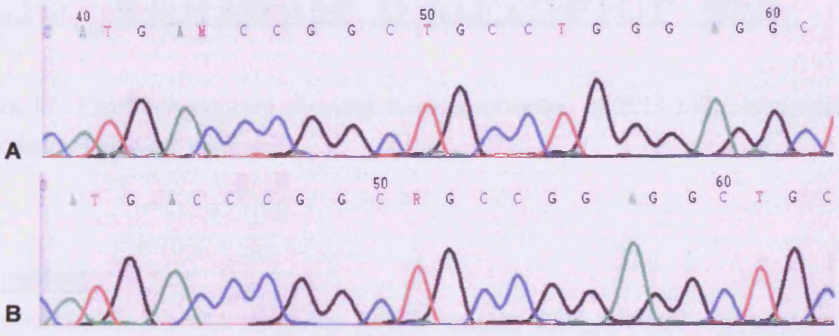

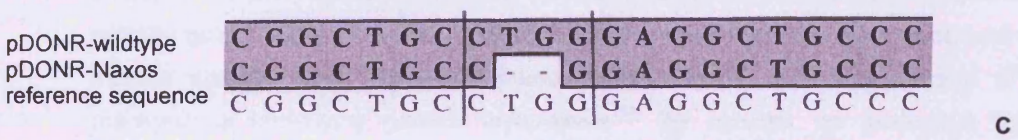

Figure 36: Electropherograms showing the wildtype (A) and 2057del2-plakoglobin (B) sequences cloned into the pDONR221 vector. When the sequences are aligned the 2-nucleotide deletion is clearly evident (C).

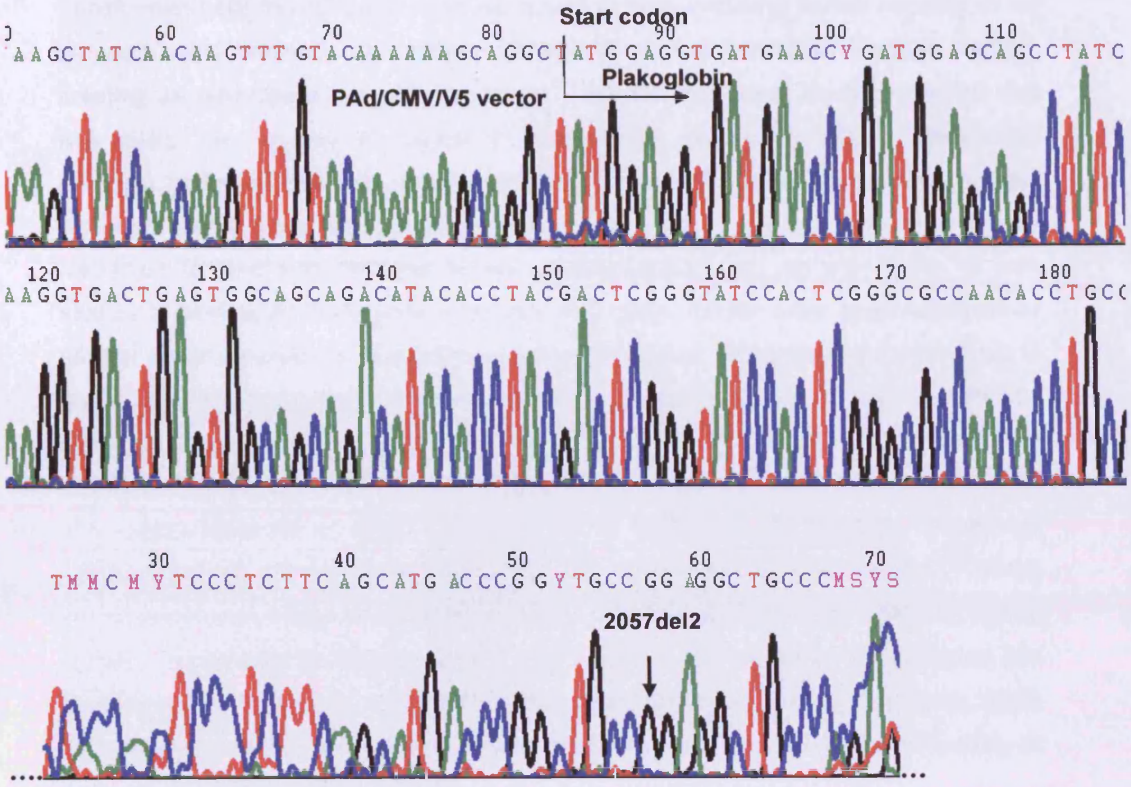

Figure 37: Electropherogram showing the incorporation of 2057del2 plakoglobin in the pAd/CMV/V5-pDEST vector.

Discussion:

To characterize the effects of the ARVC-causing S39_K40insS mutation in cardiac myocytes, a recombinant adenoviral construct expressing the mutant plakoglobin sequence was generated. Cardiomyocytes exit the cell cycle and terminally differentiate in vivo in the peri-natal period. Unlike skeletal muscle, the myocardium does not have satellite cells capable of proliferating. Studies of skeletal myoblast cultures derived from muscle satellite cells have contributed significantly to our understanding of the mechanisms underlying genetic myopathies.[355] By contrast, no analogous human ventricular cardiomyocyte cell line is available for similar studies, since cultures of cardiac tissue have a finite lifespan in vitro.[356] Attempts to establish immortalized cardiomyocyte cell lines that can proliferate in culture include AT-1 cells, established from a mouse atrial tumor,[357] MC29, a quail cell line from a rhabdomyosarcoma tumor,[358] cell lines established from transgenic mice that express the SV40 T-ag[359] and by transformation of fetal cardiomyocytes with the SV40 oncogene.[360] These

transformed cells though suffer from numerous deficits including limited capacity to be passaged and tendency to undergo morphological and functional changes thereby creating an heterogeneous cell population.[356] As no permanent cardiac myocyte cell line exists, the majority of cardiac myocyte gene expression studies have used transient gene transfer into primary cultures of fetal and neonatal cardiomyocytes. Although useful, this methodology has several limitations, including low efficiency and restriction to fetal and neonatal stages of development. As an alternative, in vivo studies of cardiac myocyte gene regulation and gene transfer have been successfully carried out in transgenic mice. However, the generation of transgenic mouse lines is costly and time-consuming. Another approach to cardiac gene transfer in vivo has relied on injecting plasmid DNA into the myocardium and measuring reporter gene expression in the cells which have successfully taken up sufficient quantities of DNA. The major drawback of direct DNA injection is its relative insufficiency, since only 0.02% of the myocytes in the adult rat heart take up and express injected DNA.[361] Many of the above-mentioned disadvantages though can be solved through adenoviral gene delivery. Adenoviral expression vectors have been in use for over two decades and more recently, thoroughly exploited for the purpose of gene therapy. Features which make these vectors attractive include very efficient uptake into cells, and their ability to carry up to 7.5kb of foreign DNA.[361]

S39_K40insS plakoglobin was cloned into the pAd/CMV/V5-pDEST vector. Benefits of the chosen vector include the presence of the CMV promoter, which ensures high-level constitutive expression of the gene of interest and the presence of the V5 epitope sequence, which allows detection of the recombinant protein using anti-V5 antibodies. Transfection efficiency was determined both by immunostaining and Western immunoblotting. When neonatal rat ventricular cardiomyocytes were transfected with a concentration of 10 viral particles per cell, >90% of the cultured cells took up and expressed the recombinant protein. Transfected NRVMs were subsequently subjected to linear pulsatile stretch. Myocytes transfected with an adenoviral recombinant wildtype plakoglobin construct, non-transfected and non-stretched myocytes were used for control purposes. It is well-established that under conditions of stretch, cells seem to be maturing and developing faster. Furthermore, when cells are subjected to chronic stretch they even tend to orient in the direction of the applied vector.[362] Consequently, efforts to re-constitute conditions of heart failure through application of increased, continuous mechanical load with the custom-designed system described in the methodology section of this chapter, have been unsuccessful. Still, though mechanical load does seem to "improve" myocytes in vitro, it also tends to induce morphological and functional changes, one of which is hypertrophy.[363] Indeed, early studies with animal models using the technique of aortic banding have shown that mechanical

stress and neurohumoral activation are the two major stimuli for cardiac hypetrophy.[364] Such alterations in cell physiology would render our system disadvantageous for studying the effects of desmosomal gene mutations. However, previous studies have shown that 1 hour of pulsatile stretch does not alter the morphology and physiology of cultured myocytes, while it does induce dramatic responses at the desmosomal sites.[334] In non-transfected control myocytes, N-cadherin, plakoglobin and Cx43 were all significantly up-regulated in response to 1 hour of pulsatile stretch as quantified by confocal microscopy. These observations are in agreement with those described by *Yamada et al.* in 2000.[353] Moreover, transfection of myocytes with the wildtype recombinant plakoglobin does not affect the stretch-induced cellular responses. In marked contrast though, stretch-induced up-regulation of all three proteins is significantly inhibited in the presence of the S39_K40insS mutation. Furthermore, in cells bearing the ARVC-causing mutation, even the baseline levels of expression of Cx43 and plakoglobin at junctional sites is significantly reduced. Down-regulation of plakoglobin and Cx43 expression at intercalated discs was also observed in myocardial tissue obtained from the patient carrying S39_K40insS (Chapter 2), and in HEK293 cells induced to stably express the mutant protein (Chapter 4.1). Interestingly, although myocytes were transfected with the same concentration of the wildtype and mutant adenoviral constructs, the S39_K40insS recombinant protein was expressed at higher levels at cell-cell junctions than the wildtype construct, as shown by immunostaining using an anti-V5 antibody. This observation may indicate that S39_K40insS plakoglobin acts in a dominant negative manner displacing and replacing the endogenous wildtype protein that is naturally expressed by the cardiac myocytes. Collectively, the results obtained from NRVMs are consistent with those obtained from HEK293 cells rendering the human embryonic kidney-derived cell model advantageous for similar studies.

Finally, in order to compare S39_K40insS with 2057del2, a recombinant adenoviral construct bearing the Naxos disease-causing plakoglobin molecule was generated. Experiments to determine the transfection efficiency of the "Naxos" virus and to investigate the effects of 2057del2 on cardiomyocyte responses to mechanical load are currently underway. Future plans also include the generation of recombinant adenoviral constructs expressing the *firefly luciferase* and *Renilla* reporter proteins. Transfection of NRVMs with these reporter genes would allow us to study the effects of ARVC-causing mutations on signaling pathways under conditions closely mimicking their "naturally-acting environment", the heart.

SUMMARY & CONCLUSIONS:

Arrhythmogenic right ventricular cardiomyopathy (ARVC) is an inherited heart muscle disease that may result in arrhythmia, heart failure and sudden cardiac death. The main pathological feature is the progressive loss of myocardial cells, which become replaced by adipose and fibrous tissue. Characteristic clinical abnormalities include delayed depolarization, epsilon waves and inverted T-waves in the right precordial leads on a baseline ECG, late potentials on a SA-ECG and ventricular dilatation, systolic impairment and wall motion abnormalities on imaging. Arrhythmia is predominantly of right ventricular origin and ranges from frequent premature ventricular contractions to ventricular tachycardia and fibrillation. The natural history of the disease is sub-divided into four phases based on clinical and pathological correlations. Early ARVC is often described as "concealed" owing to the frequent absence of clinical findings, although minor arrhythmia and subtle structural changes may still be present. Patients are mostly asymptomatic but may nonetheless be at risk of sudden cardiac death particularly during or immediately after intense physical activity. The "overt electrical disorder" that subsequently develops is characterized by symptomatic arrhythmia, while morphological changes are usually detectable by imaging. In the third stage, extension of the disease through the right ventricle causes impaired contractility and isolated right ventricular failure. Left ventricular involvement with consequent biventricular heart failure occurs in the end-stage, which may be difficult to distinguish from DCM. It must be emphasized though that this clinical picture is representative of severe forms of typical ARVC only. Recent studies suggest a far broader spectrum of disease expression.

The prevalence of familial ARVC is usually cited as 30-50% although this is likely to be a conservative estimate for a number of reasons. Since the disease may be clinically silent, elucidation of family history alone, without clinical assessment of relatives may be insufficient. Another major factor is the reduced penetrance that often accompanies autosomal mode of inheritance. In some kindreds, penetrance may be as low as 20%. Therefore, evaluation of small families at clinical practice may create the false impression of sporadic disease. In the past, the predilection for the right ventricle had been considered the principal distinguishing factor of ARVC from overlapping clinical syndromes such as DCM. Recent years however have seen pathological descriptions of fibrofatty replacement exclusive to the left ventricle of sudden cardiac death victims. The existence of this entity, best described as arrhythmogenic left ventricular cardiomyopathy (ALVC), was subsequently confirmed in the clinical setting. Family members of patients with ALVC may have the classic right ventricular variant, highlighting the genetic affiliation of the two entities. Predominant right ventricular involvement is therefore not a necessary attribute; nor is the presence of myocardial fat pathognomonic of ARVC. Significant fatty infiltration has been documented in >50% of

hearts in normal elderly subjects. The most important finding in the diagnostic management of the disease to date is that there is no single diagnostic test. Diagnosis remains a puzzle including data from different imaging techniques, electrocardiographic examination tests and family history. The conflicts that still remain in the diagnostic arena constitute the predominant reason for the underestimation of the disease prevalence. Originally, the prevalence was estimated to be 1 in 5000 inhabitants. Meanwhile, data showed that the disease affected in fact 1 in 1000 inhabitants. After the original publication of diagnostic criteria in 1994, there was an agreement among international experts in the field of ARVC that a re-evaluation of diagnostic methods and a correction/modification of criteria were necessary. The introduction of these revised criteria represented a major step towards better characterization of individuals at risk. A tremendous step however was also made by molecular genetics.

Although ARVC is most commonly inherited in an autosomal dominant fashion, the molecular studies that led to the identification of the first disease-causing gene were preformed on a recessive variant known as Naxos disease. One of the major syndromic forms of ARVC, Naxos disease is characterized by non-epidermolytic palmoplantar keratoderma and wooly hair. The cutaneous manifestations, coupled with nearly 100% penetrance in cardiac disease, facilitated the recognition of affected individuals in this population. In 2000, a 2-base pair deletion in the plakoglobin gene (2057del2) was identified as the cause of Naxos disease. Plakoglobin, a major constituent of cell adhesion junctions, and its isolation in Naxos disease paved the way for the search of related genes. Within months of the identification of 2057del2, a deletion in the desmoplakin gene was identified as the causative mutation in another syndromic form of ARVC, known as Carvajal syndrome. Since then, a variety of mutations in desmoplakin and in a further cell adhesion molecule; plakophilin2 have been identified in a number of ARVC probands. It therefore became obvious that unraveling the pathogenesis of ARVC was dependent on understanding the function and interplay of cell adhesion junctions. ARVC was emerging as a disease of the desmosome.

Skeletal muscle consists of long multi-nucleated myofibrils that originate from fusion of mono-nucleated myoblasts. Cardiac myocytes in contrast do not form a syncytium. Instead they rely on specialized structures known as intercalated discs for both mechanical and electrical coupling. Intercalated discs contain three distinct types of connections: gap junctions, adherens junctions and desmosomes. Gap junctions mediate ion transfer between cells. Each channel is composite of two hemi-channels known as connexons, while each connexon is in turn formed by 6 connexin sub-units. Connexin43 is the major gap junction protein expressed in the heart, while connexin40 and connexin45 are also expressed but in lower levels. The transmembrane component of an adherens junction, which provides inter-cellular connection in the

heart, is N-cadherin. Attached to the cytoplasmic tail of N-cadherin are plakoglobin and beta-catenin, both of which bind α-catenin, which in turn interacts with actin microfilaments. Desmosomes share with adherens junctions the responsibility for providing mechanical attachment between cells. In contrast to adherens junctions though, desmosomes are associated with the intermediate filament network. In a desmosome, the intracellular portions of desmosomal cadherins, namely desmogleins and desmocollins, interact with members of the armadillo family, namely plakoglobin and plakophilins. These in turn bind desmoplakin, whose C-terminus anchors the intermediate filaments to the cell surface. It should be noted that both plakoglobin and beta-catenin have additional non-adhesive functions as regulators of transcription. A new model for the pathogenesis of ARVC was arising; impaired desmosome functioning under conditions of mechanical stress is thought to cause myocyte detachment and death. Since regeneration of cardiac myocytes is limited, repair by fibrofatty replacement occurs. However, is loss of mechanical integrity, injury and repair, the whole story? The initial purpose of this project was to identify novel mutations in known disease-causing genes as well as further candidate genes. More importantly though, a journey subsequently began to understand the complex mechanisms of ARVC pathogenesis, moved a step ahead of the "loss of mechanical integrity" hypothesis in an attempt to unravel the "rest of the story"...

Mutation analysis was performed on a large cohort of patients of English, German, Greek and Cypriot origin. A large number of novel mutations were identified in desmoplakin and plakophilin2, rendering these molecules as the two major players in the ARVC arena known to date. A single plakoglobin mutation was identified in an ARVC family of German origin (S39_K40insS). Both desmoglein2 and desmocollin2 were shown to have a causative role in the disease accounting for ~20% of positively genotyped cases. Though not disease-causing *per se*, sequence changes in the gene coding for desmin were shown to have a role in ARVC pathogenesis, possibly acting synergistically with pathogenetic mutations to modify phenotypic expression. Wherever possible, relatives were examined, pedigrees were constructed and the pattern of inheritance was established. Consistent with previous reports, the vast majority of the novel mutations identified were inherited in an autosomal dominant manner. The degree of penetrance though was highly variable and in certain cases very low, particularly in kindreds bearing plakophilin2 mutations. Collectively, ~40% of all probands screened were positively genotyped. Logically though, one may wonder: what of the rest?

Subsequently, a number of heart autopsy/biopsy samples from individuals diagnosed with ARVC were subjected to histological examination. The results obtained added further evidence to the existing argument that ARVC is not merely a matter of fat. In the

majority of the cases examined, myocardial cells were gradually being replaced by fibrous tissue first in the right and then in the left ventricle, which turned into fat as the disease progressed. A small number of skin samples were also subjected to histological and ultrastructural examination. Interestingly, only one individual, identified as a compound heterozygous for two nonsense desmoplakin mutations, showed profound cutaneous abnormalities, consistent with loss of epidermal integrity, while all heterozygous mutation carriers examined showed no evidence of ultrastructural skin defects. A number of heart and skin samples from ARVC patients were subsequently stained for selected mechanical and electrical coupling proteins and examined by quantitative confocal microscopy. The results obtained indicated that disruption of one desmosomal protein leads to down-regulation of expression of its interacting protein partners at intercalated discs. The spectrum of proteins affected depended on the mutated gene in each case. However, irrespective of the mutated gene, plakoglobin distribution at junctional sites was universally disrupted, suggesting a final common pathogenetic pathway. Furthermore, in all samples examined, Cx43 at intercalated discs was significantly re-distributed, consistent with gap junction remodeling. These observations suggest another pathway that could be acting synergistically with the anatomic defects characterizing ARVC to promote arrhythmogenesis. Interestingly, junctional protein re-distribution was also evident in the skin samples examined, irrespective of whether or not the affected individual manifested any cutaneous abnormalities. Finally, expression of β-catenin at the cell surface was significantly increased, possibly compensating for the reduced levels of plakoglobin. One may wonder again: what are the implications of these findings in diagnosing and managing ARVC?

The functional effects of a single ARVC-causing mutation were subsequently examined. To our knowledge, S39_K40insS is the only autosomal dominant ARVC-causing mutation in plakoglobin to be reported to date. Yeast-two-hybrid analysis was used to investigate the effects of the novel mutation on the protein interactions established by plakoglobin. Two novel interacting partners for the mutant armadillo protein were hence recognized: histidine-rich calcium binding protein and TGFβ induced apoptosis protein2, raising questions about the role of S39_K40insS and of plakoglobin itself in calcium release and programmed cell death regulation. A human embryonic kidney 293 cell line induced to stably express S39_K40insS plakoglobin was generated and used to study the effects of the mutation on desmosomal structure, cell proliferation, cell death and subcellular localization. Cells expressing the mutant plakoglobin variant showed higher proliferation and lower caspase activity than wildtype cells highlighting the effects that ARVC-causing mutations may have on signaling pathways. Moreover, differences in the electrophoretic mobility of the mutant protein as

well as in its sub-cellular localization introduced the hypothesis that S39_K40insS may be acting through altering the turnover kinetics of plakoglobin, increasing its degradation by the ubiquitin-proteasomal system. Increased degradation could result in reduced amounts of the armadillo protein being available for incorporation into inter-cellular junctions. This hypothesis was also supported by the observation that cells bearing S39_K40insS formed fewer and smaller desmosomes than wildtype cells. The same *in vitro* model was used to study the effects of S39_K40insS on cellular responses to defined mechanical load and cellular biomechanics and compare them to those of 2057del2. The two ARVC-causing plakoglobin mutations have dramatic but similar effects on wound-healing and cell migration rates compared to wildtype cells. In contrast, S39_K40insS and 2057del2 have disparate effects on intercalated disc protein expression in response to stretch, cell-cell adhesion and cell stiffness. Finally, a recombinant adenoviral construct bearing S39_K40insS plakoglobin was generated and used to study the effects of the mutation on neonatal rat ventricular myocytes. Consistent with the results obtained from HEK293 cells, both mobilization/targeting of existing molecules to the membrane and gene expression in response to stretch were significantly disrupted in the presence of S39_K40insS. Collectively, the third part of this project presented the vast spectrum of effects that a mutation may have, rendering ARVC as "much more than a disease of compromised cell-cell adhesion". The mere involvement of plakoglobin in ARVC, a molecule holding both structural and signaling positions, suggests that we are in fact battling in more than one fields. Still, one may wonder; where do we go from here?

Approximately 40% of the ARVC probands subjected to mutation screening were positively genotyped. So, what of the rest? Plectin, like desmoplakin, is a member of the plakin family of proteins also present in desmosomes. While its absence does not alter the structure of desmosomes, plectin appears to contribute significantly to the mechanical stengthening of cells.[365] Mutations in the plectin gene result in skin fragility, demonstrating blister formation at the level of hemidesmosomes. These blistering disorders belong to the spectrum of epidermolysis bullosa (EB) phenotypes. Three distinct variants of this condition have been identified. EB with muscular dystophy is an autosomal recessive condition frequently caused by premature termination codon-causing mutations leading to the absence of plectin both in skin and muscle. Secondly, heterozygous missense mutations in the plectin gene have been documented in patients with EB simplex of the Ogna type, a rare autosomal dominant disorder. Finally, recent studies have disclosed plectin mutations in patients with EB with pyloric atresia, an autosomal recessive condition frequently with lethal consequences.[366] Though not associated with ARVC yet, plectin's role in maintaining mechanical integrity renders it a plausible candidate gene. Recent mutation analysis performed by our group has

identified plectin missense mutations in a small number of ARVC probands. Though not present in a large number of ethnically-matched control individuals also tested, *in vitro* studies are required prior to drawing conclusions as to their potential role in ARVC pathogenesis (*unpublished data*).

And what if we looked beyond the desmosomal model? An obvious extra-desmosomal candidate gene is GJA1, the gene coding for connexin43. Mutations in Cx43 have not been identified in conjuction with cardiac disease, but have the obvious potential to be arrhytmogenetic. The capacity of Cx43 defects to produce structural abnormalities is evidenced by its association with oculo-dento-digital dysplasia; an autosomal dominant syndrome presented with craniofacial and limb dysmorphisms, spastic paraplegia and neurodegeneration. Ventricular tachyarrythmia and sudden deaths have been recorded in some families affected by the disorder.[367]

Sarcoendoplasmic reticulum Ca^{+2}-ATPase (SERCA) is expressed at its highest levels in the cardiac muscle, where it controls calcium levels in the sarcoplasmic reticulum and therefore regulates the excitation-contraction coupling. SERCA2 knockout mice do not survive birth. On the contrary, heterozygous knockout animals are viable, fertile and do not show any sign of disease. When subjected to increased mechanical load though, these animals show largely impaired cardiac function, heart dilatation, evidence of hypertrophy and fibrosis and high incidence of sudden cardiac death.[368,369] Could SERCA2 therefore constitute another candidate ARVC-causing gene?

Infants with Neterton syndrome typically present with a generalized exfoliative erythroderma.[370] Histologically, they show acantholysis with super-imposed parakeratosis. Their stratum corneum is usually thin, often detached from the underlying epidermis and sometimes even absent. Mutations in SPINK5 have previously been associated with the syndrome. SPINK5 codes for a serine protease inhibitor (LEKT1) localized in the most differentiated layers of stratified epithelial tissues. Defects in LEKT1 allow for hyper-activity of the stratum corneum tryptic enzyme SCTE, which leads to increased desmosomal cleavage. Immunohistochemical analysis on skin from SPINK5 -/- mice showed significant reduction in expression levels of desmoglein1 and desmoplakin stemming from abnormal protein degradation.[370] Could mutations in the cardiac isoform of SPINK5 account for the desmosomal defects observed in the setting of ARVC? Finally, a large set of proteins are currently recognized that link the intermediate filaments to other cytoskeletal components in many tissue types.[371] Given their key position and their well-recognized role in maintaining tissue integrity, this class of proteins could also be underlying "loss of integrity" conditions, such as ARVC.

Phenocopies of ARVC may provide additional insight into its genetic heterogeneity. Surprisingly, very convincing phenocopies of ARVC may reside amongst the muscular

dystrophies. Skeletal muscle degeneration with fibrous and adipose replacement is characteristic of this group of disorders. Similar histological changes may be observed in the heart, while myocardial disease may even occur in the absence of significant skeletal myopathy. *Melacini et al.* found evidence of cardiomyopathy in 68% of patients with sub-clinical Becker's muscular dystrophy, undergoing routine cardiac evaluation.[372] ECG features included T-wave inversion in the right precordial leads, while right ventricular dilatation was a common finding on echocardiography. Serial evaluation of a single patient suggested preferential involvement of the right ventricle in early disease, followed by progression to a DCM-like phenotype.[372] The dystrophin-glycoprotein complex provides a mechanical connection between the cytoskeleton and the extra-cellular matrix.[373] Mutations in dystrophin may initially compromise cellular adherence to the matrix and thereby predispose to sarcolemmal damage by shear stress. As with desmosomal abnormalities, this process is more likely to primarily affect the thin-walled right ventricle. Subsequent involvement of the cytoskeleton could lead to left ventricular impairment. Defects of the dystrophin-glycoprotein complex should therefore be considered in families with right ventricular cardiomyopathy progressing to a DCM-like phenotype.

The histopathological appearances of the heart in X-linked Emery-Dreifuss muscular dystrophy (EDMD) mirror those of ARVC.[374] There is myocardial atrophy with fibrofatty replacement, with preponderance for the right heart.[375] The disease-causing gene codes for emerin,[376] a protein that localizes to the inner nuclear membrane, desmosomes and adherens juctions.[377] Novel mutations in emerin and related proteins could conceivably result in an ARVC phenotype. Perhaps the closest phenocopy of ARVC is the cardiac disease of myotonic dystrophy, which shares the propensity toward tachyarrhythmia in the absence of overt ventricular dysfunction. The disease is caused by expansion of an unstable CTG trinucleotide repeat in the 3' untranslated region of the DMPK gene. The affected protein, myotonic dystrophy protein kinase, localizes to the intercalated discs of cardiac muscle. Immunohistochemical analysis has demonstrated close proximity to gap junctions and co-sedimentation with Cx43.[378] Significant clinical overalp, suggests that novel mutations in the DMPK gene may produce an ARVC phenotype.[378] The presence of disease phenocopies though, may make one wonder: is what we are dealing with really ARVC?

In clinical practice, the disease that most frequently mimics ARVC is idiopathic right ventricular outflow tract tachycardia (RVOTT). A benign arrhythmic disorder, with no familial basis, RVOTT may nonetheless be extremely diffucult to distinguish from the concealed phase of ARVC, in which typical ECG and imaging abnormalities are absent.[379] Furthermore, although most patients with Brugada syndrome have structurally normal hearts, it appears that some individuals with the clinical features of

Brugada syndrome may in fact have structural heart disease broadening the area of overlap between "conduction diseases" and ARVC and making their differentation even harder.[380] Clinical diagnosis of ARVC is impeded by the non-specific nature of disease features and marked phenotypic diversity. Molecular genetics analysis will eventually assume a pivotal role in the clinical area by facilitating timely diagnosis, guiding interpretation of borderline investigations and enabling cascade screening of relatives. However, early identification of genetically affected individuals raises complex management issues in its own right while risk stratification remains elusive. A small number of patients may suffer arrhythmic events without warning symptoms or clinical evidence of overt disease. Conversely, a sizable proportion of gene carriers will not develop clinically significant disease owing to reduced penetrance. Furthermore, among relatives with disease expression, the majority are likely to follow a benign course. The ICD confers optimal protection against sudden cardiac death, but the notable complication rate and psychological impact especially in the younger age group argue stongly against indiscriminate device placement in all gene-positive patients. Similarly, the adverse prognostic impact of harboring an ARVC-causing mutation is too small to justify the use of mutation analysis in prenatal diagnosis. At present, there is little evidence to support the notion that certain mutations may portend a less favorable outcome than others.[186] Until definitive genotype-phenotype correlations are developed, the role of genetic analysis in ARVC diagnosis and management is limited and should be used with caution.

And what of sporadic gene-negative ARVC cases? Are all of these familial cases masquerading as sporadic owing to reduced penetrance? Are all of these stemming from *de novo* non-yet-identified mutations? Antibodies to the β1-adrenergic receptor are detected in a substantial number of patients with idiopathic dilated cardiomyopathy. *Jane-wit et al.* recently showed that these specific auto-antibodies elicit DCM by agonistically inducing cardiomyocyte apoptosis.[381] Equivalently, could a subset of ARVC cases be autoimmune? Loss of epidermal cell-cell adhesion, also known as acantholysis, in pemphigus may be caused by binding of auto-antibodies to the extra-cellular domains of desmoglein1 or desmoglein3 at the keratinocyte membrane.[382] Although widely expressed in the skin, these two desmosomal cadherin isoforms are not found in the myocardium. In the heart, the major isoform expressed is desmoglein2. In a similar fashion, could autoantibodies directed against the extracellular portion of desmoglein2 or desmocollin2 account for ARVC? To investigate this possibility, an immunostaining approach is currently being undertaken. Serum is being collected from patients with severe forms of what appears to be non-familial ARVC. All these patients have been screened previously for mutations in all known disease-causing genes and found negative. The serum will subsequently be applied to heart muscle specimens

obtained from control individuals with no history of heart disease. In essense, the serum will act as a "primary antibody". The specimens will then be incubated with appropriate secondary antibodies and examined by fluorescent microscopy. To eliminate the possibility of auto-antibodies developing as a secondary degenerative phenomenon in the setting of ARVC, serum from gene-positive ARVC patients is also being collected and will be used for control purposes.

When myocardial tissue is examined under an electron microscope, only very few desmosome-like structures appear interspersed at the adjoining membranes. Conversely, when tissue is immunostained for so-called "desmosomal molecules", such as desmoplakin or plakophilin2, numerous areas of high signal intensity are observed at the cell membranes under a fluorescent microscope. Under a high resolution scanning electron microscope, the intra-cellular surface of an intercalated disc appears like an extremely erose structure with peaks and valleys. The fact that particles of different sizes are distributed at random at the intercalated disc surface makes their separation into desmosomes and adherens junctions impossible.[383] The term "area composita" was hence given to ID regions occupied by cadherin-based cell adhesion structures.[384] Immunoelectron microscopy studies have shown that molecules known to be components of epithelial desmosomes such as desmoglein2, desmocollin2, desmoplakin, plakoglobin and plakophilin2 are not only confined to junctions with a typical desmosome morphology but are also found in junctions with a more fascia adhaerens-like appearance. It was also shown that typical molecular components of fascia adhaerens can have the same localization as desmosomal molecules regardless of whether the junction has a more desmosome-like or a more fascia adhaerens-like appearance. The question arises then whether the area composita represents the major part of the cardiomyocyte intercalated discs and whether there is only a low proportion in which true desmosomes or true fascia adhaerens exist separately. This seems to be the case at least in some amphibian and fish species.[384] The idea of "mixed" junction types is further supported by recent studies showing α-catenin to have a pivotal regulatory role in desmosomal formation[385] and studies showing N-cadherin interacting to a certain degree with plakophilin2.[154] If in fact there are no "true" desmosomes, or at least not according to the model currently accepted, could the genes coding for classical adherens junction proteins also be underlying ARVC pathogenesis?

Based on both previous reports and the results presented herein, it appears that plakoglobin expression at intercalated discs is universally down-regulated in all cases of ARVC examined. Myocardial samples from patients with hypertrophic, dilated or ischemic cardiomyopathy are currently being immunostained for desmosomal proteins. This approach has showed that plakoglobin re-distribution is in fact specific to ARVC.

Though preliminary, these observations are highly promising potentially rendering immunostaining as a powerful tool in diagnosis of borderline ARVC cases.

When it comes to ARVC, a lot of questions still remain unanswered and a lot of issues need to be re-visited. One such question concerns the observed right ventricular predilection, and one such issue concerns the very name of the disease. During embryonic development, the heart is initially formed as a simple linear tube located at the ventral midline of the organism. During subsequent development, the tube undergoes a complex series of movements and tissue remodeling events that lead to the formation of the mature, four-chambered, septated organ. The morphologic events are accompanied by an equally complex series of cellular and molecular processes that lead different regions of the heart to express different genes and to adopt different physiological properties. The atrial and ventricular chambers, for instance, contain distinct isoforms of the myosin light chain genes, MLC2a and MLC2v respectively, which contribute to distinct contractile properties of the chambers. [386,387] Were the two ventricles to be expressing different isoforms of desmosomal genes, the "preference" that ARVC is showing to the right ventricle, would have been easier to explain. Yet, both the left and the right ventricle express the same set of "adhesive" genes, and as shown by immunohistochemical approaches, they also appear to have equivalent protein expression and distribution patterns. On the other hand, if we accept that the predilection is driven merely by the right ventricle having a thinner wall than the left ventricle, we would not be able to explain the increasing number of arrhythmogenic left ventricular cardiomyopathy cases that are being recognized. What is the factor that decides which ventricle is to be primarily affected in each case? Could differential expression of non-desmosomal cardiac genes across the ventricles determine which chamber is more susceptible to the disease in each case? Or similarly, could genetic polymorphisms in desmosomal or even non-desmosomal genes have a role in "directing" the "primary site of action" of the disease? It is now well-established that cases of ALVC do exist both in the pathology arena and in the clinical setting. Also, since ARVC and ALVC may exist in the same kindred, it is recognized that they are in fact different "expressions" of the same entity. Does that mean that the ground under the mere name "ARVC" is shaking? Leading experts in the field met in Colorado, USA in May 2007 to discuss among others, the possibility of changing the name originally given to the disorder over a decade ago. "Desmosomal cardiomyopathy" could very efficiently describe the ~40% of ARVC cases that are positively genotyped but would at least at the moment be largely inaccurate for the remaining cases.

Collectively this project described the effects that ARVC-causing mutations may have far beyond disrupting mechanical integrity, hence highlighting the deeply complex nature of this disease. The novel disease-causing pathways presented herein do not

preclude the mechanisms previously suggested. On the contrary, they underscore how multiple routes can combine and intersect to bring about a disease. What would the next step be though? Although investigating the effects of pathogenic mutations in cardiac myocytes provides highly physiologically significant results, transfecting NRVMs with recombinant adenoviral constructs still comprises an *in vitro* model. The next step would be to study animal models expressing S39_K40insS or 2057del2 plakoglobin. Though a time-consuming, expensive and laborious procedure, the generation of such transgenic animals would give us a different and even superior perspective in understanding and subsequently managing ARVC. Steps towards the development of these *in vivo* models are currently being undertaken. With an efficient collaboration between the clinical arena, improving diagnosis and applying more effective therapies, the genetic arena, identifying the root of ARVC, and molecular biology explaining how we can get from the "root to the branches", from the mutation to the disease, understanding and fighting ARVC is finally becoming a reality.

Journal publications related to this project:

Tandri H, **Asimaki A**, Halushka M, Sinha S, Saffitz JE, Calkins H. A case of arrhythmogenic right ventricular dysplasia due to plakophilin-2 mutation: arrhythmic, structural and functional deterioration leading to transplantation (manuscript submitted to Circulation).

Ward D, Syrris P, Guereta L, **Asimaki A**, Sheppard MN, Moon JC, Sen-Chowdhry S, Evans A, Pantazis A, Elliott PM, McKenna WJ. Multiple desmosomal gene mutations in familial arrhythmogenic right ventricular cardiomyopathy cause severe phenotypes (manuscript submitted to Circulation).

Huang H, **Asimaki A**, Lo D, McKenna WJ, Saffitz JE. Disparate effects of different mutations in plakoglobin on cell mechanical behaviour (manuscript submitted to the American Journal of Physiology: Cell Physiology).

Asimaki A, Syrris P, Ward D, Guereta L, Saffitz JE, McKenna WJ. Compound heterozygosity for two novel nonsense mutations in desmoplakin underlies a unique cardiocutaneous syndrome. (manuscript submitted to Journal of the American Academy of Dermatology)

Asimaki A, Syrris P, Wichter T, Matthias P, Saffitz JE, McKenna WJ. A novel mutation in plakoglobin causes arrhythmogenic right ventricular cardiomyopathy. American Journal of Human Genetics, November 2007.

Sen-Chowdhry S, Syrris P, Ward D, **Asimaki A**, Sevdalis E, McKenna WJ. Clinical and genetic characterization of families with arrhythmogenic right ventricular dysplasia/ cardiomyopathy provides novel insights into patterns of disease expression. Circulation. 2007 Apr;115(13):1710-20.

Syrris P, Ward D, **Asimaki A**, Evans A, Sen-Chowdhry S, Hughes SE, McKenna WJ. Desmoglein-2 mutations in arrhythmogenic right ventricular cardiomyopathy: a genotype-phenotype characterization of familial disease. Eur Heart J. 2007 Mar;28(5):581-8

Syrris P, Ward D, Evans A, **Asimaki A**, Gandjbakhch E, Sen-Chowdhry S, McKenna WL. Mutations in the desmosomal gene desmocollin-2 associated with arrhythmogenic

right ventricular dysplasia/ cardiomyopathy. The American Journal of Human Genetics. 2006 Nov; 79(5): 978-84

Antoniades L, Tsatsopoulou A, Anastasakis A, Syrris P, **Asimaki A**, Panagiotakos D, Zambartas C, Stefanadis C, McKenna WJ, Protonotarios N. Arrhythmogenic right ventricular cardiomyopathy caused by deletions in plakophilin-2 and plakoglobin (Naxos disease) in families from Greece and Cyprus: genotype-phenotype relations, diagnostic features and prognosis. European Heart Journal. 2006 Sep ;27 (18): 2208-16

Syrris P, Ward D, **Asimaki A**, Sen-Chowdhry S, Ebrahim HY, Evans A, Hitomi N, Norman M, Pantazis A, Shaw AL, Elliott PM, McKenna WJ. Clinical expression of plakophilin-2 mutations in familial arrhythmogenic right ventricular cardiomyopathy. Circulation. 2006 Jan 24;113(3):356-64

Presentations related to this project:

Asimaki A. Mutations in plakoglobin. **Invited talk**. 9th Biennial world congress on cardiac arrhythmias, Cardiostim 2008. 18-21 June 2008, Nice, French Riviera.

Huang H, **Asimaki A**, Lo Denise, McKenna WJ, Saffitz JE. Disparate effects of different plakoglobin mutations cell mechanics. **Poster presentation:** American Society for Cell Biology 47th Annual Meeting, 1-5 December 2007, Washington DC.

Asimaki A. Novel plakoglobin mutations in ARVC. **Invited talk.** II Meeting of the Spanish working group on hypertrophic cardiomyopathy, 16-17 November 2007, Murcia, Spain.

Asimaki A, Huang H, McKenna WJ, Saffitz JE. Disparate biomechanical effects of two ARVC-causing mutations in plakoglobin. **Poster presentation**: American Heart Association Scientific Sessions 2007, November 4-7, Orlando, Florida.

Asimaki A, Syrris P, Wichter T, Matthias P, Saffitz JE, McKenna MJ. A novel mutation in plakoglobin causes arrhythmogenic right ventricular cardiomyopathy. **Oral presentation at the Young Investigator Award Competition.** Heart Rhythm Society Scientific Sessions 2007, May 9-12 2007, Denver. Colorado.

Tsatsopoulou A, Anastasakis A, Antoniades L, Theopistou A, Syrris P, **Asimaki A**, Christodoulou A, Stefanadis C, McKenna WJ, Protonotarios N. Incidence and penetrance of dominant desmosomal mutations in arrhythmogenic right ventricular dysplasia/cardiomyopathy from Greece and Cyprus. **Oral Presentation.** European Society of Cardiology Congress 2007, September 1 –5 2007, Vienna, Austria.

Anastasakis A, Theopistou A, Christodoulou A, Syrris P, Tsatsopoulou A, Antoniades L, **Asimaki A**, Stefanadis C, McKenna WJ, Protonotarios N. Broad clinical phenotype of desmoplakin mutations in families with dominant arrhythmogenic right ventricular dysplasia/cardiomyopathy. **Oral Presentation.** European Society of Cardiology Congress 2007, September 1 –5 2007, Vienna, Austria.

Asimaki A, Syrris P, Wichter T, Matthias P, Saffitz JE, McKenna MJ. A novel mutation in plakoglobin causes arrhythmogenic right ventricular cardiomyopathy. **Poster presentation.** Cardiovascular, Diabetes and Metabolic Disorders Research Center

Retreat, Brigham and Women's Hospital and Biomedical Research Institute, Harvard Medical School, MA, February 13 2007.

Asimaki A, Syrris P, Wichter T, Matthias P, Saffitz JE, McKenna MJ. A novel mutation in plakoglobin causes arrhythmogenic right ventricular cardiomyopathy. **Poster presentation.** Third Annual Research Retreat, Center for vascular biology research, Beth Israel Deaconess Medical Centre, Harvard Medical School, MA, February 9 2007.

Asimaki A, Yamada Hames K, McKenna WJ, Saffitz JE. A novel mutation in plakoglobin blocks up-regulation of intercellular junction proteins in response to mechanical load. **Poster presentation**. American Heart Association scientific sessions 2006, November 12-15 2006, Chicago, Illinois

Asimaki A, Mutation in the desmosomal gene desmoglein 2 causes familial arrhythmogenic right ventricular cardiomyopathy. **Oral presentation**. UCL Cardiovascular Science and Medicine Day. Institute of Child Health. 5 May 2005.

Asimaki A, Syrris P, Shaw AL, Hughes S, Ward D, Sen-Chowdhry S, McKenna WJ. Novel mutation in plakophilin II causes arrhythmogenic right ventricular cardiomyopathy. **Poster presentation**. UCL Cardiovascular Science and Medicine Day. Institute of Child Health. 5 May 2005.

Asimaki A, Syrris P, Shaw AL, Hughes S, Ward D, Sen-Chowdhry S, McKenna WJ. Arrhythmogenic right ventricular cardiomyopathy: desmosomes to blame? **Poster presentation**. UK National Science Week 2005. Annual Presentations by Britain's Top Younger scientists, engineers and technologists, at the House of Commons, London, 14 March 2005.

Asimaki A, Syrris P, Shaw AL, Hughes S, Ward D, Sen-Chowdhry S, McKenna WJ. Novel mutation in plakophilin II causes arrhythmogenic right ventricular cardiomyopathy. **Poster presentation**. UCL Graduate school research poster competition 9-10 March 2005.

Asimaki A, Novel ARVC-causing mutations? **Oral presentation**. Seminar series, Queen Mary University of London, Biological Sciences department. 10 October 2004.

APPENDIX I: List of primers used for mutation analysis

Desmoplakin I

Exon	Primer sequence	Length	GC%	Size exon/PCR (base pairs)	Annealing T °C
DPex1R	AGTCGTCCAGAGGAGGACGGT	21	62		
DPex2F	GCAAGTTTGAAATTATTTCAG	21	28	103/245	48
DPex2R	AGAAGCTAACCAGAGGACAGT	21	48		
DPex3F	CTTGCTTCCATTAATGCCCATGAA	24	41	149/291	60
DPex3R	AGTGTAACTGGTTATGAGGAGTTC	24	41		
DPex4F	CCAGAACGGGTTTTCATAGGC	21	52	175/314	55
DPex4R	CACACAAACACATGGGCTGAC	21	52		
DPex5F	GGTGTGCGTAAGTGAAACAGGT	22	50	129/260	55
DPex5R	GTAATTACACGATCCTTCGGTAG	23	43		
DPex6F	AGGAGGCTTAGAAGGGCCACTC	22	59	51/218	55
DPex6R	TCCCCGCCAGGATGTGCTTGAT	22	59		
DPex7F	CAGAGAACACCAGTCACTGCA	21	52	162/282	60
DPex7R	CCAGCTCTTCAAGGCAACAGG	21	57		
DPex8F	AACAGCGTGATTCTTTGGCA	21	38	105/237	50
DPex8R	CCAACCCCTGGTGTAGGGTA	21	33		
DPex9F	TGGTGTTCATGCATCTGTACAA	22	41	96/214	50
DPex9R	CAAAAGATTAGGTATTAAGACC	22	53		
DPex10F	CTACTAGATGAAATTGCTCAT	21	33	126/254	55
DPex10R	TCCAAGGCATGTGTTTTATCT	21	38		
DPex11F	TGCAGGTTGAAAATCTCCTCT	21	43	153/302	55
DPex11R	AATGTTGCTTTCTTGATGGAC	21	38		
DPex12F	CATCTCTGTTTCCATCATTGAG	22	41	155/313	55
DPex12R	TATAAACACCTGCCCTCTTCCT	22	45		
DPex13F	TCCCATTTGGGATGAAGTGTG	22	45	127/263	60
DPex13R	AACTGTTGGACACAGGCACTG	22	52		
DPex14F	CTCTTCTTGATTGCATTGTGG	21	43	202/340	55
DPex14R	AGTTTTATGCAAACTCCCTTC	21	38		
DPex15F	TAGCACCTTGATACCTAGGTAT	22	41	227/377	60
DPex15R	GCCTACAAACATTTAAACCAGG	22	41		
DPex16F	CAGCATATTGTACACCTTAAAT	22	32	167/340	55
DPex16R	AGAAACTGTAAGGCAAGCATCT	22	41		
DPex17F	GTGAGAGGCAAATCTTCACAGA	22	45	139/270	55

DPex17R	TGGGAGCTCAGATCTGAATTAG	22	45		
DPex18F	AGTGTAGCATACAATGGGAGAA	22	41	194/319	55
DPex18R	GACATTATCTTGTGAACAACCA	22	36		
DPex19F	TCAAGTGAATTTCTGGGTGA	22	36	163/298	55
DPex19R	AAGCCTTCACAAAATGGGTT	22	36		
DPex20F	AAGGGTACAAATAACAGTGGTA	22	36	84/246	52
Dpex20R	ATCAGCAAGTCATGCAGTTAAT	22	36		
DPex21F	GTGGAACTGTAGCTGTTAGTGA	22	45	108/265	55
DPex21R	GAAAAGGGAAGAGGCAGGAGAC	22	54		
DPex22F	ATCGGTCAAATTACATAGGACT	22	36	99/257	48
DPex22R	CCAAATCCATGTTATAATGTGG	22	36		
DPex23.1F	CTTCTTTCTTGGAATGTGAGGT	22	41	2295/420	55
DPex23.1R	ACATTGCCTTGCTTTCTGCAGT	22	45		
DPex23.2F	GACCAACAGAAGAATGACTATG	22	41	2295/381	60
DPex23.2R	CTGCTCAGTGGCCTGCAAGAT	21	57		
DPex23.3F	GGATGAAATTGTCAGGCTCAA	21	43	2295/415	58
DPex23.3R	TATCCTCTTCCTTCTGCATGG	21	47		
DPex23.4F	ACCAAGACCACCATCCACCAG	21	54	2295/416	55
DPex23.4R	TGGACCCTTTGTAATCTCGCG	21	52		
DPex23.5F	ACCGGAAATGCCTGGAAGATG	21	52	2295/397	55
DPex23.5R	CTCTTCTTAACAATGGATGCC	21	43		
DPex23.6F	ATCACCAACCTGACCCAGCAG	21	54	2295/351	55
DPex23.6R	CCTCAGGTTCCGCAGTTCTTC	21	54		
DPex23.7F	CTCACAGAGAACCTGACCAAG	21	52	2295/333	58
DPex23.7R	GAGCACAGTTCAGATGAGATA	21	56		
DPex24.1F	GTTAAGTCGTGATAGTAATATG	22	32	3931/420	55
DPex24.1R	CTTGATCTCTGCTTGGAGTCTT	22	45		
DPex24.2F	GAAGAACAGTCTTAGGAGTGA	21	43	3931/409	55
DPex24.2R	TCCTTAGGAGAAGCAGATGCT	21	47		
DPex24.3F	CCTTCTGGGTGCAGGATCTAT	21	57	3931/466	60
DPex24.3R	TCGGGGATCATTCAGGGATCG	21	52		
DPex24.4F	GTAGACCCTGTGAACAGTGTC	21	52	3931/417	65
DPex24.4R	CGGAAGCTTCTGTTTTGTGGT	21	48		
DPex24.5F	CAAGCTGCATAGCAGGCATAT	21	48	3931/410	55
DPex24.5R	CTTATATGCTATGTCAACTGG	21	38		
DPex24.6F	ATTGACCCAAAGGAGAGCCAT	21	48	3931/406	55
DPex24.6R	CATCTGATCCCGTGATGGTTA	21	48		

DPex24.7F	TGTGAGCAGGAATGTGAATGG	21	48	3931/413	55
DPex24.7R	GTAATGGAGATTTTCTCCAGG	21	43		
DPex24.8F	TTGCAGCCATCTTTGACACAG	21	48	3931/416	60
DPex24.8R	ATCTATGAACCCCTTCCGGAT	21	48		
DPex24.9F	AGGATAAGCACCGAAGAAGC	21	48	3931/480	60
DPex24.9R	CTGCAAGCACCGGGATTTTCT	21	53		

Plakoglobin

Exon	Primer Sequence	Length	GC%	SizeExon/PCR (base pairs)	Annealing T °C
JUPex2F	CTGGGCCAGGTGACTTCCTGCT	22	63	216/323	65
JUPex2R	TCTCTCCAGGACCCAGGCAGGT	22	63		
JUPex3F	AGTGTCTGCCCAGCCCACTGC	21	66	260/372	67
JUPex3R	ACAATGTCCCTCCCCTGAGGACATCT	21	66		
JUPex4F	GCCTCTCCTTAGTGCTCACGTC	22	59	239/344	58
JUPex4R	AGGGGAGAGGCCCAAGTGAGAG	22	63		
JUPex5F	GCTCACATGTATGCCAGGCCTC	22	59	202/323	60
JUPex5R	GCAGGATAGAAGATGGCGCAAG	22	54		
JUPex6F	CCCGCGCTTCCTTGTTCCTGTCA	22	66	145/293	62
JUPex6R	CATCAGCCACGGGGAGCATGGCT	21	62		
JUPex7F	CCATTGTGGAGGCTGGTGAGTATG	21	52	104/295	65
JUPex7R	AGATGCCCAGACAGGAGGCTGGAT	21	52		
JUPex8F	TGGAGTTGGCTGCTCCCTGAC	21	62	339/434	62
JUPex8R	ACCTAAGCCTGCTGCAGGGTG	21	62		
JUPex9F	AAGCTGGGATCCTTCAGATGTC	21	50	156/289	55
JUPex9R	ATTCACACACACACCCACAGAG	22	50		
JUPex10F	CATTCGGCTGTCATGGGGAGGA	22	59	120/266	55
JUPex10R	CTGGGACTCCTAACCTTGCCCT	22	59		
JUPex11F	TGTCCGGCCTGCCTCACCCCTT	22	68	151/276	65
JUPex11R	ACGTCGGCCAGCCTCCATCGTG	22	68		
JUPex12F	CACGATGGAGGCTGGCCGACGT	22	68	122/234	65
JUPex12R	CCATGGGCAGTGCCCAACTTGC	22	63		
JUPex13F	AGAAGCATCTCTCCCTGCCCAC	22	59	40/223	55
JUPex13R	CCTCTGGCCCCGGAGACATAAT	22	59		

JUPex14F	GACTGCTCCCTGCAGGGTAGCT	22	63	166/288	58
JUPex14R	GAGGGCCTCCAACAGAAGGAGG	22	63		

Plakophilin II a

Exon	Primer Sequence	Length	GC%	Size Exon/PCR (base pairs)	Annealing T °C
PKP2ex1R	ACTCCCAGCACGCGGGGTGAG	21	71		
PKP2ex2F	CTGTAAATATTAATTAGCCTAC	22	27	113/219	55
PKP2ex2R	CATGGTAGTAATCTGATCACTA	22	36		
PKP2ex3AF	AGTCCTCAGCAAAGTTGAAATTTG	24	38	698/423	53
PKP2ex3AR	GTCAAAAACGGTGTCGCTAACAGA	24	46		
PKP2ex3BF	CACATACCACAGACAGTACCAG	22	50	698/443	58
PKP2ex3BR	TGTGCTGGCAATGACTGAACTG	22	50		
PKP2ex4F	AGTATTCGCTGAGTCGTCTCT	21	48	136/291	55
PKP2ex4R	GCAAAGTCACCATAATAGAAG	21	38		
PKP2ex5F	TGAATGCCTTGATGCCACATC	21	48	208/333	60
PKP2ex5R	GATGATGTAAGGCATCTGGCT	21	48		
PKP2ex6F	TTGCTGTGTTCATAAAGGAGCC	22	45	132/258	55
PKP2ex6R	ATTACAGGCGCAGACCACGACA	22	54		
PKP2ex7F	TTCAGCGGTCATTTTGGTCCCA	22	50	178/305	55
PKP2ex7R	TGACTTCCTTGGGGCTACCTAA	22	50		
PKP2ex8F	CAAAGACCTGTTGGATACACA	21	43	118/250	55
PKP2ex9R	GCCGATATATACCAAGTACTT	21	38		
PKP2ex10F	GTGAAATTATAGCCATCACCTG	22	41	174/303	55
PKP2ex10R	CTGAATTGAATGTAGGTAAGTC	22	36		
PKP2ex11F	CATCTTCATCAACCTCTGGTA	21	43	154/322	58
PKP2ex11R	GGTGATACAGACAACATTTCA	21	38		
PKP2ex12F	TGGGATCTTGGGATTAAGAAAC	22	41	190/321	62
PKP2ex12R	GATTATTTACACACAGGCTGGT	22	41		
	sequencing was performed with nested primers				
12F nested	AAGAAACTCTCCCTGATTTGGT				
12R nested	TTACGCATCGCCTGCACTAATG				
PKP2ex13F	AGGCCGCATCCAGAAGCCTCA	21	62	88/224	55
PKP2ex13R	TTCCCAGGGTCAAGTCAAGTGG	22	54		
PKP2ex14F	CCACTTGACTTGACCCTGGGAA	22	54	1639/246	58
PKP2ex14R	GGTTTCTTGGGCTGGGTAGTAG	22	54		

Desmoglein 2

Exon	Primer Sequence	Length	GC%	SizeExon/PCR (base pairs)	Annealing T ^{0}C
DSG2ex1F	CCAGGGAGGAGCCGAGTGCGCGCT	24	75	55/226	60, GC rich
DSG2ex1R	AACGCGCACAAGGGCGGCGGGCAA	24	70		
DSG2ex2F	CAATGCAGTAGGTTATTCATGA	22	36	36/220	55
DSG2ex2R	CAACATGTGTCTTCAATCTAGT	22	36		
DSG2ex3F	TAGGACAGCATACTAATGTTC	21	38	135/266	55
DSG2ex3R	AAAGTCCTCTCACACCACATT	21	42		
DSG2ex4F	TGGCTAAGATCAAATCTAGTAA	22	31	162/292	52
DSG2ex4R	CAAATGACACTTATTATGACAG	22	31		
DSG2ex5F	GTTACCAGCATTCTTGATCGAG	22	45	145/436	52
DSG2ex5R	TGTTCTGTAGGTAATACTCAAC	22	36		
DSG2ex6F	AGGTAAATATGCTTAAAGTTGA	22	27	167/323	55
DSG2ex6R	AGGAATACAGAACAAAATAAGA	22	27		
DSG2ex7F	GAAAGCCAGATGTAAGAGTGA	22	40	138/315	53
DSG2ex7R	CTGCAAAACATGAACACATGA	22	36		
DSG2ex8AF	GGATGTCAATGACAATATACCTGT	24	37	186/315	58
DSG2ex8AR	GTTTGAGCATCTGTTTCTATGTGG	24	41		
DSG2ex8BF	AATAGGTTCTGATAATTGGCTGGC	24	41	186/295	52
DSG2ex8BR	TAGTGTGACCACTTCCTAACCACA	24	46		
DSG2ex9F	GTATCTAACATTAAAACCACAC	22	32	266/455	55
DSG2ex9R	TTGAAGGAATGAAGTGTTCAG	22	36		
DSG2ex10F	TGTTAGAGGTTTCCAATTCATG	22	36	143/285	58
DSG2ex10R	CAATCAAATCAATGGTTTCTGA	22	32		
DSG2ex11F	GTCCTAAGTGGTTAGTACCTTC	22	45	228/485	60
DSG2ex11R	TGTCAGTAGGTTCAGGACCTCA	22	50		
DSG2ex12F	ATGTTGCCTCATCCTTGGTAAT	22	41	228/357	55
DSG2ex12R	ATAGTAACACATCTCCAGGAGT	22	41		
DSG2ex13F	AAGTCCAGGAAGGGACATGCAA	22	50	122/321	55
DSG2ex13R	GATCACTTTACTCACTCAACCA	22	41		
DSG2ex14F	AAGGATGAAGGATTCCCTCCAT	22	45	333/484	58
DSG2ex14R	GATCCAAGGCAATGATTACCCT	22	45		
DSG2ex15.1F	ACATTACTGCATTTTGAACAGG	22	36	1023/412	52
DSG2ex15.1R	TCTCTGCATTGGCTTCTTGCA	21	47		
DSG2ex15.2F	GAGAATACCTACTCCTCTGGCA	22	50	1023/420	55
DSG2ex15.2R	TTCCCTCACCATGACGTAAGGT	22	50		
DSG2ex15.3F	AAGGCACTCAGCATCTTCAAGA	22	45	1023/395	50
DSG2ex15.3R	GTCACTGCTAATTAAACTCTGG	22	41		

Desmocollin II a

Exon	Primer sequence	Length	GC%	Size Exon/PCR (base pairs)	Annealing T °C
DSC2ex1R	GTTTTCCTCTGCACCCTAGGCG	22	59		
DSC2ex2F	GCCTTTTTATGTGTATATCAT	21	28	85/245	58
DSC2ex2R	TTCCTTTTTATGGCTGTGTAG	21	33		
DSC2ex3F	CACGTGCATACATTACTGTTAA	22	36	200/335	55
DSC2ex3R	GTAATGTTGATTACGTCTGAAG	22	36		
DSC2ex4F	GTCATTGTTTAATGTTTGAGAA	22	27	120/246	50
DSC2ex4R	ATAATGGTAAGAGATGGAAACT	22	31		
DSC2ex5F	ATAGATGAAAGCTCTGCTGAA	21	38	156/268	50
DSC2ex5R	AAATGGCCAAGCATCATCATT	21	38		
DSC2ex6F	TGAATTTGAAGCATACCTCAT	21	33	145/267	50
DSC2ex6R	TGTATGAATTGAAACACAGTT	21	28		
DSC2ex7F	ATAAAGGGAACATAGAACATGT	22	32	167/286	50
DSC2ex7R	GAGTTATACAGGTACTATTGAA	22	32		
DSC2ex8F	GGAGTGTAAAGTAAGATTTCAA	22	32	135/278	50
DSC2ex8R	CAGAGATGTGCATATTAAACAA	22	32		
DSC2ex9F	GATTTACTTCACATCGTGTTCA	22	36	186/319	50
DSC2ex9R	ATTCTAGCATGCTATTCTATGA	22	32		
DSC2ex10F	GCATTGCCAAATATTAAATGA	21	28	257/378	48
DSC2ex10R	GCTAAATTATAATAACGTAAC	21	23		
DSC2ex11F	GGTACTTACCATTCTATTTTAG	22	32	143/299	50
DSC2ex11R	ATGTATGTAGCCAAGGAAGTAT	22	36		
DSC2ex12F	TCAGTGCATACTTTTGTGGTGA	22	41	225/347	50
DSC2ex12R	AGTATCGCAGACATCCTGATGT	22	45		
DSC2ex13F	AGAAGAAATCAGTGACATTGTA	22	32	237/347	48
DSC2ex13R	CTTGAAAGTTACTTTAAAGGGT	22	32		
DSC2ex14F	TGTGTGTATTAACCATTGTACA	22	32	125/259	60
DSC2ex14R	TACGCATTATAAGCGAATTCAT	22	32		
DSC2ex15F	TTGTGTTCCTCTCTGTATTATC	22	36	258/384	60
DSC2ex15R	ATAGTCAGAATCCAGTTAGTTA	22	32		
DSC2ex16F	GCTATACTGAATTTATAGTGTGAT	24	29	198+36/438	55
DSC2ex16R	TAAAAGTCATAAAGCCACTGGCTT	24	37		

Desmin

Exon	Primer sequence	Length	GC%	Size Exon/PCR (base pairs)	Annealing T °C
DESex1aR	CGGTGAACCAGGAGTTTCTGAC	22	55		
DESex1bF	CTACGGCGCAGGCGAGCTGCTG	22	72	578/339	68
DESex1bR	CAGGAGGCTAGGCCTGGGGTCT	22	68		
DESex2F	GGCCAGTCGTTTCCACTGCCAG	22	63	61+96/384	65
DESex3R	AGCAGCCGGAAAGTGGGGTTGG	22	63		
DESex4F	TGAGGCTCTGGCTGGGAATAGG	22	59	162/310	65
DESex4R	CAGCTTGGATGTGCTGCCTGTG	22	59		
DESex5F	CCAGAGGCTTCATGCTCCCTTG	22	59	126/285	65
DESex5R	CTCACTTTGTGACCTTGGGCCC	22	59		
DESex6F	GTTGCCTGCCAGCCCCAAAGC	21	66	221/296	65
DESex6R	TGCGGGGTGCTGGGTGGTCCAT	22	68		
DESex7F	ATGGTCTCGATCTCCTGACCT	21	52	44/226	68
DESex7R	AGGAGTCCAGCATGGGCACT	20	60		
DESex8F	CCTGGTATAGCCCAGCCTGGA	21	62	83+784/455	68
DESex9R	TGCTCCCTGAAGCCAGCCTTC	21	62		

"F" stands for forward and "R" stands for reverse. All primers are in the 5' – 3' direction.

BIBLIOGRAPHY:

[1] P. Richardson, W. McKenna, M. Bristow, B. Maisch, B. Mautner, J. O'Connell, E. Olsen, G. Thiene, J. Goodwin, I. Gyarfas, I. Martin, and P. Nordet. Report of the 1995 World Health Organization/International Society and Federation of Cardiology Task Force on the Definition and Classification of cardiomyopathies. Circulation 93 (5):841-842, 1996

[2] M. J. Davies. The cardiomyopathies: an overview. Heart 83: 469-474, 2000

[3] D. Fatkin and R. M. Graham. Molecular mechanisms of inherited cardiomyopathies. Physiol Rev 82: 945-980, 2002

[4] J. Schonberger and C. Seidman. Many roads lead to a broken heart: the genetics of dilated cardiomyopathy. Am J Hum Genet 69: 249–260, 2001

[5] S. Karkkainen and K. Peuhkurinen. Genetics of dilated cardiomyopathy. Ann Med 39: 91-107, 2007

[6] S. DePalma, B. R. N. McDonough, C. Seidman, J. G. Seidman and L. Smoot. Mutations in sarcomere protein genes as a cause of dilated cardiomyopathy. N Engl J Med 343:1688-96, 2000

[7] D. Li, S. B. Parks, J. D. Kushner, D. Nauman, D. Burgess, S. Ludwigsen, J. Partain, R. R. Nixon, C. N. Allen, R. P. Irwin, P. M. Jakobs,M. Litt and R. E. Hershberger. Mutations of presenilin genes in dilated cardiomyopathy and heart failure. Am J Hum Genet79:1030-9, 2006

[8] E. Rubin and J. Doria. Alcoholic cardiomyopathy. Alcohol Health and Research World 14:277–284, 1990

[9] J. E. Towbin and N. E. Bowles. The failing heart. Nature 415: 227-233, 2002

[10] W. M. Franz, O. J. Muller and H. A. Katus. Cardiomyopathies: from genetics to the prospect of treatment. The lancet 358: 1627-1637, 2001

[11] http://www.mayoclinic.org/hypertrophic-cardiomyopathy/

[12] P. Elliott and W. J. McKenna. Hypertrophic cardiomyopathy. The Lancet 363: 1881-1891, 2004

[13] S. E. Hughes and W. J. McKenna. New insights into the pathology of inherited cardiomyopathy. Heart 91: 257-264, 2005

[14] http://www.healthnewsflash.com/conditions/cardiomyopathy.php#Restrictive%20Cardiomy

[15] S. Dalla Volta, G. Battaglia and E. Zerbini. 'Auricularisation' of the right ventricular pressure curve. Am Heart J 61: 25-33, 1961

[16] G. Fontaine, G. Guiraudon, R. Frank et al. Stimulation studies and epicardial mapping in ventricular tachycardia: study of mechanisms and selection for surgery. In: Kulbertus HE, ed. Reentrant arrhythmias: mechanisms and treatment. Lancaster: MTP Press Limited: 334-350, 1977

[17] F. I. Marcus, G. Fontaine, G. Guiraudon et al. Right ventricular dysplasia: a report of 24 cases. Circulation 65: 384-399, 1982

[18]G. Thiene, A. Nava, D. Corrado, L. Rossi and N. Pennelli. Right ventricular cardiomyopathy and sudden death in young people. The New England Journal of Medicine 318: 129-133, 1988

[19] A. Nava, G. Thiene, B. Canciani, R. Scognamiglio, L. Daliento, G. Buja, B. Martini, P. Stritoni and G. Fasoli. Familial occurrence of right ventricular dysplasia: a study involving nine families. J Am Coll Cardiol 12:1222-8, 1988

[20]D. Corrado, C. Basso, G. Thiene, W. J. McKenna, M. J. Davies, F. Fontaliran, A. Nava, F. Silvestri, C. Blomstrom-Lundqvist, E. K. Wlodarska, G. Fontaine, and F. Camerini. Spectrum of clinicopathologic manifestations of arrhythmogenic right ventricular cardiomyopathy/dysplasia: a multicenter study. J.Am.Coll.Cardiol. 30:1512-1520, 1997

[21] D. Corrado, C. Basso, G. Thiene, W. J. McKenna, M. J. Davies, F. Fontaliran, A. Nava, F. Silvestri, C. Blomstrom-Lundqvist, E. K. Wlodarska, G. Fontaine, and F. Camerini. Spectrum of clinicopathologic manifestations of arrhythmogenic right ventricular cardiomyopathy/dysplasia: a multicenter study. J.Am.Coll.Cardiol. 30:1512-1520, 1997

[22]Sen-Chowdhry, M. D. Lowe, S. C. Sporton, and W. J. McKenna. Arrhythmogenic right ventricular cardiomyopathy: clinical presentation, diagnosis, and management. Am.J.Med. 117:685-695, 2004

[23] W. J. McKenna, G. Thiene, A. Nava, F. Fontaliran, C. Blomstrom-Lungvist, G. Fontaine and F. Camerini. Diagnosis of arrhythmogenic right ventricular dysplasia/cardiomyopathy. Task Force of the Working Group Myocardial and Pericardial Disease of the European Society of Cardiology and of the Scientific Council on Cardiomyopathies of the International Society and Federation of Cardiology. Br Heart J 71: 215-218, 1994

[24] S. Peters and M. Trummel. Diagnosis of arrhythmogenic right ventricular dysplasia-cardiomyopathy: value of standard ECG revisited. Ann.Noninvasive.Electrocardiol. 8:238-245, 2003

[25] R. Anan, T. Takenaka, and C. Tei. Epsilon waves in a patient with arrhythmogenic right ventricular cardiomyopathy. Heart 88:444, 2002

[26] M. T. Tome Esteban, J. M. Garcia-Pinilla and W. J. McKenna. Update in arrhythmogenic right ventricular cardiomyopathy: genetic, clinical presentation and risk stratification. Rev Esp Cardiol 57: 757-67, 2004

[27] G. Fontaine, F. Fontaliran, J. L. Hebert, D. Chemla, O. Zenati, Y. Lecarpentier, and R. Frank. Arrhythmogenic right ventricular dysplasia. Annu.Rev.Med. 50:17-35, 1999

[28] M. S. Hamid, M. Norman, A. Quraishi, S. Firoozi, R. Thaman, J. R. Gimeno, B. Sachdev, E. Rowland, P. M. Elliott, and W. J. McKenna. Prospective evaluation of relatives for familial arrhythmogenic right ventricular cardiomyopathy/dysplasia reveals a need to broaden diagnostic criteria. J.Am.Coll.Cardiol 40:1445-1450, 2002

[29] J. B. White, R. Razmi, H. Nath, G. N. Kay, V. J. Plumb, and A. E. Epstein. Relative utility of magnetic resonance imaging and right ventricular angiography to diagnose arrhythmogenic right ventricular cardiomyopathy. J.Interv.Card Electrophysiol 10:19-26, 2004

[30]L. Lindstrom, U. M. Wilkenshoff, H. Larsson, and B. Wranne. Echocardiographic assessment of arrhythmogenic right ventricular cardiomyopathy. Heart 86:31-38, 2001

[31]H. Tandri, H. Calkins, and F. I. Marcus. Controversial role of magnetic resonance imaging in the diagnosis of arrhythmogenic right ventricular dysplasia. Am.J.Cardiol 92:649, 2003

[32]C. Basso and G. Thiene. Adipositas cordis, fatty infiltration of the right ventricle, and arrhythmogenic right ventricular cardiomyopathy. Just a matter of fat? Cardiovasc.Pathol 14:37-41, 2005

[33] S. Abbara, R. Q. Migrino, D. E. Sosnovik, J. A. Leichter, T. J. Brady, and G. Holmvang. Value of fat suppression in the MRI evaluation of suspected arrhythmogenic right ventricular dysplasia. AJR Am.J.Roentgenol 182:587-591, 2004

[34]M. Eguchim K. Tsuchihashi, A. Hashimoto, K. Uno, M. Kyuma, T. Takahashi, S. Shimoshige, T. Wakabayashi, N. Nahahara, T. Nakata and K. Shimamoto. Quantitative assessment of tight ventricular abnormalities by right ventricular polar mapping of signle photon emission computer tomogram. Nuclear Medicine Communications 23: 943-950, 2002

[35] S. Matsuo, Y. Sato, I. Nakae, D. Masuda, M. Yomota, T. Ashihara and M. Horie. Left ventricular involvement in arrhythmogenic right ventricular cardiomyopathy demonstrated by multi-detector row computer tomography. Int J Cardiol 115: 3129-131, 2007

[36] S. Peters. Advances in the diagnostic management of arrhythmogenic right ventricular dysplasia-cardiomyopathy. Int J Cardiol 113: 4-11, 2006

[37] C. Gemayel, A. Pelliccia and P. D. Thompson. Arrhythmogenic right ventricular cardiomyopathy. Journal of the American college of cardiology 38: 1773-1781, 2001

[38] S. Peters, M. Trummel and W. Meyners. Prevalence of right ventricular dysplasia-cardiomyopathy in a non-referral hospital. International journal of cardiology 97: 499-501, 2004

[39] Y. Cho, T. Park, D. H. Yang, H. S. Park, J. Chae, S. C. Chae, J. E. Jun, J. S. Kwak, and W. H. Park. Arrhythmogenic right ventricular cardiomyopathy and sudden cardiac death in young Koreans. Circ.J. 67:925-928, 2003

[40] A. Nava, B. Bauce, C. Basso, M. Muriago, A. Rampazzo, C. Villanova, L. Daliento, G. Buja, D. Corrado, G. A. Danieli, and G. Thiene. Clinical profile and long-term follow-up of 37 families with arrhythmogenic right ventricular cardiomyopathy. J.Am.Coll.Cardiol. 36: 2226-2233, 2000

[41] G. A. Danieli and A. Rampazzo. Genetics of arrhythmogenic right ventricular cardiomyopathy. Current opinion in cardiology 17: 218-221, 2002

[42] W. H. Fung and J. E. Sanderson. Clinical profile of arrhythmogenic right ventricular cardiomyopathy in Chinese patients. Int.J.Cardiol. 81:9-18, 2001

[43] M. Smith, M. R. Kichuk and N. B. Ratliff. Clinical and pathologic study of two siblings with arrhythmogenic right ventricular cardiomyopathy. Cardiovascular Pathology 8: 273-278, 1999

[44] J. Nemec, B.S. Edwards, M. J. Osborn and W. D. Edwards. Arrhythmogenic right ventricular dysplasia masquerading as dilated cardiomyopathy. Am J Cardiol 84: 237-239, 1999

[45] H. Suzuki, M. Sumiyoshi, S. Kawai, A. Takagi, A. Wada, Y. Nakazato, H. Daida, H. Sakurai and H. Yamaguchi. Arrhythmogenic right ventricular cardiomyopathy with an initial manifestation of severe left ventricular impairment and normal contraction of the right ventricle. Jpn Circ J 64: 209-213, 2000

[46] C. Basso, A. Tsatsopoulou, G. Thiene, A. Anastasakis, M. Valente and N. Protonotarios. "Petrified right ventricle in long-standing Naxos arrhythmogenic right ventricular cardiomyopathy. Circulation 104: e132-e133, 2001

[47] P. Bjerregaard and H. Molgaard. Electrocardiographic curiosities: a patient with biventricular dysplasia. Journal of electrocardiology 35: 289-290, 2002

[48] S. I. Khalil, A. Kamal and S. Ahmad. Arrhythmogenic right ventricular dysplasia presenting as acute coronary syndrome: a case report. Eur J Echocardiography 5: 394-398, 2004

[49] V. Barriales, J. A. Tamargo, M. G. Aguado, M. Martin, J. Rondan and I. S. Posada. Electrical storm as initial presentation of arrhythmogenic right ventricular cardiomyopathy in an elderly woman. Int J Cardiol 94: 331-333, 2004

[50] C. Bomma, J. Rutberg, H. Tandri, K. Nasir, A. Roguin, C. Tichnell, R. Rodriguez, C. James, E. Kasper, P. Spevak, D. A. Bluemke, and H. Calkins. Misdiagnosis of arrhythmogenic right ventricular dysplasia/cardiomyopathy. J.Cardiovasc.Electrophysiol. 15 :300-306, 2004

[51] G. Fontaine, F. Fontaliran, G. Lascault, R. Frank, J. Tonet, G. Chomette and Y. Grosgogeard. Congenital and acquired right ventricular dysplasia. Arch Mal Coeur Vaiss 83: 915-920, 1990

[52] F. Calabrese, A. Angelini, G. Thiene, C. Basso, A. Nava, and M. Valente. No detection of enteroviral genome in the myocardium of patients with arrhythmogenic right ventricular cardiomyopathy. J.Clin.Pathol. 53: 382-387, 2000

[53] A. Matsumori, C. Kawai, S. Sawada, and K. Yamamoto. Experimental coxsackievirus B3 perimyocarditis in the right ventricle in BALB/c mice: a one-year follow-up study. Jpn.Circ.J. 44: 842-847, 1980

[54] C. Chimenti, M. Pieroni, A. Maseri, and A. Frustaci. Histologic findings in patients with clinical and instrumental diagnosis of sporadic arrhythmogenic right ventricular dysplasia. J.Am.Coll.Cardiol. 43: 2305-2313, 2004

[55] Z. Mallat, A. Tedgui, F. Fontaliran, R. Frank, M. Durigon, and G. Fontaine. Evidence of apoptosis in arrhythmogenic right ventricular dysplasia. N.Engl.J.Med. 335:1190-1196, 1996

[56] N. Protonotarios, A. Tsatsopoulou, P. Patsourakos, D. Alexopoulos, P. Gezerlis, S. Simitsis, and G. Scampardonis. Cardiac abnormalities in familial palmoplantar keratosis. Br.Heart J. 56:321-326, 1986

[57] N. Narin, M. Akcakus, T. Gunes, A. Celiker, A. Baykan, K. Uzum, and A. Ferahbas. Arrhythmogenic right ventricular cardiomyopathy (Naxos disease): report of a Turkish boy. Pacing Clin.Electrophysiol. 26:2326-2329, 2003

[58] I. Bukhari and N. Juma'a. Naxos disease in Saudi Arabia. JEADV 18: 614-616, 2004

[59] N. Protonotarios, A. Tsatsopoulou, and G. Fontaine. Naxos disease: keratoderma, scalp modifications, and cardiomyopathy. J.Am.Acad.Dermatol. 44:309-311, 2001

[60] N. Protonotarios and A. Tsatsopoulou. Naxos disease: cardiocutaneous syndrome due to cell adhesion defect. Orphanet Journal of rare diseases 1: 1-5, 2006

[61] A. S. Coonar, N. Protonotarios, A. Tsatsopoulou, E. W. Needham, R. S. Houlston, S. Cliff, M. I. Otter, V. A. Murday, R. K. Mattu, and W. J. McKenna. Gene for arrhythmogenic right ventricular cardiomyopathy with diffuse nonepidermolytic palmoplantar keratoderma and woolly hair (Naxos disease) maps to 17q21. Circulation 97:2049-2058, 1998

[62] L. Carvajal-Huerta. Epidermolytic palmoplantal keratoderma with woolly hair and dilated cardiomyopatht. J Am Acad Dermatol 39: 418-421, 1998

[63] E. E. Norgett, S. J. Hatsell, L. Carvajal-Huerta, J. C. Cabezas, J. Common, P. E. Purkis, N. Whittock, I. M. Leigh, H. P. Stevens, and D. P. Kelsell. Recessive mutation in desmoplakin disrupts desmoplakin-intermediate filament interactions and causes dilated cardiomyopathy, woolly hair and keratoderma. Hum.Mol.Genet. 9:2761-2766, 2000

[64] S. R. Kaplan, J. J. Gard, L. Carvajal-Huerta, J. C. Ruiz-Cabezas, G. Thiene, and J. E. Saffitz. Structural and molecular pathology of the heart in Carvajal syndrome. Cardiovasc.Pathol. 13:26-32, 2004

[65] T. Kilic, K. Babaoglu, F. Aygun, A. Vural, D. Ural, A. Agacdiken, Y. Anik and B. Komsuoglu. Biventricular involvement in a Turkish boy with palmoplantal hyperkeratosis and curly hair; an unusual presentation of Naxos-Carvajal syndrome. Int J Cardiol 115_ e122-e125, 2007

[66] R. Alcalai, S. Metzger, S. Rosenheck, V. Meiner, and T. Chajek-Shaul. A recessive mutation in desmoplakin causes arrhythmogenic right ventricular dysplasia, skin disorder, and woolly hair. J.Am.Coll.Cardiol. 42:319-327, 2003

[67] R. J. Whittington and R. W. Cook. Cardiomyopathy and wooly haircoat syndrome of Poll Hereford cattle: electrocardiographic findings and un-affected calves. Aust Vet J 65: 341-344, 1988

[68] N. Protonotarios and A. Tsatsopoulou. Naxos disease and Carvajal syndrome; Cardiocutaneous disorders that highlight the pathogenesis and broaden the spectrum of arrhythmogenic right ventricular cardiomyopathy. Cardiovasc.Pathol. 13:185-194, 2004

[69] P. R. Fox, B. J. Maron, C. Basso, S. K. Liu and G. Thiene. Spontaneously occurring arrhythmogenic right ventricular cardiomyopathy in the domestic cat: a new animal model similar to the human disease. Circulation 102: 1863-1870, 2000

[70] C. Basso, P. R. Fox, K. M. Meurs, J. A. Towbin, A. W. Spier, F. Calabrese, B. J. Maron and G. Thiene. Arrhythmogenic right ventricular cardiomyopathy causing sudden cardiac death in Boxer dogs. Circulation 109: 1180-1185, 2004

[71] Y. Hiroi, K. Fujiu, S. Komatsu, M. Sonoda, Y. Sakomura, Y. Imai, Y. Oishi, F. Nakamura, K. Ajiki, N. Hayami, Y. Murakawa, M. Ohno, Y. Hirata, K. Ohtomo, and R. Nagai. Carvedilol therapy improved left ventricular function in a patient with arrhythmogenic right ventricular cardiomyopathy. *Jpn.Heart J.* 45 (1):169-177, 2004.

[72] C. Chachques, P. G. Argyriadis, G. Fontaine, J. L. Hebert, R. A. Frank, N. D'Attellis, J. N. Fabiani, and A. F. Carpentier. Right ventricular cardiomyoplasty: 10-year follow-up. Ann.Thorac.Surg. 75:1464-1468, 2003

[73] G. McKoy, N. Protonotarios, A. Crosby, A. Tsatsopoulou, A. Anastasakis, A. Coonar, M. Norman, C. Baboonian, S. Jeffery, and W. J. McKenna. Identification of a deletion in plakoglobin in arrhythmogenic right ventricular cardiomyopathy with palmoplantar keratoderma and woolly hair (Naxos disease). Lancet 355:2119-2124, 2000

[74] C. Bierkamp, K. J. Mclaughlin, H. Schwarz, O. Huber, and R. Kemler. Embryonic heart and skin defects in mice lacking plakoglobin. Dev.Biol. 180:780-785, 1996

[75] A. Rampazzo, A. Nava, S. Malacrida, G. Beffagna, B. Bauce, V. Rossi, R. Zimbello, B. Simionati, C. Basso, G. Thiene, J. A. Towbin, and G. A. Danieli. Mutation in human desmoplakin domain binding to plakoglobin causes a dominant form of arrhythmogenic right ventricular cardiomyopathy. Am.J.Hum.Genet. 71:1200-1206, 2002

[76] K. S. Grossmann, C. Grund, J. Huelsken, M. Behrend, B. Erdmann, W. W. Franke, and W. Birchmeier. Requirement of plakophilin 2 for heart morphogenesis and cardiac junction formation. J.Cell Biol. 167:149-160, 2004

[77] B. Gerull, A. Heuser, T. Wichter, M. Paul, C. T. Basson, D. A. McDermott, B. B. Lerman, S. M. Markowitz, P. T. Ellinor, C. A. Macrae, S. Peters, K. S. Grossmann, B. Michely, S. Sasse-Klaassen, W. Birchmeier, R. Dietz, G. Breithardt, E. Schulze-Bahr, and L. Thierfelder. Mutations in the desmosomal protein plakophilin2 are common in arrhythmogenic right ventricular cardiomyopathy. Nat.Genet. 36:1162-1164, 2004

[78] A. Rampazzo, A. Nava, GA Danieli, G. Buja, L. Daliento, G. Fasoli, R. Scognamiglio, D. Corrado and G. Thiene. The gene for arrhythmogenic right ventricular cardiomyopathy maps to chromosome 14q23-q24. Hum Mol Genet 3:959-962, 1994

[79]A. Rampazzo, G. Beffagna, A. Nava, G. Occhi, B. Bauce, M. Noiato, C. Basso, G. Frigo, G. Thiene, J. Towbin, and G. A. Danieli. Arrhythmogenic right ventricular cardiomyopathy type 1 (ARVD1): confirmation of locus assignment and mutation screening of four candidate genes. Eur.J.Hum.Genet. 11:69-76, 2003

[80]G.M. Severini, M. Krajinovic, B. Pinamonti , G. Sinagra, P. Fioretti, M.C. Brunazzi, A. Falaschi, F. Camerini, M. Giacca and L. Mestroni. A new locus for arrhythmogenic right ventricular cardiomyopathy on the long arm of chromosome 14. Genomics. 31: 193-200, 1996

[81]A. Rampazzo, A. Nava, M. Miorin, P. Fonderico, B. Pope, N. Tiso, B. Livolsi, R. Zimbello, G. Thiene and G.A. Danieli. ARVD4, a new locus for arrhythmogenic right ventricular cardiomyopathy, maps to chromosome 2 long arm. Genomics. 45: 259-63, 1997

[82] F. Ahmad, D. Li, A. Karibe, O. Gonzalez, T. Tapscott, R. Hill, D. Weilbaecher, P. Blackie, M. Furey, M. Gardner, L. L. Bachinski, and R. Roberts. Localization of a gene responsible for arrhythmogenic right ventricular dysplasia to chromosome 3p23. Circulation 98 :2791-2795, 1998

[83] D. Li, F. Ahmad, M. J. Gardner, D. Weilbaecher, R. Hill, A. Karibe, O. Gonzalez, T. Tapscott, G. P. Sharratt, L. L. Bachinski, and R. Roberts. The locus of a novel gene responsible for arrhythmogenic right-ventricular dysplasia characterized by early onset and high penetrance maps to chromosome 10p12-p14. Am.J.Hum.Genet. 66 :148-156, 2000

[84]A. Melberg, A. Oldfors, C. Blomstrom-Lundqvist, E. Stalberg, B. Carlsson, E. Larrson, C. Lidell, K.E. Eeg-Olofsson, G. Wikstrom, G. Henriksson and N. Dahl. Autosomal dominant myofibrillar myopathy with arrhythmogenic right ventricular cardiomyopathy linked to chromosome 10q. Ann Neurol. 46 : 684-92, 1999

[85]N. Tiso, D. A. Stephan, A. Nava, A. Bagattin, J. M. Devaney, F. Stanchi, G. Larderet, B. Brahmbhatt, K. Brown, B. Bauce, M. Muriago, C. Basso, G. Thiene, G. A. Danieli, and A. Rampazzo. Identification of mutations in the cardiac ryanodine receptor gene in families affected with arrhythmogenic right ventricular cardiomyopathy type 2 (ARVD2). Hum.Mol.Genet. 10:189-194, 2001

[86]B. Bauce, A. Rampazzo, C. Basso, A. Bagattin, L. Daliento, N. Tiso, P. Turrini, G. Thiene, G. A. Danieli, and A. Nava. Screening for ryanodine receptor type 2 mutations in families with effort-induced polymorphic ventricular arrhythmias and sudden death: early diagnosis of asymptomatic carriers. J.Am.Coll.Cardiol. 40:341-349, 2002

[87]M. Scoote and A. J. Williams. The cardiac ryanodine receptor (calcium release channel): emerging role in heart failure and arrhythmia pathogenesis. Cardiovasc.Res. 56:359-372, 2002

[88]D. M. Bers. Cardiac excitation-contraction coupling. Nature 415 (6868):198-205, 2002.

[89]N. Tiso, M. Salamon, A. Bagattin, G. A. Danieli, F. Argenton, and M. Bortolussi. The binding of the RyR2 calcium channel to its gating protein FKBP12.6 is oppositely affected by ARVD2 and VTSIP mutations. Biochem.Biophys.Res.Commun. 299:594-598, 2002

[90]G. Beffagna, G. Occhi, A. Nava, L. Vitiello, A. Ditadi, C. Basso, B. Bauce, G. Carraro, G. Thiene, J. A. Towbin, G. A. Danieli, and A. Rampazzo. Regulatory mutations in transforming growth factor-beta3 gene cause arrhythmogenic right ventricular cardiomyopathy type 1. Cardiovasc.Res. 65:366-373, 2005

[91]S. Nattel and J. J. Schott. Arrhythmogenic right ventricular dysplasia type 1 and mutations in transforming growth factor beta3 gene regulatory regions: a breakthrough? Cardiovasc.Res. 65:302-304, 2005

[92]Y. Asano, S. Takashima, M. Asakura, Y. Shintani, Y. Liao, T.minamino, H. Asanuma, S. Sanada, J. Kim, A. Ogai, T. Fukushima, Y. Oikawa, Y. Okazaki, Y. Kaneda, M. Sato, J. Miyazaki, S. Kitamura, H. Tomoike, M. Kitakaze, and M. Hori. Lamr1 functional retroposon causes right ventricular dysplasia in mice. Nat.Genet. 36:123-130, 2004

[93] K. J. Green and C. A. Gaudry. Are desmosomes more than tethers for intermediate filaments? Nat.Rev.Mol.Cell *Biol.* 1:208-216, 2000

[94] B.Alberts, D.Bray, J.Lewis, K.Roberts, and J.D.Watson. Molecukar Biology of the cell. Third edition. Garland Publishing, 1994

[95] A. P. South. Plakophilin 1: an important stabilizer of desmosomes. Clin.Exp.Dermatol. 29:161-167, 2004

[96] S. Getsios, A. C. Huen, and K. J. Green. Working out the strength and flexibility of desmosomes. Nat.Rev.Mol.Cell Biol. 5:271-281, 2004

[97] A. J. North, W. G. Bardsley, J. Hyam, E. A. Bornslaeger, H. C. Cordingley, B. Trinnaman, M. Hatzfield, K. J. Green, A. I. Magee and D. R. Garrod. Molecular map of the desmosomal plaque. Journal of cell science 112: 4325-4336, 1999

[98] T. Yin and K. J. Green. Regulation of desmosome assembly and adhesion. Semin.Cell Dev.Biol. 15:665-677, 2004

[99] Y. Kitajima. Mechanisms of desmosome assembly and disassembly. Clin.Exp.Dermatol. 27 (8):684-690, 2002.

[100] R. Windoffer, M. Borchert-Stughltrager and R. E. Leube. Desmosomes: interconnected calcium-dependent structures of remarkable stability with significant integral membrane protein turnover. Journal of cell science 115: 1717-1732,2002

[101] J. Kartenbeck, W. W. Franke, J. G. Moser and U. Stoffels. Specific attachment of desmin filaments to desmosomal plaques in cardiac myocytes. EMBO J 2: 735-742, 1983

[102] S. Getsios, A. C. Huen, and K. J. Green. Working out the strength and flexibility of desmosomes. Nat.Rev.Mol.Cell Biol. 5:271-281, 2004

[103] Z. Hu, J. M. Bonifas, J. Beech, G. Bench, T. Shigihara, H. Ogawa, S. Ikeda, T. Mauro, and E. H. Epstein, Jr. Mutations in ATP2C1, encoding a calcium pump, cause Hailey-Hailey disease. Nat.Genet. 24:61-65, 2000

[104] J. Dhitavat, R. J. Fairclough, A. Hovnanian, and S. M. Burge. Calcium pumps and keratinocytes: lessons from Darier's disease and Hailey-Hailey disease. Br.J.Dermatol. 150:821-828, 2004

[105]B. S. Hahn and M. Labouesse. Tissue integrity: hemidesmosomes and resistance to stress. Curr.Biol. 11:R858-R861, 2001

[106] K. J. Cavanaugh, Jr., J. Oswari, and S. S. Margulies. Role of stretch on tight junction structure in alveolar epithelial cells. Am.J.Respir.Cell Mol.Biol. 25:584-591, 2001

[107] M. Delmar. The intercalated disc as a single functional unit. Heart Rhythm 1: 12-13, 2004

[108] J. E. Saffitz and K. A. Yamada. Closing the gap in understanding the regulation of intercellular communication. Cardiovascular research 45: 807-809, 2000

[109] M. G. Shubich, B. G. Ermoshenko, I. M. Perov and I. V. Dorofeeva. Gap junctions-major structures promoting intercellular communication. Morfologiia 127: 65-71, 2005

[110] J. E. Saffitz. Biology and pathobiology of cardiac connexins: from cell to bedside. Heart Rhythm 3: 102-107, 2006

[111] C. A. L. S. Colaco and W. H. Evans. A biochemical dissection of the cardiac intercalated disc: isolation of subcellular fractions containing fascia adherents and gap junctions. Journal of Cel Science 52: 313-325, 1981

[112] http://www.colorado.edu/kines/Class/IPHY3430-200/image/figure3k.jpg

[113] S. Kostin, S. Hein, E. P. Bauer, and J. Schaper. Spatiotemporal development and distribution of intercellular junctions in adult rat cardiomyocytes in culture. *Circ.Res.* 85 (2):154-167, 1999.

[114] C. Zuppinger, M. Eppenberger-Eberhardt and H. M. Eppenberger. N-cadherin: structure, function and importance in the formation of new intercalated disc-like cell contacts in cardiocyocytes. Heart Failure reviews 5: 251-257, 2000

[115] D. E. Gutstein, F. Y. Liu, M. B. Meyers, A. Choo, and G. I. Fishman. The organization of adherens junctions and desmosomes at the cardiac intercalated disc is independent of gap junctions. J.Cell Sci. 116:875-885, 2003

[116] D. M. Hunt, V. K. Sahota, K. Taylor, D. Simrak, N. Hornigold, J. Arnemann, J. Wolfe, and R. S. Buxton. Clustered cadherin genes: a sequence-ready contig for the desmosomal cadherin locus on human chromosome 18. Genomics 62:445-455, 1999

[117]C. M. Cowley, D. Simrak, M. D. Marsden, I. A. King, J. Arnemann, and R. S. Buxton. A YAC contig joining the desmocollin and desmoglein loci on human chromosome 18 and ordering of the desmocollin genes. Genomics 42:208-216, 1997

[118] A. Kljuic, R. C. Bauer, and A. M. Christiano. Genomic organization of mouse desmocollin genes reveals evolutionary conservation. DNA Seq. 15:148-152, 2004

[119] N. V. Whittock and C. Bower. Genetic evidence for a novel human desmosomal cadherin, desmoglein 4. J.Invest Dermatol. 120:523-530, 2003

[120] O. Huber. Structure and function of desmosomal proteins and their role in development and disease. Cell Mol.Life Sci. 60:1872-1890, 2003

[121] M. D. Marsden, J. E. Collins, M. D. Greenwood, M. J. Adams, T. P. Fleming, A. I. Magee, and R. S. Buxton. Cloning and transcriptional analysis of the promoter of the human type 2 desmocollin gene (DSC2). Gene 186:237-247, 1997

[122] D. R. Garrod, A. J. Merritt, and Z. Nie. Desmosomal cadherins. Curr.Opin.Cell Biol. 14:537-545, 2002

[123] N. A. Chitaev and S. M. Troyanovsky. Direct Ca2+-dependent heterophilic interaction between desmosomal cadherins, desmoglein and desmocollin, contributes to cell-cell adhesion. J.Cell Biol 138:193-201, 1997

[124] W. He, P. Cowin and D. L. Stokes. Untagling desmosomal knots with electron tomography. Science 302: 109-113, 2003

[125] K. Ishii, S. M. Norvell, L. J. Bannon, E. V. Amargo, L. T. Pascoe, and K. J. Green. Assembly of desmosomal cadherins into desmosomes is isoform dependent. J.Invest Dermatol. 117:26-35, 2001

[126] P. B. Cserhalmi-Friedman, J. A. Frank, W. Ahmad, A. A. Panteleyev, V. M. Aita, and A. M. Christiano. Structural analysis reflects the evolutionary relationship between the human desmocollin gene family members. Exp.Dermatol 10:95-99, 2001

[127] N. V. Whittock and C. Bower. Targetting of desmoglein 1 in inherited and acquired skin diseases. Clin.Exp.Dermatol. 28:410-415, 2003

[128] H. Wu, Z. H. Wang, A. Yan, S. Lyle, S. Fakharzadeh, J. K. Wahl, M. J. Wheelock, H. Ishikawa, J. Uitto, M. Amagai, and J. R. Stanley. Protection against pemphigus foliaceus by desmoglein 3 in neonates. N.Engl.J.Med 343:31-35, 2000

[129] L. Pulkkinen, Y. W. Choi, A. Simpson, X. Montagutelli, J. Sundberg, J. Uitto, and M. G. Mahoney. Loss of cell adhesion in Dsg3bal-Pas mice with homozygous deletion mutation (2079del14) in the desmoglein 3 gene. J.Invest Dermatol 119:1237-1243, 2002

[130] A. Kljuic, L. Gilead, A. Martinez-Mir, J. Frank, A. M. Christiano, and A. Zlotogorski. A nonsense mutation in the desmoglein 1 gene underlies striate keratoderma. Exp.Dermatol 12 :523-527, 2003

[131] E. Allen, Q. C. Yu, and E. Fuchs. Mice expressing a mutant desmosomal cadherin exhibit abnormalities in desmosomes, proliferation, and epidermal differentiation. J.Cell Biol 133:1367-1382, 1996

[132] J. A. McGrath and V. Wessagowit. Human hair abnormalities from inherited desmosome gene mutations. Keio J Med 54: 72-79, 2005

[133] R. L. Dusek, L. M. Godsel and K. J. Green. Discriminating roles of desmosomal cadherins: beyond desmosomal adhesion. Journal of desmatological science 45: 7-21, 2007

[134] T. M. Rowlands, J. M. Symonds, R. Farookhi, and O. W. Blaschuk. Cadherins: crucial regulators of structure and function in reproductive tissues. Rev.Reprod. 5:53-61, 2000

[135] S. K. Runswick, M. J. O'Haret, L. Jones, C. H. Streuli and D. R. Garrod. Desmosomal adhesion regulates epithelial morphogenesis and cell positioning. Nature cell biology 3: 823-830, 2001

[136] W. W. Franke, M. D. Goldschmidt, R. Zimbelmann, H. M. Mueller, D. L. Schiller and P. Cowin. Molecular cloning and aminoacid sequence of human plakoglobin, the common junctional plaque protein. PNAS 86: 4027-4031, 1989

[137] A. Schmidt, L. Langbein, M. Rode, S. Pratzel, R. Zimbelmann, and W. W. Franke. Plakophilins 1a and 1b: widespread nuclear proteins recruited in specific epithelial cells as desmosomal plaque components. Cell Tissue Res. 290:481-499, 1997

[138] M. A. Warren, A. Koshoffer, B. J. Aronow, A. G. Jegga, and R. Brackenbury. Structure of the 5' portion of the human plakoglobin gene. J.Invest Dermatol. 119:196-197, 2002

[139] P.Ruiz and W. Birchmeier. The plakoglobin knock-out mouse: a paradigm for the molecular analysis of cardiac cell junction formation. TMC. 8: 97 – 101. 1998

[140] C. M. Isac, P. Ruiz, B. Pfitzmaier, H. Haase, W. Birchmeier, and I. Morano. Plakoglobin is essential for myocardial compliance but dispensable for myofibril insertion into adherens junctions. J.Cell Biochem. 72:8-15, 1999

[141] R. Caldelari, A. de Bruin, D. Baumann, M. M. Suter, C. Bierkamp, V. Balmer, and E. Muller. A central role for the armadillo protein plakoglobin in the autoimmune disease pemphigus vulgaris. J.Cell Biol. 153:823-834, 2001

[142] M. Kofron, J. Heasman, S. A. Lang, and C. C. Wylie. Plakoglobin is required for maintenance of the cortical actin skeleton in early Xenopus embryos and for cdc42-mediated wound healing. J.Cell Biol. 158:695-708, 2002

[143] J. M. Merriam, A. B. Rubenstein, and M. W. Klymkowsky. Cytoplasmically anchored plakoglobin induces a WNT-like phenotype in Xenopus. Dev.Biol. 185:67-81, 1997

[144] A. Karnovsky and M. W. Klymkowsky. Anterior axis duplication in Xenopus induced by the over-expression of the cadherin-binding protein plakoglobin. Proc Natl Acad Sci 92: 4522-4526, 1995

[145] L. DeMarchis, C. Cropp, Z. M. Sheng, S. Bargo, and R. Callahan. Candidate target genes for loss of heterozygosity on human chromosome 17q21. Br.J.Cancer 91:1001, 2004

[146] H. Aberle, C. Bierkamp, D. Torchard, O. Serova, T. Wagner, E. Natt, J. Wirsching, C. Heidkamper, M. Montagna, H. T. Lynch, and . The human plakoglobin gene localizes on

chromosome 17q21 and is subjected to loss of heterozygosity in breast and ovarian cancers. Proc.Natl.Acad.Sci.U.S.A 92:6384-6388, 1995

[147] K. Caca, F. T. Kolligs, X. Ji, M. Hayes, J. Qian, A. Yahanda, D. L. Rimm, J. Costa, and E. R. Fearon. Beta- and gamma-catenin mutations, but not E-cadherin inactivation, underlie T-cell factor/lymphoid enhancer factor transcriptional deregulation in gastric and pancreatic cancer. Cell Growth Differ. 10:369-376, 1999

[148] R. A. Winn and L. E. Heasley. Gamma catenin expression is reduced or absent in a subset of human non-small cell lung cancers, and its re-expression inhibits cell growth. Chest 125: 122S-123S, 2004

[149] X-J Liang, D-W. Shen and M. M. Gottesman. Down-regulation and altered localization of γ-catenin in cisplatin-resistant adenocardinoma cells. Mol Pharmacol 65: 1217-1224, 2004

[150] D. Canes, G. J. Chiang, B. R. Billmeyer, C. A. Austin, M. Kosakowski, K. M. Rieger-Christ, J. A. Libertino and I. C. Summerhayes. Histone deacetylase inhibitors upregulate plakoglobin expression in bladder carcinoma cells and display antineoplastic activity in vitro and in vivo. Int J Cancer 113: 841-848, 2005

[151] J. S. Shim, D. H. Kim, and H. J. Kwon. Plakoglobin is a new target gene of histone deacetylase in human fibrosarcoma HT1080 cells. Oncogene 23:1704-1711, 2004

[152] M. Hatzfeld. Plakophilins: multifunctional proteins or just regulators of desmosomal adhesion? Biochimica et Biophysica Acta 1773: 69-77, 2007

[153] C. Mertens, C. Kuhn, and W. W. Franke. Plakophilins 2a and 2b: constitutive proteins of dual location in the karyoplasm and the desmosomal plaque. J.Cell Biol 135:1009-1025, 1996

[154] X. Chen, S. Bonne, M. Hatzfeld, F. van Roy, and K. J. Green. Protein binding and functional characterization of plakophilin 2. Evidence for its diverse roles in desmosomes and beta -catenin signaling. J.Biol.Chem 277:10512-10522, 2002

[155] A. Schmidt and S. Jager. Plakophilins-hard work in the desmosome, recreation in the nucleus. European Journal of Cell Biology 84: 189-204, 2005

[156] J. A. McGrath, J. R. McMillam, C. S. Shemanko, S. K. Runswick, I. M. Leigh, E. B. Lane, D. R. Garrod and R. A. Eady. Mutations in the plakophilin 1 gene result in ectodermal dysplasia/ skin fragility syndrome. Nat Genet 17: 240-244, 1997

[157]C. Mertens, I. Hofmann, Z. Wang, M. Teichmann, Chong S. Sepehri, M. Schnolzer, and W. W. Franke. Nuclear particles containing RNA polymerase III complexes associated with the junctional plaque protein plakophilin 2. *Proc.Natl.Acad.Sci.U.S.A* 98 (14):7795-7800, 2001

[158] M. Hatzfeld, C. Haffner, K. Schulze, and U. Vinzens. The function of plakophilin 1 in desmosome assembly and actin filament organization. J.Cell Biol 149:209-222, 2000

[159] S. Getsios, A. C. Huen, and K. J. Green. Working out the strength and flexibility of desmosomes. Nat.Rev.Mol.Cell Biol. 5:271-281, 2004

[160] M. L. Virata, R. M. Wagner, D. A. Parry, and K. J. Green. Molecular structure of the human desmoplakin I and II amino terminus. Proc.Natl.Acad.Sci.U.S.A 89:544-548, 1992

[161] P. A. Coulombe. A new fold on an old story: attachment of intermediate filaments to desmosomes. Nat.Struct.Biol. 9:560-562, 2002

[162] D. K. Armstrong, K. E. McKenna, P. E. Purkis, K. J. Green, R. A. Eady, I. M. Leigh, and A. E. Hughes. Haploinsufficiency of desmoplakin causes a striate subtype of palmoplantar keratoderma. Hum.Mol.Genet. 8:143-148, 1999

[163] N. V. Whittock, G. H. Ashton, P. J. Dopping-Hepenstal, M. J. Gratian, F. M. Keane, R. A. Eady, and J. A. McGrath. Striate palmoplantar keratoderma resulting from desmoplakin haploinsufficiency. J.Invest Dermatol. 113:940-946, 1999

[164] N. V. Whittock, H. Wan, S. M. Morley, M. C. Garzon, L. Kristal, P. Hyde, W. H. McLean, L. Pulkkinen, J. Uitto, A. M. Christiano, R. A. Eady, and J. A. McGrath. Compound heterozygosity for non-sense and mis-sense mutations in desmoplakin underlies skin fragility/woolly hair syndrome. J.Invest Dermatol. 118:232-238, 2002

[165] J. E. L. Cheong, V. Wessagowit and J. A. McGrath. Molecular abnormalities of the desmosomal protein desmoplakin in human disease. Clinical and experimental dermatology 30: 261-266, 2004

[166] G. I. Gallicano, P. Kouklis, C. Bauer, M. Yin, V. Vasioukhin, L. Degenstein, and E. Fuchs. Desmoplakin is required early in development for assembly of desmosomes and cytoskeletal linkage. J.Cell Biol. 143 (7):2009-2022, 1998.

[167] G. I. Gallicano, C. Bauer, and E. Fuchs. Rescuing desmoplakin function in extra-embryonic ectoderm reveals the importance of this protein in embryonic heart, neuroepithelium, skin and vasculature. Development 128:929-941, 2001

[168] V. Vasioukhin, E. Bowers, C. Bauer, L. Degenstein, and E. Fuchs. Desmoplakin is essential in epidermal sheet formation. Nat.Cell Biol. 3:1076-1085, 2001

[169] X. Zhou, A. Stuart, L. E. Dettin, G. Rodriguez, B. Hoel and G. I. Gallicano. Desmoplakin is required for microvascular tube formation in culture. Journal of Cell Science 117: 3129-3140, 2004

[170] E. L. Davies, J. M. Gee, R. A. Cochrane, W. G. Jiang, A. K. Sharma, R. I. Nicholson, and R. E. Mansel. The immunohistochemical expression of desmoplakin and its role in vivo in the progression and metastasis of breast cancer. Eur.J.Cancer 35:902-907, 1999

[171] J. J. Jefferson, C. L. Leung, and R. K. Liem. Plakins: goliaths that link cell junctions and the cytoskeleton. Nat.Rev.Mol.Cell Biol. 5:542-553, 2004

[172] A. Sonnenberg and R. K. H. Liem. Plakins in development and disease. Exp Cell Res, 2007 Epub ahead of print

[173] L. Pulkkinen and J. Uitto. Mutation analysis and molecular genetics of epidermolysis bullosa. Matrix Biol. 18:29-42, 1999

[174] H. Nakamura, D. Sawamura, M. Goto, G. Nakamura, J. R. McMillan, S. Park, S. Kono, S. Hasegawa, S. Paku, T. Nakamura, Y. Ogiso and H. Shimizu. Epidermolysis bullosa simplex associated with pyloric atresia is a novel clinical subtype caused by mutations in the plectin gene. J Mol Diagn 7: 28-356, 2005

[175] A. D. Irvine and W. H. I. McClean. Human keratin diseases: the increasing spectrum of disease and subtlety of the phenotype-genotype correlation. British Journal of Dermatology 140: 815-828, 1999

[176] J. M. Paramio and J. L. Jorcano. Beyond structure: do intermediate filaments modulate cell signalling? Bioessays 24:836-844, 2002

[177] E. Fuchs. Intermediate filaments and disease: mutations that cripple cell strength. J.Cell Biol. 125:511-516, 1994

[178] N. V. Whittock, F. J. Smith, H. Wan, R. Mallipeddi, W. A. Griffiths, P. Dopping-Hepenstal, G. H. Ashton, R. A. Eady, W. H. McLean, and J. A. McGrath. Frameshift mutation in the V2 domain of human keratin 1 results in striate palmoplantar keratoderma. J.Invest Dermatol. 118:838-844, 2002

[179] E. Fuchs and D. W. Cleveland. A structural scaffolding of intermediate filaments in health and disease. Science 279:514-519, 1998

[180] L. G. Goldfarb, P. Vicart, H. H. Goebel, and M. C. Dalakas. Desmin myopathy. Brain 127 (Pt 4):723-734, 2004.

[181] X. Wang, H. Osinska, A. M. Gerdes, and J. Robbins. Desmin filaments and cardiac disease: establishing causality. J.Card Fail. 8:S287-S292, 2002

[182] Z. Li, E. Colucci-Guyon, M. Pincon-Raymond, M. Mericskay, S. Pournin, D. Paulin, and C. Babinet. Cardiovascular lesions and skeletal myopathy in mice lacking desmin. Dev.Biol. 175:362-366, 1996

[183] J. P. van Tintelen, R. M. W. Hofstra, A. C. P. Wiesfeld, M. P. van den Berg, R. N. W. Hauer and J. D. H. Jongbloed. Molecular genetics of arrhythmogenic right ventricular cardiomyopathy: emerging horizon? Current opinion in cardiology 22: 185-192, 2007

[184] E. A. Bornslaeger, C. M. Corcoran, T. S. Stappenbeck, and K. J. Green. Breaking the connection: displacement of the desmosomal plaque protein desmoplakin from cell-cell interfaces disrupts anchorage of intermediate filament bundles and alters intercellular junction assembly. J.Cell Biol. 134:985-1001, 1996

[185] K. Lapouge, L. Fontao, M. F. Champliaud, F. Jaunin, M. A. Frias, B. Favre, D. Paulin, K. J. Green and L. Borradori. New insights into the molecular basis of desmoplakin- and desmin-related cardiomyopathies. Journal of cell science 119: 4974-4985, 2006

[186] S. Sen-Chowdhry, P. Syrris and W. J. McKenna. Genetics of right ventricular cardiomyopathy. J. Cardiovasc Electrophysiol 16: 927-935, 2005

[187] L. Fontao, B. Favre, S. Riou, D. Geerts, F. Jaunin, J. H. Saurat, K. J. Green, A. Sonnenberg, and L. Borradori. Interaction of the bullous pemphigoid antigen 1 (BP230)

and desmoplakin with intermediate filaments is mediated by distinct sequences within their COOH terminus. Mol.Biol.Cell 14:1978-1992, 2003

[188] H. Wan, P. J. Dopping-Hepenstal, M. J. Gratian, M. G. Stone, G. Zhu, P. E. Purkis, A. P. South, F. Keane, D. K. Armstrong, R. S. Buxton, J. A. McGrath, and R. A. Eady. Striate palmoplantar keratoderma arising from desmoplakin and desmoglein 1 mutations is associated with contrasting perturbations of desmosomes and the keratin filament network. Br.J.Dermatol. 150:878-891, 2004

[189] N. Satoh and T. Deno. Periodic appearance and disappearance of microvilli associated with cleavage cycles in the egg of the ascidian, Halocynthia roretzi. Dev Biol 102: 488-92, 1984

[190] I. Hofmann, C. Mertens, M. Brettel, V. Nimmrich, M. Schnolzer and H. Herrmann. Interaction of plakophilins with desmoplakin and intermediate filament proteins: an in vitro analysis. J Cell Sci. 113: 2471-83, 2000

[191] S. Hatsell and P. Cowin. Deconstructing desmoplakin. Nature cell biology 3: E270-E272, 2001

[192] E. Charpentier, R. M. Lavker, E. Acquista, and P. Cowin. Plakoglobin suppresses epithelial proliferation and hair growth in vivo. J.Cell Biol. 149:503-520, 2000

[193] M. F. Jonkman, A. M. Pasmooij, S. G. Pasmans, M. P. van den Berg, H. J. Ter Horst, A. Timmer, and H. H. Pas. Loss of desmoplakin tail causes lethal acantholytic epidermolysis bullosa. Am J Hum Genet 77: 653-60, 2005

[194] M. Norman, M. Simpson, J. Mogensen, A. Shaw, S. Hughes, P. Syrris, S. Sen-Chwdhry, E. Rowland, A. Crosby and W. J. McKenna. Novel mutation in desmoplakin causes arrhythmogenic left ventricular cardiomyopathy. Circulation 112: 636-642, 2005

[195] A. Uzumcu, E. E. Norgett, A. Dindar, O. Uyguner, K. Nisli, H. Kayserili, S. E. Sahin, E. Dupont, N. J. Severs, I. M. Leigh, M. Yuksel-Apak, D. P. Klesell and B. Wollnik. Loss of desmoplakin isoform I causes early onset cardiomyopathy and heart failure in a Naxos-like syndrome. J. Med Genet 43: e5-e13, 2006

[196] Z. Yang, N. E. Bowles, S. E. Scherer, M. D. Taylor, D. L. Kearney, S. Ge, V. V. Nadvoretskiy, G. DeFreitas, B. Carabello, L. I. Brandon, L. M. Godsel, K. J. Green, J. E. Saffitz, H. Li, G. A. Danieli, H. Calkins, F. Marcus and J. A. Towbin. Desmosomal dysfunction due to mutations in desmoplakin causes arrhythmogenic right ventricular dysplasia/ cardiomyopathy. Circ Res 99: 646-655, 2006

[197] P. Syrris, D. Ward, A. Asimaki, S. Sen-Chowdhry, H. Y. Ebrahim, A. Evans, N. Hitomi, M. Norman, A. Pantazis, A. L. Shaw, P. M. Elliott and W. J. McKenna. Clinical expression of plakophilin-2 mutations in familial arrhythmogenic right ventricular cardiomyopathy. Circulation 113: 356-364, 2006

[198] L. Antoniades, A. Tsatsopoulou, A. Anastasakis, P. Syrris, A. Asimaki, D. Panagiotakos, C. Zambartas, C. Stefanadis, W. J. McKenna and N. Protonotarios. Arrhythmogenic right

ventricular cardiomyopathy caused by deletions in plakophilin-2 and plakoglobin (Naxos disease) in families from Greece and Cyprus: genotype-phenotype relations, diagnostic features and prognosis. European Heart Journal 27: 2208-2216, 2006

[199] A. P. Kowalczyk, M. Hatzfield, E. A. Bornslaerger, D. S. Kopp, J. E. Borgwardt, C. M. Corcoran, A. Settler and K. J. Green. The head domain of plakophilin-1 binds to desmoplakin and enhances its recruitment to desmosomes. The Journal of Biological Chemistry 274: 18145-18148, 1999

[200] D. Dalal, L. Molin, J. Piccini, C. Tichnell, C. James, C. Bomma, K. Prakasa, J. A. Towbin, F. I. Marcus, P. J. Spevak, D. A. Bluemke, T. Abraham, S. D. Russell, H. Calkins and D. P. Judge. Clinical features of arrhythmogenic right ventricular dysplasia/cardiomyopathy associated with mutations in plakophilin-2. Circulation 113: 1641-1649, 2006

[201] P. J. Kannankeril, Z. A. Bhuiyan, D. Darbar, M. M. A. M. Manners, A. A. M. Wilde and D. M. Roden. Arrhythmogenic right ventricular cardiomyopathy due to a novel plakophilin 2 mutation: wide spectrum of disease in mutation carriers within a family. Heart Rhythm 3: 939-944, 2006

[202] I. Nagaoka, K. Matsui, T. Ueyama, M. Kanemoto, J. Wu, A. Shimizu, M. Matsuzaki and M. Horie. Novel mutation of plakophilin-2 associated with arrhythmogenic right ventricular cardiomyopathy. Circ J 70: 933-936, 2006

[203] J. P. Van Tintelen, M. M. Entius, Z. A. Bhuiyan, R. Jongbloed, A. C. P. Wiesfeld, A. A. M. Wildre, J. van der Smagt, L. G. Boven, M. M. A. M. Manners, I. M. van Langen, R. M. W. Hofstra, L. C. Otterspoor, P. A. F. M. Doevendans, L. M. Rodriguez, I. C. van Gleder and R. N. W. Hauer. Plakophilin-2 mutations are the major determinant of familial arrhythmogenic right ventricular dysplasia/ cardiomyopathy. Circulation 113: 1650-1658, 2006

[204] P. Syrris, D. Ward, A. Asimaki, A. Evans, S. Sen-Chowdhry, S. E. Hughes and W. J. McKenna. Desmoglein-2 mutations in arrhythmogenic right ventricular cardiomyopathy: a genotype-phenotype characterization of familial disease. European Heart Journal 28: 581-588, 2007

[205] Kozak M. Emerging links between initiation of translation and human diseases. Mamm Genome 13: 401-410, 2002

[206] K. Pilichou, A. Nava, C. Basso, G. Beffagna, B. Bauce, A. Lorenzon, G. Frigo, A. Vettori, M. Valente, J. Towbin, G. Theien, G. A. Daniele and A. Rampazzo. Mutations in desmoglein-2 gene are associated with arrhythmogenic right ventricular cardiomyopathy. Circulation 113: 1171-1179, 2006

[207] M. M. Awad, D. Dalal, E. Cho, N. Amat-Alarcon, C. James, C. TIchnell, A. Tucker, S. D. Russell, D. A. Bluemke, H. C. Dietz, H. Calkins and D. P. Judge. DSG2 mutations contribute to arrhythmogenic right ventricular dysplasia/cardiomyopathy. The American journal of human genetics 79: 136-142, 2006

[208] P. Syrris, D. Ward, A. Evans, A. Asimaki, E. Gandjbakhch, S. Sen-Chowdhry and W. J. McKenna. Arrhythmogenic right ventricular dysplasia/cardiomyopathy associated with mutations in the desmosomal gene desmocollin2. The American Journal of Human Genetics 79: 978-984, 2006

[209] T. Hashimoto, C. Kiyokawa, O. Mori, M. Miyasato, M. A. Chidgey, D. R. Garrod, Y. Kobayashi, K. Komori, K. Ishii, M. Amagai and T. Nishikawa. Human desmocollin 1 (Dsc1) is an autoantigen for the subcorneal pustular dermatosis type of IgA pemphigus. J Invest Dermatol 109: 127-131, 1997

[210] D. R. Garrod, A. J. Merritt and Z. Nie. Desmosomal adhesion: structural basis, molecular mechanism and regulation. Mol Membr Biol 19: 81-94, 2002

[211] S. M. Troyanovsky, R. B. Troyanovsky, L. G. Eshkind,. R.E. Leube and W. W. Franke. Identificatiojn of amino acid sequence motifs in desmocollin, a desmosomal glycoprotein, that are required for plakoglobin binding and plaque formation. Proc Natl Acad Sci USA 91: 10790-10794, 1994

[212] V. Kimonis, J. J. DiGiovanna, J. M. Yang, S. Z. Doyle, S. J. Bale and J. G. Compton. A mutation in the V1 end domain of keratin 1 in non-epidermolytic palmar-plantal keratoderma. J. Invest Dermatol 103: 764-769, 1994

[213] K. Y. Park, M. C. Dalakas, C. Semino-Mora, H. S. Lee, S. Litvak, K. Takeda, V. J. Ferrans, and L. G. Goldfarb. Sporadic cardiac and skeletal myopathy caused by a de novo desmin mutation. Clin.Genet. 57:423-429, 2000

[214] A. Kaminska, S. V. Strelkov, B. Goudeau, M. Olive, A. Dagvadorj, A. Fidzianska, M. Simon-Casteras, A. Shatunov, M. C. Dalakas, I. Ferrer, H. Kwiecinski, P. Vicart, and L. G. Goldfarb. Small deletions disturb desmin architecture leading to breakdown of muscle cells and development of skeletal or cardioskeletal myopathy. Hum.Genet. 114:306-313, 2004

[215] L. G. Goldfarb, K. Y. Park, L. Cervenakova, S. Gorokhova, H. S. Lee, O. Vasconcelos, J. W. Nagle, C. Semino-Mora, K. Sivakumar and M. C. Dalakas. Missense mutations in desmin associated with familial cardiac and skeletal myopathy. Nature Genetics 19: 402-403, 1998

[216] M. C. Dalakas, A. Dagvadorj, B. Goudeau, K. Y. Park, K. Takeda, M. Simon-Casteras, O. Vasconcelos, N. Sambuughin, A. Shatunov, J. W. Nagle, K. Sivakumar, P. Vicart and L. G. Goldfarb. Progressive skeletal myopathy, a phenotypic variant of desmin myopathy associated with desmin mutation. Neuromuscular disorders 13: 252-258, 2003

[217] D. Li, T. Tapscoft, O. Gonzalez, P. E. Burch, M. A. Quinones, W. A. Zoghbi, R. Hill, L. L. Bachinski, D. L. Mann, and R. Roberts. Desmin mutation responsible for idiopathic dilated cardiomyopathy. Circulation 100:461-464, 1999

[218] K. Y. Park, M. C. Dalakas, C. Semino-Mora, H. S. Lee, S. Litvak, K. Takeda, V. J. Ferrans, and L. G. Goldfarb. Sporadic cardiac and skeletal myopathy caused by a de novo desmin mutation. Clin.Genet 57:423-429, 2000

[219] N. E. Bowles, S. Jimenez, M. Vatta, M. Chrisco, J. Szmuszkoviez and Y. Capetanaki. Familial restrictive cardiomyopathy caused by a missense mutation in the desmin gene. Pediatric Res 51 Suppl: 2, 2002

[220] B. Goudeau, F. Rodrigues-Lima, D. Fischer, M. Casteras-Simon, N. Sambuughin, M. de Visser, P. Laforet, X. Ferrer, F. Chapon, G. Sjöberg, A. Kostareva, T. Sejersen, M. C. Dalakas, L. G. Goldfarb and P. Vicart. Varying pathogenic potentials of mutations localted in the desmin alpha-helical domains. Hum Mutat 27: 906-913, 2006

[221] A. Melberg, A. Oldfors, C. Blomstrom-Lundqvist, E. Stalberg, B. Carlsson, E. Larsson, C. Lidell, K. E. Eeg-Olofsson, G. Wikstrom, K. G. Henriksson, and N. Dahl. Autosomal dominant myofibrillar myopathy with arrhythmogenic right ventricular cardiomyopathy linked to chromosome 10q. Ann.Neurol 46:684-692, 1999

[222] S. L. Van Driest, V. C. Vasile, S. R. Ommen, M. L. Will, A. J. Tajik, B. J. Gersh and M. J. Ackerman. Myosin binding protein C mutations and compound heterozygosity in hypertrophic cardiomyopathy. J Am Coll Cardiol 44: 1903-1910, 2004

[223] R. H. Lekanne Deprez, J. J. Muurling Vlietman, J. Hruda. M. J. Baars, L. C. Wijnaendts. I. Stolte Dijkstra. M. Alders and J. M. Van Hagen. Two cases of severe neonatal hypertrophic cardiomyopathy caused by compound heterozygous mutations in the MYBPC3 gene. J. Med Genet 43: 829-832, 2006

[224] A. F. Wright. A searchlight through the fog. Nat Genet 17: 132-134, 1997

[225] J. A. McGrath. Inherited disorders of desmosomes. Australasian Journal of Dermatology 46: 221-229, 2005

[226] S.R.Kaplan, J.J.Gard, N.Protonotarios, A.Tsatsopoulou, C.Spiliopoulou, A.Anastasakis, C.P.Squarcioni, W.J.McKenna, G.Thiene, C.Basso, N.Brousse, G.Fontaine and J.E.Saffitz. Remodeling of myocyte gap junctions in arrhythmogenic right ventricular cardiomyopathy due to a deletion in plakoglobin (Naxos disease). Heart Rhythm 1: 3-11, 2004

[227] J. E. Saffitz, K. G. Green, W. J. Kraft, K. B. Schechtman and K. A. Yamada. Effects of diminished expression of connexin43 on gap junction number and size in ventricular myocardium. Am J Physiol Heart Circ Physiol 278: H1662-H1670, 2000

[228] C. Basso and G. Thiene. Adipositas cordis, fatty infiltration of the right ventricle and arrhythmogenic right ventricular cardiomyopathy. Just a matter of fat? Cardiovascular pathology 14: 37-41, 2005

[229] C. Kawai, A. Matsumori and K. Kawamura. Myocardial biopsy. Annu Rev Med 31: 139-157, 2000

[230] C. Basso, G. Thiene, D. Corrado, A. Angelini, A. Nava and M. Valente. Arrhythmogenic right ventricular cardiomyopathy: dysplasia, dystrophy or myocarditis? Circulation 94: 983-991, 1996

[231] G. Thiene and C. Basso. Arrhythmogenic right ventricular cardiomyopathy: an update. Cardiovascular pathology 10: 109-111, 2001

[232] A. P. Burke, A. Farb, G. Tashko and R. Virmani. Arrhythmogenic right ventricular cardiomyopathy and fatty replacement of the right ventricular myocardium. Circulation 97: 1571-1580, 1998

[233] A. P. Burke, D. Robinson, S. Radentz, J. Smialek and R. Virmani. Sudden death in right ventricular dysplasia withminimal gross abnormalities. J Forensic Science 44: 438-443, 1999

[234] G. D'Amati, P. Leone, C. R. Tiziana di Gioia, C. Magelli, G. Arpesella, P. Grillo, B. Marion , F. Fiore and P. Gallo. Arrhythmogenic right ventricular cardiomyopathy: clinicopathologic correlation based on a revised definition of pathologic patterns. Hum Pathol 32: 1078-1086, 2001

[235] D. K. Tansey, Z. Aly and M. N. Sheppard. Fat in the right ventricle of the normal heart. Histopathology 46: 98-104, 2005

[236] A. Fletcher, S. Y. Ho, K. P. McCarthy and M. N. Sheppard. Spectrum of pathological changes in both ventricles of patients dying suddenly with arrhythmogenic right ventricular dysplasia. Relation of changes to age. Histopathology 48: 445-452, 2006

[237] G. Fontaine, F. Fontaliran and R. Frank. Arrhythmogenic right ventricular cardiomyopathies; clinical forms and main differential diagnoses. Circulation 97: 1532-1535, 1998

[238] F. Calabrese, C. Bassom, E. Carturan, M. Valente and G. Thiene. Arrhythmogenic right ventricular cardiomyopathy/dysplasia: is there a role for viruses? Cardiovascular patholohy 15: 11-17, 2006

[239] B. F. Hoffman, S. J. Feinmark and S. D. Guo. Electrophysiologic effects of interactions between activated canine neutrophils and cardiac myocytes. J. Cardiovascular Electrophysiology 8: 679-687, 1997

[240] G. Fontaine, P. Fornes and F. Fontaliran. Myocarditis as a cause of sudden death. Circulation 103: e12, 2001

[241] G. D'Amati, C. R. T. di Gioia, C. Giordano and P. Gallo. Myocyte transdifferentiation: a passible pathogenetic mechanism for arrhythmogenic right ventricular cardiomyopathy. Arch Pathol Lab Med 124: 287-290, 2000

[242] T. N. James, M. M. Nichols, D. W. Sapire, P. L. DiPatre and S. M. Lopez. Complete heart block and fatal right ventricular failure in an infant. Circulation 93: 1588-1600, 1996

[243] D. Wencker, M. Chandra, K. Nguen, W. Miao, S. Garantziotis, S. M. Factor, J. Shirani. R. C. Armstrong and R. N. Kitsis. A mechanistic role for cardiac myocyte apoptosis in heart failure. J. Clin Invest 111: 1497-1504, 2003

[244] T. Nishikawa, S. Ishiyama, M. Nagata, Y. Sakomura, M. Nakazawa, K. Momma, M. Hiroe and T. Kasajima. Programmed cell death in the myocardium of arrhythmogenic right

ventricular cardiomyopathy in children and adults. Cardiovascular pathology 8: 185-189, 1999

[245] Q. Chu, D. T. Lee, S. W. Tsao, X. Wang and Y. C. Wong. S-allylcysteine, a water soluble garlic derivative, suppresses the growth of a human androgen-independent prostate cancer xenograft, CWR22R, under in vivo conditions. BJU Int 99: 925-932, 2007

[246] J. Kanitakis. Anatomy, histology and immunohistochemistry of normal human skin. Eur Journal of Dermatology 12: 390-399, 2002

[247] J. E. Lewis, J. K. Wahl, K. M. Sass, P. J. Jensen, K. R. Johnson and M. J. Wheelock. Cross talk between adherens junctions and desmosomes depends on plakoglobin. J. Cell Biol 136: 919-934, 1997

[248] I. Hoffman, C. Mertens, M. Brettel, V. Nimmrich, M. Schnolzer and H. Herrman. Interaction of plakophilins with desmoplakin and intermediate filament proteins: an in vitro analysis. Journal of Cell Science 113: 2471-2483, 2000

[249] T. Yin, S. Getsios, R. Caldelari, L. M. Godsel, A. P. Kowalczyk, E. J. Muller and K. J. Green. Mechanisms of plakoglobin-dependent adhesion: desmosome specific functions in assembly and regulation by epidermal growth factor receptor. The journal of biological chemistry 280: 40355-40363, 2005

[250] E. A. Bornslaeger, L. M. Godsel, C. M. Corcoran, J. K. Park, M. Hatzfeld, A. P. Kowalczyk and K. J. Green. Plakophilin1 interferes with plakoglobin binding to desmoplakin, yet together with plakoglobin promotes clustering of desmosomal plaque complexes at cell-cell borders. Journal of cell science 114: 727-738, 2000

[251] M. Mathur, L. Goodwin and P. Cowin. Interactions of the cytoplasmic domain of the desmosomal cadherin Dsg1 with plakoglobin. J. Biol Chem 269: 14075-14080, 1994

[252] S. E. Syed, B. Trinnaman, S. Martin, S. Major, J. Hutchinson and A. I. Magee. Molecular interactions between desmosomal cadherins, Biochem J 362: 317-327, 2002

[253] C. Marcozzi, I. D. J. Burdett, R. S. Buxton and A. I. Magee. Coexpression of both types of desmosomal cadherin and plakoglobin confers strong intercellular adhesion. Journal of Cell science 111: 495-509, 1998

[254] P. Navaroo, E. Lozano and A. Cano. Expression of E- or P-cadherin is not sufficient to modify the morphology and the tumorigenic behavior of murine spindle carcinoma cells: possible involvement of plakoglobin. Journal of Cell science 105: 923-934, 1993

[255] H. J. Choi, S. Park-Snyder, L. T. Pascoe, K. J. Green and W. I. Weis. Structures of two intermediate filament-binding fragments of desmoplakin reveal a unique repeat motif structure. Nature structural biology 9: 612-620, 2002

[256] A. P. Kowalczyk, E. A. Bornslaeger, J. E. Borgwardt, H. L. Palka, A. S. Dhaliwal, C. M. Corcoran, M. F. Denning and K. J. Green. The amino-terminal domain of desmoplakin binds to plakoglobin and clusters desmosomal cadherin-plakoglobin complexes. J Cell Biol 139: 773-84, 1997

[257] J. E. Saffitz. Adhesion molecules: why are they important to the electrophysiologist? J Cardiovasc Electrophysiol, 17: 225-229, 2006

[258] H. Yamasaki, M. Mestril, Y. Omori, N. Mironov and V. Krutovskikh. Intercellular communication and carcinogenesis. Mutat Res 333: 181-188, 1995

[259] J. E. Trosko and R. J. Ruch. Cell-cell communication in carcinogenesis. Front Biosci 15: 208-236, 1998

[260]C. Zuppinger, M. C. Schaub and H. M. Eppenberger. Dynamics of early contact formation in cultured adult rat cardiomyocytes studied by N-cadherin fused to green fluorescent protein. J. Mol Cell Cardiol 32: 539-555, 2000

[261] J. E. Saffitz, K. G. Green, W. J. Kraft, K. B. Schechtman and K. A. Yamada. Effects of diminished expression of connexin43 on gap junction number and size in ventricular myocardium. Am J Physiol Heart Circ Physiol 278: H1662-1670, 2000

[262] J. E. Saffitz, R. B. Schuessler and K. A. Yamada. Mechanisms of remodelling of gap junction distributions and the development of anatomic substrates for arrhythmias. Cardiovascular research 42: 309-317, 1999

[263] M. J. T. DeBakker, F. J. L. van Capelle, M. J. Janse, S. Tasserron, J. T. Vermeulen, N. de Jonge and J. R. Lahpor. Slow conduction in the infracted human heart. Zig-zag course of activation. Circulation 88: 915-926, 2993

[264] N. S. Peters, J. Coromilas, N. J. Secers and A. L. Wit. Disturbed connexin43 gap junction distribution correlated with the location of reentrant circuits in the epicardial border zone of healing canine infarcts that cause ventricular tachycardia. Circulation 95: 988-996, 1997

[265] B. C. Eloff, D. L. Lerner, K. A. Yamada, R. B. Shuessler, J. E. Saffitz and D. S. Rosenbaum. High resolution optical mapping reveals conduction slowing in connexin43 deficient mice. Cardiovasc Res 51: 681-690, 2001

[266] D. L. Lerner, K. A. Yamada, R. B. Shuessler and J. E. Saffitz. Accelerated onset and increased incidence of ventricular arrhythmias induced by ischemia in Cx43-deficient mice. Circulation 101: 547-552, 2000

[267] J. Li, V. V. Patel and G. L. Radice. Dysregulation of cell adhesion proteins and cardiac arrhythmogenesis. Clinical medicine and research 4: 42-52, 2006

[268] T. Wichter, M. Schafers, C. G. Rhodes, M. Borggrefe, H. Lerch, A. L. Mammertsma, F. Hermansen, O. Schober, G. Breithardt and P. G. Camici. Abnormalities of cardiac sympathetic innervation in arrhythmogenic right ventricular cardiomyopathy. Circulation 101: 1552-1558, 2000

[269] T. Wichter, G. Hindricks, H. Lerch, P. Bartenstein, M. Borggrefe, O. Schober and G. Breithardt. Regional myocardial sympathetic dysinnervation in arrhythmogenic right ventricular cardiomyopathy. Circulation 89: 667-683, 1994

[270] M. Kretz, K. Maass and K. Willecke. Expression and function of connexins in the epidermis, analysed with transgenic mouse mutants. Eur J Cell Biol 83: 647-654, 2004

[271] P. R. Holden, B. McGuire, A. Stoler, A. Balmain and J. D. Pitts. Changes in gap junctional intercellular communication in mouse skin carcinogenesis. Carcinogenesis 18: 15-21, 1997

[272] K. Maass, A. Ghanem, J. S. Kim, M. Shaathoff, S. Urschel, G. Kirfel, R. Grummer, M. Kretz, T. Lewalter, K. Tiemann, E. Winterhager, V. Herzog and K. Willecke. Defective epidermal barrier in neonatal mice lacking the C-terminal region of connexin43. Mol Biol Cell 15: 4597-4608, 2004

[273] R. Sepp, N. J. Severs and R. G. Gourdie. Altered patterns of cardiac intercellular junction distribution in hypertrophic cardiomyopathy. Heart 76: 412, 417, 1996

[274] X. Chen and Y. Zhang. Myocardial Cx43 expression in the cases of sudden death due to dilated cardiomyopathy. Forensic Sci Int 162: 170-173, 2006

[275] R. Schulz and G. Heusch. Connexin43 and ischemic preconditioning. Cardiovas Res 62: 335-344, 2004

[276] H. Haegel, L. Larue, M. Ohsugi L. Fedorov, K. Herrenknecht and R. Kemler. Lack of beta-catenin affects mouse development at gastrulation. Development 121: 3529-3537, 1995

[277] J. Zhurinsky, M. Shtutman and A. Ben-Ze'ev. Plakoglobin and beta-catenin: protein interactions, regulation and biological roles. Journal of Cell Science 113: 3127-3139, 2000

[278] C. Bierkamp, H. Schawarz, O. Huber and R. Kemler. Desmosomal localization of beta-catenin in the skin of plakoglobin-null mutant mice. Development 126: 371-381, 1999

[279] J. Zhou, J. Qu, X. P. Ti, K. Graber, L. Huber, X. Wang, A. M. Gerder and F. Li. Upregulation of gamma-catenin compensated for the loss of beta-catenin in adult cardiomyocytes. Am J Physiol Heart Circ Physiol 292: H270-H276, 2007

[280] J. Travis. Old drug, new hope for Marfan syndrome. Science 312: 36-37, 2006

[281] R. B. Troyanovsky, N. A. Chitaev and S. M. Troyanovsky. Cadherin binding sites of plakoglobin: localization, specificity and role in targeting to adhering junctions. Journal of Cell Science 109: 3069-3078, 1996

[282] N. A. Chitaev, R. E. Leube, R. B. Troyanovsky, L. G. Eshkind, W. W. Franke and S. M. Troyanovsky. The binding of plakoglobin to desmosomal cadherins: patterns of binding sites and topogenic potential. The journal of cell biology 133: 359-369, 1996

[283] L. L. Witcher, R. Collins, S. Puttagunta, S. E. Mechanic, M. Munson, B. Gumbiner and P. Cowin. Desmosomal cadherin binding domains of plakoglobin. The journal of biological chemistry 271: 10904-10909, 1996

[284] P. A. Sacco T. M. McGranahan, M. J. Wheelock and K. R. Johnson. Identification of plakoglobin domains required for association with N-cadherin and a-catenin. The journal of biological chemistry 270: 20201-20206, 1995

[285] J. K. Wahl, P. A. Sacco, T. M. McGranahan-Sadler, L. M. Sauppe, M. J. Wheelock and K. R. Johnson. Plakoglobin domains that define its association with the desmosomal cadherins and the classical cadherins: identification of unique and shared domains. Journal of Cell science 109: 1143-1154, 1996

[286] H. L. Palka and K. J. Green. Roles of plakoglobin end domains in desmosome assembly. Journal of Cell Science 110: 2359-2371, 1997

[287] J. P. Anderson, E. Dodou, A. B. Heidt, S. J. De Val, E. J. Jaehnig, S. B. Greene, E. N. Olson and B. L. Black. HRC is a direct transcriptional target of MEF2 during cardiac, skeletal and arterial smooth muscle development in vivo. Molecular and cellular biology 24: 3757-3768, 2004

[288] D. A. Arvanitis, E. Vafiadaki, G. C. Fan, B. A. Mitton, K. N. Gregory, F. Del Monte, A. Kontrogianni-Konstantopoulos, D. Sanoudou and E. G. Kranias. The histidine rich calcium binding protein interacts with sarcoplasmic reticulum calcium ATPase. Am J Physiol Heart Circ Physiol, Epub ahead of print, 2007

[289] H. Milting, N. Lukas, B. Klauke, R. Korfer, A. Perrot, K. J. Osterziel, J. Vogt, S. Peters, R. Thieleczek and M. Varsanyi. Composite polymorphisms in the ryanodine receptor 2 gene associated with arrhythmogenic right ventricular tachycardia. Cardiovascular research 71: 496-505, 2006

[290] T. Kumagai, T. Miki, M. Kikucki, T. Fukuda, N. Miyasaka, R. Kamiyama and S. Hirosawa. The proto-oncogene Bcl6 inhibits apoptotic cell death in differentiation-induced mouse myogenic cells. Oncogene 18: 467-475, 1999

[291] O. Albagli-Curiel. Ambivalent role of BCL6 in cell survival and transformation. Oncogene 22: 507-516, 2003

[292] N. Weisleder, G. E. Taffet and Y. Capetanaki. Bcl-2 overexpression corrects mitochondrial defects and ameliorates inherited desmin null cardiomyopathy. PNAS 101: 769-774, 2004

[293] S. Hakimelahi, H. R. Parker, A. J. Gilchrist, M. Barry, Z. Li, R. C. Bleackley and M. Pasdar. Plakoglobin regulates the expression of the anti-apoptotic protein BCL-2. The journal of biological chemistry 275: 10905-10911, 2000

[294] E. Sadot, I. Simcha, K. Iwai, A. Ciechanover, B. Geiger and A. Ben-Ze'ev. Differential interaction of plakoglobin and beta-catenin with the ubiquitin-proteasome system. Oncogene 19: 1992-2000, 2000

[295] R. S. Haltiwanger, G. D. Holt and G. W. Hart. Enzymatic addition of O-GlcNAc to nuclear and cytoplasmic proteins. The journal of biological chemistry 265: 2563-2568, 1990

[296] R. S. Haltiwanger, M. A. Blomberg and G. W. Hart. Glycosylation of nuclear and cytoplasmic proteins. The journal of biological chemistry 267: 9005-9013, 1992

[297] S. Hatsell, L. Medina, J. Merola, R. Haltiwanger and P. Cowin. Plakoglobin is O-glycosylatged close to the N-terminal destruction box. The journal of biological chemistry 278: 37745-37752, 2003

[298] S. R. Powell. The ubiquitin-proteasome system in cardiac physiology and pathology. Am J Physiol Heart Circ Physiol 291: 1-19, 2006

[299] H. Aberle, A. Bauer, J. Stappert, A. Kispert and R. Kemler. B-catenin is a target for the ubiquitin-proteasome pathway. The EMBO Journal 16: 3797-3804, 1997

[300] J. T. Winston, P. Strack, P. Beer-Romero, C. Y. Chu, S. J. Elledge and J. W. Harper. The $SCF^{\beta\text{-}TRCP}$ –ubiquitin ligase complex associated specifically with phosphorylated destruction motifs in IkBa and β-catenin and stimulates IkBa ubiquitination in vitro. Genes & Development 13: 270-283, 1999

[301] C. Liu, Y. Li, M. Semenov, C. Han, G-H. Baeg, Y. Tan, Z. Zhang, X. Lin and X. He. Control of β-catenin phosphorylation/degradation by a dual-kinase mechanism. Cell 108: 837-847, 2002

[302] M. Kitagawa, S. Hatakeyama, M. Shirane, M. Matsumoto, N. Ishida, K. Hattori, I. Nakamichi, A. Kikuchi, K. Nakayama and K. Nakayama. An F-box protein, FWD1, mediates ubiquitin-dependent proteolysis of β-catenin. The EMBO Jounral 18: 2401-2410, 1999

[303] M. Hart, J-P. Concordet, I. Lassot, I. Albert, R. del los Santos, H. Durnad, C. Perret, B. Rubinfeld, F. Margottin, R. Benarous and P. Polakis. The F-box protein β-TRCP associated with phosphorylated β-catenin and regulates its activity in the cell. Current biology 9: 207-210, 1999

[304] E. Sdot, M. Conacci-Sorrell, J. Zhurinsky, D. Shnizer, Z. Lando, D. Zharhary, Z. Kam, A. Ben-Ze'ev and B. Geiger. Regulation of S33/S37 phosphorylated β-catenin in normal and transformed cells. Journal of cell science 115: 2771-2780, 2002

[305] D. Salomon, P. A. Sacco, S. G. Roy, I. Simcha, K. R. Johnson, M. J. Wheelock and A. Ben-Ze'ev. Regulation of β-catenin levels and localization by over-expression of plakoglobin and inhibition of the ubiquitin-proteasome system. The journal of cell biology 139: 1325-1335, 1997

[306] C. A. Gaudry, H. L. Palka, R. L. Dusek, A. C. Huen, M. J. Khandekar, L. G. Hudson and K. J. Green. Tyrosine-phosphorylated plakoglobin is associated with desmogleins but not desmoplakin after epidermal growth factor receptor activation. The journal of biological chemistry 276: 24871-24880, 2001

[307] J. R. Miller and R. T. Moon. Signal transduction through β-catenin and specification of cell fate during embryogenesis. Genes & development 10: 2527-2539, 1996

[308] P. Polakis. The oncogenic activation of β-catenin. Current opinion in genetics & development 9: 15-21, 1999

[309] P. Polakis. Wnt signaling and cancer. Genes & Development 14: 1837-1851, 2000

[310] H. Wan, A. P. South, I. R. Hart. Increased keratinocyte proliferation initiated through downregulation of desmoplakin by RNA interference. Experimental Cell Research 313: 2336-2344, 2007

[311] S. Polychronopoulou, A. Tsatsopoulou, S. I. Papadhmitriou, J. P. Panagiotou, A. Anastasakis, G. Paterakis, D. Anagnostou, N. Protonotarios and S. A. Haidas. Myelodysplasia and Naxos disease: a novel pathogenetic association? Leukemia 16: 2335-2337, 2002

[312] R. L. Dusek, L. M. Godsel, F. Chen, A. M. Strohecker, S. Getsios, R. Harmon, E. J. Muller, R. Caldelari, V. L. Cryns and K. J. Green. Plakoglobin deficiency protects keratinocytes from apoptosis. Journal of investigative dermatology 127: 792-801, 2007

[313] E. Garcia-Gras, R. Lombardi, M. J. Giocondo, J. T. Willerson, M. D. Schneider, D. S. Khoury and A. J. Marian. Suppression of canonical Wnt/β-catenin signaling by nuclear plakoglobin recapitulated phenotype of arrhythmogenic right ventricular cardiomyopathy. Journal of Clinical investigation 116: 2012-2021, 2006

[314] C. A. MacRae, W. Birchmeier and L. Thierfelder. Arrhythmogenic right ventricular cardiomyopathy: moving towards mechanism. The journal of clinical investigation 116: 1825-1828, 2006

[315] X. He, M. Semenov, K. Tamai and X. Zeng. LDL receptor-related proteins 5 and 6 in Wnt/β catenin signaling: arrows point the way. Development 131: 1663-1677, 2004

[316] K. Tamai, X. Zeng, C. Liu, X. Zhang, Y. Harada, Z. Chang and X. He. A mechanism for Wnt coreceptor activation. Molecular cell 13: 149-156, 2004

[317] K. Tamai, M. Semenov, Y. Kato, R. Spokony, C. Liu, Y. Katsuyama, F. Hess, J-P. Saint-Jeannet and X. He. LDL-receptor-related proteins in Wnt signal transduction. Nature 407: 530-535, 2000

[318] O. Huber, R. Korn, H. McLaughlin, M. Ohsugi, B. G. Herrman and R. Kemler. Nuclear localization of β-catenin by interaction with transcription factor LEF-1. Mechanisms of develop,ent 59: 3-10, 1996

[319] N. S. Tolwinski and E. Wieschaus. A nuclear function for armadillo/β-catenin. PLOS Biology 2: 1-8, 2004

[320] A. Hecht, C. M. Litterst, O. Huber and R. Kemler. Functional characterization of multiple transactivating elements in β-catenin, some of which interact with the TATA-binding protein in vitro. The journal of biological chemistry 274: 18017-18025, 1999

[321] I. Simcha, M. Shtutman, D. Salomon, J. Zhurinsky, E. Sdot, B. Geiger and A. Ben-Ze'ev. Differential nuclear translocation and transactivation potential of β-catenin and plakoglobin. The journal of cell biology 141: 1433-1448, 1998

[322] S. Miravet, J. Piedra, F. Miro, E. Itarte, A. Garcia de Herreros and M. Dunach. The transcriptional factor Tcf-4 contains different binding sites for β-catenin and plakoglobin. The journal of biological chemistry 277: 1884-1891, 2002

[323] J. Zhurinsky, M. Shtutman and A. BenZe'ev. Differential mechanisms of LEF/TCF family-dependent transcriptional activation by β-catenin and plakoglobin. Molecular and cellular biology 20: 4238-4252, 200

[324] P. Hu, P. Berkowitz, E. J. O'Keffe and D. S. Rubenstein. Keratinocyte adherens junctions initiate nuclear signaling by translocation of plakoglobin from the membrane to the nucleus. Journal of investigative dermatology 121: 242-251, 2003

[325] A. Rubenstein, J. Merriam and M. W. Klymkowsky. Localizing the adhesive and signaling functions of plakoglobin. Developmental genetics 20: 91-102, 1997

[326] O. Maeda, N. Usami, M. Kondo, M. Takahashi, H. Goto, K. Shimokata, K. Kusugami and Y. Sekido. Plakoglobin (γ-catenin) has TCF/LEF family-dependent transcriptional activity in β-catenin-deficient cell line. Oncogene 23: 964-972, 2004

[327] F. T. Kolligs, B. Kolligs, K. M. Hajra, G. Hu, M. Tami, K. R. Cho and E. R. Fearon. Γ-catenin is regulated by the APC tumor suppressor and its oncogenic activity is distinct from that of β-catenin. Genes & Development 14: 1319-1331, 2000

[328] E. K. Wlodarska, M. Konka, T. Zaleska, R. Ploskin, K. Cedro, B. Pucilowska, M. Bekiesinska-Figatowska, W. Rydlewska-Sadowska, W. Ruzyllo and P. Hoffman. Arrhythmogenic right ventricular cardiomyopathy in two pairs of monozygotic twins. International journal of cardiology 105: 125-133, 2005

[329] P. Kirchhof, L. Fabritz, M. Zwiener, H. Witt, M. Schafers, S. Zellerhoff, P. Matthias, T. Athai, K. H. Hiller, H. A. Baba, G. Breithardt, P. Ruiz, T. Wichter, B. Levkau. Age- and training-dependent development of arrhythmogenic right ventricular cardiomyopathy in heterozygous plakoglobin-deficient mice. Circulation 114: 1799-1806, 2006

[330] S. Firoozi, S. Sharma, M. S. Hamid and W. J. McKenna. Sudden death in young athletes: HCM or ARVC? Cardiovascular drugs and therapy 16: 11-17, 2002

[331] B. J. Maron, J. Shirani, L. C. Poliac, R. Mathenge, W. C. Roberts, F. P. Mueller. Sudden death in young competitive athletes. Clinical, demographic and pathological profiles. JAMA 276: 199-204, 1996

[332] D. Corrado, C. Basso, G. Rizzoli, M. Schiavon and G. Thiene. Does sports activity enhance the risk of sudden death in adolescents and young athletes? Journal of the American college of cardiology 42: 1959-1963, 2003

[333] N. Protonotarios, A. Tsatsopoulou, A. Anastasakis, E. Sevdalis, G. McKoy, K. Stratos, K. Gatzoulis, K. Tnetolouris, C. Spiliopoulou, D. Panagiotakos, W. J. McKenna and P. Toutouzas. Genotype-phenotype assessment in autosomal recessive arrhythmogenic right ventricular cardiomyopathy (Naxos disease) caused by a deletion in plakoglobin. Journal of the American college or cardiology 38: 1477-84, 2001

[334] J. Zhuang, K. A. Yamada, J. E. Saffitz and A. G. Kleber. Pulsatile stretch remodels cell-to-cell communication in cultured myocytes. Circulation research 87: 316-322, 2000

[335] R. C. Pimentel, K. A. Yamada, A. G. Kleber and J. E. Saffitz. Autocrine regulation of myocyte Cx43 expression by VEGF. Circulation research 90: 671- 677, 2002

[336] S. Rohr, D. M. Scholly and A. G. Kleber. Patterned growth of neonatal rat heart cells in culture. Circulation research 68: 114-130, 1991

[337] H. Huang, R. D. Kamm, P. T. So and R. T. Lee. Receptor-based differences in human aortic smooth muscle cell membrane stiffness. Hypertension 38:1158-1161, 2001

[338] H. Huang, J. Sylvan, M. Jonas, R. Barresi, P.T. So, K. P. Campbell and R. T. Lee. Cell stiffness and receptors: evidence for cytoskeletal subnetworks. Am J Physiol Cell Physiol 288:C72-80, 2005

[339] J. Lammerding, H. Huang, P.T. So, R. D. Kamm and R. T. Lee. Quantitative measurements of active and passive mechanical properties of adult cardiac myocytes. IEEE Eng Med Biol Mag 22:124-127, 2003

[340] J. Lammerding, A. R. Kazarov, H. Huang, R.T. Lee and M. E. Hemler. Tetraspanin CD151 regulates alpha6beta1 integrin adhesion strengthening. Proc Natl Acad Sci USA 100:7616-7621,2003

[341] H. Huang, F. Cruz and G. Bazzoni. Junctional adhesion molecule-A regulates cell migration and resistance to shear stress. J Cell Physiol 209:122-130,2006

[342] D. Hakuno, T. Takahashi, J. Lammerding and R.T. Lee. Focal adhesion kinase signaling regulates cardiogenesis of embryonic stem cells. J Biol Chem 280:39534-39544, 2005

[343] S. Kippenberger, A. Berndm S. Loitsch, M. Guschel, J. Muller, J. Hahn-Bereiter and R. Kaufmann. Signaling of mechanical stretch in human keratinocytes via MAP kinases. Journal of investigative dermatology 114: 408-412, 2000

[344] C. H. Turner and F. M. Pavalko. Mechanotransduction and functional response of the skeleton to physical stress: the mechanisms and mechanics of bone adaptation. J. Orth Sci 3: 346-355, 1998

[345] Y. Sawada, K. Nakamura, K. Doi, K. Takeda, K. Tobiume, M. Saitoh, K. Morita, I. Komuro, K. De Vos, M. Sheetz and H. Ichijo. Rap1 is involved in cell stretching modulation of p38 but not ERK or JNK MAP kinase. Journal of cell science 114: 1221-1227, 2001

[346] G. E. Morley and J. Jalife. Cardiac gap junction remodeling by stretch: is it a good thing? Circulation research 87: 272-274, 2000

[347]M. Stula, H. D. Orzechowski, S. Gschwend, R. Vetter, R. von Harsdorf, R. Dietz and M. Paul. Influence of sustained mechanical stress on Egr-1 mRNA expression in cultured human endothelial cells. Molecular and Cellular biochemistry 210: 101-108, 2000

[348] Y. Seko, Y. Seko, N. Takahaski, K. Tobe, T. Kadowaki and Y. Yazaki. Pulsatile stretch activated mitogen-activated protein kinase (MAPK) family members and focal adhesion kinase ($p125^{FAK}$) in cultured rat cardiac myocytes. Biochemical and biophysical research communications 259: 8-14, 1999

[349] S. Kudoh, H. Akazawa, H. Takano, Y. Zou, H. Toko, T. Nagai and I. Komuro. Stretch-modulation of second messengers: effects on cardiomyocyte ion transport. Progress in biophysics & molecular biology 82: 57-66, 2003

[350] T. Tsuruda, J. kato, K. Kitamura, T. Imamura, T. Koiwaya, K. Kangawa, I. Komuro, Y. Yazaki and T. Eto. Enhanced adrenomedullin production by mechanical stretching in cultured rat cardiomyocytes. Hypertension 35: 1210-1214, 2000

[351] X. D. Liao, X. H. Wang, H. J. Jin, L. Y. Chen and Q. Chen. Mechanical stretch induces mitochondria-dependent apoptosis in neonatal rat cardiomyocytes and G_2/M accumulation in cardiac fibroblasts. Cell research 14: 16-26, 2004

[352] Y. Seko, Y. Seko, N. Takahashi, M. Shibuya and Y. Yasaki. Pulsatile stretch stimulated vascular endothelial growth factor (VEGF) secretion by cultured rat cardiac myocytes. Biochemical and biophysical research communications 254: 462-465, 1999

[353] K. Yamada, K. G. Green, A. M. Samarel and J. E. Saffitz. Distinct pathways regulate expression of cardiac electrical and mechanical junction proteins in response to stretch. Circulation research 97: 346-353, 2005

[354] W. Chamulitrat, R. Schmidt, W. Chunglok, A. Kohl and P. Tomakidi. Epithelium and fibroblast-phenotypes derived from HPV16 E6/E7 immortalized human gingival keratinocytes following chronic ethanol treatment. European journal of cell biology 82: 313-322, 2003

[355] C. E. Murry, R. W. Wiseman, S. M. Schwartz and S. D. Hauschka. Skeletal myoblast transplantation for repair of myocardial necrosis. J Clin Invest 98: 2512-2523, 1996

[356] M. M. Davidson, C. Nesti, L. Palenzuela, W. F. Walker, E. Hernandez, L. Protas, M. Hirano and N. D. Isaac. Novel cell lines derived from adult human ventricular cardiomyocytes. Journal of molecular and cellular cardiology 39: 133-147, 2005

[357] M. E. Steinhelper, N. A. Lanson Jr, K. P. Dresdner, J. B. Delcarpio, A. L. Wit and W. C. Claycomb. Proliferation in vivo and in culture of differentiated adult atrial cardiomyocytes from transgenic mice. Am J Physiol 259: H1826-H1834, 1990

[358] T. Jaffredo, A. Chestier, N. Bachnou and F. Dieterlen-Lievre. MC29-immortalized clonal avian heart cell lines can partially differentiate in vitro. Exp Cell Res 192: 481-491, 1991

[359] E. B. Katz, M. E. Steinhelper, J. B. Delcarpio, A. I. Daud, W. C. Claycomb and L. J. Field. Cardiomyocyte proliferation in mice expressing alpha-myosin heavy chain-SV40-T-antigen transgenes. Am J Physiol 262: H1867-G1876, 1992

[360] Y. C. Wang, N. Neckelmann, A. Mayne, A. Herskowitz, A. Srinivasan and K. W. Sell. Establishment of a human fetal cardiac myocyte cell line. In vitro cell dev biol 27: 63-74, 1991

[361] A. Kass-Eisler, E. Falck-Pedresen, M. Alvira, J. Rivera, P. M. Buttrick, B. A. Wittenberg, L. Cipriani and L. A. Leinwand. Quantitative determination of adenovirus-mediated gene delivery to rat cardiac myocytes in vitro and in vivo. Proc Natl Acad Sci USA 90: 11498-11502, 1993

[362] Ji-Guo Yu and B. Russell. Cardiomyocyte remodeling and sarcomere addition after uniaxial static strain in vitro. Journal of histochemistry and cytochemistry 53: 839-844, 2005

[363] C. Fink, S. Ergun, D. Kralisch, U. Remmers, J. Weil and T. Eschenhagen. Chronic stretch of engineered heart tissue induces hypertrophy and functional improvement. FASEB J 14: 669-679, 2000

[364] B. Swynghedauw. Molecular mechanisms of myocardial remodeling. Physiol rev 79: 215-262, 1999

[365] K. Andra, H. Lassmann, R. Bittner, S. Shorny, R. Fassler, F. Propst and G. Wiche. Targeted inactivation of plectin reveals essential function in maintaining the integrity of skin, muscle and heart cytoarchitecture. Genes and development 11: 3143-3156, 1997

[366] E. Pfender, F. Rouan and J. Uitto. Progress in epidermolysis bullose: the phenotypic spectrum of plectin mutations. Experimental dermatology 14: 241-249, 2005

[367] W. A. Paznekas, S. A. Boyadjiev, R. E. Shapiro, O. Daniels, B. Wollnik, C. E. Keegan, J. W. Innis, M. B. Dinulos, C. Christian, M. C. Hannibal and E. W. Jabs. Connexin 43 (GJA1) mutations cause the pleiotropic phenotype of oculodentodigital dysplasia. Am J Hum Genet 72: 408-418, 2003

[368] J. E. J. Schultz, B. J. Glascock, S. A. Witt, M. L. Nieman, K. J. Nattamai, L. H. Liu, J. N. Lorenz, G. E. Shull, T. R. Kimball and M. Periasamy. Accelerated onset of heart failure in mice during pressure overload with chronically decreased SERCA2 calcium pump activity. Am J Physiol Heart Circ Physiol 296: H1146-H1153, 2004

[369] M. Periasamy, T. D. Reed, L. H. Liu, Y. Ji, E. Loukianov, R. J. Paul, M. L. Nieman, T. Riddle, J. J. Duffy, T. Doetschman, J. N. Lorenz and G. E. Shull. Impaired cardiac performance in heterozygous mice with a null mutation in the sarco(endo)plasmic reticulum Ca^{+2}-ATPase isoform 2 (SERCA2) gene. The journal of biological chemistry 2745: 2556-2562,1999

[370] P. Descargues, C. Deraison, C. Bonnart, M. Kreft, M. Kishibe, A. Ishida-Yamamoto, P. Elias, Y. Barrandon, G. Zambruno, A. Sonnenberg and A. Hovnarian. Spink5-deficient mice mimic Netherton syndrome through degradation of desmoglein 1 by epidermal protease hyperactivity. Nature genetics 37: 56-65, 2005

[371] A. Jazwinska, E. Ehler and S. M. Hughes. Intermediate filament-co-localized molecules with myosin heavy chain epitopes define distinct cellular domains in hair follicles and epidermis. Cell Biology 4, 2003

[372] P. Melacini, M. Fanin, G. A. Danieli, C. Villanova, F. Martinello, M. Miorin, M. P. Freda, M. Miorelli, M. L. Mostacciuolo, G. Fasoli, C. Angelini and S. Dalla Volta. Myocardial involvement is very frequent among patients with sub-clinical Becker's muscular dystrophy. Circulation 94: 3168-3175, 1996

[373] K. A. Lapidos, R. Kakkar and E. M. McNally. The dystrophin glycoprotein complex: signaling strength and integrity for the sarcolemma. Circulation research 94: 1023-1031, 2004

[374] A. A. Carvalho, J. A. Levy, P. S. Gutierrez, S. K. Marie, E. A. Sosa and M. Scanavaca. Emery-Dreifuss muscular dystrophy: anatomical-clinical correlation (case report). Arq Neuropsiquiatr 58: 1123-1127, 2000

[375] M. C. Fishbein, R. J. Siegel, C. E. Thompson and L. C. Hopkins. Sudden death of a carrier of X-linked Emery-Dreifuss muscular dystrophy. Ann intern Med 119: 900-905, 1993

[376] S. Bione, E. Maestrini, S. Rivella, M. Mancini, S. Regis, G. Romeo and D. Toniolo. Identification of a novel X-linked gene responsible for Emery-Dreifuss muscular dystrophy. Nature Genetics 8: 323-327, 1994

[377] L. Cartegni, M. R. di Barletta, R. Barresi, S. Squarzoni, P. Sabatelli, N. Maraldi, M. Mora, C. di Blasim F. Cornelio, L. Merlini, A. Villa, F. Cobianchi and D. Toniolo. Heart-specific localization of emerin: new insights into Emery-Dreifuss muscular dystrophy. Hum Mol Genet 6: 2257-2264, 1997

[378] G. Schiavon, S. Furlan, P. Marin and S. Salvatori. Myotonic dystrophy protein kinase of the cardiac muscle: evaluation using an immunochemical approach. Microsc Res Tech 58: 404-411, 2002

[379] S. Peters. Advances in the diagnostic management of arrhythmogenic right ventricular dysplasia-cardiomyopathy. International Journal of Cardiology 113: 4-11, 2006

[380] J. E. Saffitz. Structural heart disease, SCN5A gene mutations and Brugada syndrome: a complex ménage a trios. Circulation 112: 3672-3674, 2005

[381] D. Jane-wit, C. Z. Altuntas, J. M. Johnson, S. Yong, P. J. Wickley, P. Clark, Q. Wang, Z. B. Popovic, M. S. Penn, D. S. Damron, D. M. Perez and V. K. Tuohy. B1-adrenergic receptor autoantibodies mediate dilated cardiomyopathy by agonistically inducing cardiomyocyte apoptosis. Circulation 116: 399-410, 2007

[382] S. A. Grando. Pemphigus in the XXI century: new life to an old story. Autoimmunity 39: 521-530, 2006

[383] B. Tandler, L. Riva, F. Loy, G. Conti and R. Isola. High resolution electron microscopy of the intracellular surface of intercalated disks in human heart. Tissue and Cell 38: 417-420, 2006

[384] C. M. Borrmann, C. Grund, C. Kuhn, I. Hofmann, S. Pierperhoff and W. W. Franke. The area composita of adhering junctions connecting heart muscle cells of vertebrates. II. Colocalizations of desmosomal and fascia adhaerens molecules in the intercalated disk. European journal of cell biology 85: 469-485, 2006

[385] T. Taniguchi, M. Miyazakim Y. Miyashita, T. Arima and M. Ozawa. Identification of regions of alpha-catenin required for desmosome organization in epithelial cells. Int J Mol Med 16: 1003-1008, 2005

[386] E. M. Small and P. A. Krieg. Molecular regulation of cardiac chamber-specific gene expression. TCM 14: 13-18, 2004

[387] S. Sharma, P. Razeghi, A. Shakir, B. J. Keneson 2nd, F. Clubb and H. Taegtmeyer. Regional heterogeneity in gene expression profiles: a transcript analysis in human and rat heart. Cardiology 100: 73-79, 2003